ISSN 2519-8521 (Print)
ISSN 2520-2588 (Online)

Regulatory Mechanisms in Biosystems

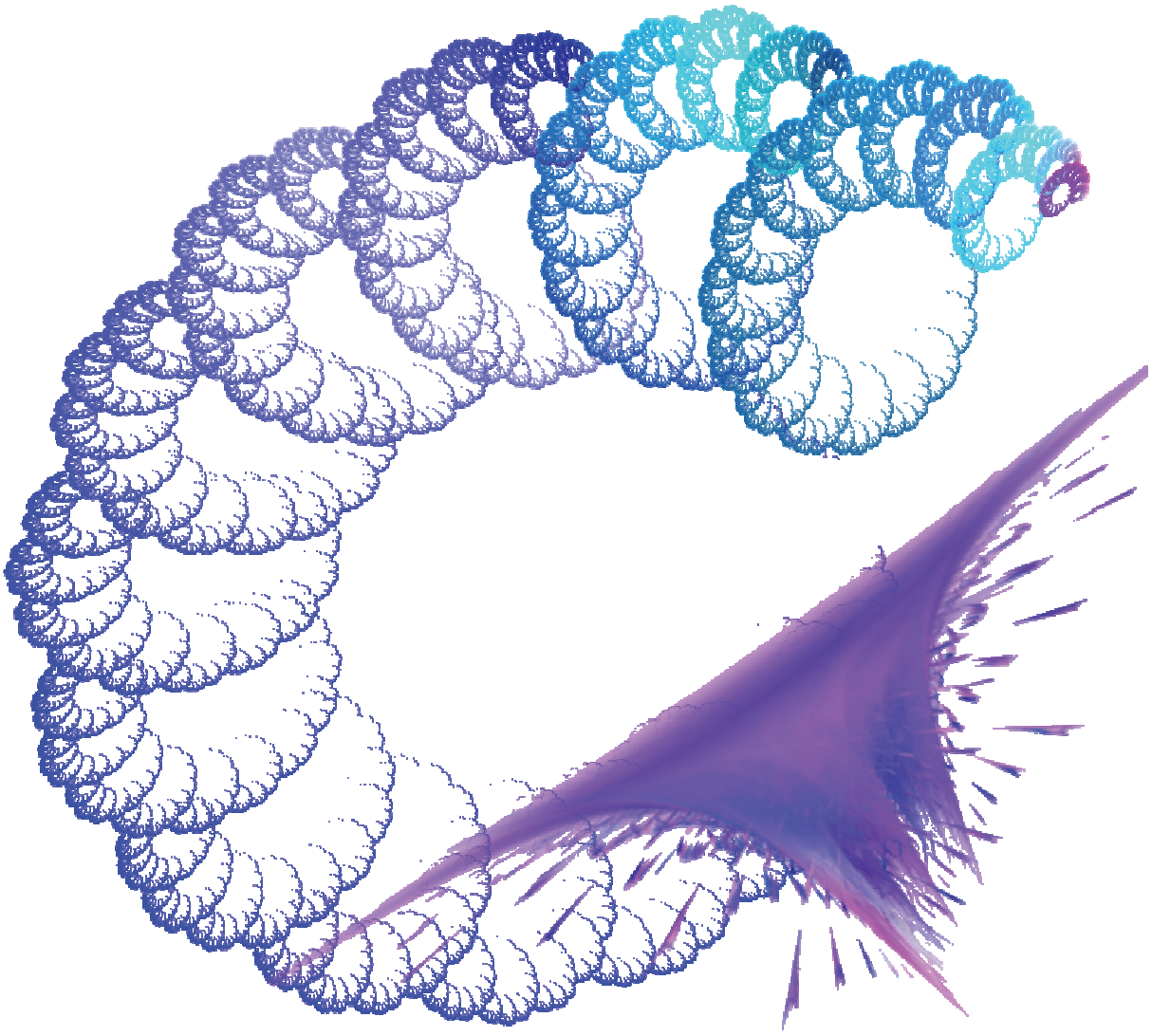

Volume 9(3)

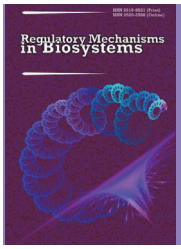

Regulatory Mechanisms in Biosystems

ISSN 2519-8521 (Print)
ISSN 2520-2588 (Online)

Aims and scope. *Regulatory Mechanisms in Biosystems* publishes peer-reviewed original research and review articles across all aspects of regulatory mechanisms in biological systems from the molecular level of organisation to the level of the organism. This journal mostly focuses on physiological mechanisms of regulation of metabolic processes, biochemical and physiological features of any species including human beings. This journal covers a wide range of regulatory mechanisms in biological systems that are associated both with natural processes and those transformed under the influence of chemicals and drugs, and any other man-made factors. We will publish papers concerned solely with clinical case studies and clinical trials if such articles address important questions in regulatory mechanisms in biosystems. *Regulatory Mechanisms in Biosystems* focuses on good-quality research, reporting scientifically sound observations and valid conclusions, which bring new and important information to the attention of the wider international scientific community. The journal publishes contributions in the following basic areas: biochemistry, bioinformatics, biophysics, cell biology, endocrinology, genetics, immunology, microbiology, molecular biology, physiology, neuroscience, pharmacology, toxicology.

Publication information. *Regulatory Mechanisms in Biosystems*, ISSN 2519-8521 (Print), ISSN 2520-2588 (Online). Subscription prices are available upon request from the Publisher or from the journal's website (www.medicine.dp.ua). Subscriptions are accepted on a prepaid basis only and are entered on a calendar year basis. Issues are sent by standard mail (surface within Europe, air delivery outside Europe). Priority rates are available upon request. Claims for missing issues should be made within six months of the date of dispatch.

Approved by the Scientific Council of Oles Honchar Dnipro National University, Gagarin Ave., 72, Dnipro, 49010, Ukraine

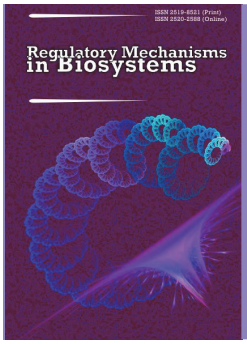

Regulatory Mechanisms in Biosystems

ISSN 2519-8521 (Print)
ISSN 2520-2588 (Online)
Regul. Mech. Biosyst., 9(3), 309–314
doi: 10.15421/021845

Effect of trypanosomiasis on hematologic characteristics of bream (*Abramis brama*)

T. B. Lapirova, E. A. Zabotkina

I. D. Papanin Institute for Biology of Inland Waters RAS, Borok, Russia

Article info

Received 19.04.2018
Received in revised form 07.05.2018
Accepted 10.05.2018

I. D. Papanin Institute for Biology of Inland Waters RAS, Borok, 152742, Russia.
Tel.: +748-547-24-042
E-mail: ltb@ibiw.yaroslavl.ru

Lapirova, T. B., & Zabotkina, E. A. (2018). Effect of trypanosomiasis on hematologic characteristics of bream (Abramis brama). Regulatory Mechanisms in Biosystems, 9(3), 309–314. doi:10.15421/021845

Trypanosomes are flagellated protozoa; they parasitize in the blood of a wide range of vertebrates and invertebrates, including fish, for which leeches are carriers. The metabolites released by trypanosomes are toxic to the host, cause disruption of homeostasis, which leads to illness and even death. Parasites in fish living in hot climates are the most common and better studied. Trypanosomes were first detected in common bream (*Abramis brama* L.) from the Uglich Reservoir (Upper Volga) in August 2015. The aim of this work is to study the effect of these parasites on the hematological parameters of the fish. As a control, blood indices of uninfected fish were used. The condition factor of infected fish did not differ from that of healthy fish. There were no significant differences between the two groups of fish in contents of total serum protein and glycemia. This may indicate a low level of bream parasitemia. At the same time, a significant increase in the leukocyte abundance index was detected, which indirectly indicates an increase in the number of these cells in the infected fish compared with the control ones, statistically significant differences were found in the leukogram: the proportion of eosinophils in the diseased fish increased almost 6 times while the relative number of lymphocytes decreased. The pattern of red blood also changed: the proportion of immature erythrocytes increased in the infected fish; a small number of microcytes and amitoses of erythrocytes and differences in the cytometric characteristics of red blood cells were found. The level of hemoglobin significantly decreased. A sharp increase in the content of circulating immune complexes indicates a shift in antigenic homeostasis caused by the presence of parasites. A similarity in the reaction of a number of indicators of the blood system of bream with trypanosomiasis to that of animals of higher systematic groups was revealed. The interpretation of the results obtained during the study of the effect of parasites on the host organism requires consideration of its physiological status and habitat conditions, the stage of the disease and the mechanism of adaptation of the parasite to the host defense system.

Keywords: *Trypanosoma* sp.; common bream; blood cells; hemoglobin; total protein; glucose; circulating immune complexes.

Introduction

Trypanosoma are a large group of flagellate protozoa, which parasitize in the blood of many vertebrate and some invertebrate animals (Goodwin, 1985; Ranzani-Paiva et al., 1997; Haag et al., 1998; Fermino et al., 2015). In fish, *Trypanosoma* have been found both in marine and fresh water species, representatives of Cyprinidae (Grybchuk-Ieremenko et al., 2014), eels (Islam & Woo, 1991a; Zintl et al., 1997), gobies, esocids, Pleuronectidae (Woo, 2001), Gadidae (Khan, 1977), Schilbeidae and Clariidae (Ferreira & Avenant-Oldewage, 2013), Serranidae (Wang et al., 2015), *Tilapia* (de Jesus et al., 2018), Characidae (Rodrigues et al., 2018). Fish living in hot climates are the most affected. Trypanosomes are very small, their length, depending on the species, ranges from 2 to 30 μm. They consume food in the form of dissolved organic and other substances using the entire surface of their body. The products of the metabolism of these parasites can be highly toxic and cause serious, and in many cases lethal diseases to their hosts (Bienek et al., 2002).

The life cycles of most trypanosomes have been insufficiently studied, but it has been established that among the invertebrates, their hosts are leeches, which therefore are the carriers of these protozoa for many fresh water as well as the marine species of fish, (Qadri, 1962; Mork, 2011; Hayes et al., 2014; Lemos et al., 2015). In water bodies with a high number of leeches, fish are often infected by *Trypanosoma*, around 200 species of piscine trypanosomes being currently known (Gupta & Gupta, 2012). During the cultivation of fish in ponds, disease outbreaks are rare due to absence of carriers, whereas in open water bodies inhabited by leeches, trypanosomiasis of fish can be a serious problem. According to some authors, at the initial stage of infestation, stimulation of humoral and cell immunity occurs (Ribeiro et al., 2010; Oladiran et al., 2011). The extent of the impact of the parasites on the organism of fish is mostly determined by the energetic resources of the host, and also the conditions of the environment (water temperature, feeding, competition, etc.) (Gupta & Gupta, 2012). It has been demonstrated that trypanosomes decrease the vitality and the growth tempi of fish, cause anemia (Dykova & Lom, 1979; Clauss et al., 2008), shifts of physiological and biochemical parameters, disorders in metabolic processes (Lom & Dykova, 1984; Gupta & Gupta, 1987). Histopathological analyses of infected fish, compared to healthy fish, have indicated the following disorders; damaged vessels of spleen, degenerative and infiltrational changes in hepatocytes and epithelium of the kidney tubules, hypertrophy of epithelium cells of secondary lamellae of the gills (Osman et al., 2009).

Despite the fact that trypanosomiasis of fish was determined long ago, data on the parasites` impact on physiological and hematological parameters of infected fish are fragmented, and the problem of the influence of these protozoa on the commercial species which live in the Volga has not been studied. The objective of this paper is the study of the morphophysiological and hematological parameters of fish infected by trypanosomes. The scope of the study included determining the condition factor, hemoglobin concentration, the content of total protein, glucose and circulating immune complexes, leukogram, and also the ratio of different age stages and sizes of the erythrocytes of common bream from the Uglich Reservoir.

Materials and methods

For the study, we used common bream *Abramis brama* L. caught in the Uglich Reservoir in August 2015. For the study, we selected 20 mature fish of 294 ± 25 mm and 547 ± 142 g length and weight respectively. Trypanosomes were found in the blood smear of all 20 individuals. Systematically, they belong to Protozoa kingdom; Euglenozoa type; Kinetoplastida class; Trypanosomatida order; Trypanosomatidae family; *Trypanosoma* genus. No identification of the parasitic species was made. As the control, we used non-infected fish (15 individuals) with similar linear-weight parameters selected during the same period in the Ivankovo Reservoir located upstream of the Volga (Fig. 1).

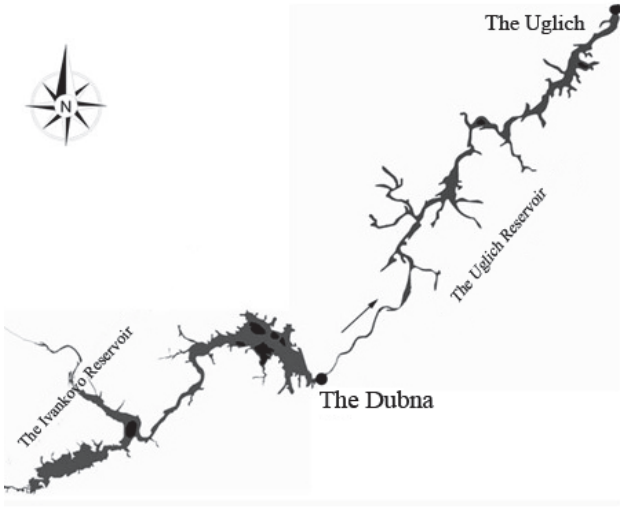

Fig. 1. Scheme of the Reservoirs

The main hydrochemical parameters of the water bodies where the fish was caught (pH, BOD, the content of the main cations and anions, nutrients) have similar values (Debol'skij et al., 2010). According to the results of the final evaluation of the quality of the water in the Uglich Reservoir, the water is considered "dirty" by most of the integral hydrochemical indices (Lazareva, 2016). The water in the Ivankovo Reservoir, in area where the fish were caught, is also considered "dirty" according to the main hydrochemical parameters (Debol'skij et al., 2010). Therefore, no principal difference in the quality of water in the two reservoirs was found.

We measured the body length, weight of the fish, and after the caudectomy, obtained blood. The smears were made, part of the blood was stabilized by heparin and was used for identification of hemoglobin. The remaining blood was used for making blood serum. Then, the fish was anatomized and weighed after the internal organs were removed. The condition factor was calculated according to Clark. The concentration of hemoglobin was analyzed using the HPP-01 [Hemoglobinometer photometric portative] miniHEM+ hemoglobinometer in accordance with the hemichrome method. The level of circulating immune complexes (CIC) was determined using a standard method of sedimentation with polyethylene glycol. The results are given in conventional units. The content of total protein and glucose in the serum was determined according to the biuret and glucose oxidase methods respectively, using the "Agat-Med" standard sets of reagents for clinical analysis.

The smears were processed according to the standard method, we established the leukocyte formula, and also the relative number of erythroblasts, immature and mature erythrocytes, amitosis. During the calculation of the red blood cells, we took into account no less than 500 cells in the smears, the results were expressed as a % of total number of erythrocytes. The anomalous forms of erythrocytes were considered microcytes and cells without a nucleus. The amitosis were calculated also for 500 erythrocytes and expressed as a %.

In determining the proportion of the leukocytes, we calculated no less than 200 cells in a smear. We identified hematopoietic stem cells, lymphocytes, monocytes, myelocytes, metamyelocytes, stab neutrophils and segmented neutrophils, eosinophils. The results of the calculation were expressed as a %. The abundance index of leukocytes (without thrombocytes) was calculated as the number of the leukocytes in the microscope field of view at $^{x}1000$ magnification. The number of thrombocytes was calculated in relation to the total number of leukocytes and was expressed as a %.

We measured the small (h) and large (l) diameter of the erythrocytes and their nuclei, calculated the index of form, area of cells and nuclei, nuclear-cytoplasmic ratio. The index of form (If) was calculated as a ratio of the small diameter (h) of the cell to the large (l): If = h/l. The area of the cell and nucleus was calculated using the formula ellipse equation: $S = \pi hl/2$, μm^2. Nuclear-cytoplasm ratio was calculated using the formula: $N/C = S_n/(S_c–S_n)$, where S_n – the area of nucleus, S_c – the area of cell. The research was conducted using a Keyence VHX-1000 microscope using a Z-500 R objective at ×2000–3000 magnification.

The results were analyzed in the Statistica package at the significance level of $P < 0.05$. The data are presented as mean values and standard errors (x ± SE), for the assessment of the values` reliability, we used ANOVA, taking into account the normal distribution of the parameters.

Results

Trypanosomes were found for the first time in the peripheral blood of common bream from the Uglich Reservoir. The parasites were found in the smears of all analyzed fish to the amount of 1–3 individuals per 10 and more view fields (at $^{x}1000$ magnification) (Fig. 2).

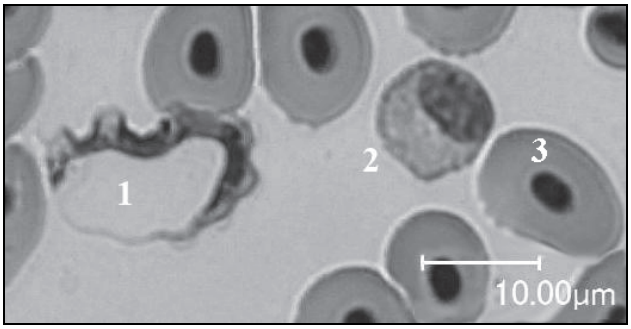

Fig. 2. Peripheral blood of common bream from the Uglich Reservoir: *1* – trypanosome, *2* – neutrophil metamyelocyte, *3* – erythrocyte

Condition factor. The presence of parasites did not affect the fatness coefficient, in both groups of the fish it was the same, equaling 1.8 ± 0.1.

Physiological-biochemical parameters of the blood. The results are presented in Table 1.

Table 1
Physiological-biochemical parameters of the peripheral blood of bream (x ± SE)

Parameters	Infected fish, n = 20	Control, n = 15
Total protein, g/l	44.9 ± 2.4	40.6 ± 1.2
Glucose, mmol/l	5.0 ± 0.5	5.4 ± 1.0
Hemoglobin, g/l	67.8 ± 3.3*	80.6 ± 1.6
CIC, conventional units	37 ± 4*	18 ± 3

Note: hereinafter, * – symbol in tables indicates the values which are statistically reliably different compared to the control.

As the obtained data demonstrated, the content of the total protein in the serum of the infected fish was slightly higher than in the control, though this difference was not statistically reliable. The level of glycemia the fish of the both groups practically did not differ. The hemoglobin concentration of the infected fish was reliably lower than among the healthy fish, and the CIC content of the fish from the first group was twice as high compared to the control.

Blood cells. Despite the relatively low level of infection, the blood leukogram was sharply shifted towards the granular forms of

the cells (Table 2), mostly due to 6 times increase in the content of eosinophils.

Table 2
The ratio of the forms of leukocytes and erythrocytes in the peripheral blood of bream (x ± SE)

Parameter	Infected fish, n = 20	Control, n = 15
Erythrocytes		
Erythroblasts	3.51 ± 1.43	1.73 ± 0.81
Immature erythrocytes	4.52 ± 1.24*	2.11 ± 1.51
Mature erythrocytes	93.33 ± 2.01	97.60 ± 1.82
Amitosis	0.53 ± 0.21	0.00
Microcytes	1.23 ± 1.03	0.00
Leukocytes		
Lymphocytes	50.04 ± 0.52*	67.30 ± 2.41
Monocytes	2.92 ± 0.21	0.89 ± 0.89
Blasts	2.38 ± 0.26	1.09 ± 0.78
Myelocytes	5.11 ± 0.67*	14.22 ± 3.24
Metamyelocytes	14.21 ± 1.11	10.38 ± 4.52
Stab neutrophils	5.89 ± 0.09	6.83 ± 2.37
Segmented neutrophils	0.30 ± 0.30	1.03 ± 0.77
Eosinophils	19.26 ± 1.91*	2.83 ± 1.77
Shift of leukocytes	0.77 ± 0.05*	0.53 ± 0.21
Index of leukocyte abundance	20.00 ± 2.00*	8.00 ± 5.00
Thrombocytes	63.52 ± 0.68*	52.08 ± 4.48

We should mention the increase in the index of leukocyte abundance, and also reliable increase in the relative number of thrombocytes in the infected fish compared to the control. The ratio of immature and mature erythrocytes was higher among the infected fish, in their peripheral blood, we also found an insignificant amount of amitosis and microcytes.

The analysis of the cytometric characteristics of erythrocytes indicated that the erythrocytes of the infected fish had a more rounded shape, had a smaller area, but greater nuclear-cytoplasmic ratio (Table 3).

Table 3
Cytometric parameters of the erythrocytes of bream (x ± SE)

Parameter	Infected fish, n = 20	Control, n = 15
Cell		
H, μm	8.85 ± 0.04	9.24 ± 0.03
L, μm	11.81 ± 0.03	12.62 ± 0.06
Sc, μm^2	82.04 ± 0.87*	91.52 ± 0.64
I_f	0.75 ± 0.06	0.73 ± 0.04
Nucleus		
H, μm	4.84 ± 0.05	4.64 ± 0.04
L, μm	6.08 ± 0.03	5.76 ± 0.06
Sn, μm^2	23.09 ± 0.22	20.98 ± 0.32
Nuclear-cytoplasmic ratio	0.39 ± 0.01*	0.30 ± 0.02

Discussion

The difference which consisted in the presence or absence of infection of bream in the Uglich and Ivankovo Reservoirs may be caused by the peculiarities of these water bodies. The main fattening places of the fish are shallow-water areas up to 3 m depth. The shallow water area in the Uglich Reservoir is almost 2 times smaller compared to the Ivankovo (90 and 160 km^2, respectively), which is by 12% lower in relation to the total area of the reservoir (48 and 36%). At the same time, ichthyomass of the demersal fish in the Uglich Reservoir since 1985 has been higher than in the Ivankovo Reservoir (Ehdel'shtejn, 1998).

The number of leeches (intermediate hosts of trypanosomes) on fish in the Uglich Reservoir is higher compared to the Ivankovo (Lapkina et al., 2002), therefore the probability of infection of the fish is higher in the Uglich Reservoir than in the Ivankovo Reservoir.

Trypanosomes grow to the full length in 60 days after penetrating the blood of fish (Lom & Dykova, 1984), therefore the occurrence of individuals of more than 80 μm length and 3 to 5 individuals per mm^3 in the bloodstream of the bream indicate that the bream of the Uglich Reservoir were exposed to the chronic stage of the disease. The literature contains very few data on the impact of trypanosomes on the linear-weight parameters of fish. The are reports that the parasites can cause decrease in growth and weight (Kharat & Kothavade, 2012), at the same time, the analysis of the impact of the extent of infestation by *T. percea* on length and weight of perch revealed differences only in the juvenile groups (Hamnueva, 2001).

Referring to the literature data, Islam & Woo (1991b) provide several reasons for the decrease in food consumption among fish infected by trypanosomes: slowing of food passage through the intestine, damage to the mucous membrane of the intestine, which leads to disorders in metabolism and absorption, disruption in the balance of hormones which regulate the sense of hunger, and development of anorexia. However, in their own studies, the authors did not find any significant decrease in the body weight of the infected fish. They think that the fish with developed anorexia either die or survive a crisis, after which they return to normal feeding. The absence of differences according to the condition factor in our research most likely occurred due to relatively low level of infection.

The literature data on the changes in the level of total serum protein of the infected fish are also contradictory. There are reports about decrease in the parameters of African sharptooth catfish (Osman et al., 2009). According to the authors, the significant decrease in the total protein in the serum and its fractions (albumin and globulin) of the infected fish, which they found, could be caused by hemodilution. The representatives of 7 species of ornamental loricariids, infected by trypanosomes were observed to have both decrease and insignificant increase, as well as absence of the changes in the parameter compared to the control (Fudjimoto et al., 2013).

On the whole, literature data and our own study allow us to draw the conclusion that the level of total serum protein in fish with trypanosomiasis depends on many factors, including the extent of invasion, species and physiological condition of fish, etc.

Disorders in the carbohydrate metabolism of the host infected with protozoa were mentioned by von Brand (1973). He made the assumption that trypanosomes consume such an amount of sugar in the blood that the carbohydrate reserves of the host become depleted, causing a heavy load on the liver and disorders in its functioning. Such phenomenon occurs both among amniotes and fish. At the same time, the extent of depletion of the carbohydrate reserves of the host depends on the species of parasite and extent of infestation (Gupta & Gupta, 1987). According to the results of our studies, the average level of glucose in the blood of infested fish practically did not differ from that of the control fish, which was most likely caused by the low extent of invasion.

We found no literature data on the impact of protozoa on the level of CIC of fish. However, taking into account that the formation of immune complexes is an important and indispensable component of the mechanism of supporting the antigene homeostasis, and they are constantly present in blood stream, one should expect a reaction of the indicator to the parasites` penetration to organism. The CIC concentration is determined by the conditions of the fish` habitat. They are removed as with the amniotes – by cells of the mononuclear phagocyte system (MPS) (Levinsky, 1981).

It has been demonstrated that birds suffer the development of pathological process when subject to helminthiases with accompanying formation of CIC which take an important part in pathogenesis of the disease, and the period of their circulation in the host`s organism correlates with the time and severity of the pathological process (Kuklina & Kuklin, 2011). Increase in the content of CIC by 59% was also determined among horses suffering from strongyloidiasis (Tkachenko, 2009).

Because trypanosomes, as mentioned above, produce toxic metabolic products in the blood of the host, their neutralization requires an additional number of non-specific antibodies, which can also cause increase in the CIC level. Increased production of antibodies, including specific antibodies, by the host organism was noted by a number of authors during introduction of hemoflagellates (Evans & Gratzek, 1989; Plouffe & Belosevic, 2006; Joerink et al., 2007; Sitia-Bobadilla, 2008; Wiegertjes & Forlenza, 2010). Intensity of production of antibodies depends on the extent of the invasion and the temperature of the habitat (Woo, 1981; Sypek & Burreson, 1983). Therefore, literature

data and our study suggest that the immune complexes take an active part in an organism`s reaction to parasites.

Most researchers mention a decrease in the level of total number of erythrocytes among infected fish (Steinhagen et al., 1990; Hamnueva, 2001; Klauss et al., 2008; Shahi et al., 2013). It is considered that this parameter is the most vulnerable hematological parameter during trypanosomiasis. At the same time, apart from decrease in the total number of erythrocytes, a decrease in the content of hemoglobin has been mentioned (Shahi et al., 2013), and anemia in a number of cases (Gupta & Gupta, 2012). Anemia is considered the most typical symptom of trypanosomiasis, the fish are often slow and apathetic (Shahi et al., 2013).

On the basis of their own and literature data, Islam & Woo (1991a) came to the conclusion that decrease in the total number of erythrocytes in cases of trypanosomiasis is caused by at least two factors: first of all, hemolysin produced by the parasite, which causes direct lysis of erythrocytes; secondly, by hemodilution (increase in the blood volume), a process which correlates with the protozoa number. It was experimentally demonstrated that the hemolysis of erythrocytes is also caused by metalloproteinases produced by *Criptobia salmonocida* (Zuo & Woo, 2000).

The decrease in the proportion of mature and, correspondingly, increase in the immature erythrocytes that we observed has also been mentioned by other authors (Maqbool & Ahmed, 2016). Most likely, this phenomenon is related to stimulation of erythropoiesis caused by the accelerated death of mature cells.

The literature contains very few data on the change in morphometric characteristics of erythrocytes of fish with trypanosomiasis. There is information about decrease in hematocrit and increase in the cell volume of the infected fish (Shahi et al., 2013; Maqbool & Ahmed, 2016). On contrary, during direct counting of cell sizes, we determined a decrease in their area, increase in the area of the nucleus, and therefore increase in nuclear-cytoplasmic ratio. Perhaps, this decrease in the cell sizes is related to reduction of the time of their presence in the bloodstream.

We can draw a conclusion that cytometric parameters are affected by a number of factors, including the extent of the invasion, stage of disease, etc. The differences between the data we obtained and the literature data, is probably connected with the different methods of counting the volume (area) of cells. With recounting from hematocrit volume and number of erythrocytes to ml of blood, one will obtain average cell volume, without consideration of the stage of development, whereas during direct measurement of cells, one considers only the sizes of mature erythrocytes.

On the whole, measuring the morphometric parameters explains the rather steep decrease in the hemoglobin level: decrease in the share of mature erythrocytes, decrease in their area, including the area of cytoplasm, where hemoglobin is concentrated.

The leukocytes` reaction to parasites is similar to that occurring in guinea pigs and fresh water fish in cases of both acute and chronic processes. Usually, there is a steep increase in the total number of leukocytes and shift of the leukogram towards granular forms of cells (Shahi et al., 2013; Correa et al., 2016; Maqbool & Ahmed, 2016), which was also found in our study. Some authors mention that the reaction of phagocytes to trypanosome infection depends on the intensity of the invasion, its stage, and also the species of parasite and fish (Forlenza et al., 2008). We determined that the factors produced by monocytes (macrophages) in peripheral blood can stimulate growth and development of trypanosomes in hosts (Bienek & Belosevic, 1999). In its turn, transferrins which penetrate the blood during lysis of erythrocytes significantly activate the killer ability of macrophages (Stafford & Belosevic, 2003).

The significant increase which we found in the share of eosinophils among the infected fish coincides with the assumption that eosinophils are cells "responsible for the organism`s reaction to parasites" (Clauss et al., 2008). Eosinophilia was also observed in cases of infestation of fish by flat worms and nematodes (Kutyrev et al., 2011).

The reaction of thrombocytes to the invasion of parasites is not usually analysed, and data in the literature on the reaction of these cells in cases of parasitemia appear rarely and are contradictory. Therefore, protozoa caused no change in the share of thrombocytes in loricariid *Hypostomus* sp. (Correa et al., 2016), but carp with severe tryponosomiasis were observed to have a decrease in population of these cells in the spleen and blood and their apoptosis caused by increase in the level of nitrogen oxide in the blood (Fink et al., 2015), during our study, the bream showed a reliable increase in the share of these cells. Contradictions in the abovementioned data could most likely indicate insufficient study of this parameter in the response reaction of the host organism to parasitemia.

On the whole, the data we obtained indicate that the trypanosomes which have penetrated the organism of fish produce compounds that destroy erythrocytes, cause decrease in the level of hemoglobin, increase in the share of immature erythrocytes and stimulate production of eosinophils, and also cause increase in the level of CIC.

It is worth noting the similarity between the determined shifts of the hematological parameters in fish with trypanosomiasis and those caused by different species of parasites in different systematic groups of vertebrates: inhibition of erythropoiesis, eosinophilia, lymphopenia, increase in the CIC level among horses with strongloidiasis (Tkachenko, 2009), according to a number of parameters, the pattern of changes was similar to that of birds suffering from cestode invasion (Kuklina & Kuklin, 2011).

The ambivalence of the reaction of some parameters in different species of fish to trypanosome` invasion is caused by the fact that "parasite – host" is a complicated system of interdependence, which is determined by many factors, of which the most important are age, immune-physiological status and conditions of the fish habitat on the one hand and mechanisms of interaction of parasite and immune system of host on the other hand (Khan, 2012).

Conclusion

The absence of deviations in fatness, level of total serum protein and blood sugar level of the infected fish prove the conclusion drawn on the basis of analysis of blood smears that the level of parasitemia was low. The presence of a relatively low number of parasites and their sizes indicate the chronic stage of disease. The clear reaction of the CIC level in these conditions allows one to presume that using this parameter is promising for diagnosing parasitic infections, including those of protozoa. We determined changes in the condition of red blood, which allows one to assume a decrease in the lifespan of the erythrocytes, and also a reliable decrease in the concentration of hemoglobin in the blood. At higher levels of infestation, such shifts cause anemia. Change in the composition and ratio of the leukocytes accompanied increase in their total number. Shift of the leukocytes was caused mostly by growth of the share of eosinophils. On the whole, it could be stated that the reaction of the hematological parameters of bream to trypanosome infection is in general similar to the reaction of animals of higher systematic groups to presence of parasites.

The work was conducted within the framework of the budget topic AAAA-A18-118012690123-4.

References

Bienek, D. R., & Belosevic, M. (1999). Macrophage or fibroblast-conditioned medium potentiates growth of *Trypanosoma danilewskyi* Laveran & Mesnil 1904. Journal of fish diseases, 22(5), 359–367.

Bienek, D. R., Plouffe, D. A., Wiegertjes, G. F., & Belosevic, M. (2002). Immunization of goldfish with excretory/secretory molecules of *Trypanosoma danilewskyi* confers protection against infection. Developmental and Comparative Immunology, 26(7), 649–657.

Brand, T. von (1973). Biochemistry of parasites. Academic Press, New York.

Clauss, T. M., Dove, A. D. M., & Arnold, J. E. (2008). Hematologic disorders of fish. Veterinary Clinics: Exotic Animal Practice, 11, 445–462.

Correa, L. L., Oliveira, M. S. B., Tavares-Dias, M., & Ceccarelli, P. S. (2016). Infections of *Hypostomus* spp. by *Trypanosoma* spp. and leeches: A study of hematology and record of these hirudineans as potential vectors of these hemoflagellates. Brazilian Journal of Veterinary Parasitology, 25(3), 299–305.

Debol'skij, V. K., Grigor'eva, I. L., & Komissarov, A. B. (2010). Sovremennaja gidrohimicheskaja harakteristika reki Volga i ee vodohranilisch [Modern hydrochemical characteristics of the Volga River and its reservoirs]. Voda: Himija i Ekologija, 11, 2–12 (in Russian).

Dyková, I., & Lom, J. (1979). Histopathological changes in *Trypanosoma danilewskyi* Laveran & Mesnil, 1904 and *Trypanoplasma borelli* Laveran & Mesnil, 1902 infections of goldfish, *Carassius auratus* (L.). Journal of Fish Diseases, 2(5), 381–390.

Ehdel'shtejn, K. K. (1998). Vodohranilishcha Rossii: Ekologicheskie problemy, puti ih resheniya [Reservoirs of Russia: Environmental problems, ways to solve them]. GEOS, Moscow (in Russian).

Evans, D. L., & Gratzek, J. B. (1989). Immune defense mechanisms in fish to protozoan and helminth infections. Integrative and Comparative Biology, 29(2), 409–418.

Fermino, B. R., Paiva, F., Soares, P., Tavares, L. E. R., Viola, L. B., Ferreira, R. C., Botero-Arias, R., De-Paula, C. D., Campaner, M., Takata, C. S. A., Teixeira, M. M. G., & Camargo, E. P. (2015). Field and experimental evidence of a new caiman trypanosome species closely phylogenetically related to fish trypanosomes and transmitted by leeches. International Journal for Parasitology: Parasites and Wildlife, 4(3), 368–378.

Ferreira, M. L., & Avenant-Oldewage, A. (2013). Notes on the occurrence of *Trypanosoma* sp. (Kinetoplastida: Trypanosomatidae) in freshwater fishes from South Africa. Onderstepoort Journal of Veterinary Research, 80(1), 529.

Fink, I. R., Ribeiro, C. M. S., Forlenza, M., Taverne-Thiele, A., Rombout, J. H. W. M., Savelkoul, H. F. J., & Wiegertjes, G. F. (2015). Immune-relevant thrombocytes of common carp undergo parasite-induced nitric oxide-mediated apoptosis. Developmental and Comparative Immunology, 50(2), 146–154.

Forlenza, M., Scharsack, J. P., Kachamakova, N. M., Taverne-Thiele, A. J., Rombout, J. H. W. M., & Wiegertjes, G. F. (2008). Differential contribution of neutrophilic granulocytes and macrophages to nitrosative stress in a host – parasite animal model. Molecular Immunology, 45, 3178–3189.

Fudjimoto, R. Y., Neves, M. S., Santos, R. F. B., Souza, N. C., Do Couto, M. V. S., Lopes, J. N. S., Diniz, D. G., & Eiras, J. C. (2013). Morphological and hematological studies of *Trypanosoma* spp. infecting ornamental armored catfish from Guamá River-Pa, Brazil. Anais da Academia Brasileira de Ciências, 85(3), 1149–1156.

Goodwin, L. G. (1985). Trypanosomiasis: Introduction. British Medical Bulletin, 41(2), 103–104.

Grybchuk-Ieremenko, A., Losev, A., Kostygov, A. Y., Lukeš, J., & Yurchenko, V. (2014). High prevalence of trypanosome co-infections in freshwater fishes. Folia Parasitologica, 61(6), 495–504.

Gupta, N., & Gupta, D. K. (1987). Dimorphism in *Trypanoplasma* (*Cryptobia*) *maguri* n. sp.: Effect on blood glucose level of host. Revista Iberica de Parasitologia, 47(4), 317–324.

Gupta, N., & Gupta, D. K. (2012). Erythropenia in piscine trypanosomiasis. Trends in Parasitology, 1, 1–6.

Haag, J., O'h Uigin, C., & Overath, P. (1998). The molecular phylogeny of trypanosomes: Evidence for an early divergence of the Salivaria. Molecular and Biochemical Parasitology, 91(1), 37–49.

Hamnueva, T. R. (2001). Raznoobrazie i ekologija kinetoplastid (Kinetoplastida: Kinetoplastidea) – parazitov ryb ozera Bajkal [Diversity and ecology of Kinetoplastidae (Kinetoplastida: Kinetoplastidea) – parasites of fish of Lake Baikal]. Ulan-Ude (in Russian).

Hayes, P. M., Lawton, S. P., Smit, N. J., Gibson, W. C., & Davies, A. J. (2014). Morphological and molecular characterization of a marine fish trypanosome from South Africa, including its development in a leech vector. Parasites and Vectors, 7, 50.

Islam, A. K. M. N., & Woo, P. T. K. (1991a). Anemia and its mechanism in goldfish *Carassius auratus* infected with *Trypanosoma danilewskyi*. Diseases of Aquatic Organisms, 8, 37–43.

Islam, A. K. M. N., & Woo, P. T. K. (1991b). Anorexia in goldfish *Carassius auratus* infected with *Trypanosoma danilewsky*. Diseases of Aquatic Organisms, 11, 45–48.

Jesus, R. B., Gallani, S. U., Valladão, G. M. R., Pala, G., Silva, T. F. A., Costa, J. C., Kotzent, S., & Pilarski, F. (2018). *Trypanosomiasis* causing mortality outbreak in Nile tilapia intensive farming: Identification and pathological evaluation. Aquaculture, in press.

Joerink, M., Groeneveld, A., Ducro, B., Savelkoul, H. F. J., & Wiegertjes, G. F. (2007). Mixed infection with *Trypanoplasma borreli* and *Trypanosoma carassii* induces protection: Involvement of cross-reactive antibodies. Developmental and Comparative Immunology, 31(9), 903–915.

Khan, R. A. (1977). Blood changes in atlantic cod (*Gadus morhua*) infected with *Trypanosoma murmanensis*. Journal Fisheries Research Board Canada, 34(11), 2185–2192.

Khan, R. A. (2012). Host-parasite interactions in some fish species. Review article. Journal of Parasitology Research, 2012, article ID 237280.

Kharat, S., & Kothavade, S. (2012). Hematological study of *Clarias batrachus* with reference to trypanosomiasis. Trends in Fisheries Research, 1(1), 6–9.

Kuklina, M. M., & Kuklin, V. V. (2011). Biohimicheskie i gematologicheskie pokazateli moevki *Rissa tridactyla* (Linnaeus, 1758) pri invazii tsestodami *Alcataenia larina* (Krabbe, 1869) (Cestoda: Dilepididae) [Biochemical and haematological parameters of the kittiwake *Rissa tridactyla* (Linnaeus, 1758) during the invasion of cestodes *Alcataenia larina* (Krabbe, 1869) (Cestoda: Dilepididae)]. Rossijskij Parazitologicheskij Zhurnal, 3, 62–67 (in Russian).

Kutyrev, I. A., Pronin, N. M., & Dugarov, Z. N. (2011). Composition of leucocytes of the head kidney of the crucian carp (*Carassius auratus gibelio*, Cypriniformes: Cyprinidae) as affected by invasion of cestode *Digramma interrupta* (Cestoda; Pseudophyllidea). Biology Bulletin, 38(6), 653–657.

Lapkina, L. N., Zharikova, T. I., Svirskij, A. M. (2002). Zarazhennost' ryb pijavkami (sem. Piscicolidae) v volzhskih vodohranilischah [Infection of fish with leeches (family Piscicolidae) in the Volga reservoirs]. Parazitologija, 36(2), 132–139 (in Russian).

Lazareva, G. A. (2016). Otsenka kachestva vod Uglichskogo vodohranilischa po integral'nym gidrohimicheskim pokazateljam [Assessment of the Uglich reservoir water quality by integral hydrochemical indicators]. Vestnik Moskovskogo Gosudarstvennogo Oblastnogo Universiteta, Serija Estestvennye Nauki, 2, 158–164 (in Russian).

Lemos, M., Fermino, B. R., Simas-Rodrigues, C., Hoffmann, L., Silva, R., Camargo, E. P., Teixeira, M. M. G., & Souto-Padrón, T. (2015). Phylogenetic and morphological characterization of trypanosomes from Brazilian armoured catfishes and leeches reveal high species diversity, mixed infections and a new fish trypanosome species. Parasites and Vectors, 8, 573.

Levinsky, R. (1981). Role of circulating immune complexes in renal diseases. Journal of Clinical Pathology, 34, 1214–1222.

Lom, J., & Dykova, I. (1984). Pathogenicity of some protozoan parasites of cyprinid fishes. Symposia Biological Hungarica, 23, 99–118.

Maqbool, A., & Ahmed, I. (2016). Haematological response of snow barbell, *Schizothorax plagiostomus* Heckel, naturally infected with a new *Trypanosoma* species. Journal of Parasitic Diseases, 40(3), 791–800.

Mork, J. (2011). Prevalence of the haemoflagellate *Trypanosoma* sp. in some common Norwegian marine fish species. Sarsia, 73(4), 263–266.

Oladiran, A., Beauparlant, D., & Belosevic, M. (2011). The expression analysis of inflammatory and antimicrobial genes in the goldfish (*Carassius auratus* L.) infected with *Trypanosoma carassii*. Fish and Shellfish Immunology, 31(4), 606–613.

Osman, H. A. M., Fadel, N. G., & Ali, A. T. (2009). Biochemical and histopathological alterations in catfish, *Clarias gariepinus*, infected with trypanosomiasis with special reference to immunization. Egypt Journal of Comparative Pathology and Clinical Pathology, 22, 164–181.

Plouffe, D. A., & Belosevic, M. (2006). Antibodies that recognize α- and β-tubulin inhibit *in vitro* growth of the fish parasite *Trypanosoma danilewskyi*, Laveran and Mesnil, 1904. Developmental and Comparative Immunology, 30(8), 685–697.

Qadri, S. S. (1962). An experimental study of the life cycle of *Trypanosoma danilewskyi* in the Leech, *Hemiclepsis marginata*. Journal of Eukaryotic Microbiology, 9(3), 254–258.

Ranzani-Paiva, M. J. T., Ishikawa, C. M., Campos, B. E. S., & Eiras, A. C. (1997). Haematological characteristics associated with parasitism in mullets, *Mugil platanus* Günther, from the estuarine region of Cananéia, São Paulo, Brazil. Revista Brasileira de Zoologia, 14(2), 329–339.

Ribeiro, C. M. S., Pontes, M. J. S. L., Bird, S., Chadzinska, M., Scheer, M., Verburg-van Kemenade, B. M. L. (2010). Trypanosomiasis-induced Th17-like immune responses in carp. PLoS One, 5(9), e13012.

Rodrigues, R. N., Oliveira, M. S. B., Tavares-Dias, M., & Corrêa, L. L. (2018). First record of infection by *Trypanosoma* sp. of *Colossoma macropomum* (Serrasalmidae), a neotropical fish cultivated in the Brazilian Amazon. Journal of Applied Aquaculture, 30(1), 29–38.

Shahi, N., Yousuf, A. R., Rather, M. I., Ahmad, F., & Yaseen, T. (2013). First report of blood parasites in fishes from Kashmir and their effect on the haematological profile. Open Veterinary Journal, 3(2), 89–95.

Sitja-Bobadilla, A. (2008). Living off a fish: A trade-off between parasites and the immune system. Fish and Shellfish Immunology, 25, 358–372.

Stafford, J. L., & Belosevic, M. (2003). Transferrin and the innate immune response of fish: Identification of a novel mechanism of macrophage activation. Developmental and Comparative Immunology, 27(6–7), 539–554.

Steinhagen, D., Kruse, P., & Körting, W. (1990). Some haematological observations on carp, *Cyprinus carpio* L., experimentally infected with *Trypanoplasma borreli* Laveran & Mesnil, 1901 (Protozoa: Kinetoplastida). Journal Fish Diseases, 13(2), 157–162.

Sypek, J. P., & Burreson, E. M. (1983). Influence of temperature on the immune response of juvenile summer flounder, *Paralichthys dentatus*, and its role in the elimination of *Trypanoplasma bullocki* infections. Developmental and Comparative Immunology, 7(2), 277–286.

Tkachenko, A. V. (2009). Vlijanie strongiloidoznoj invazii na morfologicheskie, biohimicheskie i immunobiologicheskie pokazateli krovi i razrabotka me-

todov ih korrektsii pri terapii loshadej [Influence of strongyloid infection on morphological, biochemical and immunobiological indicators of blood and development of methods for their correction in the therapy of horses]. Tjumen' (in Russian).

Wang, M., Yan, S., Wang, Y., Lun, Z. R., & Yang, T. B. (2015). Occurrence of trypanosomiasis in net cage cultured groupers (*Cromileptes altivelis* and *Epinephelus fuscoguttatus*) in Nanshan port of Sanya, Hainan province, China. Aquaculture Research, 46(5), 1039–1043.

Wiegertjes, F. G., & Forlenza, M. (2010). Nitrosative stress during infection-induced inflammation in fish: Lessons from a host-parasite infection model. Current Pharmaceutical Design, 16(38), 4194–4202.

Woo, P. T. K. (1981). Acquired immunity against *Trypanosoma danilewskyi* in goldfish, *Carassius auratus*. Parasitology, 83, 343–346.

Woo, P. T. K. (2001). Cryptobiosis and its control in North American fishes. International Journal for Parasitology, 31, 566–574.

Zintl, A., Poole, W. R., Voorheis, H. P., & Holland, C. V. (1997). Naturally occurring *Trypanosoma granulosum* infections in the european eel, *Anguilla anguilla* L. from County Mayo, Western Ireland. Journal of Fish Diseases, 20(5), 333–341.

Zuo, X., & Woo, P. T. K. (2000). *In vitro* haemolysis of piscine erythrocytes by purified metallo-protease from the pathogenic haemoflagellate, *Cryptobia salmositica* Katz. Journal of Fish Diseases, 23, 227–230.

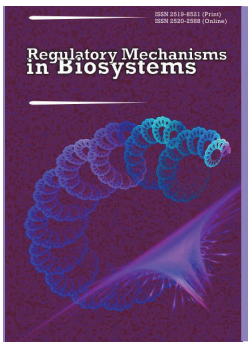

Regulatory Mechanisms in Biosystems

ISSN 2519-8521 (Print)
ISSN 2520-2588 (Online)
Regul. Mech. Biosyst., 9(3), 315–321
doi: 10.15421/021846

Diagnostic value of biochemical markers of bone metabolism in treatment of generalized periodontitis in patients with age-related osteoporosis

O. O. Fastovets, I. V. Masheiko, H. B. Peleshenko

Dnipro Medical Academy of the Ministry of Health of Ukraine, Dnipro, Ukraine

Article info

Received 24.05.2018
Received in revised form 20.06.2018
Accepted 23.06.2018

Dnipro Medical Academy of the Ministry of Health of Ukraine, Vernadsky st., 9, Dnipro, 49027, Ukraine.
Tel.: +38-097-992-11-24
E-mail: fastovets.e@ex.ua

Fastovets, O. O., Masheiko, I. V., & Peleshenko, H. B. (2018). Diagnostic value of biochemical markers of bone metabolism in treatment of generalized periodontitis in patients with age-related osteoporosis. Regulatory Mechanisms in Biosystems, 9(3), 315–321. doi:10.15421/021846

The topicality of the problem of periodontal diseases is due to their significant prevalence. The purpose of this work is to study the dynamics of markers of bone metabolism in the process of treatment of generalized periodontitis of the II–III levels of severity in patients with age-related osteoporosis and without osteoporotic changes in the skeleton. The examination and treatment of 104 patients, aged 63–78, equal ratio of men and women, was conducted. Among the selected patients, 49 persons had normal bone mineral density, while the remaining 55 had osteoporotic changes in the bone tissue of involutory genesis. All subjects were assessed for the following indicators ; mineral density of jaw bone tissue (BMD) according to the results of the computer tomography, the concentration of C-Propeptide of Type I Procollagen (CICP) in blood plasma, the activity of tartrate-resistant acid phosphatase (TRAP), bone alkaline phosphatase (BAP), osteocalcin, parathyroid hormone in blood serum, concentration of β-CrossLaps in urine, total calcium and inorganic phosphorus content in blood with calculation of the Ca/P index. It was established that in patients with periodontitis of the II–III degree there was a decrease in the BMD of the alveolar bone in comparison with the control values ($P < 0.05$), whereas the presence of systemic osteopenia worsened the indices ($P < 0.001$). The least osteoregenerative activity, which was characterized by the decrease in BAP, TRAP and CICP levels, was registered in patients with generalized periodontitis of the III degree on the background of age-related osteoporosis ($P < 0.05$). In the patients with generalized periodontitis of the III degree of severity, at the beginning of treatment, a weak negative correlation was found between BMD and TRAP activity ($r = –0.292$, $P < 0.05$) and mean strength correlation – with β-CrossLaps in urine ($r = –0.348$, $P < 0.01$). The concentration of CICP positively correlated with the mineral density of bone tissue from the third month after the start of treatment ($r = 0.312$, $P < 0.05$). As a conclusion, the mineral density of alveolar bone in the process of treatment varies unevenly depending on the severity of generalized periodontitis and the character of osteoporotic changes in the skeleton. The biochemical markers of bone metabolism allow the balance of processes of bone resorption and formation to be determined in order to correct treatment of generalized periodontitis.

Keywords: periodontal diseases; osteopenia; bone mineral density; biomarkers.

Introduction

The problem of inflammatory-dystrophic diseases of periodontal tissues is highly relevant on account of the wide distribution of this disease among the population of Ukraine, complicated by delayed diagnostics; the rapidly progressing development of the pathological process; and also by the necessity of integrated and prolonged treatment. Moreover, generalized periodontal disease is a serious socio-economic problem caused by a significant loss of teeth and decrease in the quality of life (Lu et al., 2016; Frencken et al., 2017). Currently, the diseases are classified as multi-factor diseases which are the result of interaction of the organism with the environment (Tsepov et al., 2016). Milder forms of generalized periodontal disease usually are nosologies, whereas severe forms are related to different systemic diseases which are characterized by general disorders of homeostasis (Fastovets, 2000; Linden et al., 2013). Practically always, hormonal disorders such as diabetes mellitus (Wu et al., 2015; Winning &Linden, 2017), endemic goiter (Chornij & Shmanko, 2017), menopause (Kolte et al., 2017; Goyal et al., 2017), states of immune deficiency, especially HIV infection (Souza et al., 2017), leukemia (Rinčić et al., 2016), and disorders of the development of connective tissue, for example its dysplasia (Kirova et al., 2009, are associated with generalized periodontal disease.

Currently, the pathogenic relation between the inflammatory process in the periodontal tissues and destructive changes in the alveolar cyst is proved (Wang & McCauley, 2016; Kinane et al., 2017). However, recent research is not unanimous regarding the peculiarities of the development of periodontal disease during osteoporotic changes in the skeleton (Darcey et al., 2013; Chambrone, 2016), and also regarding the leading mechanism of destruction of the osseous component of periodontal disease (Bernal et al., 2018). It has been mentioned that with aggressive forms of periodontal disease, the number of osseous tooth deposits is minimum, whereas the resorption of bone tissue is significant (Clark et al., 2017).

The bone tissue is a connective tissue with a high level of mineralization of organic intercellular substance which contains around 70% of non-organic compounds, mostly calcium phosphate. Despite the high level of mineralization, constant renewal of the matrix and adaptive restructuration occurs in the bone tissues depending on the conditions of their functioning (Sims & Gooi, 2008). The bone tissue`s resistance to resorption depends on the level of its mineralization, which is determined by the main factors (Penoni et al., 2016). The main factors which

influence the metabolism of bone tissue are the levels of calcium, phosphorus and hormones, which regulate their metabolism, circulating in the extracellular fluid (Naot & Cornish, 2008). The most informative markers of bone metabolism, often used in clinical studies, are considered to be the tartrate-resistant acid phosphatase (TRAP) of blood serum and C-terminal Telopeptide of Type-1 Collagen (β-CrossLaps) of urine, which reflect the activity of resorptive processes. At the same time, osteocalcin (OC), bone alkaline phosphatase (BAP), procollagen type 1 C-terminal propeptide (CICP) of blood serum are most representative of the activity of processes of bone formation (Lu et al., 2016; Garnero, 2017). On the whole, the determination of the dynamics of concentration of the markers of resorption and formation of bone tissue in biological fluids is required in order to assess the success of treatment in effecting remission of the destructive processes in the bone tissue.

Apart from the abovementioned biochemical studies, numerous noninvasive apparatus methods of diagnostics have been developed and broadly introduced into clinical practice. They allow accurate determination of the mineral density of the bone tissue (Dobrovol'skaja et al., 2017). Thus, the usage of roentgenological investigation allows not only study of the structure of bone tissue of the periodontal complex, but also determination of whether the patient is in the risk group of development of periodontal disease (Gajdarova et al., 2006; Ignasiak et al., 2016), whereas the data from orthopatomography are a reason for roentgenological densitometery (Nakamoto et al., 2008).

Finally, considering that systemic osteoporosis is a significant mechanism which leads to the development and complication of generalized periodontal disease (Bodduru et al., 2016), it is necessary to prescribe specific pathogenic therapy depending on the character of the metabolic disorders in the bone tissue (Gorb-Gavril'chenko & Strel'chenja, 2013; Aspalli et al., 2014; Mordasov & Ivanjuta, 2016). As a result of the close relationship between the mineral metabolism and the pattern of systemic osteoporosis, many clinicians recommend combined pharmacotherapy using anti-resorptive preparations, calcium and vitamins (Karakov, 2016). Selecting the optimum medicamental protocol, monitoring of the efficiency of treatment in dynamics, which includes timely correction, is impossible without determining and monitoring the structural-functional condition of the bone tissue (Masheiko, 2017; Roschger et al. 2008).

Therefore, considering everything stated above, the objective of this study was to determine the dynamics of biochemical markers of metabolism of bone tissue in the process of treatment of generalized periodontal disease of II–III degree among patients with age-related osteoporosis and no osteoporotic changes in the skeleton.

Materials and methods

For realisation of the goal, we conducted an integrated study and treatment of 104 patients with generalized periodontal disease of II–III degree, aged between 63–78 years, with an equal number of men and women. To diagnose periodontal disease, we used the classification of M. F. Danilevskij (Danilevskij & Borisenko, 2000).

Among the selected patients, 49 had normal mineral density in the bone tissue, whereas 55 had osteoporotic changes in bone tissue of involute genesis. The condition of bone tissue was determined on the bases of the results of studying the mineral density of the bone tissue (BMD) using the method of dual-energy X-ray absorptiometry using the Lunar Prodigy apparatus. Measurements were made in the lumbar vertebrae (LI-LIV), in the area of femoral neck (Neck), greater trochanter (Troch), and Ward's triangle (Ward). Diagnosing osteoporotic changes in the skeleton was conducted in accordance with the recommendations of the WHO, criteria T, i.e. in relation to the value of standard deviation (SD) from the normal parameters of peak bone mass of healthy individuals of a corresponding age. The SD value below 1 was considered normal, between 1 and 2.5 SD – osteopenia, below 2.5 SD – osteoporosis (Siris et al., 2014).

Criteria for excluding patients from the scope of the study were as follows: the general diseases in the anamnesis, which could influence the mineral density of bone tissue; usage of medical preparations which contain mineral components; traumas and inflammatory diseases of the bone-joint system, breach of the treatment protocol.

Prior to the study, the patients gave written approval for being involved in the study.

The patients were divided as follows: 55 patients with senile osteoporosis were included in the first main group, group I (12 men and 15 women, who had generalized periodontal disease of II degree of severity) and the second main group, group II, which included 10 men and 18 women with aggressive (III type) disease. The comparison group was formed similarly to the main group in relation to gender-age and clinical criteria from people who had normal parameters of mineral bone density. Therefore, the comparison group I included 14 men and 9 women with periodontal disease of the II type; the comparison group II – 16 men and 10 women with periodontal disease of the III type. Also, as the control, we involved 20 people of the same age group with an equal number of men and women, with conditionnally healthy periodontal tissues, who had no diagnosed osteoporotic changes in the bone tissue.

All patients suffering from generalized periodontal disease received complex treatment according to the generally accepted protocol (Borysenko et al., 2005). Prior to the treatment the patients underwent a professional hygiene regime of the oral cavity, which consisted of removing the sediments above and under the gums using the "Piezon-Master" ultrasonic system and the "Vektor" system. For providing long term stabilization of the pathological process, the dental treatment included therapeutic, surgical and orthopedic methods, and also consultations and treatment recommended by an endocrinologist.

In the scope of the presented study, all the observed patients were monitored using computer tomographic scanning of the jaw bones (Morita, Japan, 2008) to determine destructive changes in the compacted and trabecular bone, and at the same time determine the parameters of BMD in the following zones: alveolar, middle and apical horizontal, septal vertical. Alveolar horizontal was considered a conventional line which lay along the crest of alveolar process; middle horizontal – line which lay across the central part of interdental septum; apical horizontal – line which connects the tops of the roots, septal vertical – line which divides the alveolar line into equal parts in lengthwise direction. The density of the bone tissue was expressed in Hounsfield numbers (H).

The conclusions on the activity of the processes of destructive bone tissue were made according to the level of the resorption markers. In the blood serum, we determined the activity of tartrate-resistant acid phosphatase (TRAP) (u/l) using a set of Bone-TRAP (IDS). The concentration of β-CrossLaps fragments in the urine were determined using the Serum CrossLaps (Osteometer) test-system.

For standard excretion of β-CrossLaps, we used the second spontaneous morning sample of urine with following normalization of its concentration to the amount of creatinine in the analyzed sample. The results were converted into ng β-CrossLaps to 1 g of creatinine.

The activity of recovery of the bone tissue was determined according to the concentration of procollagen type 1 C-terminal propeptide (CICP) in the blood serum, which was determined using the method of immune-enzymic analysis with Metra CIPC EIA Kit («Quidel Corporation», USA) diagnostic set, bone alkaline phosphatase (BAP) in the blood serum using kinetic colorimetric method (U/l), osteocalcin with N-MID Osteocalcin ELISA (USA) test set.

In addition, we calculated the parameters of mineral metabolism – concentration of parathyroid hormone in the blood serum using the "I-PTH ELISA" (DSL, USA) test-system; the content of total calcium in the blood by the colorimetric method with Ortho-CresolPhthalein (Kapitanenko & Dochkin, 1988); the content of total non-organic phosphorus in the blood by the colorimetric method according to the reaction with Molybdenum-Vanadium reagent (mmol/l) (Kondrahin, 2004) with following calculation of the Ca/P proportion.

The obtained data were statistically analyzed in Statistica 6.0 (Statsoft Inc., USA) pack using the calculation of the Student`s t-criterion at normal distribution of the data and non-parametric Mann-Whitney test criterion at not normal distribution. The normal distribution was calculated using the Shapiro-Wilk test criterion. Differences

at $P < 0.05$ were considered statistically reliable (Filimonova et al., 2004; Filimonova & Fil', 2005).

Results

As we see from the data provided in Table 1, in each group, the most significant changes in the bone tissue density which occurred as a result of the course of treatment were observed in the septal vertical, and also in the alveolar and middle horizontals, i.e. in the areas directly involved in the pathological process of generalized periodontal disease. At the same time, in the alveolar horizontal, the BMD parameters were higher ($P < 0.05$), though the dynamics of the changes in the process of treatment were similar to other areas of the jaw bones ($P > 0.05$). The lowest changes in BMD were observed in the apical horizontal, which is explained by the remoteness of this area from the inflammation source localized in the interalveolar septa ($P < 0.001$).

Separate mention should be made of the significant dependency of the peculiarities of localization of the destructive process on the BMD parameters among the patients with generalized periodontitis. In patients suffering from generalized periodontitis of the III type with predominant vertical type of destruction of the bone tissue, the BMD parameters in certain areas were reduced to 600 H. The determined reduction of the mineral density was followed by disorders in the bone structure manifested by loss of clarity in the trabecular pattern, which was clearer in the upper part of the septa, enlargement of the intratrabecular cavities; thinning of the trabeculae. The described pattern of the pathological process is related to its localization mostly in the areas of cancellous bone tissue, where the metabolic processes take place very actively. Thus, in the abovementioned observations, the bone tissue was affected by active resorption, which was manifested in rapid decrease in the BMD parameters.

The greatest decrease in the BMD parameters was observed in the alveolar horizontal among the patients suffering from generalized periodontitis which developed following systemic osteoporotic changes in the bone tissue (main groups I and II). The determined parameters of these groups were higher compared to the comparison groups I and II by 12.3 ± 3.2% ($P > 0.05$) and 14.1 ± 3.5% ($P > 0.05$) on average respectively and by 24.0 ± 4.1% ($P < 0.01$) and 32.1 ± 4.6% ($P < 0.001$) respectively compared to the control group.

However, later, in the process of treatment, we observed gradual normalization of the parameters of mineral bone density among the patients of both experimental groups ($P < 0.001$). One month after the beginning of the treatment, the BMD parameters of the II group of comparison had practically normalized and were close to the parameters of the control, maintaining at this level throughout the monitoring ($P > 0.05$). In the II group of comparison, the BMD parameters recovered gradually, which was manifested in clinical-X-ray stabilization of the pathological process in the periodontal tissues, though they did not equalize with the parameters of the control ($P > 0.05$).

At the same time, mineral density of the bone tissue of the patients with generalized periodontitis of the II type (main group I), despite the treatment, remained practically unchanged, and 3 months after the beginning of the treatment it had increased only by 6.1 ± 1.8% from the initial parameters ($P > 0.05$). A similar insignificant increase was recorded in the next monitoring period. By contrast, during the treatment, the patients of main group II were observed to have a negative dynamic of the BMD parameters. Therefore, 1 month after the beginning of the treatment, the mineral density of the bone tissue had decreased by 4.2 ± 1.2% on average from the initial parameters, and after 3 months – by 6.5 ± 1.8%, having stabilized and demonstrating an insignificant positive dynamic 6 months after the beginning of the treatment ($P > 0.05$).

The results of the conducted biochemical studies, presented in Table 2, indicated that the level of total calcium in the blood before the treatment of generalized periodontitis in the comparison groups was within the norm, whereas in the main groups, we recorded a statistically reliable decrease of this indicator compared to the control ($P < 0.05$). A similar difference was observed during 3 months after the beginning of treatment in main group I. Moreover, in main group II, the normalization of the calcium level in the blood serum was not recorded even 6 months after the beginning of the treatment.

Table 1

The dynamic of parameters of the mineral density of bone tissue (BMD) in different areas of the alveolar process among the patients of the main groups (n = 49) and the groups of comparison (n = 55) during the treatment compared to the control (M ± m, n = 20)

Group			Alveolar horizontal	Middle horizontal	Apical horizontal	Septal vertical
Control			1244.2 ± 78.6	1397.7 ± 106.1	1324.1 ± 84.3	1276.3 ± 98.4
Comparison	I	before treatment	1077.6 ± 127.2	1285.8 ± 107.3	1301.8 ± 142.4	1126.6 ± 152.7
		after 1 month	1024.6 ± 131.4	1257.8 ± 96.8	1328.7 ± 153.5	1103.8 ± 111.9
		after 3 months	1037.6 ± 118.4	1287.8 ± 129.9	1355.5 ± 162.1	1174.6 ± 98.8
		after 6 months	1193.3 ± 95.9	1341.4 ± 124.2	1343.8 ± 146.6	1216.7 ± 139.8
	II	before treatment	983.9 ± 10.3*	1131.4 ± 95.3	1298.1 ± 118.1	982.5 ± 102.4*
		after 1 month	978.4 ± 182.2	1145.2 ± 88.9	1316.4 ± 125.7	969.7 ± 96.8*
		after 3 months	1027.1 ± 18.3	1257.4 ± 120.1	1311.6 ± 131.5	1096.4 ± 128.3
		after 6 months	1144.6 ± 118.4	1314.2 ± 129.9	1320.8 ± 176.6	1177.6 ± 119.4
Main	I	before treatment	945.4 ± 78.1**	1101.7 ± 100.6*	1139.4 ± 145.3	982.7 ± 106.5*
		after 1 month	958.2 ± 148.3	1145.8 ± 97.3	1032.6 ± 117.4*	1002.3 ± 93.4*
		after 3 months	967.7 ± 132.6	1159.6 ± 134.6	1150.1 ± 120.9	1020.8 ± 114.7
		after 6 months	1046.1 ± 84.5	1201.1 ± 107.8	1158.3 ± 14.7	1059.7 ± 138.2
	II	before treatment	844.8 ± 79.6***	978.3 ± 135.8*	1025.4 ± 115.1*	880.4 ± 125.3*
		after one month	812.7 ± 140.9*	936.1 ± 123.2**	1048.2 ± 105.4*	829.4 ± 136.1*
		after 3 months	795.6 ± 151.2*	922.8 ± 147.5*	1109.6 ± 123.6	826.3 ± 122.3**
		after 6 months	887.3 ± 133.8*	1020.5 ± 158.1	1143.5 ± 128.7	893.8 ± 133.4*

Note: * – the difference is statistically reliable at $P < 0.05$, ** – $P < 0.01$, *** – $P < 0.001$ compared to the parameters of the control.

In the experimental groups, at the beginning of the treatment, the level of phosphorus in the blood of patients with generalized periodontitis of the III type was higher than the control parameters ($P < 0.05$), indicating the prevalence of the bone resorption over the processes of bone tissue formation, unrelated to the mineral density of the skeleton.

However, in comparison group II, we recorded a decrease in the concentration of phosphorus in the blood serum to its normalization already in the 3rd month since the treatment began ($P < 0.05$). By contrast, in all patients of the main groups the level of blood phosphates remainned significantly lower than the parameters of the control throughout the study. Also, the prevailing of bone tissue resorption over the processes of its regeneration was indicated by the Ca/P proportion which was much lower than 1.0. In the patients with generalised periodontitis in the main groups I and II this indicator equaled 0.82 ± 0.08 and 0.63 ± 0.07 respectively ($P < 0.05$ compared to the control).

As we see in Table 2, the systemic osteoporotic phenomenon among the patients with generalized periodontitis was manifested in increase in the concentration of β-CrossLaps fragments in the urine ($P < 0.05$). And despite the fact that during the study, the patients of the main groups I and II were observed to exhibit a tendency towards decrease in its secretion, this parameter remained heightened even during the period remote from the beginning of the treatment, which indicates

resorption which gradually involved previously unaffected areas of the alveolar bone, and also possible progression of osteoporotic changes in other areas of bone.

A positive change in the process of bone recovery among the patients with generalized periodontitis was the normalization of the level of acid bone phosphatase a month after the treatment started in the I main group and 3 months after the beginning – in main group II ($P < 0.001$). Similar dynamic indicates gradual transformation of progressive resorption of bone tissue in its latent process with following decrease in the total proinflammatory potential as a result of the treatment.

Table 2

Changes in the biochemical parameters of metabolism of bone tissue in the blood and urine of the patients of the main groups (n = 49) and comparison groups (n = 55) over the treatment process compared to the control (M ± m, n = 20)

Group			TRAP, U/l	β-CrossLaps, ng/g creatinine	Osteocalcin, ng/mol	BAP, U/l	CICP, ng/mol	Parathormone, pg/mol	Total blood calcium, mmol/l	Total non-organic phosphorus of blood, mmol/l
Control			4.86 ± 0.14	1.02 ± 0.05	16.64 ± 0.43	10.73 ± 0.34	61.82 ± 2.45	47.84 ± 3.27	2.32 ± 0.11	1.91 ± 0.16
Comparison	I	before treatment	5.20 ± 0.16	1.12 ± 0.09	16.45 ± 0.44	11.82 ± 0.43	60.73 ± 2.56	46.78 ± 3.41	2.21 ± 0.12	2.05 ± 0.21
		after 1 month	5.11 ± 0.17	1.09 ± 0.07	18.22 ± 0.48*	11.59 ± 0.33	68.02 ± 2.48	47.12 ± 3.37	2.18 ± 0.14	1.98 ± 0.18
		after 3 months	5.15 ± 0.08	1.04 ± 0.08	17.93 ± 0.57	11.52 ± 0.38	71.09 ± 2.63*	46.84 ± 2.82	2.38 ± 0.11	2.07 ± 0.15
		after 6 months	5.05 ± 0.13	1.06 ± 0.09	18.64 ± 0.65*	11.45 ± 0.34	64.30 ± 2.57	47.51 ± 3.25	2.29 ± 0.13	1.86 ± 0.12
	II	before treatment	5.68 ± 0.21*	1.22 ± 0.08*	15.31 ± 0.55	9.01 ± 0.58*	51.93 ± 2.89*	48.15 ± 2.92	2.12 ± 0.19	2.38 ± 0.14*
		after 1 month	5.34 ± 0.26	1.14 ± 0.11	16.97 ± 0.45	9.23 ± 0.67	75.42 ± 3.01**	48.02 ± 3.19	2.37 ± 0.14	2.31 ± 0.23
		after 3 months	5.24 ± 0.24	1.12 ± 0.09	19.14 ± 0.62**	9.55 ± 0.51	71.72 ± 2.92*	47.48 ± 3.91	2.41 ± 0.16	2.24 ± 0.19
		after 6 months	5.18 ± 0.17	1.09 ± 0.07	17.97 ± 0.56	9.76 ± 0.46	66.76 ± 2.61	47.12 ± 4.06	2.25 ± 0.14	2.03 ± 0.17
Main	I	before treatment	5.59 ± 0.32*	1.26 ± 0.10*	14.61 ± 0.63*	8.69 ± 0.58**	47.85 ± 3.04**	59.22 ± 3.87*	1.85 ± 0.18*	2.04 ± 0.20
		after 1 month	5.02 ± 0.30	1.23 ± 0.12	16.31 ± 0.44	9.08 ± 0.56*	53.17 ± 2.58*	56.75 ± 3.09	1.95 ± 0.16	2.14 ± 0.16
		after 3 months	4.74 ± 0.27	1.27 ± 0.11*	15.57 ± 0.56	9.31 ± 0.53*	58.73 ± 2.85	53.16 ± 2.64	2.09 ± 0.15	1.92 ± 0.14
		after 6 months	4.81 ± 0.24	1.22 ± 0.08*	16.03 ± 0.48	9.42 ± 0.56	59.35 ± 2.63	53.73 ± 3.03	2.23 ± 0.17	1.85 ± 0.15
	II	before treatment	5.83 ± 0.28**	1.33 ± 0.10**	13.31 ± 0.59***	8.39 ± 0.52***	45.75 ± 2.93***	61.49 ± 4.42*	1.74 ± 0.21*	2.35 ± 0.11*
		after 1 month	5.73 ± 0.25**	1.28 ± 0.11*	13.65 ± 0.62***	8.58 ± 0.51**	48.23 ± 3.02**	58.61 ± 4.15*	1.79 ± 0.23*	2.30 ± 0.10*
		after 3 months	5.23 ± 0.33	1.30 ± 0.11*	14.15 ± 0.64**	8.80 ± 0.48**	54.37 ± 2.76*	48.03 ± 3.89	1.86 ± 0.21	2.18 ± 0.18
		after 6 months	5.16 ± 0.31	1.25 ± 0.10*	14.88 ± 0.59*	8.97 ± 0.45**	55.11 ± 2.54	47.22 ± 3.95	1.90 ± 0.19	2.16 ± 0.22

Note: * – difference is statistically significant at $P < 0.05$, ** – $P < 0.01$, *** – $P < 0.001$ compared to the parameters of the control.

The highest level of alkaline phosphatase, which indicates the active processes of collagen synthesis in the bone tissue, was observed among the patients of comparison group I, whereas, the patients of the main groups and comparison group II had low values of this parameter ($P < 0.05$). In the patients with generalized periodontitis of the III type, which followed osteoporotic changes in the skeleton, the activity of the bone alkaline phosphatase decreased from the control values by 21.8 ± 4.2% ($P < 0.001$). The latter, perhaps, was caused by the inhibition of the functional activity of the osteoblasts which accompanied the damage to a large volume of the bone tissue, which occurred among the patients.

At the same time, the level of parathormone in all the experimental groups remained within the norm, though in the main groups, we observed a tendency towards the increase of its level to the upper border of the norm, caused by low level of calcium in the blood. Excessive secretion of parathormone following the hypocalcaemia additionally activates osteoprotegerin, which justifies the prescription of the calcium preparations and vitamin complexes during treatment of destructive forms of generalized periodontal disease (Leonova et al., 2013; Hellstein et al., 2011).

It is interesting that the dynamic of changes in the level procollagen type 1 C-terminal propeptide (CICP) in the blood plasma, which describes the activity of osteoblasts, was different from the pattern of changes of other parameters of osteoregeneration. The highest CICP level observed in comparison groups I and II indicates that despite that decrease in the mineral density of bone tissue of bones of the jaw and significant prevalence of bone resorption over osteosynthesis among the abovementioned patients, the process of bone tissue recovery is developing at a sufficient level. Also, we should mention that the CICP level in the blood plasma normalized 1–3 months after the beginning of the treatment among the patients of the comparison groups. However, in the patients of the main groups the initial CICP level, which was lower by 22.6 ± 4.0% compared to the control (by 26.0 ± 4.3% for the main group II), normalized only 3–6 months after the treatment ($P < 0.05$).

The same dynamic was observed for the parameters of bone alkaline phosphatase and osteocalcin (Table 2). However, due to significant variation of its parameters, the determined differences compared to the control were statistically unreliable ($P > 0.05$). On the whole, the determined difference of the parameters of the bone formation reflects the decrease in the activity of the osteoregeneration processes among the patients with generalized periodontitis, who had osteoporotic changes in the entire skeleton.

After generalization and analysis of the quantitative parameters determined for the experimental groups during different periods of the treatment, we conducted a correlation-regressional analysis for determining the most significant relations between the indicators of mineral density of the bone tissue (BMD) and biochemical markers of bone metabolism. For the abovementioned analysis, we selected the parameters which changed the most during the treatment: mineral density of the bone tissue in the alveolar and middle horizontal, concentration of tartrate-resistant acid phosphatase (TRAP), bone alkaline phosphatase, procollagen type 1 C-terminal propeptide (CICP) in the blood and β-CrossLaps fragments in urine. The calculated correlational relations are presented in the Table 3 and 4.

Table 3

Correlational relationships (r) between the parameters of bone tissue mineral density of the lower jaw in alveolar horizontal and biochemical parameters of bone tissue metabolism among the patients of the experimental groups during the treatment (n = 104)

Group			TRAP	β-CrossLaps	BAP	CICP
Comparison	I	before treatment	–0.325*	–0.315*	0.205	0.232
		after 1 month	–0.282	–0.275*	0.252*	0.268
		after 3 months	–0.216	–0.246	–0.178	0.271*
		after 6 months	–0.188	–0.163	0.211	0.234
	II	before treatment	–0.368*	–0.386**	–0.188	0.214
		after 1 month	–0.327	–0.325	0.155	0.247
		after 3 months	–0.264*	–0.341*	0.236*	0.281*
		after 6 months	–0.180	–0.307	–0.146	0.319**
Main	I	before treatment	–0.325*	–0.345*	0.172	0.283
		after 1 month	–0.276	–0.308*	–0.134	0.250
		after 3 months	–0.294	–0.286	0.180	0.341*
		after 6 months	–0.209	–0.262	0.216*	0.294*
	II	before treatment	–0.292*	–0.348**	0.208	0.217
		after 1 month	–0.267*	–0.312*	0.141	0.194
		after 3 months	–0.283	–0.285*	–0.187	0.312*
		after 6 months	–0.227	–0.251	0.235	0.282*

Note: * – the difference is statistically reliable at $P < 0.05$, ** – $P < 0,01$.

After the relationships between the mineral density of the jaws in the alveolar horizontal (BMD) and parameters of bone tissue metabolism were calculated, in the main groups and comparison groups, we found a relatively low and average negative relation between this parameter and TRAP concentration in the blood and β-CrossLaps in the urine during the first three months of monitoring ($P < 0.05$). It is interesting that the further correlation of the abovementioned parameters had a low level of probability ($P > 0.05$), which indicates the impact of proinflammatory markers on the destruction of bone tissue, and, therefore, the values of the BMD parameters at the beginning of the treatment. However, during the treatment, the levels of the abovementioned markers gradually decreased and their impact on the parameters of bone mineral density was reduced (see Table 3).

For both experimental groups, we calculated a low positive correlational relationship between bone mineral density and CICP concentration in the blood plasma, which had a sufficient level of significance, beginning from the third month of monitoring ($P < 0.05$). In our opinion, it was present due to the BMD dependency on the balance between the proinflammatory and osteoregenerating factors, and its changes were caused by the increase in the activity of the processes of bone tissue mineralization which occurred in the final stage of osteoregeneration a few months after the beginning of treatment. At the same time, in comparison group I, the correlational relation was less significant due to lower loss of the bone mass, i.e. a lower impact of these markers on the bone mineral density parameter.

During the comparison of bone mineral density of the alveolar process in the middle horizontal and the indicators of bone tissue metabolism (see Table 4) among the patients of the main group, we determined a statistically significant average negative relation in the main groups with β-CrossLaps concentration throughout the monitoring and a low relation with TRAP at the beginning of the treatment ($P < 0.05$). In comparison group II, a similar pattern was determined until the third month of monitoring.

Perhaps, the presence of the abovementioned relations is due to the fact that bone tissue of the alveolar process in the middle horizontal is not directly involved in the inflammatory process in patients with generalized periodontitis, i.e., its resorption level is less than TRAP-conditioned, therefore following osteoporosis, the bone mineral density depends also on other components of the bone homeostasis. This is proved by the extent of correlation of this parameter, which remained quite high with the β-CrossLaps concentration ($P < 0.05$).

Table 4

Correlation relations (r) between the parameters of bone mineral density of the lower jaw in the middle horizontal and biochemical parameters of bone tissue metabolism among the patients of experimental groups in the process of treatment (n = 104)

Group			TRAP	β-CrossLaps	BAP	CICP
Comparison	I	before treatment	–0.218*	–0.242*	0.145	0.232
		after 1 month	–0.223	–0.197	0.242*	0.261*
		after 3 months	–0.148	–0.236*	–0.173	0.284*
		after 6 months	–0.167	–0.192	0.215	0.220
	II	before treatment	–0.203*	–0.328*	0.262	0.237
		after 1 month	–0.176*	–0.222*	0.125	0.277*
		after 3 months	–0.144	–0.291*	–0.136	0.291*
		after 6 months	–0.159	–0.247	0.182	0.269*
Main	I	before treatment	–0.274*	–0.302*	0.153	0.186
		after 1 month	–0.240	–0.268*	0.164	0.217
		after 3 months	–0.193	–0.227	0.207	0.251*
		after 6 months	–0.162	–0.245	–0.118	0.234*
	II	before treatment	–0.217*	–0.343**	0.151	0.226
		after 1 month	–0.182*	–0.322*	0.170	0.254*
		after 3 months	–0.168	–0.279*	0.183*	0.272*
		after 6 months	–0.151	–0.258*	–0.174	0.308*

Note: * – difference was statistically reliable at $P < 0.05$.

Finally, a low positive correlational relationship between BMD and CICP concentration was determined in the comparison groups from the first month of monitoring, whereas in the main groups this began in the third month ($P < 0.05$). This allows us to conclude that the CICP is good at reflecting the processes of osteoregeneration and remineralization of bone tissue which was not directly involved in the inflammatory-dystrophic process.

Finally, we should summarize the data obtained over the treatment of the patients with generalized periodontitis in the different experimental groups. The highest percentage of stable remissions 6 months after the treatment begun was recorded in the Ist main group and the Ist comparison group, i.e. among the patients with generalized periodontitis of the II type, who had osteoporotic changes in the skeleton, or did not have them. The treatment efficiency parameters equaled 74.1 ± 8.4% (20 of 27) respectively for the Ist main group and 78.3 ± 8.6% (18 of 23) for the I comparison group ($P > 0.05$). Far worse results were observed in the II comparison group (patients with generalized periodontitis of the III type with no systemic involutory osteoporotic changes of bones), where the clinical-X-ray stabilization of the disease was observed only in 53.8 ± 9.8% (14 of 26) of the observations ($P < 0.05$). In the II main group, i.e. the patients with the periodontitis of the III type, which had developed following systemic osteoporotic disorders in the bone tissue, the stable remission 6 months from the beginning of the treatment was recorded only in 8 of 28 patients (28.6 ± 8.5%, $P < 0.05$). Therefore, the efficiency of the treatment significantly decreases in patients with advanced development of the inflammatory-dystrophic process in the tissues around the teeth. At the same time, the presence of systemic disorders in the bone metabolism complicates the clinical symptomatic, causes more significant imbalance of the resorption-regeneration processes in the alveolar bone, and, therefore complicates the treatment.

Discussion

Generalized periodontitis should be analyzed as an inflammatory-dystrophic multi-factor process in the tissues around the teeth, the development of which depends both on genetic predisposition and external factors, and also individual peculiarities of the metabolic profile of the patient, and finally, the systemic diseases suffered by this patient (Wu et al., 2015; Tsepov et al., 2016; Souza et al., 2017).

Osteoporosis of involutary genesis is a non-favourable factor which complicates generalized periodontal disease, which, first of all, manifests in decrease of the bone mineral density (BMD), particularly the alveolar process (Bodduru et al., 2016). Considering the fact that the alveolar bone is within the source area of the inflammatory-destructive process initiated by the microbial invasion of the periodontal tissues, rapid progression of the bone resorption develops. Also, bone tissue with decreased mineral density has lower reserve potential for recovery, even after eradication of the main periodontopathogenic factors.

Therefore, it is pretty clear that without determining the causes of systemic disorders in the bone tissue, and also their elimination, it is practically impossible to achieve prolonged remission of generalized periodontal disease and eliminate the risk of development of relapse and progression of the pathological process (Mordasov & Ivanjuta, 2016). Thus, it is recommended to supplement the main complex treatment of generalized periodontosis by calcium preparations, mineral complexes, and preparations which normalize metabolic processes, particularly in bone tissue (Hellstein et al., 2011; Leonova et al., 2013). Moreover, in cases of diagnosed osteoporosis of patients with generalized periodontal disease, it is recommended to prescribe antiosteoporotic preparations (Gorb-Gavril'chenko & Strel'chenja, 2013; Aspalli et al., 2014). In our opinion, such an approach is entirely justified. However, treatment of osteoporosis cannot be within the competency of only a periodontist and requires participation of specialists in the field.

Certainly, prescribing antiresorptive preparations, as with monitoring the dynamic of changes in bone tissue as a result of treatment is impossible without determining the parameters of bone mineral density (BMD) and study of biochemical markers of bone metabolism.

As the results of our study indicate, bone mineral density changes in a nonuniform manner depending on the severity of generalized periodontosis and manifestation of osteoporotic changes in bone density. In our opinion, this is caused by the fact that the pattern of processes of destruction and recovery of the bone matrix is determined by

proinflammatory, osteomodeling and osteoregeneration factors, the proportion of which changes and determines the condition of bone tissue at different stages of treatment.

The results we obtained indicate a close relationship between the treatment results and initial periodontal status of patients, i.e. much worse prognosis of treatment outcome in groups with higher level of disease severity, which is proved by the works by our colleagues (Bodduru et al., 2016; Bernal et al., 2018). On the other hand, we demonstrated that the systemic disorders in bone metabolism, particularly involutory genesis, radically complicate the inflammatory-dystrophic process in the tissues around the teeth, decreasing the efficiency of treatment. Therefore, there is a need to adjust the treatment protocol for the abovementioned patients.

Conclusions

The most diagnostically valuable indicators of the condition of bone tissue of patients with generalized periodontal disease of II–III type of severity following involutory osteoporosis with no systemic changes in mineral bone density are the parameters of bone mineral density of the alveolar bone (BMD), and also the β-CrossLaps level in urine and activity of tartrate-resistant acid phosphatase (TRAP) and bone alkaline phosphatase in the blood serum.

The most representative indicator of the inflammatory-destructive process in periodontal disease is decrease in bone mineral density in the alveolar part of jaw bones. This parameter decreases in patients with II type of severity by 13.4 ± 3.2% compared to the control, and in patients with III type by 20.1 ± 3.5% ($P < 0.05$). Systemic osteopenic phenomena cause even greater decrease in this parameter to values which in patients with generalized periodontosis of II type of severity were 24.0 ± 4.1% lower than the control level, and lower by 32.1 ± 4.6% ($P < 0.001$) in patients with III type.

The lowest osteoregenerative activity occurred at the beginning of treatment of patients with generalized periodontal disease of III type, which followed systemic involutory osteoporosis. Therefore, the activity of bone alkaline phosphatase decreased by 21.8 ± 4.0% compared to the control; tartrate-resistant acid phosphatase (TRAP) – by 20.0 ± 3.9% respectively; concentration of procollagen type 1 C-terminal propeptide (CICP) – by 26.0 ± 4.3% ($P < 0.05$).

The main proinflammatory markers on the BMD parameters gradually decrease in the process of treatment, whereas the positive dynamic of osteogenerative parameters indicate processes of bone tissue recovery, which is recorded only from the third month of monitoring. The mineral metabolism parameters have only supportive significance for assessing bone metabolism.

The patients suffering from generalized periodontal disease of III type of severity have a low negative relationship between mineral density of the alveolar part of the jaw bones and activity of TRAP in the blood ($r = –0.292$, $P < 0.05$) and relationship of average extent with concentration of β-CrossLaps in the urine ($r = –0.348$, $P < 0.01$). At the same time, concentration of procollagen type 1 C-terminal propeptide positively correlates with bone mineral density from the third month after the start of the treatment ($r = 0.312$, $P < 0.05$).

The diagnostic value of biochemical markers of bone tissue metabolism consists in determining the balance in the processes of resorption and formation, at different stages of generalized periodontal disease, which allows one to correctly select the treatment tactics, prescribe the correct pharmacotherapy and prevent the development of complications.

References

Aspalli, S. S., Shetty, V. S., Parab, P. G., Nagappa, G., Devnoorkar, A., & Devarathnamma, M. V. (2014). Osteoporosis and periodontitis: Is there a possible link? Indian Journal of Dental Research, 25(3), 316–320.

Bernal, M., Elenkova, M., Evensky, J., & Stein, S. H. (2018). Periodontal disease and osteoporosis – shared risk factors and potentiation of pathogenic mechanisms. Current Oral Health Reports, 5(2), 26–32.

Bodduru, R., Deshmukh, K., Chintawa, S., & Nayyar, A. S. (2016). Osteoporosis and periodontal disease: Association and mechanisms: An in-depth review. International Journal of Therapeutic Applications, 32, 11–19.

Borysenko, A. V., Politun, A. M., Nesin, O. F., & Sydelnykova, L. F. (2005). Terapevtychna stomatolohiia. Rozdil 1. Protokoly nadannia stomatolohichnoi dopomohy [Therapeutic dentistry. Part 1. Protocols for the provision of dental care]. Medytsyna, Kyiv (in Ukrainian).

Chambrone, L. (2016). Current status of the influence of osteoporosis on periodontology and implant dentistry. Current Opinion in Endocrinology and Diabetes and Obesity, 23(6), 435–439.

Chornij, A. V., & Shmanko, V. V. (2017). Index assessment of the state of periodontal tissues in individuals with primary hypothyroidism. Clinical Dentistry, 3, 17–23.

Clark, D., Febbraio, M., & Levin, L. (2017). Aggressive periodontitis: The unsolved mystery. Quintessence International, 48(2), 103–111.

Danilevskij, N. F., & Borisenko, A. V. (2000). Zabolevanija parodonta [Periodontal diseases]. Zdorovye, Kyiv (in Russian).

Darcey, J., Devlin, H., Lai, D., Walsh, T., Southern, H., Marjanovic, E., & Horner, K. (2013). An observational study to assess the association between osteoporosis and periodontal disease. British Dental Journal, 215(12), 617–621.

Dobrovol'skaya, O. V., Toroptsova, N. V., & Smirnov, A. V. (2017). Instrumental'naya diagnostika osteoporoza na sovremennom etapye [Instrumental diagnostics of osteoporosis at the present stage]. Meditsinskiy Alfavit, 1(12), 11–15 (in Russian).

Fastovets, O. O. (2000). Systemni porushennia metabolizmu kistkovoi tkanyny u khvorykh na heneralizovanyi parodontyt [Systemic disorders of bone tissue metabolism in patients with generalized periodontitis]. Visnyk Stomatolohii, 2, 15–17 (in Ukrainian).

Filimonova, N. B., & Fil', I. O. (2005). Statystychnyy analiz danykh vidpovidno do zasad naukovo obgruntovanoyi medytsyny. Porivnyannya hrup za kil'kisnymy pokaznykamy [Statistical analysis of data according to the principles of science-based medicine. Comparison of groups in quantitative terms]. Medytsyna Zaliznychnoho Transportu Ukrayiny, 4, 86–93 (in Ukranian).

Filimonova, N. B., Fil', I. O., & Mykhaylova, T. S. (2004). Statystychnyy analiz danykh vidpovidno do zasad naukovo obgruntovanoyi medytsyny. Pervynnyy analiz kil'kisnykh danykh, podannya rezul'tativ eksperymentu [Statistical analysis of data according to the principles of science-based medicine. Initial analysis of quantitative data, presentation of experimental results]. Medytsyna Zaliznychnoho Transportu Ukrayiny, 4, 30–38 (in Ukranian).

Frencken, J. E., Sharma, P., Stenhouse, L., Green, D., Laverty, D., & Dietrich, T. (2017). Global epidemiology of dental caries and severe periodontitis – A comprehensive review. Journal of Clinical Periodontology, 44 (18), 94–105.

Gajdarova, T. A., Fedotova, M. V., Eremina, N. A., Inshakov, D. V., & Litvinova, T. K. (2006). Metod ispol'zovanija rentgenomorfometrii dlja ocenki mineral'noj plotnosti kostnoj tkani al'veoljarnoj kosti [The method of using X-ray morphometry to evaluate the mineral density of bone tissue of the alveolar bone]. Bulletin VSSC of the RAMS, 51, 23–30 (in Russian).

Garnero, P. (2017). The utility of biomarkers in osteoporosis management. Molecular Diagnosis and Therapy, 21(4), 401–418.

Gorb-Gavril'chenko, I. V., & Strel'chenja, T. N. (2013). Opyt lechenija generalizovannogo parodontita na fone ovariojektomii osteotropnymi preparatami [Experience in the treatment of generalized periodontitis against ovariectomy with osteotropic drugs]. Ukrainskyi Stomatolohichnyi Almanakh, 3, 42–46 (in Russian).

Goyal, L., Goyal, T., & Gupta, N. D. (2017). Osteoporosis and periodontitis in postmenopausal women: A systematic review. Journal of Midlife Health, 8(4), 151–158.

Hellstein, J. W., Adler, R. A., Edwards, B., Edwards, B., Jacobsen, P. L., Kalmar, J. L., Koka, S., Migliorati, C. A., & Ristic, H. (2011). Managing the care of patients receiving antiresorptive therapy for prevention and treatment of osteoporosis: Executive summary of recommendations from the American Dental Association Council on Scientific Affairs. Journal of American Dental Association, 142(11), 1243–1251.

Ignasiak, Z., Radwan-Oczko, M., Rozek-Piechura, K., Cholewa, M., Skrzek, A., Ignasiak, T., & Slawinska T. (2016). Analysis of the relationships between edentulism, periodontal health, body composition, and bone mineral density in elderly women. Clinical Interventions in Aging, 11, 351–356.

Kapitanenko, A. M., & Dochkin, I. I. (1988). Klinicheskij analiz laboratornyh issledovanij [Clinical analysis of laboratory studies]. Voennoe izdatel'stvo, Moscow (in Russian).

Karakov, K. G. (2016). Terapevticheskij podhod k lecheniju hronicheskogo generalizovannogo parodontita na fone sistemnogo osteoporoza [Therapeutic approach to the treatment of chronic generalized periodontitis in

the context of systemic osteoporosis]. Meditsinskiy Alfavit, 2(9), 12–16 (in Russian).
Kinane, D. F., Stathopoulou, P. G., & Papapanou, P. N. (2017). Periodontal diseases. Nature Reviews. Disease Primers, 22, 170–188.
Kirova, E. G., Konev, V. P., & Suncova, T. V. (2009). Osobennosti techenija vospalitel'nyh zabolevanij parodonta u pacientov s displaziej soedinitel'noj tkani: Morfologicheskija harakteristika, principy klinicheskogo podhoda [Features of the course of inflammatory periodontal diseases in patients with connective tissue dysplasia: Morphological characteristics, principles of the clinical approach]. Institute of Stomatology, 4(45), 68–69 (in Russian).
Kondrahin, I. P. (2004). Metody veterinarnoj klinicheskoj laboratornoj diagnostiki [Methods of veterinary clinical laboratory diagnostics]. Kolos, Moscow (in Russian).
Kolte, R. A., Kolte, A. P., & Potey, A. M. (2017). Risk assessment of osteoporosis in pre- and postmenopausal periodontally healthy and chronic periodontitis women with digital panoramic radiographs. Journal of Indian Society of Periodontology, 21(6), 461–465.
Leonova, L. E., Kovtun, A. A., & Pavlova, G. A. (2013). Sravnitel'naja ocenka effektivnosti lechenija bol'nyh parodontitom s primeneniem osteotropnyh preparatov [Comparative evaluation of the effectiveness of treatment of patients with periodontitis with the use of osteotropic drugs]. Parodontology, 18(1), 32–35 (in Russian).
Linden, G. J., Lyons, A., & Scannapieco, F. A. (2013). Periodontal systemic associations: Review of the evidence. Journal of Clinical Periodontology, 40(14), 8–19.
Lu, R. F., Feng, X. H., Xu, L., & Meng, H. X. (2015). Clinical and putative periodontal pathogens features of different sites with probing depth reduction after non-sergicalperiodontal treatment of patients with aggressive periodontitis. Beijing Da Xue Xue Bao, 47(1), 13–18.
Lu, H., Jiang, F., Guan, D., Lu, C., Guo, B., Chan, C., Peng, S., Liu, B., Guo, W., Zhu, H. L., Xu, X., Lu, A., & Zhang, G. (2016). Metabolomics and its application in the development of discovering biomarkers for osteoporosis research. In: Mobasheri, A. (ed.). International Journal of Molecular Sciences, 17(12), 2018–2040.
Masheiko, I. V. (2017). Biohimicheskie markery v ocenke processov remodelirovanija kostnoj tkani pri osteopenii i osteoporoze [Biochemical markers in the evaluation of bone remodeling processes in osteopenia and osteoporosis]. Journal of Grodno State Medical University, 2, 149–153 (in Russian).
Mordasov, N. A., & Ivanjuta, I. V. (2016). Sravnitel'noe issledovanie dvuh antirezorbtivnyh preparatov s raznym mehanizmom dejstvija pri lechenii hronicheskogo generalizovannogo parodontita na fone vtorichnogo osteoporoza [A comparative study of two antiresorptive drugs with different mechanisms of action in the treatment of chronic generalized periodontitis in the context of secondary osteoporosis]. Scientific Almanah, 5(3), 319–323 (in Russian).
Nakamoto, T., Taguchi, A., Ohtsuka, M., Suei, Y., Fujita, M., Tsuda, M., Sanada, M., Kudo, Y., Asano, A., & Tanimoto, K. (2008). A computer-aided diagnosis system to screen for osteoporosis using dental panoramic radiographs. Dental Maxillofacial Radiology, 37, 274–281.
Naot, D., & Cornish, J. (2008). The role of peptides and receptors of the calcitonin family in the regulation of bone metabolism. Bone, 43(5), 813–818.
Penoni, D. C., Torres, S. R., Farias, M. L. F., Fernandes, T. M., Luiz, R. R., & Leão, A. T. T. (2016). Association of osteoporosis and bone medication with the periodontal condition in elderly women. Osteoporosis International, 27(5), 1887–1896.
Rinčić, N., Božić, D., Rinčić, G., Gaćina, P., & Plančak, D. (2016). Evaluation of periodontal parameters in patients with early stage chronic lymphocytic leukemia. Acta Stomatologica Croatica, 50(1), 23–33.
Roschger, P., Paschalis, E. P., Fratzl, P., & Klaushofer, K. (2008). Bone mineralization density distribution in health and disease. Bone, 42(3), 456–466.
Sims, N. A., & Gooi, J. H. (2008). Bone remodeling: Multiple cellular interactions required for coupling of bone formation and resorption. Seminars in Cell and Developmental Biology, 19(5), 444–451.
Siris, E. S., Adler, R., Bilezikian, J., Bolognese, M., Dawson-Hughes, B., Favus, M. J., Harris, S. T., Jan de Beur, S. M., Khosla, S., Lane, N. E., Lindsay, R., Nana, A. D., Orwoll, E. S., Saag, K., Silverman, S., & Watts, N. B. (2014). The clinical diagnosis of osteoporosis: A position statement from the National Bone Health Alliance Working Group. Osteoporosis International, 25(5), 1439–1443.
Souza, A. J., Gomes-Filho, I. S., Silva, C. A. L., Passos-Soares, J. S., Cruz, S. S., Trindade, S. C., Figueiredo, A. C. M. G., Buischi, Y. P., Seymour, G. J., & Cerqueira, E. M. M. (2017). Factors associated with dental caries, periodontitis and intra-oral lesions in individuals with HIV/AIDS. AIDS Care, 1–8.
Tsepov, L. M., Tsepova, E. L., & Tsepov, A. L. (2016). Sochetannaja patologija: Vospalitel'nye zabolevanija parodonta, osteoporoz, deficit vitamina D [Combined pathology: Inflammatory periodontal diseases, osteoporosis, vitamin D deficiency]. Parodontology, 21(4), 4–9 (in Russian).
Wang, C. W. J., & McCauley, L. K. (2016). Osteoporosis and periodontitis. Current Osteoporosis Reports, 14(6), 284–291.
Winning, L., & Linden, G. J. (2017). Periodontitis and systemic disease: Association or causality? Current Oral Health Reports, 4(1), 1–7.
Wu, Y. Y., Xiao, E., & Graves, D. T. (2015). Diabetes mellitus related bone metabolism and periodontal disease. International Journal of Oral Science, 7(2), 63–72.

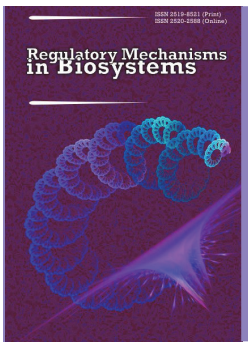

Regulatory Mechanisms in Biosystems

ISSN 2519-8521 (Print)
ISSN 2520-2588 (Online)
Regul. Mech. Biosyst., 9(3), 322–328
doi: 10.15421/021847

Fibrin-blood clot as an initial stage of formation of bone regeneration after a bone fracture

O. K. Popsuishapka*, N. O. Ashukina**, V. O. Litvishko***,
V. V. Grigorjev****, O. O. Pidgaiska**, K. O. Popsuishapka**

**Kharkiv Medical Academy for Postgraduate Education of the Ministry of Health of Ukraine, Kharkiv, Ukraine*
***Sytenko Institute of Spine and Joint Pathology National Academy of Medical Sciences of Ukraine, Kharkiv, Ukraine*
****Kononenko Chuguyev Central District Hospital», Chuguyev, Ukraine*
*****Cherkasy City Accident and Emergency Hospital No 3, Cherkasy, Ukraine*

Article info

Received 19.05.2018
Received in revised form 07.07.2018
Accepted 10.07.2018

Kharkiv Medical Academy of Postgraduate Education, Amosov st., 58, Kharkiv, 61176, Ukraine.
Tel.: +38-067-933-51-71
E-mail: alexeycorn@gmail.com

Popsuishapka, O. K., Ashukina, N. O., Litvishko, V. O., Grigorjev, V. V., Pidgaiska, O. O., & Popsuishapka, K. O. (2018). Fibrin-blood clot as an initial stage of formation of bone regeneration after a bone fracture. Regulatory Mechanisms in Biosystems, 9(3), 322–328. doi:10.15421/021847

This study focuses on mechanisms which regulate the process of fracture healing. We studied the form and position of the fibrin-blood clots (FBC) in the zone near the fragments among patients with limb fractures: macroscopically (during open surgical operations to reposition bone fragments) and using sonography. We conducted a histological and immunohistochemical analysis of biopsy material obtained from the zone around the fracture during surgical procedures on 16 patients in 1–18 days after the fracture. We determined that the density of FBC and their form depends on the volume of damage to the periosteum-muscular fascia and the extent of the shift of fragments. In most cases, with a closed fracture, fibrin-blood clots had a spindle-shaped form. Fibrin along the periphery and in the zone between the fragments has a dense structure, and becomes cellular in central zones. The cells surrounded by fibrin partitions contain blood cells and serum. In many places, fibrin partitions had a one-direction orientation position, and the cells were oval-elongated, which indicated hydrostatic pressure in them. Proliferation of mesenchymal cells began in the vital tissues around the FBC, then during reproduction they pentrated to fibrin. Lengthwise axis of the cells was parallel to fibrin partitions. The bone trabeculae which form on the third week after fracture repeated the orientation of the fibrin partitions. It was determined that the vascular endothelial growth factor (VGEF) concentrates in fibrin and remains in it over the first week after the fracture, later it was found in endotheliocytes, fibroblasts and osteoblasts. The process of filling of the cells with around-fracture FBC lasted 12–18 days and during this period, their osteogenic differentiation occurred. Such tempi and orientation of the process is caused by fibrin with a concentration of growth factors in it. Using the results of the study, it could be assumed that the main conditions for osteogenic differentiation of cells are high concentration of VGEF in the fibrin, which initiates neoangiogenesis and internal tension of fibrin partitions. The formation of structured FBC around the ends of the fragments, which contain VGEF should be considered an initial stage of the process of forming of bone regeneration.

Keywords: structure of fibrin; vascular endothelial growth factor; reproduction of mesenchymal cells; orientation of mesenchymal cells; orientation of bone trabeculae.

Introduction

In traumatology, there has recently been a tendency towards surgical treatment of fractures of limb bones. This could be related to the intense impact of the powerful industry of preparations for advanced osteosynthesis. At the same time, it would be wrong to state that technically advanced devices and methods of their use are in harmony with formation of the regenerated bone. Most of them are designed for an open cutaneous approach to the fractured bone, which increase the risk of disrupting the regeneration process and development of pus-necrotic infectious complications.

In cases of multiple closed fractures, especially if the fragments are shifted over an insignificant distance, there are two possible methods of treatment – closed reduction of the fragments and fixation by an external device or open reduction and stabilization using a internal fixating device. The question which of the mentioned variants causes fewer complications and has a higher clinical efficiency is still to be solved. Some researchers present different frequencies of nonunion of shaft fractures after internal osteosynthesis (Gaebler et al., 2001). According to the results of an independent study, it is significantly higher (Antonova et al., 2013). In the conditions of intense development of the industry of preparations for healing fractures, the selection of the approach for fixating the fragments is significantly affected by factors of an economic-commercial character, which can sometimes infringe biological regulations.

Understanding of the pattern of bone healing is necessary for choosing an adequate method of restoration of bone fragments, which would cause the least damage to the natural processes of bone regeneration. This requires knowledge and understanding of the mechanisms that organize this process. Currently the data is still insufficient.

Recent scientific publications present the following stages in the process of bone regeneration: I – inflammation (1–7 days), II – formation of soft callus (2–3 weeks), III – formation of hard callus (3–4 months), IV – remodeling of the new formed bone (5 months and

longer) (Sfieretal., 2005; Ito & Perren, 2007). In our opinion, the basis of the division of regeneration process into stages should be determined by the mechanisms which regulate the natural process. Maximum activity occurs during the initial stages of the processes and phenomena which take place. Researchers have different opinions on this topic. Some focus on the inflammatory as the factor which initiates the process (Marsell & Einhom, 2012), other focus on the role of hematoma (Schell et al., 2017) or on the process of formation of the fibrin-collagen carcass (Popsuishapka et al., 2013; Echeverri et al., 2015; Wang et al., 2016).

Significant progress in the understanding of the process of bone regeneration was made by the studies of clinical use of fibrin enriched with thrombocytes (platelet-rich fibrin, PRF) in dental implantology (Ehrenfest et al., 2010; Kobayashi et al., 2015; Aydemir Turka et al., 2016; Bastami & Khojasteh, 2016). As we know, neoangenesis and differentiation of osteoblasts are regulated by biologically active factors: the vascular endothelial growth factor (VEGF) (Ramasamy et al., 2016; Hu & Olsen, 2016), transforming growth factor (TGF) (van Meeteren et al., 2011), bone morphogenetic proteins (BMP) (Moreno-Miralles et al., 2009), platelet-derived growth factor (PDGF) (Raica et al., 2010). The abovementioned factors (except BMP) are contained in the granules of platelets and some other white blood cells which possibly become released from fibrinogen in the process of forming fibrin. The discovery that mesenchymal cells can differentiate to osteoblasts if the regeneration object has vessels is highly significant (Maes et al., 2010; Marsell & Einhorn, 2011; Hankenson et al., 2011; Sivaraj & Adams, 2016; Ramasamy et al., 2016). Therefore, special attention should be focused on the role of VEGF in the process of osteoregeneration (Dong et al., 2016; Hu & Olsen, 2016).

In our opinion, the problem is that most of the abovementioned data were obtained mostly in theoretical-experimental studies and they do not significantly affect the existing methods of treating fractures. We mean not different commercial projects (for example, making devices for obtaining PRF), but practical suggestions regarding particular medical actions, e. g. what to do with hematoma around the fracture? Or, could anti-inflammatory preparations be prescribed in early stages after the fracture?

The objective of the study was the elaboration of the set-off mechanism and the orientation of the regenerative process after the bone fracture through the study of structural-morphological peculiarities of fibrin-blood clots in the space around the fracture, its biological activity and mechanical impacts related to the fixation regime.

Materials and methods

The study was conducted in accordance with the current ethical requirements. The protocol of the study was approved at the meeting of the Committee of Bioethics of the Sytenko Institute of Spine and Joint Pathology, Academy of Medical Science of Ukraine (protocol No 109 from 29.10.2012). A macroscopic study was conducted of the morphology of the fibrin-blood clot around the fracture among patients with diaphyseal fractures of long bones. During open reduction of the fragments for 45 patients with closed diaphyseal fracture, we assessed the form and peculiarities of positions of fibrin-blood clots in the area around the fracture.

Histological study. Biopsy material from the area around the fracture was taken from 16 patients over 1–18 days during surgical procedures and was fixated for 24 hours in 10% neutral formalin. Then the material was decalcified (if bone fragments were present) in 10% solution of formic acid, dehydrated in spirits (70%, twice 96%), mixture of 96% spirit with diethyl ether (1 : 1) and poured into celloidin. Histological sections of 5 μm thickness were made using a Reichert rotary microtome (Austria), stained using hematoxylin and eosin (H&E) and picrofuchsin solution according to Van Gieson (Van Gieson's stain). For the analysis, we used a BX63 microscope (Olympus, Japan) and the photographs were taken using a DP73 digital camera (Olympus) and "Cell Sens Dimention 1.8.1" (Olympus, 2013) software.

The zone of interest was the border between the maternal vital tissue and the fibrin-blood clot adjacent to it. We assessed the structure of fibrin, orientation of its fibrin bundles, places and periods of appearance of mesenchymal cells, vessels and spatial orientation. We assessed the number of spindle-shaped cells (per 100 cells in the microscope view, lens $^{x}40$, eyepiece $^{x}10$) which orientated with the long axis from the adjacent tissues to the centre of the fibrin-blood clot along the fibrin fibres, on the 3, 5, 8 and 12th day after the injury. Using the IBM SPSS Statistics 20 program, we calculated the mean value (x) and standard error (SE). The significance of the differences between the periods of monitoring was assessed using a single factor dispersal analysis.

Immunohistological study of the expression of the vascular endothelium growth factor (VEGF) in the tissues adjacent to the area of the fracture. The biopsy material was taken from 9 patients, from the tissues which surrounded the fragments, during their open reduction. The periods after the trauma: 1–5 days – 4 patients, 8–15 days – 5. Using a lancet, we cut the fibrin-blood clot with the adjacent periosteum, muscles and adipose tissue as a single block. Biopsy material was fixated in 10% buffered formalin and processed in accordance with the generally accepted method in a Mikrom CP-120 histoprocessor, and poured into paraffin wax. Histological sections of 3 μm thickness were made on the rotary microtome LeikaRM 2125, deparaffinated, and some were stained using hematoxylin and eosin. Other sections were analysed on VEGF with mouse antibody of VEGF (VG1 clone, Diagnostic Bio Systems) using the indirect peroxidase method with high-temperature exposure of En Vision (Dako) antigens. A brown colour corresponded to a positive result. The preparations were made in the laboratory of the Cherkasy Regional Oncological Dispensary (head of the dispensary – F. M. Halkin), the analysis was made in the Laboratory of Morphology of Connective Tissue of Sytenko Institute of Spine and Joint Pathology.

The results of immune-histological reaction were evaluated by the following points: 0 – reaction is absent; 1 - insignificant reaction (lower than 25% of the microscopic field), 2 – moderate (over 25%, but no higher than 50%), 3 – clear (over 50%), 4 – maximum (100%).

Ultrasonography of the zone around the fracture. Ultrasound analysis was conducted for 25 patients with shaft fractures of the humerus (13), tibia (4), femur (8). The periods of monitoring after the fracture: 2–6th day – 4, 7–14th – 16, 15–21st – 10. In total, 30 examinations were made, one patient was examined three times, and two patients were examined twice. We used a ToshibaAplio-500 sonograph with a linear 5–12 Hz transducer and a SLE-100 (Lithuania) mobile sonograph with 5.0–7.5 Hz transducer. The transducer was positioned alongside the fragment axis, exogeneity of the tissues was examined in the front and sagittal planes. We assessed the form of the external contour of the hematoma (or fibrin-blood clot) and recorded lengthwise and transversal sizes.

Results

Results of macroscopic (during surgical operation) and ultrasonographic examination. At the moment of opening the area of fracture, blood which filled the posttraumatic space had already changed its biological condition. It partly saturated adjacent tissues, and the rest of the blood had turned into a fibrin-blood clot. Taking to account these transformations, over first days after the fracture, we observed the following zones (Fig. 1):

– fibrin-blood clot zone;

– zone of serums with erythrocytes (blood fluid) (sometimes present);

– zone of muscles saturated with blood.

Depending on the magnitude of the shift of fragments and destruction of the surrounding tissues, the configuration of the fibrin-blood clot was different. We observed three variants:

I – the fibrin-blood clot fully filled the space around the fracture, and was limited by detached and hardly damaged periosteum. This variant occurred when the fragments were positioned along the width at an insignificant distance, approximately 1/3 of bone diameter (Fig. 2*a*). The periosteum with muscles under the pressure of blood deformed as a membrane, forming a spindle-shaped space filled with blood;
II – fibrin-blood clot retained spindle-like shape as a periphery barrier; was limited by muscles, but had a serum with erythrocytes (blood

fluid) in its central zone (Fig. 2, b); III – periosteum-muscular fascia was damaged, spindle-like shape was absent, fibrin-blood clots were in the form of fragments and were positioned in different places (not forming solid structure), the blood saturated the surrounding tissues in large areas, the fragments were shifted to full diameter and along the length (Fig. 2, c).

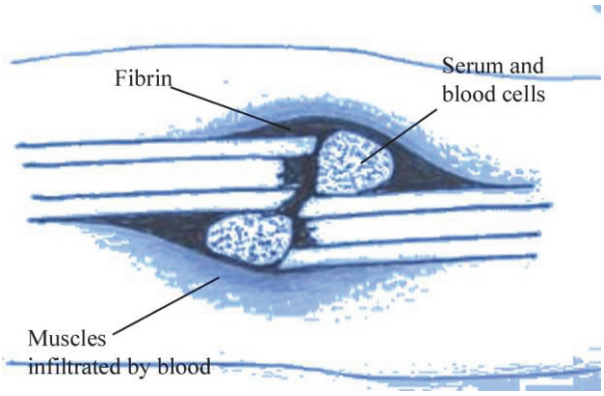

Fig. 1. Schematic image of the identified zones around the fracture

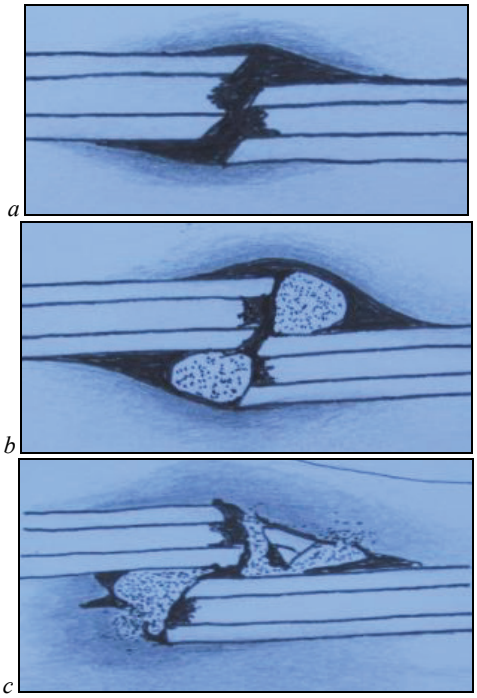

Fig. 2. Schematic illustration of the variant of the form and volume of the fibrin-blood clot in the area around the fracture after diaphyseal fracture: *a* – I, *b* – II, *c* – III

The zone of perifocal infiltration of muscles (or other tissues) with blood depended on the extent of destruction of the periosteum barrier – the greater the disruption, the wider the distribution of broadly its infiltration. This was determined visually by change in colour of the muscles and proved by histological examination. In this zone between the muscle fibres, there were accumulations of erythrocytes. Fibrin-blood clots which filled the space around the fragments were dark-brown, had elastic consistency and were also closely connected to the surrounding tissues (bone, periosteum, myeloid and adipose tissue). Their most typical localizations were: the fractured surface of the bone, including the bone-marrow canal, then the internal surface of the detached periosteum, mostly in border zones of the spindle. If the shift of fragments was insignificant, the clot filled the space directly between the areas of fracture, as we see in the patient during a surgical operation (Fig. 3).

Results of ultrasonographic examination. During ultrasonographic examination of the fracture zone, on the 2-6th days after its appearance, 72% of the patients (18 of 25) were observed to have an anechogenic zone with a bow-shaped external contour (Fig. 4) above the fragments. It indicated the presence of the hematoma around the fragments or a fresh fibrin-blood clot with no organization. To determine the level of echogenicity of freshly formed fibrin, we put a two or three day fibrin-blood clot obtained from the venous blood of patients on the transducer of the sonograph. The freshly formed clot did not resist the ultrasound and was identified by the sonograph as an anechogenic medium. Seven and more days later, at the site of the former hematoma (mostly along the peripheral part, and also directly between the fragments), a bow-shaped zone of hypoechogenicity appeared, which connected the fragments in an arc (bridge). This symptom indicated the growth of the cells in fibrin with formation of collagen. This coincided with the results of our histological studies of the clot around the fragments and other data (McNally, 2011).

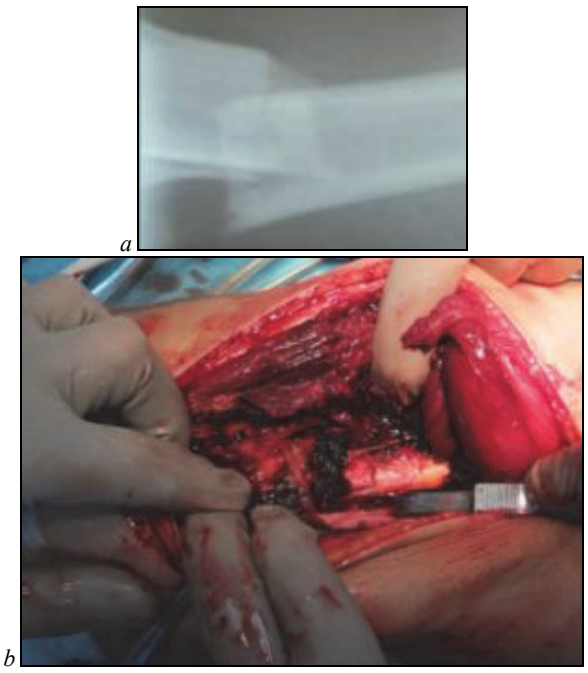

Fig. 3. Radiography of the zone of femur fracture (*a*) and photo of positioning of fibrin-blood clot between fragments (*b*) of patient III, 21 years, 12th day after the trauma

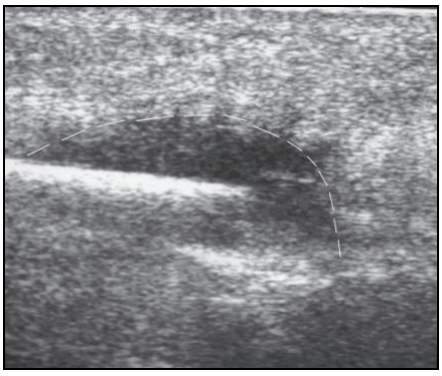

Fig. 4. Ultrasonographic image of the fracture zone of tibia: 2nd day after the trauma; anechogenic zone with bow-shaped external contour (white line)

Results of histological examinations. On histological preparation of biopsy material obtained during a surgical operation, in the first 1–3 days after the trauma, we found fibrin-blood clots represented by a system of fibrin membranes of different density in the zone around the fragments. In some areas, they were positioned in parallel, in others they formed a cellular structure. Cells limited by fibrin partitions were rounded or oval-elongated orientated in one-direction and filled with blood cells (mostly erythrocytes) (Fig. 5).

Fig. 5. Fragment of fibrin-blood clot with the zone surrounding the bone fragments, 2nd day after the fracture: the pointers indicate the orientation of the parallel fibrin membranes, dashed line – oval-elongated cell filled with erythrocytes; bar – 50 µm

Starting from the 3d day after the fracture, we observed capillaries developing into a fibrin-blood clot and its penetration to the blast cells of stretched shape, the long axis of which was orientated towards their direction of movement – from adjacent tissues to the center of the clot. Such cells had large hypochromic nuclei and elongated basophil cytoplasm. The density of cells (among them – insignificantly differentiated mesenchymal, fibroblasts, macrophages) was the highest on the side of damaged muscle tissue infiltrated with blood and decreased closer to the central areas of the clot (Fig. 6). Between the muscle fibers, we found bleeding in the form of accumulation of erythrocytes, mesenchymal cells, mitotic figures (2–3 in the microscope view, eyepiece $^{x}10$, lens $^{x}40$). Proliferation of insignificantly differenttiated cells was observed also in the bone-marrow canal.

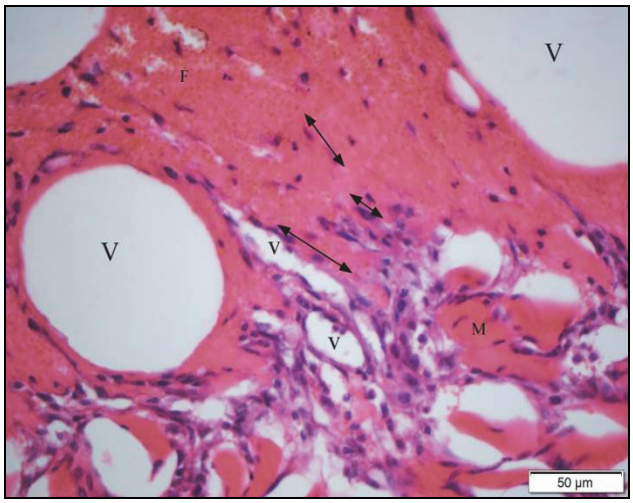

Fig. 6. Fragment of fibrin-blood clot and the muscle adjacent to it, which is infiltrated with blood, 5th day after the trauma: high cellular density at the "clot-muscle" border; the pointers indicate the orientation of growing of blood capillaries (v) and cells, 4th day after the fracture of a sheep

The longer the territory of the clot was monitored, the smaller it became due to the number of cells which penetrated to it from the surrounding tissues. Particularly, on the 3d day after the fracture, only 3.7 ± 0.66 cells out of 100 located at the border between damaged tissues and the clot had a spindle-like shape and penetrated to it, 5 days later, their number insignificantly increased (7.1 ± 0.93), after 8 and 12 days, it had increased compared to the previous period of study by 3.08 and 1.50 times respectively – 21.9 ± 2.0 and 33.2 ± 2.88 ($P < 0.001$) (Fig. 7). The cells formed pod-like bundles which started from the zone of their accumulation and grew into fibrin.

8–12 days after the trauma, the restructuring of the fibrin-blood clot continued: insignificantly differentiated cells penetrated to it, fibro- and osteoblasts, blood capillaries which formed granular and fibroreticular tissues, and osteoids near the bone fragments. In the areas remote from the maternal damaged cells, the number of cells was lower, also we found remains of fibrin. The elongated cells on some areas of the preparation were positioned in parallel to one another and to the fibrin partitions (Fig. 8).

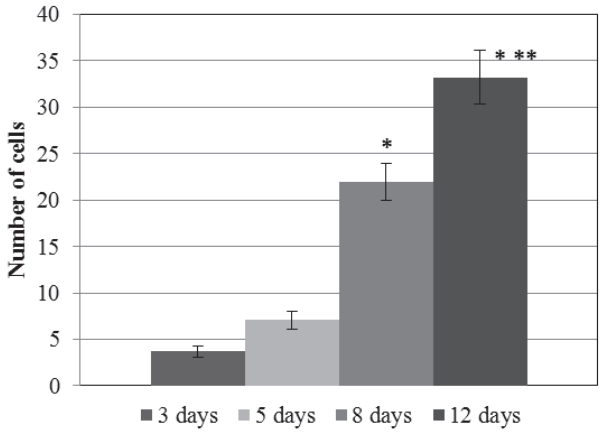

Fig. 7. Number of elongated cells which penetrated to the fibrin-blood clot, depending on the period of study: the graph demonstrates the standard error of the arithmetic mean (SE – Standard Error), the probability of the differences $P < 0.001$; * – compared to the period of 3 and 5 days, ** – compared to the period of 8 days

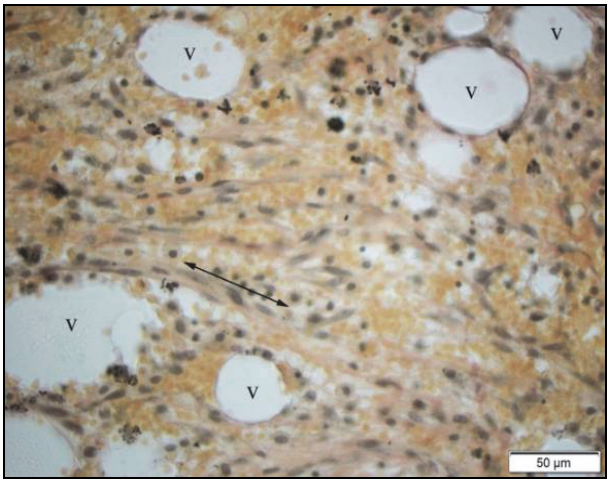

Fig. 8. Fragment of the regeneration between the fragments 9 days after the fracture of humerus: Ribbon-like proliferates of fibroblastic cells (the pointer indicates the orientation of long axis of the cells), the vessels of the capillary type (V); Van Gieson's stain

14–18 days after the fracture, at the place of the fibrin-blood clot, granular tissue formed, which had a high density of cells, vessels, areas of fibroreticular tissues of osteogenic type, and large-fiber bone tissue in the form of separate bone trabeculae. On their external surface, there were functionally active osteoblasts with large hypochromatic nuclei. Between the bone trabeculae, there was a fibroreticular tissue of osteogenic type with significant number of osteoblasts and fibroblasts. Lengthwise axis of these cells corresponded to the axis of the trabeculae (Fig. 9).

Results of immunohistological examination of VEGF in the tissues of the zone around the fragments after fractures of long bones. In the biopsy material taken on the 1–2nd day after the fracture, in the fibrin-blood clot, we found maximum reaction to VEGF (4 degrees), and in the surrounding tissues – minimum (0 degrees in the adipose tissue) and low (1 degree – in the muscle tissue) (Fig. 10).

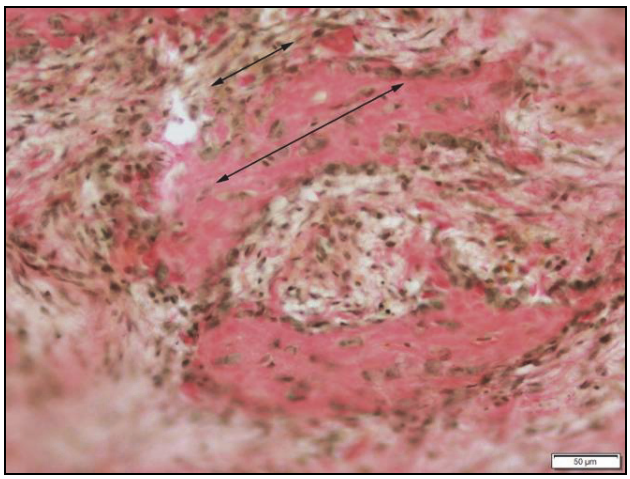

Fig. 9. Fragment of biopsy material with the surrounding area, 18th day after the fracture of tibia: the new formed bone trabeculae with active osteoblasts on the external surface; reticular fiber tissue of osteogenic type; long axis of fibroblasts is parallel to the trabeculae axis (pointers); Van Gieson's stain

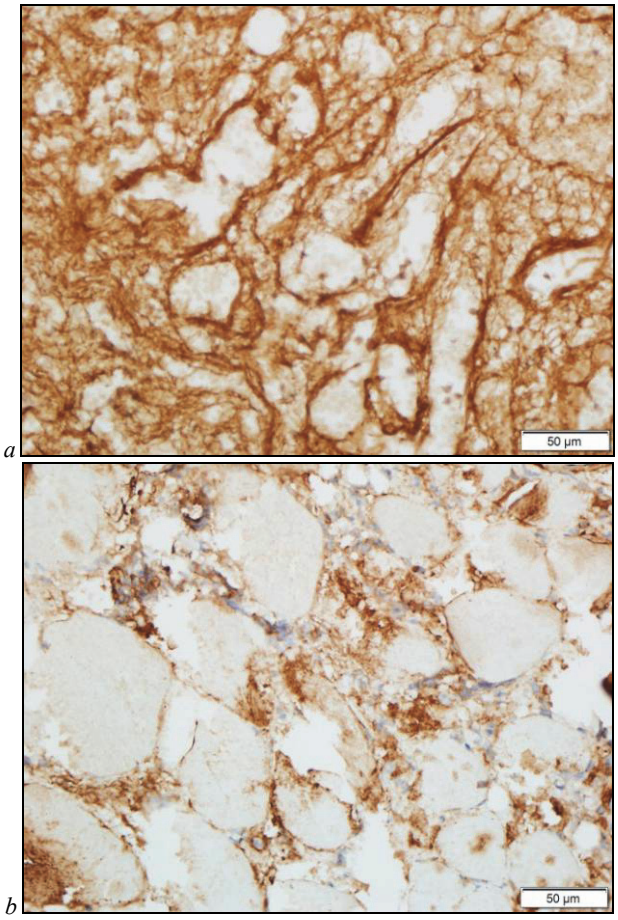

Fig. 10. Positive reaction to VEGF on 100% of the territory of a fibrin-blood clot (*a*) and less than 25% in the muscle tissue (*b*); 2nd day after the fracture

5 days after the fracture, the change in the structure of the regeneration manifested also in the VEGF. The highest reaction retained in the fibrin, though was the least clear – 3 points. Also, the expression of VEGF was observed in endotheliocytes, insignificantly differentiated cells and fibroblasts, which was in general assessed at 2 points.

On the 8 and 12th days after the fracture, the VEGF expression in the regeneration zone was generally moderate or clear (2–3 points). Positive reaction was observed in the regeneration cells – fibroblasts, endotheliocytes, osteoblasts and osteocytes. The matrix of the new formed bone trabeculae was characterized by absence of reaction to VEGF (0 points) (Fig. 11).

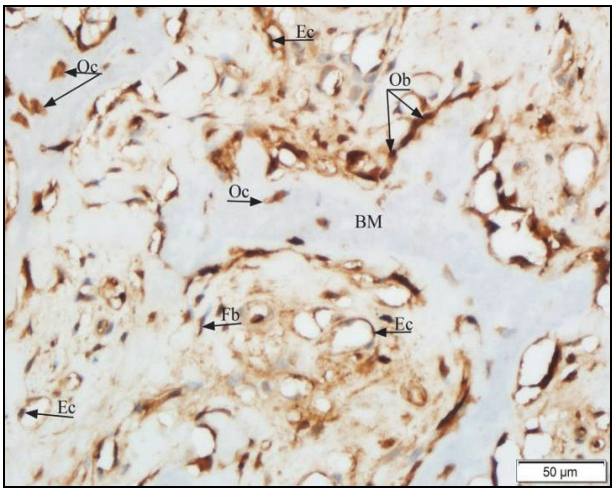

Fig. 11. Reaction to VEGF in the area surrounding the regeneration: the absence of reaction in bone matrix (BM), presence – in the cells; Oc – osteocyte, Ob – osteoblast, Fb – fibroblast, Ec – endotheliocyte; bar – 20 μm

Thus, the filling of the fibrin-blood clot around the fragments develops in the direction from the surrounding tissues and lasts 12–18 days among humans. During this period, the cells become osteogenically differentiated. Such tempi and orientation of the process occur due to the presence of fibrin with growth factors` concentration in it.

Discussion

Traditionally, bone regeneration is divided into the following stages: inflammation (1–7 days), migration and proliferation of cells, formation of the cellular blastema (soft callus, 2–3 weeks), formation of regenerated bone or bone-cartilage (hard callus, 3–4 months), remodeling of the new formed bone tissue (5 months and more) (Sfier et al., 2005; Korzh & Dedukh, 2006; Ito & Perren, 2007). In our opinion, the inflammatory process is a general reaction of the organism and follows the recovery of any tissue to the end, and the first important stage of bone regeneration at the local level is formation of the fibrin-blood clot, the structure of which stabilizes approximately in 12 to 24 hours (Popsuishapka et al., 2015; Wang et al., 2016).

It should be mentioned that in normal condition, compact bone has a highly organized microstructure in the form of dense lengthwise positioned osteons. Every osteon consists of concentric layers, where the collagen fibers lie in parallel and in a certain direction (Figurskaya, 2007). For the recovery of such structure of the compact bone, the 4–6 months prescribed for treatment are not enough. In the process of bone regeneration after a fracture, first, trabecular tissue forms, then, under the impact of loads, transforms along the periphery to compact bone. Insufficient density of the trabecular bone on the first stages of suppuration in the fracture is compensated by its form and internal structure. Therefore, it was important for us to analyse the mechanisms of formation of trabecular regeneration between the fragments and determine the conditions necessary for this.

As we have seen during an open reduction of the fragments, the bleeding after the bone fracture is caused by two phenomena – saturation of the surrounding tissues with blood and formation of fibrin-blood clot from the blood which fills the space around the fracture. There is always a border between the space filled with blood and the surrounding tissues. It is logical to presume that the bleeding from the damaged vessels will last while the blood pressure in the closed cavity around the fracture does not stabilize with the pressure in the vessels. Heightened blood pressure deforms the surrounding tissues as a membrane, therefore causing the spindle-like shape of the hematoma (Litvishko et al., 2016). At first, part of the blood, while in liquid state, penetrates to the surrounding soft tissues. We found accumulations of

erythrocytes in the muscles, therefore there might have been other elements of blood (thrombocytes, monocytes, etc). At the same time, we observed no formation of fibrin in this zone, despite the fact that fibrogen could be transported here with the blood plasma.

In vitro studies have proved that the structural organization of fibrin-blood clots is affected by mechanical and chemical factors (Popsuishapka et al., 2013; Wang et al., 2016). Among the mechanical factors, the surface pressure is important. It was proved that on the surface of the contact with the trabecular layer which causes pressure, a layer of dense fibrin forms, and in the central part – its structure is cellular (Popsuishapka et al., 2013). A similar structure of fibrin clot was determined in microscopic examination of the biopsy material received from experimental animals (Popsuishapka et al., 2015). This made it possible to represent the general structure of a fibrin-blood clot around a fracture, which occurs after a closed fracture (Fig. 12).

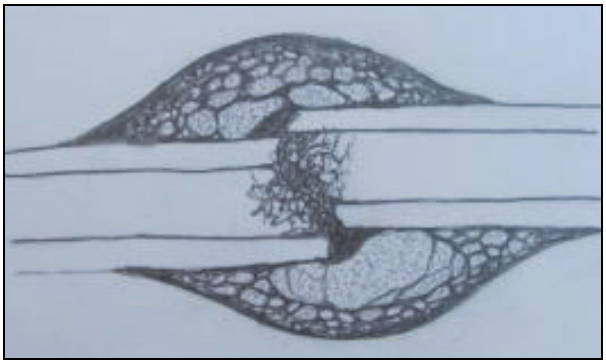

Fig. 12. Schematic image of the structure of a fibrin-blood clot after a closed diaphyseal bone fracture

There is a presumption that a fibrin-blood clot is a "network of closely intertwined fibers of fibrin and blood cells, thrombocytes and blood plasma involved in this network" (https://dic.academic.ru/dic.nsf/medic2/49113). On the basis of the examinations conducted, we determined that fibrin fibers form membranes of different thickness, positioned at different densities. It could be important that in a three-dimensional plane, fibrin membranes form closed cells containing cells of blood serum. The oval shape of the cells indicates the pressure of the fluid inside. During the retraction of fibrin or additional external loads, tension and deformations (including the fact that the fluid does not compress) form in these membranes. They can have a significant effect on the processes of the cell orientation and differentiation.

The process of formation of fibrin takes place first of all due to thrombocytes which are the source of VEGF (Hu & Olsen, 2016). Using the immunohistological method, we determined the highest reaction to VEGF in the fibrin-blood clot around the fragments, which occurred due to release of growth factors (including VEGF) from the thrombocytes in the process of blood coagulation on the one hand, and mechanical stimuli which increase the content of VEGF, on the other hand (Groothuis et al., 2010). This causes a strong localized signal which activates and orientates the formation of capillaries, which in its turn is a precondition of bone regeneration (Street et al., 2002; Hu & Olsen, 2016; Ramasamy et al., 2016). The impact of VEGF is determined in time: at the very beginning of the healing, process it concentrates in fibrin and activates neoangeogenesis, later – stimulates the formation of osteoblasts and mineralization of regeneration (Hu & Olsen, 2016; Grosso et al., 2017).

Blood which at first saturated the surrounding vital tissues provides a signal for proliferation of the cells. Their source, as we know, is the cells of the vessels` adventitia, perimysium cells, the cambium layer of the periosteum. Insignificantly differentiated mesenchymal cells come from the side of the adjacent tissues into the formed clot which over a week transforms in cellular blastema along the perimeter. Fibrin carcass functions as a flexible matrix, through which the cells first develop collagen and then bone regeneration.

The mechanisms which orientate the differentiation of cells in an osteogenic direction are still not fully understood. Currently, a common presumption is that the osteogenic differentiation of cells is related to angiogenesis and VEGF (Maes et al., 2010; Hu & Olsen, 2016; Grosso et al., 2017). We have also observed formation of osteoblasts and osteoid near the blood capillaries. However, at the same time, we found an increased number of vessels also in the young connective tissue. We think that the mechanism of osteogenic differentiation works when the formation of vessels and conditions of oxygenation occur before or coincide in time with the phase of proliferation and differentiation of cells. Perhaps, the high content of VEGF in fibrin over the first 5 days after a fracture causes initial osteogenesis in this particular area.

It is very likely that the osteogenic differentiation of cells is caused also by sufficient level of tension in fibrin-collagen partitions. The elastic properties were proved and the fibrin fiber`s elastic modulus was found to equal 1.6–8.0 MPa (Janmey et al., 2009). If the periosteum detached from the ends of the fragments remains, the clot becomes surrounded by a pressurized membrane due to the higher elastic modulus of the periosteum (Evans, 2012), which increases the tension-deformed condition of fibrin (Litvishko et al., 2016). The forces of internal pressure of the fibrin carcass determine the orientation of mechanocytes which form trabeculae of the corresponding form (Claes et al., 1998; Popsuishapka et al., 2015), and, perhaps, initiate the osteogenic differentiation of cells. The more dense (solid) is the partition, the higher is its ability to tense compared to a less dense one in the conditions of similar deformations. The internal forces which developed in it influence the cell cytoplasm and therefore "inform" it about the orientation of the tissue differentiation. The higher the pressure on the cell, the higher the necessity to resist it by formation of a base mechanical substation around to prevent its destruction.

Earlier, we demonstrated that the form and sizes of the formed periosteum bone regeneration after diaphyseal fracture are similar in form and are close in size to the hematomas around the fragments (fibrin-blood clot) in sonographic image (Litvishko & Popsuishapka, 2017).

We can imagine a development of the process when the function of fibrin-formation is decreased, which often occurs in clinical practice at the condition of hemodilution, consumption of aspirin or non-steroid anti-inflammatory preparations. In this case, blood in liquid state infiltrates the surrounding tissues, becoming remote from the spot where the bone regeneration should take place. In this situation, regeneration occurs in the surrounding tissues through formation of connective tissue (fibrosis).

The described conception involves proving the priority of these phenomena of fibrin-formation in the zone between the fragments after the fracture, which is the initial stage of the fracture healing process. It is wrong to consider the inflammatory stage the beginning of the process. It is not logical at least due to the fact that "inflammation" is a general term and does not indicate a particular phenomenon or factor. Each clinically identified stage of the process should indicate its essence and have practical significance. If the beginning of the fracture healing is inflammation, then why do all doctors inhibit it with all available measures? That is not logical.

Our principles of treatment of fractures are based on the suggested conception, the validity of which is substantiated by clinical results (Litvishko, 2017). They prove that fractures heal faster, and also have a lower frequency of complications if the treatment tactics includes maintaining the integrity of tissues around the fragments with initial formation of a fibrin-blood clot, and also creating a regime of their elastic seaming.

Conclusion

Formation of a structured fibrin-blood clot around the fragments should be considered the initial stage of the process of formation of bone regeneration after fracture. It is an initial biologically active mechanical carcass for proliferation and osteogenic differentiation of cells. Such conception is a reason for introducing updated principles of fracture treatment, which are related to preserving the surrounding tissues, the formed fibrin-blood clot and creating conditions which provide a manageable regime of regeneration tensions.

References

Antonova, E., Le, T. K., Burge, R., & Mershon, J. (2013). Tibia shaft fractures: Costly burden of nonunions. BMC Musculoskeletal Disorders, 14(1), 42.

Aydemir Turkal, H., Demirer, S., Dolgun, A., & Keceli, H. G. (2016). Evaluation of the adjunctive effect of platelet-rich fibrin to enamel matrix derivative in the treatment of intrabony defects. Six-month results of a randomized, split-mouth, controlled clinical study. Journal of Clinical Periodontology, 43(11), 955–964.

Bastami, F., & Khojasteh, A. (2016). Use of leukocyte-and platelet-rich fibrin for bone regeneration: A systematic review. Regeneration, Reconstruction and Restoration, 1(2), 47–68.

Claes, L. E., Heigele, C. A., Neidlinger-Wilke, C., Kaspar, D., Seidl, W., Margevicius, K. J., & Augat, P. (1998). Effects of mechanical factors on the fracture healing process. Clinical Orthopaedics and Related Research, 355S, S132–S147.

Dohan Ehrenfest, D. M., Del Corso, M., Diss, A., Mouhyi, J., & Charrier, J. (2010). Three-dimensional architecture and cell composition of a choukroun's platelet-rich fibrin clot and membrane. Journal of Periodontology, 81(4), 546–555.

Dong, L., Yin, H., Wang, C., & Hu, W. (2014). Effect of the timing of surgery on the fracture healing process and the expression levels of vascular endothelial growth factor and bone morphogenetic protein-2. Experimental and Therapeutic Medicine, 8(2), 595–599.

Echeverri, L. F., Herrero, M. A., Lopez, J. M., & Oleaga, G. (2015). Early stages of bone fracture healing: Formation of a fibrin – collagen scaffold in the fracture hematoma. Bulletin of Mathematical Biology, 77(1), 156–183.

Maes, C., Kobayashi, T., Selig, M. K., Torrekens, S., Roth, S. I., Mackem, S., & Kronenberg, H. M. (2010). Osteoblast precursors, but not mature osteoblasts, move into developing and fractured bones along with invading blood vessels. Developmental Cell, 19(2), 329–344.

Marsell, R., & Einhorn, T. A. (2011). The biology of fracture healing. Injury, 42(6), 551–555.

McNally, E. G. (2011). The development and clinical applications of musculoskelet alultrasound. Skeletal Radiology, 40(9), 1223–1231.

Moreno-Miralles, I., Schisler, J. C., & Patterson, C. (2009). New insights into bone morphogenetic protein signaling: Focus on angiogenesis. Current Opinion in Hematology, 16(3), 195–201.

Popsuishapka, A. K., Lytvyshko, V. A., & Ashukina, N. A. (2015). Klinikomorfolohichni stadiyi zroshchennya vidlamkiv pislya perelomu kistky [Clinical and morphological stages of bone fragments fusion]. Orthopaedics, Traumatology and Prosthetics, 1, 12–20 (in Ukrainian).

Popsuishapka, A. K., Lytvyshko, V. A., Ashukina, N. A., & Danyshchuk, Z. N. (2013). Osobennosti formirovaniya, strukturno-mekhanicheskiye svoystva fibrin-krovyanogo sgustka i yego znacheniye dlya regeneratsii kosti [Peculiarities in the formation, structural-mechanical properties of a fibrin-blood clot and its importance for bone regeneration in fractures]. Orthopaedics, Traumatology and Prosthetics, 4, 5–12 (in Russian).

Raica, M., & Cimpean, A. M. (2010). Platelet-derived growth factor (PDGF)/PDGF receptors (PDGFR) axis as target for antitumor and antiangiogenic therapy. Pharmaceuticals, 3(12), 572–599.

Ramasamy, S. K., Kusumbe, A. P., Schiller, M., Zeuschner, D., Bixel, M. G., Milia, C., & Adams, R. H. (2016). Blood flow controls bone vascular function and osteogenesis. Nature Communications, 7, 13601.

Schell, H., Duda, G. N., Peters, A., Tsitsilonis, S., Johnson, K. A., & Schmidt-Bleek, K. (2017). The haematoma and its role in bone healing. Journal of Experimental Orthopaedics, 4(1), 5.

Sfeir, C., Ho, L., Doll, B. A., Azari, K., & Hollinger, J. O. (2005). Fracture repair. In: Bone regeneration and repair: Biology and clinical applications. Humana Press. Pp. 21–44.

Sivaraj, K. K., & Adams, R. H. (2016). Blood vessel formation and function in bone. Development, 143(15), 2706–2715.

Street, J., Bao, M., de Guzman, L., Bunting, S., Peale, F. V., Ferrara, N., Steinmetz, H., Hoeffel, J., Cleland, J. L., Daugherty A., van Bruggen, N., Redmond, H. P., Carano, R. A. D., & Filvaroff, E. H. (2002). Vascular endothelial growth factor stimulates bone repair by promoting angiogenesis and bone turnover. Proceedings of the National Academy of Sciences of the United States of America, 99(15), 9656–9661.

van Meeteren, L. A., Goumans, M., & Ten Dijke, P. (2011). TGF-β receptor signaling pathways in angiogenesis: Emerging targets for anti-angiogenesis therapy. Current Pharmaceutical Biotechnology, 12(12), 2108–2120.

Wang, X., Friis, T. E., Masci, P. P., Crawford, R. W., Liao, W., &Xiao, Y. (2016). Alteration of blood clot structures by interleukin-1 beta in association with bone defects healing. Scientific Reports, 6, 35645.

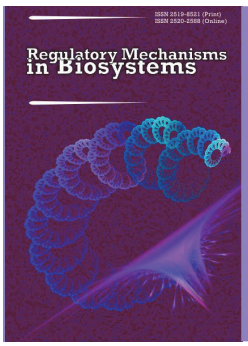

Regulatory Mechanisms in Biosystems

ISSN 2519-8521 (Print)
ISSN 2520-2588 (Online)
Regul. Mech. Biosyst., 9(3), 329–334
doi: 10.15421/021848

The parasitofauna of the Siberian sterlet *Acipenser ruthenus marsiglii* of the Lower Irtysh

E. L. Liberman*, E. L. Voropaeva**

**Tobolsk Complex Scientific Station UD RAS, Tobolsk, Russia*
***Center for Parasitology of the A. N. Severtsov Institute of Ecology and Evolution of the RAS, Moscow, Russia*

Article info

Received 19.05.2018
Received in revised form 24.06.2018
Accepted 28.06.2018

Tobolsk Complex Scientific Station UD RAS, Y. Osipova st., 15, Tobolsk, 626152, Russian Federation. Tel.: +7-905-826-23-47 E-mail: eilat-tymen@mail.ru

Center for Parasitology of the A. N. Severtsov Institute of Ecology and Evolution of the RAS, Leninsky Prospect, 33, Moscow, 119071, Russian Federation. Tel.: +7-925-509-40-96 E-mail: kts2@yandex.ru

Liberman, E. L., & Voropaeva, E. L. (2018). The parasitofauna of the Siberian sterlet Acipenser ruthenus marsiglii of the Lower Irtysh. Regulatory Mechanisms in Biosystems, 9(3), 329–334. doi:10.15421/021848

In the Ob-Irtysh basin, studies on the parasitofauna of the Siberian sterlet are very limited and confined to the middle of the twentieth century. The decrease in the numbers of sterlet over the past half century may have led to a change in the qualitative and quantitative composition of the parasitofauna. The aim of this work is to study the parasitofauna of the Siberian sterlet in the rivers Irtysh and Tobol. 85 specimens of Siberian sterlet (L = 27.8–51.5 cm, 2+ – 6+) from the Tobol and Irtysh rivers were examined by the method of complete parasitological dissection during the periods from 5 to 21 June and from 14 to 22 July 2017. A comparison of the biodiversity of parasites was performed using the indices: Berger-Parker. 11 species of parasites were found, including four species specific to sturgeons: *Cryptobia acipenseris* (Joff, Lewashow, Boschenko, 1926), *Haemogregarina acipenseris* (Nawrotzky, 1914), *Crepidostomum auriculatum* (Wedl, 1858), *Capillospirura ovotrichura* (Skrjabin, 1924). Seven broadly specific species: *Trichodina* sp., *Proteocephalus* sp. (plerocercoids), *Diplostomum chromatophorum* mtc. (Vrown, 1931), *Echinorhynchus cinctulus* (Porta, 1905), *Piscicola geometra* (Linnaeus., 1761), *Ergasilus sieboldi* (Nordmann, 1832), Unionidae gen. sp. *Cryptobia acipenseris* and *H. acipenseris* were recorded for the first time in the Ob-Irtysh basin. *C. acipenseris* was found only in three fish from the total number of examined sterlet (3.5%). In the River Tobol the extent of infestation *H. acipenseris* was higher (22.7%) than in the River Irtysh 11.1%. The carriers of *C. acipenseris* and *H. acipenseris* in the Lower Irtysh are allegedly leeches of *Piscicola geometra* (10.6%). The most common parasites found were *C. auriculatum* (32.9%) and *C. ovotrichura* (15.3%). In the River Irtysh, metacercariae of *Diplostomum chromatophorum* (Vrown, 1931) (metacercariae) were discovered in the lens of the eye in the studied fish. The maximum EI of this parasite was noted in the fish sample near the city of Tobolsk – 12.5% with AI – 1 and IO – 0.12. In the Gornoslinkino area in June and July, the infection level was low (EI 4.3% and 8.3%, respectively). In the June sample of fish from the River Tobol no metacercariae of this species were detected. Single cases of infection of *Proteocephalus* sp. (plerocercoid), *E. cinctulus*, *E. sieboldi*, Unionidae gen. sp. were found. In the River Irtysh the parasitofauna was dominated by *C. ovotrichura*, in the River Tobol – *C. auriculatum*. The number of parasite species noted in the Siberian sterlet in the Ob-Irtysh basin according to our own and literary data is greater than that found in sterlet from the River Yenisei: 18 and 11 respectively. Common to the sterlet of the two basins are 8 species of parasites: *Cryptobia acipenseris*, *Diclybothrium armatum*, *Crepidostomum auriculatum*, *Capillospirura ovotrichuria*, *Truttaedacnitis clitellarius*, *Echinorhynchus cinctulus*, *Piscicola geometra*, Unionidae gen. sp. The fauna of the Ob-Irtysh basin was enriched by the "southern" narrowly specific parasite of sturgeon – *H. acipenseris*. For many years the infection of *C. auriculatum* has practically not changed.

Keywords: parasites; *Haemogregarina acipenseris*; *Cryptobia acipenseris*; *Capillospirura ovotrichuria*; Siberian sterlet; Tobol; Irtysh.

Introduction

Sturgeons are one of the oldest groups of fish, the biology and cultivation of which is a subject of interest all around the world (Guénette et al., 1992; Israel & May, 2010; Wuertz et al., 2011; Akbulut et al., 2013; Vasil'ev et al., 2014). The smallest representative of sturgeons is the sterlet (*Acipenser ruthenus* (Linnaeus, 1758)). It is a nonmigratory species, inhabits the rivers of the following basins: Azov, Caspian, Black, Adriatic and Baltic seas, and also the Northern Dvina River and its tributaries – Suhona and Vychegda. It is common in the basins of the Siberian rivers: Ob and Yenisei, where it forms a subspecies – *Acipenser ruthenus marsiglii* (Brandt, 1833) (Zhuravlev, 2000). Sterlet quite like warm water, winter in river pockets, and are typical benhtophages – the basis of their food is chironomid larvae, Simuliidae, mayflies, dragonflies, molluscs, and other representatives of macrozoobenthos (Strel'nikova, 2012). Because of the high industrial value of sterlet, and therefore their intensive fishing, and also change in hydrological and hydrochemical regimes of water bodies (places of spawning and fattening), by the end of the 1970s, the reserves of sterlet in the Ob-Irtysh basin had become critical (Liberman, 2017). Currently, there is no industrial fishing of sterlet in this basin, catching takes place only for scientific purposes.

Studies on the morphology and biology of parasites of sturgeons in natural and artificial water bodies have been conducted by a number of scientists (Appy & Anderson, 1982; George & McCabe, 1993; Choudhury & Dick, 2001; Sepúlveda et al., 2010; Lysenko, 2013). The species composition of the parasitofauna of the sterlet has been best studied in the Volga basin, where the species is represented by the nominative subspecies (Dubinin, 1952; Ivanov, 1968; Izyumova, 1977; Lyubarskaya & Lavrent'eva, 1985; Fedotkina &, Shinkarenko, 2015). In the rivers of the basins of the Azov and the Black seas, parasites of sterlet were studied by Kazarnikova & Shestakovskaya (2006), Cakic et al. (2008),

Lenhardt et al. (2009). Parasites of sterlet have been well studied in the Yenisei and Ob-Irtysh basins (Zahvatkin, 1938; Volkova, 1941; Bauer, 1948; Petrushevskij et al., 1948; Shul'man, 1954; Dobrohotova, 1960; Titova, 1965; Skryabina, 1974). However, the last publication with original data on sterlet parasites in the Ob-Irtysh basin was published more than 50 years ago (Titova, 1965).

The decrease in the number of sterlet over the last half-century could have led to change in qualitative and quantitative composition of their parasitofauna. Therefore, due to absence of the corresponding studies over many years, the presentation of new data on the species composition of parasites of sterlet is relevant.

The objective of this research was to study the current condition of the parasitofauna of the Siberian sterlet in the Irtysh and Tobol rivers.

Materials and methods

The material was collected during the periods from 5th to 21st June and from 14th to 22st July of 2017 from the Tobol and Irtysh rivers, located within the Tobol and Uvatsky districts of the Tyumen oblast.

Using the method of full parasitological autopsy, we examined 85 specimens of sterlet: 22 specimens with absolute body length (L) 30.8–51.5 cm from the Tobol River (Karachino village, 58°02'50" N, 68°06'35" E; June), 23 specimens with L = 29.2–37.6 cm from the Irtysh near Gornoslinkino village (58°43'54" N, 68°41'54" E; June), 24 specimens with L = 27.8–36.2 cm from the Irtysh near Gornoslinkino (July) and 16 specimens with L = 31.5–46.0 cm from the Irtysh in the area of the city of Tobolsk (58°11'04" N, 68°12'59" E; July). We studied individuals of different sex and age range 2+ – 6+.

Full parasitological analysis, standard methods of fixation and staining of parasites were conducted according to the methods of I. E. Byhovskaya-Pavlovskaya (1985). Blood was drawn from the tail vein, a smear was prepared, dried in the air, and then fixated in a mixture of 95% ethyl spirit and diethyl ether (1 : 1) during 30 minutes, the fixated smears were then dried in the air at room temperature, stained using azure-eosine in a 1 : 10 solution during 40 minutes. For identifying the nematodes, we used the work of Moravec (2013), for the remaining groups of parasites – identification guides to parasites of fresh water fish of the fauna of the USSR (Opredelitel' …, 1984, 1987).

We calculated the extensity of the invasion (EI, %), intensity of the invasion (II, minimum – maximum, specimens), abundance index (AI, specimens per fish), for intra-erythrocytic parasites – parasitemia index (X) (Bush et al., 1997; Woo et al., 2006).

$$E = \frac{n}{N} \times 100\%;$$

where E – invasion extensivity, n – number of host individuals infested with parasites, N – number of studied host individuals.

$$M = \frac{m}{N};$$

where M – abundance index, m – number of parasites found in the studied selection of hosts, N – number of examined host individuals.

$$X = \frac{A}{B \times C} \times 100\%;$$

where A – number of affected erythrocytes, B – number of erythrocytes in one microscope field, C – number of examined microscope fields. No less than 50 microscopic fields were examined for each preparation.

For identifying the dominant species in the communities, we used the Berger-Parker dominance index (d) (Mehgarran, 1992):

$$d = \frac{\mathrm{Nmax}}{\mathrm{N}};$$

where N_{max} – number of the most abundant species, N – total number of parasites in the community.

Results

In the basin of the Lower Irtysh, the Siberian sterlet was found to have 11 species of parasites (Table 1), represented by different systematic groups: Ciliophora – 1, Kinetoplastida – 1, Apicomplexa – 1, Cestoda – 1, Trematoda – 2, Chromadorea – 1, Palaeacanthocephala – 1, Hirudinea – 1, Copepoda – 1, Bivalvia – 1. Among them, 4 species are specific to sturgeon – *Cryptobia acipenseris* (Joff, Lewashow, Boschenko, 1926), *Haemogregarina acipenseris* (Nawrotzky, 1914), *Crepidostomum auriculatum* (Wedl, 1858), *Capillospirura ovotrichura* (Skrjabin, 1924) (Table 1). *Cryptobia acipenseris* and the intra-erythrocytic parasite *Haemogregarina acipenseris* were found as a result of microscopic analysis of the smears. *C. acipenseris* (Fig. 1) was recorded in June, one specimen from the Tobol and in July, two specimens from the Irtysh (in one of each of the researched stretches). We assessed 2–4 parasites in each blood smear.

H. acipenseris has an oval body shape, is 6.5–8.2 × 2.2–3.0 μm in size, with two rounded ends or one rounded and one sharpened end (Fig. 2). The nucleus is composed of a few chromatin granules. It is positioned both in the middle of the body and in one of its ends. Most often, one parasite is found in an erythrocyte, more rarely two, and we also found parasites outside erythrocytes due to their decomposition. The highest EI of this parasite was recorded in a selection of fish caught in July in the Irtysh River in the area of Tobolsk – 31.2% at average value of parasitemia of 0.06 ± 0.02%. The lowest EI was in fish caught in the same month in the Irtysh in the area of Gornoslinkino village (8.3%) at average value of parasitemia equaling 0.12 ± 0.11%. The highest average values of parasitemia were observed in sterlet from the Tobol River – 0.19 ± 0.13%. It is interesting that these parasites were not found at all in the selection of fish from the Irtysh, collected in the same month as the fish from the Tobol (June).

Table 1
Species composition of parasites and parameters of infestation of Siberian sterlet in the Lower Irtysh basin

Species of parasite	Localization	The Tobol River n = 22 specimens			The Irtysh River n = 63 specimens		
		EI, %	II, specimens	AI, specimens	EI, %	II, specimens	AI, specimens
Cryptobia acipenseris	blood	4.5	–	–	3.2	–	–
Haemogregarina acipenseris	erythrocytes	22.7	–	–	11.1	–	–
Trichodina sp.	body surface, fins, gills	100.0	–	–	9.5	–	–
Proteocephalus sp., pl	intestine	–	–	–	1.6	1	0.02
Diplostomum chromatophorum, mtc*	lens	–	–	–	7.9	1	0.08
Crepidostomum auriculatum	intestine	40.9	1–23	3.1	30.2	1–36	1.50
Capillospirura ovotrichura	stomach	9.1	2–28	1.4	17.5	1–93	3.80
Echinorhynchus cinctulus	intestine	–	–	–	1.6	1	0.02
Piscicola geometra	gills, fins	4.5	1	0.04	12.7	1–2	0.20
Ergasilus sieboldi	gills	–	–	–	1.6	1	0.02
Unionidae gen. sp.*	gills	–	–	–	1.6	1	0.02

Note: EI – extensity of invasion, II – intensity of invasion min–max, AI – abundance index, mtc – metacercariae, pl – plerocercoid,* – larvae stage.

Crepidostomum auriculatum trematode (Fig. 3) and *Capillospirura ovotrichura* nematode (Fig. 4) were found in all examined selections of fish. All specimens found of *C. auriculatum* and *C. ovotrichura* were mature. The nematode parasitized mostly in the stomach, more rarely – in the intestine, trematodes were found throughout the length of intestine. The highest infestation with *C. auriculatum* was recorded in fish from the Tobol River in June (Table 1). In the Irtysh, maximum EI equaled 37.5%, with infestation intensity of 1–36 specimens per fish and AI – 3.9 (area of Tobolsk, July). Maximum extensivity of infestation with *Capillospirura ovotrichura* was observed in fish from the Irtysh River near Gornoslinkino (July) – 25% at II of 1–21 specimens per fish and AI – 1.7, whereas maximum intensity of invasion – 93 specimens per fish at 5.9 abundance index was recorded near Tobolsk (EI – 12.5%). On the whole, *Capillospirura ovotrichura* is the most abundant parasite of sterlet in the Irtysh (d = 0.680), whereas in the Tobol River, the dominant was *Crepidostomum auriculatum* trematode (d = 0.690).

In the Irtysh river, in the lenses of the studied fish, we found *Diplostomum chromatophorum* (Brown, 1931) metacercariae. Maximum EI with this parasite was recorded in the fish selection from the area of

Tobolsk – 12.5% and II – 1 and AI – 0.12. In the area of Gornoslinkino in June and July, the infestation was low (EI – 4.3% and 8.3% respectively). In the June selection of fish from the Tobol River, no metacercariae of this species were found.

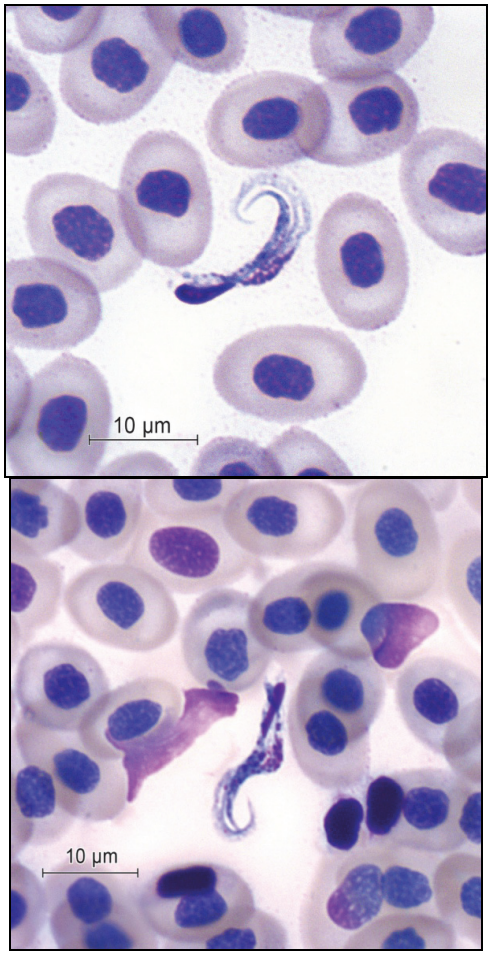

Fig. 1. *Cryptobia acipenseris* (Joff, Lewashow, Boschenko, 1926) in blood of Siberian starlet

Among the rest of the recorded species, parasites of sterlet which belong to *Trichodina* sp. were frequently found, parasitizing the body surface, gills and fins. The identification to species level was impossible due to the poor condition of the material. All fish species were infested with this parasite only in the June selection from the Tobol (Table 1). In each preparation of slime scrape, we found 1–3 trichodinids. At the same time, fish from the Irtysh (June) was found to be freer from this parasite. In July, in the Irtysh River, the extensity of invasion, depending on the area of the study, ranged from 8.3% (Gornoslinkino) to 25.0% (Tobolsk). Rare parasite species were *Proteocephalus* sp. cestode (plerocercoid), *Diplostomum chromatophorum* (Brown, 1931) trematode (metacercaria), *Echinorhynchus cinctulus* (Porta, 1905) acanthocephala (immature female), *Ergasilus sieboldi* (Nordmann, 1832) copepod crustacean, *Piscicola geometra* (Linnaeus, 1761) leech and Unionidae gen. sp. mollusc (glochidium).

Discussion

Most of the parasite species found (6) are reliably known to have a complex life cycle: *Haemogregarina acipenseris*, *Proteocephalus* sp., *Diplostomum chromatophorum*, *Crepidostomum auriculatum*, *Capillospirura ovotrichura*, *Echinorhynchus cinctulus* .Four species have a direct life cycle – widely distributed and insignificantly specific to any hosts: *Trichodina* sp., *Piscicola geometra*, *Ergasilus sieboldi*, Unionidae gen. sp.

Cryptobia acipenseri were recorded in different sturgeon in the basins of Don, Volga, Donau and Yenisei (Dubinin, 1952; Bauer et al., 2002). Most often, this parasite was recorded in sterlet (Shul'man, 1954; Lyubarskaya & Lavrent'eva, 1985; Baska, 1990; Bauer et al., 2002). According to Shul'man (1954), the range of *C. acipenseris* should coincide with the range of sterlet. However, the absence of data on the records of this parasite in the Ob-Irtysh basin could not prove this supposition. Our data verify the hypothesis of this author. The studies by Pazooki and Masoumian (2004), conducted on mature *Acipenser gueldenstaedtii* and *A. persicus* from the Caspian Sea, demonstrated a significantly different occurrence of *Cryptobia acipenseri* during examination of humid and stained blood smears (EI – 45% and 55% compared to 15% and 25%). These authors recommend assessing the infestation of fish with kinetoplastids and flagellates by humid blood smears. The evidence presented by Pazooki and Masoumian (2004) should be checked by referring to additional material. The life cycle of *C. acipenseri* has not been studied completely. According to the literature data, transmission of Cryptobia to fish is possible by direct transmission from leeches (Woo, 2003).

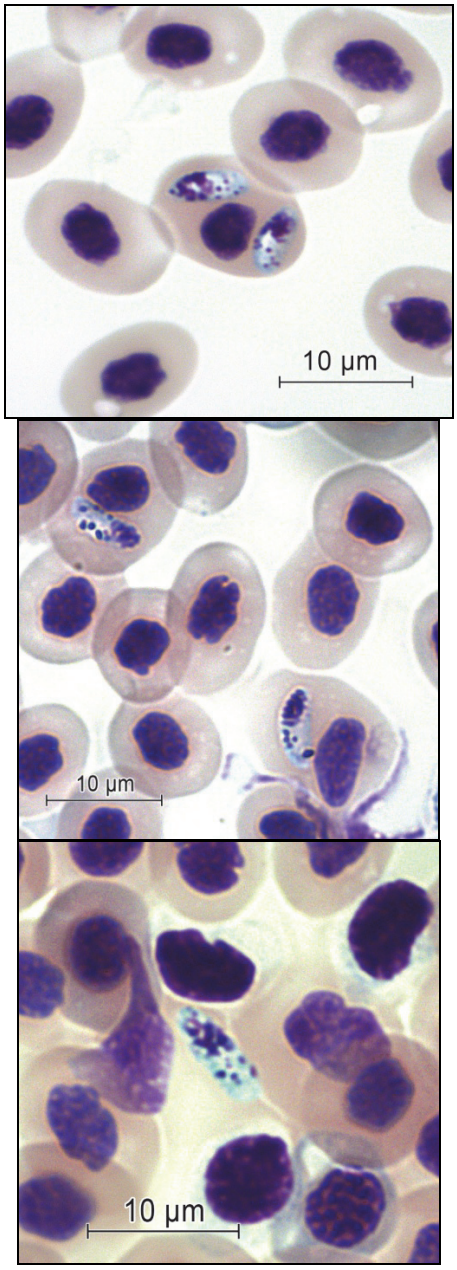

Fig. 2. Blood smears of Siberian sterlet with intra-erythrocytic *Haemogregarina acipenseris* (Nawrotzky, 1914)

Haemogregarina acipenseris was previously recorded only in sturgeon in the basin of the Caspian and the Black Seas. It was recorded in sterlet in the Volga and Danube (Perekropov, 1930; Baska, 1990), and also in Russian sturgeon and Persian sturgeon, and beluga from the

Lower Volga, Northern and Southern Caspian Sea (Ivanov, 1968; Pazooki & Masoumian, 2004). The sizes of *H. acipenseris* merozoites from Siberian sterlet coincide with equivalent parameters from Volga sterlet (Perekropov (1930), but significantly differ from merozoites from sturgeon (Pazooki & Masoumian, 2004): 6.5–8.2 × 2.2–3.0 µm compared to 4.0–5.0 × 1.5–3.0 µm. The identification of haemogregarine species found by Pazooki & Masoumian (2004) needs to be proved.

Fig. 3. *Crepidostomum auriculatum* (Wedl, 1858)

Perekropov (1930) thought that the entire life cycle of *H. acipenseris* takes place in the blood of sterlet. Shul'man (1954) doubted the reliability of this study, for he assumed that transmission of haemogregarines from one fish to another is not possible without participation of blood-sucking invertebrates. It seems that as a result of experimental studies, it was determined that haemogregarines of fish are transmitted by leeches of the Piscicolidae family (Khan, 1980; Woo, 2006). Carriers of *H. acipenseris* in the Lower Irtysh are *Piscicola geometra* leeches, which were found on sterlets` pharyngeal arches and fins.

The most abundant helmiths of Siberian sterlet in the Lower Irtysh basin were *C. auriculatum* trematode and *C. ovotrichura* nematode, both specific to sturgeon. It should be mentioned that *C. ovotrichura* in the Irtysh basin were recorded earlier only in the Zaysan Lake (Zahvatkin, 1938; Dobrohotova, 1960). The distribution of these parasites coincides with the range of sturgeon (Skryabina, 1974; Appy & Anderson, 1982). Molecular-genetic data do not prove that *C. auriculatum* belongs to the *Crepidostomum* (Braun, 1900) genus (Atopkin & Shedko, 2014; Soldanova et al., 2017). The genus status of this parasite requires confirmation. Their life cycle is still incompletely studied. Presumably, the intermediary hosts for these species (the second for *C. auriculatum* and the only one for *C. ovotrichura*) are benthos invertebrates, particularly Gammaridae and mayfly larvae (Caira, 1989; Moravec, 1994). The Tobol River is a tributary of the Irtysh, there are both artificial and natural barriers between them, which limits the freedom of movement of fish between the water currents. The differences in the dominance of *Crepidostomum auriculatum* and *Capillospirura ovotrichura* in the Tobol and Irtysh are, perhaps, related to the intensity of consumption of the abovementioned components of the zoobenthos.

It is interesting that without an account of the abovementioned local differences, the extent of sterlet infestation with *C. auriculatum* in the Lower Irtysh was practically similar to that recorded by Petrushevskij et al. (1948) for this host in the region over 70 years ago (Table 2). Anderson (1982) demonstrated that a high number of the intermediary host when there is a decrease in the number of the final host leads to higher resistance of the "host – parasite" system than at increase in the number of the latter. And, if a higher number of parasite individuals concentrate in a small number of host individuals, then it is enough for survival of the parasites` population due to the larva forms which live in intermediary hosts (Anderson & May, 1978; May & Anderson, 1978).

Metacercariae of *Diplostomum chromatophorum* trematodes were recorded in Siberian sterlet for the first time. Infestation with this common and low-specific parasite was insignificant and causes no great damage to fish (Marcogliese et al., 2001; Voutilainen et al., 2008).

According to the literature data, sterlet in the Ob-Irtysh basin were found to host 11 species of parasites (Table 2), of which, 7 species were not observed by us : *Hexamita truttae* (Schmidt, 1920), *Trichodina domerguei* (Wallengren, 1897), *Trichodina carassii* (Dogiel, 1940), *Diclybothrium armatum* (Leuckart, 1835), *Diplostomum spathaceum* (Rudolphi, 1819), *Truttaedacnitis clitellarius* (Ward & Magath, 1917), *Cystidicoloides ephemeridarum* (von Linstow, 1872) (Moravec, 1981).

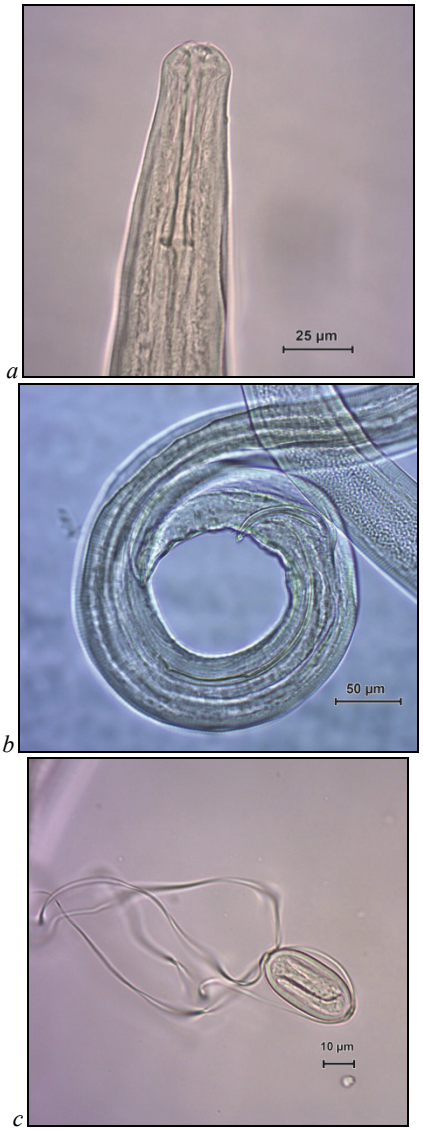

Fig. 4. *Capillospirura ovotrichura* (Skrjabin, 1924):
a – head end, *b* – back end of male, *c* – egg

We would like to emphasise the rarity of *Diclybothrium armatum* monogenea in the Siberian sterlet, the parasite being common in other sturgeon species, including the nominative subspecies of sterlet (Zahvatkin, 1938; Volkova, 1941; Petrushevskij et al., 1948; Bauer, 1948, 1959; Shul'man, 1954; Skryabina, 1974). Shul'man (1954) suggests the presence of several mechanisms, either physiological or biochemical, and an ecological peculiarity of the Siberian sterlet subspecies, which prevent infestation with *D. armatum*. This aspect should be studied further.

The species composition of non-specific parasites which occur in sturgeon depends on the local ecological conditions and differs in each particular water body. In water bodies of Siberia (Ob, Yenisei, Lena), sturgeon become infested with species typical for northern fish: Salmonidae, Coregonus and burbot (Shul'man, 1954). This was proved by our

discovery of the acanthocephalan *E. cinctulus*. This parasite was recorded for the first time in sterlet of the Ob-Irtysh basin.

Table 2
Species composition of parasites of sterlet in the rivers of Siberia and the extensivity of invasion (%)

Parasitofauna	Yenisei Basin (Bauer, 1948; Skryabina, 1974[1])	R. Irtush (Petrushevskij et al., 1948)	Lake Zaysan and the Black Irtush (Zahvatkin, 1938; Dobrohotova, 1960)	R. Ob (Titova, 1965; Razmashkin, 1976[2])	Lower Irtysh (our own research)
	Number of researched specimens of sterlet				
	96 and 2[1]	40	4	148 and 5[2]	85
Hexamita truttae	–	20.0	–	–	–
Cryptobia acipenseris	7.7–33.3	–	–	–	3.5
Haemogregarina acipenseris	–	–	–	–	14.1
Trichodina domerguei	–	6.6	–	–	
Trichodina carassii	–	13.2	–	–	–
Trichodina sp.					32.9
Diclybothrium armatum	*	*	*	–	–
Amphilina foliacea	20.0–92.4	–	–	–	–
Proteocephalus sp.	–	–	–	–	*
Cyathocephalus truncates	7.7–33.3	–	–	–	–
Diplostomum chomatophorum mtc	–	–	–	–	5.9
Diplostomum spathaceum	–	–	–	*[2]	–
Crepidostomum auriculatum	30.8–100.0	33.0	*	10.0–27.0	32.9
Capillospirura ovotrichuria	20.0–53.0	–	*	–	15.3
Truttaedacnitis clitellarius	15.4	–	–	40.0	–
Cystidicoloides ephemeridarum	–	–	–	15.0	–
Echinorhynchus cinctulus	6.6–23.1	–	–	–	*
Echinorhynchus salmonis	*[1]	–	–	–	–
Piscicola geometra	6.6–26.6	–	–	–	10.6
Ergasilus sieboldi	–	–	–	–	*
Unionidae gen. sp.	7.0	–	–	–	*
Total number of species	11	4	3	4	11

Note: * – single specimens of the parasite found.

The total number of species recorded for the Siberian sterlet in the Ob-Irtysh basin was higher than that for sterlet from the Yenisei: 18 and 11 respectively (Table 2). The species found in fish of two basins were the following: *Cryptobia acipenseris*, *Diclybothrium armatum*, *Crepidostomum auriculatum*, *Capillospirura ovotrichuria*, *Truttaedacnitis clitellarius*, *Echinorhynchus cinctulus*, *Piscicola geometra*, Unionidae gen. sp. To a large extent, the interbasin parasitological differences are related to the lower extent of study of parasitofauna of sterlet in the Yenisei. However, the absence of *Amphilina foliacea*, which is parasite specific to sturgeon, in the Ob-Irtysh basin, and the high infestation with this species in the Yenisei, and also its presence in Siberian sturgeon in the Ob-Irtysh basin indicates that there are other factors.

In the water bodies of Siberia, the species composition of parasites of the Siberian sterlet is significantly poor compared to that of sterlet in the Volga-Caspian basin, where the species is recorded as hosting 44 species of parasites, 20 of which are specific to sturgeon (Kazarnikova & Shestakovskaya, 2006).

Conclusion

During the summer of 2017, *Acipenser ruthenus marsiglii* in the Lower Irtysh basin was found to host 11 species of parasites, the most abundant of which are specific parasites of sturgeon: the trematode *Crepidostomum auriculatum* and the nematode *Capillospirura ovotrichura*. Compared to the data obtained for this region over 70 years ago (Petrushevskij et al., 1948), infestation of sterlet with *Crepidostomum auriculatum* almost has not changed, and blood parasites *Cryptobia acipenseris* and *Haemogregarina acipenseris* were recorded in the Ob-Irtysh basin for the first time.

The article was prepared with financial support of the Federal Agency of Scientific Organizations of Russia in the scope of the topic of fundamental scientific research R&D No AAAA-A17-117041910049-9 "Biodiversity of parasitic communities among the fish population of the Lower Irtysh and species interaction between them".

References

Akbulut, B., Feledi, T., Lengyel, S., & Ronyai, A. (2013). Effect of feeding rate on growth performance, food utilization and meat yield of sterlet (*Acipenser ruthenus* Linne, 1758). Journal of Fisheries Sciences, 7(3), 216–224.

Anderson, R. M., & Gordon, D. M. (1982). Processes influencing the distribution of parasite numbers within host populations with special emphasis on parasite-induced host mortalities Parasitology, 85(2), 373–398.

Anderson, R. M., & May, R. M. (1978). Regulation and stability of host-parasite population interactions: I. Regulatory Processes Journal of Animal Ecology, 47(1), 219–247.

Appy, R. G., & Anderson, R. C. (1982). The genus *Capillospirura* Skrjabin, 1924 (Nematoda: Cystidicolidae) of sturgeons. Canadian Journal of Zoology, 60(2), 194–202.

Appy, R. G., & Anderson, R. C. (1982). The genus *Capillospirura* Skrjabin, 1924 (Nematoda: Cystidicolidae) of sturgeons. Canadian Journal of Zoology, 60(2), 194–202.

Atopkin, D. M., & Shedko, M. B. (2014). Genetic characterization of far eastern species of the genus *Crepidostomum* (Trematoda: Allocreadiidae) by means of ^{28}S ribosomal DNA sequences. Advances in Bioscience and Biotechnology, 5, 209–215.

Baska, F. (1990). *Chloromyxum inexpectatum* n. sp. and *Sphaerospora colomani* n. sp. (Myxozoa: Myxosporea) parasites of the urinary system of the sterlet, *Acipenser ruthenus* L. Systematic parasitology, 16, 185–193.

Bauer, O. N. (1948). Parazity ryb r. Enisej [Fish parasites of the Yenisei River]. Izvestiya VNIORH, 27, 97–157 (in Russian).

Bauer, O. N. (1959). Biologiya *Diclybothrium armatum* Leuckart (Monogenoidea) – parazita osetrovyh ryb [Biology of *Diclybothrium armatum* Leuckart (Monogenoidea) – sturgeon parasite]. Voprosy Ekologii, 3, 142–153 (in Russian).

Bauer, O. N., Pugachev, O. N., & Voronin, V. N. (2002). Study of parasites and diseases of sturgeons in Russia: A review. Journal of Applied Ichthyology, 18, 420–429.

Bush, A. O., Lafferty, K. D., Lotz, J. M., & Shostak, A. W. (1997). Parasitology meets ecology on its own terms: Margolis et al. revisited. Journal of Parasitology, 83(4), 575–583.

Byhovskaya-Pavlovskaya, I. E. (1985). Parazity ryb. Rukovodstvo po izucheniyu [Fish parasites. Study Guide]. Nauka, Leningrad (in Russian).

Caira, J. N. (1989). A revision of the North American papillose Allocreadiidae (Digenea) with independent cladistic analyses of larvaland adult forms. Bulletin of the University of Nebraska State Museum, 11, 1–58.

Cakic, P., Djikanovic, V., Kulisic, Z., Paunovic, M., Jakovčev-Todorovic, D., & Milosevic, S. (2008). The fauna of endoparasite fauna in *Acipenser ruthenus* Linneaus 1758 from the Serbian part of the Danube River. Archives of Biological Sciences, 60(1), 103–107.

Choudhury, A., & Dick, T. A. (2001). Sturgeons (Chondrostei: Acipenseridae) and their metazoan parasites: Patterns and processes in historical biogeography. Journal of Biogeography, 28, 1411–1439.

Dobrohotova, O. V. (1960). Parazity ryb oz. Zajsan [Fish parasites of the lake Zaisan]. Trudy Instituta Zoologii Kazahskoj SSR, 14, 109–127 (in Russian).

Dubinin, V. B. (1952). Parazitofauna molodi osetrovyh ryb Nizhnej Volgi [Parasitofauna of juvenile sturgeon fish of the Lower Volga]. Uchenye Zapiski LGU. Seriya Biologicheskie Nauki, 141, 238–251 (in Russian).

Fedotkina, S. N., & Shinkarenko, A. N. (2015). Vopros izucheniya gel'mintofauny sterlyadi vodoemov Volgogradskoj oblasti [The study of the helminthofauna of sterlet reservoirs in the Volgograd Region]. Teoriya i Praktika Parazitarnyh Boleznej Zhivotnyh, 16, 453–455 (in Russian).

George, T., & McCabe, J. (1993). Prevalence of the parasite *Cystoopsis acipenseri* (Nematoda) in juvenile white sturgeons in the Lower Columbia River. Journal of Aqualic Animal Health, 5, 313–316.

Guénette, S., Rassart, E., & Fortin, R. (1992). Morphological differentiation of Lake Sturgeon (*Acipenser fulvescens*) from the St. Lawrence River and Lac des Deux Montagnes (Quebec, Canada). Canadian Journal of Fisheries and Aquatic Sciences, 49(9), 1959–1965.

Israel, J. A., & May, B. (2010). Indirect genetic estimates of breeding population size in the polyploid green sturgeon (*Acipenser medirostris*). Molecular Ecology, 19, 1058–1070.

Ivanov, V. P. (1968). Parazitofauna osetrovyh ryb pri estestvennom i iskusstvennom ih vosproizvodstve v izmennenoj Volge [Parasitofauna of sturgeon fishes with natural and artificial reproduction in the changed Volga]. Volgograd (in Russian).

Izyumova, N. A. (1977). Parazitofauna ryb vodohranilishch SSSR i puti ee formirovaniya [Parasitofauna of fish in reservoirs of the USSR and ways of its formation]. Nauka, Leningrad (in Russian).

Kazarnikova, A. V., & Shestakovskaya, E. V. (2006). Sravnitel'nyj analiz fauny parazitov osetrovyh ryb Azovskogo i Kaspijskogo bassejnov. Ehkosistemnye issledovaniya sredy i bioty Azovskogo moria [Comparative analysis of fauna of parasites of sturgeon fish of the Azov and Caspian basins. Ecosystem research of the environment and biota of the Sea of Azov]. MMBI RAN, YUNC RAN, Murmansk, Apatity. Pp. 252–263 (in Russian).

Khan, R. A. (1980). The leech as a vector of a fish piroplasm. Canadian Journal of Zoology, 58(9), 1631–1637.

Lenhardt, M., Jarić, I., Cakić, P., Cvijanović, G., Gačić, Z., & Kolarević, J. (2009). Seasonal changes in condition, hepatosomatic index and parasitism in sterlet (*Acipenser ruthenus* L.). Turkish Journal of Veterinary and Animal Sciences, 33(3), 209–214.

Liberman, E. L. (2017). Analiz linejno-vesovyh pokazatelej i meristicheskih priznakov sibirskoj sterlyadi *Acipenser ruthenus marsiglii* (Brandt, 1833) bassejna reki Irtysh [Analysis of linear-weight indicators and meristic characters of the siberian sterlet *Acipenser ruthenus marsiglii* (Brandt, 1833) in the Irtish river basin]. Vestnik AGTU, 64, 83–89 (in Russian).

Lyubarskaya, O. D., & Lavrent'eva, Y. I. (1985). Parazitofauna sterlyadi Srednej Volgi i Kujbyshevskogo vodohranilishcha [The parasitofauna of the sterlet of the Middle Volga and the Kuibyshev reservoir]. Parazitologiya, 19(4), 320–323 (in Russian).

Marcogliese, D. J., Dumont, P., Gendron, A. D., Mailhot, Y., Bergeron, E., & McLaughlin, J. D. (2001). Spatial and temporal variation in abundance of *Diplostomum* spp. in walleye (*Stizostedion vitreum*) and white suckers (*Catostomus commersoni*) from the St. Lawrence River. Canadian Journal of Zoology, 79(3), 355–369.

May, R. M., & Anderson, R. M. (1978). Regulation and stability of host-parasite population interactions: II. Destabilizing Processes Anderson Journal of Animal Ecology, 47(1), 249–267.

Moravec, F. (2013). Parasitic nematodes of freshwater fishes of Europe. Academia, Praha.

Opredelitel' parazitov presnovodnyh ryb fauny SSSR (1984). Paraziticheskie prostejshie [The determinant of parasites of freshwater fish of the USSR (1984). Parasitic Protozoa]. Nauka, Leningrad. Vol. 1 (in Russian).

Opredelitel' parazitov presnovodnyh ryb fauny SSSR (1987). Paraziticheskie mnogokletochnye [The determinant of parasites of freshwater fish fauna of the USSR. Parasitic multicellular]. Nauka, Leningrad. Vol. 3 (in Russian).

Pazooki, J., & Masoumian, M. (2004). *Cryptobia acipenseris* and *Haemogregarina acipenseris* infections in *Acipenser guldenstadti* and *A. persicus* in the southern part of the Caspian Sea. Journal of Agricultural Science and Technology, 6, 95–101.

Perekropov, T. I. (1930). *Haemogregarinen beim* Wolga und Kama Sterlet (*Acipenser ruthensis*). Zentralblatt für Bakteriologia, 80, 253–259.

Petrushevskij, G. K., Mosevich, M. V., & Shchupakov, I. G. (1948). Fauna parazitov Obi i Irtysha [Fauna of the parasites of the Ob and the Irtysh]. Izvestiya VNIORH, 27, 67–97 (in Russian).

Razmashkin, D. A. (1976). O lichinkah trematod, parazitiruyushchih u ryb vodoemov Ob'-Irtyshskogo bassejna. Bolezni i parazity ryb Ledovitomorskoj provincii (v predelah SSSR) [On the larvae of trematodes parasitizing fish of the reservoirs of the Ob-Irtysh basin. Diseases and parasites of fish from the Arctic Ocean (within the USSR)]. Sverdlovsk. Pp. 80–103 (in Russian).

Sepúlveda, M. S., Stefanavage, T., & Goforth, R. (2010). First record of a *Polypodium* sp. parasitizing eggs of Shovelnose Sturgeon from the Wabash River, Indiana. Journal of Aquatic Animal Health, 22, 36–38.

Shul'man, S. S. (1954). Obzor fauny parazitov osetrovyh ryb [Overview of fauna of parasites of sturgeon]. Zoologicheskij Zhurnal, 33(1), 190–254 (in Russian).

Skryabina, E. S. (1974). Gel'minty osetrovyh ryb (Acipenseridae Bonaparte, 1831) [Helminths of sturgeon fishes (Acipenseridee Bonaparte, 1831)]. Nauka, Moscow (in Russian).

Soldanova, M., Georgieva, S., Rohacova, J., Knudsen, R., Kuhn, J. A., Henriksen, E. H., Siwertsson, A., Shaw, J. C., Kuris, A. M., Amundsen, P. A., Scholz, T., Lafferty, K. D., & Kostadinova, A. (2017). Molecular analyses reveal high species diversity of trematodes in a sub-Arctic lake. International Journal for Parasitology, 47, 327–345.

Strel'nikova, A. P. (2012). Feeding of juvenile sterlet (*Acipenser ruthenus*, Acipenseridae) in the Danube River midstream. Journal of Ichthyology, 52(1), 85–90.

Titova, S. D. (1965). Parazity ryb Zapadnoj Sibiri [Fish parasites of Western Siberia]. Izdatel'stvo Tomskogo Universiteta, Tomsk (in Russian).

Vasil'ev, V. P., Rachek, E. I., Lebedeva, E. B., & Vasil'eva, E. D. (2014). Karyological study in backcross hybrids between the sterlet, *Acipenser ruthenus*, and kaluga, *A. dauricus* (Actinopterygii: Acipenseriformes: Acipenseridae): *A. ruthenus* × (*A. ruthenus* × *A. dauricus*) and *A. dauricus* × (*A. ruthenus* × *A. dauricus*). Acta Ichthyologica et Piscatoria, 44(4), 301–308.

Volkova, M. M. (1941). Parazitofauna ryb bassejna r. Obi [Parasitofauna of fish in the Ob River Basin]. Uchenye Zapiski LGU, 74(18), 20–36 (in Russian).

Voutilainen, A., Figueiredo, K., & Huuskonen, H. (2008). Effects of the eye fluke *Diplostomum spathaceum* on the energetics and feeding of Arctic charr *Salvelinus alpines*. Journal of Fish Biology, 73(9), 2228–2237.

Woo, P. T. K. (2003). *Cryptobia* (*Trypanoplasma*) *salmositica* and salmonid cryptobiosis. Journal of Fish Diseases, 26, 627–646.

Woo, P. T. K. (2006). Fish diseases and disorders. Protozoan and Metazoan infections. CABI, 1, 191–194.

Wuertz, S., Reiser, S., Gessner, J., & Kirschbaum, F. (2011). Morphological distinction between juvenile stages of the european sturgeon *Acipenser sturio* and the atlantic sturgeon *Acipenser oxyrinchus*. Biology and Conservation of the European Sturgeon *Acipenser sturio* L. 1758. Pp. 53–64.

Zahvatkin, V. A. (1938). Parazitofauna ryb oz. Zajsan i r. Chernogo Irtysha [Parasitofauna of fish of the Lake. Zaisan and the river. Black Irtysh]. Uchenye Zapiski Permskogo Universiteta, 3(2), 193–249 (in Russian).

Zhuravlev, V. B. (2000). K voprosu o taksonomicheskom statuse sterlyadi *Acipenser ruthenus* reki Obi [On the question of the taxonomic status of the sterlet *Acipenser ruthenus* of the Ob River]. Izvestiya Altajskogo Gosudarstvennogo Universiteta, 3, 77–88 (in Russian).

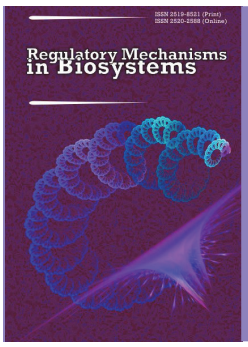

Regulatory Mechanisms in Biosystems

ISSN 2519-8521 (Print)
ISSN 2520-2588 (Online)
Regul. Mech. Biosyst., 9(3), 335–339
doi: 10.15421/021849

Methods for increasing the accuracy of recording the parameters of the cardiovascular system in double-beam photoplethysmography

Y. M. Snizhko, O. O. Boiko, N. P. Botsva, D. V. Chernetchenko, M. M. Milyh

Oles Honchar Dnipro National University, Dnipro, Ukraine

Article info

Received 12.06.2018
Received in revised form 20.07.2018
Accepted 24.07.2018

Oles Honchar Dnipro National University, Gagarin ave., 72, Dnipro, 49010, Ukraine.
Tel.: +38-056-373-12-63.
E-mail: nbotsva@gmail.com

Snizhko, Y. M., Boiko, O. O., Botsva, N. P., Chernetchenko, D. V., & Milyh, M. M. (2018). Methods for increasing the accuracy of recording the parameters of the cardiovascular system in double-beam photoplethysmography. Regulatory Mechanisms in Biosystems, 9(3), 335–339. doi:10.15421/021849

Photoplethysmography has recently become more widespread among non-invasive methods for obtaining information on the state of physiological systems of the human body. Serial photoplethysmographs are intended for use in clinics and require special care, therefore, interest in portable media developed on the basis of modern sensors and microcontrollers is growing, which would not only make this method available for individual use, but also expand its capabilities through the use of light of various spectral ranges. Such devices require modified signal processing techniques that allow them to be used in mobile applications. The aim of the work is to develop methods for processing signals from a modern two-beam sensor operating in the red and infrared ranges for the analysis of photoplethysmography on a mobile device (smartphone or tablet). A device using the microcontroller and radio module in the Bluetooth standard allows you to continuously record pulse waves, determine the level of oxygen in the blood, calculate peak-peak intervals and heart rate. The use of the two-beam sensor for registration and the implementation of the developed signal processing methods in the Android operation system application increase the accuracy of setting the maximums on pulse curve and provide a relative error in determining the heart rate and pulse-to-pulse intervals relative to the certified electrocardiograph at 9.2% and 9.6% respectively, with an average level of interference and an average activity. An Android operation system mobile device (tablet, smartphone) allows you to visualize the measurement results, store data in the internal memory, and transfer them to the server for further processing.

Keywords: photoplethysmography; absorption spectra; pulse oximetry; photoplethysmography analysis; oxygenation; continuous registration of oxygen saturation in peripheral vessels.

Introduction

Photoplethysmography is a method for recording the optical density of tissue using a photoelectric plethysmograph. It is used to study the individual properties of regional blood circulation, the spectral properties of blood flowing through the investigated area of the body. Recently, single-beam and two-beam photoplethysmography have been widely used to determine a number of parameters of the cardiovascular system, in particular, the frequency of breathing, the heart rate, the duration of pulse-to-pulse intervals. The method of pulse oximetry, which is used in birefringence photoplethysmography, also determines the level of oxygen in the blood.

The assessment of respiratory rate, which is an important indicator for ambulatory care, can be done in real time with a signal from a portable one-beam pulse oximeter (Karlen et al., 2011; Lin et al., 2017). In this case, the definition of respiration frequency according to photoplethysmography is more reliable and has a lower error than the electrocardiography signal.

As a contactless method for determining the heart rate, photoplethysmography with a camera, is used for recording the instantaneous pulsations in the change in face skin colour during the cardiovascular wave, invisible to the eye, but measured during video recording (Aarts et al., 2013; Alghoul et al., 2017).

The variability of heart rhythm is widely used for early diagnosis of cardiovascular diseases and the evaluation of the functions of the autonomic nervous system (Bulvestre et al., 2013; Cygankiewicz et al., 2015; Goldkorn et al., 2015). The predictive value of heart rate variability has been demonstrated by numerous studies in recent years (Al-Zaiti et al., 2014; O'Neal et al., 2016; Botswa et al., 2017). The signal from which both the time domain and the frequency domain of heart rate variability are measured requires an accurate determination of the interval between consecutive cardiac contractions (Blood et al., 2015; Ha et al., 2015). The classical method involves analysing the numerical R-R intervals for electrocardiogram signals which are obtained in a laboratory (Task Force, 1996; ChuDuc et al., 2013). However, certain methodological problems associated with the recording and analysis of electrocardiograms create a barrier to the collection of large amounts of data, which are necessary for a statistically reliable comparison of the status of various subjects.

Some authors have recently preferred an alternative method for analysing variability of heart rhythm – instead of R-R intervals in the electrocardiogram, they are using time intervals between peak values in the photoplethysmography signal, which also reflects the heart rate, since the mechanical activity of the heart is related to its electrical activity (Schäfer & Vagedes, 2013; Kavsaoğlu et al., 2016). In this case, in place of an electrocardiogram a portable photoplethysmograph is used, which operates on an optical pulse oximeter based on a smartphone or similar portable device and can serve as the basis for a new tool for screening heart rate variability indices in a nonclinical environment (Dehkordi et al., 2016; Orphanidou, 2017). A similar system typically has a photosensor on the finger for measuring the intensity of reflection, after which the signal is selected, filtered, processed and sent via a wireless channel for further processing. The system is often used on the wrist in the cuffs to make it wearable and easy to wear (Sudin et al., 2015).

The analysis shows a high level of agreement between the peak-peak intervals obtained from an electrocardiogram and photoplethysmography (Weinschenk et al., 2016), that's why the changes in pulse rate which are determined by the photoplethysmography can be used instead of variability of heart rhythm, for a more complete evaluation of the autonomic nervous system's functions. Numerous studies suggest that photoplethysmography using pulse oximetery as a simple non-invasive method for determining the interval between successive heart contractions and the calculation of heart rate variability is more practical and reliable not only in ideal conditions for healthy subjects (Lu et al., 2009; Karlen et al., 2011; Chen et al., 2015), but also for elderly patients (Chuang et al., 2015), in non-stationary conditions (Gil et al., 2010) and in conditions of motion (Sudin et al., 2015). Such a system allows for an approximation sufficient for analyses of the temporal and frequency regions of the heart rate variability, which creates conditions for studying of heart rate variability by the photoplethysmography signal for a large number of subjects in cardiological and psychophysiological studies (Heathers, 2013), e.g. in the interpretation of emotions (Alghoul et al., 2017; Costa et al., 2018) and for the care of certain groups of patients with electrocardiogram's artefacts.

However, during the analysis it should be borne in mind that the changes in the photoplethysmography signal have some delay in time with respect to the electrocardiogram signal, which is needed for passing the wave (Selvaraj et al., 2008). In addition, physical activity and some psychological stressors decrease correlation level between the values of heart rate for photoplethysmography and heart rate variability (Schäfer & Vagedes, 2013) as a result of changes during stressful loadings of heart rate variability parameters (Lin et al., 2014). Moreover, the effect of the breathing process also has an influence. Recently, for eliminating the influence the frequency of breathing on photoplethysmography, a new method has been proposed for patients wearing sensors (Orphanidou, 2017), but for determination of more accurate values of R-R intervals it is recommended to use the registration of photoplethysmography and electrocardiogram at the same time.

Some researchers pay attention to the fact that the heart rate variability analysis by photoplethysmography signal which is taken from wearable sensors makes the influence of noise and trends more powerful, which is why for achieving more reliable results of photoplethysmography analysis, decreasing of effect of this artefact and creating more accurate determination methods are very important tasks (Alian & Shelley, 2014). This adds to the relevance of research into finding hardware and software methods for making more accurate recording of the photoplethysmography signal and for improving the obtaining of necessary parameters for subsequent processing.

Recently a reliable algorithm was created for fast online evaluation of the quality of the photoplethysmographic signals, which has the advantage of being used in mobile devices with low technical power (Pflugradt et al., 2015). For removing the influence of artefacts of physical motion on the results of analysis of photoplethysmography from wearable devices, a suggestion was made for recording at the same time the signal from an accelerometer with following filtration and processing methods of spectral analysis (Han & Kim, 2012; Islam et al., 2017). It has been established that the trends of photoplethysmographic signals which occur in the low frequency range are changed during the spectral analysis, that's why they must be removed using methods of filtrations in the primary processing before starting analysis of heart rate variability (Akdemir et al., 2013). For assessing respiratory rate using the method of single-beam photoplethysmography, the algorithm which is based on Wavelet transform is very appropriate.

Among the software for the processing of signals of photoplethysmography, also it should be noted that new algorithms for the allocation of peaks in the photoplethysmography signal are based on the median method (Firoozabadi et al., 2017) and the adaptive segmentation method (Kavsaoğlu et al., 2016). The latter, according to the authors, allows you to correctly determine peaks from photoplethysmographic signals at rest even without pre-processing.

Thus, in the meantime, the interest of researchers in the registration and processing of photoplethysmography with wearable sensors based on simple mobile devices is increasing. Available hardware-software and processing algorithms allow one to perform the initial signal processing and improve its quality at the stage of preparation for the analysis of single-beam photoplethysmography. However, in the literature there is not enough information on the algorithms for improving the quality of the processing of the results of two-beam photoplethysmography. The aim of the research presented in this article is the development of methods for processing signals from a modern two-beam sensor, which work in red and infrared ranges for the analysis of photoplethysmography on a mobile device (smartphone or tablet).

Materials and methods

For registration of parameters of the cardiovascular system by the method of two-beam photoplethysmography, a device was created which contains two light-emitting diodes in a sensor, the first one is red, the second one is infrared (Fig. 1). The light-emitting diodes alternately emit pulse wavelengths of 680 nm (RED) and 950 nm (IR). After reflection from biological tissues which contain blood vessels, these pulses are recorded by a photodetector, converted into a digital signal and sent to a microcontroller. The microcontroller manages the sensor, performs the initial processing of the received signal and sends it for further processing to a mobile device which uses the operation system of Android. Transmission of processing results to a phone or tablet is made by wireless Bluetooth at a distance of up to 5 m. The main processing of signals is carried out on the microcontroller, visualization and storage of results on a mobile device. This allows one to collect a lot of data from many experiments for further analysis. The developed device allows one to register the signal continuously for two hours.

The photoplethysmography is analysed using two algorithms: the first one can determine the level of oxygen saturation in peripheral vessels (SpO_2), the second one is the time value of systolic peaks which is needed for calculation of pulse-to-pulse intervals and heart rate.

The algorithm for determining the level of oxygen in the blood is based on the dependence of the absorption coefficient of light by different states of hemoglobin from the light-emitting diode wavelength: at a wavelength of 660 nm (RED), hemoglobin is absorbed about 10 times more than oxyhemoglobin and at a wavelength of 940 nm (IR) the absorption of oxyhemoglobin is more than hemoglobin (Fig. 2).

For non-invasive determination of the level of oxygen saturation in human blood, the sensor is placed next to the portion of the tissue which contains arterial vessels. Under these conditions, the level of the signal from the sensor is proportional to the absorption of light in the tissues and due to the presence of arterial blood circulation has two component's the constant (A_{DC}) and the variable (A_{AC}) (Fig. 3).

Signal valuation is used to increase the accuracy of the determination of saturation by pulse oximetry. The normalized signal S for each of the two wavelengths is defined as the ratio of the variable component of the corresponding A_{AC} signal to the constant component of the A_{DC}, which are measured at the time of diastole,

$$S = A_{AC} / A_{DC}.$$

Normed signals S_{RED} and S_{IR} do not depend on the intensity of light from light-emitting diodes, but are determined only by optical properties of living tissue (Fig. 4). By their values, the ratio R is calculated

$$R = S_{RED} / S_{IR}.$$

The value of R is related to the definition of SpO_2 saturation by empirical dependence

$$SpO_2 = a - b \cdot R,$$

where a, b are coefficients determined empirically during calibration depending on the certificated device (Kalakutskij & Manelis, 1999). In this case, following the calibration of the Heaco CMS50C "Pulse Oximeter" certified device, the following coefficients are set: a = 109.0, b = 11.3. The value of R varies from 0.8 for 100% saturation and 9.6 for 0% saturation; 85% saturation corresponds to the value of R = 2.12.

The algorithm for detecting the peaks of systolic elevation on photoplethysmography is based on the principle of state machine, which is to monitor the state of the current signal value in time. This machine follows the loop of states, which allows us to separate parts of the photoplethysmography signal in real-time mode into five parts and research each of them individually (Fig. 5).

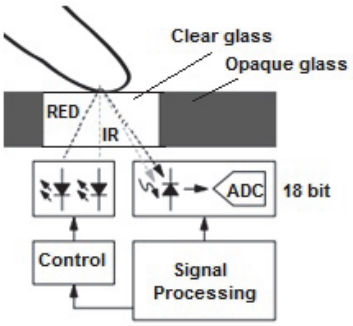

Fig. 1. Scheme of registration of photoplethysmography based on the sensor that works on the principle of reflection of light from tissues

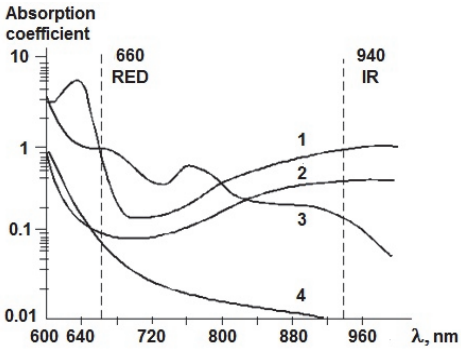

Fig. 2. Dependence of the absorption coefficient of light in different forms hemoglobin on the wavelength λ of radiation: *1* – methemoglobin, *2* – oxyhemoglobin, *3* – hemoglobin, *4* – carboxyhemoglobin

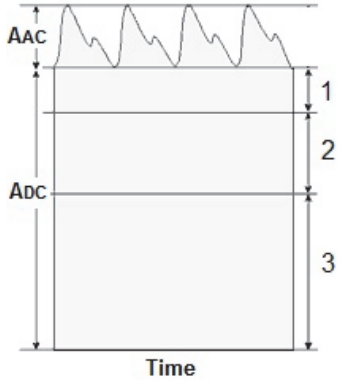

Fig. 3. Components of the signal from the sensor of the photoplethysmography: A_{AC} is a variable component, A_{DC} is a constant component: *1* – arterial blood, *2* – venous blood, *3* – tissue

The first state – STATE_INIT – is responsible for initializing and indicates the start of the algorithm.

The second state – STATE_WAITING – is responsible for adapting all required boundaries of the passage and seeing whether the transition to the next state has begun.

The third state – STATE_FOLLOWING_SLOPE – corresponds to the signal region where the systolic rise occurs and the transition to the next state, where the top of the systolic lift may be detected.

The fourth state – STATE_MAYBE_DETECTED – checks if the vertex of the systolic lift is actually recorded or the signal is still in state STATE_FOLLOWING_SLOPE. If the systolic peak is fixed, its time coordinate is stored in memory, and the algorithm goes to the next state.

The fifth state – STATE_MASKING – masks (holds) the algorithm's work for a while, after which it is re-executed.

The algorithms for determining the saturation level and the detection of peaks of photoplethysmography are developed and implemented in the Java programming language for the Android operating system. For further analysis of the cardiovascular system, according to the time coordinates of the systolic peaks, the programmed R-R intervals and heart rate are determined.

The table shows the general characteristics of a mobile device for the registration of two-beam photoplethysmography.

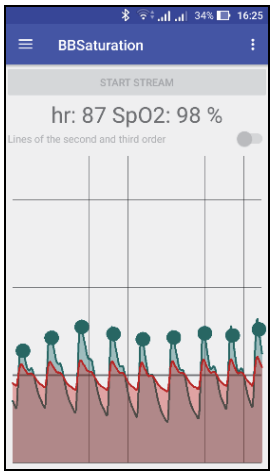

Fig. 4. View of the photoplethysmography on a mobile device: the lower signal wave corresponds to red (RED) range, and upper – to infrared (IR); the values of heart rate and saturation are calculated at the top

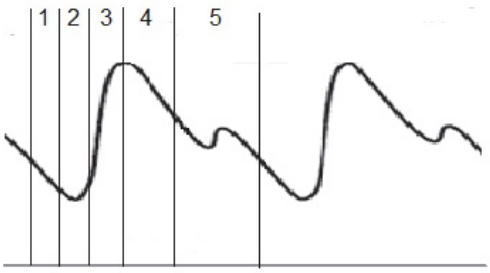

Fig. 5. The states of the algorithm for detecting the peaks of systolic lift on photoplethysmography

Table
General characteristics of the mobile device for photoplethysmography measurement

Parameter	Value
Sampling frequency, Hz	50
Duration of one measurement, min	2–3
Power supply, V	3.3 < U < 5.0
Battery capacity, mA/h	160
Dimensions, mm	60 x 35 x 10

Results

During the preliminary testing of the algorithm for detecting the peaks of systolic lift and determining the heart rate on a mobile device, along with the results similar to those shown in Figure 4, it was possible to observe cases of registration of peaks that looked false (Fig. 6).

The developed algorithm can be sufficiently precise and flexible in use. For checking and analysis of the developed systolic peak detection algorithm we performed research which determined peak-peak intervals and heart rate with mobile devices for photoplethysmography and compared this with results of R-R intervals which was determined by the certified electrocardiograph CONTEC8000GW ECG Workstation.

For the experiment we took nine volunteers aged from 20 to 40 without any disorders of the cardiovascular system. For each participant about 2–3 measurements were carried out with duration 2–3 minutes using both devices for registration of the appropriate intervals and heart rate. According to the results of each measurement, pairs of mean values of intervals and heart rate were determined (Fig. 7, 8).

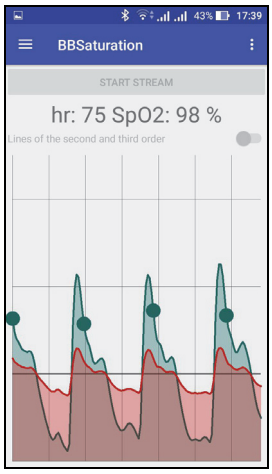

Fig. 6. Photoplethysmography with expectation interval relative to peak peak, where green dot is a peak of systolic lift

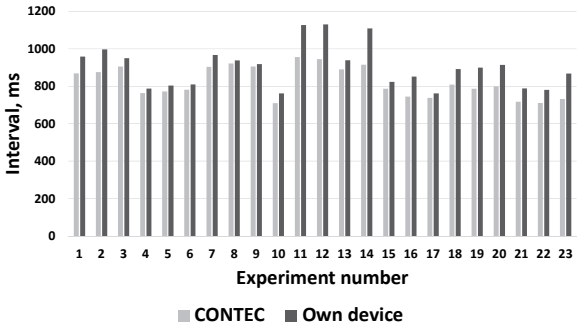

Fig. 7. Results of measurement of R-R intervals (light colour) and peak-peak intervals (dark colour) with two devices

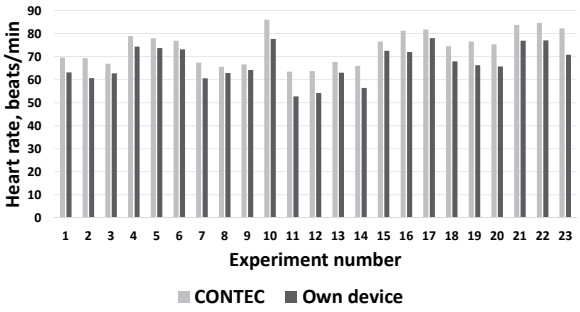

Fig. 8. Results of measurement of heart rate by two devices

Calculated from experimental data, the mean absolute and relative errors are respectively: for peak-peak intervals 79.7 ms and 9.6%, for heart rate 9.6 beats/min and 9.2%.

Discussion

However, it should be noted that precisely in the state where the peak of systolic lifting is detected, the algorithm provides protection against signal noise at the peaks of the wave. That is why in state STATE_MAYBE_DETECTED there is a so-called waiting interval, belonging to the current time coordinate and verified by the algorithm. If the conditions are true, this point is recorded as the peak of the systolic wave. Such a check is a significant advantage of the developed algorithm, which precisely increases its accuracy and allows one to perform the functions of determining peaks at any quality of the input signal of the photoplethysmography.

During the testing, certain weaknesses of the algorithm were also found. Firstly, the value of the waiting interval should be set depending on the quality of the output signal from the wearer. Secondly, the STATE_MASKING state duration value also needs an initial definition and is significantly dependent on the peak-peak intervals. However, this disadvantage is not critical, since such a duration is sufficient to set 1/4–1/6 of the average statistical value of the peak-peak interval. The obtained results confirm the conformity of the proposed methods of processing the signal of the photoplethysmography and the performance of the device as a whole. It is seen that the developed device does not have many differences in the determination of absolute values of parameters relative to the certified electrocardiograph, and it can be noted that all deviations are unidirectional. The relative error value is almost the same as the results of comparative studies comparing electrocardiography and photoplethysmography with a relative error of 10.3% (Orphanidou, 2017).

The existing discrepancies between the results for photoplethysmography and electrocardiogram may be due to the fact that comparisons of measurements were from instruments which are used for different objects and methods of research: the cardiograph records the electrical signals of the heart, and the photoplethysmograph analyses the cardiovascular system as a whole, whose state, in particular, depends on the state of vessels. Therefore, the results can be considered acceptable.

In general, the obtained results are in agreement with the results of other authors, which determine the possibility of substituting heart rate variability analysis for electrocardiogram signals by analysis of pulse variability according to the results of photoplethysmography, but at the same time emphasize the fact that the differences between these indicators can be caused by respiration, in particular respiratory delusions and rhythmic breathing (Chen et al., 2015). There are also some differences in the spectral values of heart rate variability and pulse wave changes, mainly in the area of high respiratory rates (Gil et al., 2010). Therefore, it is obvious that the influence of breathing on the accuracy of determining the parameters of the cardiovascular system for photoplethysmography requires further research.

Studies have shown that although the photoplethysmographic signals provides accurate data for analysing the parameters of heart rate variability in ideal conditions, it is less reliable due to its vulnerability to artefacts of movements (Lu & Yang, 2009). Along with this, it is believed that the pulse wave can be used as an electrocardiogram substitute for the analysis of heart rate variability in non-stationary conditions (Gil et al., 2010).

The development of tools for modelling realistic photoplethysmographic signals for the development and testing of photoplethysmograph-specific arrhythmia detectors can also be considered promising, taking into account the lack of annotated public databases of photoplethysmograph with arrhythmias (Soloshenko et al., 2017).

Conclusion

We developed methods of analysis of photoplethysmographic signals with modes for determination of the level of oxygination and the setting of heart rate parameters on a mobile unit that contains a two-beam sensor with red and infrared light-emitting diodes, a microcontroller and a radio module in the Bluetooth standard. The device allows you to continuously record pulse waves, determine the level of oxygen saturation, peak-peak intervals and heart rate. The use of two-beam sensors for registration and implementation of developed signal processing methods in the Android operation system application allow one not only to calculate the saturation of blood but also to increase the accuracy of setting the maximum of the corresponding pulse curves and to provide a relative error in determining the heart rate and peak-peak intervals relative to a certified electrocardiograph at 9.2% and 9.6% with an average level of interference and average muscle activity. An Android operation system mobile device (tablet, smartphone) allows one to visualize the measurement results, store data in the internal memory, and transfer them to the server for further processing.

It is possible to use the device to determine other parameters associated with different physiological processes, such as breathing rate.

References

Aarts, L. A. M., Jeanne, V., Cleary, J. P., Lieber, C., Nelson, J. S., Bambang Oetomo, S., & Verkruysse, W. (2013). Non-contact heart rate monitoring

utilizing camera photoplethysmography in the neonatal intensive care unit – A pilot study. Early Human Development, 89(12), 943–948.
Akdemir Akar, S., Kara, S., Latifoğlu, F., & Bilgiç, V. (2013). Spectral analysis of photoplethysmographic signals: The importance of preprocessing. Biomedical Signal Processing and Control, 8(1), 16–22.
Alghoul, K., Alharthi, S., Al Osman, H., & El Saddik, A. (2017). Heart rate variability extraction from videos signals: ICA vs. EVM Comparison. IEEE Access, 5, 4711–4719.
Alian, A. A., & Shelley, K. H. (2014). Photoplethysmography. Best Practice and Research Clinical Anaesthesiology, 28(4), 395–406.
Al-Zaiti, S. S., Fllavollita, J. A., Canty, J. J. M., & Carey, M. G. (2014). Electrocardiographic predictors of sudden and non-sudden cardiac death in patients with ischemic cardiomyopathy. Heart and Lung: The Journal of Acute and Critical Care, 43(6), 527–533.
Blood, J. D., Wu, J., Chaplin, T. M., Hommer, R., Vazquez, L., Rutherford, H. J. V., Mayes, L. C., & Crowley, M. J. (2015). The variable heart: High frequency and very low frequency correlates of depressive symptoms in children and adolescents. Journal of Affective Disorders, 186, 119–126.
Botsva, N., Naishtetik, I., Khimion, L., & Chernetchenko, D. (2017). Predictors of aging based on the analysis of heart rate variability. Pacing and Clinical Electrophysiology, 40(11), 1269–1278.
Bulvestre, M., Leprêtre, P. M., & Ghannem, M. (2013). 243: Heart rate variability analysis could help to determine the ventilatory threshold in patients with heart failure. Archives of Cardiovascular Diseases Supplements, 5(1), 82.
Chen, X., Huang, Y. Y., Yun, F., Chen, T. J., & Li, J. (2015). Effect of changes in sympathovagal balance on the accuracy of heart rate variability obtained from photoplethysmography. Experimental and Therapeutic Medicine, 10(6), 2311–2318.
Chuang, C. C., Ye, J. J., Lin, W. C., Lee, K. T., & Tai, Y. T. (2015). Photoplethysmography variability as an alternative approach to obtain heart rate variability information in chronic pain patient. Journal of Clinical Monitoring and Computing, 29(6), 801–806.
ChuDuc, H., NguyenPhan, K., & NguyenViet, D. (2013). A review of heart rate variability and its applications. APCBEE Procedia, 7, 80–85.
Costa, A., Rincon, J. A., Carrascosa, C., Julian, V., & Novais, P. (2018). Emotions detection on an ambient intelligent system using wearable devices. Future Generation Computer Systems. In press.
Cygankiewicz, I., Corino, V., Vazquez, R., Bayes-Genis, A., Mainardi, L., Zareba, W., de Luna, A. B., & Platonov, P. G. (2015). Reduced irregularity of ventricular response during atrial fibrillation and long-term outcome in patients with heart failure. The American Journal of Cardiology, 116(7), 1071–1075.
Dehkordi, P., Garde, A., Karlen, W., Petersen, C. L., Wensley, D., Dumont, G. A., & Mark Ansermino, J. (2016). Evaluation of cardiac modulation in children in response to apnea/hypopnea using the Phone Oximeter TM. Physiological Measurement, 37(2), 187–202.
Firoozabadi, R., Helfenbein, E. D., & Babaeizadeh, S. (2017). Efficient noise-tolerant estimation of heart rate variability using single-channel photoplethysmography. Journal of Electrocardiology, 50(6), 841–846.
Gil, E., Orini, M., Bailón, R., Vergara, J. M., Mainardi, L., & Laguna, P. (2010). Photoplethysmography pulse rate variability as a surrogate measurement of heart rate variability during non-stationary conditions. Physiological Measurement, 31(9), 1271–1290.
Goldkorn, R., Naimushin, A., Shlomo, N., Dan, A., Oieru, D., Moalem, I., Rozen, E., Gur, I., Levitan, J., Rosenmann, D., Mogilewsky, Y., Klempfner, R., & Goldenberg, I. (2015). Comparison of the usefulness of heart rate variability versus exercise stress testing for the detection of myocardial ischemia in patients without known coronary Artery Disease. The American Journal of Cardiology, 115(11), 1518–1522.
Ha, J. H., Park, S., Yoon, D., & Kim, B. (2015). Short-term heart rate variability in older patients with newly diagnosed depression. Psychiatry Research, 226, 484–488.
Han, H., & Kim, J. (2012). Artifacts in wearable photoplethysmographs during daily life motions and their reduction with least mean square based active noise cancellation method. Computers in Biology and Medicine, 42(4), 387–393.
Heathers, J. A. J. (2013). Smartphone-enabled pulse rate variability: An alternative methodology for the collection of heart rate variability in psychophysiological research. International Journal of Psychophysiology, 89(3), 297–304.
Islam, M. T., Zabir, I., Ahamed, S. T., Yasar, M. T., Shahnaz, C., & Fattah, S. A. (2017). A time-frequency domain approach of heart rate estimation from photoplethysmographic (PPG) signal. Biomedical Signal Processing and Control, 36, 146–154.
Kalakutskij, L. I., & Manelis, J. S. (1999). Apparatura i metody klinicheskogo monitoringa [Apparatus and methods of clinical monitoring]. Samara State Aerospace University, Samara (in Russian).
Kavsaoğlu, A. R., Polat, K., & Bozkurt, M. R. (2016). An innovative peak detection algorithm for photoplethysmography signals: An adaptive segmentation method. Turkish Journal of Electrical Engineering and Computer Sciences, 24(3), 1792–1796.
Lin, F., Heffner, K., Mapstone, M., Chen, D.-G. (Din), & Porsteisson, A. (2014). Frequency of mentally stimulating activities modifies the relationship between cardiovascular reactivity and executive function in old age. The American Journal of Geriatric Psychiatry, 22(11), 1210–1221.
Lin, Y.-D., Chien, Y.-H., & Chen, Y.-S. (2017). Wavelet-based embedded algorithm for respiratory rate estimation from PPG signal. Biomedical Signal Processing and Control, 36, 138–145.
Lu, G., & Yang, F. (2009). Limitations of oximetry to measure heart rate variability measures. Cardiovascular Engineering, 9(3), 119–125.
Lu, G., Yang, F., Taylor, J. A., & Stein, J. F. (2009). A comparison of photoplethysmography and ECG recording to analyse heart rate variability in healthy subjects. Journal of Medical Engineering and Technology, 33(8), 634–641.
O'Neal, W. T., Chen, L. Y., Nazarian, S., & Soliman, E. Z. (2016). Reference ranges for short-term heart rate variability measures in individuals free of cardiovascular disease: The multi-ethnic study of atherosclerosis (MESA). Journal of Electrocardiology, 49(5), 686–690.
Orphanidou, C. (2017). Derivation of respiration rate from ambulatory ECG and PPG using ensemble empirical mode decomposition: Comparison and fusion. Computers in Biology and Medicine, 81, 45–54.
Pflugradt, M., Moeller, B., & Orglmeister, R. (2015). OPRA: A fast on-line signal quality estimator for pulsatile signals. IFAC-PapersOnLine, 48(20), 459–464.
Schäfer, A., & Vagedes, J. (2013). How accurate is pulse rate variability as an estimate of heart rate variability?: A review on studies comparing photoplethysmographic technology with an electrocardiogram. International Journal of Cardiology, 166(1), 15–29.
Selvaraj, N., Jaryal, A., Santhosh, J., Deepak, K. K., & Anand, S. (2008). Assessment of heart rate variability derived from finger-tip photoplethysmography as compared to electrocardiography. Journal of Medical Engineering and Technology, 32(6), 479–484.
Sološenko, A., Petrėnas, A., Marozas, V., & Sörnmo, L. (2017). Modeling of the photoplethysmogram during atrial fibrillation. Computers in Biology and Medicine, 81, 130–138.
Sudin, S., Aziz, F., Mohd Hishamuddin, N. A., Ahmad Saad, F. S., Md Shakaff, A. Y., Zakaria, A., & Salleh, A. F. (2015). Wearable heart rate monitor using photoplethysmography for motion. In: IECBES 2014, Conference Proceedings – 2014 IEEE Conference on Biomedical Engineering and Sciences. Pp. 1015–1018.
Task force of the European Society of Cardiology and the North American Society of Pacing and Electrophysiology. Heart rate variability. Standards of measurement, physiological interpretation and clinical use (1996). Circulation, 93, 1043–1065.
Verma, A., Cabrera, S., Mayorga, A., & Nazeran, H. (2013). A robust algorithm for derivation of heart rate variability spectra from ECG and PPG signals. In: Proceedings – 29th Southern Biomedical Engineering Conference, SBEC 2013. Pp. 35–36.
Weinschenk, S. W., Beise, R. D., & Lorenz, J. (2016). Heart rate variability (HRV) in deep breathing tests and 5-min short-term recordings: agreement of ear photoplethysmography with ECG measurements, in 343 subjects. European Journal of Applied Physiology, 116(8), 1527–1535.

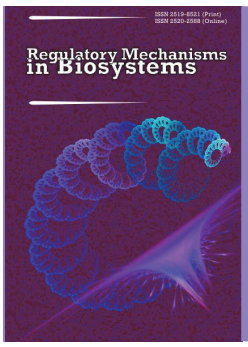

Regulatory Mechanisms in Biosystems

ISSN 2519-8521 (Print)
ISSN 2520-2588 (Online)
Regul. Mech. Biosyst., 9(3), 340–346
doi: 10.15421/021850

Effect of clonal reproduction on quantitative indices and component composition of essential oil of peppermint varieties

T. E. Talankova-Sereda*, J. V. Kolomiets*, A. F. Likhanov**, A. V. Sereda***, N. I. Kucenko****, E. O. Shkopinskiy*****

*National University of Life and Environmental Sciences of Ukraine, Kyiv, Ukraine
**Institute for Evolutionary Ecology of NAS of Ukraine, Kyiv, Ukraine
***Chinese-Ukrainian Life Sciences Research Institute, Zhuji City, China
****Experimental Station of Medicinal Plants at the Institute of Agroecology and Nature Management of NAAS, Beresotocha, Ukraine
*****Zaporizhzhia National University, Zaporizhzhia, Ukraine

Article info

Received 14.06.2018
Received in revised form 20.07.2018
Accepted 28.07.2018

National University of Life and Environmental Sciences of Ukraine, Heneral Rodimtsev st., 19/4, Kyiv, 03041, Ukraine.

Institute for Evolutionary Ecology NAS Ukraine, Lebedev st., 37, Kyiv, 03143,Ukraine.

Sino-Ukrainian Institute of Life Sciences, South Wenzhou st., 26, Zhuji City, Prov. Zhejiang, Republic of China.

Experimental Station of Medicinal Plants at the Institute of Agroecology and Nature Management of NAAS, Lenin ave., 16a, Beresotocha, 37535, Ukraine.

Zaporizhzhia National University, Zhukovskogo st., 66, Zaporizhzhya, 69600, Ukraine. Tel.: +38-050-983-58-53. E-mail: tatazp77@gmail.com

Talankova-Sereda, T. E., Kolomiets, J. V., Likhanov, A. F., Sereda, A. V., Kucenko, N. I., & Shkopinskiy, E. O. (2018). Effect of clonal reproduction on quantitative indices and component composition of essential oil of peppermint varieties. Regulatory Mechanisms in Biosystems, 9(3), 340–346. doi:10.15421/021850

Quantitative and qualitative composition of essential oils of peppermint breeds Lebedinaya Pesnya, Lubenchanka, Lidiya, Ukrainskaya Perechnaya, Mama, Chornolista was investigated before and after clonal microreproduction by the method of isolated tissues and bodies culture *in vitro*. Methods of essential oil steam distillation, capillary gas chromatography and statistical analysis were used in the research. It is established that increase in essential oil quantity was observed for peppermint breeds on which reproduction and improvement in vitro technology was applied. As a result of clonal microreproduction of peppermint plants in culture *in vitro* on nutrient medium Murasige and Skug, in which the growth regulators 0.75 mg/l of 6-benzylaminopurine, 0.1 mg/l of adenine, 0.05 mg/l of indolil-3-acetic acid and 0.5 mg/l of gibberellins acid were added and virocide Ribavirin in concentration 10 mg/l, improvement was obtained in comparison with vegetatively reproduced plants; increase in essential oil quantity per hectare was established for the following breeds; Chornolista by 54.2%, Lebedinaya pesnya by 38.2%, Ukrainskaya Perechnaya by 36.7%, Mama by 28.5%, Lubenchanka by 17.1% and Lidiya by 11.6%. For oil content the highest indices were noted for Lubenchanka, Mama and Lebedinaya Pesnya peppermint breeds with product yield 4.02%, 3.98% and 3.84% respectively. It was established that the essential oil component composition in non-clonal peppermint plants raw materials and plants-regenerants after culture *in vitro* is variable depending on breed. Limonene, cineole, menthone, menthofuran, iso-menthone, menthyl acetate, β-caryophyllene, iso-menthol, menthol, pulegone, germacren, piperitone, carvone were identified in peppermint essential oil. High content of menthol, low content of carvone, piperitone, pulegone (except for Chornolista, Ukrainskaya Perechnaya breeds) and menthofuran (except for Chornolista, Ukrainskaya Perechnaya and Lubenchanka breeds) are characteristic for Ukrainian selection peppermint investigated breeds. A clear tendency to menthol and menthone content ratio increase is observed in plants which were improved in conditions in vitro. Pulegone was not detected in essential oil samples of Lebedinaya Pesnya, Lidiya and Mama breeds. Biochemical markers of Lebedinaya Pesnya, Lubenchanka, Mama breeds, which differentiate them within the group of investigated breeds, are higher limonene, piperitone and menthol pool; for Ukrainskaya Perechnaya and Chornolista breeds – pulegone, cineole and menthone; for Lidiya breed – iso-menthone.

Keywords: *Mentha piperita*; *in vitro*; capillary gas chromatography; menthol; menthone; pulegone.

Introduction

According to State Statistics Service data nearly 50 species of plants whose raw materials are used for medicinal preparation manufacture are cultivated in Ukraine. Structural parts of these plants contain biologically active substances which positively influence the human organism. Peppermint is one of the most widespread and traditionally cultivated species. It is cultivated as industrial culture in all climatic zones of Ukraine, Moldova, Russia (Krasnodar territory and North Caucasus), Belarus, and also in many countries of Europe, Central Asia, Africa, India and the North America. Such soil-climatic variety of cultivation zones testifies to the considerable adaptive potential of this culture. The demand for medicinal preparations on the basis of natural vegetative raw materials has increased in the last 10–15 years and the Ukraine home market does not satisfy the needs of the domestic chemical-pharmaceutical industry, which requires every year nearby 50 tonnes of *M. piperita* essential oil and 20–25 tonnes of natural menthol (Shelud'ko, 2004). Mint is a source for obtaining pharmaceutic leaf, essential oil and its components, which are widely used in the chemical-pharmaceutical, perfume-cosmetic, confectionery, food, liqueur and spirits, tobacco, paint and coatings industries and medicine (Vojtkevich, 1999; Tkachenko, 2011).

The biologically active substances of peppermint are complex and its essential oil shows anti-inflammatory, antimicrobial, antifungal, antiviral, anthelmintic, antiparasitic, analgetic, spasmolytic, cholagogic, mucolytic and broncholytic, antihistaminic action, normalises central and vegetative nervous system activity, limits rotting and fermentation processes, strengthens motor secretory intestinal tract function, prevents peptic ulcer development, expands coronary vessels, improves heart blood supply, reduces pressure in blood circulation small circle, and also shows

antiarrhythmic and hypertensive action, improves sports results, attention, working memory, cognitive activity, visual motor reactions (Grigoleit & Grigoleit, 2005; Mi-Hyun et al., 2005). The biologically active substances complex of mint oil is primarily responsible for the therapeutic action of peppermint. About 100 components are identified in mint essential oil according to Lawrence (2006) , basic of which are menthol, and also α-pinene, β-pinene, limonene, sabinene, isoamyl alcohol, phelandrene, 1.8-cineole, γ-tarpinene cis-3-hexanol, trans-sabinene hydrate, menthone, menthofuran, isomenthone, menthyl acetate, neomenthol, terpinene-4-ol, caryophyllene, germacrene, dipentene, pulegone and other terpenoids. Monoterpenic alcohol menthol, the action of which is sufficiently selective, has substantial significance in the substances complex. The substance irritates first of all mucous membranes and skin thermoreceptors, which causes cooling sensation, which is accompanied by reflex vessels constriction, after which burning sensations develop and then easy anaesthesia comes (Magge & Lembo, 2011). Thanks to such properties, peppermint is a part of many pharmaceutical preparations. Herbage, leaves and essential oil, concentration of which fluctuates in peppermint leaves according to Shelud'ko (2004) data from 1.2% to 4.8% and in inflorescences reaches 6.0%, are used for their manufacturing.

The *Mentha* species breeds collection is collected, studied and registered in the National Centre of Genetic Resources in Ukraine. 269 samples are in the collection structure, from which over 11% belong to *M. piperita* L., and about 40% are hybrids which have been created in the course of selection research. The collection is stored in Experimental Station of Medicinal Plants of the Institute of Agroecology and Nature Management of National Academy of Agricultural Sciences (NAAS) of Ukraine and is used by selectionists in creation of new breeds with better essential oil indices (Kolosovich et al., 2008). Five pepper mint grades are registered in the Register of Breeds Suitable for Distribution in Ukraine (Derzhavnij reestr sortiv roslyn pridatnyh do poshyrennja v Ukrajini, 2016). The majority of priority breeds, except the breed Lada, were created 10 and more years ago. Considering that pepper mint breeds are bred in vegetative way, a decrease in their raw productivity is marked during the long period of their cultivation. It is known that the essential oil quantity and quality in raw materials depends on a plant organs proportion, age, climatic conditions, agricultural techniques, extra nutrition, degree of contamination and protection systems. In Brazil, research by Costa et al. (2013) with colleagues revealed that various organic amendments sources and influence of doses on plants and essential oil biomass manufacture, changes in menthone, pulegone and menthyl acetate quantitative composition were observed in essential oil chemical composition, although menthol indices were stable. Growth regulators at application on a green leaf differently influence pepper mint essential oil productivity and qualitative characteristics. Salicylic acid turned out to be the best for increase in quantity yield of oil, concentration of menthol and menthyl acetate in *M. piperita*, 6-benzylaminopurine (BAP) increased yield of menthone; gibberellic acid (GA) increased menthyl acetate content (Dmitrieva & Dmitriev, 2011; Khanam & Mohammad, 2017).

It is established on the basis of research by Mishhenko et al. (2016) in the joint work of the Viruses Ecology and Virus Diseases Diagnostics Research Laboratory of the Education Scientific Centre "Biology Institute" of Taras Shevchenko National University of Kyiv with colleagues of National University of Bioresources and Nature Management of Ukraine and the Research Sstation of Medicinal Plants of the Institute of Agroecology and Nature Management of NAAS of Ukraine that over the last 10–15 years peppermint has been affected by 23 viruses, in particular on the territory of Ukraine P. virus Y, P. virus X and an unidentified filariform virus, which considerably reduces the quality of the raw materials, owing to such symptoms arising as growth inhibition, lamina deformity, leaf curl, savoyed leaf and frenching. Certified seeds improvement by the apical meristems method and chemotherapy, which is based on explants cultivation in vitro on nutrient mediums with viricides addition, is one of the most effective ways to combat the viruses (Mel'nichuk et al., 2003).

Santoro et al. (2013) has shown that addition of BAP to nutrient medium Murasige and Skug (MS) in concentration of 0.6 mg/l increases the general essential oil yield and some its components: menthone, menthol, pulegone and menthofuran by secondary metabolites biosynthesis induction. It is shown in the research of Slovak scientists that in the essential oil composition of *M. piperita* breed Kristinka in culture *in vitro* the menthofuran content increased after addition of 2,4-dichlorophenoxyacetic acid (2,4-D) and $CoCl_2$ to the nutrient medium and after BAP and zeatin application pulegone content increased (Fejer et al., 2018).

Therefore, the topicality of the given work consists in studying for plants at clonal microreproduction *in vitro* the influence of the improvement process on the further secondary metabolites synthesis, in particular terpenoids, which are a part of the essential oils of mint. In this connection, the purpose of our work is to investigate within three years the quantitative content and qualitative composition of essential oil components of peppermint breeds of the Ukrainian selection Lebedina Pisnya, Lubenchanka, Lidiya, Ukrainska Perechna, Mama, Chornolista, received from plants after vegetative reproduction and clonal microreproduction *in vitro*.

Materials and methods

The research objects are the essential oil samples of pepper mint breeds Lebedina Pisnya (5), Lubenchanka (7), Lidiya (8), Ukrainska Perechna (9), Mama (10), Chornolista (11). The breed Lebedina Pisnya is cultivated for obtaining pharmaceutic leaves and for essential oil processing. The breed Lubenchanka is cultivated for pharmaceutical industry technical purposes – obtaining essential oil and menthol. The breeds Lidiya, Chornolista, Mama are used for obtaining pharmaceutic leaves (Grodzins'kij, 1992; Shelud'ko, 2004).

The research was conducted during 2014–2017 within the framework of the scientific theme "Lamiaceae family essential oil medicinal plants. Biotechnological reproduction foundations for receiving high-quality planting material" (number of the state registration 0116U001994).

Methods of isolated tissues and organs culture *in vitro* and chemotherapy were used for pepper mint improvement in 2014. Murashige and Skoog (Murashige & Skoog, 1962) nutrient medium, in which 0.75 mg/l BAP, 0.1 mg/l adenine, 0.05 mg/l indolebutyric acid (IAA) and 0.5 mg/l gibberellic acid (GA), and also virucide Ribavirin (1-β-D-ribofuranosyl-1,2,4-triazole-3-carboxamide, "Sigma-Aldrich", USA) in 10 mg/l concentration were added, paravariation was used for above mentioned peppermint breeds of Ukrainian selection explants introduction and microreproduction (Talankova-Sereda et al., 2016).

The experiment was conducted four times in Lubensky district of Poltava region in the territory of the Research Station of Medicinal Plants of the Institute of Agroecology and Nature Management of NAAS of Ukraine annually since 2015 in field conditions, in which the influence of clonal microreproduction and chemotherapy was investigated on the quantitative indices and componental composition of essential oil of pepper mint breeds Lebedina Pisnya, Lubenchanka, Lidiya, Ukrainska Perechna, Mama, Chornolista. Vegetatively reproduced planting material of the mint breeds was used as the control variants. Mint sprouts, which were used for trial establishment, met the requirements of the standard document "Mint Sprouts" (Technic Specifications 10-04-13-48-88 "Mint Sprouts. Technic Specifications").

The research was conducted according to Moloc'kij et al. (2006), Eshhenko et al. (2014), Shelud'ko & Kucenko (2013) techniques. Pepper mint raw materials for obtaining essential oil were selected annually with time requirements compliance, which is defined in technology regulations for the investigated kind. In particular, the investigated breeds overground part was cut in the mass flowering phase as numerous researches specify a tendency to increase in essential oil content during this period (Tanasienko, 1985; Kirichenko, 2008; Morozov & Hazieva, 2013). Raw materials from plants after vegetative reproduction and plants to which clonal microreproduction in vitro was applied were selected on each of plots with the use of the linear metre method.

Essential oil was received by steam distillation by A. S. Ginzberg's technique (Hefendehl et al., 1967) with the subsequent recalculation on dry weight. For this purpose, 50 g milled raw materials were placed in wide neck flask with 3,000 ml capacity, then 1,500 ml water was added and it was closed with a rubber stopper with a ball check refrigerator. The calibrated receiver was suspended on metal hooks on the stopper

underside in such way that the refrigerator end was directly under the receiver funneled widening on distance of about 1–2 mm. The receiver was not less than on 50 mm from the water level. A flask with contents was heated up to boiling and the boiling was sustained for 1.5 hours. Water steam and essential oil after condensation in the refrigerator flowed down into the receiver in liquid form. Essential oil remained in the receiver's graduated knee, and water through a smaller receiver knee followed back into the flask. Essential oil volume in the receiver was measured after cooling the device and essential oil content was measured in volume-mass percent in relation to air-dry medicinal raw materials weight.

Essential oil received from pepper mint breeds Lebedina Pisnya, Lubenchanka, Lidiya, Ukrainska Perechna, Mama and Chornolista plants was a transparent liquid, light-yellowish colour, with a strong menthol smell, which remained in the glassware in the refrigerator at temperature 4 °C.

The essential oil components analysis was conducted by the capillary gas chromatography method on chromatograph Agilent 7890A with flame ionization detector with automatic test input. A column: DB-WAX (Agilent) 60 g * 0.25 mm, an immovable phase macrogol 20000 (0.25 um). Carrier-gas: helium 1.5 ml/min, stream division 1 : 50. For chromatography 25 mcl essential oil was dissolved in 1.5 ml n-hexane, injecttion volume: 1 mcl. Chromatography program: column temperature – 15 minutes at 70 °C, then rise in temperature to 240 °C over 85 minutes and kept for 5 minutes at 240 °C; the block of tests input – 250 °C, the detector – 270 °C.

Components identification was conducted by comparison of the chromatogramms with typical mint oil chromatogramm which meets the requirements of monography EP "Peppermint oil" (Ph. Eur. 8, 2014). Calculation of percentage components proportion was performed by the method of internal normalisation of essential oil composition and these results were compared with corresponding intact plants.

Statistically average values and their standard errors are shown in the text and tables (x ± SE). The results were statistically processed with the help of the program Statistica 7.0 (StatSoft Inc., USA). Differences between average values were calculated by the method ANOVA.

Results

The highest indices of essential oil content among investigated pepper mint breeds of Ukrainian selection were noted for Lubenchanka, Mama and Lebedina Pisnya – 4.02%, 3.98% and 3.84% respectively (Table 1). These indices are especially important for breeds Lubenchanka and Lebedina Pisnya, which are cultivated for obtaining essential oil as the basic product.

Table 1
Essential oil content (%) in medicinal peppermint breeds of the Ukrainian selection raw materials (2015–2017, n = 5, x ± SE)

Peppermint breeds	Variants	2015	2016	2017
Lebedina Pisnya	VR	3.79 ± 0.010	3.82 ± 0.013	3.82 ± 0.006
	in vitro	3.83 ± 0.013 **	3.85 ± 0.008 *	3.85 ± 0.008 **
Lubenchanka	VR	3.98 ± 0.008	4.01 ± 0.014	3.99 ± 0.010
	in vitro	4.00 ± 0.013	4.03 ± 0.017	4.02 ± 0.015 *
Lidiya	VR	3.20 ± 0.013	3.24 ± 0.016	3.23 ± 0.013
	in vitro	3.33 ± 0.010 **	3.35 ± 0.008 **	3.34 ± 0.017 **
Ukrainska Perechna	VR	3.63 ± 0.014	3.67 ± 0.013	3.63 ± 0.015
	in vitro	3.66 ± 0.010	3.71 ± 0.014 **	3.70 ± 0.010 **
Mama	VR	3.90 ± 0.013	3.94 ± 0.008	3.91 ± 0.010
	in vitro	3.95 ± 0.010 **	3.99 ± 0.010 **	3.99 ± 0.008 **
Chornolista	VR	3.74 ± 0.014	3.78 ± 0.010	3.77 ± 0.013
	in vitro	3.81 ± 0.016 **	3.86 ± 0.013 **	3.83 ± 0.010 **

Notes: VR – vegetatively reproduced plants; *in vitro* – plants treated in culture *in vitro*; * – differences are statistically signicant at P < 0.05, ** – at P < 0.01 comparing with the control.

The Lidiya breed of vegetative reproduced plants contained the least essential oil quantity 3.22%, however this index increased by 0.12% in plants after culture *in vitro* and was 3.34%. Essential oil quantity in vegetatively reproduced plants of the breed Ukrainska Perechna after culture *in vitro* was accordingly 3.64% and 3.69%. It is important also, that plants of this breed in culture in vitro had the maximum rate of reproduction 1:15 for one passage. Essential oil quantity in vegetatively reproduced plants of breed Chornolista was 3.77%, and in plants after culture *in vitro* it increased to 3.83%. It is necessary to note that the breed Chornolista is recognised by the State Commission of Strain Test in Ukraine as a peppermint meeting the state standard for the purpose of obtaining pharmaceutic leaves and manufacturing phytocompositions.

Essential oil componental composition and its separate fractions proportion are defined for peppermint breeds Lebedina Pisnya, Lubenchanka, Lidiya, Ukrainska Perechna, Mama and Chornolista. Limonene, cineole, menthone, menthofuran, isomenthone, menthyl acetate, β-caryophyllene, isomenthol, menthol, pulegone, germacrene, piperitone, carvone were identified among compounds which are components of pepper mint essential oil (Table 2, 3).

Table 2
Essential oil componental composition (%) in peppermint breeds of the Ukrainian selection without culture in vitro application (2016)

Essential oil component	European Pharmacopoeia standard	Peppermint breeds: Lebedina Pisnya	Lubenchanka	Lidiya	Ukrainska Perechna	Mama	Chornolista
Limonene	1.0–5.0	3.2	3.5	1.3	0.9	3.2	1.1
Cineole	3.05–14.0	0.2	0.3	0.1	2.8	0.2	3.8
Menthone	14.0–32.0	14.9	9.3	12.6	18.8	12.6	23.5
Menthofuran	1.0–9.0	0.5	4.4	0.0	9.3	0.5	4.8
Isomenthone	1.5–10.0	2.8	2.5	17.6	5.3	2.7	4.0
Menthyl acetate	2.8–10.0	2.4	3,3	2.9	8.5	2,6	3.1
Menthol	30.0–55.0	70.1	68.0	60.5	38.4	72.0	30.7
Isomenthol	–	2.0	3.1	1.1	2.5	2.0	6.5
Pulegone	Up to 4.0	0.0	0.0	0.0	6.1	0.0	11.1
Carvone	Up to 1.0	0.0	0.1	0.2	0.1	0.0	0.6
Minor compounds	–	3.8	5.5	3.9	7.4	4.2	11.0

Table 3
Essential oil componental composition (%) in peppermint breeds of the Ukrainian selection after culture *in vitro* (2016)

Essential oil component	European Pharmacopoeia standard	Peppermint breeds: Lebedina Pisnya	Lubenchanka	Lidiya	Ukrainska Perechna	Mama	Chornolista
Limonene	1.0–5.0	2.9	3.5	1.5	0.7	1.9	1.0
Cineole	3.1–14.0	0.2	0.3	0.1	3.3	0.5	3.1
Menthone	14.0–32.0	8.8	8.9	11.0	20.1	12.9	21.8
Menthofuran	1.0–9.0	0.3	3.8	0.2	6.8	0.3	4.5
Isomenthone	1.5–10.0	2.8	2.8	16.8	6.8	1.5	3.3
Menthyl acetate	2.8–10.0	3.7	3.1	2.8	5.8	1.0	2.9
Menthol	30.0–55.0	74.1	68.8	61.4	44.2	72.6	33.3
Isomenthol	–	2.0	2.8	1.2	2.5	4.3	6.4
Pulegone	up to 4.0	0.0	0.0	0.0	3.1	0.0	11.9
Carvone	up to 1.0	0.0	0.2	0.2	0.1	0.2	0.9
Minor compounds	–	5.1	5.8	4.8	6.7	4.8	11.0

Breeds Lebedina Pisnya – 70.1–74.1% (Fig. 1), Lubenchanka – 68.0–68.8%, Lidiya – 60.5–61.4% and Mama – 72.0–72.6% contain the maximum menthol content as the basic marking essential oil component according to the received data.

Essential oil contained almost half the abovementioned content of menthol , 38.4–44.2% and 30.7–33.3% , respectively in vegetatively reproduced after culture *in vitro* breeds Ukrainska Perechna and Chornolista plants, which correlates with the high menthone content in these samples. The proportion of menthone was 18.8% in the essential oil of plants of the breed Ukrainska Perechna without culture *in vitro* application, after clonal microreproduction – 20.1%, and in the breed Chorno-

lista – 23.5–21.8%, but total menthol and menthone content in these plants was high enough and was in the breed Ukrainska Perechna – 57.2–64.3%, Chornolista – 54.1–55.0%. Total menthol and menthone content in high menthol breeds was considerably higher, in particular in Lebedina Pisnya – 85.0–82.9%, Lubenchanka – 77.3–77.7%, Lidiya – 73.1–72.3% and Mama – 85.5–82.5%.

Menthone quantity decreased in essential oil of four breeds of vegetatively reproduced plants and after culture *in vitro*, in particular in the pepper mint breed Lebedina Pisnya by 6.15%. In the breeds Ukrainska Perechna and Mama it slightly increased. The quantity of such major essential oil components as menthol and menthone in different breeds fluctuated.

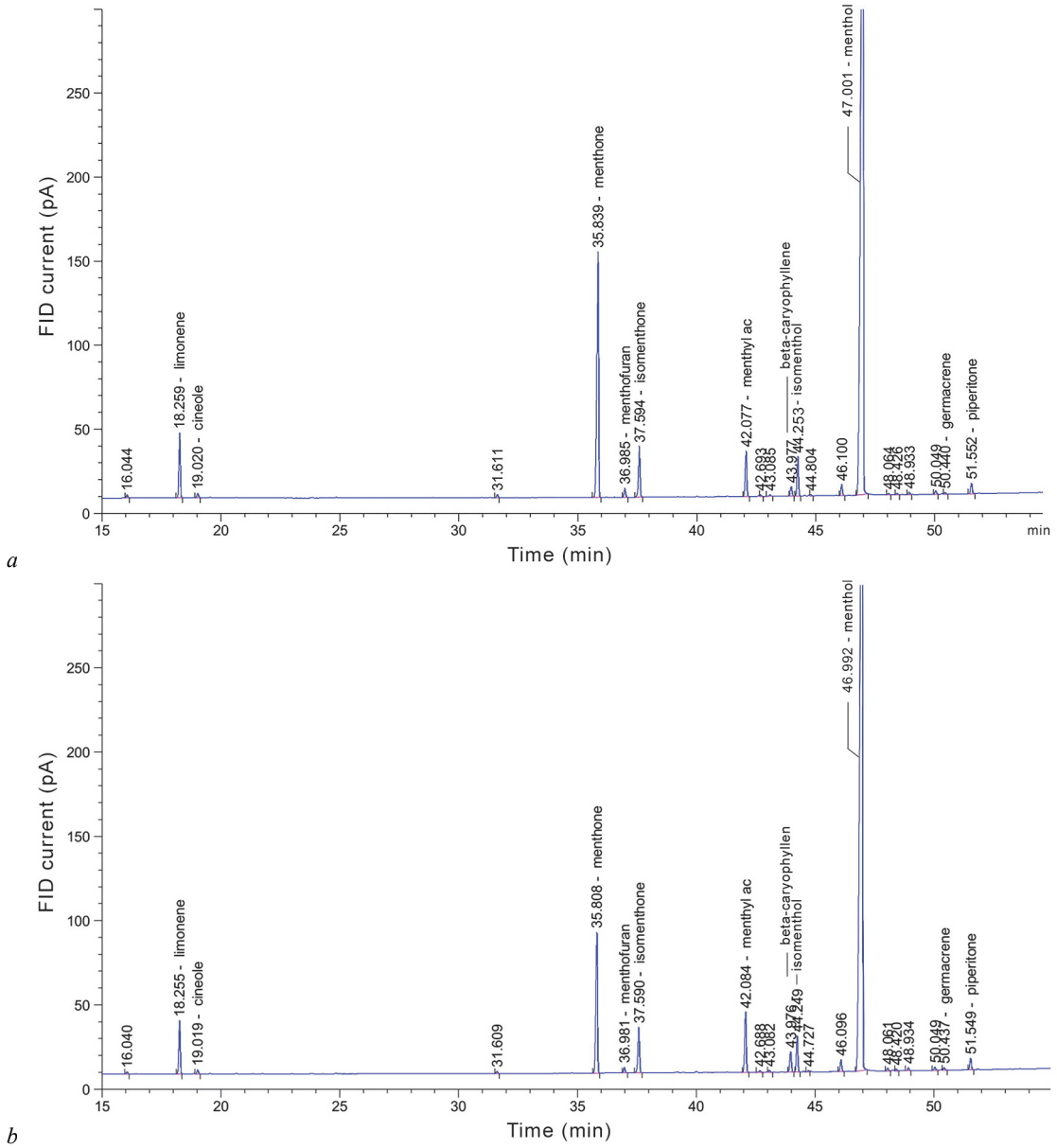

Fig. 1. Essential oil peppermint breed Lebedina Pisnya leafage chromatogram before *in vitro* (*a*) and after *in vitro* (*b*)

Limonene concentration in all essential oil samples was within the range of the recommended European pharmacopoeia (Ph. Eur.) values, under which requirements this non-toxic monocyclic terpene representtative should be in the range of 1.0–5.0% . Only in both essential oils of plant samples of the breed Ukrainska Perechna was it was lower than the European Pharmacopoeia standard by 0.1–0.4% (Ph. Eur. 8, 2014). The insignificant reduction in this essential oil component was observed in all pepper mint plants breeds after culture *in vitro* application by 0.1–1.3%, except for the breed Lidiya in which the proportion of limonene increased by 0.3%.

Analysis of the amount of cineole contained in the essential oil samples showed that for the majority of breeds this component amounted to less than 1%, except for two breeds – Ukrainska Perechna and Chornolista, but its quantity nevertheless is below European pharmacopoeia requirements. Only the essential oil which was received from vegetatively reproduced plants of the breed Chornolista corresponded to the European pharmacopoeia standards (3.5–14.0%) (Ph. Eur. 8, 2014). It is necessary to notice that essential oil received by steam distillation by A. S. Ginzberg's technique can yield underestimated results on more volatile components, which include limonene and cineole, in comparison with the technique which is used in the European pharmacopoeia.

An insignificant excess of menthofuran content over the established standard European pharmacopoeia requirements was noted only in the breed Ukrainska Perechna among investigated essential oil samples. Menthofuran content did not exceed 1% in essential oil breeds Lebedina Pisnya, Lidiya, Mama. The breeds Lubenchanka and Chornolista indices correspond to Ph. Eur. (1.0–9.0%). The general tendency to menthofuran reduction on average by 0.2–2.5% among essential oil peppermint plants samples, which were treated in culture *in vitro*, except for the breed Lidiya, was observed. In the essential oil of vegetatively reproduced plants this component was not revealed by us, and in plants-regenerants raw materials its share was 0.2%. It is known, that mint flowers contain a significant menthone and menthofuran amount (Tanasienko, 1985). Menthofuran content of less then 9% does not worsen essential

oil quality, but usually it is accompanied by other substances with an unpleasant smell.

Essential oil of the uncloned breed Ukrainska Perechna had increased pulegone content – 6.1%, at the same time in this breed essential oil of plants after culture *in vitro* content of this component decreased by 50%, which corresponds to the European pharmacopoeia requirements. In essential oil samples of vegetatively reproduced plants of the breed Chornolista, pulegone amounted to 11.1% and after culture *in vitro* application its content increased to 11.9%, but such quantity exceeds European pharmacopoeia standards by three times (to 4%). These breeds were created in Ukraine as English peppermint analogues, and pulegone presence is a characteristic feature for them, and its content, according to our data, considerably varies depending on weather conditions, collecting period of raw materials and other factors. Essential oil of pepper mint samples of other breeds of Ukrainian selection, Lebedina Pisnya, Lubenchanka, Lidiya and Mama did not contain pulegone at all, which in excessive quantity (more than 4%) introduces an appreciable shade of standard English peppermint aroma.

All pepper mint essential oil plants of Ukrainian selection samples correspond to European pharmacopoeia standards for content of the terpenoids carvone and piperitone, and in the essential oil of pepper mint breed Mama, to which culture *in vitro* was not applied, and of the pepper mint breed Lebedina Pisnya (Fig. 1) carvone, which can give unpleasant caraway aroma to the essential oil and which under European pharmacopoeia recommendations should have a concentration of no more than 1%, was completely absent. The low carvone content is a characteristic feature for all pepper mint breeds investigated by us.

Cineole/limonen proportion is an important peppermint essential oil quality index. Two breeds among the investigated essential oil samples correspond to European pharmacopoeia requirements. For Ukrainska Perechna without culture in vitro application this index is 2.9 and after culture *in vitro* application – 5.0, and also in breed Chornolista 3.5 – in uncloned plants and 3.0 – in plants after culture *in vitro*. According to Ph. Eur. this proportion should be more than 2.0.

If total marking of mint essential oil compounds content will be counted in all essential oil samples, specifically menthone, isomenthone, menthol and isomenthol, it is possible to arrange breeds in such sequence as: Lidiya – 90.3–91.7%; Mama – 89.3–90.3%; Lebedina Pisnya – 87.7–89.8%; Lubenchanka – 82.9–83.2%; Chornolista – 61.3–64.5%, Ukrainska Perechna – 61.6–64.9%.

Main components analysis of qualitative composition and isoprenoid content in pepper mint breeds Lebedina Pisnya (5), Lubenchanka (7), Lidiya (8), Ukrainska Perechna (9), Mama (10), Chornolista (11) leaves established that the first main components axis (F1) was 58.4% from the general dispersion in indices complex, from which the greatest value was for menthol, pulegone, cineole. A slightly smaller contribution to the general dispersion is noted on menthone, germacrene, carvone and limonene content indices (Table 4).

Table 4
Main components analysis indices

Essential oil indices	Main components weighting		
	F_1	F_2	F_3
Limonene	0.589 *	0.261	0.054
Cineole	0.889 *	0.003	0.058
Menthone	0.826 *	0.006	0.001
Menthofuran	0.453	0.037	0.455 *
Isomenthone	0.004	0.595 *	0.329
Menthyl acetate	0.141	0.315	0.435 *
B-caryophyllene	0.302	0.226	0.044
Isomenthol	0.569 *	0.370	0.006
Menthol	0.944 *	0.036	0.002
Pulegone	0.936 *	0.033	0.001
Germacrene	0.678 *	0.012	0.003
Piperitone	0.392 *	0.247	0.261
Carvone	0.602 *	0.131	0,182
Minor compounds	0.852 *	0.055	0.003

Notes: * – the greatest contribution to main components weighting.

Axis F_1 separates cloned and not cloned in vitro breeds Ukrainska Perechna and Chornolista from Lebedina Pisnya, Lubenchanka, Lidiya and Mama. The last differ by absence of pulegone in the leaves and rather high menthol content, which is the key vegetative raw materials quality feature. For breeds Ukrainska Perechna and Chornolista, the rather high menthone content accumulation, on the contrary, is characteristic. The second main components axis (F_2) was 16.6% from the general dispersion in which the greatest value was for isomenthone. In the investigated breeds group second components axis separates breeds Lidiya and Ukrainska Perechna. Axis F_3 is 25% from the general dispersion. Menthofuran and menthyl acetate have the greatest value by the third component. The total 1 and 2 main components dispersion is 75% (Fig. 2). Biplot analysis use allows us to show a number of indices which characterise the investigated breeds by essential oil componental composition specificity.

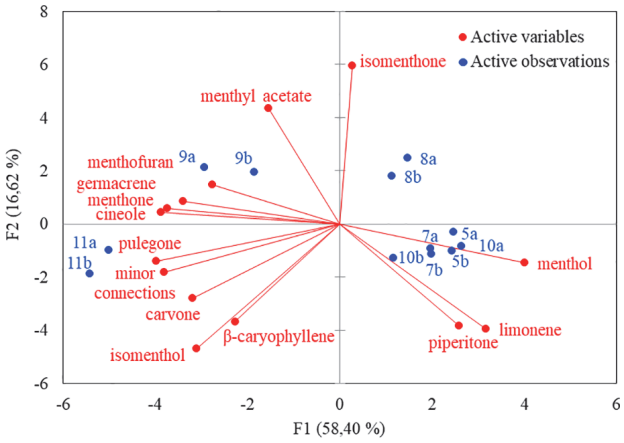

Fig. 2. Vegetatively reproduced plants (*a*), and after clonal microreproduction (*b*) pepper mint breeds Lebedina Pisnya (*5*), Lubenchanka (*7*), Lidiya (*8*), Ukrainska Perechna (*9*), Mama (*10*), Chornolista (*11*) biplot analysis

It is established that in the Lebedina Pisnya, Lubenchanka, Mama breeds the predominate components which differentiate them within the group of investigated breeds, are limonene, piperitone, menthol; for Ukrainska Perechna and Chornolista breeds – pulegone, cineole and menthone; for Lidiya breed – iso-menthone.

Discussion

Essential oil composition is genetically caused. However the proportion of its components depends on many factors, in particular the plant's age, ontogenesis stage, agroprocessing methods, climatic conditions, plants pathogenic organisms and viruses contamination etc. Besides, growth regulators application during the clonal microreproduction *in vitro*, in turn, is capable of changing the intensity and character of plants' tissues metabolism, but does not cause considerable qualitative differences in these plants landed *in vivo* essential oil composition, which can be caused by specific fermental systems work stability and genes expression which are responsible for terpenoid synthesis regulation.

It is established by us that yield of essential oil increases in improved plants after methods of tissues and organs culture, chemotherapy *in vitro* and clonal microreproduction application. Improvement of the plants in culture *in vitro* can be considered as the reason for this increase in yield. As a clonal microreproduction result, better planting material was received, with better sprout tillering, their leaf cover and accordingly considerable inflorescences quantity, and, as is known (Oceania et al., 2015), intensive second level sprouts development and their dense flowering lead to increase in content of essential oil ketones (Tanasienko, 1985). From Fejer et al. (2018) article it is known that 0.5 mg/l cytokinin BAP addition increases sprouts quantity *de novo*.

Our research found that the quantity of menthol increased in all plants after culture *in vitro* application, which concurs with the findings presented in Santoro et al. (2013) publication, which studied growth regulators' influence on *Mentha piperita* plants *in vitro* aiming at growth and essential oil synthesis maximalisation in microreproducted plants-regenerants. Base nutrient medium was supplemented with 4-indolil-3-

acetic acid (IAA) and BAP separately and in combination in our experiment. Only BAP in 0.6 mg/l concentration addition had led to the highest roots length, their dry weight, sprouts length and internode number, leaves and branching values. Only 0.6 mg/l IAA or simultaneously IAA and 0.6 mg/l BAP processing led to increase in sprouts weights by 50%. Secondary metabolites synthesis increased only in the case of BAP addition,which resulted in 40% increase in the general yield of essential oil and the basic components (menthone, menthol, pulegone and menthofuran).

Fluctuations in menthol and menthone quantity of different breeds of peppermint were caused by plant genotype, and also connected with continuous synthesis processes, their biochemical transformation and evaporation. Menthone synthesis can occur by pulegone or piperitone restoration, and also in the course of menthol oxidation. Thus, the rather high accumulation of menthone content in the breeds Ukrainska Perechna and Chornolista specifies that for these two breeds there is high activity of fermental systems, which are involved in menthone synthesis pulegone ways.

We have confirmed the precise tendency of menthol to increase by 0.6–5.8% in essential oil of peppermint plants to which we applied culture *in vitro*, which corresponds to the research of Paric et al. (2017) which has revealed secondary metabolites production stimulation as a result of BAP in concentration from 0.1 to 4.0 mg/l and 0.1 mg/l indole-3-butyric acid (IBA) separately and in combination application, which underlines the great value of the optimum growth regulator and its concentration choice. Also, we have verified that their application led to increase in sprouts and roots quantity.

In the publication of Ivanova et al. (1996) it is shown that menthol and menthone production reduces in plants after culture *in vitro*, to which cytokinins from purine and phenyl carbamide preparations were applied, but they led to increase in the amount of pulegone and menthofuran, and the highest pulegone content was observed after BAP application. In our research an insignificant increase in pulegone content was characteristic only for the breed Chornolista. Other investigated pepper mint breeds before and after improvement did not contain pulegone, which testifies to the absence of this component in the biochemical essential oil synthesis chain of peppermint plants of Ukrainian selection – most likely this is caused by their genotype.

Also, in an article by Slovak scientists culture of *M. piperita* breed Kristinka *in vitro* is described, where they had cultivated node segments on nutrient medium and showed that after BAP and zeatin addition in the nutrient medium, the pulegone content increased, and after 2.4–D and $CoCl_2$ application, menthofuran content in the essential oil composition increased. Our research found that menthofuran was present at 0.2% in the essential oil of cloned plants of the pepper mint breed Lidiya, though in vegetatively reproduced plants this component was absent. In all other investigated breeds at the same time a general tendency was observed to reduction in menthofuran content on the average by 0.2–2.5 %.

Thus, it is established that two components – menthol and menthone are the predominant components of the essential oil of plants of the breeds Lebedina Pisnya, Lubenchanka and Mama, and their total content was: Lebedina Pisnya – 82.9–85.0%, Lubenchanka – 77.3–77.7%, Mama – 82.5–84.6%. In the essential oil of plants of the breed Lidiya three components – menthol, menthone, isomenthone – prevail, and their total content is 89.1–90.6%; in the breed Ukrainska Perechna five compounds – menthone, menthyl acetate, menthofuran, menthol, pulegone – prevail, and their total content is 68.9–81.1%; in the breed Chornolista four compounds – menthone, menthol, isomenthol and pulegone – prevail, and their total content is 69.9–70.1% from the total essential oil indices sum.

Menthol, menthyl acetate, cineole and menthone should be present in peppermint leaves (Peppermint leaf) according to the European pharmacopoeia. Also, isomenthone, pulegone and carvone can be determined on a chromatogram. Thymol presence is not required. The optimum for peper mint essential oil components (Peppermint oil) has to be in the proportion – limonene from 1.0 to 5.0%, cineole 3.5–14.0%, menthone 14.0–32.0%, menthofuran 1.0–9.0%, isomenthone 1.5–10.0%, menthyl acetate 2.8–10.0%, menthol 30.0–55.0%, pulegone maximum of 4.0%, carvone no more than 1.0%, isopulegol no more than 0.2% according to European pharmacopoeia standards (Ph. Eur. 8, 2014).

The breed Lidiya was the most productive among the investigated breeds in 2015–2017, its indices were at 2,820 kg/ha level after improvement *in vitro* and 2,620 kg/ha in the control group. Increase in raw materials productivity after improvement was minimal for the breed Lidiya among investigated breeds and was 7.6%. This can be explained by the fact that culture *in vitro* and chemotherapy promote mainly the plants' improvement, protecting their tissues from pathogenic and potentially pathogenic microorganisms, endophytic and epiphytic mushrooms and viruses. Besides, according to existing data, pepper mint breed Lidiya plants have complex resistance to illnesses, which was confirmed in Mishhenko et al. (2015, 2016) publications concerning this breed's resistance to powdery mildew, rust, anthracnose and to virus diseases.

Differences in productivity indices in breeds Chornolista and Lebedina Pisnya between variants are essential and accordingly are 51.4% and 37.1%. Owing to improvement, culture productivity considerably increased and was 2,120 kg/ha for breed Lebedina Pisnya and 2,550 kg/ha for breed Chornolista. The last is one of the oldest peppermint breeds cultivated in Ukraine, which was created over thirty years ago and for a long time was cultivated in manufacture conditions. The breed Ukrainska Perechna increased productivity by 34.9%, and breed Mama by 26.6%, and this was 1,880 and 2,380 kg/ha accordingly.

Productivity indices analysis by air-dry foliage weight and pepper mint essential oil quantity determined that in plants after culture *in vitro*, in comparison with vegetatively reproduced plants, the essential oil quantity per hectare considerably increased in the breed Chornolista by 54.2%, Lebedina Pisnya – by 38.2%, Ukrainska Perechna – by 36.7%, Mama – by 28.5%, Lubenchanka – by 17.1 %, Lidiya – by 11.6 %.

Thus, the characteristic features of the investigated peppermint breeds of Ukrainian selection are the high menthol content, low carvone, piperitone, pulegone (except breeds Chornolista, Ukrainska Perechna) and menthofuran (except breeds Chornolista, Ukrainska Perechna and Lubenchanka) content. It is necessary to specify, that in the essential oil samples of the breeds Lebedina Pisnya, Lubenchanka, Lidiya and Mama pulegone was completely absent, and in essential oil samples of vegetatively reproduced plants of the breed Mama and both samples from the breed Lebedina Pisnya carvone was absent, which is caused by breed-specific genotypic features and action of fermentative systems, which are connected with given components synthesis.

Conclusions

The qualitative composition of essential oil of vegetatively reproduced peppermint plants raw materials and plants after culture *in vitro* essentially does not differ and it is within the measures which are characteristic for their genotypes. All raw material samples of improved peppermint plants had increased essential oil quantity. The maximum essential oil content exceeding 4% was received from vegetative raw materials of the breed Lubenchanka. The componental composition of essential oil of mint which was received from vegetatively reproduced plants and plants after culture *in vitro* varies depending on the breed. In improved *in vitro* plants a clear tendency to increase in menthol and menthone content is revealed.

A high content of menthol (except for Chornolista, Ukrainska Perechna breeds), and low content of menthofuran (except for Chornolista, Ukrainska Perechna and Lubenchanka breeds) and of carvone, piperitone, pulegone (except the breeds Chornolista and Ukrainska Perechna) are characteristic for the investigated breeds of Ukrainian selection pepper mint. Pulegone was not detected in essential oil samples of the Lebedina Pisnya, Lidiya and Mama breeds. In the Lebedina Pisnya, Lubenchanka and Mama breeds the dominant components which differentiate them in the group of investigated breeds, are limonene, piperitone, menthol; for the Ukrainska Perechna and Chornolista breeds – pulegone, cineole and menthone; for Lidiya breed – iso-menthone.

As a result of clonal microreproduction in culture *in vitro* of pepper mint plants and improvements by virocide Ribavirin (1-β-D-ribofuranosyl-1.2.4-triazole-3-carboxamide, "Sigma-Aldrich", USA), the essential oil, in comparison with vegetatively reproduced plants, increased per

hectare in the breed Chornolista by 54.2%, Lebedina Pisnya – by 38.2%, Ukrainska Perechna – by 36.7%, Mama – by 28.5%, Lubenchanka – by 17.1%and in Lidiya – by 11.6%.

References

Costa, A. G., Bertolucci, S. K. V., Chagas, J. H., Ferraz, E. O., & Pinto, J. E. (2013). Biomass production, yield and chemical composition of peppermint essential oil using different organic fertilizer sources. Ciencia e Agrotecnologia, 37(3), 202–210.

Council of Europe (2014). European Pharmacopoeia 8th Edition (Ph. Eur. 8). Strasbourg.

Dmitrieva, V. L., & Dmitriev, L. B. (2011). Izuchenie sostava jefirnyh masel jefiromaslichnyh rastenij nechernozjomnoj zony Rossii [Study of the composition of essential oils of essential oil plants of the Non-chernozem zone of Russia]. Izvestija Timirjazevskoj Sel'skohozjajstvennoj Akademii, (3), 106–119.

Eshhenko, V. O., Kopitko, P. G., Kostogriz, P. V., & Oprishko, V. P. (2014). Osnovy naukovykh doslidzhen' v agronomiji [Fundamentals of research in agronomy]. TD Edel'vejs & K, Vinnytsya (in Ukrainian).

Fejer, J., Grul'ova, D., De Feo, V., Ürgeova, E., Obert, B., & Pret'ova, A. (2018). *Mentha × piperita* L. nodal segments cultures and their essential oil production. Industrial Crops and Products, 112, 550–555.

Grigoleit, H.-G., & Grigoleit, P. (2005). Pharmacology and preclinical pharmacokinetics of peppermint oil. Phytomedicine, 12, 612–616.

Grodzins'kij, A. M. (1992). Likars'ki roslyny: Enciklopedychnyj dovidnyk [Medicinal plants: An encyclopedic guide]. Ukrajins'ka enciklopedija imeni M. P. Bazhana, Ukrajins'kyj Vyrobnycho-Komercijnyj Centr Olimp, Kyiv (in Ukrainian).

Hefendehl, F. W., Underhill, R. W., & Rudlof, F. (1967). The biosynthesis of the originated monoterpenes in mint. Phytochemistry, 6, 823–835.

Ivanova, K., Manov, M., Iliev, L., & Stefanov, B. (1996). Effect of cytokinins on the essential oil composition of *in vitro* produced peppermint plants. Biotechnology and Biotechnological Equipment, 10(2–3), 44–48.

Khanam, D., & Mohammad, F. (2017). Effect of structurally different plant growth regulators (PGRs) on the concentration, yield, and constituents of peppermint essential oil. Journal of Herbs, Spices and Medicinal Plants, 23(1), 26–35.

Kirichenko, E. B. (2008). Ekofiziologija miaty: Produkcionnyj process i adaptacionnyj potencial [Ecophysiology of mint: Production process and adaptive potential]. Main Botanical Gardens Named after N. V. Tsitsin. Nauka, Moscow (in Russian).

Kolosovich, M. P., Shelud'ko, L. P., & Kolosovich, N. R. (2008) Stvorennja bazovoji ta uchbovoji kolekciji m'jaty v Doslidnij stanciji likars'kyh roslyn [Creation of a basic and educational mint collection at the experimental station of medicinal plants]. Genetychni Resursy Roslyn, 2, 62–68 (in Ukrainian).

Lawrence, B. M. (2006). Mint: The genus *Mentha*. CRC Press Taylor & Francis Group, Boca Raton, London, New York.

Magge, S., & Lembo, A. (2011). Complementary and alternative medicine for the irritable bowel syndrome. Gastroenterology Clinics, 40(1), 245–253.

Mel'nichuk, M. D., Novak, T. V., & Kunah, V. A. (2003). Biotehnologija roslyn [Biotechnology of plants]. Poligrafkonsalting, Kyiv (in Ukrainian).

Mi-Hyun, K., Eun-Hye, C., Hang-Sook, C., & Kwang-Geun, L. (2005). Antioxidative activity of volatile extracts isolated from *Angelica tenuissimae* roots, peppermint leaves, pine needles and sweet flag leaves. Journal of Agricultural and Food Chemistry, 53(10), 4124–4129.

Mishhenko, L. T., Kucenko, N. I., & Talankova-Sereda, T. E. (2016). Osobennosti diagnostiki virusnyh boleznej (*Mentha piperita* L.) i optimizacija mikroklonal'nogo razmnozhenija dlja ozdorovlenija [Features diagnosis of viral diseases of (*Mentha piperita* L.) and optimization of microclonal breeding for improvement of plants]. Sbornik nauchnyh trudov Mezhdunarodnoj nauchno-prakticheskoj konferencii "Biologicheskie osobennosti lekarstvennyh i aromaticheskih rastenij i ih rol' v medicine". Shherbinskaja Tipografija, Moscow. Pp. 282–287 (in Russian).

Moloc'kij, M. J., Vasil'kivs'kij, S. P., Knjazjuk, V. I., & Vlasenko, V. A. (2006). Selekcija i nasinnyctvo sil's'kogospodars'kyh roslyn [Selection and seed production of agricultural plants]. Vishha Osvita, Kyiv (in Ukrainian).

Morozov, A. I., & Hazieva, F. M. (2013). Biomorfologicheskie osobennosti i sroki uborki u sortov *Mentha piperita* L. raznogo celevogo naznachenija [Biomorphological features and harvesting time in *Mentha piperita* L. varieties of different designation]. Agricultural Biology, 1, 113–118 (in Russian).

Murashige, T., & Skoog, F. A. (1962). Revised medium for rapid growth and bio assay with tobacco tissue culture. Plant Physiology, 15(3), 473–497.

Mishhenko, L. T., Dunich, A. A., Dashhenko, A. V., & Polishhuk, V. P. (2015). Virusni hvoroby likars'kyh roslyn [Viral diseases of medicinal plants]. Fitosociocentr, Kyiv (in Ukrainian).

Oceania, C., Doni, T., Tikendra, L., & Nongdam, P. (2015). Establishment of efficient *in vitro* culture and plantlet generation of tomato (*Lycopersicon esculentum* Mill.) and development of synthetic seeds. Journal of Plant Sciences, 10(1), 15–24.

Paric, A., Karalija, E., & Cakar, J. (2017). Growth, secondary metabolites production, antioxidative and antimicrobial activity of mint under the influence of plant growth regulators. Acta Biologica Szegediensis, 61(2), 189–195.

Santoro, M. V., Nievasv, F., Zygadlo, J., Giordano, W., & Banchio, E. (2013). Effects of growth regulators on biomass and the production of secondary metabolites in peppermint (*Mentha piperita*) micropropagated *in vitro*. American Journal of Plant Sciences, 4, 49–55.

Shelud'ko, L. P. (2004). M'jata perceva (selekcija i nasinnyctvo) [Mint pepper (breeding and seedling)]. Vydavnyctvo Poltava, Poltava (in Ukrainian).

Shelud'ko, L. P., & Kucenko, N. I. (2013). Likars'ki roslyny (selekcija i nasinnyctvo) [Medicinal plants (breeding and seed production)]. Kopi-Centr, Poltava (in Ukrainian).

Talankova-Sereda, T. E., Kolomiec, J. V., & Grigorjuk, I. P. (2016). Klonal'ne mikrorozmnozhennia sortiv m'jaty percevoji (*Mentha piperita* L.) Ukrajins'koji selekciji [Clonal micropropagation of peppermint (*Mentha piperita* L.) varieties of Ukrainian breeding]. Plant Varieties Studying and Protection, 2(31), 50–56 (in Ukrainian).

Tanasienko, F. S. (1985). Efirnye masla. Soderzhanie i sostav v rastenijah [Essential oils. Content and composition in plants]. Naukova Dumka, Kyiv (in Russian).

Tkachenko, K. G. (2011). Efirnomaslichnye rastenija i efirnye masla: Issledovanija i perspektivy, sovremennye tendencii izuchenija i primenenija [Essential oil plants and essential oils: Research and perspectives, modern trends in studying and application]. Bulletin of Udmurt University. Series Biology. Earth Sciences, 1, 88–100 (in Russian).

Vojtkevich, S. A. (1999). Jefirnye masla dlja parfjumerii i aromaterapii [Essential oils for perfumery and aromatherapy]. Food Industry, Moscow (in Russian).

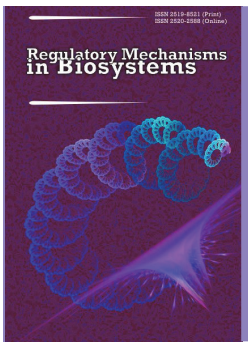

Regulatory Mechanisms in Biosystems

ISSN 2519-8521 (Print)
ISSN 2520-2588 (Online)
Regul. Mech. Biosyst., 9(3), 347–352
doi: 10.15421/021851

Effect of photostimulation on biopotentials of maize leaves in conditions of thermal irritation

M. P. Motsnyj, O. V. Elina, N. P. Botsva, S. O. Kochubey

Oles Honchar Dnipro National University, Dnipro, Ukraine

Article info

Received 02.07.2018
Received in revised form 10.08.2018
Accepted 12.08.2018

Oles Honchar Dnipro National University, Gagarin ave., 72, Dnipro, 49010, Ukraine.
Tel.: +38-066-204-32-24.
E-mail: elina.elena5@gmail.com

Motsnyj, M. P., Elina, O. V., Botsva, N. P., & Kochubey, S. O. (2018). Effect of photostimulation on biopotentials of maize leaves in conditions of thermal irritation. Regulatory Mechanisms in Biosystems, 9(3), 347–352. doi:10.15421/021851

Plant biopotentials can be used to evaluate their functional state and mechanisms for adaptation to changes in external conditions of their cultivation. The paper is devoted to the experimental study of the dynamics of total potential of maize leaves caused by cold and heat stimuli on the background of photopotential during continuous light stimulation. In the experiments, a specially designed stimulator was used that allowed simultaneous exposure of the plant to light and to thermal irritation. Studies have shown that background continuous light stimulation with white light with a brightness of 250 lux results in an increase in the amplitude of total action potentials caused by rhythmic cold stimulation. The amplitudes of "cold" potentials grew synchronously with the growth of the potential of hyperpolarization under the influence of photostimulation. With the termination of light stimulation, the amplitude of "cold" potentials stabilized. It is assumed that this effect is due to an increase in the amplitude of potentials of action, which correspond to the total potential due to the hyperpolarization of the membranes of the cells that generate them. Such hyperpolarization is due to an increase in the active transport of H^+ ions through the membrane of cells in the light phase of photosynthesis. It has been shown that during pulsed heat stimulation, the preliminary continuous background light stimulation results in a decrease in the amplitude of "heat" potentials, a reduction in their duration, and the appearance of a short latent hyperpolarization potential in their initial phase. It is established that these changes correlate with the growth of the potential of hyperpolarization caused by background light stimulation. Based on the analysis of the detected changes, it was deduced that an increase in the level of hyperpolarization increases the threshold of excitability of cell membranes generating these potentials. When the photostimulation was switched off, the level of hyperpolarization decreased, but the amplitudes of the "heat" potentials increased. At the same time, the duration of the potentials increased sharply, and the elements characteristic of the variable potentials appeared in them. This may indicate a significant increase in sensitivity to heat irritation with a decrease in the level of hyperpolarization.

Keywords: registration of bioelectric potentials; impulse stimulation; photostimulation; functional state; hyperpolarization, repolarisation.

Introduction

According to researchers, plant biopotentials can be used to evaluate their functional state (Pjatygin et al., 2008; Vodeneev et al., 2016) and mechanisms for adaptation to changes in external conditions of their cultivation (Pjatygin et al., 2006; Volkov et al., 2013b). Changes in environmental parameters affect the morphological and physiological characteristics of plants and consequently alter their electrical activity (Álvarez & Sánchez-Blanco, 2015; Gallé et al., 2015; Vuralhan-Eckert et al., 2018). It is also advisable to assess the adaptability of plants to various stress factors such as deficiency and water solubility, ultra high and extremely low temperatures, insufficient light, high radiation, and electrical conductivity (Bendaly et al., 2016; Lyu & Lazár, 2017). The results of the research show a slowing down of the photosynthesis processes under stress conditions, which together with damage to cell membranes delay the renewal of electrical activity of plants and their normal functioning (Surova et al., 2016).

Over the past decades, a technology has been developed to use modern technical solutions for real-time control and to optimize the influence of external factors on the plants under study. It should also be taken into account that different types of stimulation trigger characteristic electrical signals, each of which has a certain effect on physiological processes (Ríos-Rojas et al., 2014). The use of automated systems for controlling the processes of external exposure to plants (Chernetchenko et al., 2013; Zheng et al., 2015) and quantitative assessment of existing factors with various irritations (Das et al., 2016; Berk et al., 2016; Wijewardana et al., 2016) are very important in understanding the processes of biogenesis of plants.

In today's conditions, the task of finding effective scientific methods for increasing the productivity of agricultural crops is relevant. In this sense, the study of biopotentials caused by light, in particular continuous, stimulation is useful (Trebacz & Sievers, 1998; Chernetchenko et al., 2015). It is also important to use simultaneously other stimuli, such as temperature, including impulse stimulation (Volkov et al., 2013a; Zhou et al., 2014; Tao et al., 2016). Metabolic acclimatization of plants to heat or cold stress affects their development and livelihoods. At the same time, high temperature stress prevents the increase of crop yields, therefore, an understanding of the physiological processes which under adverse temperature conditions negatively affects photosynthesis is important (Lyu & Lazár, 2017; Tao et al., 2016). Adequate stimulation allows for both temperature and light irritation.

Temperature stimulation is convenient for use during experiments; because using thermoelements based on the Peltier effect can be applied to plant tissues dosed with thermostimulants. The duration of these thermostimulants ΔT is determined by the duration of the current pulse through the thermocouple, the change in temperature Δt (°C) – the magnitude of the current in the pulse. The temperature difference is measured by a miniature differential thermocouple.

The application of the described thermostimulation method allows one to change the modulus of the thermo pulse. To do this, it is enough

to change the direction of current through the thermocouple with a simple mechanical switch.

Thermostimulation can be of two types: dose reduction or increase in temperature. In practice, lower temperatures are more often used as less traumatic, because at elevated temperatures, even in a zone of intact temperatures, potentials of action with obvious signs of variable potential are often generated. Temperature stimuli act directly on plasmolma cells, causing changes in its permeability.

Cooling depolarizes the cell membrane, reduces its potential to a threshold level, which leads to the potential of action, while heating in the physiological range increases the membrane potential. The emergence of the action potential occurs when the physiological range is already overheated, and, apparently, is associated with the development of the initial reversal phase of thermal damage. Sometimes, the potential for action in the case of heating occurs also in the physiological range of temperatures, but not at elevated temperatures, and when the temperature decreases to the initial level when the thermometer is switched off, the stimulator. This is most strongly manifested when the current is turned on.

Light stimulation is also adequate, but unlike thermal, the change in leaf illumination does not produce potential for action and is not a reflection of electrical processes in chloroplasts under photosynthesis (Szechyńska-Hebda & Karpiński, 2013; Hasegawa et al., 2016). The stimulation during experiments is quite easy to ask and control its parameters with the help of a luxmetre. As a light source, a light-emitting diode is used which emits light of a known fixed wavelength. Duration of the stimulus ΔT is given by the duration of the current pulse through the light-emitting diode, and the source illumination of the photodiode is the magnitude of the current through it.

The purpose of the work presented here is to study the dynamics of total potential of maize leaves caused by cold and heat stimuli on the background of photopotential during continuous light stimulation.

Materials and methods

Research on biopotentials was carried out on well-developed and prepared maize sprouts (type Spirit H7). The selected maize corn was sown in special containers filled with soil and sprouted in a humid environment. Seedlings were used in experiments in 20–25 days after the emergence of shoots. Experiments were carried out on a universal automated system for the study of plant biopotentials (Fig. 1).

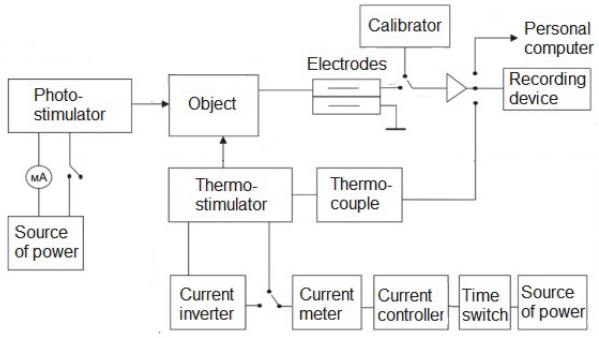

Fig. 1. Block diagram of universal automated system for the study of plant biopotentials

The seedlings in a container with soil were placed in a shielded thermostatted chamber in which a stable temperature of 20 °C was maintained. In the experiment, a special universal stimulator was used, which allowed simultaneously creation of both temperature and light irritating stimuli. To do this, the device for fixing the sheet on the thermostimulator was fitted with a miniature light-emitting diode with a special infrared filter to eliminate the heating of the sheet with an light-emitting diode.

The maize sheet was fixed on the stimulator and non-polarized electrodes applied (EVL-1m). The active electrode was located on the active surface of the thermostimulator and the light-emitting diode of the photostimulator. Thus, the active zone of potential output could simultaneously be subjected to two types of stimulation – continuous light and pulsed thermal. The indifferent electrode is located on the sheet over the stimulation zone. The outputs of the electrodes were connected to the input of the previous amplifier. The signal from its output was fed to the terminals of the Endim recorder and the digitizing device for data processing on the personal computer.

The experimental method was to use dosed pulsed thermal stimuli against the background of light stimulation. Thermopotentials were called with a thermostimulator, and the duration and frequency of thermostimulation were set using a time relay. This thermostimulation method allows one to change the modulus of thermocouples. The required temperature was regulated by the current value via a thermostimulator, which was measured by a digital ammeter. The temperature on the working surface of the thermostimulator was measured using a miniature differential thermocouple.

For light stimulation, a white light with a brightness of 250 lux was used. Amplitude calibration was calibrated by a generator.

Results

In the first series of experiments, changes in the potential of maize leaves caused by rhythmic cold irritations with frequency f = 1/15 Hz were studied. Cold stimuli were used with a temperature difference Δt = –6 °C duration of 5 seconds. A typical result from this series of experiments is shown in Figure 2.

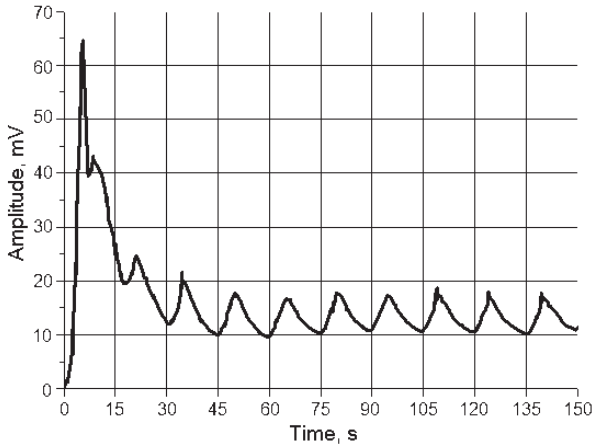

Fig. 2. Potentials of maize leaves at rhythmic stimulation (frequency f = 1/15 Hz) with cold impulses duration of 5 seconds with temperature difference Δt = –6 °C

From Figure 2 it is evident that with this variant of irritation on the maize leaf, action potentials are recorded, the amplitude of which in the interval of 5 to 45 seconds after the start of stimulation drops sharply from 65 to 18 mV and at the 45th second stabilizes at this level.

According to the results of 12 such experiments, the dependence of the amplitude of the "cold" potential on the time between the first and the next cold impulses is obtained (Fig. 3). To reveal general patterns of potential dynamics at different absolute values of amplitudes during construction of this graph, the amplitudes of the potentials were expressed as a percentage of the amplitude of the first response. Based on the results obtained, it is evident that over a period of about 60 seconds, the average response amplitude for rhythmic cold stimuli drops sharply, and then stabilizes at 20% of the amplitude of the first response.

In the second series of experiments for stimulating maize leaves, heat stimuli were used with a temperature difference Δt = 7 °C duration of 5 seconds and two frequencies f_1 = 1/15 Hz and f_2 = 1/30 Hz. Typical results from this series of experiments are shown in Figure 4 and 5, respectively. In the case of heat stimulation, two-phase potentials that have a phase of hyperpolarization and a phase of depolarization are recorded. Figure 4 shows that under conditions of stimulation with frequency f_1 = 1/15 Hz, the phase of hyperpolarization has a maximum of 14 mV at the 5th second, then the potential level passes through zero to the phase of depolarization, which remains until the appearance of the next stimulus.

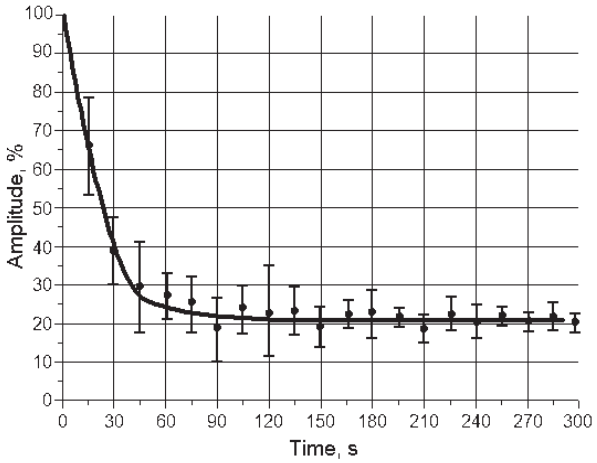

Fig. 3. Dynamics of relative "cold" potential of maize leaves depending on the time between the first and subsequent stimuli (frequency of stimuli f = 1/15 Hz): vertical lines indicate reliable intervals for the average, calculated with a reliability of 0.85

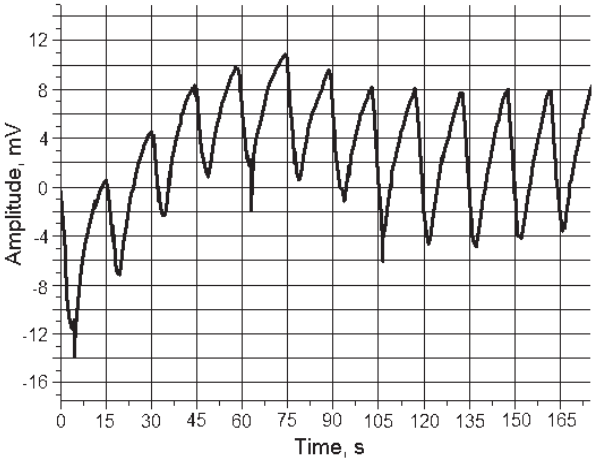

Fig. 4. Potentials of maize leaves at rhythmic stimulation (frequency f_1 = 1/15 Hz) with heat impulses duration of 5 seconds with temperature difference $\Delta t = 7\ ^{o}C$

In Figure 5 it is evident that under conditions of stimulation with frequency f_2 = 1/30 Hz, the phase of hyperpolarization has a maximum of 10 mV. The level of potential reaches zero faster than with stimulateon with frequency f_1 = 1/15 Hz. At the 15th second the amplitude of the depolarization is 4 mV. Potential is stabilized at this level until the next stimulus is irritating.

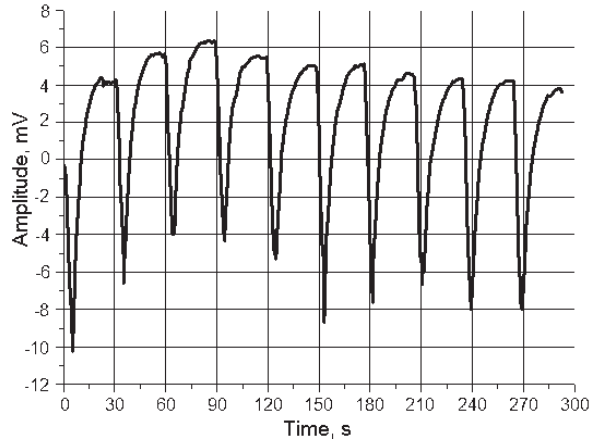

Fig. 5. Potentials of maize leaves at rhythmic stimulation (frequency f_2 = 1/30 Hz) with heat impulses duration of 5 seconds with temperature difference $\Delta t = 7\ ^{o}C$

According to the results of 8 similar experiments with the frequency of stimulation f_1 = 1/15 Hz and 7 experiments with frequency f_2 = 1/30 Hz, the dependences of the relative amplitude of the "heat" potential on the time between the first and subsequent stimulations of heat stimulation were obtained (Fig. 6, 7). The amplitudes of potentials, as in the previous series, were calculated as a percentage of the amplitude of the first response.

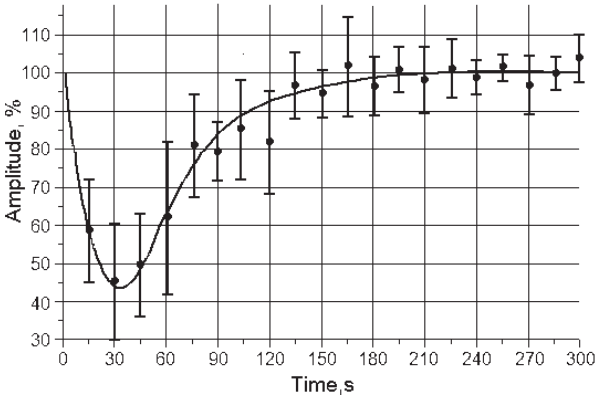

Fig. 6. Dynamics of relative "heat" potential of maize leaves depending on the time between the first and subsequent stimuli (frequency of stimuli f_1 = 1/15 Hz): vertical lines indicate reliable intervals for the average, calculated with a reliability of 0.85

The dynamics of "heat" potentials at the frequency of heat stimuli f_1 = 1/15 Hz is such that the response amplitude after a certain decrease during the first 30 seconds increases again and after 180 seconds stabilizes at the initial level.

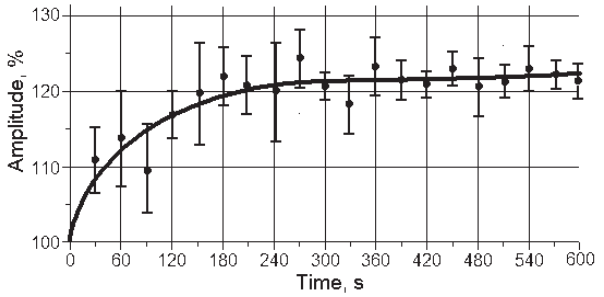

Fig. 7. Dynamics of relative "heat" potential of maize leaves depending on the time between the first and subsequent stimuli (frequency of stimuli f_2 = 1/30 Hz): vertical lines indicate reliable intervals for the average, calculated with a reliability of 0.85

At the frequency of heat stimuli f_2 = 1/30 Hz, the amplitude of the potentials in 180 seconds stabilizes at 120%, and then even more with respect to the amplitude of the first response.

In the next series of experiments, the interaction of the potential caused by the continuous illumination of the sheet with white light with a brightness of 250 lux, with potentials caused by rhythmic cold stimulation with a temperature difference $\Delta t = -5\ ^{o}C$ and duration of 5 seconds was investigated. The rate of decrease of temperature –1 ^{o}C/s. During the experiment, a recorder was started at a speed of 50 cm/s, a photostimulator was turned on, and then cold spots were applied to the sheet at an interval of 60 seconds. One of the typical results of this series of experiments is shown in Figure 8. It is evident that light stimulation leads to the development of a slow photopotential of hyperpolarization, on the background of which are recorded the total potentials of action caused by cold irritation.

On the basis of the obtained data, a plot of the dependence of the amplitude of "cold" potentials on time was constructed (Fig. 9). The duration of the potentials was 30 seconds, the amplitude depends on the time that elapses from the beginning of stimulation to the moment of registration. The analysis of the results shows that the first "cold" response was registered at the background of hyperpolarization at +1.6 mV and is –3.3 mV. The second, caused by the stimulus in 60 seconds, has a minimum amplitude of –2 mV and is recorded at a hyperpolarization

level of +3 mV. With increasing hyperpolarization, the amplitude of the potentials increases and at the moment of switching off the photostimulator (600 seconds) the level of hyperpolarization is +6 mV, and the amplitude of the "cold" biopotential reaches –4 mV. From this it follows that an increase in the level of hyperpolarization leads to an increase in the amplitude of "cold" potentials.

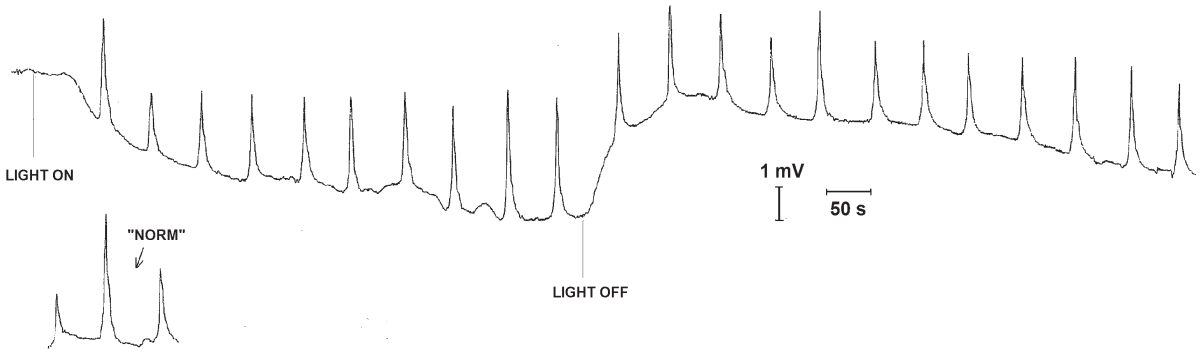

Fig. 8. Dynamics of the amplitude of "cold" potentials caused by rhythmic cold irritations Δt = –5 °C duration 5 seconds against the background of photopotential with continuous light stimulation with white light with illumination of 250 lux

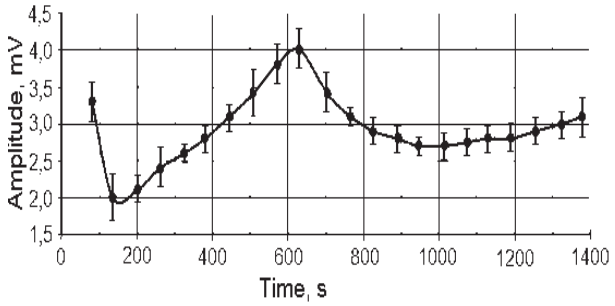

Fig. 9. The dynamics of "cold" potentials of maize leaves depending on the time between the first and subsequent cold stimuli with continuous light stimulation: vertical lines indicate reliable intervals for the average, calculated with a reliability of 0.85

After turning off the photostimulant, a sharp repolarization of the membrane from the level +6 mV to +3 mV was observed. The amplitude of the first recorded after this response is –3.5 mV, and when the level of hyperpolarization reaches a minimum of +1 mV, the amplitude of the response is –3 mV. Starting from the 750th second after the start of stimulation, there is a second wave of increasing hyperpolarization. At the same time, the amplitude of responses increases.

In the next series of experiments, on the background of continuous photostimulation, heat stimulation was used. To do this, the direction of the current was changed through the thermostimulator. The results of one of the typical experiments of this series are shown in Figure 10. From Figure 10 it is evident that at the beginning of photostimulation there is a depolarization phase with a duration of 100 seconds with a maximum of –7 mV at the 70th second, followed by a phase of hyperpolarization. The first response is the potential of depolarization with a duration of 20 seconds with an amplitude of –3 mV against a background of +1 mV hyperpolarization.

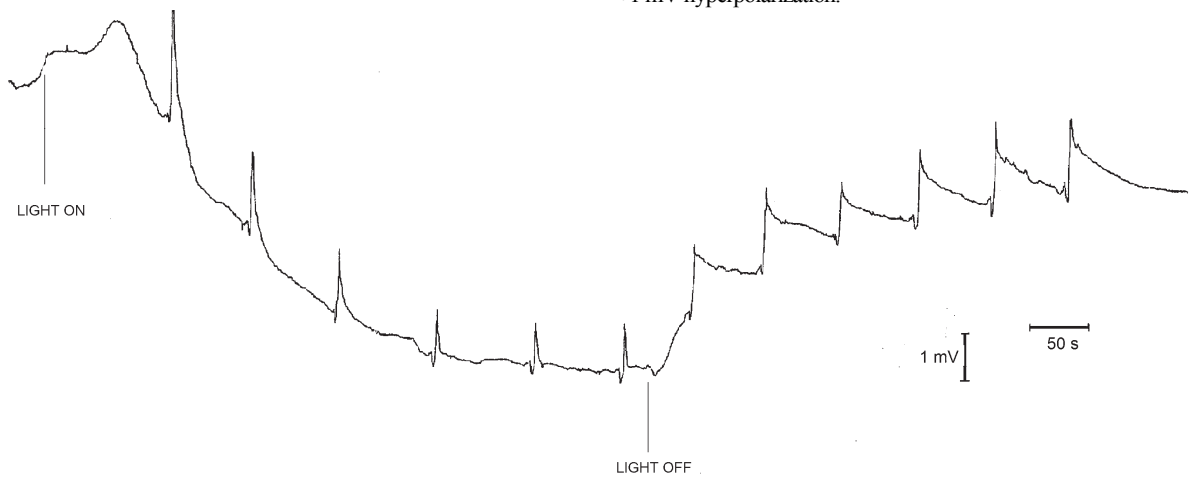

Fig. 10. Dynamics of potentials caused by rhythmic heat stimulation Δt = + 6.5 °C duration 5 seconds, on the background of photopotential with continuous light stimulation with white light with illumination of 250 lux

On the basis of the obtained data, a plot of the dependence of the amplitude of the "heat" potentials on time was constructed (Fig. 11).

With further heat stimuli, the level of hyperpolarization increases, and the potential amplitude decreases. Then, at the 300th second, hyperpolarization stabilizes at +8.5 mV, and the potential amplitude is –1.2 mV. Note that this significantly reduces the duration of the potential up to 10 seconds. After turning off the photostimulator at 500 seconds, rapid repolarization is observed. The first response of the "heat" potential after turning off of the photostimulator (at 560th second) occurs at the background of hyperpolarization at +7 mV and has an amplitude of –1.5 mV. Over time, hyperpolarization decreases, and the potential amplitude increases. By the end of the registration, the level of hyperpolarization is +3 mV, and the amplitude of the potential is –2 mV, respectively.

Note that after turning off the photostimulator in the phase of repolarization, the shape of the potentials changes substantially, their duration is significantly increases (more than 60 seconds) and characteristic features of the variational potential appear.

Discussion

It is known that in the absence of background photostimulation, in particular under these conditions, the first series of experiments were carried out, stabilization of the potential amplitude was observed over time (Pjatygin et al., 2008; Motsnyj et al., 2017). The essence of the stabilization is that the next response falls into the phase of the relative refractoriness of the previous recall. In the presence of continuous light

stimulation, the picture changes substantially, as the background potential causes hyperpolarization of the membrane by increasing the active transport of H^+ ions that occurs during the light phase of photosynthesis. The transformation of energy caused by the active transport of ions is due to the change in the electrical potentials of the membrane of the plant cell (Pjatygin et al., 2008). The obtained results give grounds to assert that the hyperpolarization of the illuminated part of the sheet that was in contact with the active electrode causes the growth of the metabolic component of the membrane potential of the cell against the background of light stimulation. This component is related to the activity of the proton H^+ pump. The total flow of H^+ ions from the intercellular medium to the middle of the cell may be due to the depolarization of the cell caused by the action of light (Pjatygin et al., 2006; Hasegawa et al., 2016; Lyu & Lazár, 2017).

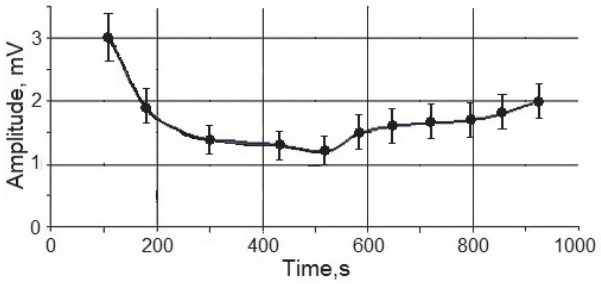

Fig. 11. Dynamics of "heat" potentials of maize leaves depending on the time between the first and subsequent thermal stimuli with continuous light stimulation: vertical lines indicate reliable intervals for the average, calculated with a reliability of 0.85

The results of experiments, however, do not exclude the possibility of absorption of light by chloroplasts, which leads to the activation of zones in plasmolma ion channels penetrating to protons, and can cause a change in pH on the cell surface (Vodeneev et al., 2012).

As is known, increasing the membrane potential leads to an increase in the amplitude of the potential of the action of individual cells, which form the "cold" potential recorded in these experiments (Volkov et al., 2013a). That is why with the increase in the level of hyperpolarization caused by background light stimulation, the total cell potential is also increased due to cold irritation (Álvarez & Sánchez-Blanco, 2015). After turning off the photostimulator, rapid repolarization is observed, which is associated with the inactivation of the active transport of H^+ ions, which leads to a decrease in the registered potentials. This assumption is confirmed by the fact that under the action of the second wave of hyperpolarization (after turning off the photostimulator) the amplitude of the potentials increases again (Pjatygin et al., 2006; Pjatygin et al., 2008).

From the analysis of the data obtained in the last series of experiments, it follows that when using thermal stimuli on the background of light stimulation, the parameters of the obtained potentials are significantly dependent on the temperature difference Δt (°C).

At $\Delta t = +5.0$ °C there is a potential, with the parameter similar to "cold", and at $\Delta t = +7.0$ °C the potential has signs of the variable potential. In our experiments, $\Delta t = +6.5$ °C is used. As we see from Figure 10, when the photostimulator is turned on, pulses are recorded, with parameters similar to "cold", and when the photostimulator is turned off, in the phase of the repolarization, the pulse parameters are similar to the parameters of the variable potentials. This suggests that in the phase of repolarization the cells' sensitivity to thermal irritation is significantly increased.

Hyperpolarization of the membranes leads to the reverse effect. Reducing the amplitude of "thermal" potentials may be due to the fact that the hyperpolarization of membranes leads to an increase in the excitatory threshold of cells that generate the potential of action. As a result, the total amplitude of the potential decreases. In support of this assumption, the decrease in the duration of registered potentials is indicated. We note that with increasing hyperpolarization in the light phase, the amplitude and duration of the positive jump increases in front of the "thermal" potential. This confirms the hypothesis that the potential effect does not occur if the part of the plant's leaf is heated, and when the thermostimulator is turned off, which is consistent with the literature data (Vodeneev et al., 2012).

Thus, the results of the experiments support the existing view that plant cell responses to different physical stimuli are combined (Vuralhan-Eckert et al., 2018) and indicate that maize leaves can process at least two simultaneously applied stimuli.

Conclusions

Studies have shown that background light continuous stimulation leads to an increase in the amplitude of the total action potentials caused by rhythmic cold stimulation. The increase in the amplitude of these potentials occurs synchronously with the growth of the hyperpolarization potential, caused by photostimulation. When the photostimulator is turned off, the amplitude of the potentials is stabilized. This effect may be associated with an increase in the amplitude of potentials due to hyperpolarization of cell membranes. The indicated hyperpolarization can be caused by continuous light stimulation due increasing the active transport of H^+ protons in the light phase of photosynthesis.

During pulsed heat stimulation the background continuous light stimulation results in a decrease in the amplitude of "heat" potentials, a significant reduction in their duration, and the appearance in the initial phase of the short-acting potential of hyperpolarization. The experiments have shown that these changes correlate with the growth of the potential of hyperpolarization, caused by photostimulation.

All of the changes described may indicate that an increase in the level of hyperpolarization leads to an increase in the threshold of excitability of cell membranes, generating these potentials. When the photostimulator is turned off, the level of hyperpolarization decreases and the potential amplitude increases. The duration of potentials in which elements of variable potentials appear also increase. This may be a sign of a significant increase in sensitivity to heat irritation with a decrease in the level of hyperpolarization.

References

Álvarez, S., & Sánchez-Blanco, M. J. (2015). Comparison of individual and combined effects of salinity and deficit irrigation on physiological, nutritional and ornamental aspects of tolerance in *Callistemon laevis* plants. Journal of Plant Physiology, 185, 65–74.

Bendaly, A., Messedi, D., Smaoui, A., Ksouri, R., Bouchereau, A., & Abdelly, C. (2016). Physiological and leaf metabolome changes in the xerohalophyte species *Atriplex halimus* induced by salinity. Plant Physiology and Biochemistry, 103, 208–218.

Berk, P., Hocevar, M., Stajnko, D., & Belsak, A. (2016). Development of alternative plant protection product application techniques in orchards, based on measurement sensing systems: A review. Computers and Electronics in Agriculture, 124, 273–288.

Chernetchenko, D. V., Motsnyj, M. P., Botsva, N. P., Elina, O. V., & Milykh, M. M. (2013). Avtomitizovana systema reestraciy bioelectrichnih potencialiv [Automated experiment for bioelectrical potentials registration]. Visnyk of Dnipropetrovsk University. Biology, Ecology, 21(2), 70–75 (in Ukrainian).

Chernetchenko, D. V., Motsnyj, M. P., Botsva, N. P., & Elina, O. V. (2015). Doslidzhennja fotoindukovanyh potencialiv lystja percju [Research of photoinduced potentials of pepper leaves]. Visnyk of Dnipropetrovsk University. Biology, Ecology, 23(2), 225–229 (in Ukrainian).

Das, S., Ajiwibawa, B. J., Chatterjee, S. K., Ghosh, S., Maharatna, K., Dasmahapatra, S., Vitaletti, A., Masi, E., & Mancuso, S. (2015). Drift removal in plant electrical signals via IIR filtering using wavelet energy. Computers and Electronics in Agriculture, 118, 15–23.

Gallé, A., Lautner, S., Flexas, J., & Fromm, J. (2015). Environmental stimuli and physiological responses: The current view on electrical signalling. Environmental and Experimental Botany, 114, 15–21.

Hasegawa, Y., Murohashi, F., & Uchida, H. (2016). Plant physiological activity sensing by bioelectric potential measurement. Procedia Engineering, 168, 630–633.

Lyu, H., & Lazár, D. (2017). Modeling the light-induced electric potential difference ($\Delta\Psi$), the pH difference (ΔpH) and the proton motive force across the thylakoid membrane in C_3 leaves. Journal of Theoretical Biology, 413, 11–23.

Motsnyj, M. P., Botsva, N. P., Elina, O. V., Chernetchenko, D. V., Sadovskaya, L. Y., & Tykhomyrov, O. Y. (2017). Effect of external lighting on biopotential of maize leaves caused by pulsed temperature stimulation. Regulatory Mechanisms in Biosystems, 8(2), 179–184.

Pjatygin, S. S., Vodeneev, V. A., & Opritov, V. A. (2006). Depoljarizacija plazmaticheskoj membrany kak universal'naja pervichnaja biojelektricheskaja reakcija rastitel'nyh kletok na dejstvie razlichnyh faktorov [Depolarization of the plasma membrane as a universal primary bioelectric reaction of plant cells to the action of various factors]. Uspehi Sovremennoj Biologii, 126(5), 492–502 (in Russian).

Pjatygin, S. S., Opritov, V. A., & Vodeneev, V. A. (2008). Signal'naja rol' potenciala dejstvija u vysshih rastenij [Signal role of the action potential in higher plants]. Fiziologija Rastenij, 55, 312–319 (in Russian).

Ríos-Rojas, L., Tapia, F., & Gurovich, L. A. (2014). Electrophysiological assessment of water stress in fruit-bearing woody plants. Journal of Plant Physiology, 171(10), 799–806.

Surova, L., Sherstneva, O., Vodeneev, V., Katicheva, L., Semina, M., & Sukhov, V. (2016). Variation potential-induced photosynthetic and respiratory changes increase ATP content in pea leaves. Journal of Plant Physiology, 202, 57–64.

Szechyńska-Hebda, M., & Karpiński, S. (2013). Light intensity-dependent retrograde signalling in higher plants. Journal of Plant Physiology, 170(17), 1501–1516.

Tao, Z., Chen, Y., Li, C., Zou, J., Yan, P., Yuan, S., Wu, X., & Sui, P. (2016). The causes and impacts for heat stress in spring maize during grain filling in the North China Plain – A review. Journal of Integrative Agriculture, 15(12), 2677–2687.

Trebacz, K., & Sievers, A. (1998). Action potentials evoked by light in traps of *Dionaea muscipula* Ellis. Plant Cell Physiology, 39, 369–372.

Vodeneev, V. A., Katicheva, L. A., & Sukhov, V. S. (2016). Electrical signals in higher plants: Mechanisms of generation and propagation. Biophysics, 61, 505–512.

Vodeneev, V., Orlova, A., Morozova, E., Orlova, L., Akinchits, E., Orlova, O., & Sukhov, V. (2012). The mechanism of propagation of variation potentials in wheat leaves. Journal of Plant Physiology, 169(10), 949–954.

Volkov, A. G., O'Neal, L., Volkova, M. I., & Markin, V. S. (2013a). Morphing structures and signal transduction in *Mimosa pudica* L. induced by localized thermal stress. Journal of Plant Physiology, 170(15), 1317–1327.

Volkov, A. G., Vilfranc, C. L., Murphy, V. A., Mitchell, C. M., Volkova, M. I., O'Neal, L., & Markin, V. S. (2013b). Electrotonic and action potentials in the Venus flytrap. Journal of Plant Physiology, 170(9), 838–846.

Vuralhan-Eckert, J., Lautner, S., & Fromm, J. (2018). Effect of simultaneously induced environmental stimuli on electrical signalling and gas exchange in maize plants. Journal of Plant Physiology, 223, 32–36.

Wijewardana, C., Henry, W. B., Gao, W., & Reddy, K. R. (2016). Interactive effects on CO_2, drought, and ultraviolet-B radiation on maize growth and development. Journal of Photochemistry and Photobiology B: Biology, 160, 198–209.

Zheng, L., Wang, Z., Sun, H., Zhang, M., & Li, M. (2015). Real-time evaluation of corn leaf water content based on the electrical property of leaf. Computers and Electronics in Agriculture, 112, 102–109.

Zhou, H., Sun, Y., Cheng, Q., Schulze Lammers, P., Damerow, L., Schumann, H., Norton, T., & Wen, B. (2014). *In situ* observation of thermal and hydraulic responses of sunflower stem to cold water irrigation using embedded thermocouples. Computers and Electronics in Agriculture, 109, 195–199.

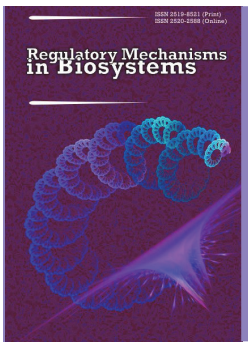

Regulatory Mechanisms in Biosystems

ISSN 2519-8521 (Print)
ISSN 2520-2588 (Online)
Regul. Mech. Biosyst., 9(3), 353–362
doi: 10.15421/021852

Pharmacological correction of the hemostasis system for the surgical treatment of bitches with tumours of the mammary gland

D. D. Bely*, M. V. Rublenko**, S. V. Rublenko**, I. D. Yevtushenko***, N. I. Suslova*, V. V. Samoyuluk*

*Dnipro State Agrarian and Economic University, Dnipro, Ukraine
**Bila Tserkva National Agrarian University, Bila Tserkva, Ukraine
***Kharkiv State Veterinary Academy, Kharkiv, Ukraine

Article info

Received 06.07.2018
Received in revised form 14.08.2018
Accepted 17.08.2018

Dnipro State Agrarian and Economic University, Sergiy Efremov st., 25, Dnipro, 49000, Ukraine.
Tel.: +38-056-713-51-74.
E-mail: info@dsau.dp.ua

Bila Tserkva National Agrarian University, Soborna sq., 8/1, Bila Tserkva, 09100, Ukraine.
Tel.: +38-045-635-12-88.

Kharkiv State Veterinary Academy, Mala Danylivka, 1, Derhachivsky Raion, Kharkiv oblast, 62341, Ukraine.
Tel: +38-057-635-74-23.
E-mail: zoovet@zoovet.kharkov.ua

Bely, D. D., Rublenko, M. V., Rublenko, S. V., Yevtushenko, I. D., Suslova, N. I., & Samoyuluk, V. V. (2018). Pharmacological correction of the hemostasis system for the surgical treatment of bitches with tumours of the mammary gland. Regulatory Mechanisms in Biosystems, 9(3), 353–362. doi:10.15421/021852

We carried out the clinical validation of pathogenetically substantiated protocols for the treatment of female dogs with tumour lesions of the mammary gland. The positive effect of corrective therapy was characterized by a decrease in the physiological level of fibrinogen: in benign tumours in 10 days, malignant – in 14 days against the background of its stable high level in control animals with malignant neoplasia. In the postoperative period in experimental animals, the functioning of the internal coagulation unit was restored, as evidenced by the normalization of the activated partial thromboplastin time for benign tumours by days 10–14, malignant – by 14 days. In control patients, these changes were detected only for benign neoplasms. Shifts of the external mechanism of blood coagulation in the experimental groups were eliminated in benign neoplasia cases in 10 days, malignant cases in 14 days against the background of severe disorders in this link in control patients throughout the observation period. The positive effect of complex treatment regimens is confirmed by the restoration of total fibrinolytic activity by days 10–14 due to the normalization in the same terms of the plasminogen activator and tissue plasminogen activator by days 3–7. In control animals, the total fibrinolytic activity was consistent with those of clinically healthy animals only for benign neoplasms. The balancing of coagulation and fibrinolytic mechanisms was accompanied by a decrease in the activity of proteolytic inhibitors: α_2-macroglobulin in experimental groups with benign neoplasia by day 10, malignant – by days 10–14, and control – respectively, by days 3 and 14; α_1-proteinase inhibitor in all groups by day 3. Concentration of nitric oxide after extirpation of benign tumors already at day 3 of the postoperative period in all groups corresponded to the indexes of clinically healthy dogs, with the removal of malignant tumours – in experimental animals at day 3, control – at day 14. The content of malondialdehyde and ceruloplasmin against the background of pharmacological correction was restored by days 10–14, whereas in control animals – only with benign neoplasms by day 14. Postoperative pharmacological correction of the hemostasis system can significantly improve the results of treatment in cancer patients.

Keywords: neoplasia; electrocoagulation; dogs; low molecular weight heparins; non-steroidal anti-inflammatory drugs; hemostatic status.

Introduction

Currently, among the surgical pathologies of small domestic animals, neoplasia is attracting interest from researchers due to the significant increase in registration and inadequate efficacy in treatment of such cases. This situation is related to the increase in the population of small domestic animals, an increase in the unfavourable impact of the environment, the broad use of hormone preparations and high level of metastasis and recurrence. Tumour diseases are one of the commonest causes of the death of dogs and humans (Bonnett et al., 2005).

The difficulty in solving the problem of increasing the effectiveness of therapeutic measures against neoplasia of the mammary gland is caused by the absence of a unified statistical basis, discussion of the pathogenetic mechanisms of this process and low efficiency of early diagnosis, which does not allow one to form the complete chain of formation, development and subsequent behaviour of the tumour source.

A complicated situation in oncopathology, the level of morbidity, the similarity of nonplastic mechanisms of humans and dogs is established (Shafiee et al., 2013; Fürdös et al., 2015) and requires the united efforts of human and veterinary medicine (Ostrander & Engl, 2012) for coordinating research orientated towards optimizing diagnosis and developing new effective ways of preventing cancer and treating cancer patients (Gardner et al., 2016). Current and previous veterinary records of animals that have been diagnosed with neoplasms of various tissues and organs are few and not systematized. Different inclusion criteria, different methods of collecting and assessing create obstacles for the analysis of available information (Brønden et al., 2007).

At the same time, the most commonly used combination regimen for treating neoplasia, including mammary cancer in dogs, is treatment using a combination of surgical removal and adjuvant and non-adjuvant chemotherapy (Tripp et al., 2011; Leach et al., 2012; Khanna et al., 2015) which, even with the use of modern metronomic protocols, is accompanied by a toxic response of the body (Heading et al., 2011; Marchetti et al., 2012), while the levels of metastasis and relapse remain quite high – within 20–50% (Sarrau et al., 2007).

The research on changes in the blood of animals with cancer only focuses on particular clinical and biochemical blood parameters (Grandi et al., 2016) without analyzing their diagnostic significance in mechanisms of carcinogenesis. Detected relationships between the clinical signs (Sorenmo et al., 2009), pathomorphic (Gundim et al., 2016), cellular, immunohistochemical structures (Beha et al., 2012) and malignancy do not allow us to fully reveal the mechanisms of development and progression of the neoplastic process. At the same time, it has been proved that the main cause of death of animals with tumours is the metastasis

and thrombosis which accompanies it (Khamis et al., 2012). According to the various statistics, tumour of the mammary gland of dogs is the second commonest among all neoplasms, being recorded on average in 31.9–39.9% of cases, even reaching 52% and 56% (Eierskyte et al., 2011; Abdullah et al., 2014).

Currently, a number of studies focus on the search for an alternative way of influencing neoplasms, which, in combination with surgical intervention, would reduce the possibility of relapse and metastasis. One of the possible directions, considering the role of hemostasis in oncogenesis (Levine et al., 2005; Boccaccio et al., 2006), is influencing the mechanisms of blood coagulation, which would minimise the unfavourable effect of tumour extirpation on hemostasis status and help improve the treatment outcomes.

Thus, the wide distribution of mammary tumours of dogs in the conditions of the tendency to increase in number of cases recorded, discussion of the issues of etiology and pathogenesis, and insufficient effectiveness of therapeutic measures give relevance to and justify the need to study the role of hemostasic status in the mechanisms of tumour development in order to improve diagnostic approaches and optimize antithrombotic therapy for this pathology.

The objective of the study is to assess the effectiveness of pharmacological correction of hemostasic systems, which follows the electrocoagulation of mammary tumours of female dogs.

Material and methods

The research was conducted at the Department of Surgery and Obstetrics of Farm Animals of the Dnipro State Agrarian and Economic University and the Department of Surgery and Animal Diseases of the Bila Tserkva National Agrarian University. Monitoring of oncological morbidity among dogs was carried out during 2010–2017 on the basis of veterinary hospitals under different forms of ownership in the city of Dnipro, other cities, district centers and villages of Dnipropetrovsk Oblast.

Out of the dogs with mammary tumours, two experimental and one control groups were formed, which included 7–10 year old females with single tumours of the mammary gland of the 2nd ($T_2N_0M_0$) and 3rd ($T_3N_0M_0$) stages: the size of the growths was 5–10 cm in the absence of metastases in the regional lymph nodes and distant tissues. At the same time, 40 animals were included in each experimental group, 20 of which were diagnosed with benign tumours, and 20 – malignant neoplasias, and in the control – 32 patients with benign (n = 16) and malignant (n = 16) tumours of the mammary gland.

Removal of mammary growths of all of the patients was performed electrosurgically, using an EC-150 electrocoagulator. Unlike the control animals, dogs from the experimental groups, from the second day were prescribed corrective therapy which included: roncoleukin (subcutaneously, in a dose of 15,000 OD/kg, 5 injections at 24 hours intervals) and trannexes (intravenously, at a dose of 15 mg/kg, 2 times/day for 10 days) that were combined for the patients of the first experimental group with nonsteroidal anti-inflammatory preparations (acelizin – intramuscularly, in a dose of 20 mg/kg, 2 times/day for 10 days), the second experimental group – with low molecular weight heparins (phenotype – subcutaneously, in a dose of 1.5 mg (1500 anti-Xa MO)/kg once a day over 10 days).

The efficacy of the treatment protocols was determined by the dynamics of biochemical and hemostac parameters of blood prior to the surgical intervention and in the postoperative period on the 3, 7, 10, 14th days.

The coagulation potential of blood plasma was determined by the content of fibrinogen (Belicer et al., 1997) and its metabolite – soluble fibrin (Vareckaja et al., 1992), during activated partial thromboplastin time (a set of reagents manufactured by the company "Simko LTD ", Lviv). The state of the fibrinolysis system was investigated using the method of fibrin plates according to Astrup & Millertz (1952), with the definition of total fibrinolytic activity of blood plasma, plasmin activity and tissue plasminogen activator activity, by the lysis area (mm2) of the fibrin blood clot.

The inhibitory potential of the blood was determined by the content of α_1-proteinase inhibitor and α_2-macroglobulin in the plasma (Veremeenko et al., 1978).

In the blood plasma or serum, we determined the content of the total protein by the biuretic reaction using a set of reagents manufactured by the "Reagent" company, the content of albumin – by the reaction with bromocresol green, the content of ceruloplasmin – using the method of Ravin, malonic dialdehyde (Andreeva, 1988), and nitric oxide (Golikov, 2004).

The statistical analysis of the results was carried out using the Statistica 10 program (StatSoft Inc., USA, 2011). The reliability of the differences between the samples was determined using ANOVA, considered significant at $P < 0.05$.

Results

Monitoring research included a survey of 10,118 dogs, including 1,063 cancer patients with various clinical and pathomorphological forms of mammary gland neoplasia.

In the comparative analysis of the prevalence of mammary tumours of dogs in conditions of industrial cities, district centers and rural areas of Dnipropetrovsk Oblast (Table 1), it was found that the lowest level of occurrence of mammary tumours was recorded in villages: they were diagnosed in every fifth cancer patient. In district centers which are represented by small towns or urbanized settlements and in the city of Dnipro, neoplastic growths in the mammary gland were detected in every third dog of the total number of animals with tumours. At the same time, the frequency of neoplastic lesions of the mammary gland in ecologically polluted cities (Kamianske, Kryvy Rih, Marhanets, Zhovti Vody) reached 42%. This difference in the latter case occurs due to the unfavourable impact of environmental factors. At the same time, it should be mentioned that the relatively low level of detection of mammary neoplasia in rural areas is conditioned by the low frequency of contacting veterinary hospitals, and in the conditions of the city of Dnipro – the prevalence of sterilization measures, including an intensive programme of sterilization of homeless animals.

Table 1
Monitoring of tumour lesions of female dogs in Dnipropetrovsk region (%)

Characteristics	Dnipro	Environmentally polluted cities*	District centers	Villages
Tumors, all	100	100	100	100
Neoplasia of the mammary gland	29	42	30	20

Note: *– Kamianske, Kryvy Rih, Marhanets, Zhovti Vody.

Comparative morphological analysis of pathological material (Table 2) indicates a significant prevalence of malignant neoplasia over benign neoplasia among dogs in industrial, environmentally polluted cities (the ratio is 2.5 : 1). A similar situation, but with a smaller difference, was recorded in the villages (1.4 : 1) in the absence of a pronounced difference in the district centers (1.1 : 1), while in the city of Dnipro, benign neoplasms (1 : 1.2) prevail. Other clinical parameters were similar and independent of the area where the animals lived: the fifth pair of mammary glands was the most often affected (33% of cases), the fourth pair – more rarely (21%), and also the third (19%) and the second (18%). Only 9% of animals were diagnosed with tumour process in the first pair of mammary glands. At the same time, multiple lesions were recorded for benign neoplasms in 21% of dogs, malignant – only in 8%.

Table 2
Prevalence of breast tumours in dogs in different regions of Dnipropetrovsk region (%)

Breast tumours	Dnipro	Environmentally polluted cities*	District centers	Villages
Benign	54	29	47	41
Malignant	46	71	53	59
Together	100	100	100	100

Note: *– Kamianske, Kryvy Rih, Marhanets, Zhovti Vody.

Studies on the hemostastic status of animals with tumours allowed us to identify certain patterns that reflect the adverse effect of the tumour

on the system of coagulation and fibrinolysis and the corresponding protective response of the organism (Table 3). In most cases, they are characterized by increased blood coagulation following the inhibition of its lysis, which indicates the development of DIC-syndrome. In particular, we recorded excessive accumulation of fibrinogen, soluble fibrin, shortening of activated partial thromboplastin time, decrease of total fibrinolytic activity following the increase in the level of its inhibitors (α_1-inhibitor of proteases and α_2-macroglubulin) and increased nitrogen oxide content. These changes were manifested more clearly in cases of malignant neoplasm. At the same time, it should be mentioned that there were significant fluctuations in the markers which reflect the extent of imbalance in the processes of blood coagulation and lysis, their different vector orientation, and in some cases – the lack of changes compared to the clinically healthy animals.

Table 3

Hemostatic status of female dogs with tumours of the mammary gland (x ± SD)

Indicator	Clinically healthy (n = 30)	Tumours	
		benign (n = 35)	malignant (n = 35)
Fibrinogen, g/l	2.20 ± 0.12	2.62 ± 0.15*	5.09 ± 0.19***•••
Soluble fibrin, mg/100 ml	0	30.73 ± 4.17***	49.87 ± 5.22***••
Activated partial thromboplastin time, s	46.13 ± 1.35	46.08 ± 5.16	69.53 ± 4.82**••
Total fibrinolytic activity, mm^2	607.76 ± 22.85	482.69 ± 40.19**	417.42 ± 36.24**
Plasma activator, mm^2	284.42 ± 11.61	214.86 ± 21.25**	241.80 ± 19.09**
Tissue plasminogen activator, mm^2	323.34 ± 25.24	267.83 ± 23.17*	175.62 ± 16.95**••
α_1- proteinase inhibitor, µmol/l	78.62 ± 1.93	89.80 ± 7.53*	105.89 ± 8.19**•
α_2-macroglobulin, g/l	1.43 ± 0.05	1.72 ± 0.21*	2.25 ± 0.07***•
Nitric oxide, µmol/l	32.19 ± 1.82	29.74 ± 4.03	42.85 ± 4.89**••

Note: * – P < 0.05, ** – P < 0.01, *** – P < 0.001 compared to clinically healthy dogs; • – P < 0.05, •• – P < 0.01, ••• – P < 0.001 with respect to indicators in females with benign tumours.

Regardless of the structure of the neoplastic tissue, the tumour process caused excessive accumulation of fibrinogen. In cases of the malignant course, the fibrinogen level in the blood was over 3.3 g/l (1.5 times more than the physiological index) in 93% of the animals, and with benign tumours of the mammary gland – in 68% of patients. The absence of changes in this marker was determined for malignant neoplasia of the mammary gland in 6%, for benign tumours – in 3% of bitches. Thus, the main characteristic of the malignant course is the excessive accumulation of fibrinogen in the blood of 80% of patients when a significant difference obtained (P < 0.01) compared to the clinically healthy animals and dogs with benign tumours.

In correlation with fibrinogen, the early phase of hypercoagulative process and the degree of expression of inflammation during tumours characterizes the content of soluble fibrin, which in an absolute majority of cases exceeded the parameters of clinically healthy animals. However, the wide range of fluctuations in the concentration of soluble fibrin in the blood should be mentioned: 2.0 to 97.5 mg/100 ml in the cases of malignant tumours, 1.3 to 58.1 mg/100 ml – with benign tumours. The averages determined allow one to assume a statistically higher level of soluble fibrin in bitches with malignant lesions of the mammary gland (P < 0.01).

The obtained results indicate that with benign growths, no dissolved fibrin was found in the blood of 20% of the dogs, while with malignant tumours, its content was over the norm in all cases. Thus, the content of soluble fibrin correlates with fibrinogen, indicating the presence of hypercoagulative changes and determining the level of malignancy of the neoplasia process.

The mean values of the activated partial thromboplastin time, which characterizes the internal and general cascade of the blood coagulation system, allows us to estimate the initial stage of coagulation – the formation of thromboplastin indicates its lengthening in the case of malignant neoplasms (P < 0.01) and the absence of clearly manifested changes in benign tumours in the conditions of the statistical difference between the groups depending on the malignancy of the lesion (P < 0.01). The duration of the activated partial thromboplastin time among all patients significantly differed from the physiological parameters with the fluctuation of parameters in a wide range.

In cases of malignant neoplasia, the prolongation and shortening of this marker were observed in approximately the same number of cases (51% and 49% respectively), and in cases of benign tumours, a typical feature was the prevalence of the number of animals in which this indicator had a reduced duration (71% vs 29%). It was determined that the borders of the fluctuations of this indicator were: 30.7–106.1 s for malignant neoplasms, 28.7–89.3 s – for benign tumours.

The results of the study of the state of the fibrinolytic element of the hemostasic system in animals with mammary tumours indicate a decrease in its activity in patients of both groups (P < 0.01) due to plasmin activity (P < 0.05) and tissue plasminogen activator (P < 0.05) following the statistical difference between malignant and benign tumors only in the parameters of tissue plasminogen activator (P < 0.01). Regardless of the morphological structure of the tumours, in the vast majority of cases, the inhibition of the level of total fibrinolytic activity was observed: 88.9% for benign tumours, 82.9% – malignant tumours at fluctuations within 50% from the physiological parameters.

In animals with tumours of the mammary gland, an increase in the proteolytic activity of the blood was recorded. The analysis of the results allowed us to determine a reliable difference between the mean levels of α_1-proteinase inhibitor and α_2-macroglobulin in female dogs with benign (P < 0.05) and malignant (P < 0.01) mammary tumours and clinically healthy animals. Moreover, the activity of these inhibitors of proteolysis was statistically higher in the patients with a malignant process (P < 0.05).

The examination of the oxidative system of the dogs with mammary tumours revealed a statistically significant difference in the nitrogen oxide content between the clinically healthy animals and the patients with malignant lesions (P < 0.01). At the same time, in the cases of the benign neoplastic process, the average content of its stable metabolites did not differ significantly from the physiological parameters, although some animals were observed to have a reduction to 23.7 µmol/l and increase to 43.5 µmol/l in nitric oxide concentration.

Thus, the study of the hemostatic status of female dogs with spontaneous tumours of the mammary gland has revealed that during the development of neoplasia, metastasis of tumour cells, a certain dynamic occurs in the ratios of procoagulant, anticoagulant mechanisms and system of fibrinolysis, which determine the prognostically unfavourable background for this pathology.

The need for pharmacological correction in dogs with mammary tumours is conditioned by the following facts:

– insufficient effectiveness of surgical intervention;

– disorders in the coagulation and fibrinolytic links of hemostasis;

– proven significance of hemostasis mechanisms in the pathogenesis of tumour growth and progression;

– absence of normalization of indicators of coagulation and lysis of blood 14 days after removal of neoplasia.

Therefore, subsequent research focused on determining the effectiveness of correction of mechanisms of hemostasis after using EC-150 electrocoagulator for this pathology.

The practical testing of the developed schemes was evaluated, first of all, by the change in the concentration of fibrinogen (Table 4), which reflects the level of disorders in coagulation mechanisms and the intensity of the inflammatory reaction (as an osteophatic protein).

The content of this marker in the blood of dogs after the removal of benign tumours and the corrective therapy, in contrast to the samples of the control animals, during the first 7 days was at the preoperative level.

From the 10th day, the normalization of the fibrinogen content was recorded in all groups of patients. Thus, the main determined differences are related to the first week after the surgical intervention. They manifested in the fact that in this period of time, the females of the control group had a significantly decreased concentration of fibrinogen in relation to both clinically healthy dogs and to primary parameters ($P < 0.01$). At the same time, in the animals of the experimental groups this indicator remained significantly higher than the physiological norms, not significantly differing from the level of this marker among the dogs with tumours.

Changes in the concentration of fibrinogen in the patients with extirpation of malignant neoplasia were similar, but with certain peculiarities. In particular, the restoration of its level occurred only in the cases of using the corrective schemes for 14 days after surgery. It should be mentioned that the dynamics of this indicator did not depend on the prescribed correction scheme. The dynamics of the level of accumulation of soluble fibrin in the blood are confirmed by the influence of the proposed protocols of the pharmacological correction of the hemostasis system on the coagulation level.

Table 4

Dynamics of fibrinogen for pharmacological correction in bitches with tumours of the mammary glands (g/l, x ± SD)

Period of observation, day	Group		
	control (n = 32) coagulator	first experimental (n = 40) coagulator + non-steroidal anti-inflammatory drugs	second experimental (n = 40) coagulator + low molecular weight heparins
Clinically healthy	2.20 ± 0.12		
Benign tumours			
Before surgery	2.62 ± 0.15*		
3	1.28 ± 0.08***	3.07 ± 0.44*••	2.95 ± 0.41*••
7	1.43 ± 0.16*	2.87 ± 0.38*••	2.77 ± 0.29*••
10	2.05 ± 0.11	2.35 ± 0.26	2.52 ± 0.32
14	2.47 ± 0.14	2.24 ± 0.51	2.47 ± 0.17
Malignant neoplasms			
Before surgery	5.09 ± 0.19**		
3	1.17 ± 0.06***	3.00 ± 0.31*••	3.09 ± 0.51*••
7	1.31 ± 0.17***	2.92 ± 0.42*••	2.87 ± 0.38*••
10	1.52 ± 0.14**	2.53 ± 0.29••	2.64 ± 0.42•
14	1.89 ± 0.13*	2.26 ± 0.33	2.38 ± 0.46

Note: see Table 3.

The analysis of the concentration of soluble fibrin in the blood of patients after the removal of mammary tumours and prescription of preparations for correcting the hemostasis system, regardless of the malignancy of the process was characterized by the following features (Table 5). In all groups, the excess accumulation of the mentioned marker, was conditioned by the presence of neoplasia; after its extirpation, a gradual decrease in its level occurred. However, both in cases of benign and malignant tumours, conducting only surgical intervention was not enough for restoring the parameters of the content of soluble fibrin during 14 days: it exceeded the parameters of clinically healthy dogs by two times.

Combining electrosurgical excision of neoplasms with directed pharmacological therapy allowed us to maximally approximate its concentration to the parameters of clinically healthy animals. At the same time, the dynamics of the level of soluble fibrin in the experimental groups did not differ significantly. Particularly, the prescription of nonsteroidal anti-inflammatory preparations and low molecular weight heparins allowed reduction in the content of this marker in cases of benign tumours to 0.3–0.4 mg/100 ml, and to 0.9–1.0 mg/100 ml – in cases of malignant tumours. That is, the patients who were prescribed pharmacological correction of hemostatic status in the postoperative period were observed to have a significantly lower level of soluble fibrin in the blood compared to the control animals, whereas no significant difference occurred between the experimental groups.

Analysing the results obtained (Table 6), we can assess the effectiveness of the developed correction courses for benign neoplasia of the mammary gland: the normalization of the level of soluble fibrin indicates the bringing of blood coagulation and fibrinolysis into balance. Thus, the research conducted has confirmed the effectiveness of the schemes of complex pharmacological correction in dogs with tumour lesions of the mammary gland, which was reflected in the normalization of the concentration of fibrinogen and soluble fibrin in the blood, which are markers of hypercoagulative disorders of the hemostasis system. In this case, it would be logical to assume a mediation (through the mechanisms of blood coagulation and lysis) optimization of the course of healing of surgical wounds, as well as the reduction of the risk of postoperative complications: both local inflammatory purulent, and also possible relapse and metastasis complications.

Table 5

Influence of pharmacological correction on the content of soluble fibrin in bitches after extirpation of mammary gland neoplasia (mg/100 ml, x ± SD)

Period of observation, day	Group		
	control (n = 32) coagulator	first experimental (n = 40) coagulator + non-steroidal anti-inflammatory drugs	second experimental (n = 40) coagulator + low molecular weight heparins
Before surgery	0		
Benign tumours			
Before surgery	30.73 ± 4.17***		
3	5.41 ± 0.39***	2.35 ± 0.24***•••	2.81 ± 0.43***••
7	4.08 ± 0.27***	1.98 ± 0.35***••	1.57 ± 0.36***•••
10	2.39 ± 0.16***	1.49 ± 0.22***••	0.81 ± 0.12***•••
14	2.12 ± 0.19***	0.32 ± 0.21*••	0.34 ± 0.25*••
Malignant neoplasms			
Before surgery	49.87 ± 5.22**		
3	7.19 ± 0.52***	4.85 ± 0.69***••	3.23 ± 0.16***•••
7	6.18 ± 0.33***	3.42 ± 0.56***••	2.15 ± 0.67***•••
10	4.59 ± 0.24***	2.08 ± 0.31***•••	1.64 ± 0.24***•••
14	3.01 ± 0.27***	0.85 ± 0.32*••	0.94 ± 0.47**••

Note: see Table 3.

Table 6

Change in activated partial thromboplastin time after extirpation of breast cancer neoplasia in dogs (s, x ± SD)

Period of observation, day	Group		
	control (n = 32) coagulator	first experimental (n = 40) coagulator + non-steroidal anti-inflammatory drugs	second experimental (n = 40) coagulator + low molecular weight heparins
Clinically healthy	46.13 ± 1.35		
Benign tumours			
Before surgery	46.08 ± 5.16		
3	35.24 ± 1.94**	31.67 ± 1.53***	34.54 ± 5.21*
7	33.15 ± 1.22***	36.05 ± 3.81*	38.27 ± 4.03*
10	37.28 ± 1.61**	40.21 ± 3.24*	42.82 ± 3.45•
14	43.99 ± 2.17	44.53 ± 3.89	43.41 ± 4.98
Malignant neoplasms			
Before surgery	69.53 ± 4.82**		
3	25.25 ± 1.16***	24.13 ± 2.63***	36.50 ± 2.38*••
7	23.05 ± 0.97***	27.23 ± 1.98***•	37.89 ± 2.47*••
10	29.52 ± 0.96***	33.60 ± 2.85**	39.67 ± 3.04*••
14	38.74 ± 0.78**	41.27 ± 3.12	40.05 ± 3.31

Note: see Table 3.

The study of the duration of activated partial thromboplastin time in animals which were prescribed postoperative corrective therapy indicates a greater efficacy of the pharmacological course which included low molecular weight heparins, regardless of the structure of the neoplasia.

The dogs after extirpation of benign tumours were observed to experience normalization of the duration of activated partial thromboplastin time in the control and the first experimental groups on the 14th day of the postoperative period, and in the second experimental group – on the 10th day. Indicators of the duration of activated partial thromboplastin time in females after the removal of malignant neoplasia differed significantly between the groups depending on the protocol used for correction. After 14 days, in the animals of the control group the activated

partial thromboplastin time was accelerated ($P < 0.05$), and a stabilization of this marker was recorded with the experimental animals, both in the cases of prescription of non-steroidal anti-inflammatory preparations and low molecular weight heparins.

It should be mentioned that during the first 10 days after the surgical intervention in dogs with malignant neoplasms, the parameters of the second experimental group significantly differed from those of the first experimental ($P < 0.05$) and the control group ($P < 0.01$). The duration of activated partial thromboplastin time in patients which were prescribed low molecular weight heparins was statistically higher ($P < 0.05$) compared to animals prescribed nonsteroidal anti-inflammatory preparations. Thus, the postoperative period was characterized by shortened activated partial thromboplastin time in all animals with a subsequent tendency of prolongation. Regarding the normalization of this marker, the best results were obtained when low molecular weight heparins were added to the pharmacological correction course, although the advantage was not significant.

The dynamics of the total fibrinolytic activity of blood after the excision of mammary tumours of dogs the confirms the feasibility of the corrective therapy (Table 7). Reduced intensity of proteolytic mechanisms, even after removal of tumorrs, restores in two weeks only in cases of benign tumours. Prescribing preparations for correcting the hemostasic system allows its activity to be restored. After introducing low molecular weight heparins, these changes were observed on the 10th day in cases of benign neoplasias, and on the 14th day – in cases of malignant tumours; with use of nonsteroidal anti-inflammatory preparations – on the 14th day in both cases.

It should be mentioned that the total fibrinolytic activity in patients of the control group was significantly lower than the corresponding parameters in the experimental groups in cases of benign tumours on the 7th and 10th days of monitoring, and on the 3d, 10th and 14th days – in cases of malignant tumours ($P < 0.05$).

The disorders among different elements of the hemostasis system which were found in the previous studies, particularly disorders in the levels of proteinase inhibitors, indicate a high risk of hemocoagulation complications, therefore prescribing postoperative corrections is necessary. Therefore, we studied the dynamics of their changes in the case of using low molecular weight heparins and nonsteroidal anti-inflammatory agents after usage of EC-150 electrocoagulator.

Table 7

Influence of pharmacological correction
on total fibrinolytic activity of blood in oncopatients (mm^2, x ± SD)

Period of observation, day	Group		
	control (n = 32) coagulator	first experimental (n = 40) coagulator + non-steroidal anti-inflammatory drugs	second xeperimental (n = 40) coagulator + low molecular weight heparins
Clinically healthy		607.76 ± 22.85	
Benign tumours			
Before surgery		482.69 ± 40.19**	
3	409.58 ± 17.15***	458.21 ± 36.97**	418.13 ± 18.29***
7	412.72 ± 19.38***	509.16 ± 27.39**••	496.32 ± 37.04**•
10	484.29 ± 23.03**	548.67 ± 30.52*•	597.45 ± 23.16••
14	590.03 ± 25.12	614.93 ± 29.34	609.15 ± 20.47
Malignant neoplasms			
Before surgery		417.42 ± 36.24**	
3	372.21 ± 21.15***	420.91 ± 28.67***•	473.68 ± 28.94**••
7	488.34 ± 16.59**	529.14 ± 30.51*	517.62 ± 23.42**
10	443.56 ± 29.25**	553.48 ± 21.84*••	548.96 ± 24.53*••
14	491.38 ± 15.87**	603.62 ± 24.63••	618.92 ± 31.05••

Note: see Table 3.

Unlike the patients in the control group, whose treatment measures consisted of extirpating tumours using the electrosurgical technique, the postoperative period in the case of prescribing the corrective therapy, the content of α_2-macrogluculin did not significantly change during the first seven days (Table 8), exceeding the parameters of the clinically healthy dogs on average by 50–70%. Later, the concentration of this marker decreased to the physiological level. The exceptions were females with malignant tumours, which were prescribed low molecular weight heparins (these changes were observed after ten days).

Table 8

Influence of different courses of treatment
of mammary tumours on the level of α_2-macroglobulin (g/l, x ± SD)

Period of observation, day	Group		
	control (n = 32) coagulator	first experimental (n = 40) coagulator + non-steroidal anti-inflammatory drugs	second experimental (n = 40) coagulator + low molecular weight heparins
Clinically healthy		1.43 ± 0.05	
Benign tumours			
Before surgery		1.72 ± 0.21*	
3	1.28 ± 0.11	2.16 ± 0.52*•	2.24 ± 0.34*•
7	1.37 ± 0.05	1.97 ± 0.36*•	2.05 ± 0.49*•
10	1.39 ± 0.04	1.63 ± 0.21	1.65 ± 0.22
14	1.42 ± 0.06	1.20 ± 0.34	1.41 ± 0.15
Malignant neoplasms			
Before surgery		2.25 ± 0.07**	
3	1.24 ± 0.02**	2.14 ± 0.37*•	2.84 ± 0.67*•
7	1.27 ± 0.05*	1.98 ± 0.19**••	2.43 ± 0.45*•
10	1.19 ± 0.04*	1.52 ± 0.21•	2.06 ± 0.38*•
14	1.36 ± 0.05	1.33 ± 0.12	1.98 ± 0.46•

Note: see Table 3.

Also, we should mention a statistically significant difference between the parameters of the experimental groups and control: on the third and seventh day ($P < 0.05$) among the dogs with benign tumours, and on the 3–10th day ($P < 0.05$) in cases of malignant tumours, and also on the 14th day ($P < 0.05$) in cases of using low molecular weight heparin.

The function of inhibiting the invasion and metastasis of tumours by limiting the activity of proteolytic enzymes is carried out by proteolytic inhibitors. Despite the manifested changes in the α1-proteinase inhibitor in female dogs with mammary tumours, indeed only surgical intervention using an electrocoagulant (control) resulted in its restoration to the physiological level, starting from 3d day of the postoperative period (Table 9). Reduction of the intensity of proteolytic reactions in the organism as a result of removing the neoplasias, which synthesize a wide range of matrix metalloproteinases and different groups of cathepsins necessary for infiltration of tumour tissue, promotion of the invasion and metastasis, led to obtaining similar results after combining electrosurgical technique and pharmacological correction. At the same time, there was no statistically significant difference between the groups.

Table 9

Dynamics of activity of α_1-inhibitor of proteinases
in dogs with growths in the mammary glands (μmol/l, x ± SD)

Period of observation, day	Group		
	control (n = 32) coagulator	first experimental (n = 40) coagulator + non-steroidal anti-inflammatory drugs	second experimental (n = 40) coagulator + low molecular weight heparins
Clinically healthy		78.62 ± 1.93	
Benign tumours			
Before surgery		89.80 ± 7.53*	
3	75.08 ± 6.15	82.16 ± 5.48	83.81 ± 5.62
7	79.22 ± 7.26	83.09 ± 7.14	80.94 ± 6.23
10	88.09 ± 4.21	87.27 ± 7.53	84.51 ± 4.64
14	85.38 ± 4.53	81.11 ± 5.61	86.62 ± 4.77
Malignant neoplasms			
Before surgery		105.89 ± 8.19**	
3	80.35 ± 4.19	77.35 ± 4.92	80.43 ± 2.70
7	71.02 ± 6.55	84.19 ± 7.68	81.26 ± 9.12
10	79.82 ± 6.17	76.16 ± 5.86	84.33 ± 6.98
14	82.91 ± 4.83	83.40 ± 7.27	83.23 ± 5.08

Note: see Table 3.

During the study of the level of oxidative stress, which is an integral part of the neoplasia process, in cases of using different approaches to the treatment of this pathology, it was determined that the best results were

obtained after using a combination operative-conservative course which included excision of neoplasms followed by prescription of a pharmacological correction (Table 10).

Table 10
Level of accumulation of malondialdehyde
in patients after removal of mammary tumour (μmol/l, x ± SD)

Period of observation, day	Group		
	control (n = 32)	first experimental (n = 40)	second experimental (n = 40)
	coagulator	coagulator + non-steroidal anti-inflammatory drugs	coagulator + low molecular weight heparins
Clinically healthy	9.8 ± 0.4		
Benign tumours			
Before surgery	14.5 ± 0.5**		
3	16.4 ± 0.3***	17.2 ± 0.2***	15.9 ± 0.4***
7	15.1 ± 0.2**	12.4 ± 0.3**••	13.6 ± 0.3**
10	12.2 ± 0.3**	10.6 ± 0.2•••	12.4 ± 0.3*
14	9.3 ± 0.5	11.2 ± 0.4	9.9 ± 0.5
Malignant neoplasms			
Before surgery	21.0 ± 0.7***		
3	23.5 ± 0.6***	23.6 ± 0.5***	24.6 ± 0.4***
7	17.1 ± 0.5***	19.8 ± 0.2***••	21.2 ± 0.6***••
10	13.0 ± 0.3**	15.1 ± 0.4**••	14.7 ± 0.3**••
14	12.1 ± 0.3**	10.8 ± 0.3•••	10.5 ± 0.2•••

Note: see Table 3.

Prescribing nonsteroidal anti-inflammatory agents led to normalization of the mechanisms of peroxidation of lipids in benign tumours on the 10th day of monitoring, and on the 14th day in malignant tumours. Using low molecular weight heparins caused the normalization of the level of malondialdehyde in blood on the 14th day irrespective of the pathomorphological type of neoplasm.

At the same time, the control dogs with benign neoplasms had the stabilization of the content of the products of lipid peroxidation on the 14th day in cases of their excessive accumulation in the blood (30%) in malignant neoplasia ($P < 0.01$). It should be mentioned that in malignant neoplasms, the content of malondialdehyde in the patients of the experimental groups was significantly different compared to the control animals on the 7th ($P < 0.01$), 10th ($P < 0.01$) and 14th ($P < 0.001$) days of the postoperative period.

The dynamics of the malonic aldehyde content in the cases of mammary tumours among female dogs is a marker of the activation of lipid peroxidation, and development of endogenous intoxication which accompanies carcinogenesis. Pharmacological correction of the hemostasis system, which regulates the intensity of the formation of free radicals, excessive accumulation of which negatively affects the cells, led to a decrease in their concentration and, therefore, damage to the tissues.

Nitrogen oxide, which participates in the regulation of inflammation and regeneration of the tissues, has a positive value for organisms suffering the neoplasia process. Its impact causes vasodilation, which increases the permeability and forms tissue swelling with the subsequent development of inflammatory reaction.

The study on the saturation of the blood with nitrogen oxide in animals with mammary tumours (Table 11) allowed us to draw a conclusion that its level in the patients of all groups with benign neoplasms varied at the level of clinically healthy dogs throughout the monitoring. In malignant neoplasms of the control animals, the restoration of the nitrogen oxide content was observed on the 14th day; in the earlier period, there was observed its excessive accumulation ($P < 0.05$). Conducting corrective therapy was followed by the normalization of the level of nitric oxide in the blood after using nonsteroidal anti-inflammatory and low molecular weight heparins, starting from the three day after the neoplasia was removed.

The stability of the homeostasis in the organism is to a great extent caused by nitrogen oxide, which is the main regulator of the intra- and intercellular processes related to free radical oxidation. Thus, considering that the tumour process is accompanied by clearly manifested inflammatory reaction, we can assume the positive role of the combined method of treating mammary tumours, which includes electro-surgical removal of tumours and postoperative pharmacological correction of the hemostasis system.

Table 11
Dependence of the content of nitrogen oxide on the treatment course of femaledogs with neoplasias of mammary gland (μmol/L, x ± SD)

Period of observation, day	Group		
	control (n = 32)	first experimental (n = 40)	second experimental (n = 40)
	coagulator	coagulator + non-steroidal anti-inflammatory drugs	coagulator + low molecular weight heparins
Clinically healthy	32.19 ± 1.82		
Benign tumours			
Before surgery	29.74 ± 4.03		
3	33.35 ± 2.98	32.69 ± 3.71	34.37 ± 2.50
7	28.39 ±2.33	29.83 ± 3.95	31.20 ± 2.45
10	29.42 ± 2.54	30.57 ± 4.13	30.61 ± 3.58
14	30.07 ± 2.98	29.21 ± 2.76	28.15 ± 2.57
Malignant neoplasms			
Before surgery	42.85 ± 4.89*		
3	38.36 ± 3.19*	35.77 ± 2.64	34.96 ± 0.85
7	37.78 ± 2.47*	32.19 ± 1.91	33.56 ± 2.48
10	36.08 ± 1.13*	31.20 ± 4.51	32.18 ± 3.09
14	34.11 ± 1.74	29.34 ± 1.24	30.46 ± 4.55

Note: see Table 3.

The corrective effect of the proposed treatment protocols was demonstrated by a positive effect on the hemostatic status, thereby confirming its normalizing effect on the processes of lipid peroxidation after the removal of mammary tumours in dogs. Reducing the endogenous intoxication leads to optimization of the reparative regeneration processes in the postoperative period and minimizes the possibility of further development and spread of tumour cells in the body. The body's reproductive capacity reflects the content of protein molecules and their fractions in the blood. It should be mentioned that according to the reference data, the physiological concentration of total protein in dogs is 50–70 g/l. We determined that in clinically healthy females, it equals 63.07 ± 3.21 g/l. This indicator was a starting point for further research.

The level of total protein in the previous studies in the preoperative period had significant differences between the groups of patients with malignant and benign tumours of the mammary gland by 25% (Table 12). That is, according to the results, the development of mammary tumours was followed by decrease in the content of total protein, which was observed more clearly in patients with malignant lesions.

Table 12
Dynamics of the total protein content
in dogs with mammary tumours (g/l, x ± SD)

Period of observation, day	Group		
	control (n = 32)	first experimental (n = 40)	second experimental (n = 40)
	coagulator	coagulator + non-steroidal anti-inflammatory drugs	coagulator + low molecular weight heparins
Clinically healthy	63.07 ± 3.21		
Benign tumours			
Before surgery	44.19 ± 4.37**		
3	42.77 ± 2.25***	51.07 ± 1.76***••	55.29 ± 5.62•
7	45.63 ± 3.56**	53.28 ± 3.59*	57.16 ± 3.12•
10	45.86 ± 3.58**	55.67 ± 4.35•	54.39 ± 4.98
14	52.74 ± 6.24	57.78 ± 5.14	55.54 ± 6.08
Malignant neoplasms			
Before surgery	54.89 ± 2.64*		
3	38.39 ± 2.09***	51.96 ± 5.74*•	57.03 ± 4.77••
7	40.43 ± 5.01**	54.25 ± 4.86*•	56.61 ± 3.92•
10	46.56 ± 4.13**	58.10 ± 3.15•	54.68 ± 4.35
14	45.88 ± 4.47**	57.43 ± 4.77•	54.13 ± 5.25

Note: see Table 3.

Extirpation of neoplasia was followed by changes in the content of total protein, which were characterized by its gradual increase. At the same time, on the 14th day of the monitoring, in the dogs of the control

group, restoration of the physiological parameters was observed only in cases of benign lesions. In patients of the experimental groups the total protein concentration was observed to normalize starting from the 10th day of the postoperative period with use of nonsteroidal anti-inflammatory preparations and from the 3d day in cases of using low molecular weight heparins. Unlike animals of the control group, in the blood of which during 10 days after the surgical removal of benign tumours of the mammary gland a low content of total protein was recorded (by 30%), the state of hypoproteinemia lasted the first 7 days of postoperative treatment with nonsteroidal anti-inflammatory drugs, and the use of low molecular weight heparins removed the changes in the protein metabolism on the 3d day.

Extirpation of malignant tumours using the electrosurgical method did not significantly affect the content of total protein in patients: throughout the monitoring, its level remained stably low (by 30–40%) compared to the clinically healthy dogs. Prescribing corrective therapy with nonsteroidal anti-inflammatory preparations allowed normalization of the content of total protein in 10 days, and immediately after the surgery after using low molecular weight heparin. Thus, we can assume that the proposed protocols of pharmacological correction of the hemostasis system optimize regenerative processes in the organism reducing the recovery period.

The main proteins that provide transportation of hydrophobic metabolites in the circulatory system of the organism, particularly cellular metabolism products, mediators and other compounds, the total amount of which reflects the pattern and intensity of the physiological and pathological processes in the body, are albumins. The obtained results indicate that there are no disorders in the level of albumin both in the preoperative period and after the surgery: it ranged within the limits of physiological parameters in all groups of animals in the absence of a significant difference between them (Table 13). Only on the 14th day, were the animals of the control group recorded to have a insignificant decrease to 24.05 ± 2.76 g/l ($P < 0.05$), which is probably related to the complicated process of reparative regeneration of surgical wounds. Albumin belongs to the negative proteins of the acute phase of inflammation. Considering that they are highly hydrophilic and bind a large amount of water, one can predict that in cases of tumours, an increase in the coagulation processes occurs due to the disorders of hemostasis mechanisms, and is not related to dehydration.

Table 13
Albumin concentration in patients with mammary neoplasia (g/l, x ± SD)

Period of observation, day	Group		
	control (n = 32) coagulator	first experimental (n = 40) coagulator + non-steroidal anti-inflammatory drugs	second experimental (n = 40) coagulator + low molecular weight heparins
Clinically healthy		31.17 ± 2.23	
Benign tumours			
Before surgery		29.25 ± 5.81	
3	27.73 ± 2.53	27.84 ± 5.57	25.87 ± 1.50*
7	27.14 ± 4.05	26.84 ± 4.71	27.23 ± 2.61
10	26.28 ± 3.75	28.94 ± 5.15	28.03 ± 3.18
14	24.05 ± 2.76*	29.28 ± 6.04	27.84 ± 5.67
Malignant neoplasms			
Before surgery		30.53 ± 4.88	
3	32.17 ± 4.22	34.70 ± 1.87	31.86 ± 2.98
7	31.53 ± 4.19	33.65 ± 4.91	31.08 ± 2.77
10	29.79 ± 3.62	31.51 ± 3.21	29.52 ± 3.46
14	30.23 ± 2.11	34.01 ± 3.77	29.78 ± 2.95

Note: see Table 3.

The determination of ceruloplasmin, one of the mediators which regulate the activity of proteolytic enzymes in the presence of inflammatory reaction in the tumour for assessing the intensity of the inhibitory system, shows (Table 14) that in the dogs with benign tumours of the mammary gland it decreased on average by 15% in the absence of changes in the patients with malignant tumours in the conditions of significant difference in its levels, depending on the pathomorphological type of neoplasms.

Table 14
Concentration of ceruloplasmin in dogs with tumours of the mammary glands in relation to the treatment method (mg/l, x ± SD)

Period of observation, day	Group		
	control (n = 32) coagulator	experimental first (n = 40) coagulator + non-steroidal anti-inflammatory drugs	experimental second (n = 40) coagulator + low molecular weight heparins
Clinically healthy		28.77 ± 0.34	
Benign tumours			
Before surgery		24.74 ± 0.36***	
3	39.37 ± 3.45**	37.94 ± 3.27**	35.86 ± 1.54**
7	35.89 ± 3.31**	34.11 ± 2.34*	33.61 ± 4.17*
10	35.63 ± 2.47**	28.47 ± 3.19•	32.31 ± 2.27*
14	31.08 ± 3.46	26.20 ± 2.47	27.67 ± 2.34
Malignant neoplasms			
Before surgery		28.31 ± 0.42	
3	43.27 ± 1.87***	38.35 ± 2.68**	44.10 ± 5.57***
7	41.48 ± 3.39**	37.11 ± 4.26*	39.43 ± 4.84*
10	37.94 ± 4.26*	32.18 ± 3.47	34.22 ± 2.86*
14	36.27 ± 3.58*	26.33 ± 4.85	31.20 ± 3.44

Note: see Table 3.

The postoperative period for benign neoplasms is characterized by accumulation of ceruloplasmin during 7 days in the first experimental group, 10 days in the control and second experimental groups. The patients with malignant neoplasias had excessive accumulation of this marker in the control groups during 14 days, 7 days – in cases of using nonsteroidal anti-inflammatory preparations, 10 days in cases of using low molecular weight heparins, which is related to its main function as an osteopathic protein – the protection of biological membranes by inhibition of proteolytic cascade systems, complement, coagulation and fibrinolysis in conditions of inflammation.

The presented results indicate the effectiveness of using corrective courses after the extirpation of mammary tumours of dogs. Conducting pharmacological correction after excision of the tumour resulted in the normalization of the content of ceruloplasmin in cases of prescribing nonsteroidal anti-inflammatory agents on the 10th day, and on the 14th day in cases of using low molecular weight heparins. The obtained results suggest that the use of pharmacological correction of hemostasis status recovers the balance of proteins due to their rational use, reducing the intensity of reactions in which they take part directly or indirectly, except for inflammation, normalizes the ratio of synthesis/disintegration, initiates increase in the production of immunoproteins.

Summarizing the data obtained during the study of the effects of nonsteroidal anti-inflammatory and low molecular weight heparins on the system of hemostasis in dogs that had been operated on for breast tumours, we can state the following. The markers indicated deep disorders of the hemostasis balance during the postoperative period in the patients in cases of using the electrosurgical method of extirpation of tumours. Optimization of the processes of reparative regeneration is possible during the course of corrective therapy which is based on nonsteroidal anti-inflammatory drugs or low molecular weight heparins. Restoration of hemostasis equilibrium in such animals indicates a higher intensity of regenerative processes compared to alteration.

The presented results allow us to supplement the methodological basis of veterinary medicine with new effective protocols which improve the efficiency of treating mammary tumours of dogs and form a basis for further research orientated to development of alternative methods of preventing relapses and metastasis.

Discussion

Currently, despite the wide distribution of mammary tumours among small domestic animals, there is no united information base for cancer patients, which would include the data on patients, description of general and pathological changes, treatment protocols and the results of their use. At the same time (Talahadze et al., 2012), there is no general methodological approach to the verification of tumours, and Owen's histological classification for animals (1980) is insufficient to cover the

pathogenesis of neoplasms and therefore requires a correction based on the latest studies on the mechanisms of development of this pathology. Clinical TNM classification requires taking into account the immunohistochemical profile of tumours, molecular genetic characteristics, which would allow us to not only make a more accurate prognosis of the course of the disease, but also recommend optimal treatment tactics (Ferreira et al., 2011; Losiewicz et al., 2014). The research conducted confirms the widespread distribution of tumour lesions of the mammary gland, which is also typical for other regions (Dhami et al., 2010; Mysak, 2010; Glazunova et al., 2014).

The study of the pathogenesis is characterized by low activity of scientists in this area and a similarity in their studies (Mischke et al., 2005). In most cases, one or several indicators are being determined, which only reflect the orientation of changes in the coagulation and proteolytic mechanisms, but do not reveal the nature of the changes (Vilar Saavedra et al., 2011). The diseases, treatment of which requires the study of hemostatic status as an important element of the pathogenesis, are, first of all, tumours.

An important role in the carcinogenesis of the mammary gland is played by inflammation which causes release of signaling molecules (cyclooxygenase-2, tumour epidermal growth factor, angiogenic vascular endothelial growth factor, other proangiogenic factors, chemokines, cytokines) which exacerbate the inflammation and contribute to survival, reproduction and spread of the tumour cells (Pinho et al., 2012).

The information given above confirms the presence of disorders in the coagulation system in dogs with mammary tumours, characterized by high probability of bleeding in cases of malignant course (prolongation of activated partial thromboplastin time in 50% of patients) due to consumption coagulopathy; in cases of benign tumours there is significant risk of thrombosis (it decreased in 71.4% of the animals).

The activation of the proteolytic systems, particularly the fibrinolytic, plays an important part in the invasion of the malignant cells and the development of metastases, the mechanisms of which involve several classes of proteases, first of all the plasminogen activation proteolytic cascade with the formation of a plasmin that activates the matrix metalloproteases which destroy collagen and other components of the tumour stroma (Corte et al., 2005; Salman et al., 2009; Jessen et al., 2010).

The average level of the inhibitors of proteolysis indicates an increase in their activity in neoplasms. It was significantly higher in cases of malignant neoplasms compared to benign neoplasms. The obtained data indicate that the development of neoplasms in the mammary gland of dogs in most cases is accompanied by excessive activation of the α_1-proteinase inhibitor and α_2-macroglubulin. The abovementioned changes in the content of acute-phase proteins, which follow the suppression of fibrinolytic activity characterize the organism's attempts to eliminate the threat of thrombosis and localize the inflammatory process which accompany the development of neoplasms.

Our previous studies (Rublenko & Bilyj, 2012) indicate significant disorders in the hemostatic status of bitches with mammary tumours, in particular the presence of oxidative stress in cases of malignant lesions (Rublenko & Bilyj, 2014), justifying the usefulness of its pharmacological correction in the postoperative period, and also the advantage of an electrosurgical technique over the generally accepted one.

The results obtained on the possibility of restoring the hemostasis status in animals with mammary tumours by their removal followed by prescription of the correcting protocols, are confirmed by the studies conducted in human medicine (Masljakova et al., 2017), according to which the disorders in the mechanisms of coagulation in tumours has a reverse pattern. A promising direction for further research is the use of nonsteroidal anti-inflammatory agents for the prevention of mammary tumours of dogs: this is indicated by the results of the monitoring conducted in human medicine (Harris et al., 2003).

The results of clinical testing of non-steroidal anti-inflammatory agents in dogs with cancer confirm the conclusions (Tran-Thanh et al., 2010) about the ability to prevent the growth of mammary tumours using a selective inhibitor of cyclooxygenase-2. The conclusions are based on research in which the animals were used as biological models, although information on the use of nonselective agents of this pharmacological group is controversial.

At the same time, in human medicine, the use of nonsteroidal anti-inflammatory preparations and low molecular weight heparins was justified (Koh et al., 2013; Hevia et al., 2017), and in veterinary oncology, this correction is not used. Only roncoleukin monotherapy was proposed (Korobova, 2005), but the efficacy was determined using only the clinical criteria, which does not allow one to make an objective prognosis of the course of the disease. That is, the problem of postoperative treatment of animals with cancer is not solved, hence the necessity of studies orientated to the development and clinical implementation of pathogenetically justified courses of pharmacological correction of hemostasis for such patients and the criteria for their evaluation.

The positive effect of the proposed protocol for breast cancer in female dogs can be explained by its influence on the main element of carcinogenesis, which was proved by the study of the effects of the immunostimulants, hemostatic preparations, nonsteroidal anti-inflammatory drugs and low molecular weight heparins on the development of neoplasms in human medicine.

The main direction of the pharmacological influence on the neoplasia process is the stimulation of the immune response of the organism, in particular the direct and indirect effects on the immune-competent cells (Hegmans & Aerts, 2014). In the proposed protocol, the antitumour activity was induced by roncoleukin, which directly damages the tumour cells, and significantly stimulates the local immune reaction and activates the immune defense organs, and also indirectly affects the carcinogenesis by activating different cells of the immune system (Zlatnik et al., 2012).

The use of nonsteroidal anti-inflammatory agents has been shown to reduce the inflammatory process caused by tumours as well as surgical intervention. This coincides with its proven anti-inflammatory, analgesic and antipyretic action (Brown et al., 2001). Some researchers (Hussain et al., 2012) described their immunomodulatory effects related to the influence on the immune cells, and also to macrophages, dendritic, T-effector and regulatory T cells related to the growths.

The results obtained confirm the antitumour effect of nonsteroidal anti-inflammatory preparations, which, perhaps, occur as a result of strengthening of apoptosis, as was determined in a study using cellular lines of tumours in dogs (Wilson et al., 2012). Considering the similarity of the development of tumours in human and dogs, it can be assumed that the prophylactic effect of non-steroidal anti inflammatory preparations on the development of neoplasms is related to decrease in the level of estradiol (Horn et al., 2010), presence of HER2 gene and the receptors in the tumour cells (Dierssen-Sotos et al., 2016).

The results obtained coincide with the data presented in human medicine (Marchetti et al., 2008; Promzeleva et al., 2012) on the efficiency of using low molecular weight heparins against growths in the mammary gland in the postoperative period. In this case, the inhibition of the development and distribution of tumours is explained by the activation of apoptosis of neoplastic cells and inhibition of the expression of the vascular endothelial growth factor (Yin et al., 2014), by inflammation through NFkappaB, the main enzymes which negatively affect the matrix, platelet and adherence cell interaction, and the effect on the release of the tissue pathway inhibitor factor, inhibition of selective modulation (Mousa, 2010; Heyman & Yang, 2016).

Despite discussion on the use of nonsteroidal anti-inflammatory preparations and low molecular weight heparins, on the basis of the pathogenesis of breast cancer and the results obtained, it can be stated that they have been proven to be efficient in case of this pathology.

In our opinion, the proposed therapeutic direction for breast tumours has certain advantages over the generally accepted protocols. The courses we recommend, which affect the key pathogenetic mechanisms of the neoplastic process, create unfavourable conditions for tumour transformation, activate and enhance antitumour protection without causing toxic effects on the organism. At the same time, selecting preparations for pharmacological correction is carried out in accordance with the peculiarities of hemostasic changes in a particular patient, and not by the pathomorphological type of a tumour, which permits an individual approach to blocking the key pathogenetic mechanisms of the neoplastic transformation.

Conclusions

High coagulation potential for breast tumours in female dogs causes an increased risk of vascular thrombosis and promotes dissemination of the neoplastic cells. The presence of prolonged postoperative coagulopathy proves the need for a pharmacological correction aimed at restoring the hemostasis equilibrium, which is an important factor for improving the long-term prognosis for patients with cancer.

Using the protocol of pharmacological correction of the hemostasis system (roncoleukin, trannexam and acelysin or phenox) after electrosurgical removal of mammary tumours of female dogs facilitates normalization of the hemostasis mechanisms within 14 days of surgery, thus reducing the risk of thrombosis and the probability of relapse and metastasis. The proven efficiency of the combined method of treating dogs with the mammary tumours, which includes electrocoagulation of tumours and the pharmacological correction of the hemostasis status, allows us to recommend it for broad introduction into clinical veterinary practice.

References

Andreeva, L. I., Kozhemjakin, L. A., & Kishkun, A. A. (1988). Modifikacija metoda opredelenija perekisej lipidov v teste s tiobarbiturovoj kislotoj [Modification of the method for determination of lipid peroxides in the test with thiobarbituric acid]. Laboratornoe Delo, 11, 41–43 (in Russian).

Abdullah, M. A., Almufty, B. I., Yasin, M. I., & Hassan, N. J. (2014). Clinical and histopathological study of mammary tumors in foreing dogs breeds in Kurdistan region of Iraq. Basrah Journal of Veterinary Research, 1(1), 11–19.

Astrup, T., & Mullertz, S. (1952). The fibrin plate metod for estimating fibrinolitic activity. Archives of Biochemistry and Biophysics, 40, 346–351.

Beha, G., Brunetti, B., Asproni, P., Muscatello, L., Millanta, F., Poli, A., Sarli, G., & Benazzi, C. (2012). Molecular portrait-based correlation between primary canine mammary tumor and its lymph node metastasis: Possible prognostic-predictive models and/or stronghold for specific treatments? Biomed Central Veterinary Research, 8, 219–228.

Belicer, V. O., Varec'ka, T. V., & Veremjejenko, K. M. (1997). Kil'kisne vyznachennja fibrynogenu v plazmi krovi ljudyny [Quantitative determination of fibrinogen in human plasma]. Laboratorna Diagnostyka, 2, 53–55 (in Ukrainian).

Boccaccio, C., & Medico, E. (2006). Cancer and blood coagulation. Cellular and Molecular Life Sciences, 63(9), 1024–1027.

Bonnett, B. N., Egenvall, A., Hedhammar, A., & Olson, P. (2005). Mortality in over 350,000 insured Swedish dogs from 1995–2000: I. Breed-, gender-, age- and cause-specific rates. Acta Veterinaria Scandinavica, 46(3), 105–120.

Brønden, L. B., Flagstad, A., & Kristensen, A. T. (2007). Veterinary cancer Registries in companion animal cancer: A review. Veterinary and Comparative Oncology, 5(3), 133–144.

Brown, W. A., Skinner, S. A., Malcontenti-Wilson, C., Vogiagis, D., & O'Brien, P. E. (2001). Non-steroidal anti-inflammatory drugs with activity against either cyclooxygenase 1 or cyclooxygenase 2 inhibit colorectal cancer in a DMH rodent model by inducing apoptosis and inhibiting cell proliferation. British Medical Journal, 48, 660–666.

Corte, M. D., Vérez, P., Rodríguez, J. C., Roibás, A., Domínguez, M. L., Lamelas, M. L., Vázquez, J., García Muñiz, J. L., Allende, M. T., González, L. O., Fueyo, A., & Vizoso, F. (2005). Tissue-type plasminogen activator (tPA) in breast cancer: Relationship with clinicopathological parameters and prognostic significance. Breast Cancer Research, 90(1), 33–40.

Dhami, M. A., Tank, P. H., Karle, A. S., Vedpathak, H. S., & Bhatia, A. S. (2010). Epidemiology of canine mammary gland tumours in Gujarat. Veterinary World, 3(6), 282–285.

Dierssen-Sotos, T., Gómez-Acebo, I., Pedro, M., Pérez-Gómez, B., Servitja, S., Moreno, V., Amiano, P., Fernandez-Villa, T., Barricarte, A., Tardon, A., Diaz-Santos, M., Peiro-Perez, R., Marcos-Gragera, R., Lope, V., Gracia-Lavedan, E., Alonso, M. H., Michelena-Echeveste, M. J., Garcia-Palomo, A., Guevara, M., Castaño-Vinyals, G., Aragonés, N., Kogevinas, M., Pollán, M., & Llorca, J. (2016). Use of non-steroidal anti-inflammatory drugs and risk of breast cancer: The Spanish Multi-Case-Control (MCC) study. BioMed Central Cancer, 16, 660.

Eierskyte, A., Zamokas, G., Grigonis, A., & Juodiiukyniene, N. (2011). The retrospective analysis of mammary tumors in dogs. Veterinarija ir Zootechnika, 53, 3–8.

Ferreira, E., Gobbi, H., Saraiva, B. S., & Cassali, G. D. (2011). Histological and immunohistochemical identification of atypical ductal mammary hyperplasia as a preneoplastic marker in dogs. Veterinary Pathology, 49(2), 322–329.

Fürdös, I., Fazekas, J., Singer, J., & Jensen-Jarolim, E. (2015). Translating clinical trials from human to veterinary oncology and back. Journal of Translational Medicine, 13, 265.

Gardner, H. L., Fenger, J. M., & London, C. A. (2016). Dogs as a model for cancer. Annual Review of Animal Biosciences Journal Impact, 4, 199–222.

Glazunova, L. A., & Koneva, A. V. (2014). Sravnitel'naja effektivnost' razlichnyh prijomov pri lechenii novoobrazovanij molochnoj zhelezy u sobak i koshek [Comparative effectiveness of various methods in the treatment of neoplasms of the breast in dogs and cats]. Sovremennye Problemy Nauki i Obrazovanija, 6, 18–24 (in Russian).

Golikov, P. P. (2004). Oksid azota v klinike neotlozhnyh zabolevanij [Nitric oxide in the clinic for urgent diseases]. Medpraktika, Moscow (in Russian).

Grandi, F., Colodel, M. M., Monteiro, L. N., Leão, J. R., & Rocha, N. S. (2016). Extramedullary hematopoiesis in a case of benign mixed mammary tumor in a female dog: Cytological and histopathological assessment. Biomed Central Veterinary Research, 6, 45.

Gundim, L. F., de Araújo, C. P., Blanca, W. T., Guimarães, E. C., & Medeiros, A. A. (2016). Clinical staging in femaleses with mammary tumors: influence of type and histological grade. Canadian Journal of Veterinary Research, 80(4), 318–322.

Harris, R. E., Chlebowski, R. T., Jackson, R. D., Frid, D. J., Ascenseo, J. L., Anderson, G., Loar, A., Rodabough, R., White, E., & McTiernan, A. (2003). Breast cancer and nonsteroidal anti-inflammatory drugs prospective results from the women's health initiative. Cancer Research, 63, 6096–6101.

Heading, K. L., Brockley, L. K., & Bennett, P. F. (2011). CCNU (lomustine) toxicity in dogs: A retrospective study (2002–07). Australian Veterinary Journal, 89(4), 109–116.

Hegmans, J. P., & Aerts, J. G. (2014). Immunomodulation in cancer. Current Opinion in Pharmacology, 17, 17–21.

Heyman, B., & Yang, Y. (2016). Mechanisms of heparanase inhibitors in cancer therapy. Experimental Hematology, 44(11), 1002–1012.

Hevia, G., Pablos, I., Clavell, M., Raymond, J., Labrada, M., & Fernández, L. E. (2017). Cyclooxygenase inhibition in cancer immunotherapy: Combination of indomethacin with cancer vaccines is not always beneficial. Journal of Cancer Therapy, 8, 188–209.

Horn, S. L., & Fentiman, I. S. (2010). The role of non-steroidal anti-inflammatory drugs in the chemoprevention of breast cancer. Pharmaceuticals, 3, 1550–1560.

Hussain, M., Javeed, A., Ashraf, M., Al-Zaubai, N., Stewart, A., & Mukhtar, M. M. (2012). Non-steroidal anti-inflammatory drugs, tumour immunity and immunotherapy. Pharmacological Research, 66(1), 7–18.

Jessen, L. R., Wiinberg, B., Kjelgaard-Hansen, M., Jensen, A. L., Rozanski, E., & Kristensen, A. T. (2010). Thrombin-activatable fibrinolysis inhibitor activity in healthy and diseased dogs. Veterinary Clinical Pathology, 39(3), 296–301.

Khamis, Z. I., Sahab, Z. J., & Sang, Q.-X. A. (2012). Active roles of tumor stroma in breast cancer metastasis. International Journal of Breast Cancer, 2012, 1–10.

Khanna, C., Rosenberg, M., & Vail, D. M. (2015). A review of paclitaxel and novel formulations including those suitable for use in dogs. Journal of Veterinary Internal Medicine, 29(4), 1006–1012.

Koh, Y. W., Park, C, Yoon, D. H., Suh, C., & Huh, J. (2013). Prognostic significance of COX-2 expression and correlation with Bcl-2 and VEGF expression, microvessel density, and clinical variables in classical Hodgkin lymphoma. The American Journal of Surgical Pathology, 37(8), 1242–1251.

Korobova, N. V. (2005). Opyt primenenija Ronkolejkina na pozdnih stadijah onkologicheskih zabolevanij molochnyh zheljoz [Experience in the use of Roncoleukin in the late stages of oncological diseases of the mammary glands]. Veterinarnaja Klinika, 34, 21 (in Russian).

Leach, T. N., Childress, M. O., Greene, S. N., Mohamed, A. S., Moore, G. E., Schrempp, D. R., Lahrman, S. R., & Knapp, D. W. (2012). Prospective trial of metronomic chlorambucil chemotherapy in dogs with naturally occurring cancer. Veterinary and Comparative Oncology, 10(2), 102–112.

Levine, M. N., Lee, A. Y., & Kakkar, A. K. (2005). Thrombosis and cancer. Proceedings of the Annual Meeting of the American Society for Clinical Oncology, 13–17, 748–747.

Losiewicz, K., Chmielewska-Krzesinska, M., Socha, P., Jakimiuk, A., & Wąsowicz, K. (2014). MiRNA-21, miRNA-10b, and miRNA-34a expression in canine mammary gland neoplasms. Bulletin of the Veterinary Institute in Pulawy, 58, 447–451.

Marchetti, M., Vignoli, A., Russo, L., Balducci, D., Pagnoncelli, M., Barbui, T., & Falanga, A. (2008). Endothelial capillary tube formation and cell proliferation induced by tumor cells are affected by low molecular weight heparins and unfractionated heparin. Thrombosis Research, 121(5), 637–645.

Marchetti, V., Giorgi, M., Fioravanti, A., Finotello, R., Citi, S., Canu, B., Orlandi, P., Desidero, T. D., Danesi, R., & Bocci, G. (2012). First-line metronomic chemotherapy in a metastatic model of spontaneous canine tumours: A pilot study. Investigational New Drugs, 30(4), 1725–1730.

Masljakova, G. N., Fedorov, V. J., Krekova, N. J., & Cheburkaeva, M. J. (2017). Izmenenija gemokoaguljacii pri progressirovanii raka molochnoj zhelezy [Changes in hemocoagulation in the progression of breast cancer]. Medicinskij Al'manah, 2, 151–154 (in Russian).

Mischke, R., Fehr, M., & Nolte, I. (2005). Efficacy of low molecular weight heparin in a canine model of thromboplastin-induced acute disseminated intravascular coagulation. Research in Veterinary Science, 79(1), 69–76.

Mousa, S. A. (2010). Heparin and low-molecular weight heparins in thrombosis and beyond. Anticoagulants, Antiplatelets, and Thrombolytics, 663, 109–132.

Mysak, A. R. (2010). Porivnjal'ni aspekty monitoryngu neoplazij u sobak [Comparative aspects of neoplasia monitoring in dogs]. Naukovyj Visnyk Veterynarnoi' Medycyny, 76(4), 75–80 (in Ukrainian).

Ostrander, E. A., & Engl, N. (2012). Both ends of the leash – the human links to good dogs with bad genes. The New England Journal of Medicine, 367, 636–646.

Owen, L. N. (Ed.). (1980). TNM classification of tumors in domestic animals. Geneva, World Health Organization.

Pinho, S. S., Carvalho, S., Cabral, J., Reis, C. A., & Gärtner, F. (2012). Canine tumors: A spontaneous animal model of human carcinogenesis. American Journal of Translational Research, 3, 165–172.

Promzeleva, N. V., Zorina, V. N., & Zorin, N. A. (2012). Belki semejstva macroglobulinov pri rake molochnoj zhelezy [Proteins of the family of macroglobulins in breast cancer]. Voprosy Onkologii, 5, 688–690 (in Russian).

Rublenko, M. V., & Bilyj, D. D. (2012). Funkcional'ni porushennja ta systemni rozlady gemostazu za novoutvoren' u sobak [Functional disorders and systemic haemostasis disorders due to neoplasms in dogs]. Naukovo-Tehnichnyj Bjuleten', 13, 142–145 (in Ukrainian).

Rublenko, M. V., & Bilyj, D. D. (2014). Znachennja oksydantnogo stresu v patogenezi puhlyn molochnoi' zalozy u sobak [Significance of oxidative stress in the pathogenesis of breast cancer in dogs]. Problemy Zooinzhenerii' ta Veterynarnoi' Medycyny, 29(2), 75–78 (in Ukrainian).

Salman, T., Bilici, A., & Ustaalioglu, B. O. (2009). The correlation of thrombin-activated fibrinolysis inhibitor (TAFI) levels and clinicopathologic factors in advanced colorectal cancer patients. Journal of Clinical Oncology, 27, 27–32.

Sarrau, S., Jourdan, J., Dupuis-Soyris, F., & Verwaerde, P. (2007). Effects of postoperative ketamine infusion on pain control and feeding behaviour in femaleses undergoing mastectomy. Journal of Small Animal Practice, 48, 670–676.

Shafiee, R., Javanbakht, J., Atyabi, N., Kheradmand, P., Kheradmand, D., Bahrami, A., Daraei, H., & Khadivar, F. (2013). Diagnosis, classification and grading of canine mammary tumours as a model to study human breast cancer: An clinico-cytohistopathological study with environmental factors influencing public health and medicine. Cancer Cell International, 13, 469.

Sorenmo, K. U., Kristiansen, V. M., Cofone, M. A., Shofer, F. S., Breen, A. M., Langeland, M., Mongil, C. M., Grondahl, A. M., Teige, J., & Goldschmidt, M. H. (2009). Canine mammary gland tumours; A histological continuum from benign to malignant; clinical and histopathological evidence. Veterinary and Comparative Oncology, 7(3), 162–172.

Talahadze, N. T., Zurrida, S., Vorotnikov, I. G., Chhikvadze, N. V., Nechushkin, M. I., Petrovskij, A. V., Paolo, A., Dzhjermana, L., Dzhuzeppe, V., Dzhjermana, L., & Umberto, V. (2012). Klassifikacija zlokachestvennyh opuholej molochnoj zhelezy po sisteme TNM: Neobhodimost' peremen [Classification of malignant tumors of the breast by the TNM system: The need for changes]. Vestnik RONC imeni N. N. Blohina, 23(1), 69–76 (in Russian).

Tran-Thanh, D., Buttars, S., Wen, Y., Wilson, C., & Done S. J. (2010). Cyclooxygenase-2 inhibition for the prophylaxis and treatment of preinvasive breast cancer in a HER-2/Neu mouse model. Cancer Prevention Research, 3(2), 202–211.

Tripp, C. D., Fidel, J., Anderson, C. L., Patrick, M., Pratt, C., Sellon, R., & Bryan, J. N. (2011). Tolerability of metronomic administration of lomustine in dogs with cancer. Journal of Veterinary Internal Medicine, 25(2), 278–284.

Vareckaja, T. V., Mihajlovskaja, L. I., & Svital'skaja, L. A. (1992). Opredelenie rastvorimogo fibrina v plazme krovi [Determination of soluble fibrin in blood plasma]. Klinicheskaja Laboratornaja Diagnostika, 7–8, 10–14 (in Russian).

Veremeenko, K. N., Volohonskaja, L. I., & Kizim, A. I. (1978). Metody opredelenija prekallikrein-kallikreinovoj sistemy v krovi cheloveka [Methods for the determination of prekallikrein-kallikrein system in human blood]. Kyiv (in Russian).

Vilar Saavedra, P., Lara García, A., Zaldívar López, S., & Couto, G. (2011). Hemostatic abnormalities in dogs with carcinoma: A thromboelastographic characterization of hypercoagulability. Veterinary Journal, 190(2), 78–83.

Wilson, H., Chadalapaka, G., Jutooru, I., Sheppard, S., Pfent, C., & Safe, S. (2012). Effect of tolfenamic acid on canine cancer cell proliferation, specificity protein (sp) transcription factors, and sp-regulated proteins in canine osteosarcoma, mammary carcinoma, and melanoma cells. Journal of Veterinary Internal Medicine, 26(4), 977–986.

Yin, W., Zhang, J., Jiang, Y., & Juan, S. (2014). Combination therapy with low molecular weight heparin and Adriamycin results in decreased breast cancer cell metastasis in C_3H mice. Experimental and Therapeutic Medicine, 8(4), 1213–1218.

Zlatnik, E. A., & Nikipelova, O. F. (2012). Regressija opuholi i lokal'nye immunenye reakcii pri razlichnyh sposobah vvedenija ronkolejkina v jeksperimente [Tumor regression and local immune responses in various ways of administering Roncoleukin in the experiment]. Nauchnye Vedomosti. Serija Medicina, Farmacija, 129(10), 147–151 (in Russian).

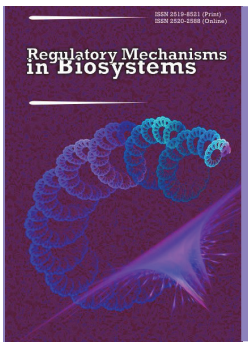

Regulatory Mechanisms in Biosystems

ISSN 2519-8521 (Print)
ISSN 2520-2588 (Online)
Regul. Mech. Biosyst., 9(3), 363–368
doi: 10.15421/021853

BoLA-DRB3 gene as a marker of susceptibility and resistance of the Ukrainian black-pied and red-pied dairy breeds to mastitis

T. M. Suprovych, M. P. Suprovych, T. V. Koval, T. M. Karchevska, V. A. Chepurna, I. O. Chornyi, A. P. Berezhanskyi

State Agrarian and Engineering University in Podilya, Kamianets-Podilskyi, Ukraine

Article info

Received 01.08.2018
Received in revised form 29.08.2018
Accepted 02.09.2018

State Agrarian and Engineering University in Podilya, Shevchenko st., 13, Kamianets-Podilskyi, 32300, Ukraine.
Tel.: +38-098-57-63-018.
E-mail: suprovycht@gmail.com

Suprovych, T. M., Suprovych, M. P., Koval, T. V., Karchevska, T. M., Chepurna, V. A., Chornyi, I. O., & Berezhanskyi, A. P. (2018). BoLA-DRB3 gene as a marker of susceptibility and resistance of the Ukrainian black-pied and red-pied dairy breeds to mastitis. Regulatory Mechanisms in Biosystems, 9(3), 363–368. doi:10.15421/021853

The major histocompatibility complex (MHC) determines the immune response, and the MHC genes are promising candidate genes for identifying associations with diseases. The decisive role in the resistance of cattle to diseases belongs to the major histocompatibility complex of (BoLA). The BoLA system consists of several jointly operating genes that provide antigen presentation by MHC system molecules followed by an immune response to pathogenic microorganisms. The most functional is the BoLA-DRB3 gene. Its exon 2 is highly polymorphic and encodes the peptide antigen-binding cleft. Alleles, for which a close connection with disease susceptibility or disease resistance has been detected, are considered as DNA markers. These play a decisive role in the breeding of cattle to create herds resistant to diseases, including mastitis. This paper presents the results of a study of BoLA-DRB3 gene polymorphism in two commercial cattle breeds: the Ukrainian black-pied dairy (UBPD) and the Ukrainian red-pied dairy (URPD) and its association with mastitis. The UBPD and the URPD cows were genotyped at the bovine lymphocyte antigen DRB3.2 locus by a genotyping system that used polymerase chain reaction and restriction fragment length polymorphisms (PCR-RLFP). In 276 UBPD cows, 32 BoLA-DRB alleles have been found. Six alleles (*03, *08, *10, *22, *24 and *28) were identified with a frequency of more than 5% (total amount of 50.4%). The allele BoLA-DRB3.2*24 was the most frequent (19.2%). In the UBPD population (n = 162), four BoLA-DRB3.2 alleles are truly associated with mastitis: *24 and *26 with susceptibility and *13 and *22 with resistance. In 117 URPD cows, 22 alleles were identified, of which the most frequent were *07, *22, *11, *24, *01, *03 and *16 (total frequency 64.5%). Allele BoLA-DRB3.2*07 (present in 25.6% of cows) was the most commonly found. In the URPD population studied, four alleles truly associated with mastitis were identified. Animals susceptible to the disease had alleles *07 and *08, and resistant animals had alleles *22 and *24. Breeding activities for the creation of cattle resistant to mastitis using alleles of the BoLA-DRB3 gene are much more effective than treatment and special care for animals. Similar research should be carried out for other Ukrainian breeds in relation to various diseases (leukemia, necrobacteriosis, etc.).

Keywords: polymorphism; PCR-RLFP; allele-specific PCR; alleles; udder, cattle.

Introduction

Udder diseases of cows lead to significant economic loss for the dairy business. That loss is greater than any damage from all non-contagious diseases in cattle farming. Mastitis in cattle imposes a significant financial burden on milk producers (the dairy industry worldwide loses $16–26 billion annually) (Abdel Hameed et al., 2006). Dairy production in Ukraine is the main branch of cattle farming. In 2016, 10,329 thousand tons of milk were received from 2,100 thousand cows (Chajkova & Foshhij, 2016). Mastitis of cows represents the biggest challenge for milk producers. The analysis of data from different publications shows that cases of mastitis amount to 18.8–34.7% of livestock, including 3.62–12.6% of clinically manifested cases. The loss due to the disease is about $75 per animal (Hanjejev & Janchuk, 2011).

The search for disease resistance markers includes the screening of candidate genes that are associated with the disease resistance caused by DNA polymorphisms. The major histocompatibility complex plays a crucial role in the immune response, and MHC genes are promising candidate genes to establish associations with various diseases (Abdel Hameed et al., 2006). MHC is a polymorphic genetic system that is a cluster of closely coupled genes. It is responsible for the formation of the immune response, macrophage, T-and B-lymphocyte interactions and for the immunological homeostasis support in general. The binding of peptides to MHC molecules triggers acquired immune responses. Therefore, MHC molecule polymorphism forms the diversity of the immune response. In particular, the major histocompatibility complex genes (BoLA) of cattle play an important role in the resistance of the host to diseases (Ibeagha-Awemu et al., 2008).

The BoLA system is located on the chromosome 23. It includes three classes: class I (locus A); class II, divided into IIa (includes DRA, DRB1, DRB3, DRB2, DQA DQB et al. loci) and IIb (includes DOB, DYA, DYB, DIB et al. loci); class III (including TNF, 21-OH, C4, BF, HSP70-1 and -2, EAM, PRL et al. loci). The first two groups of loci encode surface molecules that are related to the induction and regulation of immune responses.

The BoLA-DRB3 gene encoding antigens of Class II MHC is quite polymorphic (Van Eijk et al., 1992; Sharif et al., 1998). It is located in the IIa region of the sublocus of the DR system BoLA. The gene consists of six exons encoding the leader and the terminal sequence, the hydrophobic transmembrane region, the cytoplasmic and extracellular domain of the protein. The second exon of the BoLA-DRB3 gene encoding the β_1-domain of class II antigens is highly polymorphic. This is

necessary for binding of a wide range of foreign antigens (Behl et al., 2012). Analysis of the BoLA-DRB3.2 gene polymorphism is performed by PCR-RLFP (54 alleles) or PCR-SBT (107 alleles according to www.ebi.ac.uk/ipd/mhc/group/BoLA).

The functions of MHC antigens, associated with immune response to foreign antigens, determine numerous associations with specific diseases. Therefore, most studies are devoted to the establishment of the relation of the alleles of BoLA-DRB3.2 gene to various diseases: mastitis (Dietz et al., 1997; Sharif et al., 1998; Rupp et al., 2007; Kulberg et al., 2007; Duangjinda et al., 2009; Firouzamandi et al., 2010), dermatophilosis (Maillard et al., 1996), lameness (Sun et al., 2013), FMD (foot-and-mouth disease) (Lei et al., 2012), leukemia (Udina et al., 2003; Nikbakht Brujeni et al., 2016; Latypova et al., 2017), tick-borne disease (Duangjinda et al., 2013).

The BoLA-DRB3.2 gene polymorphism has been studied in more than 30 cattle populations (Takeshima et al., 2014) and the research is on-going. The allelic spectrum of the gene for most commercial breeds has been identified. The greatest attention of researchers is given to the purebred Holstein in the USA and Canada (Dietz et al., 1997; Sharif et al., 1998; Rupp et al., 2007) and to the breeds in other countries with a significant proportion of heredity from the Holstein (Duangjinda et al., 2009; Yoshida et al., 2012; Sun et al., 2013; Takeshima et al., 2015; Nikbakht Brujeni et al., 2016). There are numerous reports on the study of allelic diversity of indigenous breeds: Norwegian Red (Kulberg et al., 2007), Russian Ayrshire and Black-Pied (Udina et al., 2003), Japanese Shorthorn (Takeshima et al., 2002), USA Jersey (Gilliespie et al., 1999). Considerable attention is given to the study of the BoLA-DRB3.2 gene polymorphism in indigenous and native breeds: China Wanbei (Lei et al., 2012), Philippine native cattle (Takeshima et al., 2014), cattle of South American (Giovambattista et al., 2001; Takeshima et al., 2015), Mongolian, Kalmyk and Yakut breeds (Ruzina et al., 2010), Iranian native cattle (Firouzamandi et al., 2010), Indian native cattle (Behl et al., 2009), Egyptian cows (Ibrahim et al., 2012).

There are many breeds for which polymorphism of the BoLA-DRB3 gene and its connection with diseases has not been studied. The present study is aimed at analyzing the polymorphism of the BOLA-DRB3 gene exon 2 of the most common Ukrainian dairy breeds, black-pied dairy and red-pied and establishing associations between the alleles of this gene and mastitis.

Materials and methods

The research was carried on farms in Khmelnitsky and Chernivtsi regions from 2009 until 2015. Blood samples from the UBPD breed (5 farms, n = 276) and the URPD breed (2 farms, n = 117) were examined. Practical studies we conducted at the Animal Genetics Laboratory at the Institute of General Genetics Vavilov Russian Academy of Sciences (Moscow) and in the Genetics Laboratory of the Institute of Animal Breeding and Genetics of National Academy of Agrarian Science of Ukraine.

The maximum accuracy of the alleles of the gene BoLA-DRB3 definition was achieved by using three independent approaches (Sulimova, 2004):

– restriction analysis of PCR-RFLP amplification products;

– allele-specific PCR (AS-PCR) with primers ER-17 and VD-19;

– allele-specific PCR with primers HLO-07 and HLO-24d.

Isolation of DNA was carried out using "DIAtomTMDNA Prep200" kits (Isogen Laboratory Ltd.) in accordance with the manufacturer's instructions. DNA isolated from fresh biological material (yield was 5–10 mg from 200 ml of whole blood) high molecular weight (40–50 bp) and pure (OD 260/280 nm = 1.6–2.0) substance. The DNA concentration was determined visually. With this purpose, 25, 50, and 100 ng of λ phage DNA and aliquots of solution with an unknown concentration were applied to 1% agarose gel.

Electrophoresis was performed in 1^x Trisborate (TBE) buffer (89 mM Tris-OH, 89 mM H_3BO_3, 2 mM EDTA) with ethidium bromide (1 μg/ml) added to the gel to stain DNA at a constant voltage of 120 V. To avoid contamination, electrophoresis was performed in a separate room.

The DNA concentrations of the test samples were determined by comparing the fluorescence intensity of the aliquots from solutions of unknown concentration and control λ phage DNA. For further nested PCR analysis, the exon 2 region of the BoLA-DRB3 gene, 284 bp in size, was amplified (281 bp for alleles with deletion) (Van Eijk et al., 1992).

The PCR was carried out using ready-made sets of "GenPakR PCR Core", LLC "Izogen Laboratory", Russia. The final volume of the reaction mixture was 20 μl. The mixture contained 60 mM Tris-HCL (pH 8.8), 2.5 mM $MgCl_2$, 20 mM KCl, 15 mM $(NH_4)_2SO_4$, 10 mM mercaptoethanol, 0.1% Triton X-100, 0.2 mM dNTP, 10 units of Klentaq DNA polymerase, 10 pM of each primer, template DNA. Oligonucleotide primers used for amplified of the exon 2 of BoLA-DRB3 were previously published (Van Eijk et al., 1992). The primers HLO-30 (5'-3': TCCTCTCTCTGCAGCACATTTCC) and HLO-31 (5'-3': ATTCGCGCTCACC TCGCCGCT) for the first round of the reaction were used. 5 μl DNA was used as a template, regardless of its concentration. For the second round, PCR primers HLO-30 (5'-3': TCCTCTCTCTGCAGCACATTTCC) and HLO-32 (5'-3': TCGCCGCTGCACAGT GAAACTCTC) were used. 2 μl of the first round PCR products were used for the second round.

Amplification. The first stage was started from DNA denaturation at 95 °C for 5 min. followed by 10 cycles with denaturation (94 °C for 1 min), annealing (62.5 °C for 2 min) and elongation (72 °C for 1 min) and a final extension at 72 °C for 7 min. The second stage was started initial denaturation (95 °C for 5 min), was followed by 35 cycles of denaturation (68 °C for 30 s), and annealing-extension (72 °C for 30 s) and a final extension (72 °C for 7 min). Contamination and self-priming controls were included in each PCR round and 5 μL of the last PCR product were electrophoresed on 1.5% agarose gels in order to check the quality and specificity of DNA fragment amplification.

For the restriction analysis of the exon 2 fragment of the BoLA-DRB3 gene, endonucleases RsaI, HaeIII, XhoII (Promega, USA, New England BioLabs and SibEnzim, Russia) were used. The restriction fragments were separated by electrophoresis in a 4% agarose gel (Fig. 1). Amplification of exon 2 of the gene by means of a PCR followed by the analysis of restriction fragment length polymorphism and comparison of DNA patterns obtained using the three specified restriction endonucleases allows the identification of 54 alleles of the BoLA-DRB3 gene.

In cases where it was impossible to determine the genotype of the animal using restriction analysis, the AS-PCR method was used (Fig. 2). Allelic variants differ because the 3'-terminal nucleotide of one of the primers hybridizes directly to the variable nucleotide (SNP position), which causes the presence or absence of PCR. The specificity of the reaction can be increased by introducing an additional, not paired, nucleotide in the second or third position from the 3'-end of the same primer or using a competitive PCR in the same tube. Allele-specific PCR was performed using ready-made sets of "GenPakR PCR Core" (Isogen Laboratory). The PCR products of the first round of nested PCR were used as a template. A more detailed description of the method for typing the DRB3-alleles was reported by other sources (Udina et al., 2003; Firouzamandi et al., 2010; Ruzina et al., 2010).

Cows which repeatedly suffered during 2–3 lactations from various forms of mastitis were considered susceptible to mastitis. Animals which had no disease during this period were considered resistant.

In order to detect which cows were resistant and which were sensitive to mastitis, we conducted regular monthly studies. Special control plates with four deepenings were used. In these deepenings 1 ml of milk from each udder quarter and equal amounts of reagent were added. If the reaction was positive, a jelly-like clot formed, which indicated the presence of at least 500 thousand somatic cells per 1 ml of milk. Clinical manifestations of mastitis were diagnosed during milking based on several factors, such as: proportionality of udder quarters, pain sensitivity, local and general temperature increases, swelling, udder induration, secretion and presence of blood or pus in the secretrion.

Allele frequencies for the experimental sample were calculated taking into account the number of homozygotes and heterozygotes. In order to identify the associations between BoLA-alleles and the disease, it is necessary to establish the strength of association and the statistical significance between the frequency of gene carriers in the groups of susceptible and resistant animals. The force of the associative relationship is determined on the basis of relative risk (RR – relative risk, f_b –

frequency of gene carriers among susceptible animals, f_k – frequency of gene carriers in resistant animals):

$$RR = \frac{f_b(1-f_k)}{f_k(1-f_b)} \quad (1)$$

The RR value shows how many times the risk of developing the disease is greater in the presence of a certain allele in the genotype than in its absence (Zaretskaya, 1983).

Test χ^2 indicates a statistically significant difference between the frequency of alleles among susceptible and resistant animals. The allele is considered as associated with the disease if the condition $RR \geq 2$ and $\chi^2 > 3.84$ ($P < 0.05$) is satisfied. If the value $RR \leq 0.5$, then the presence of the allele in the animal genotype indicates a close association with the disease resistance. In this case, in order to highlight a positive association, relative risk values are set as 1/RR with a minus sign. Test χ^2 makes sense if the sample involves at least 20 animals and the respective conditions are met (a, c – susceptible to animal disease, having or not having an appropriate allele; b, d – resistant to animal disease, having or not having an appropriate allele; N – sample size):

$$(a+b)\times(a+c)/N > 5,\ (a+b)\times(b+d)/N > 5,$$
$$(c+d)\times(a+c)/N > 5,\ (c+d)\times(b+d)/N > 5. \quad (2)$$

If an allele is not detected in groups of susceptible or resistant animals, one of the values a or b is zero. Then the value of RR is determined by the Haldane formula (Kleinbaum et al., 1982). Woolf-Haldane correction is a modification of data, which allows for the verification of statistical significance in cases where one of the values is zero. Numeric 0.5 to warn the division by zero and make the calculation possible increases the 0 value.

Results

Polymorphism of BoLA-DRB3.2 gene in Ukrainian black-pied and red-pied dairy breeds

Ukrainian black-pied dairy breed. Table 1 summarizes the allele frequencies of the BoLA-DRB3.2 gene for 276 cows. The total number of the alleles found was 32.

Table 1
The distribution of the frequencies of the BoLA-DRB3.2 alleles in the population of UBPD cows (n = 276)

Allele BoLA-DRB3.2	Number of alleles	Frequency P(A), %	Allele BoLA-DRB3.2	Number of alleles	Frequency P(A), %
*01	7	1.27	*20	5	0.9
*02	12	2.17	*21	9	1.6
*03	31	5.62	*22	57	10.3
*04	11	1.99	*23	16	2.9
*06	1	0.18	*24	79	14.3
*07	26	4.71	*25	3	0.5
*08	38	6.88	*26	19	3.4
*10	31	5.62	*28	42	7.6
*11	7	1.27	*31	3	0.5
*12	18	3.26	*32	15	2.7
*13	25	4.53	*36	17	3.1
*14	2	0.36	*37	19	3.4
*15	10	1.81	*41	3	0.5
*16	14	2.54	*42	4	0.7
*18	12	2.17	*48	12	2.2
*19	2	0.36	*51	2	0.4

Six alleles had frequency of more than 5% (such alleles are termed «informative»). They are alleles *03, *08, *10, *22, *24 and *28. Their total frequency is 50.4%. The allele BoLA-DRB3.2*24 was the most frequent in the sample and was found in 53 cows. This allele was carried by 19.2% of animals (including homozygotes). Four alleles *06, *14, *19 and *51 (P (A) < 0.5%) were the least frequent.

Ukrainian red-pied dairy breed. We studied the allelic spectrum of this breed in two herds on farms in Khmelnitsky and Chernivtsi regions. Twenty-two alleles were detected in 117 blood samples (Table 2).

Seven alleles had frequency of more than 5%. They make up 64.5% of the total alleles fund of the sample studied. The most "informative" for the breed studied is the allele BoLA-DRB3.2*07, which was identified in 36 cases (15.4%), almost every fourth animal carries it. Seven alleles (*04, *09, *12, *20, *32, *35, and *43) were detected only thrice (1.6%).

Table 2
The distribution of the frequencies of the BoLA-DRB3.2 alleles in the population of URPD cows (n = 117)

Allele BoLA-DRB3.2	Number of alleles	Frequency P(A), %	Allele BoLA-DRB3.2	Number of alleles	Frequency P(A), %
*01	18	7.7	*20	3	1.3
*03	12	5.1	*22	31	13.3
*04	3	1.3	*24	20	8.6
*07	36	15.4	*25	6	2.6
*08	11	4.7	*27	6	2.6
*09	3	1.3	*28	8	3.4
*10	11	4.7	*32	4	1.7
*11	22	9.4	*35	3	1.3
*12	3	1.3	*42	11	4.7
*15	4	1.7	*43	3	1.3
*16	12	5.1	*45	4	1.7

Determination of associative relationships between alleles and mastitis

Ukrainian black-pied dairy breed. The sample studied included 62 cows susceptible and 100 cows resistant to mastitis. In this research, we identified 28 BoLA-DRB3.2 alleles, of which 24 were present in the group of susceptible cows. Five alleles were identified with a frequency of more than 5%, occupying together 53.6% of the total allele spectrum. In animals susceptible to mastitis, the allele *24 was the most frequent – 20 cases (16.1%). They were found in 17 animals (27.4%). Alleles frequently found also include *28 (9.7%), *26 (8.1%), *22 (7.3%), and *03 (6.5%). The alleles *01, *20, and *42 (0.8% for each) were found to a limited extent.

Among the cows resistant to mastitis, 27 alleles were found. The total frequency of eight "informative" alleles was 65.5%. The most frequent was BoLA-DRB3.2*22 allele. It was carried by 24% of cows. The peculiarity of this allele is that it forms a homozygous genotype most often spread throughout a whole population (40% of the total number of homozygotes detected).

The association between the disease and the allele is detected by comparing the frequencies of alleles in sick and healthy cows based on relative risk (RR), which reflects multiplicity of the association, that is, how many times the risk of developing the disease is greater in the presence of a specific allele in the genotype than in its absence. The significance of the detected association is determined by the test χ^2. According to the relative risk associated with mastitis, there are 17 alleles, of which eight are associated with susceptibility and nine with resistance (Table 3).

Table 3
Detection of BoLA-DRB3.2 alleles of UBPD cows associated with mastitis

Allele BoLA-DRB 3.2*	Frequency P(A), %	χ^2	RR	Test χ^2_{min} on the limited sample			
				(a+b)× (a+c)/N	(a+b)× (b+d)/N	(c+d)× (a+c)/N	(c+d)× (b+d)/N
*01	0.0154	0.729	–2.54	1.91	2.99	60.1	96.9
*08	0.0741	2.1	–2.05	9.19	13.0	52.8	85.2
*11	0.0154	3.85	6.83	1.91	3.18	60.1	96.9
*13	0.0525	5.65	–5.29	6.51	9.13	55.5	89.5
*15	0.0185	2.13	3.38	2.3	3.78	59.7	96.3
*16	0.0062	1.26	–3.17	0.77	1.21	61.2	98.8
*18	0.0247	4.81	5.25	3.06	5.14	58.9	95.1
*21	0.0185	2.13	3.38	2.3	3.78	59.7	96.3
*22	0.1204	5.02	–2.52	14.9	19.0	47.1	75.9
*24	0.1173	4.33	2.17	14.5	23.9	47.5	76.5
*25	0.0062	1.26	–3.17	0.77	1.21	61.2	98.3
*26	0.0432	7.13	4.62	5.36	9.16	56.6	91.4
*31	0.0062	1.26	–3.17	0.77	1.21	61.2	98.8
*32	0.0309	1.51	–2.61	3.83	5.8	58.2	93.8
*36	0.0309	6.61	–14.5	3.83	5.56	58.2	93.8
*41	0.0062	3.27	8.31	0.77	1.26	61.2	98.8
*48	0.0247	4.81	5.25	3.06	5.14	58.9	95.1

Notes: * – The Table shows the alleles for which one of the following conditions holds: 1) $\chi 2 \geq 3.8$; 2) $RR \geq 2$ or $RR \leq -2$; 3) both conditions 1 and 2.

Test χ^2 determines eight alleles that have a sufficient level of reliability: *26 and *36 ($P < 0.01$); *11, *13, *18, *22, *24, *48 ($P < 0.05$). Only four alleles of the above withstood the check for limited sample size. Thus, four BoLA-DRB3.2 alleles were found to have a strong and true association with mastitis in the UBPD population studied. Susceptible to mastitis are cows with alleles:

BoLA-DRB3.2*24 (RR = 2.17; P(A) = 0.117; $\chi^2 = 4.33$); χ^2_{min} = true;
BoLA-DRB3.2*26 (RR = 4.62; P(A) = 0.043; $\chi^2 = 7.13$); χ^2_{min} = true;
resistant are:
BoLA-DRB3.2*13 (RR = –5.29; P(A) = 0.053; $\chi^2 = 5.65$); χ^2_{min} = true;
BoLA-DRB3.2*22 (RR = –2.52; P(A) = 0.12; $\chi^2 = 5.02$); χ^2_{min} = true.

It is necessary to pay attention to alleles *18 and *48 with high relative risk (RR = 5.25) and sufficient significance in the test χ^2, but which do not satisfy the test for small sample size (χ^2_{min} = false), because they are rarely found in healthy animals. Such a restriction, as a rule, can withstand a check for small samples according to Fisher's criterion, with a slight decrease in the overall reliability of the study.

Due to the resistance to mastitis, it is necessary to pay attention to the allele *08 (RR = –2.05; P (A) = 0.074), which does not withstand the test χ^2 ($P > 0.05$) but meets the requirements of reliability by other criteria. In case of competent biological studies, it is permissible to lower the threshold of reliability, which makes it possible to use this allele in further analysis.

Ukrainian red-pied dairy breed. Blood samples were taken from 117 animals. Fifty-nine cows were resistant and 58 susceptible to mastitis.

Twenty-one alleles were detected in the samples of diseased animals. Eight alleles with a frequency exceeding 5% were identified, which embrace in total 74.9%. The most common allele was BoLA-DRB3.2*07. It was detected in almost every third cow (32.8%), or in 21.6% of cases among all detected alleles.

In the group of resistant animals, 20 alleles were identified, among which the most "informative" is BoLA-DRB3.2*22. It embraces 19.5% of the allelic spectrum. Six alleles other were found with a frequency of more than 5%: *24 (11.7%), *11 (11.0%), *07 (9.3%), *01 and *16 (5.9%), *28 (5.1%). The other 13 alleles embrace in total 30.5%. All alleles have only the heterozygous genotype.

Relative risk calculations show that 13 alleles of BoLA-DRB3.2 have a close association with mastitis, of which eight are associated with susceptibility and five with resistance to this disease (Table 4). The test χ^2 indicates five alleles that have a sufficient level of significance: *22 ($P < 0.001$); *07 ($P < 0.01$); *08, *24 i *45 ($P < 0.05$), of which only the latter cannot withstand a check for limited sample size.

Table 4
Detection of BoLA-DRB3.2 alleles of URPD cows associated with mastitis

Allele BoLA-DRB 3.2*	Frequency P(A), %	χ^2	RR	Test χ^2_{min} on the limited sample			
				(a+b)× (a+c)/N	(a+b)× (b+d)/N	(c+d)× (a+c)/N	(c+d)× (b+d)/N
*03	0.051	1.56	2.20	5.95	6.46	52.05	52.95
*04	0.013	0.36	2.07	1.49	1.54	56.51	57.49
*07	0.154	8.21	3.31	17.85	22.46	40.15	40.85
*08	0.047	5.05	5.24	5.45	6.21	52.55	53.45
*12	0.013	0.36	2.07	1.49	1.54	56.51	57.49
*20	0.013	0.36	2.07	1.49	1.54	56.51	57.49
*22	0.131	11.11	–4.66	14.87	11.03	43.13	43.87
*24	0.087	4.52	–2.96	10.41	8.97	47.59	48.41
*27	0.026	2.74	–5.28	2.97	2.82	55.03	55.97
*28	0.034	1.03	–2.08	4.46	4.31	53.54	54.46
*35	0.013	3.03	–7.25	1.49	1.44	56.51	57.49
*43	0.013	3.13	7.51	1.49	1.59	56.51	57.49
*45	0.017	4.21	9.83	1.98	2.15	56.02	56.98

Note: * – the Table shows the alleles for which one of the following conditions is met: 1) $\chi^2 \geq 3.8$; 2) RR ≥ 2 or RR ≤ –2; 3) both conditions 1 and 2 are met.

Thus, in the investigated population of the Ukrainian red-pied dairy breed, two alleles have a close association with cow susceptibility to mastitis:

*07 (RR = 3.31; P(A) = 0.154; $\chi^2 = 8.21$); χ^2_{min} = true;
*08 (RR = 5.24; P(A) = 0.047; $\chi^2 = 5.05$); χ^2_{min} = true;
and two alleles indicate resistance to the disease:
*22 (RR = –4.66; P(A) = 0.131; $\chi^2 = 11.1$); χ^2_{min} = true;
*24 (RR = –2.96; P(A) = 0.087; $\chi^2 = 4.16$): χ^2_{min} = true;

In further studies, it will be necessary to pay attention to the allele BoLA-DRB3.2*03 (RR = 2.2; P (A) = 0.051; χ^2_{min} = true), for which the null hypothesis (χ^2 = false) is not confirmed and BoLA-DRB3.2*45, which is practically not manifested in cows resistant to mastitis.

Discussion

In our study we established that high allele diversity of BoLA-DRB3 gene is characteristic for UBPD livestock. This breed has a diverse genetic structure. Most researchers identify this breed as an open population. The UBPD cattle have similarity to Dutch, Estonian, Lithuanian, Moscow, black and red and other breeds. Nowadays when crossbreeding with Holstein bulls is spreading actively, the presence of 32 alleles BoLA-DRB3.2 is fully consistent with its genealogy. The same large number of RLFP-alleles has been found in Mongolian (35 alleles) and Kalmyk (34 alleles) breeds (Ruzina et al., 2010), as well as Iranian Sistani (30 alleles) cattle (Behl et al., 2009).

The Ukrainian red-pied dairy breed is the second commonest dairy breed in Ukraine after the black-pied one. It is derived from reproductive crossbreeding of the Simmentals (maternal breed) with red-pied Holstein. The breed develops according to the principle of open populations and also has a heterogeneous structure. In our study, 22 alleles were detected in URPB, which is significantly less than in UBPB. This result of our study is caused by limited range and the small sample size. Most commercial breeds have a wide range of alleles – from 13 in Canadian Jersey to 28 in Iranian Holstein (Behl et al., 2009). This number of alleles in these populations is likely a consequence of maternal breed features and selection actions.

There is a low consolidation of "informative" alleles for UBPD cattle (50.4%). The same low level of consolidation was found for UBPB (64.5%). Commercial breeds, as a rule, are characterized by a higher consolidation of "informative" alleles. For example, there are seven alleles *22 and *24 (14.3%), *08 (14.1%), *16 (10.0%), *23 (9.1%), *11 (8.5%) and *07 (5.3%) with a frequency of more than 5% in Holstein cows (n = 1100) from 93 dairy herds in the states of Iowa, Wisconsin, Minnesota and Illinois (USA) (Dietz et al., 1997). Their sum is 75.6%. Similar studies in the Holstein cows (n = 835) in Ontario (Canada) (Sharif et al., 1998) showed that seven "informative" alleles *08 (20.1%), *24 (19.2%), *11 (14.9%), *22 (13.7%), *16 (9.2%), *23 (6.4%) and *03 (5.2%) occupied 88.7% of the allelic spectrum. In another study carried out on Iranian Holstein cows, the most frequent alleles were BoLA-DRB3.2*08, *11, *16 and *24 (Mohammadi et al., 2009).

Our study has identified alleles of cows susceptible and resistance UBPD and UBPB to mastitis. Significant research was carried out (Table 5) in detecting associations between alleles BoLA-DRB 3.2 and various aspects of mastitis, such as clinical and subclinical forms, specific pathogens (*Staphylococcus aureus*, *Streptococcus agalactiae*, *E. coli*) and somatic count cells (Dietz et al., 1997; Kelm et al., 1997; Sharif et al., 1998, 2000; Rupp et al., 2007; Duangjinda et al., 2009; Ruzina et al., 2010; Ibrahim et al., 2012).

Sulimova, Ruzina et al. (2010) believes that generalization and analysis research of different authors indicate three groups of alleles BoLA-DRB3.2 in connection with mastitis: susceptibility – *16, *23 and *26; resistance – *07, *11, *13, *18 and *27; have opposite associations in different studies – *08, *22 and *24. Data indicate that alleles in different populations have opposite associations more: *11, *16, *22, *23 and *24. The conditions for the emergence of mastitis are very diverse. Many factors promote the development of mastitis, including the feeding environment, care conditions and genetic background. Infectious mastitis occurs because of the penetration of the udder by *Streptococcus*, *Staphylococcus*, coliform bacterium and other pathogens. Infection of the udder occurs through the galactogenous path (through the teat channel), the lymphogenous way (through the wounds of the teats and udder), less often by the hematogenous way (from other organs). Non-infectious mastitis is widespread. It occurs when milking is done incorrectly, when poor hygiene of the udder is maintained, when damaged milking equipment is used, etc. In milk of cows with mastitis, due to the

development of the immune response to inflammation, SCC increases. Multifactorial effects influence different types of immune responses, which implies the peculiarity of its formation in different populations of cattle. Therefore, the possibility of finding deterministic BoLA-DRB3.2 alleles indicating resistance or susceptibility of cows to mastitis is unlikely for the whole world dairy herd.

Table 5
Summary of data on the detection of associations between alleles BoLA-DRB3.2 and various aspects of mastitis

Authors, source	Associations	Breed	Alleles DRB3.2
Dietz et al., 1997	increased risk of mastitis	Holstein	*16
Kelm et al., 1997	increased EBV* for CM**	Holstein	*08
Sharif et al., 1998	occurrence of mastitis	Holstein,	*23
	lower SCC and risk of mastitis	Jersey	*16
Sharif et al., 2000	mastitis caused by *Staphylococcus* spp.		*22,*23,*24
Rupp et al., 2007	lower SCC	Holstein	*03,*11
	higher SCC		*22,*23
	less risk of CM		*03
	high risk of CM		*08
Kulberg et al., 2007	increased clinical mastitis	Norwe-	*22,*26
	mastitis resistance	gian	*07,*11,
		Red	*18,*24
Duangjinda et al., 2009	occurrence of CM	Holstein	*01,*52
	resistance to CM	× Zebu	*15,*51,*22
Firouzamandi et al., 2010	resistance for CM	Sarabi	*16
Ibrahim et al., 2012	susceptibility to mastitis	Holstein	*11
	susceptibility to *E. coli*	Egypt	*24
	resistant to *St. aureus*		*16
Yoshida et al., 2012	susceptibility to mastitis	Japanese	*8,*16
	resistant to mastitis	Holstein	*22,*23,*24
Own research	susceptibility to mastitis	UBPD	*24,*26
	resistant to mastitis		*13,*22
	susceptibility to mastitis	URPD	*07,*08
	resistant to mastitis		*22,*24

Note: *EBV – estimated breeding value; **CM – clinical mastitis.

Our study has identified alleles associated with mastitis which are different from alleles identified by other researchers in similar studies. This is due to the multifactoral nature of the immune response to various pathogens that cause mastitis. The condition for the emergence of mastitis is not only the penetration of the pathogen into the udder, but also its ability to survive there, and then to multiply in sufficient quantities to cause the disease. Therefore, in cases of occurrence of mastitis the natural resistance of an organism of the animal and the mammary gland is of great importance.

Conclusions

The results obtained in this study confirmed the hypothesis of DRB3 being a marker for susceptibility (resistance) to mastitis in dairy cows. In summary, it is necessary to note that the results of this study demonstrated that BoLA-DRB3.2 in the Ukrainian black-pied and the Ukrainian red-pied breeds of dairy cattle is highly polymorphic and depends on the breed and population, as a result of the founder population and selection actions. The identified BoLA-DRB3.2 alleles can be recommended as a marker used to select the animals at a young age preceding the appearance of the traits of interest for the investigated breeds. Selection of cows for resistance to mastitis with the help of DNA markers based on the alleles of the BoLA-DRB3 gene is much more effective than treatment and use of costly animal maintenance and care. Similar research should be continued in order to achieve significant results that could be applied to one breed and one disease.

References

Abdel Hameed, K. G., Sender, G., & Mayntz, M. (2006). Major histocompatibility complex polymorphism and mastitis resistance – A review. Animal Science Papers and Reports, 24(1), 11–25.

Behl, J. D., Verma, N. K., Behl, R., & Sodhi, M. (2009). Genetic variation of the major histocompatibility complex DRB3.2 locus in the native *Bos indicus* cattle breeds. Asian-Australasian Journal of Animal Sciences, 22(11), 1487–1494.

Behl, J. D., Verma, N. K., Tyagi, N., Mishra, P., Behl, R., & Joshi, B. K. (2012). The major histocompatibility complex in bovines: A review. ISRN Veterinary Science, article ID 872710.

Chajkova, O. I., & Foshhij, M. D. (2016). Analiz rynku molochnoi' galuzi Ukrai'ny ta prognoz jogo rozvytku [Market analysis of the dairy industry of Ukraine and forecast of its development]. Bulletin of National Technical University "Kharkiv Polytechnic Institute" (Economic Sciences), 47, 26–29 (in Ukrainian).

Dietz, A. B., Cohen, N. D., Timms, L., & Kehrli, M. E. (1997). Bovine lymphocyte antigen class II alleles as risk factors for high somatic cell counts in milk of lactating dairy cows. Journal of Dairy Science, 80(2), 406–412.

Duangjinda, M., Buayia, D., Pattarajinda, V., Phasuk, Y., Katawatin, S., Vongpralub, T., & Chaiyotvittayakul, A. (2009). Detection of bovine leukocyte antigen DRB3 alleles as candidate markers for clinical mastitis resistance in Holstein×Zebu. Journal of Animal Science, 87, 469–476.

Duangjinda, M., Jindatajak, Y., Tipvong, W., Sriwarothai, J., Pattarajinda, V., Katawatin, S., & Boonkum, W. (2013). Association of BoLA-DRB3 alleles with tick-borne disease tolerance in dairy cattle in a tropical environment. Veterinary Parasitology, 196(3–4), 314–320.

Firouzamandi, M., Shoja, J., Bazegari, A., & Roshani, E. (2010). Study on the association of BoLA-DRB3.2 alleles with clinical mastitis in Iranian Holstein and Sarabi (Iranian native) cattle. African Journal of Biotechnology, 9(15), 2224–2228.

Gilliespie, B. E., Jayarao, B. M., Dowlen, H. H., & Oliver, S. P. (1999). Analysis and frequency of bovine lymphocyte antigen DRB3.2 alleles in Jersey cows. Journal of Dairy Science, 82, 2049–2053.

Giovambattista, G., Ripoli, M. V., Peral-Garcia, P., & Bouzat, J. L. (2001). Indigenous domestic breeds as reservoirs of genetic diversity: The Argentinean Creole cattle. Animal Genetics, 32, 240–247.

Hanjejev, V. V., & Janchuk, T. V. (2011). Zahvorjuvannja koriv na mastyt: Rahujemo zbytky [Disease of cows for mastitis: Count losses]. Veterynarna Medycyna Ukrai'ny, 189, 36–37 (in Ukrainian).

Ibeagha-Awemu, E. M., Kgwatalala, P., Ibeagha, A. E., & Zhao, X. (2008). A critical analysis of disease-associated DNA polymorphisms in the genes of cattle, goat, sheep, and pig. Mammalian Genome, 19, 226–245.

Ibrahim, E. A., Allam, N. A. T., Kotb, E. E. Z., El-Rafey, G. A., El-Deen, M. M. A., & Fadlallah, M. G. (2012). Sequence-based typing-study on the relationship between subclinical mastitis and BoLA-DRB3.2* allelic polymorphism in Egyptian cows. Global Veterinaria, 9(1), 8–22.

Kelm, S. C., Detilleux, J. C., Freeman, A. E., Kehrli, M. E., Dietz, A. B., Fox, L. K., Butler, J. E., Kasckovics, I., & Kelley, D. H. (1997). Genetic association between parameters of inmate immunity and measures of mastitis in periparturient Holstein cattle. Journal of Dairy Science, 80, 1767–1775.

Kleinbaum, D. G., Kupper, L. L., & Morgenstern, H. (1982). Epidemiologic research lifetime learning publication. Lifetime Learning Publications, Belmont.

Kulberg, S., Heringstad, B., Guttersrud, O. A., & Olsaker, I. (2007). Study on the association of BoLA-DRB3.2 alleles with clinical mastitis in Norwegian Red cows. Journal of Animal Breeding and Genetics, 124(4), 201–217.

Latypova, Z., Sarbakanova, S., Mamanova, S., Sultanov, A., Nam, I., Smaznova, I., Zayakin, V., & Kozlov, A. (2017). Comparison between populations of black pied and holstein cows and stud bulls from Russia, Belarus and Kazakhstan by the genetic markers for resistance to leukemia. International Journal of Current Research in Biosciences and Plant Biology, 4(8), 1–7.

Lei, W., Liang, Q., Jing, L., Wang, C., Wu, X., & He, H. (2012). BoLA-DRB3 gene polymorphism and FMD resistance or susceptibility in Wanbei cattle. Molecular Biology Reports, 39(9), 9203–9209.

Maillard, J. C., Martinez, D., & Bensaid, A. (1996). An amino acid sequence encoded by the exon 2 of the BoLA-DRB3 gene associated with a BoLA class 1 specificity constitutes a likely genetic marker of resistance to dermatophilosis in Brahman zebu cattle in Martinique (FWI). Annals of the NY Academy of Science, 791, 185–197.

Mohammadi, A., Nassiry, M. R., Mosafer, J., Mohammadabadi, M. R., & Sulimova, G. E. (2009). Distribution of BoLA-DRB3 allelic frequencies and identification of a new allele in the Iranian cattle breed sistani (*Bos indicus*). Russian Journal of Genetics, 45(2), 224–229.

Nikbakht Brujeni, G., Ghorbanpour, R., & Esmailnejad, A. (2016). Association of BoLA-DRB3.2 alleles with BLV infection profiles (Persistent lymphocytosis / Lymphosarcoma) and Lymphocyte Subsets in Iranian Holstein Cattle. Biochemical Genetics, 54(2), 194–207.

Rupp, R., Hernandez, A., & Mallard, B. (2007). Association of bovine leukocyte antigen (BoLA) DRB3.2 with immune response, mastitis, and production and type traits in Canadian Holsteins. Journal of Dairy Science, 90(2), 1029–1038.

Ruzina, M. N., Shtyfurko, T. A., Mohammad Abadi, M. R., Gendzhieva, O. B., Cedev, C., & Sulimova, G. E. (2010). Polimorfizm gena BoLA DRB 3 u

krupnogo rogatogo skota mongol'skoj, kalmyckoj i jakutskoj porod [Polymorphism of the BoLA-DRB3 gene in the Mongolian, Kalmyk, and Yakut Cattle Breeds]. Russian Journal of Genetics, 46(4), 517–525 (in Russian).

Sharif, S., Mallard, B. A., Wilkie, B. N., Sargeant, J. M., Scott, H. M., Dekkers, J. C., & Leslie, K. E. (1998). Associations of the bovine major histocompatibility complex DRB3 (BoLA-DRB3) alleles with occurrence of disease and milk somatic cell score in Canadian dairy cattle. Animal Genetics, 29, 185–193.

Sharif, S., Mallard, B. A., & Sargeant, J. M. (2000). Presence of glutamine at position 74 of pocket 4 in the BoLA-DR antigen-binding groove is associated with occurrence of clinical mastitis caused by *Staphylococcus* species. Veterinary Immunology and Immunopathology, 76, 231–238.

Sulimova, G. E. (2004). DNK-markery v geneticheskih issledovanijah: Tipy markerov, ih svojstva i oblasti primenenija [DNA markers in genetic research: Marker types, their properties and applications]. The Success of Modern Biology, 124(3), 260–271 (in Russian).

Sun, L., Song, Y., Riaz, H., & Yang, L. (2013). Effect of BoLA-DRB3 exon 2 polymorphisms on lameness of Chinese Holstein cows. Molecular Biology Reports, 40(2), 1081–1086.

Takeshima, S. N., Giovambattista, G., Okimoto, N., Matsumoto, Y., Rogberg-Muñoz, A., Acosta, T. J., Onuma, M., & Aida, Y. (2015). Characterization of bovine MHC class II DRB3 diversity in South American Holstein cattle populations. Tissue Antigens, 86(6), 419–430.

Takeshima, S., Nakai, Y., Ohta, M., & Aida, Y. (2002). Characterization of DRB3 alleles in the MHC of Japanese Shorthorn cattle by polymerase chain reaction sequence based typing. Journal of Dairy Science, 85, 1630–1632.

Takeshima, S. N., Miyasaka, T., Polat, M., Kikuya, M., Matsumoto, Y., Mingala, C. N., Villanueva, M. A., Salces, A. J., Onuma, M., & Aida, Y. (2014). The great diversity of major histocompatibility complex class II genes in Philippine native cattle. Meta Gene, 2, 176–190.

Udina, I. G., Karamysheva, E. E., Turkova, S. O., Sulimova, G. E., & Orlova, A. R. (2003). Genetic mechanisms of resistance and susceptibility to leukemia in Ayrshire and Black-pied cattle breeds determined by allelic distribution of gene BoLA-DRB3. Genetika, 39(3), 306–317.

Van Eijk, M. J. T., Stewart-Haynes, J. A., & Lewin, H. A. (1992). Extensive polymorphism of the BoLA-DRB3 gene distinguished by PCR-RFLP. Animal Genetics, 23(6), 483–496.

Yoshida, T., Furuta, H., Kondo, Y., & Mukoyama, H. (2012). Association of BoLA-DRB3 alleles with mastitis resistance and susceptibility in Japanese Holstein cows. Animal Science Journal, 83(5), 359–366.

Zaretskaya, Y. M. (1983). Klinicheskaja immunogenetika [Klinicheskaya immunogenetika]. Meditsina, Moscow. Pp. 70–74 (in Russian).

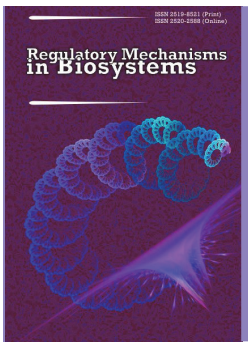

Regulatory Mechanisms in Biosystems

ISSN 2519-8521 (Print)
ISSN 2520-2588 (Online)
Regul. Mech. Biosyst., 9(3), 369–373
doi: 10.15421/021854

Antifungal activity of 5-(2-nitrovinyl) imidazoles and their derivatives against the causative agents of vulvovaginal candidiasis

N. D. Yakovychuk, S. Y. Deyneka, A. M. Grozav, A. V. Humenna, V. B. Popovych, V. S. Djuiriak

Bukovinian State Medical University, Chernivtsi, Ukraine

Article info

Received 12.06.2018
Received in revised form 14.07.2018
Accepted 17.07.2018

Bukovinian State Medical University, Teatralna Square, 2, Chernivtsi, 58002, Ukraine.
Tel.: +38-050-691-03-12.
E-mail: yakovychuk.nina@bsmu.edu.ua

Yakovychuk, N. D., Deyneka, S. Y., Grozav, A. M., Humenna, A. V., Popovych, V. B., & Djuiriak, V. S. (2018). Antifungal activity of 5-(2-nitrovinyl) imidazoles and their derivatives against the causative agents of vulvovaginal candidiasis. Regulatory Mechanisms in Biosystems, 9(3), 369–373. doi:10.15421/021854

Development of resistance of yeast-like fungi belonging to the *Candida* genus to the existing antifungal medicines as well as the high toxicity and low tolerance of these medicines in many cases stipulate the acute need for new antibiotic compounds. In this context, an extremely promising group of chemical substances is imidazole derivatives. Therefore, the search for more active and less toxic medical preparations based on imidazole is a relevant and important issue for medical practice. Considering the urgent demand for new antifungal preparations, four new nitro containing imidazole derivatives were synthesized – 5-(2-nitrovinyl) imidazoles and their derivatives. Then *in vitro* by means of double serial dilution in Saburo liquid nutritious medium we examined their antifungal action against eight clinical strains of yeast-like fungi belonging to the *Candida* genus: *C. albicans*, *C. guillermondii*, *C. krusei*, *C. glabrata*, *C. kefyr*, *C. tropicalis*, *C. inconspicua* and *C. zeylanoides*). They were isolated and identified from the vulvovaginal content of women suffering from vulvovaginal candidiasis. 3-methyl-4-[1-(1-naphthyl-4-chloro-1H-imidazole-5-yl)-2-nitroethyl-]-1H-pyrazole-5-ole and 2,4-dichloro-5-(2-nitrovinyl)-1-(4-fluorophenyl)-1H-imidazole were found to be the most active compounds – mean values of minimal fungistatic concentrations of these compounds against all the eight examined strains were 34.9 and 39.7 μg/mL (with the ranges of these concentrations 5.2–83.3 μg/mL) respectively. 2,4-dichloro-3-methyl-4-{2-nitroethyl-1-[1-(4-fluorophenyl)-1H-imidazole-5-yl]}-1H-pyrazole-5-ole and 1-naphthyl-5-(2-nitrovinyl)-4-chloro-1H-imidazole were found to possess lower anti-*Candida* activity – mean values of their minimal fungistatic concentrations against all the eight clinical strains were 48.8 and 51.4 μg/mL (with the ranges of these concentrations 10.4–166.7 μg/mL) respectively. The highest antifungal activity of 5-(2-nitrovinyl) imidazoles and their derivatives was found to be against the clinical strains *C. krusei*, *C. kefyr* and *C. inconspicua* – mean values of minimal fungistatic concentrations concerning the indicated strains were 11.7–26.0 μg/mL. The examined nitro containing imidazole derivatives were found to manifest a slightly lower anti-*Candida* action against the clinical strains *C. tropicalis* and *C. guilliermondii* (mean values of minimal fungistatic concentrations 31.3 and 36.5 μg/mL). The lowest antifungal activity of the examined compounds was detected against the clinical strains *C. albicans* and *C. glabrata* – mean values of minimal fungistatic concentrations against these strains were 85.9 and 79.4 μg/mL. Comparison of anti-*Candida* activity of different 5-(2-nitrovinyl) imidazoles and their derivatives enabled us to select their most promising representatives and give recommendations for further synthesis of new nitro containing imidazole derivatives with pronounced antifungal properties.

Keywords: nitro containing imidazole derivatives; yeast-like fungi; *Candida*; clinical strains; antifungal means; anti-*Candida* action; antimycotic agents.

Introduction

Candidiasis is the most widespread fungal infection in the world. Causative agents of candidiasis – *Candida* spp. are the 4th most widespread microorganisms, being often recorded among patients who take broad-spectrum antibacterial drugs, after immunosuppressive therapy, parenteral nutrition, undergoing various invasive medical procedures, in HIV-infected newborns and AIDS patients, and most frequently in patients suffering from vulvovaginal candidiasis (Hani et al., 2015).

Nowadays more and more publications are appearing which report the development of resistance of yeast-like fungi of the *Candida* genus to new and existing antifungal preparation (Whaley et al., 2016). Studies conducted in 98 laboratories in 34 countries have demonstrated that the sensitivity to 7 antifungal remedies known in therapeutic practice of clinical strains of yeast-like fungi depends on epidemiological value and geographic existence of isolates (Pfaller, 2012; Posteraro et al., 2015). Mostly, fungal diseases are treated with azoles (fluconazole, itraconazole, voriconazole, posaconazole) (Pfaller et al., 2013; Posteraro et al., 2015; Xiao et al., 2015), which in a number of cases demonstrate a high toxicity, have low tolerance and are characterized by a narrow spectrum of effect and cause formation of azole-resistant strains (Xiao et al., 2015; Jensen et al., 2016; Karabıçak & Alem, 2016; Whaley et al., 2016).

Therefore, the treatment of candidiasis was and remains a topical issue, especially considering the fact that due to administration of broad-spectrum antimycotic agents, a clear resistance of pathogens of fungal diseases is observed. Also, over many years, using antifungal imidazole derivatives has been relevant in medical practice. Apart from antifungal properties, these preparations have other pharmaceutical properties untypical for classic imidazole derivatives, including antiviral, anticancer, antituberculous and analgesic (Verma et al., 2013; Chen et al., 2014). Also, a relevant and important task is developing a methodology of structural modification of known imidazole derivatives by pharmacophore groups, which would provide a broad spectrum of structurally similar compounds – a basis for systemic investigation of "structure – activity" relations.

In this respect, an interesting preparation is a hybrid modification of the known imidazole derivatives by a fragment which plays an important part in the formation of antimicrobial properties of these compounds (Chornous et al., 2014).

The objective of our study was to investigate antifungal activity of new nitro-containing imidazole derivatives – 5-(2-nitrovinyl) imidazoles and their derivatives in relation to clinical strains of yeast-like fungi of the *Candida* genus isolated from the vulvovaginal content of women suffering from vulvovaginal candidiasis.

Materials and methods

During the determination of antifungal activity, we took into consideration the recommendations of the European Committee on Antimicrobial Susceptibility Testing (EUCAST), and the USA National Committee for Clinical Laboratory Standards. These recommendations were suggested by Clinical and Laboratory Standards Institute – document CLSI M27-A3, 2008, developed and recommended for examinations of antifungal activity of yeast-like fungi in liquid nutrient medium (Castanheira et al., 2014). We studied the antifungal action of four new nitro containing imidazole derivatives – two 5-(2-nitrovinyl) imidazoles (compounds I, II) and their two derivatives (compounds III, IV) synthesized at the Department of Medical and Pharmaceutical Chemistry, Bukovinian State Medical University with the following structural formulas:

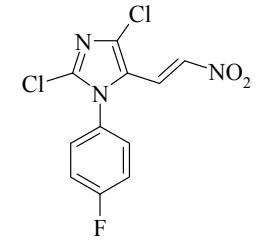

I

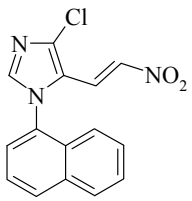

II

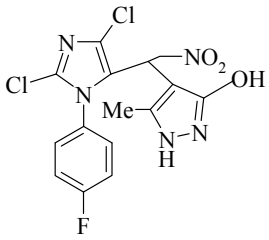

III

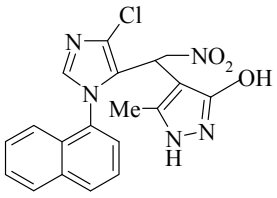

IV

Synthesis of the mentioned imidazole derivatives was done by the method (Chornous et al., 2014) in the following way.

1-aryl-4-chloro-5-(2-nitrovinyl)imidazoles I and II. 0.39 g (0.005 mole) of ammonium acetate was added to the solution of 0.01 mole of 2,4-dichloro-5-formylimidazole (for compound I) or 1-naphthyl-4-chloro-5-formylimidazole (for compound II) in 5 ml of nitromethane, and then boiled for 4 hours. The nitromethane excess was evaporated at reduced pressure, and the residue was crystallized from ethanol.

4-[1-(1-aryl-4-chloro-1H-imidazole-5-yl)-2-nitrovinyl]-5-methyl-1H-pyrazole-3-oles III and IV. The mixture of 0.005 mole (2-nitrovinyl) imidazole I or II and 0.6 g (0.006 mole) 3-methyl-2-pyrazoline-5-one was boiled for 3 hours in 20 ml of water. The mixture was cooled, the formed sediment was filtered, dried and crystallized from acetic acid.

Compounds I–IV – crystallized substances of yellow or maize yellow colour, well soluble in high polar organic solvents. Their content was proven by the elemental analysis, and their structure – by the results of measuring of infrared (IR) and ^{1}H nuclear magnetic resonance (^{1}H NMR) spectra. IR-spectra of the synthesized compounds were recorded on a UR-20 spectrophotometer in the table KBr. ^{1}H NMR and ^{13}C NMR spectra were recorded on a Varian-Gemini spectrophotometer (300 MHz) in the solution of dimethylsulfoxide-d6 (DMSO)-d6, internal standard – tetramethylsilane. Chromate mass spectra were obtained on the example PE SCXAPI 150 EX, UV (250 nm) and ELSOJ detectors.

In the role of testing microorganisms, we used clinical strains of yeast-like fungi belonging to *Candida* genus isolated and identified from the vulvovaginal content of women suffering from vulvovaginal candidiasis including *C. albicans*, *C. guillermondii*, *C. krusei*, *C. glabrata*, *C. kefyr*, *C. tropicalis*, *C. inconspicua* and *C. zeylanoides* (Yakovychuk et al., 2017). To assess antibiotic sensitivity of microorganisms to new chemical compounds the following successive stages were performed. First of all, solutions of new chemical compounds were prepared for the serial dilution method (in the concentration 1000 μg/ml). Due to the fact that new chemical compounds differ considerably by the degree of solubility, dimethylsulfoxide (DMSO) was used as a solvent. Twofold serial dilutions of the examined compounds were prepared (from 500 μg/ml – 1st well of the microtiter plate to 0.2 μg/ml – 12th well of the microtiter plate).

The suspension of the examined yeast-like fungi (inoculum) was prepared from twenty-four-hour culture. Using an inoculation loop, we selected several one-type isolated colonies, transferred a small amount of the material into a test tube with sterile physiological solution, and using a DEN-1 Biosan densitometer, we obtained the suspension of microorganisms in the concentration of 1.5 x 10^8 CFU/ml, which corresponded to the McFarland turbidity standard 0.5. Then, no later than 15 minutes, using a tenfold serial dilution in Saburo liquid nutrient medium, we obtained the appropriate working microbial suspension with yeast-like fungi in the concentration of 2.5 x 10^3 CFU/ml. Antifungal activity was determined using the micromethod of twofold serial dilutions in disposable polystyrene 96-well microtiter plates with application of 8-channel sampler and incubated at the temperature of 35 °C during 24 hours.

At the final stage, we conducted visual analysis of the results, comparing the growth of the microorganism in the presence of new chemical compound with the growth of culture (control) without it. Minimal fungicidal concentration (MFcC) and fungistatic concentration (MFSC) were determined using the micromethod of serial dilutions within 1.9–500 μg/ml. The minimal fungistatic concentration was considered the concentration of the examined compound, in the presence of which, no growth of the culture was observed (by the level of microbial turbidity of the growth medium). MFcC was determined using inoculation on Petri dishes with sterile 2% dense Saburo growth medium without clearly observed growth of fungi which were transparent visually, and then incubated in the thermostat at the optimal temperature for growth of fungi. The results were analyzed for the test fungi after 48–72 hours, that is, the lack of growth of colonies was observed.

The control was the rows of microtiter plate wells with the used medium – control medium, and the lines of microtiter plate wells containing the test-strain in the medium with the solvent used to prepare the solution of the examined compound. In the growth controls of the test-strains and the solvent, the growth of microorganisms was observed. The medium control was transparent, indicating its sterility.

The experiment with every compound and every clinical strain of *Candida* yeast-like fungi was replicated three times. The analysis of the obtained digital results was conducted using Biostatistics (Biostat 3.0) program, developed for statistical processing of the results of medical and biological studies. We calculated mean values (x), standard deviations (± SD) and confidence intervals.

Results

During the examination of the antifungal activity of 5-(2-nitrovinyl) imidazoles and their derivatives in relation to *Candida* clinical strains isolated from the vulvovaginal content of women suffering vulvovaginal candidiasis, the values of their minimal fungistatic concentrations were determined (Fig. 1–4). The data demonstrate that the highest anti-*Candida* activity in relation to the examined clinical strain of *C. albicans* was manifested by 3-methyl-4-[1-(1-naphthyl-4-chloro-1H-imidazole-5-yl)-2-nitroethyl-]-1H-pyrazole-5-ole (compound IV) and 2,4-dichloro-5-(2-nitrovinyl)-1-(4-fluorovenyl)-1H-imidazole (compound I). Their mean values of minimal fungistatic concentrations (MFsC) were 31.3 and 41.7 ± 10.4 μg/ml respectively. Compounds III (2,4-dichloro-3-methyl-4-{2-nitroethyl-1-[1-(4-fluorophenyl)-1H-imidazole-5-yl]}-1H-

pyrazole-5-ole and compound II (1-naphthyl-5-(2-nitrovinyl)-4-chloro-1H-imidazole) demonstrated lower anti-candida activity – their mean values of minimal fungistatic concentrations (MFsC) were 104.2 ± 20.8 and 166.7 ± 1.6 μg/ml respectively.

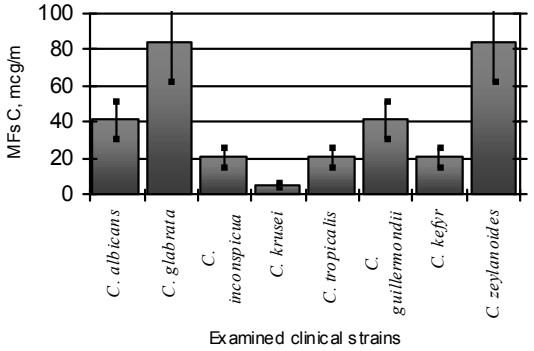

Fig. 1. Minimal fungistatic concentrations (MFsC) of 2,4-dichloro-5-(2-nitrovinyl)-1-(4-fluorophenyl)-1H-imidazole (compounds I) in relation to *Candida* clinical strains isolated from the vulvovaginal content of women suffering from vulvovaginal candidiasis (n = 3)

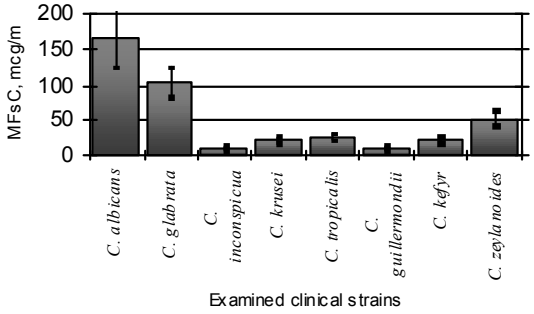

Fig. 2. Minimal fungistatic concentrations (MFsC) of 1-naphthyl-5-(2-nitrovinyl)-4-chloro-1H-imidazole (compound II) in relation to *Candida* clinical strains isolated from the vulvovaginal content of women suffering from vulvovaginal candidiasis (n = 3)

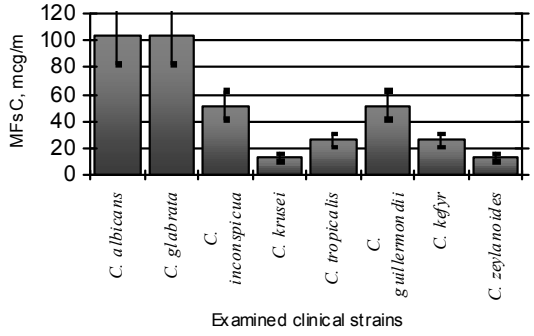

Fig. 3. Minimal fungistatic concentrations (MFsC) of 2,4-dichloro-3-methyl-4-{2-nitroethyl-1-[1-(4-fluorophenyl (compounds III) in relation to *Candida* clinical strains isolated from the vulvovaginal content of women suffering from vulvovaginal candidiasis (n = 3)

Minimal fungicidal concentrations (MFcC) of the examined compounds in relation to the abovementioned clinical strain of *C. albicans* were 2.0–3.3 times higher than their minimal fungistatic concentrations and were 104.2 ± 20.8 to 333.3 ± 3.2 μg/ml (Fig. 5–8).

The study of anti-*Candida* activity of new nitro containing imidazoles in relation to clinical strain of *C. glabrata* determined that the highest activity was demonstrated by the compound IV (MFsC is 26.0 ± 5.2), lower activity – by compound I (MFsC is 83.3 ± 20.8) (Fig. 1–4). Similarly to the case with the clinical strain of *C. albicans*, compounds II and III demonstrated the lowest anti-*Candida* activity, and against clinical strain of *C. glabrata*, their minimal fungistatic concentrations were 104.2 ± 20.8 μg/ml. It should be mentioned that fungicidal action of these compounds in relation to *C. glabrata* was rather low and equaled 208.3 ± 41.7 μg/ml for compounds I and IV and 500 μg/ml for compounds II and III (Fig. 5–8).

It was determined that 5-(2-nitrovinyl) imidazoles and their derivatives demonstrated higher antifungal activity against the examined clinical strain *C. inconspicua*. Thus, MFsC of the compound II in relation to this strain was 10.4 ± 2.6 μg/ml, compounds I and IV – 20.8 ± 5.2 μg/ml, and compound III – 52.1 ± 10.4 μg/ml (Fig. 1–4). Minimal fungicidal concentrations of these compounds against this clinical strain ranged significantly from 26.0 ± 5.2 to 208.3 ± 41.7 μg/ml (Fig. 5–8).

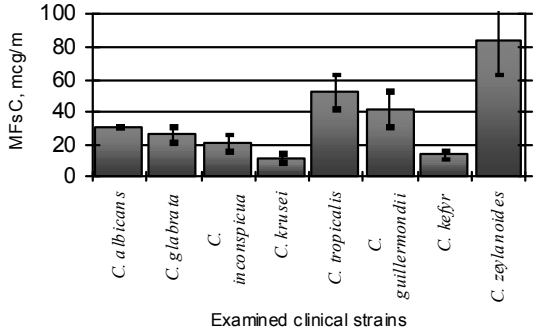

Fig. 4. Minimal fungistatic concentrations (MFsC) of 3-methyl-4-[1-(1-naphthyl-4-chloro-1H-imidazole-5-yl)-2-nitroethyl-]-1H-pyrazole-5-ole (compounds IV) in relation to *Candida* clinical strains isolated from the vulvovaginal content of women suffering from vulvovaginal candidiasis (n = 3)

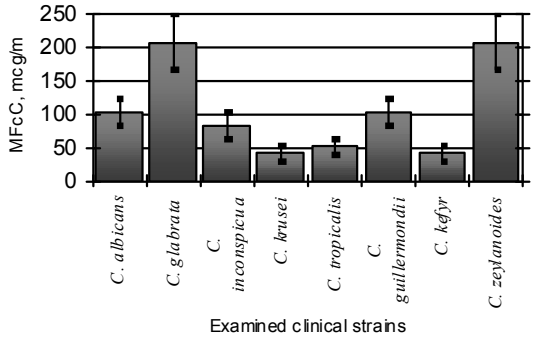

Fig. 5. Minimal fungicidal concentrations (MFcC) of 2,4-dichloro-5-(2-nitrovinyl)-1-(4-fluorovinyl)-1H-imidazole (compound I) in relation to *Candida* clinical strains isolated from the vulvovaginal content of women suffering from vulvovaginal candidiasis (n = 3)

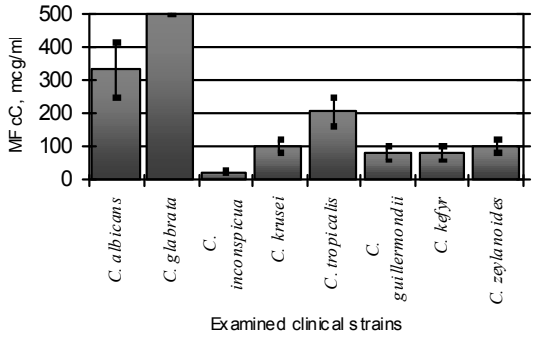

Fig. 6. Minimal fungicidal concentrations (MFcC) of 1-naphthyl-5-(2-nitrovinyl)-4-chloro-1H-imidazole (compound II) in relation to *Candida* clinical strains isolated from the vulvovaginal content of women suffering from vulvovaginal candidiasis (n = 3)

Similar patterns were found during the study of anti-*Candida* activity of the new nitro containing imidazole derivatives against strains *C. krusei* and *C. tropicalis*. Minimal fungistatic concentrations of the examined compounds in relation to clinical strain *C. krusei* ranged from 5.2 ± 1.3 μg/ml (compound I) to 20.8 ± 5.2 μg/ml (compound II), and minimal fungicidal concentrations – 20.8 ± 5.2 to 104.2 ± 20.8 μg/ml (Fig. 1–8).

Against *C. tropicalis* clinical strain, minimal fungistatic concentrations of the studied compounds ranged from 20.8 ± 5.2 (compound I) to 52.1 ± 10.4 μg/ml (compound IV), and minimal fungicidal ones from 52.2 ± 10.3 (compound I) to 208.3 ± 41.7 μg/ml (compounds II and IV) (Fig. 1–8). It was determined that the examined new nitro-containing imidazole derivatives exhibit anti-*Candida* activity against the clinical strain of *C. guilliermondii*. The highest anti-*Candida* activity was demonstrated by the compound II (MFsC of 10.4 ± 2.6 μg/ml), and lower activity – by the compounds I and IV (MFsC of 41.7 ± 10.4 μg/ml. Fungistatic concentrations of the abovementioned compounds against the clinical strain of *C. guilliermondii* were twice as high as fungistatic ones (compound III), higher by 2.5 (compounds I and IV) and 8 times (compound II) (Fig. 1–8).

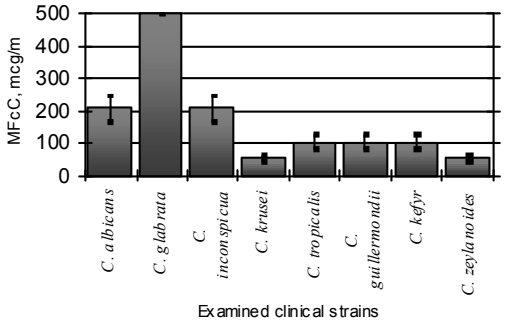

Fig. 7. Minimal fungicidal concentrations (MFcC) of 2,4-dichloro-3-methyl-4-{2-nitroethyl-1-[1-(4-fluorophenyl (compounds III) in relation to *Candida* clinical strains isolated from the vulvovaginal content of women suffering from vulvovaginal candidiasis (n = 3)

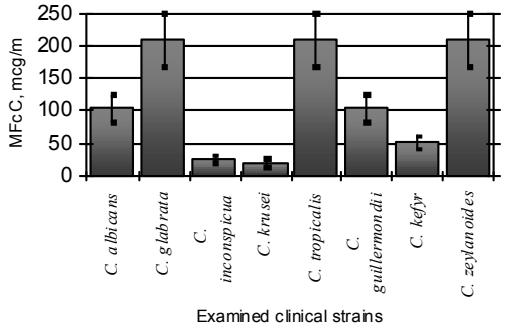

Fig. 8. Minimal fungicidal concentrations (MFcC) of 3-methyl-4-[1-(1-naphthyl-4-chloro-1H-imidazole-5-yl)-2-nitroethyl-]-1H-pyrazole-5-ole (compounds IV) in relation to *Candida* clinical strains isolated from the vulvovaginal content of women suffering from vulvovaginal candidiasis (n = 3)

Two of the four examined compounds (compounds I and II) demonstrated minimal fungistatic concentrations against the clinical strain of *C. kefyr*: at the level of 20.8 ± 5.2 μg/ml, and compounds IV and III – at the level of 13.0 ± 2.6 and 26.0 ± 5.2 μg/ml respectively (Fig. 1–4). Minimal fungicidal concentrations of these compounds against *C. kefyr* strain ranged from 41.7 ± 10.4 (compound I) to 104.2 ± 20.8 μg/ml (compound III).

Lower anti-*Candida* activity of the examined compounds was determined against the clinical strain of *C. zeylanoides*. Minimal fungistatic concentrations of the three of four examined compounds against *C. zeylanoides* clinical strain ranged from 52.1 ± 10.4 to 83.3 ± 20.8 μg/ml. Only the compound III demonstrated a slightly higher anti-*Candida* activity – its MFsC was 13.0 ± 2.6 μg/ml. Similar results were observed in the minimal fungicidal concentrations – for the three out of four examined compounds they ranged from 104.2 ± 20.8 to 208.3 ± 41.7 μg/ml, and compound III demonstrated lower MFcC – 52.1 ± 10.4 μg/ml (Fig. 5–8).

Discussion

Comparing anti-*Candida* activity of the examined 5-(2-nitrovinyl) imidazoles and their derivatives against the clinical strains of *Candida*, it should be mentioned that these compounds demonstrated the highest activity against the clinical strain of *C. krusei*. Their minimal fungistatic concentrations against this strain ranged from 5.2 ± 1.3 to 20.8 ± 5.2 μg/ml. Mean values of the minimal fungistatic concentrations of all four examined compounds against this equaled 12.5 μg/ml.

5-(2-nitrovinyl) imidazoles and their derivatives demonstrated considerably lower anti-*Candida* activity against the clinical strains of *C. kefyr* and *C. inconspicua* (mean values of MFsC 20.2 and 26.0 μg/ml), and *C. tropicalis* and *C. guilliermondii* (mean values of MFsC 31.3 and 36.5 μg/ml). The studied compounds demonstrated the lowest antifungal activity against the clinical strains of *C. albicans* and *C. glabrata* – mean values of MFsC in relation to these strains were 85.9 and 79.4 μg/ml.

The analysis of anti-*Candida* effectiveness of certain examined compounds in relation to all eight studied *Candida* clinical strains revealed the following. Compound IV was the most active (3-methyl-4-[1-(1-naphthyl-4-chloro-1H-imidazole-5-yl)-2-nitroethyl-]-1H-pyrazole-5-ole). The mean value of minimal fungistatic concentrations of this compound against all eight studied clinical strains of yeast-like *Candida* fungi was 34.9 μg/ml (with the range of MFsC against these clinical strains equaling 10.8 to 83.3 μg/ml). Compound I (2,4-dichloro-5-(2-nitrovinyl)-1-(4-fluorovinyl)-1H-imidazole) demonstrated a slightly lower mean value of minimal fungistatic concentrations against all eight studied clinical strains of yeast-like *Candida* fungi – 39.7 μg/ml (with the range of MFsC against these clinical strains equaling 5.2–83.3 μg/ml). Even lower anti-*Candida* activity was demonstrated by compound III (2,4-dichloro-3-methyl-4-[1-(1-naphthyl-4-chloro-1H-imidazole-5-yl)-2-nitroethyl-]-1H-pyrazole-5-ol) and II (1-naphthyl-5-(2-nitrovinyl)-4-chloro-1H-imidazole). Their mean values of minimal fungistatic concentrations against all eight studied clinical strains of *Candida* yeast-like fungi were 48.8 and 51.4 μg/ml respectively (with MFsC in relation to these clinical strains ranging 13.0–104.2 and 10.4–166.7 μg/ml).

Comparing anti-candida activity of the examined 5-(2-nitrovinyl)imidazoles and their derivatives with the results of other imidazole derivatives, described in the scientific literature, we determined the following.

A well-known first-line antifungal drug recommended by the World Health Organization (WHO), which has an exceptional therapeutic effect in treating infections caused by *Candida* yeast-like fungi is fluconazole. Its poor water solubility, absence of the effect in case of invasive aspergillosis and increase of fluconazole-resistant isolates of *C. albicans*, limit its clinical use and therefore its being an object of studies focused on modifying the structure of fluconazole. Synthesized fluconazole analogues demonstrated antifungal activity against *C. albicans*, *C. mycoderma* and *C. utilis* with minimal inhibiting values at the level of 32 μg/ml (Zhang, 2013).

The examined 3-methyl-4-[1-(1-naphthyl-4-chloro-1H-imidazole-5-yl)-2-nitroethyl-]-1H-pyrazole-5-ole (Compound IV) demonstrated anti-*Candida* activity against clinical strain of *C. albicans* on the level of fluconazole analogues with the value of minimal fungistatic concentration equaling 31.3 μg/ml, and compound I (2,4-dichloro-5-(2-nitrovinyl)-1-(4-fluorovinyl)-1H-imidazole) demonstrated activity close to fluconazole analogues with minimal fungistatic concentration of 41.7 ± 10.4 μg/ml.

Minimal fungistatic concentration of 1-substituted 4-chloro-5-(2-nitrovinyl)imidazoles against antibiotic-resistant strain of *C. albicans* isolated from the patients was 62.5 μg/ml, and the minimal fungicidal concentration – 125 μg/ml (Chornous et al., 2014). The examined compounds IV and I exhibited higher anti-*Candida* activity compared with 1-substituted 4-chloro-5-(2-nitrovinyl)imidazoles – their minimal fungistatic concentrations were 31.3 and 41.7 μg/ml respectively, and minimal fungicidal concentrations – 104.2 μg/ml.

Examination of anti-*Candida* activity of 3-imidazole-1-aryl-2-propene-1-ones revealed their fungistatic activity ranging 62.5–125.0 μg/ml, and the fungicidal activity – 125–250 μg/ml (Melnyk, 2016). The presented results coincide with results which we obtained on the clinical strain of *C. albicans* yeast-like fungi, isolated from the vulvovaginal content of women suffering from vulvovaginal candidiasis (MFsC ranged 31.3–166.7 μg/ml, MFcC ranging 104.2–333.3 μg/ml).

Imidazoles on the basis of chromen demonstrated anti-*C. albicans* activity with minimal inhibiting concentrations of 12.5 μg/ml, similarly to the minimal inhibiting concentration (12.5 μg/ml) of ketoconazole

(Thareja, 2010). Compound IV (3-methyl-4-[1-(1-naphthyl-4-chloro-1H-imidazole-5-yl)-2-nitroethyl-]-1H-pyrazole-5-ole) demonstrated anti-*Candida* activity against clinical strain of *C. albicans* with minimal fungistatic concentration of 31.3 μg/ml, which is 2.5 times less than the corresponding values of imidazoles on the base of chromen and ketoconazole. The examined 5-(2-nitrovinyl)imidazoles and their derivatives which we studied also exhibited lower anti-candida activity compared to clotrimazole, minimal inhibiting concentration of which was 5 μg/ml (Padmavathi, 2010), and fluconazole with minimal inhibiting concentration equaling 1 μg/ml (Gupta, 2012).

Minimal inhibiting concentrations of a number of new synthesized imidazole derivatives against *C. albicans* (ATCC 10231) and *C. albicans* (ATCC 24433) were found to be 16–32 μg/ml (Gupta, 2012). These results are also close to the data we obtained for anti-*Candida* activity of compound IV (3-methyl-4-[1-(1-naphthyl-4-chloro-1H-imidazole-5-yl)-2-nitroethyl-]-1H-pyrazole-5-ole) against the clinical strain of *C. albicans* with minimal fungistatic concentration of 31.3 μg/ml.

4-[1-(4-chloro-1H-imidazole-5-iл)-2-nitroalkyl]-5-methyl-1H-pyrazole-3-oles demonstrated fungistatic activity against an antibiotic-resistant strain of *C. albicans* isolated from the patients ranging 62.5–250 μg/ml, and fungicidal activity ranging 125–500 μg/ml (Chomous et al., 2014), which is lower compared to the antifungal activity of the compounds we studied – their fungistatic activity ranged 31.3–166.7 μg/ml, and the fungicidal activity – 104.2–333.3 μg/ml.

Similar results were obtained during comparing the anti-*Candida* activity of the examined compounds and 2-amino-4(1-aryl-4-chloro-1H-imidazole-5-yl)-7,7-dimethyl-5-oxo-5,6,7,8-tetrahydro-4H-chromen-3-carbonitryls, minimal fungistatic concentrations of which ranged 31.3–62.5 μg/ml, and minimal fungicidal concentrations 62.5–125 μg/ml (Melnyk, 2016).

Therefore, the comparison of the data we obtained with the literature data demonstrated that the examined 5-(2-nitrovinyl)imidazoles and their derivatives exhibit anti-candida activity which is higher or similar to that of the new synthetic imidazole derivatives. However, in certain cases, they demonstrate lower activity compared to the new synthetic compounds and preparations used in clinical work. On the one hand, this indicates a perspective of using 5-(2-nitrovinyl)imidazoles and their derivatives as antimicrobial agents (first of all anti-*Candida* compounds), and on the other hand, it indicates the need for the search for new representtatives of 5-(2-nitrovinyl)imidazoles and their derivatives with stronger antimicrobial properties.

Conclusions

Of the nitro-containing imadozole derivatives, the highest anti-*Candida* activity against the *Candida* clinical strains isolated from the vulvovaginal content of women suffering from vulvovaginal candidiasis was exhibited by 3-methyl-4-[1-(1-naphthyl-4-chloro-1H-imidazole-5-yl)-2-nitroethyl-]-1H-pyrazole-5-ol and 2,4-dichloro-5-(2-nitrovinyl)-1-(4-fluorophenyl)-1H-imidazole – mean values of their minimal fungistatic concentrations against the eight examined clinical strains of *Candida* yeast-like fungi were 34.9 and 39.7 μg/ml respectively.

It was determined that 5-(2-nitrovinyl)imidazoles and their derivatives demonstrated the highest activity against clinical strain of *C. krusei*, the minimal fungistatic concentrations of the examined compounds ranged from 5.2 ± 1.3 to 20.8 ± 5.2 μg/ml. New nitro containing imidazole derivatives exhibited lower anti-*Candida* activity against clinical strains of *C. kefyr*, *C. inconspicua*, *C. tropicalis* and *C. guilliermondii* (mean values of minimal fungistatic concentrations ranged 20.2–36.5 μg/ml).

References

Castanheira, M., Messer, S. A., Rhomberg, P. R., Dietrich, R. R., Jones, R. N., & Pfaller, M. A. (2014). Isavuconazole and nine comparator antifungal susceptibility profiles for common and uncommon *Candida* species collected in 2012: Application of new CLSI clinical breakpoints and epidemiological cutoff values. Mycopathologia, 178(1–2), 1–9.

Chomous, V. O., Mel′nyk, O. Y., Hroza, A. M., Yakovychuk, N. D., & Vovk, M. V. (2014). Syntez ta antymikrobna aktyvnist′ 4-khloro-5-(2-nitrovinil)-1N-imidazoliv i produktiv yikh vzayemodiyi z 3-metyl-2-pirazolin-5-onom. [Synthesis and antimicrobial activity of 4-chloro-5-(2-nitrovinyl)-1h-imidazoles and products of their interaction with 3-methyl-2-pyrazolin-5-one]. Journal of Organic and Pharmaceutical Chemistry, 47, 28–32 (in Ukrainian).

Gupta, A. K., Jain, A., Mishra, S., & Jiaswal, A. (2012). Design and synthesis of substituted imidazole derivatives as antifungal agents. International Journal of Drug Design and Discovery, 3(4), 943–954.

Hani, U., Shivakumar, H. G., Vaghela, R., Osmani, R. A., & Shrivastava, A. (2015). Candidiasis: A fungal infection-current challenges and progress in prevention and treatment. Infect Disord Drug Targets, 15(1), 42–52.

Jensen, R. H., Hagen, F., Astvad, K. M., Tyron, A., Meis, J. F., & Arendrup, M. C. (2016). Azole-resistant *Aspergillus fumigatus* in Denmark: A laboratory-based study on resistance mechanisms and genotypes. Clinical Microbiology and Infection, 22(6), 570.

Karabıçak, N., & Alem, N. (2016). Antifungal susceptibility profiles of *Candida* species to triazole: Application of new CLSI species-specific clinical breakpoints and epidemiological cutoff values for characterization of antifungal resistance. Mikrobiyoloji Bulteni, 50(1), 122–132.

Padmavathi, V., Mahesh, K., Reddy, G. D., & Padmaja, A. (2010). Synthesis and bioassay of pyrrolyl oxazolines and thiazolines. European Journal of Medicinal Chemistry, 45(7), 3178–3183.

Pfaller, M. A. (2012). Antifungal drug resistance: Mechanisms, epidemiology, and consequences for treatment. The American Journal of Medicine, 125(1), 3–13.

Pfaller, M. A., Messer, S. A., Rhomberg, P. R., Jones, R. N., & Castanheira, M. (2013). *In vitro* activities of isavuconazole and comparator antifungal agents tested against a global collection of opportunistic yeasts and molds. Journal of Clinical Microbiology, 51(8), 2608–2616.

Posteraro, B., Spanu, T., Fiori, B., De Maio, F., De Carolis, E., Giaquinto, A., Prete, V., De Angelis, G., Torelli, R., D'Inzeo, T., Vella, A., De Luca, A., Tumbarello, M., Ricciardi, W., & Sanguinetti, M. (2015). Antifungal susceptibility profiles of bloodstream yeast isolates by Sensititre Yeast One over nine years at a large Italian teaching hospital. Antimicrob Agents Chemother, 59, 3944–3955.

Thareja, S., Verma, A., Kalra, A., Gosain, S., Rewatkar, P. V., & Kokil, G. R. (2010). Novel chromeneimidazole derivatives as antifungal compounds: Synthesis and *in vitro* evaluation. Acta Poloniae Pharmaceutica, 67(4), 423–427.

Verma, A., Joshi, S., & Singh, D. (2013). Imidazole: Having versatile biological activities. Journal of Chemistry, 12, 1–12.

Whaley, S. G., Berkow, E. L., Rybak, J. M., Nishimoto, A. T., Barker, K. S., & Rogers, P. D. (2016). Azole antifungal resistance in *Candida albicans* and emerging non-albicans *Candida* species. Frontiers in Microbiology, 7, 2173.

Xiao, M., Fan X., Chen, S. C., Wang, H., Sun, Z. Y., Liao, K., Chen, S. L., Yan, Y., Kang, M., Hu, Z. D., Chu, Y. Z., Hu, T. S., Ni, Y. X., Zou, G. L., Kong, F., & Xu, Y. C. (2015). Antifungal susceptibilities of *Candida glabrata* species complex, *Candida krusei*, *Candida parapsilosis* species complex and *Candida tropicalis* causing invasive candidiasis in China: 3 year national surveillance. Journal Antimicrobial Chemotherapy, 70(3), 802–810.

Yakovychuk, N. D., Dejneka, S. Y., Sydorchuk, I. I., Sydorchuk, L. I., Humenna, A. V., & Bendas, V. V. (2017). Populyatsiynyy riven′ holovnoyi mikrobioty ta drizhdzhopodibnykh hrybiv rodu *Candida* v zhinok, yaki khvori na vul′vovahinal′nyy kandydoz [Population level of main microbiota and yeast-like fungi of genus *Candida* in women with vulvovaginal candidiasis]. Zaporiz′kyy Medychnyy Zhurnal, 19(3), 337–341 (in Ukrainian).

Zhang, S. L., Chang, J. J., Damu, G. L. V., Geng, R. X., & Zhou, C. H. (2013). Berberine azoles as antimicrobial agents: Synthesis, biological evaluation and their interactions with human serum albumin. Medicinal Chemistry Communications, 4, 839–846.

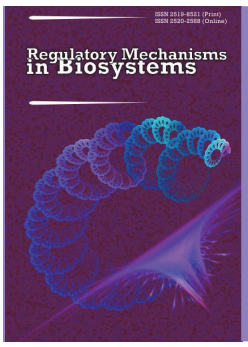

Regulatory Mechanisms in Biosystems

ISSN 2519-8521 (Print)
ISSN 2520-2588 (Online)
Regul. Mech. Biosyst., 9(3), 374–378
doi: 10.15421/021855

Antimicrobial activity of phytoextracts on opportunistic oral bacteria, yeast and bacteria from probiotics

N. M. Vorobets*, M. V. Kryvtsova**, O. Y. Rivis**,
M. Y. Spivak ***, H. V. Yavorska****, H. M. Semenova*****

**Danylo Halytsky Lviv National Medical University, Lviv, Ukraine*
***Uzhhorod National University, Uzhhorod, Ukraine*
****Danylo Zabolotny Institute of Microbiology and Virology, National Academy of Sciense of Ukraine, Kyiv, Ukraine*
*****Ivan Franko Lviv National University, Lviv, Ukraine*
******Bacteriological Laboratory of Uzhhorod District Hospital, Uzhhorod, Ukraine*

Article info

Received 03.08.2018
Received in revised form 27.08.2018
Accepted 29.08.2018

Danylo Halytsky Lviv National Medical University, Pekarska st., 69, Lviv, 79010, Ukraine.

Uzhhorod National University, Voloshyna st., 32, Uzhhorod, 88000, Ukraine.
Tel.: +38-050-278-54-97.
E-mail: maryna.krivcova@gmail.com

Danylo Zabolotny Institute of Microbiology and Virology, National Academy of Sciense of Ukraine, Acad. Zabolotny st., 154, Kyiv, D03680, Ukraine.

Ivan Franko Lviv National University, Hrushevsky st., 4, Lviv, 79004, Ukraine.

Bacteriological Laboratory of Uzhhorod District Hospital, Mynajska st., 71, Uzhhorod, 88000, Ukraine.

Vorobets, N. M., Kryvtsova, M. V., Rivis, O. Y., Spivak, M. Y., Yavorska, H. V., & Semenova, H. M. (2018). Antimicrobial activity of phytoextracts on opportunistic oral bacteria, yeast and bacteria from probiotics. Regulatory Mechanisms in Biosystems, 9(3), 374–378. doi:10.15421/021855

Developed experimental assays enable us to compare the antimicrobial activity of herbal medicinal drugs on *Lactobacillus* and *Bacillus* strains probiotics, which have been claimed to possess the ability of suppressing the growth of various oral pathogens. In the treatment of periodontal disease it is advisable to use a comprehensive approach which would include the application of herbal remedies and probiotics. The combination of such effects may be a new approach in dentistry due to their complementary antimicrobial activity. In this study, we researched antimicrobial effects of herbal medicinal drugs (tinctures of some medical plants, solutions Rotocanum and Chlorophyllipt) against collection strains and clinical strains isolated from the oral cavity of patients with periodontitis, and probiotic strains *Bacillus subtilis* UKM B-5007 and *Bacillus licheniformis* UKM B-5514 that are part of the active base of probiotic Biosporin (Ukraine), *Bacillus clausii* from the probiotic Normaflore (Hungary), as well as the strains *Lactobacillus* spp. – from probiotic *Lactobacterinum* (Biopharma, Ukraine). For investigation, the standard agar dilution method was used in modification with glass cylinders. The results of the research showed that among the studied herbal medicinal remedies, tinctures of *Eucalypthus viminalis*, *Mentha piperita* and Chlorophyllipt had the strongest antimicrobial activity. Probiotic strains are also sensitive to herbal tinctures (except the tinctura of wormwood), which indicate the possibility of only consecutive usage (with an interval of time) of herbal remedies and probiotics in combination therapy in the treatment of periodontal diseases.

Keywords: antimicrobial activity; herbal medicinal remedies; probiotics; periodontal diseases.

Introduction

Oral health influences the general quality of life, and poor oral health is linked to chronic conditions and systemic diseases. Dental caries, gingivitis and periodontitis are prominent oral disorders. The current understanding is that the etiology of oral diseases is multifactorial but, in many cases, it includes a pathogenic response to bacterial and *Candida* infection (Radulovic et al., 2013; Vorobets & Rivis, 2017). Periodontitis is a common and widespread disease, which occurs due to pathogenic microbial infection established within the gingival sulcus. Treatment of patients with periodontal diseases should include both local and general therapy. It must be based on the understanding of the mechanisms of action of the pharmaceutical or prophylactic agents, and be used to be effective and at the same time safe for the patient. Currently, the drugs of plant origin correspond to such criteria, because active compounds in their composition can act bacteriostatically and bactericidally (Rios et al., 2005; Kačániováa et al., 2014; Hleba et al., 2016). Another group of medicines – probiotics have relatively recently started to be used for periodontal treatment. Probiotics are commonly bacteria from genera *Lactobacillus* (including strains *L. salivarius* and *L. plantarum*) and Bifidobacterium (including strains *B. bifidum*, *B. longum*) or others, which could be beneficial not only to the digestive system, but to oral health too (Mishra et al., 2014; Alok et al., 2017).

The mechanisms of probiotic action are mainly unknown but the inter-microbial species interactions are supposed to play a key role in this together with their immunostimulatory effects. The proposed mechanisms of action of probiotics on oral health correspond to those shown in studies of the gastrointestinal tract. These are aid in synthesis of vitamins B, and K, and also in the breakdown of bile salts, aid in enhancing innate and acquired immunity, and assistance in inhibition of pro-inflammatory mediators (Alok et al., 2017). It is known that oral diseases, including periodontitis, are often accompanied by qualitative and quantitative changes in the microbiota (Rivis et al., 2012; Curtis, 2014). This makes probiotics an alternative means of correction of microbiota of the mouth and of reducing the number of opportunistic pathogens. On the other hand, there is evidence that the occurrence of candidiasis of the oral cavity and its chronic form is caused not only by changes in the balance of microorganisms in the mouth, but also by the influence of intestinal microbiota (Zlatkina et al., 2001).

Therefore, a complex treatment should be performed targeting the mouth and lower parts of the gastrointestinal tract. Dysbacteriosis is not only excessive growth of pathogenic microbes in the gut, but also

involves the overall decline of the immune defence of the body (Alok et al., 2017) At the same time, it can involve such diseases as atopic dermatitis, eczema, thirst, bronchial asthma, food allergy in children. To restore normal intestinal microbiota, probiotics can be used, which are often composed of bifidobacteria and lactobacilli, which are able to show antagonism against pathogenic and opportunistic microorganisms. The results of our previous studies indicate that some industrial strains of spore bacteria that are used as a basis for probiotic products show high antagonistic activity against strains of microorganisms isolated from "periodontal pockets" (Rivis et al., 2013). However, from the clinical practitioner's point of view, direct recommendations for the use of probiotics cannot yet be given (Curtis, 2014). Beside this, there is a lack of information regarding the contributions of probiotics in oral health and their compatible use with plant origin remedies (Safronova, 2009; Shipradeep, 2012). Our research is focused on the determining of the antimicrobial properties of Tinctura Eucalypti, Tinctura Calendulae, Tinctura Menthae piperitae, Tinctura Absinthii, and also Tinctures Chlorophyllipt and Rotocanum against collection and clinical strains isolated from the oral cavity of patients with periodontitis and against probiotic strains that are part of the active base of probiotics Biosporin, Lactobacterin and Normaflore.

Material and methods

The effect of herbal medicinal products such as Rotocanum, Chlorophyllipt, Tinctura Calendulae, Tinctura Eucalipti, Tinctura Menthae piperitae, Tinctura Absinthii was investigated on collection and clinical isolated strains of microorganisms. The general chemical profiles of the extracts and their pharmacological effects against oral cavity diseases are summarized in Table 1.

To determine the antimicrobial activity of the herbal medicinal remedies, as test cultures we used bacteria from the American Type Culture Collection, USA: *Escherichia coli* ATCC 25922, *Staphylococcus aureus* ATCC 25923, *Enterococcus faecalis* ATCC 29212, and yeast *Candida albicans* ATCC 885-653; clinical strains of bacteria: *Staphylococcus aureus*, *Streptococcus salivarius*, *Enterobacter* sp., *Neisseria* sp.; yeast *Candida albicans*, isolated from the oral cavity of periodontitis patients; and bacteria *Bacillus subtilis* UKM B-5007 and *Bacillus licheniformis* UKM B-5514, isolated from probiotic Biosporin (Biopharma, Ukraine), and *Bacillus clausii* from the probiotic Normaflore (Manufacturer: Uniter Laboratory, France; holder of Sanofi-aventis S.p.A., Hungary trade license), as well as the strains *Lactobacillus* spp. – from probiotic Lactobacterinum (Biopharma, Ukraine). Positive control were prepared with the same solvents, which were used to prepare the plant Tinctures. The antiseptic drug Decasan (Solution of decamethoxine dihydrochloride 0.02% by weight in water with sodium chloride, Yuria-Pharm Ltd.) also has antimicrobial properties.

The agar diffusion method as adapted earlier using glass cylinders (Vorobets & Yavorska, 2016) was used. From the daily culture of microorganisms, a suspension was made in a sterile physiological solution, and every suspension was adjusted to equal 0.5 McFarland standard. Each cup of Muller-Hinton agar was filled with 0.1 ml of a bacterial suspension. The cups were dried at room temperature for an hour. Then on the culture medium with tweezers we carefully arranged sterile glass cylinders, into which 0.1 ml of the substance was contributed. Antimicrobial activity was judged by the presence and size of the growth zone of the studied microorganisms around the cylinder with the extract. To determine the antimicrobial activity of the examined samples, the following scale was used: diameter of the growth retardation zone more than 20 mm highly sensitive, 10–20 mm – sensitive, up to 10 mm – moderately sensitive. Ethanol of various concentrations was used as solvent control. All tests were performed at least three times.

Results of laboratory tests were processed by methods of variation statistics with the calculation of averages (M) and their error (m), the criterion of authenticity difference is determined using Fisher tables and adapted to the Medical Research simplified tables.

Table 1
Characteristics of Drugs Used

Latin name of the drug. Manufacturer	Active substance. Extractant	Pharmaceutical composition, basic active substances	Mode of action
Tinctura Eucalypti. LLC "DKP "Pharmaceutical Factory", Zhytomyr, Ukraine	*Eucalypti viminalis* folia Extractant 70% ethanol	Eucalyptus leaves contain essential oil (3%), flavonoids, tannins, ellagic acid, resins and waxes	Used to treat stomatitis, gangrenous pulpitis, inflammation of the oral mucosa; in otorhinolaryngology for the treatment of sore throat, chronic rhinitis and pharyngitis. In surgery, used to treat of abscesses, osteomyelitis, purulent mastitis, open fractures, burns and frostbite (Shulga, 2011)
Tinctura Calendulae. LLC "DKP "Pharmaceutical Factory", Zhytomyr, Ukraine	*Calendulae officinalis* floridis Extractant 70% ethanol	Saponins, tannins, flavonoid and carotenoid glycosides, organic acids, essential oil, carbohydrates resins, saponins, organic acids	In tincture form, taken internally, promotes healing of ailments in the digestive tract; also has anti-inflammatory and antibacterial activity (Shulga, 2011). Calendula's high molecular weight polysaccharides stimulate the immune system activity; have anti-inflammatory, antimicrobial, and moderate choleretic effect
Tinctura Menthae piperitae. PrAT Pharmaceutical Factory "Viola", Zaporozhye, Ukraine	*Menthae piperitae* folia Extractant 90% ethanol	Glycoside tropsolin, essential oils, menthol, potassium sulfate, phytosterols, ascorbic acid, sugar, starch, mucilage, pectin, pigment sorbuzin and others	Normalizes heart rate, improves circulation, relieves spasms of blood vessels and expands them, lowers blood pressure, and relieves stress. In dentistry is widely used as a component of menthol mouthwash, toothpastes and powders, solutions for rinsing the oral cavity in purpose of breath freshening
Tinctura Absinthii or Absinthii tinctura. PrAT Pharmaceutical Factory "Viola", Zaporozhye, Ukraine	*Artemisiae absinthii* herba Extractant 70% ethanol	Bitternesses	Has anti-inflammatory, antiseptic, anti-ulcer effect; used for the treatment of gingivitis, periodontitis; stimulates appetite, activates all stages of digestion
Chlorophyllipt. Corporation "Arterium", JSC "Halychpharm", Lviv, Ukraine	Extractum chlorophyllipti spissum Extractant 96% ethanol	Chlorophylls mixture of eucalyptus leaves	Has antibacterial (bacteriostatic and bactericidal) activity against staphylococci and antiseptic and anti-inflammatory activity; used to rinse the mouth at the stage of initial periodontal treatment; for local utilization (Shulga, 2011)
Rotocanum. State Enterprise "Experimental Plant of Medicines IBONH NAS of Ukraine", Kyiv, Ukraine	A mixture of liquid extracts (2 : 1 : 1): *Matricariae recutitae extractum fluidum* + *Calendulae extractum fluidum* + *Millefolii extractum fluidum.* Extractant 40% ethanol	–	Injected into the dental pockets in patients with parodontosis; in cases of stomatitis used as oral applications or baths (Shulga, 2011)

Results

The antimicrobial activity of the herbal medicinal remedies was tested *in vitro* (Table 2). Tinctura Calendulae showed antimicrobial effect on *E. coli*, *S. aureus*, *E. faecalis*, and probiotic strains. Moreover, such activity was greater than that of the antiseptic Decasan. However, it showed no or low antifungal activity and effects on bacteria of genus *Neisseria* and *Enterobacter* compared to controls. Research has shown

that Tinctura Eucalipti has high antimicrobial activity against Gram-positive, Gram-negative microorganisms, and probiotic strains. The diameters of zones of growth retardation were the highest for staphylococci (up to 30 mm), streptococci (up to 30 mm) and *B. clausii* (up to 40 mm) and significantly exceeded the effect of Decasan on test culture. The tincture did not reveal a pronounced antifungal effect compared to the control. Tinctura Menthae piperitae produces using 90% ethanol and Chlorophyllipt 96% one, but despite the presence of the extractant revealed high antimicrobial activity of these drugs against Gram-positive microorganisms, so that diameters of growth were in the range of 20 to 40 mm. These indicators significantly exceeded the effect of Decasan on test cultures. The Tinctura of peppermint inhibited the growth of Gram-negative microorganisms too. Phytopreparations of mint and Chlorophyllipt also have a high anti-candidal effect.

Table 2
Antimicrobial activity of plant medicinal drugs to test-bacteria

Plant medicinal remedies	*C. albicans* ATCC 885-653	*S. aureus* ATCC 25923	*E. faecalis* ATCC 29212	*E. coli* ATCC 25922	*C. albicans*	*S. aureus*	*Enterobacter* sp.	*Neisseria* sp. *S. salivarius*	*B. subtilis* UKM B-5007, *B. licheniformis* UKM B-5514 (Biosporin)	*B. clausii* (Normaflore)	*Lactobcillus* sp. (Lactobacterinum)
Tinctura Absinthii	18.0 ± 1.6	8.8 ± 2.0	16.5 ± 0.6*	10.3 ± 0.3	17.6 ± 0.4	12.8 ± 2.9	13.3 ± 1.0	6.7 ± 1.9	19.6 ± 0.9**	0	21.3 ± 1.3*	18.3 ± 1.0
Tinctura Calendulae	19.5 ± 1.8	16.5 ± 0.5**	24.5 ± 0.6*	14.7 ± 2.7	15.9 ± 3.3	13.1 ± 1.9	12.5 ± 0.5*	6.0 ± 0.4	18 ± 2.1*	23.5 ± 0.6***	28.6 ± 1.3***	25.0 ± 1.7**
Tinctura Eucalypti	18.0 ± 0.0	29.3 ± 2.4***	30.0 ± 0.0*	18.0 ± 1.7	20.2 ± 0.4	30.0 ± 1.5***	17.3 ± 0.7*	21.3 ± 0.3***	28.4 ± 1.1***	26.0 ± 1.9***	37.6 ± 1.0***	28.7 ± 0.7***
70% ethanol	18.3 ± 1.1	10.0 ± 1.9	0.0 ± 0.0	12.5 ± 1.6	18.9 ± 0.7	9.4 ± 1.4	13.3 ± 0.3	10.5 ± 1.6	10.0 ± 2.5	0.0 ± 0.0	11.3 ± 3.6	17.1 ± 1.4
Rotocanum	10.3 ± 2.4	12.8 ± 0.6**	15.5 ± 0.6*	10.0 ± 0.0*	11.8 ± 0.8*	13.3 ± 1.0***	10.0 ± 0.0***	14.4 ± 1.9*	18.2 ± 1.0***	13.7 ± 0.3***	16.3 ± 1.6***	15.0 ± 2.7**
40% ethanol	8.1 ± 1.9	5.1 ±1.9	0.0 ± 0.0	0.0 ± 0.0	6.1±1.7	0.0 ± 0.0	0.0 ± 0.0	6.0 ± 0.3	0.0 ± 0.0	0.0 ± 0.0	0.0 ± 0.0	0.0 ± 0.0
Tinctura Menthae piperitae	35.7 ± 2.7**	25.8 ± 1.3**	29.0 ± 1.3*	39.3 ± 0.7***	39.5 ± 0.5***	25.7 ± 1.3**	27.0 ± 0.7*	21.0 ± 1.0**	36.3 ± 0.7*	26.4 ± 4.4***	40.5 ± 1.7***	30.3 ± 0.3*
90% ethanol	24.8 ± 1.1	20.5 ± 1.1	14.0 ± 2.7	21.5 ± 1.2	21.9 ± 0.9	19.3 ± 1.1	19.3 ± 2.4	16.5 ± 0.7	26.3 ± 2.1	0.0 ± 0.0	25.0 ± 1.6	20.2 ± 4.5
Chlorophyllipt	30.8 ± 2.1	40.0 ± 1.6***	37.5 ± 1.7*	21.7 ± 1.0	23.3 ± 1.0	34.8 ± 2.5***	19.3 ± 2.1	32.0 ± 1.2***	35.0 ± 2.7	37.2 ± 1.7***	40.4 ± 1.2***	39.3 ± 0.7***
96% ethanol	26.9 ± 0.9	22.4 ± 0.8	12.0 ± 2.5	23.3 ± 2.4	24.5 ± 1.0	19.2 ± 0.7	23.0 ± 1.7	18.4 ± 0.6	30.5 ± 0.5	6.0 ± 0.3	25.8 ± 0.8	26.0 ± 0.0

Note: mathematical reliability * – $P < 0.05$, ** – $P < 0.01$, *** – $P < 0.001$; the reliability of the difference between the plant medical remedies and the corresponding solution of alcohol P: Tinctura Absinthii, Tinctura Calendulae, Tinctura Eucalypti – 70% ethanol; Rotocanum – 40% ethanol; Tinctura Menthae piperitae – 90% ethanol; Chlorophyllipt – 96% ethanol.

Sensitive to the Tinctura Absinthii were *S. salivarius* (19.6 ± 0.9 mm), *E. faecalis* (16.5 ± 0.6 mm), and *B. clausii* (21.3 ± 1.3 mm) from the probiotic Normaflore, as well as *C. albicans*, *S. aureus* and *Lactobacillus* sp., but ethanol also had an effect on these microorganisms. Tinctura Absinthii did not affect the growth of Gram-negative microorganisms, and species of probiotic Biosporin. The drug Rotocanum, which contains in its composition extracts of chamomile, calendula and yarrow (*Calendula officinalis* floridis + *Chamomillae recutitae* floridis + *Achillea millefolii* herbae) and is used as applications or mouthparts baths for patients with periodontitis and stomatitis, did not significantly affect the microorganisms which have been studied. The largest growth retardation regions were observed for streptococci (15.5 ± 0.6 mm for *E. faecalis* ATCC 29212 and 18.2 ± 1.0 mm *S. salivarius*), staphylococci (12–14 mm), and *Neisseria* sp. (14.4 ± 1.9 mm).

It should also be noted that all remedies as extractants containing ethanol are known as disinfectants that also have antimicrobial properties. It was found that Tinctura Absinthii had no effect on bacteria that are the active Biosporin basis. However, it affected the most opportunistic microbes taken in the experiment.

Discussion

Detailed analysis of the impact of drugs on different types of microorganisms made it possible to find that no drug that would act the same way or have no effect on the growth of microorganisms. Thus, the results obtained show that use of herbal drugs in dentistry is promising, in particular to eliminate infectious processes in the mouth and suppression of vital activity of pathogenic and opportunistic microorganisms.

The subject of antimicrobial properties of essential oils and extracts from *Artemisia* L. species is very widely discussed (Erel et al., 2007; Massiha et al., 2013). Cha (2007) investigated the chemical composition and antibacterial activity of *Artemisia iwayomogi* essential oil against oral bacteria. The essential oil of the plant exhibited strong inhibitory effect against all obligate anaerobic bacteria tested, while its major compounds demonstrated various degrees of growth inhibition (Cha, 2007). In our study, ethanolic extract of *Artemisiae absinthii* herba showed moderate effect on the investigated strains. Sensitive to the Tinctura Absinthii were mainly Gram-positive oral bacteria and yeast while it did not affect the growth of Gram-negative microorganisms and probiotic strains *B. subtilis* UKM B-5007, *B. licheniformis* UKM B-5514. Moslemi et al. (2012) showed that topical application of *A. absinthium* extract on the infected wound sites in rat models produced significant antibacterial activity against *S. aureus*.

In the present study, Tinctura Calendulae showed antimicrobial effect on most Gram-positive, Gram-negative microorganisms and probiotic strains. Szakiel et al. (2008) found that oleanic acid isolated from marigold (*Calendula officinalis*) inhibited bacterial growth and survival, influenced cell morphology and enhanced the autolysis of Gram-positive bacteria, suggesting that bacterial envelopes are the target of its activity. Essential oil from *Calendula officinalis* was effective against 23 clinical fungi strains tested (Gazim et al., 2008). Other experimental data obtained showed that methanol extract of *C. officinalis* petals exhibited better antibacterial activity than ethanol exstract. However, both extracts showed high antifungal activity in comparison with fluconazole (Efstratiou et al., 2012). In our research Tinctura Calendulae has shown no or low antifungal activity in comparison with control.

Among the studied herbal medicinal products, the strongest antimicrobial activity was found in Tinctura Eucalipti, Tinctura Menthae piperitae and Chlorophyllipt. Eucalyptus oil, which is known for its antibacterial, antiviral (Cermelli et al., 2007; Astani et al., 2009) and antifungal (Ashour, 2008) properties, and has a long history of use for the treatment of colds, flu, rhinitis, sinusitis and other respiratory tract diseases. The obtained results have shown that essential oils of the leaves of *E. globulus* have antimicrobial activity against Gram-negative bacteria (*E. coli*) as well as Gram-positive bacteria (*S. aureus*) (Bachir & Benali, 2012). The effectiveness of eucalyptus oils on caries and periodontitis pathogens was also investigated. In particular, essential oils of *Eucalyptus camaldulensis* showed antibacterial activity against *Streptococcus mutans* and significantly retard its biofilm formation (Rasooli et al., 2009). Takarada et al. (2004) earlier showed that eucalyptus oil inhibited the growth of the following oral bacteria: *Porphyromonas gingivalis*, *Actinobacillus actinomycetemcomitans*, *Fusobacterium nucleatum*, *Streptococcus mutans*, *Streptococcus sorbinus* and also inhibited the adhesion of *S. mutans* (Takarada et al., 2004). The antifungal effect of eucalyptus essential oils has been investigated. Ashour et al. (2008) showed that essential oils of *E. sideroxylon* and *E. torquata* generally exhibited moderate to high antifungal activities againt *Candida albicans*, *A. flavus* and *A. niger* (Ashour et al., 2008). Agarwal et al. (2008) inves-

tigated the ability of eucalyptus essential oil to suppress the formation of *C. albicans* biofilm. Takahashi et al. (2004) reported that extracts of *Eucalyptus globulus*, *E. maculata* and *E. viminalis* significantly inhibited the growth of six Gram-positive bacteria (*Staphylococcus aureus*, MRSA, *Bacillus cereus*, *Enterococcus faecalis*, *Alicyclobacillus acidoterrestris*, *Propionibacterium acnes*), and of a fungus (*Trichophyton mentagrophytes*), but they did not show strong antibacterial activity against Gram-negative bacteria (*Escherichia coli*, *Pseudomonas putida*) (Takahashi et al., 2004). In our findings, Gram-negative bacteria showed lower sensitivity to Tinctura Eucalipti than Gram-positive bacteria.

Our results showed that the Tinctura of peppermint inhibited the growth of Gram-positive, Gram-negative microorganisms and had a high anti-candidal effect. Caretto et al. (2010) also showed antimicrobial activity of hydroalcoholic extract of *Mentha piperita* L. against *Candida* spp. (*C. albicans*, *C. tropicalis* and *C. glabrata*). Shalayel et al. (2017) showed the potential antibacterial activity for *Mentha piperita* extracts against MDR *S. pyogenes*, *E. faecalis*, MRSA, MRSE and carbapenem-resistant *E. coli*, and *Klebsiella pneumonia* clinical isolates. Sujana et al. (2013) earlier demonstrated that the organic extracts of the leaves of the plant (*Mentha piperita* L.) possessed strong antibacterial activity against a range of pathogenic bacteria, such as *Bacillus subtilis*, *Streptococcus pneumonia*, *Staphylococcus aureus*, *Escherichia coli*, *Proteus vulgaris* and *Klebsiella pneumonia* (Sujana et al., 2013). The mint leaf methanolic extract showed considerable antimicrobial activity against human oral pathogens, such as: *Escherichia coli*, *Acinetobacter* sp., *Staphylococcus aureus* and two fungi such as *Candida albicans*, *C. glabrata* (Pramila et al., 2012). Miloš Nikolić et al. reported antimicrobial activity of essential oil of pepermint *Mentha piperita* against pathogenic microorganisms isolated from the oral cavity (8 bacteria and 58 *Candida* sp.) and referent strains (Nikolić et al., 2013).

According to usage instruction, Chlorophyllipt inhibits staphylococci infections that are resistant to antibiotics and is used in washing, rinsing, lotion, wet tampons and douching, and in dental stomatitis to treat gangrenous pulpitis, abscesses, boils, inflammation of the oral mucosa. Our results suggested its antibiotic activity not only against collection and clinical strains of Gram-positive and Gram-negative bacteria, but also against investigated probiotic strains. By investigation of the antagonistic activity of probiotics it was established that bacteria, being the background of the biopreparations, have demonstrated different levels of suppression effect on various strains of test-cultures.

Conclusions

It was confirmed that each of the proposed health benefits should be studied separately for each probiotic bacterial strain, especially if the treatment protocol stipulates the use of drugs with herbal remedies. At the same time, all probiotic strains proved to be sensitive to the action of plant extracts, indicating the possibility of consecutive use (with an interval of time) of herbal remedies and probiotics in combination therapy for the treatment of periodontal disease. Screening herbal medicinal products according to their activity on the *Lactobacillus* and *Bacillus* strains of probiotics could precede the clinical efficacy studies for adjunct treatment with both in treatment of periodontal infections.

While BAS of herbal medicines suppress the vital activity of pathogenic and opportunistic microorganisms or destroy them, probiotics create conditions for the resumption of normal microbiota. Alternating drugs (of plant origin and probiotics) in the treatment of periodontal disease will prevent the formation of resistant strains of oral microbiota, and will not disturb the biological balance in the oral cavity, and, therefore, will provide recovery of the patient's health.

References

Agarwal, V., Lal, P., & Pruthi, V. (2008). Prevention of *Candida albicans* biofilm by plant oils. Mycopathologia, 165(1), 13–19.

Alok, A., Singh, I. D., Singh, S., Kishore, M., Jha, P. C., & Iqubal, M. A. (2017). Probiotics: A new era of biotherapy. Advanced Biomedical Research, 6(1), 31.

Ashour, H. M. (2008). Antibacterial, antifungal and anticancer activities of volatile oils and extracts from stems, leaves, and flowers of *Eucalyptus sideroxylon* and *Eucalyptus torquata*. Cancer Biology and Therapy, 7(3), 399–403.

Astani, A., Reichling, J., & Schnitzler, P. (2009). Comparative study on the antiviral activity of selected monoterpenes derived from essential oils. Phytotherapy Research, 24(5), 673–679.

Bachir, R. G., & Benali, M. (2012). Antibacterial activity of the essential oils from the leaves of *Eucalyptus globulus* against *Escherichia coli* and *Staphylococcus aureus*. Asian Pacific Journal of Tropical Biomedicine, 2(9), 739–742.

Carretto, C. F. P., Junqueira, J. C., Almeida, R. B. A., Furlan, M. R., & Jorge, A. O. C. (2010). Antimicrobial activity of *Mentha piperita* L. against *Candida* spp. Brazilian Dental Science, 13(1/2), 4–9.

Cermelli, C., Fabio, A., Fabio, G., & Quaglio, P. (2007). Effect of eucaliptus essential oil on respiratory bacteria and viruses. Current Microbiology, 56(1), 89–92.

Cha, J.-D. (2007). Chemical composition and antibacterial activity against oral bacteria by the essential oil of *Artemisia iwayomogi*. Journal of Bacteriology and Virology, 37(3), 129–136.

Curtis, M. A. (2014). Periodontal microbiology – The lid's off the box again. Journal of Dental Research, 93(9), 840–842.

Efstratiou, E., Hussain, A. I., Nigam, P. S., Moore, J. E., Ayub, M. A., & Rao, J. R. (2012). Antimicrobial activity of *Calendula officinalis* petal extracts against fungi, as well as Gram-negative and Gram-positive clinical pathogens. Complementary Therapies in Clinical Practice, 18(3), 173–176.

Erel, Ş. B., Yavaoğlu, N. Ü. K., & Zeybek, U. (2007). Antimicrobial activities of six artemisia species of West Anatolia. Planta Medica, 73(9), 131.

Gazim, Z. C., Rezende, C. M., Fraga, S. R., Estivaleti Svidzinski, T. I., & Garsia Cortez, D. A. (2008). Antifungal activity of the essential oil from *Calendula officinalis* L. (Asteraceae) growing in Brazil. Brazilian Journal of Microbiology, 39(1), 61–63.

Hleba, L., Kompas, M., Hutková, J., Rajtar, M., Petrová, J., Čuboň, J., Kántor, A., & Kačániová, M. (2016). Antimicrobial activity of crude ethanolic extracts from some medicinal mushrooms. Journal of Microbiology, Biotechnology and Food Sciences, 5(1), 60–63.

Kačániováa, M., Vukovic, N., Horska, E., Salamov, I., Bobkova, A., Hleba, L., Mellen, M., Vatlak, A., Petrova, J., & Bobko, M. (2014). Antibacterial activity against *Clostridium* genus and antiradical activity of the essential oils from different origin. Journal of Environmental Science and Health, Part B, 49(7), 505–512.

Massiha, A., Majid Khoshkholgh-Pahlavian, M., Issazadeh, K., Bidarigh, S., & Zarrabi, S. (2013). Antibacterial activity of essential oils and plant extracts of *Artemisia* (*Artemisia annua* L.) *in vitro*. Zahedan Journal of Research in Medical Sciences, 15(6), 14–18.

Mishra, R., Tandon, S., Rathore, M., & Banerjee, M. (2014). Antimicrobial and plaque inhibitory potential of herbal and probiotic oral rinses in children: A randomized clinical trial. Indian Journal of Dental Research, 25(4), 485–492.

Moslemi, H. R., Hoseinzadeh, H., Badouei, M. A., Kafshdouzan, K., & Fard, R. M. (2012). Antimicrobial activity of *Artemisia absinthium* against surdical wounds infected by *Staphylococcus aureus* in a rat model. Indian Journal of Microbiology, 52(4), 601–604.

Nikolić, M., Glamočlija, J., Ćirić, A., Marković, T., Marković, D., Perić, T., & Soković, M. (2013). Hemijski sastav i antimikrobna aktivnost etarskog ulja pitome nane (*Mentha piperita* L.). Lekovite Sirovane, 33, 63–72.

Pramila, D. M., Xavier, R., Marimuthu, K., Kathiresan, S., Khoo, M. L., Senthilkumar, M., Sathya, K., & Sreeramanan, S. (2012). Phytochemical analysis and antimicrobial potential of methanolic leaf extract of peppermint (*Mentha piperita*: Lamiaceae). Journal of Medicional Plants Research, 6(2), 331–335.

Radulovic, N. S., Blagojevic, P. D., Stojanovic-Radic, Z. Z., & Stojanovic, N. M. (2013). Antimicrobial plant metabolites: Structural diversity and mechanism of action. Current Medicinal Chemistry, 20(7), 932–952.

Rios, J. L., & Recio, M. C. (2005). Medicinal plants and antimicrobial activity. Journal of Ethnopharmacology, 100, 80–84.

Rasooli, I., Shayegh, S., & Astaneh, S. D. A. (2009). The effect of *Mentha spicata* and *Eucalyptus camaldulensis* essentisl oils on dental biofilm. International Journal of Dental Hygiene, 7(3), 196–203.

Rivis, O. Y., Krivtsova, M. V., Nikolaichuk, V. I., Semenova, G. M., & Barani, E. A. (2012). Mikroflora rotovoi' porozhnyny ljudej z zapal'nymy zahvorjuvannjamy tkanyny parodontu v Uzhgorods'komu rajoni [Microflora of the oral cavity of people with inflammatory diseases of periodontal tissue in Uzhgorod area]. Bulletin of Problems in Biology and Medicine, 1(3), 121–124 (in Ukrainian).

Rivis, O. Y., Krivtsova, M. V., & Nikolaichuk, V. I. (2013). Antagonistic activity of *Bacillus* probiotics against bacteria isolates of oral cavity of patients with periodontitis. Visnyk of Dnipropetrovsk University. Biology, Medicine, 4(1), 10–13.

Safronova, L. A., Osadchaya, A. I., Avdeyeva, L. V., & Ilyash, V. M. (2009). Vlijanie fitokompozicij na biologicheskuju aktivnost' probioticheskih shtammov *Bacillus subtilis*. [Influence of phytocompositions on biological activity of *Bacillus subtilis* probiotic strains]. Likarska Sprava, 3–4, 68–74 (in Russian).

Shalayel, M. H. F., Asaad, A. M., Qureshi, M. A., & Elhussein, A. B. (2017). Anti-bacterial activity of peppermint (*Mentha piperita*) extracts against some emerging multi-drug resistant human bacterial pathogens. Journal of Herbal Medicine, 7, 27–30.

Shipradeep, K. S., Khare, R. S., Ojha, S., Kundu, K., & Kundu, S. (2012). Development of probiotic candidate in combination with essential oils from medicinal plant and their effect on enteric pathogens: a review. Gastroenterology Research and Practice, 2012, 1–6.

Shulga, L. I. (2011). Fitopreparaty v stomatologii': Suchasnyj stan ta perspektyvy stvorennja [Herbal remedies in dentistry: Current status and perspectives for production]. Clinical Pharmacy, Pharmacotherapy and Medical Standardization, 3–4, 151–156 (in Ukrainian).

Sujana, P., Sridhar, T. M., Josthna, P., & Naidu, C. V. (2013). Antibacterial activity and phytochemical analysis of *Mentha piperita* L. (Peppermint) – An important multipurpose medicinal plant. American Journal of Plant Sciences, 4(1), 77–83.

Szakiel, A., Ruszkowski, D., Grudniak, A., Kurek, A., Wolska, K. I., Doligalska, M., & Janiszowska, W. (2008). Antibacterial and antiparasitic activity of oleanolic acid and its glycosides isolated from marigold (*Calendula officinalis*). Planta Medica, 74(14), 1709–1715.

Takahashi, T., Kokubo, R., & Sakaino, M. (2004). Antimicrobial activities of eucalyptus leaf extracts and flavonoids from *Eucalyptus maculata*. Letters in Applied Microbiology, 39(1), 60–64.

Takarada, K., Kimizuka, R., Takahashi, N., Honma, K., Okuda, K., & Kato, T. (2004). A comparison of the antibacterial efficacies of essential oils against oral pathogens. Oral Microbiology and Immunology, 19(1), 61–64.

Vorobets, N., & Rivis, O. (2017). Aktual'nist' ta perspektyvy vykorystannja likars'kyh roslyn dlja likuvannja kandydozu rotovoi' porozhnyny [Relevance and perspectives of using medicinal plants for the treatment of oral candidiasis]. Bulletin of Problems in Biology and Medicine, 135, 22–32 (in Ukrainian).

Vorobets, N. M., & Yavorska, H. V. (2016). Modifications of agar diffusion method to determination of the antimicrobial effect of the herbal medicinal products. Ukrainian Biopharmaceutical Journal, 43, 80–84.

Zlatkina, A. R., Isakov, V. A., & Ivanikov, I. O. (2001). Kandidoz kishechnika kak novaja problema gastrojenterologii [Candidiasis of the intestine as a new problem of gastroenterology]. Russian Journal of Gastroenterology, Hepatology, Coloproctology, 6, 33–38 (in Russian).

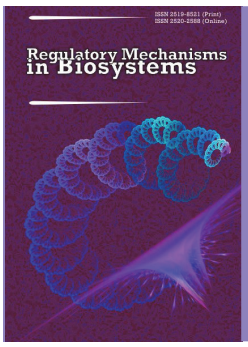

Regulatory Mechanisms in Biosystems

ISSN 2519-8521 (Print)
ISSN 2520-2588 (Online)
Regul. Mech. Biosyst., 9(3), 379–383
doi: 10.15421/021856

Changes in erythrocytopoesis indices in dogs with babesiosis

V. I. Holovakha*, O. V. Piddubnyak*, T. I. Bakhur*, N. V. Vovkotrub*, A. A. Antipov*, M. V. Anfiorova**, B. V. Gutyj***, L. G. Slivinska***, O. P. Kurdeko****, A. O. Macynovich****

**Bila Tserkva National Agrarian University, Bila Tserkva, Ukraine*
***Odessa State Agrarian University, Odessa, Ukraine*
****Stepan Gzhytskyi National University of Veterinary Medicine and Biotechnologies, Lviv, Ukraine*
*****Vitebsk Order of the Badge of Honor State Academy of Veterinary Medicine, Vitebsk, Belarus Republic*

Article info

Received 20.07.2018
Received in revised form 28.08.2018
Accepted 02.09.2018

Bila Tserkva National Agrarian University,
Pl. Soborna, 8/1,
Bila Tserkva, 09117, Ukraine.
Tel.: +38-067-693-17-73.

Odessa State Agrarian University,
Krasnova st., 3a, Odessa, 65010, Ukraine.
Tel.: +38-048-765-93-17.
E-mail: odau_vetmed@ukr.net

Stepan Gzhytskyi National University of Veterinary Medicine and Biotechnologies Lviv, Pekarska st., 50, Lviv, 79010, Ukraine.
Tel.: +38-097-290-41-51.
E-mail: maksymovych@lvet.edu.ua

Vitebsk Order of the Badge of Honor State Academy of Veterinary Medicine, 1st Dovator st., 7/11, Vitebsk, 210026, Belarus Republic.
E-mail: vsavm@vsavm.by

Holovakha, V. I., Piddubnyak, O. V., Bakhur, T. I., Vovkotrub, N. V., Antipov, A. A., Anfiorova, M. V., Gutyj, B. V., Slivinska, L. G., Kurdeko, O. P., & Macynovich, A. O. (2018). Changes in erythrocytopoesis indices in dogs with babesiosis. Regulatory Mechanisms in Biosystems, 9(3), 379–383. doi:10.15421/021856

Babesiosis is a common disease in dogs. *Babesia canis* (Piana & Galli-Valerio, 1895) (Sporozoa, Babesiidae) causes the destruction of erythrocytes, resulting in hypotensive shock and total tissue damage due to lack of oxygen. Because of babesiosis, anemia develops in dogs, and in the first hours of the disease it is normocytic, normochromic and nonregenerative, and on the 2–3rd day of the course, macrocytic, hypochromic anemia with reticulocytosis develops. Scientists have studied the most common indicators of evaluation of erythrocytopoesis during babesiosis (the number of red blood cells, hemoglobin, hematocrit index, indices of "red" blood MCH and MCV), but the age structure of erythrocytes, their acid resistance and the ferrum-transferrin complex for this parasitic pathology have not been sufficiently studied. We carried out research on dogs of service breeds, which were divided into two groups: the first (6–18 months old, n = 10) and the second (2–8 years, n = 15). According to the conducted studies, in dogs of different age groups with babesiosis revealed oligocythemia with anisocytosis and poikilocytosis, oligochromia, decreased hematocrit index and macrocytosis. Significant changes in the morpho-functional state of erythrocytes in dogs of both groups have been revealed, in particular, changes in the population (age) composition of red blood cells: the number of "old" erythrocytes increases (they are rapidly destroyed), the "young" forms of red blood cells decrease and the time for their hemolysis is reduced. As a result of the study of the ferrum-transferrin complex in dogs with babesiosis in both groups, an increase in the level of free ferrum (UIBC) and a decrease in the saturation of transferrin with the trace element was found, which makes it impossible to form a hemoglobin molecule in the bone marrow.

Keywords: erythrocytes; population composition of erythrocytes; acid resistance; hemoglobin; MCN; MCV; ferrum; transferring; ferrum-transferrin complex.

Introduction

One of the most common diseases in dogs is babesiosis. Areas of infection are found in the tropics (Jain et al., 2017; Ybañez et al., 2018), Mediterranean countries (Salem & Farag, 2014), Eastern (Davitkov et al., 2015; Bartnicki et al., 2017) and Western Europe (Eichenberger et al., 2016), Asia (Liu et al., 2016; Wang et al., 2018) and America (Di Cicco et al., 2012; Rojas et al., 2014). The analysis of recent publiccations proves that babesiosis in dogs occurs in almost all regions of Ukraine (in 18 of 24). The territory of six regions (mostly Southern and Steppe zones of Ukraine) remain free of this invasion. The infestation of dogs occurs during an attack of ixodid ticks (Arachnoidea, Ixodidae) and exposure of the pathogen with their saliva to a susceptible animal (Bajer et al., 2014).

Metabolites of *Babesia canis* (Piana & Galli-Valerio, 1895) (Sporozoa, Babesiidae), accumulating in erythrocytes, cause disorders of blood, nervous and cardiovascular systems, the gastrointestinal tract, liver, kidneys, etc. (Lobetti et al., 2012; Zygner et al., 2012; Tasaki et al., 2013). Parasites cause destruction of red blood cells, resulting in hypotensive shock and total tissue damage due to lack of oxygen (Goddard et al., 2015). Because of babesiosis in dogs, anemia appears, which is normocytic, normochromic and non-regenerative in the first hours of the disease. On the 2–3rd days of the course of the disease, macrocytic, hypochromic anemia with reticulocytosis develops.

Sources from the literature usually describe the most common indicators of evaluation of erythrocytopoesis during babesiosis (the number of erythrocytes, hemoglobin, hematocrit index, indices of "red" blood – MCH and MCV).

However, data are absent on the changes in other indicators of evaluation of erythrocytopoesis in the course of this parasitic pathology: the red blood cells' age structure, their acid resistance and the ferrum-transferin complex (FTC). Therefore, the purpose of this article is to study the changes in age composition of erythrocytes, their acid resistance and indicators of FTC in dogs with babesiosis.

Materials and methods

The objects of the study were dogs of service breeds, which were divided into two groups: the first (age from 6 to 18 months, n = 10) and the second one (from 2 to 8 years old, n = 15). Blood samples were taken in vacuum tubes of 10 ml volume (Vacutest, Italy). An anticoagulant ethylendiaminetetraacetic acid (EDTA) was used for blood tests.

In the dogs' blood, the total number of erythrocytes, hemoglobin content, hematocrit, MCV (average volume of erythrocyte) was deter-

mined by an automatic hematological analyzer Mythic 18 (Orphee S.A., Switzerland) and reagents by PZ Cormay S.A. (Poland). MCH (hemoglobin content in erythrocyte) was calculated mathematically.

Acid resistance of erythrocytes was determined by the method of A. I. Terskov and I. I. Hitelzon. Blood for research was taken into centrifuge tubes, where heparin was pre-added at a rate of 10 IU per 10 ml of blood. The plasma was separated by centrifugation (1,500 rpm for 20 minutes). The erythrocyte suspension was thoroughly cleaned with 0.85% sodium chloride solution, cooled to 4 °C (to prevent oxidation of the lipoproteins), followed by centrifugation under the same conditions. The erythrocyte suspension was taken by capillary (0.02 ml) and transferred to a test tube where 10 ml of isotonic sodium chloride solution was pre-introduced. The capillary was washed in the top layer of the solution and the contents of the test tube were thoroughly mixed. In this case 0.2% suspension of erythrocytes was obtained (Terskov & Hitelzon, 1967).

Measurement of optical density of the solutions was carried by a photometer at 540 nm wavelength (cuvettes with 10 mm process soluteon thickness). Before the study, both cuvettes were filled for 5–10 min with hemolytic solution with the abovementioned concentration. The control cuvette was filled with 4 ml of 0.85% sodium chloride, and the experimental one was filled with 2 ml of hemolytic solution and 2 ml of 0.2% erythrocytes' suspension added. Hemolytic with erythrocytes' suspension was stirred by pipette tip. The sample extinction was determined immediately after mixing. Extinction changes were recorded every 30 seconds until a constant indicator is reached, during 30 seconds (Golovakha et al., 2017).

The difference between the initial and final (after hemolysis) optical density is seen as 100% and the ΔE percentage was calculated (the next extinction index was subtracted from previous one and seen as "X"), which reflects the relative percentage of non-hemolyzed erythrocytes every 30 seconds. This calculation excludes dependence of the results on the number of erythrocytes and hemoglobin concentration. The obtained data was depicted graphically. The horizontal axis reflects time from 0 and every 30 seconds, the ordinate axis – the erythrocytes' hemolysis percentage. The left side of the diagram indicates hemolysis of "old" erythrocyte populations, the central part with the peak is formed by the destruction of "mature" and partially "young" cells, the right side is the hemolysis result of only "young" erythrocytes (Terskov & Hitelzon, 1967).

The population structure of the erythrocytes was determined by fractionation of sucrose density gradient by the I. Sizova method (Sizova et al., 1980). Blood samples were put into centrifuge tubes, with previously added heparin at 10 IU per 10 ml of blood. Plasma was separated by centrifugation (1,500 rpm for 20 minutes). The erythrocytes' suspension was washed three times by cooled to 4 °C (to prevent oxidation of lipoproteins) 0.85% sodium chloride solution followed by centrifugation under the same conditions.

The erythrocytes' suspension was taken by a 0.1 ml pipette and moved to Florinski test tubes, previously filled with 0.9 ml of isotonic sodium chloride solution. The pipette was washed in the upper layer of the solution and the tube content was thoroughly mixed (thus obtaining 10% erythrocytes suspension). 0.5 ml of erythrocytes' suspension was introduced into the 45° tilted column, and sucrose solution was put layer over layer on the column wall (the first layer – with the highest concentration, the last – with the lowest). It is provides the distribution of erythrocytes in different concentrations of sucrose, depending on the erythrocytes' age.

The column was carefully leveled at 90° to avoid mixing of the sucrose layers, and every last layer was carefully separated into a separate graded tube (7 in total). Isotonic sodium chloride solution was added into each tube, totaling volume to 10 ml. All 7 tubes were thoroughly mixed and checked for the optical density.

Measurement of the solutions' optical density was carried by the photometer at 520 nm wavelength (cuvettes with 10 mm working layer thickness). A 0.85% sodium chloride solution was a control one. The received extinction amount was seen as 100%, and each tube index was seen as "X" and thus calculating the percentage of a particular fraction. The indicators of the first three tests (in sucrose solutions of 30%, 26% and 22% concentrations) were added. The obtained result was a percentage indicator of the "old" erythrocytes' number. The same was done with the fourth and fifth indicators (18% and 14% solutions), by calculating the concentration of "mature" cells, while adding percentage of the sixth and the seventh results (10% and 6% sucrose solutions) and a relative indicator of the "young" population's content was obtained (Sizova et al., 1980; Wijk & Solinge, 2005).

In the blood serum the following were determined: the content of the ferrum, the total and unsaturated ferrum-binding ability of the serum (TIBS, UIBS), the level of transferrin and the saturation of it by ferrum (ferrosine method).

Mathematical analysis of the study results was conducted in Statistica 6.0 (StatSoft Inc., USA). Differences between average values were considered statistically significant at $P < 0.05$ (ANOVA).

Results

Clinically, babesiosis in dogs was manifested by hyperthermia (up to 41.2 °C), drowsiness, shaky stroke, anemia in the mucous membranes of the eyes and oral cavity, dull hair, thirst, vomiting. In sick animals there were: tachycardia, tachypnea, oliguria, yellow-brown urine. In dogs of first group (age up to 18 months), the number of erythrocytes was reduced and averaged 3.8 ± 0.33 T/L, which is 57.6% less than in clinically healthy animals. Oligocythemia was found in all animals. In dogs of the second group, too, oligocythemia was established – 4.7 ± 0.36 T/L (minimal norm is 5.0 T/L). Along with oligocythemia in animals, anisocytosis and poikilocytosis have been observed, indicated dystrophic changes in the structural elements of the bone marrow.

We also found changes in the population composition of erythrocytes. In particular, the number of "old" erythrocytes in dogs of the first group on average was 15.4 ± 2.46%, which is almost three times more than in the clinically healthy animals ($P < 0.05$). However, the most "old" populations of erythrocytes were found in older dogs (second group). In them, the number of "old" in the group on average was 27.9 ± 4.98%, which is 5.2 times more than in the clinically healthy animals ($P < 0.01$). Such a number of "old" erythrocytes, obviously, is evidence of an increase in aging processes of "red" cells.

Unlike "old" populations, the number of "mature" red cells in patients of both groups did not differ from the number in clinically healthy animals ($P < 0.5$, Table 1). The number of "young" forms of erythrocytes, compared with clinically healthy, in dogs with babesiosis, especially the second group, was reduced and averaged 35.0 ± 5.80%, which is 17.7% less than in clinically healthy animals. Reduction of "young" red blood cells is evidence of depletion of the "red" bone marrow and inhibition of adaptive processes for hemic hypoxia.

Table 1
Indices of the total number of erythrocytes and their population structure in dogs

Animal groups	Erythrocytes, T/l	population structure of erythrocytes, %		
		"old"	"mature"	"young"
Clinically healthy (n = 10)	5.7–7.67	1.6–11.3	33.0–58.0	35.2–62.3
	6.6 ± 0.25	5.4 ± 1.12	41.9 ± 3.25	52.7 ± 2.59
Infected, age up to 1.5 years (n = 10)	2.57–4.96	6.2–25.5	27.7–41.6	35.1–56.2
	3.8 ± 0.33	15.4 ± 2.46	36.8 ± 1.38	47.8 ± 2.26
P <	0.001	0.05	0.5	0.5
Infected, age 2–8 years (n = 15)	2.52–7.75	3.8–66.2	19.7–56.0	12.4–61.3
	4.7 ± 0.36	27.9 ± 4.98	37.1 ± 2.57	35.0 ± 5.80
P <	0.01	0.01	0.5	0.05

Changes in the population composition of erythrocytes also affect their osmotic (acid) resistance, since the time of hemolysis depends on their age, leads to the destruction of intracellular structures and lowering the resistance of the membrane to increased pressure inside the cell.

The analysis of the erythrograms (acid erythrocytes hemolysis) shows that the time of the main peak in dogs of the first group was 3.7 min; its height was 20% (Fig. 1). The whole hemolysis of erythrocytes was completed in 6.5 min. The time of hemolysis of "old" and "mature" erythrocytes in dogs of the first group was 3.5 min, which is 2 min less, compared to clinically healthy dogs of the same age. It testifies to the rapid destruction of these populations as a result of the depletion of the structural and functional state of membranes of red blood cells. Regar-

ding the hemolysis of the "young" red blood cells (right side of the graph), its duration in both patients and healthy dogs was 3 min, but in animals with babesiosis invasion there was an additional peak indicating the unstable resistance of the membranes of "young" red blood cells to the action of hemolysis due to toxic effects products of microscopic parasites' catabolism.

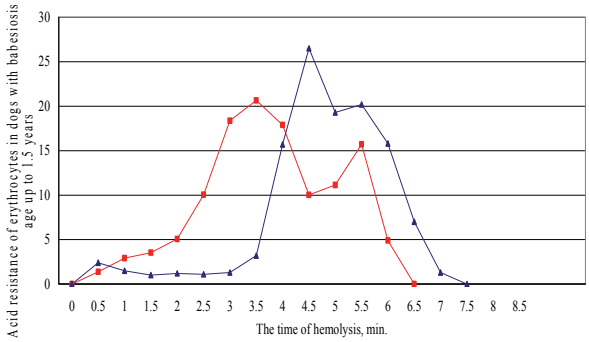

Fig. 1. Acid resistance of erythrocytes in dogs with babesiosis aged up to 1.5 years (n = 10)

Analyzing the erythrograms of dogs of the second group (Fig. 2), it should be noted that the left side of the graph (hemolysis of the "old" and "mature" populations) was more acute and expired for 3 min, while in healthy dogs, it was 2 min longer. It may indicate the blocking effect of invasive agents on the elements of the erythroid bone marrow sprout, inhibition of erythrocyte maturation processes and increased aging. The complete hemolysis time was 5.5 min, which is 1.5 min less, compared to healthy dogs, indicating a change in the functional state of the membranes of the "young" populations.

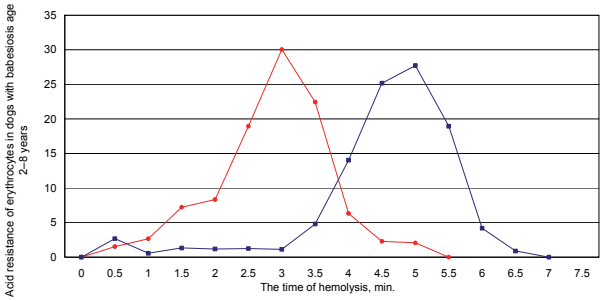

Fig. 2. Acid resistance of erythrocytes in dogs with babesiosis aged 2–8 years (n = 15)

The content of the respiratory blood enzyme (hemoglobin) in dogs with babesiosis was reduced. In particular, in young dogs (first group), its average number was 98.0 ± 6.59 g/l, which is 38.0% less than in clinically healthy ($P < 0.001$). Similar values of this chromoprotein were also found in dogs of the second group ($P < 0.001$, Table 2). It should be noted that oligochromemia was established in 90.0 and 80.0% of dogs of the first and second groups, which testifies to the increased destruction of red blood cells. If the number of erythrocytes and hemoglobin content in dogs with babesiosis are reduced, then the indices of "red" blood, in particular, the MCH, did not differ from the values in clinically healthy animals (Table 2).

One of the commonly used indicators of erythrocytopoesis is the hematocrit index, which determines the total volume of erythrocytes, characterizing certain types of anemia (Gutyj et al., 2017; Slivinska et al., 2018). In dogs with babesiosis, this indicator was lower than normal ($P < 0.01$). It should be noted that low values of hematocrit were detected in 90.0% and 73.3% of dogs from the first and second groups, respectively.

Different forms of anemia can be diagnosed using an average volume of red blood cells (MCV). MCV in dogs should not exceed 80 μm^3. However, in some of the sick dogs of both the first and the second groups, the MCV was within the range of 80.2–101.3 μm^3. That is, in such cases there is an increased inflow into the peripheral blood of immature erythrocytes.

But, it is impossible to evaluate erythrocytopoesis without indicators of the ferrum-transferin complex, the basis of which is the ferrum. It is the element that plays an important role in the transfusion of oxygen and carboxylic acid in the cells of the body. The content of ferrum in blood serum of dogs with babesiosis on average did not differ from the values in clinically healthy animals ($P < 0.5$, Table 3). However, a detailed analysis of the obtained values shows that some dogs (60.0% and 66.7% respectively) exhibit hyposideremia, which indicates a low intake of ferrum into the body.

Table 2
Changes in erythrocytopoesis in dogs with babesiosis

Animal groups	Hemoglobin, g/l	Hematocrit index, %	MCH, fmol	MCV, μm^3
Clinically healthy	145.0–168.0	46.0–57.0	20.4–28.2	64.6–82.5
(n = 10)	158.0 ± 2.84	50.0 ± 1.46	24.0 ± 0.94	74.8 ± 2.29
Infected, age up to	52,0–142.0	19.0–35.0	19.6–33.3	58.1–101.2
1.5 years (n = 10)	98.0 ± 6.59	28.1 ± 1.21	26.4 ± 1.86	76.6 ± 4.72
P <	0.001	0.001	0.5	0.5
Infected, age	72.0–148.0	17.0–46.0	18.2–30.8	57.6–101.3
2–8 years (n = 15)	100.0 ± 5.95	30.8 ± 2.33	21.7 ± 1.06	65.9 ± 2.44
P <	0.001	0.01	0.2	0.05

Table 3
Indicators of the ferrum-transferrin complex in dogs

Animal groups	Biometric indicator	Ferrum, µmol/l	TIBC, µmol/l	UIBC, µmol/l
Clinically healthy	Lim M ± m	22.4–36.7	62.5–83.2	34.6–48.7
(n = 10)		28.3 ± 1.38	70.8 ± 2.63	42.5 ± 1.64
Infected, aged up to	Lim M ± m	16.8–40.3	60.6–91.7	41.3–72.8
1.5 years (n = 10)		23.6 ± 2.70	80.2 ± 2.96	56.6 ± 4.09
	P <	0.2	0.05	0.05
Infected, aged	Lim M ± m	17.8–39.6	76.3–111.4	43.1–89.4
2–8 years (n = 15)		26.6 ± 2.52	89.5 ± 3.45	62.9 ± 2.90
	P <	0.5	0.01	0.001

In the rest of the animals (30.0% and 26.7%, respectively), hypersideremia was found (> 35 µmol/l), which obviously indicates an increased accumulation of ferrum in the blood for the destruction of red blood cells. But it is important that the value of the content of the ferrum cannot on its own reflect the state of its exchange. Therefore, it is important to determine other indicators of its metabolism, in particular, TIBC (indicating the content of a non-protein-transferrin-bound ferrum) and UIBC (toxic level indicator of the ferrum).

TIBC in dogs with babesiosis was elevated in the first and second group by 13.3% and 26.6% respectively ($P < 0.01$). High values of TIBC indicate dystrophic changes in the transferrin receptor apparatus, which leads to a reduced transport of the ferrum from the depot to the bone marrow, enhanced erythrocyte hemolysis, and the accumulation of free ferrum. An indicator of the last one is the UIBC, which indicates the non-transferring pool of the ferrum. In dogs with babesiosis, UIBC averaged 56.6 ± 4.09 and 62.9 ± 2.90 µmol/l in the first and second groups, respectively, which is by 33.2% and 48.0% more than in clinically healthy animals ($P < 0.05$ and $P < 0.001$). This value indicates the accumulation of toxic (free) ferrum and reduced binding of the protein transferrin to the trace element.

It is not advisable to evaluate the exchange of a ferrum without determining the content of transferrin in serum and its saturation with ferrum. The content of transferrin in dogs with babesiosis was elevated and was in the first and second group 3.6 ± 0.13 and 4.0 ± 0.13 g/l, respectively.

In contrast to the amount of transferrin, the coefficient of its saturation with ferrum was lower, compared with healthy animals, and was in young dogs (first group) – 29.5 ± 3.17%, in older (the second group) – 29.8 ± 2.66% ($P < 0.05$, Table 4). Reduced saturation (less than 30%) of transferrin with ferrum was detected in 30.0% and 33.3% of animals, respectively, indicating a low synthesis of the structure of the protein molecule of transferrin in the liver and slow transport of the trace element to the depot and bone marrow.

Table 4
Indicators of the ferrum-transferrin complex in dogs

Animal groups	Biometric indicator	Transferrin content, g/l	Coefficient of transferrin's saturation with ferrum, %
Clinically healthy (n = 10)	Lim M ± m	2.79–3.72 3.20 ± 0.12	33.30–44.60 39.90 ± 1.41
Infected, age up to 1.5 years (n = 10)	Lim M ± m	2.71–4.10 3.60 ± 0.13	19.80–48.70 29.50 ± 3.17
	P <	0,05	0,05
Infected, age 2–8 years (n = 15)	Lim M ± m	3.41–4.98 4.0 ± 0.13	17.60–43.50 29.80 ± 2.66
	P <	0.01	0.05

Discussion

The development of babesiosis in dogs is a complex process which is determined by a number of biological, natural-climatic and socio-economic factors (Iguchi et al., 2014). The pathogenesis of this disease is determined by the specific type of pathogen and the corresponding reactions occurring in the organism of the affected animal, which, in turn, depend on the biology and life cycle of the *Babesia canis* and the conditions in which the interaction of the macro- and microorganism occurs (Al Izzi et al., 2013; Bajer et al., 2016; Piane et al., 2016). The peculiarity of the pathogenesis of the disease is the reproduction of the causative agent of babesiosis in the organism of a susceptible animal inside the erythrocytes of the capillaries in the internal organs, and then in the erythrocytes of the blood stream. Parasites are feeding in red blood cells through osmosis. The metabolites of parasites that have been excreted during this, cause a violation of the function of the organs of the hematopoesis of the host, disturbed blood circulation, etc. That is why the leading role in pathogenesis is given to the destruction of erythrocytes and as a consequence – the development of anemia. The destruction of red blood cells occurs in the spleen, which leads to the appearance of blood in the free hemoglobin, which is excreted in the urine in the unchanged form or in the form of urobilinogen. Thus, for babesiosis, changes in the functions of the circulatory system, especially the morphological composition of blood, are adaptive (Di Mauro & Schoeffler, 2016).

As a result of hemoglobin destruction, endogenous siderosis develops, as indicated by the increased content of ferrum in serum. This can cause the trapping of the trace element in the liver and kidneys and the development of hemochromatosis. Thus, in dogs with babesiosis, regenerative-macrocytic anemia develops, which is accompanied by oligocythemia, oligochromia, macrocytosis, reticulocytosis, thrombocytopenia, and elevated erythrocyte sedimentation rate (ESR). At the same time, the decrease in the number of erythrocytes prevailed over the decrease in the content of hemoglobin, which gives grounds to consider such a process as hemolytic (Sunaga et al., 2013).

In dogs with babesiosis at the first stages of the disease, poikilocytosis with the presence of echinocytes and acanthocytes (spherical stellate cells), and stomatocytes (pelori in the form of a slit) were detected. The third stage of the disease was characterized by schizocytes (fractures of red blood cells) and basophilic granularity of erythrocytes.

Hypoxia and intoxication caused by metabolites of babesia lead to dystrophic changes in hepatocytes and disturbance of their bilirubin and protein-synthesizing functions (Crnogaj et al., 2017). It is known from literary sources that merozoites of the pathogen bind to the receptors of the caudal-lateral surface in the hepatocytes due to the presence of a protein in them, which is homologous to the connecting portion of the thrombospondin in hepatocytes. Inside the liver cell, the parasite rapidly breeds and merozoites, formed in large numbers, break the hepatocyte. Bloodparasites have a destructive effect on the vessels, including the vessels of the portal system. Violation of blood circulation in the liver leads to increased portal pressure accordingly the slowing of blood flow (Zygner et al., 2012; Sunaga et al., 2013).

Pathomorphological changes in the liver are characterized by a discomplexation of the liver beams, granular dystrophy, hepatocyte necrosis. Due to babesiosis, a mixed – hemolytic-parenchymal jaundice with a sign of cholestasis develops. The severity of the disease is determined by the presence and intensity of jaundice. The most informative indicator of the early stages of the development of liver disease is hyperfermentemia; the more severe degree of damage to hepatocytes is shown by hypo- and dysproteinemia.

Conclusions

In dogs of service breeds from different age groups with babesiosis we found oligocytemia with anisocytosis and poikilocytosis, oligochromemia, decreased hematocrit index and macrocytosis. We detected significant changes in the morpho-functional state of erythrocytes in dogs of both age groups due to the catabolic effect of ultramicroscopic invasion on their membranes and the processes of erythrocytopoesis. In dogs with babesiosis, the population (age) composition of erythrocytes varies: the number of "old" erythrocytes increases (they are rapidly destroyed) and the "young" forms of red blood cells (which do not completely provide tissue with oxygen) are reduced. It is, in turn, reflected in the acid resistance of the "red" cells and reduction in the time of hemolysis. The undeniable proof of the work of erythron and processes of transfusion of gases in the body is the ferrum-transferrin complex. As a result of its study in dogs with babesiosis from both age groups, an increase in the level of free ferrum (UIBC) was found and a reduction in the saturation of transferrin with this trace element, which makes it impossible to form hemoglobin molecules in the bone marrow.

References

Al Izzi, S., Martin, D. S., Chan, R. Y., & Leutenegger, C. M. (2013). *Babesia canis vogeli*, *Ehrlichia canis*, and *Anaplasma platys* infection in a dog. Veterinary Clinical Pathology, 42(4), 471–475.

Bajer, A., Mierzejewska, E. J., Rodo, A., & Welc-Falęciak, R. (2014). The risk of vector-borne infections in sled dogs associated with existing and new endemic areas in Poland. Part 2: Occurrence and control of babesiosis in a sled dog kennel during a 13-year-long period. Veterinary Parasitology, 202(3–4), 234–240.

Bajer, A., Mierzejewska, E. J., Rodo, A., Bednarska, M., Kowalec, M., & Welc-Falęciak, R. (2014). The risk of vector-borne infections in sled dogs associated with existing and new endemic areas in Poland: Part 1: A population study on sled dogs during the racing season. Veterinary Parasitology, 202(3–4), 276–286.

Bajer, A., Rodo, A., Mierzejewska, E. J., Tołkacz, K., & Welc-Faleciak, R. (2016). The prevalence of *Dirofilaria repens* in cats, healthy dogs and dogs with concurrent babesiosis in an expansion zone in central Europe. BMC Veterinary Research, 12(1), 183.

Bartnicki, M., Łyp, P., Dębiak, P., Staniec, M., Winiarczyk, S., Buczek, K., & Adaszek, Ł. (2017). Cardiac disorders in dogs infected with *Babesia canis*. Polish Journal of Veterinary Sciences, 20(3), 573–581.

Crnogaj, M., Cerón, J. J., Šmit, I., Kiš, I., Gotić, J., Brkljačić, M., Matijatko, V., Rubio, C. P., Kučer, N., & Mrljak, V. (2017). Relation of antioxidant status at admission and disease severity and outcome in dogs naturally infected with *Babesia canis canis*. BMC Veterinary Research, 13(1), 114.

Davitkov, D., Vucicevic, M., Stevanovic, J., Krstic, V., Tomanovic, S., Glavinic, U., & Stanimirovic, Z. (2015). Clinical babesiosis and molecular identification of *Babesia canis* and *Babesia gibsoni* infections in dogs from Serbia. Acta Veterinaria Hungarica, 63(2), 199–208.

Di Cicco, M. F., Downey, M. E., Beeler, E., Marr, H., Cyrog, P., Kidd, L., Diniz, P. P, Cohn, L. A., & Birkenheuer, A. J. (2012). Re-emergence of *Babesia conradae* and effective treatment of infected dogs with atovaquone and azithromycin. Veterinary Parasitology, 187(1–2), 23–27.

Di Mauro, F. M., & Schoeffler, G. L. (2016). Point of care measurement of lactate. Topics in Companion Animal Medicine, 31(1), 35–43.

Eichenberger, R. M., Riond, B., Willi, B., Hofmann-Lehmann, R., & Deplazes, P. (2016). Prognostic markers in acute *Babesia canis* infections. Journal of Veterinary Internal Medicine, 30(1), 174–182.

Goddard, A., Leisewitz, A. L., Kristensen, A. T., & Schoeman, J. P. (2015). Platelet activation and platelet-leukocyte interaction in dogs naturally infected with *Babesia rossi*. Veterinary Journal, 205(3), 387–392.

Golovakha, V. I., Piddubnyak, O. V., Sliusarenko, S. V., Slivinska, L. G., Maksymovych, I. A., Shcherbatyy, A. R., & Gutyj, B. V. (2017). Acid resistance and population structure of erythrocytes in trotter horses during and after exercise. Regulatory Mechanisms in Biosystems, 8(4), 623–627.

Gutyj, B., Martyshchuk, T., Bushueva, I., Semeniv, B., Parchenko, V., Kaplaushenko, A., Magrelo, N., Hirkovyy, A., Musiy, L., & Murska, S. (2017). Morphological and biochemical indicators of blood of rats poisoned by car-

bon tetrachloride and subject to action of liposomal preparation. Regulatory Mechanisms in Biosystems, 8(2), 304–309.
Gutyj, B., Khariv, I., Binkevych, V., Binkevych, O., Levkivska, N., Levkivskyj, D., & Vavrysevich, Y. (2017). Research on acute and chronic toxity of the experimental drug Amprolinsyl. Regulatory Mechanisms in Biosystems, 8(1), 41–45.
Iguchi, A., Shiranaga, N., Matsuu, A., & Hikasa, Y. (2014). Efficacy of Malarone(®) in dogs naturally infected with *Babesia gibsoni*. Journal of Veterinary Medical Science, 76(9), 1291–1295.
Jain, K. J., Lakshmanan, B., Syamala, K., Praveena, J. E., & Aravindakshan, T. (2017). High prevalence of small *Babesia* species in canines of Kerala, South India. Veterinary World, 10(11), 1319–1323.
Liu, M., Cao, S., Vudriko, P., Suzuki, H., Soma, T., & Xuan, X. (2016). *Babesia gibsoni* internal transcribed spacer 1 region is highly conserved amongst isolates from dogs across Japan. Journal of Veterinary Medical Science, 78(5), 863–865.
Lobetti, R., Kirberger, R., Keller, N., Kettner, F., & Dvir, E. (2012). NT-ProBNP and cardiac troponin I in virulent canine babesiosis. Veterinary Parasitology, 190(3–4), 333–339.
Piane, L., Théron, M. L., Aumann, M., & Trumel, C. (2016). Spurious reticulocyte profiles in a dog with babesiosis. Veterinary Clinical Pathology, 45(4), 594–597.
Rojas, A., Rojas, D., Montenegro, V., Gutiérrez, R., Yasur-Landau, D., & Baneth, G. (2014). Vector-borne pathogens in dogs from Costa Rica: First molecular description of *Babesia vogeli* and *Hepatozoon canis* infections with a high prevalence of monocytic ehrlichiosis and the manifestations of co-infection. Veterinary Parasitology, 199(3–4), 121–128.
Salem, N. Y., & Farag, H. S. (2014). Clinical, hematologic, and molecular findings in naturally occurring *Babesia canis vogeli* in egyptian dogs. Veterinary Medicine International, Article ID 270345.
Sizova, I. A., Kamenskaja, V. V., & Fedjakov, V. I. (1980). Bezapparaturnyj sposob frakcionirovanija krasnyh kletok krovi v gradiente plotnosti saharozy [The nonparametric method of fractionation of red blood cells in a sucrose density gradient]. Izvestija Sibirskogo Otdelenija Akademii Nauk SSSR, 3(15), 119–122 (in Russian).
Slivinska, L., Shcherbatyy, A., Gutyj, B., Lychuk, M., Fedorovych, V., Maksymovych, I., Rusyn, V., & Chernushkin, B. (2018). Parameters of erythrocytopoiesis, acid resistance and population composition of erythrocytes of cows with chronic hematuria. Ukrainian Journal of Ecology, 8(1), 379–385.
Sunaga, F., Arai, S., Itoh, S., & Taharaguchi, S. (2014). Protective efficacy of *Babesia gibsoni* culture-derived exoantigens against the challenge infection in dogs. Parasitology Research, 113(5), 1681–1686.
Sunaga, F., Taharaguchi, S., Arai, S., Itoh, S., & Kanno, Y. (2013). Virulence attenuation of *Babesia gibsoni* by serial passages *in vitro* and assessment of the protection provided by the immunization against the passaged isolate in dogs. Veterinary Parasitology, 197(3–4), 565–570.
Tasaki, Y., Miura, N., Iyori, K., Nishifuji, K., Endo, Y., & Momoi, Y. (2013). Generalized alopecia with vasculitis-like changes in a dog with babesiosis. Journal of Veterinary Medical Science, 75(10), 1367–1369.
Terskov, I. A., & Hitelzon, I. I. (1967). Znachenie dispersionnyh metodov analiza jeritrocitov v norme i patologii [The value of dispersion methods for erythrocytes analysis in norm and pathology]. Voprosy Biofiziki, Biohimii i Patologii Jeritrocitov. Nauka, Moscow. Pp. 41–48 (in Russian).
Wang, J., Zhang, J., Kelly, P., Zheng, X., Li, M., You, J., Huang, K., Qiu, H., Wang, Y., Zhang, R., Li, J., Dong, J., Feng, Y., Zhou, J., & Wang, C. (2018). First description of the pathogenicity of *Babesia vogeli* in experimentally infected dogs. Veterinary Parasitology, 253, 1–7.
Wijk, R., & Solinge, W. (2005). The energy-less red cell is lost: Erythrocyte enzyme abnormalities of glycolysis. Blood, 106(13), 4034–4042.
Ybañez, R. H. D., Ybañez, A. P., Arnado, L. L. A., Belarmino, L. M. P., Malingin, K. G. F., Cabilete, P. B. C., Amores, Z. R. O., Talle, M. G., Liu, M., & Xuan, X. (2018). Detection of *Ehrlichia*, *Anaplasma*, and *Babesia* spp. in dogs of Cebu, Philippines. Veterinary World, 11(1), 14–19.
Zygner, W., Gójska-Zygner, O., Norbury, L. J., & Wedrychowicz, H. (2012). Increased AST/ALT ratio in azotaemic dogs infected with *Babesia canis*. Polish Journal of Veterinary Sciences, 15(3), 483–486.

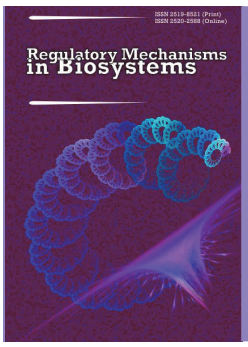

Regulatory Mechanisms in Biosystems

ISSN 2519-8521 (Print)
ISSN 2520-2588 (Online)
Regul. Mech. Biosyst., 9(3), 384–390
doi: 10.15421/021857

Biochemical screen correction possibilities in patients with non-alcoholic fatty liver disease with diabetes mellitus

S. V. Feisa, M. V. Rostoka-Reznikova, M. I. Tovt-Korshynska, L. T. Siksai

Uzhhorod National University, Uzhhorod, Ukraine

Article info

Received 10.07.2018
Received in revised form 17.08.2018
Accepted 19.08.2018

Uzhhorod National University, Sobranetska st., 148, Uzhhorod, 88000, Ukraine. Tel.: +38-050-560-08-47. E-mail: snizhana.feysa@uzhnu.edu.ua

Feisa, S. V., Rostoka-Reznikova, M. V., Tovt-Korshynska, M. I., & Siksai, L. T. (2018). Biochemical screen correction possibilities in patients with non-alcoholic fatty liver disease with diabetes mellitus. Regulatory Mechanisms in Biosystems, 9(3), 384–390. doi:10.15421/021857

The rationale for this study is the controversial data regarding the efficacy of hepatoprotectors and antioxidants for lipid profile correction in non-alcoholic fatty liver disease, the prevalence of which is increasing especially in association with diabetes mellitus. We examined 100 non-alcoholic fatty liver disease patients (40–75 years old) with concomitant type 2 diabetes mellitus (n = 73) or without it (n = 27), the groups were standardized by age and gender. In patients with non-alcoholic fatty liver disease with diabetes mellitus we revealed significantly higher rates of total cholesterol, triglycerides and atherogenic factor in association with a significantly lower high-density lipoproteins level versus the group of patients without concomitant diabetes. We recommended the modification of lifestyle as basic management of their condition to all patients, hypoglycemic therapy with metformin to persons with concomitant diabetes mellitus and rosuvastatin to patients with non-alcoholic fatty liver disease without diabetes. In addition, 25 patients received essential phospholipids (2 caps. 3 times a day) and omega-3 polyunsaturated fatty acids (1000 mg per day) for 3 months; 26 patients – α-lipoic acid (600 mg daily) for 3 months, 22 patients received rosuvastatin (10 mg daily), 27 patients with non-alcoholic fatty liver disease without diabetes mellitus received rosuvastatin (10 mg daily). We evaluated the treatment efficiency after 3 months treatment, and the remote consequences – 12 months after the start of combined treatment. After 3 months, the alanine-aminotransferase rate had decreased by 15.1% in the group taking combined essential phospholipids and ω3-polyunsaturated fatty acids and by 12.9% in the group taking alpha-lipoic acid, which was significantly larger than in the rosuvastatin group (7.5%); gamma-glutamate transpeptidase level decreased by 16.7%, 18.7% and 9.4% respectively indicating anticholestatic and hepatoprotective effect of both proposed treatment combinations. The same tendency of cytolysis and cholestasis processes inhibition was observed after 12 months as well. In conclusion, the combination of standard treatment with antioxidant and hepatoprotective agents (omega-3 polyunsaturated fatty acids with essential phospholipids or only alpha-lipoic acid) promotes both cytolysis and cholestasis syndromes inhibition in non-alcoholic fatty liver disease patients with concomitant type 2 diabetes mellitus.

Keywords: type 2 diabetes mellitus; dyslipidemia; hepatoprotectors; essential phospholipids; omega-3 polyunsaturated fatty acids; alpha-lipoic acid.

Introduction

Non-alcoholic fatty liver disease (NAFLD) is a multi-stage disease that starts with excessive (over 5%) lipids (predominantly triglycerides) accumulation in hepatocytes (hepatosteatosis stage) (Brunt & Tiniakos, 2010; Takahashi & Fukusato, 2014), progresses to the development of necrotic inflammation liver parenchyma (steatohepatitis stage) (Schleicher et al., 2014) and associated with risk factors (obesity, type 2 diabetes mellitus (DM-2), dyslipidemia, genetic predisposition) (Jonathan et al., 2016; Stepanov et al., 2018). NAFLD is the most common liver disease with 6.3–33.0% prevalence in the general population (Loomba & Sanyal, 2013; Lombardi et al., 2017; Perazzo & Dufour, 2017). NAFLD can be diagnosed in every third inhabitant of the planet (Anavi et al., 2017; Williams et al., 2011; Lazo et al., 2013). The frequency of its detection in adults depends on diagnosis method (Lee, 2017), age, gender, ethnicity (Dajani et al., 2015; Berzigotti et al., 2018) and presence of comorbidity (Dajani & Abu Hammour, 2016). NAFLD can progress to non-alcoholic steatohepatitis (NASH) in about 30% of cases (Michelotti et al., 2013; Firneisz, 2014; Sharma et al., 2015; Lee et al., 2017).

The high risk groups of NAFLD include people with abdominal obesity, DM-2, hypercholesterolemia, metabolic syndrome (Sumida et al., 2014; Stepanov et al., 2018). According to Gastaldelli (2007), NAFLD is diagnosed in 57% of obesity patients and 72% of DM-2 patients. Almost 90% of patients with severe obesity demonstrate the signs of NAFLD (Machado & Cortez-Pinto, 2014). Prevalence of NAFLD in dyslipidemia patients is estimated at 50% and characterized by increased triglycerides (TG) rate and decreased low density lipoproteins (LDL) level (Nseir & Mahamid, 2013). In the case of DM-2, NAFLD more often progresses to NASH. Prevalence of NASH in DM-2 patients is 12.2% versus 7.4% in patients without diabetes and in cases of coexistent DM-2 and obesity the rate of NASH reaches 21–40% (Ballestri, 2016).

Considering the close link of NAFLD and obesity, dyslipidemia, arterial hypertension and metabolic syndrome (MS) and their common pathogenesis based on insulin resistance (IR), NAFLD is reasonably named as hepatic manifestation of MS (Ballestri, 2016). IR can lead to NAFLD and NAFLD can cause hepatic IR, so NAFLD patients are at high risk of complete MS or its development of its components especially DM-2 (Gaggini et al., 2013; Firneisz, 2014). In addition to higher probability of death due to hepatic complications (liver failure, portal hypertension complications, hepatocellular carcinoma) (Armstrong et al., 2014), those patients are prone to higher incidence of cardiovascular diseases (Patel et al., 2017). The dangerous feature of NAFLD is an asymptomatic course especially during the initial stage (hepatosteatosis) which can be presented without lab tests showing abnormalities, which makes it

difficult and sometimes even impossible to diagnose in time and start the early treatment for prevention of both hepatic and extrahepatic complications. Often the only changes in the laboratory picture of NAFLD patients are the initial signs of prediabetes or DM-2 (often diagnosed for the first time) - diseases that create a background predisposition to liver steatosis development.

The first aspect of effective NAFLD treatment is a life style modification: low calorie diet, increase in physical activity, cessation of smoking (Verbeek et al., 2013; Kim, 2017; Newsome et al., 2018). The gradual reduction in body weight is particularly important when NAFLD is a component of MS (Federico et al., 2017; Babio, 2014). Pharmacological treatment in NAFLD patients is to be considered in case of NASH or in case of comorbidity – steatohepatosis with cardiometabolic disorders (obesity, dyslipidemia, arterial hypertension, DM-2) (Lombardi et al., 2017). According to the recommendations of the European Association for the Study of the Liver (EASL), the European Association for the Study of Diabetes (EASD) and the European Association for the Study of Obesity (EASO) (2016), a pharmacological treatment can be prescribed not only to patients with liver fibrosis of F_2 stage but in case of high probability of the disease progression (concomitant DM-2, MS, recurrent high ALT level detection, high intensity of inflammation) and includes pioglitazone, Vitamin E or their combination, statins, omega-3 polyunsaturated fatty acids (EASL-EASD-EASO, 2016).

Considering that NAFLD is characterized by comorbidity which often leads to polypharmacy (Patel et al., 2017), the medicines with multiple effects that influence different ethio-pathogenic links of clinical and laboratory presentation of NFLD should be preferred in those patients (Berlanga et al., 2014).

Although the current recommendations (EASL-EASD-EASO, 2016; Ganesh & Rustgi, 2016) don't include indications regarding prescription of hepatoprotectors (Dajani & Abu Hammour, 2016) there are publications about their advisability as well as medicines with cytoprotective (Gonciarz et al., 1988; Gundermann et al., 2016) and antioxidant (de Oliveira et al., 2011; Basu et al., 2014) effects that constitute a pathogenetically reasonable approach in case of NAFLD. It has been proven that the function of hepatocytes correction leads to enhanced treatment effect due to indirect impact on IR degree (Dajani & Abu Hammour, 2016).

Considering their combined effects, cytoprotective, anti-inflammatory, hypotrigliceridemic and antioxidant effects, essential phospholipids (EPL), omega-3 polyunsaturated fatty acids (PUFA) and alpha-lipoic (thioctic) acid (ALA) attracted our attention. The main component of EPL is a phosphocholine which contains PUFA (Dajani et al., 2015; Padma et al., 2013). Building up in the hepatocyte membranes, EPL improve membrane-dependent function, showing anti-inflammatory, antifibrotic, apoptosis-modulating, regenerative effects (Gundermann et al., 2016). ALA works as a coenzyme in the ketoacids oxidative decarboxylation, takes part in the cell energy metabolism and shows antitoxic and antioxidant effects (Kajikawa et al., 2011; Stankovic et al., 2014). In DM-2 patients ALA decreases IR, inhibits peripheral neuropathy development and glycogen accumulation in the liver, influences cholesterol metabolism, helps to reduce blood glucose level, takes part in lipid and carbohydrates metabolism regulation, improves liver function due to its hepatoprotector, antioxidant, detoxication effect. Use of omega-3 PUFA in NAFLD with DM-2 patients is advisable and reasonable for hyperlipidemia correction (Di Minno et al., 2012) since their hypotrigliceridemic effect allows this group to be considered as a possible alternative to statins. The high prevalence on NAFLD and DM-2 and the lack of consensus regarding the use of EPL, ALA and omega-3 PUFA in such patients determine the relevance of this work and justify the necessity of conducting a clinical study of their effect on patients with NAFLD and DM-2. The objective of this article is to investigate biochemical screen of liver function, lipid and carbohydrate metabolism in NAFLD patients and evaluate the effect of combined treatment with omega-3 PUFA, EPL and ALA use.

Materials and methods

We examined 73 patients with NAFLD and DM-2 who were treated at the Therapy and Family Medicine Department of Uzhhorod National University in 2011–2017. The patients were 40–71 years old (50.5 ± 5.8 years on average). 49 (67.1%) of patients were males and 24 (32.9%) – women. 30 healthy adults (20 men, 10 women with an average age of 49.5 ± 5.5 years) were examined as the control group. The groups were standardized by the age and gender.

The NAFLD diagnosis was considered according to the EASL-EASD-EASO Clinical Practice Guidelines for the Management of Non-Alcoholic Fatty Liver Disease (2016). Inclusion criteria were confirmed diagnoses of NAFLD and DM-2. Exclusion criteria were viral, autoimmune, alcohol and toxic (drug-induced, iatrogenic) liver disease, cardiovascular diseases decompensation, collagenosis (rheumatic diseases), an active or decompensated stage of any other concomitant diseases, infectious diseases (including tuberculosis), pregnancy, breast feeding and psychiatric diseases that violated the patient's ability to evaluate his / her condition and discuss the disease's management. Patients that refused to sign an informed consent for participation in the study were also excluded from the investigation.

All patients underwent the laboratory tests complex that included total, direct, indirect bilirubin level, uric acid, total protein, albumin, creatinine rates; enzymes activity (alanine-aminotransferase (ALT), aspartate-aminotransferase (AST), gamma-glutamate transpeptidase (GGT), alkaline phosphatase (ALP). The lipid profile investigation included blood levels of total cholesterol (TC), triglycerides (TG); high density lipoproteins (HDL), low density lipoproteins (LDL) and very low density lipoproteins (VLDL) cholesterol; atherogenic index of plasma (AIP) calculation. The lipid metabolism was evaluated by fasting and postprandial blood glucose levels (oral glucose tolerance test – OGTT), glycated hemoglobin (HbA1C). IR was evaluated by HOMA index according to the formula IR-HOMA = (fasting blood glucose X fasting blood insulin) / 22.5, where X – multiplication and / – division.

The LAP (Lipid Accumulation Product) index was calculated in all patients as the non-invasive liver steatosis index (Bedogni et al., 2010; Dai et al., 2017) according to the formula: LAP = (WC – 65) X TG (for men) or LAP = (WC – 58) X TG (for women), where: WC – waist circumference in cm, X – multiplication, TG – blood triglycerides level in mmol/l. LAP over 4.28 was interpreted as liver steatosis.

The average ranges of the groups of all laboratory tests were calculated in NAFLD with DM-2 patients before the start of treatment and compared to those of the control group for evaluation of NAFLD and DM-2 laboratory characteristics.

Management of all patients included life style modification with moderate exertion (walking for at least 30 min every day) and diet correction (5 food intakes daily: 3 large meals and 2 small ones; limited fast-digesting carbohydrates and animal fats consumption, adequate water intake, 15% deficit in daily caloric intake). All patients received hypoglycemic therapy with metformin, which is proven to reduce IR.

The study design required 3 groups of NAFLD patients in accordance to the proposed combined treatment. Group 1 included 25 patients who received EPL (medicine Essentiale Forte H) 2 capsules TID and omega-3 PUFA 1000 mg daily, group 2 – 26 patients who received ALA (per os) 600 mg daily. Group 3 included patients who didn't receive any medicine with hepatoprotective and antioxidant effect; they received rosuvastatin (10 mg daily) for dyslipidemia correction.

The effect of different combinations was evaluated after 3 months of treatment by comparison of average group laboratory test ranges with respective baseline tests. The remote consequences were estimated 12 months after the start of combined treatment by comparison of the laboratory tests to baseline, 3 month and control group results.

The statistical analysis included Microsoft Excel table base of patients and Statistica 10.0 (StatSoft Inc., USA) software use. Treatment group differences were evaluated using the independent sample t-test in case of normal distribution and the Mann-Whitney test for non-parametric data. The significance of changes in evaluated indices after treatment in normal distribution was evaluated using the Student two-tailed test and in case of non-normal distribution – the Wilcoxon test respecttively. The difference was considered as significant at $P < 0.05$. All quantitative indices were presented in (x ± SD) design, where x is a mean group value and SD – its standard deviation.

Results

Biochemical screen of NAFLD patients with concomitant DM-2 is shown in Table 1, where mean group values are presented in comparison to control group values and the group of patients with NAFLD without diabetes. The mentioned indices were evaluated before treatment and characterize baseline values of NAFLD patients.

Table 1
Biochemical screen of NAFLD patients with concomitant type 2 diabetes mellitus versus NAFLD patients without diabetes and control group (x ± SD)

Index	NAFLD with DM-2 (n = 73)	NAFLD without DM (n = 27)	Control group (n = 30)
Fasting blood glucose, mmol/l	11.1 ± 1.78*#	6.23 ± 0.66	4.08 ± 0.59
HbA1C, %	7.87 ± 0.52*#	6.04 ± 0.24	5.13 ± 0.44
IR-HOMA, units	9.34 ± 3.42#	6.32 ± 3.35	2.33 ± 0.23
Total cholesterol, mmol/l	5.84 ± 0.68#	5.18 ± 0.56	4.03 ± 0.66
Triglycerides, mmol/l	2.77 ± 0.60#	2.51 ± 0.41	1.84 ± 0.26
HDL, mmol/l	0.91 ± 0.10*#	1.16 ± 0.11	2.27 ± 0.76
LDL, mmol/l	3.67 ± 0.47	2.87 ± 0.41	2.71 ± 0.34
VLDL, mmol/l	1.26 ± 0.27	1.15 ± 0.19	0.83 ± 0.13
IAP, units	5.48 ± 0.68#	3.50 ± 0.64	2.15 ± 0.43
ALT, IU/l	37.90 ± 10.52#	27.40 ± 8.61	12.56 ± 3.12
AST, IU/l	33.80 ± 11.98#	22.06 ± 5.26	8.32 ± 2.89
GGT, IU/l	39.30 ± 12.55#	21.30 ± 12.68	10.24 ± 3.61
ALP, IU/l	94.81 ± 14.05*#	38.41 ± 15.73	46.57 ± 7.13
Total protein, g/l	70.60 ± 3.03	70.11 ± 5.57	73.86 ± 2.56
Bilirubin total, mcmol/l	9.74 ± 1.82	13.03 ± 4.08	10.01 ± 1.24
Bilirubin direct, mcmol/l	3.42 ± 0.90	3.70 ± 0.61	3.40 ± 0.76
Creatinine, mcmol/l	77.25 ± 11.51	78.42 ± 25.50	78.91 ± 8.22
Uric acid, mcmol/l	336.2 ± 53.97	269.3 ± 90.02	280.21 ± 22.30

Notes: * – significant difference in NAFLD and DM-2 versus NAFLD without DM-2 patients, $P < 0.05$; # – significant difference in NAFLD patients versus control group, $P < 0.05$.

We observed positive dynamics of carbohydrate metabolism indices after treatment (Table 2). The fasting blood glucose and HbA1C rates decreased the most significantly in Group 2 showing additional hypoglycemic effect of ALA. In Group 1 the changes of the mentioned indices after treatment were also significantly different but less pronounced. In Group 3 the rates of those indices decreased as well but without significant difference ($P > 0.05$). The IR-HOMA rate was reduced in all groups but significance of those changes was confirmed only in Group 2 after 12 months apart from the treatment start.

Table 2
The treatment influence on carbohydrate metabolism indices in NAFLD patients with DM-2 (x ± SD)

Index		Group 1 (essential phospholipids: 2 capsules 3 times a day + omega-3 polyunsaturated fatty acids, 1000 mg daily; n = 25)	Group 2 (alfa lipoic acid, 600 mg daily per os; n = 26)	Group 3 (rosuvastatin, 10 mg daily; n = 22)
Fasting blood glucose, mmol/l	before treatment	10.82 ± 1.91	11.27 ± 2.13	11.21 ± 1.02
	after 3 months treatment	10.08 ± 0.30*	9.60 ± 0.26*	10.10 ± 0.62
	12 months after the start of treatment	9.13 ± 1.16*	8.52 ± 0.97*	9.40 ± 0.62*
HbA1C, %	before treatment	7.88 ± 0.49	7.77 ± 0.57	7.99 ± 0.52
	after 3 months treatment	7.67 ± 0.09	7.47 ± 0.08	7.77 ± 0.91
	12 months after the start of treatment	7.46 ± 0.36*	7.26 ± 0.36*	7.56 ± 0.36
IR-HOMA (units)	before treatment	8.18 ± 2.04	9.72 ± 3.74	13.17 ± 5.15
	after 3 months treatment	7.60 ± 1.81	8.57 ± 3.53	12.10 ± 4.74
	12 months after the start of treatment	7.82 ± 2.30*	8.71 ± 3.20*	10.65 ± 2.17

Notes: * – significant changes after treatment versus before treatment, $P < 0.05$.

The lipid profile of NAFLD before treatment was characterized by hypercholesterolemia and dyslipidemia, which were presented with hypertriglyceridemia, high LDL, VLDL and significantly decreased HDL levels. It led to significantly higher AIP in NAFLD with DM-2 patients (5.48 ± 0.68) versus NAFLD without DM-2 patients (3.50 ± 0.64, $P < 0.05$). This index was 2.55 fold higher in NAFLD with DM-2 patients versus the control group (2.15 ± 0.43). The changes in lipid profile after treatment, shown in Table 3, demonstrate the good effect of the treatment of all combinations.

Table 3
The changes in lipid profile of NAFLD with DM-2 patients after treatment (x ± SD)

Index		Group 1 (essential phospholipids: 2 capsules 3 times a day + omega-3 polyunsaturated fatty acids, 1000 mg daily; n = 25)	Group 2 (alfa lipoic acid, 600 mg daily per os; n = 26)	Group 3 (rosuvastatin, 10 mg daily; n = 22)
Total cholesterol, mmol/l	before treatment	5.80 ± 0.65	5.84 ± 0.54	5.87 ± 0.87
	after 3 months treatment	5.45 ± 0.10*	5.28 ± 0.07*	5.17 ± 0.59
	12 months after the start of treatment	5.22 ± 0.31*	5.05 ± 0.44*	4.90 ± 0.44*
Triglycerides, mmol/l	before treatment	2.86 ± 0.51	2.60 ± 0.53	2.86 ± 0.74
	after 3 months treatment	2.45 ± 0.08	2.17 ± 0.08	2.28 ± 0.56
	12 months after the start of treatment	1.94 ± 0.16*	1.98 ± 0.41*	1.97 ± 0.34
HDL, mmol/l	before treatment	0.90 ± 0.11	0.90 ± 0.08	0.92 ± 0.13
	after 3 months treatment	0.98 ± 0.15	0.98 ± 0.01	0.99 ± 0.09
	12 months after the start of treatment	1.11 ± 0.09*	1.07 ± 0.70*	1.05 ± 0.07
LDL, mmol/l	before treatment	3.59 ± 0.46	3.76 ± 0.33	3.65 ± 0.62
	after 3 months treatment	3.36 ± 0.07*	3.31 ± 0.04*	3.13 ± 0.42*
	12 months after the start of treatment	3.23 ± 0.26*	3.08 ± 0.31*	2.95 ± 0.35*
VLDL, mmol/l	before treatment	1.31 ± 0.23	1.18 ± 0.24	1.30 ± 0.34
	after 3 months treatment	1.12 ± 0.04*	0.99 ± 0.04*	1.04 ± 0.26*
	12 months after the start of treatment	0.88 ± 0.07*	0.90 ± 0.18*	0.89 ± 0.15*
IAP, units	before treatment	5.45 ± 0.74	5.53 ± 0.56	5.44 ± 0.75
	after 3 months treatment	4.56 ± 0.10*	4.40 ± 0.07*	4.20 ± 0.41*
	12 months after the start of treatment	3.74 ± 0.44*	3.74 ± 0.52*	3.70 ± 0.49*

Notes: * – significant changes after treatment versus before treatment, $P < 0.05$.

In cases of NAFLD, free fats, mostly triglycerides, are accumulated in hepatocytes, which is characterized by the common ultrasound conclusion of a "fatty liver". Excessive accumulation of fats in the liver can be detected by the non-invasive method of the lipid products accumulation (LAP) index (Bedogni et al., 2010). One of the indicators of the effect of treatment is a reduction in liver fats deposits, which is represented not only by positive biochemical screen and liver ultrasound dynamics but also the LAP index reduction. Table 4 demonstrates the changes in the LAP index after treatment: in Group 1 the LAP index had decreased 1.59 times after 3 months treatment as well as in Group 2, while in Group 3 these changes were less significant and LAP index decreased only 1.44 times. The remote consequences that were evaluated 12 months after the start of treatment showed the LAP index reduction versus mean group values before treatment of 3.13 fold in Group 1; 2.67 fold in Group 2 and only 1.98 fold – in Group 3.

The liver function tests were evaluated in all NAFLD with DM-2 patients. The cytolysis, liver parenchyma inflammation and cholestasis syndromes were revealed. We investigated the influence of different treatment combination on the following liver functions: protein synthesis, pigment and purine metabolism as well as kidney function – the mean values of selected biochemical screen indices in patients with NAFLD and DM-2 after treatment, which are shown in Table 5. The hepatocytes cytolysis intensity was evaluated according to ALT and AST activity indices.

Table 4
The non-invasive LAP (Lipid Accumulation Products) index changes in NAFLD with DM-2 patients after treatment (x ± SD)

Index		Group 1 (essential phospholipids: 2 capsules 3 times a day + omega-3 polyunsaturated fatty acids, 1000 mg daily; n = 25)	Group 2 (alfa lipoic acid, 600 mg daily per os; n = 26)	Group 3 (rosuvastatin, 10 mg daily; n = 22)
LAP (Lipid accumulation products) index, units	before treatment	164.2 ± 30.4	144.1 ± 33.1	157.1 ± 39.5
	after 3 months treatment	103.5 ± 14.3	90.8 ± 13.6*	108.9 ± 11.9
	12 months after the start of treatment	52.5 ± 12.3*	54.0 ± 22.3*	79.2 ± 23.9*

Notes: * – significant changes after treatment versus before treatment, $P < 0.05$.

Table 5
Changes in selected biochemical screen indices in NAFLD and DM-2 patients after different treatment combinations, M ± m

Index		Group 1 (essential phospholipids: 2 capsules 3 times a day + omega-3 polyunsaturated fatty acids, 1000 mg daily; n = 25)	Group 2 (alfa lipoic acid, 600 mg daily per os; n = 26)	Group 3 (rosuvastatin, 10 mg daily; n = 22)
ALT, IU/l	before treatment	37.5 ± 11.9	36.6 ± 10.8	39.9 ± 8.6
	after 3 months treatment	31.8 ± 2.0	31.9 ± 1.8	36.9 ± 1.8
	12 months after the start of treatment	30.7 ± 17.0	28.5 ± 2.2*	34.5 ± 7.0*
AST, IU/l	before treatment	32.0 ± 12.7	33.1 ± 12.1	36.7 ± 11.0
	after 3 months treatment	27.2 ± 2.2	27.9 ± 1.9	33.7 ± 2.0
	12 months after the start of treatment	23.9 ± 9.0	25.1 ± 6.6*	31.4 ± 8.4
GGT, IU/l	before treatment	38.7 ± 9.4	40.8 ± 15.8	38.0 ± 11.7
	after 3 months treatment	32.2 ± 1.6*	33.2 ± 2.5	34.4 ± 2.1
	12 months apart from the treatment t	28.5 ± 6.7*	29.2 ± 8.7*	32.9 ± 9.0
ALP, IU/l	before treatment	94.1 ± 16.1	91.4 ± 15.4	99.7 ± 7.6
	after 3 months treatment	75.6 ± 3.0*	73.2 ± 2.4*	83.3 ± 3.1*
	12 months after the start of treatment	66.4 ± 12.1*	63.4 ± 9.9*	67.4 ± 7.4*
Total protein, g/l	before treatment	70.4 ± 3.6	70.1 ± 2.6	71.4 ± 2.7
	after 3 months treatment	74.4 ± 0.7*	70.6 ± 0.7	72.6 ± 0.6
	12 months apart from the treatment start	71.3 ± 13.8	71.8 ± 5.2	73.0 ± 3.4
Bilirubin total, mcmol/l	before treatment	9.28 ± 1.85	10.02 ± 2.14	9.93 ± 1.25
	after 3 months treatment	9.89 ± 0.37	14.07 ± 0.69	13.42 ± 1.89*
	12 months after the start of treatment	10.80 ± 2.76*	15.30 ± 2.84*	13.51 ± 2.23*
Bilirubin total, mcmol/l	before treatment	3.32 ± 0.55	3.59 ± 1.36	3.30 ± 0.41
	after 3 months treatment	3.79 ± 0.17*	5.34 ± 0.39*	5.14 ± 0.45*
	12 months after the start of treatment	3.71 ± 1.00	5.42 ± 1.39*	4.82 ± 1.02*
Creatinine, mcmol/l	before treatment	77.9 ± 12.3	76.9 ± 11.3	76.8 ± 11.3
	after 3 months treatment	78.3 ± 2.1	85.9 ± 1.7*	83.9 ± 3.5*
	12 months after the start of treatment	80.4 ± 10.3	89.9 ± 6.1*	86.3 ± 7.9*
Uric acid, mcmol/l	before treatment	345.6 ± 77.6	338.2 ± 46.3	322.3 ± 15.2
	after 3 months treatment	326.5 ± 8.4	343.3 ± 8.4	324.4 ± 11.6
	12 months after the start of treatment	322.7 ± 37.9	331.9 ± 35.9	325.5 ± 14.6

Notes: * – significant changes after treatment versus before treatment, $P < 0.05$.

The majority of NAFLD patients with DM-2 (50 of 73; 68.5%) presented with steatosis in the liver (the 1st stage of NAFLD) without steatohepatitis signs and only in 23 of 73 patients (31.5%) did we diagnose mild NASH (the 2nd stage of NAFLD) with a 1.5–2.0 fold increase in ALT. Mild NASH was detected in all 23 NASH patients and zero, moderate or high hepatitis activity degrees were diagnosed. The mean ALT activity in NAFLD with DM-2 patients before treatment was 37.9 ± 10.5 IU/l. In Group 1 which additionally received EPL and omega-3 PUFA, we observed the mean ALT activity reduction by 15.1% after 3 months treatment and by 18.1% after 12 months from the treatment start. In Group 2, where ALA was additionally prescribed, the mean ALT activity decreased by 12.9% and 15% respectively. The AST changes demonstrated the same tendency in the abovementioned groups.

The cholestasis intensity was evaluated by GGT and ALP activity. We observed many significant changes after treatment in the Groups 1 and 2 in comparison with Group 3: the mean GGT activity value decreased by 16.7% in Group 1; by 18.7% – in Group 2 and only by 9.4% – in Group 3 respectively after 3 months treatment. 12 months after the start of treatment the mean GGT activity had decreased by 26.4% in Group 1, by 28.5% – in Group 2 respectively in contrast to 13.6% in Group 3. The mean ALP activity decreased after treatment in all treatment groups with significant changes both after 3 month treatments and after 12 months. In Group 1 the total protein rate significantly increased after 3 months treatment without significant changes in Groups 2 and 3, showing the improvement in protein-synthetic liver function after additional prescription of EPL and omega-3 PUFA.

We did not find significant pigment metabolism violation in NAFLD patients with DM-2 confirmed by normal total, direct and indirect bilirubin levels in NAFLD patients compared to the control group. Nevertheless, the bilirubin rate was significantly higher in all groups of NAFLD patients with DM-2 versus the control group but remained within reference ranges. The mean creatinine value in NAFLD patients with DM-2 before treatment also was not significantly different in comparison to the control group. This index slightly increased after treatment especially in Group 2 and less in Group 3 but did not exceed the upper limit of normal value.

In NAFLD patients with DM-2 we revealed a tendency to purine metabolism violation but the uric acid level difference was not significant. The level of uric acid was slightly reduced in Group 1 after treatment compared to the initial level without significant difference, probably indicating an indirect impact of hepatoprotector medicines EPL and omega-3 PUFA on the purine metabolism of NAFLD patients.

Discussion

The results of our clinical trial showed the presence of significant biochemical screen changes in NAFLD and DM-2 patients with carbohydrate metabolism violation confirmed by significantly higher rates of fasting blood glucose (11.1 ± 1.78 mmol/l) and HbA1C (7.87 ± 0.52%) versus the control group (4.08 ± 0.59 mmol/l and 5.13 ± 0.44% respectively, $P < 0.05$) associated with insulin resistance of the peripheral tissues demonstrated by significantly higher rate of IR-HOMA (9.34 ± 3.42 in the examined patients versus 2.33 ± 0.23 in the control group, $P < 0.05$).

Comorbidity is characteristic for NAFLD with frequent other chronic concomitant diseases. According to Patel et al. (2017), the most common comorbidities are MS (94%), "depression" diagnosed by patients (44%), coronary heart disease (32%), obstructive sleep apnea (32%), and 59% cases of NAFLD with DM-2 are characterized by polypharmacy (Patel et al., 2017). Jonathan et al. (2016) revealed that NAFLD and DM-2 association leads to a higher rate of treatment resistant DM-2 and diabetic microangiopathy development. At the same time, NAFLD progression rate from steatohepatosis to NASH and liver cirrhosis is much higher in cases of concomitant DM-2.

We revealed dyslipidemia which is characterized by significantly higher rates of total cholesterol, triglicerydes and AIP with significantly lower LDL cholesterol level in NAFLD and DM-2 patients. These results accord with other clinical trials results (Nseir & Mahamid, 2013) and meet the current recommendations in NAFLD diagnosis and treatment data (EASL-EASD-EASO, 2016).

In NAFLD patients with DM-2, the liver function tests are characterized by the presence of cytolysis and cholestasis laboratory syndromes with preserved protein- and pigment-synthetic functions. The mean

ALT activity rate before treatment (37.9 ± 10.5 IU/l) was 3 fold higher than in the control group (12.6 ± 3.1 IU/l, $P < 0.05$) and the mean AST activity rate (33.8 ± 12.0 IU/l) was respectively 4.06 times higher than in the control group, showing cytolysis and necrotic inflammation changes of liver parenchyma. The mean GGT activity rate in NAFLD patients with DM-2 (39.3 ± 12.6 IU/l) was also significantly higher and exceeded the control group GGT rate by 3.84 times (10.2 ± 3.6 IU/l, $P < 0.05$) and the mean ALP activity rate was 2.03 fold higher in the examined patients versus the control group (94.8 ± 14.1 IU/l and 46.6 ± 7.1 IU/l respectively, $P < 0.05$) confirming the cholestasis syndrome. We did not find significant changes in total protein, bilirubin and its fractions and creatinine in NAFLD and DM-2 patients in comparison with the control group. That is why, according to our results, we cannot state that the protein-synthetic function and pigments metabolism were violated in the examined NAFLD and DM-2 patients, and kidney function impairment was also not confirmed. The mean uric acid value (336.2 ± 54.0 mmol/l) was higher than in the control group (280.2 ± 22.3 mmol/l) but this difference was not significant ($P > 0.05$). The revealed tendency to rise in uric acid level demonstrates coexistent purine metabolism impairment in NAFLD and DM-2 patients. Our results are in accordance with similar studies of metabolic changes in NAFLD patients with concomitant DM-2 (Maximos et al., 2015; Buzzetti et al., 2016; Magee et al., 2016; Hansen et al., 2017; Martin-Rodriguez et al., 2017). Lou et al. (2015) revealed that the IR-HOMA rate is significantly higher in NAFLD patients with DM-2 as well as ALT, AST, GGT, total cholesterol, LDL, triglycerides than in NAFLD patients without DM-2 or in DM-2 patients without NAFLD. The same study demonstrated negative correlation of serum omega-3 PUFA with IR-HOMA, triglycerides, LDL and total cholesterol. Most pathogenic hepatocyte damage mechanisms in NAFLD are based on damage to membrane structures (Magee et al., 2016; Hansen et al., 2017). That is why the use of medicines which can regenerate the structure and functions of cell membranes and inhibit the destruction of hepatocytes is advisable. The search of new pharmacotherapy aids is conducted in different directions: looking for hepatoprotector agents that stimulate regeneration processes and the most active detection of hepatoprotectors (Pivtorak, 2017).

Our study demonstrated the good effect of EPL and omega-3 PUFA in addition to the standard treatment for cytolysis and cholestasis inhibition and liver protein-synthetic function improvement. We revealed a tendency to reduction in ALT and AST rates in Group 1 who received EPL and omega-3 PUFA, but those changes were not significant. At the same time, in Group 2 (additional ALA prescription) the ALT and AST rates significantly ($P < 0.05$) had decreased 12 months after the start of treatment showing long duration and stability of the anticytolitic effect of this treatment combination. Similarly, in Group 3 (rosuvastatin prescription) the ALT and AST activity rates significantly decreased after treatment, which gives a reason to affirm its positive influence on liver function and partly deny hepatotoxic effect. The long-term stable anticholestatic effect was revealed in Groups 1 and 2 confirmed by significant reduction in GGT and ALP rates 2 months the start of treatment. In Group 1, both GGT and ALP rates had significantly decreased after 3 months treatment with preserved effect after 12 months, demonstrating the most prominent and stable hepatoprotector effect of EPL with omega-3 PUFA use among the prescribed combinations and in Group 2 only the ALP level had decreased significantly after 3 months treatment with additional ALA prescription, while GGT demonstrated just a tendency to reduction with significantly lower both ALP and GGT rates after 12 months compared to the initial rates before treatment. In Group 3 (rosuvastatin prescription) only ALP reduction was detected and the GGT rate was not significantly changed.

Our results are consistent with those of other similar investigations of the clinical effect of EPL and omega-3 PUFA (Li et al., 2000; Ohbayashi, 2004; Poongothai et al., 2005; Sas et al., 2013; Lou et al., 2014; Gundermann et al., 2016; Stepanov, 2016; Martinez-Rodriguez et al., 2017). The Kokran review (Lombardi et al., 2017), which includes 77 clinical trials with 6,287 NFLD patients examined, showed ambiguous data regarding efficacy of different pharmacological treatments including EPL, omega-3 PUFA and ALA use. The beneficial pathogenic effects of EPL are well-known. The complex EPL-based medicines contain multiple phospholipids in combination with vitamins and lead to appropriate biochemical reactions that meet urgent hepatocytes demands (Pivtorak, 2017). Many scientists state a positive effect of EPL represented by resolution of clinical symptoms and improvement in laboratory test results (decreasing of ALT, AST activity rates), ultrasound signs of liver fibrosis reduction (Wu, 2009; Padma, 2013). Gundermann (2016) published a review of 45 clinical trials where EPL were used in NAFLD patients, 2 of them were double-blind. The daily dose of EPL varied from 1.05 to 1.8 g and treatment course duration was from 4 weeks to 2 years. In the majority of these trials EPL were prescribed in the daily dose of 1.8 g for 3–6 months. In several studies the therapy started from 500-1000mg of EPL for 10 days – 4 weeks with further oral prescription. In one trial 500 mg of EPL were prescribed for 30 days. In an open randomized trial by Dajani et al. (2015) with 324 patients (113 were NAFLD patients, 107 – NAFLD with DM-2 and 104 – NAFLD with combined dyslipidemia patients respectively) the diet and physical exertion were combined with 1,800 mg of EPL daily for 24 weeks with the dose reduction to 900 mg per day for the following 48 weeks. The results demonstrated good general and gastrointestinal symptoms improvement in NAFLD patients with significant reduction in ALT and AST activity rates, which were high before treatment. The ultrasound showed normalization in 4.6% and shift from the 2nd to 1st NAFLD stage in 24% of patients.

Despite there being reasonable mechanisms of potential EPL influence on the main NAFLD pathogenic links, the results of some clinical trials have not confirmed their efficacy (Sanyal et al., 2014).

We obtained interesting results of the impact of treatment on lipid metabolism. In Group 3 which received rosuvastatin, the total cholesterol rate decreased by the highest degree as was expected but the lowest mean triglycerides level 12 months after the start of treatment was revealed in Group 1, not Group 3. In the same Group 1 there was a maximal (among the 3 treatment groups) HLD level rise demonstrating good effect of EPL and omega-3 PUFA on lipid metabolism improvement. In Group 1, the total cholesterol level reduction was comparable to that of Group 3; at the same time in Group 1, we observed reduction in the triglycerides level with increase in the HLD level, which demonstrates an anti-atherogenic effect. The hypotriglyceridemic effect of EPL and omega-3 PUFA combination in Group 1 is particularly important since triglycerides cause liver steatosis accumulating in heaptocytes in cases of NAFLD.

According to EASL-EASD-EASO (2016) recommendations, omega-3 PUFA can be considered as the first line treatment of triglyceridemia in NAFLD patients but cannot be recommended for the specific NAFLD therapy yet (class 1 recommendations, evidency level B). The first trial of siliphos-selenium-methionine-alpha lipoic acid effect in NAFLD patients (Martinez-Rodriguez et al., 2014) showed that combined use of selenium 15 mg, methionine 3 mg and ALA 200 mg for 24 weeks additionally to metformin 1500 mg led to the steatosis reduction by 70% according to ultrasound results versus 15% in patients who received only metformin 1500 mg daily. This combined therapy promoted better antioxidant protection, liver transaminases activity reduction, steatosis progression prevention and anti-inflammatory profile improvement in NAFLD patients.

Kajikawa et al. (2011) in a prospective double-blind placebo controlled trial in 37 North American clinical centers investigated the efficacy of ethyl-eicosapentaenic acid in different dosing, which is an omega-3 PUFA well known for its insulin resistance, lipogenesis and inflammation reduction leading to NAFLD activity inhibition. This trial demonstrated the good effect of omega-3 PUFA for NAFLD clinical course improvement, hepatocytes triglycerides level correction and ALT activity reduction. The liver oxidative stress indicators (free fatty acids, TNF-factor, serum ferritin and thioredoxin) rates were significantly reduced but the body mass, blood glucose, insulin and adiponectin levels were not changed significantly.

Di Minno et al. (2012) described 7 clinical trials of omega-3 PUFA efficacy in NAFLD patients; the largest study involved 177 NAFLD patients who received omega-3 PUFA for 6 months and showed its advisability in complex NAFLD treatment. In contrast to the abovementioned study, Sanyal et al. (2014) demonstrate an absence of significant

liver histology changes after omega-3 PUFA therapy. In a randomized, placebo-controlled open prospective clinical trial Basu et al. (2014) investigated efficacy of antioxidants in overweight and obesity patients (body mass index (BMI) 28–33 kg/m^2) with ultrasound liver steatosis signs. The patients walked 150 min per week (at least 100 steps per minute) and consumed less than 1600 calories daily. Comparison of 3 treatment groups (additional 30 mg of ALA prescription – 40 patients, Vitamin E 700 Units – 40 patients and ALA 300mg + Vitamin E 400 Units – 40 patients) to the placebo group (35 patients) after 6 months showed significant improvement of cytokine profile, steatosis, IR-HOMA, triglycerides level in all 3 treatment groups. This study demonstrated that ALA monotherapy led to reduction of IR-HOMA by 54.3%, triglycerides rate – by 34.4%, leptin level – by 44.8%, Hb1AC – by 13.6%, ALT activity – by 20.8%, fibrosis degree – by 5.9% and adiponectin concentration increased from 0.9 to 2.0 mcg/ml (by 122.2%).

Another randomized, double-blind, placebo-controlled trial (de Oliveira et al., 2011) showed similar results. The same medicines were used but the dosing and treatment duration were different: ALA 600 mg or alpha-tocopherol 800 mg or ALA 600 mg + alpha tocopherol 800 mg for 4 months but the significant lipid and biochemical profile changes were revealed only after combined ALA + Vitamin E therapy in contrast to the ALA monotherapy which led to non-significant changes probably related to insufficient treatment duration. The only significant difference after treatment vs before treatment obtained in all treatment groups was improvement in the pro / antioxidant system indices showing the good antioxidant effect of the prescribed agents.

Several clinical trials revealed the good lipid reduction effect of statins in NAFLD patients: Argo et al. (2008) showed the efficacy of atorvastatin and Riche et al. (2014) – of statins and pioglitazone respecttively. At the same time, there are different even controversial opinions regarding the use of statins in NAFLD patients. In particular, statins are not recommended in NASH patients due to possible toxic effects (Nseir & Mahamid, 2013). At the same time, Neto-Ferreira's (2013) study showed glucose tolerance improvement and insulin resistance reduction in mice after rosuvastatin use and Riche et al. (2014) showed improvement in biochemical and ultrasound NAFLD markers. We have not found toxic effects of rosuvastatin in any our patients, even the opposite – mean ALT, AST and GGT activity in patients who received rosuvastatin (Group 3) decreased after treatment versus before treatment. This result allows us to state an absence of hepatotoxic rosuvastatin effect in cases of prescription in daily dose of 10 mg. The hypolipidemic effect of EPL and omega-3 PUFA combination or ALA in Groups 1 and 2 shows the advisability of using these agents in treating NAFLD patients with DM-2 as an alternative dyslipidemia correction method in cases of low efficacy of rosuvastatin 10 mg daily and the necessity to increase the dose of rosuvastatin. The remote consequences after combined treatment used in our study can be explained by modified life style habit development in our patients during the 3 month treatment course that persists after the end of the 3 month pharmacotherapy course.

Conclusions

Along with life style modification and diet correction in patients with non-alcoholic fatty liver disease with type 2 diabetes mellitus, pharmacotherapy with essential phospholipids with omega-3 polyunsaturated fatty acids or alpha lipoic acid additionally to metformin is advisable. The abovementioned treatment combinations led to biochemical screen correction in such patients due to both cytolysis and cholestasis as well as improvement in dyslipidemia laboratory indices with reduction in hepatocytes triglycerides deposits. The combined treatment with additional prescription of essential phospholipids with omega-3 polyunsaturated fatty acids or alpha lipoic acid might become a good alternative to rosuvastatin due to their good hypolipidemic, hypotriglyceridemic and hepatoprotector effects.

Since the laboratory parameters we investigated characterize rather the conditions in which non-alcoholic fatty liver disease (carbohydrate and lipid metabolism impairment, type 2 diabetes mellitus with overweight or obesity) occurs than non-alcoholic fatty liver disease itself and manifestations of cytolysis and cholestasic laboratory syndromes are non-specific, our results can be interpreted only as the "tip of the iceberg" of non-alcoholic fatty liver disease. That's why investigation of essential phospholipids with omega-3 polyunsaturated fatty acids or alpha lipoic acid influence on the interleukin system, leptin, adyponectin and other indices that characterize molecular aspects and genetic features of non-alcoholic fatty liver disease is promising in order to determine a personalised approach for each patient and directly impact on the treatment effect. Such study will give an opportunity to avoid a "superficial" approach and give a pathogenic clarification of some of the laboratory changes revealed in this study.

References

Anavi, S., Madar, Z., & Tirosh, O. (2017). Non-alcoholic fatty liver disease, to struggle with the strangle: Oxygen availability in fatty livers. Redox Biology, 13, 386–392.

Argo, C. K., Loria, P., Caldwell, S. H., & Lonardo, A. (2008). Statins in liver disease: A molehill, an iceberg, or neither? Hepatology, 48(2), 662–669.

Armstrong, M. J., Hazlehurst, J. M., Hull, D., Guo, K., Borrows, S., Yu, J., Gough, S. C., Newsome, P. N., & Tomlinson, J. W. (2014). Abdominal subcutaneous adipose tissue insulin resistance and lipolysis in patients with non-alcoholic steatohepatitis. Diabetes, Obesity and Metabolism, 16, 651–660.

Babio, N., Toledo, E., Estruch, R., Ros, E., Martínez-González, M. A., & Castañer, O. (2014). Mediterranean diets and metabolic syndrome status in the Predimed randomized trial. Canadian Medical Association Journal, 186(17), 649–657.

Ballestri, S. (2016). Nonalcoholic fatty liver disease is associated with an almost two-fold increased risk of incident type 2 diabetes and metabolic syndrome. Evidence from a systematic review and meta-analysis. Journal of Gastroenterology and Hepatology, 31(5), 936–944.

Basu, P. P., Shah, N. J., Aloysius, M. M., & Brown Jr., R. S. (2014). Effect of vitamin E and alpha lipoic acid in nonalcoholic fatty liver disease: A randomized, placebo-controlled, open-label, prospective clinical trial (vain trial). Open Journal of Gastroenterology, 4, 199–207.

Bedogni, G., Kahn, H. S., Bellentani, S., & Tiribelli, C. (2010). A simple index of lipid overaccumulation is a good marker of liver steatosis. BMC Gastroenterology, 10, 98.

Berlanga, A., Guiu-Jurado, E., Porras, J. A., & Auguet, T. (2014). Molecular pathways in non-alcoholic fatty liver disease. Clinical and Experimental Gastroenterology, 7, 221–239.

Berzigotti, A., Ferraioli, G., Bota, S., Gilja, O. H., & Dietrich, C. F. (2018). Novel ultrasound-based methods to assess liver disease: The game has just begun. Digestive and Liver Disease, 50(2), 107–112.

Brunt, E. M., & Tiniakos, D. G. (2010). Histopathology of nonalcoholic fatty liver disease. World Journal of Hepatology, 16(42), 5286–5296.

Buzzetti, E., Pinzani, M., & Tsochatzis, E. A. (2016). The multiple-hit pathogenesis of non-alcoholic fatty liver disease (NAFLD). Metabolism, 65(8), 1038–1048.

Dai, H., Wang, W., Chen, R., Chen, Z., Lu, Y., & Yuan, H. (2017). Lipid accumulation product is a powerful tool to predict non-alcoholic fatty liver disease in Chinese adults. Nutrition and Metabolism, 1, 14–49.

Dajani, A., & Abu Hammour, A. (2016). Treatment of nonalcoholic fatty liver disease: Where do we stand? An overview. Saudi Journal of Gastroenterology, 22(2), 91–105.

Dajani, A. I., Abu Hammour, A. M., Zakaria, M. A., Al Jaberi, M. R., Nounou, M. A., & Semrin, A. I. (2015). Essential phospholipids as a supportive adjunct in the management of patients with NAFLD. Arab Journal of Gastroenterology, 16(3–4), 99–104.

de Oliveira, A. M., Rondo, P. H., Luzia, L. A., D'Abronzo, F. H., & Illison, V. K. (2011). The effects of lipoic acid and alpha-tocopherol supplementation on the lipid profile and insulin sensitivity of patients with type 2 diabetes mellitus: A randomized, double-blind, placebo-controlled trial. Diabetes Research and Clinical Practice, 92, 253–260.

Di Minno, M. N., Russolillo, A., Lupoli, R., Ambrosino, P., Di Minno, A., & Tarantino, G. (2012). Omega-3 fatty acids for the treatment of non-alcoholic fatty liver disease. World Journal of Gastroenterology, 18, 5839–5847.

EASL–EASD–EASO (2016). Clinical practice guidelines for the management of non-alcoholic fatty liver disease. Journal of Hepatology, 64(6), 1388–1402.

Federico, A., Dallio, M., Caprio, G. G., Gravina, A. G., Picascia, D., Masarone, M., Persico, M., & Loguercio, C. (2017). Qualitative and quantitative evaluation of dietary intake in patients with non-alcoholic steatohepatitis. Nutrients, 9(10), e1074.

Firneisz, G. (2014). Non-alcoholic fatty liver disease and type 2 diabetes mellitus: The liver disease of our age? World Journal of Gastroenterology, 20(27), 9072–9089.

Gaggini, M., Morelli, M., Buzzigoli, E., DeFronzo, R. A., Bugianesi, E., & Gastaldelli, A. (2013). Non-alcoholic fatty liver disease (NAFLD) and its con-

nection with insulin resistance, dyslipidemia, atherosclerosis and coronary heart disease. Nutrients, 5, 1544–1560.
Ganesh, S., & Rustgi, V. K. (2016). Current pharmacologic therapy for nonalcoholic fatty liver disease. Clinics in Liver Disease, 20(2), 351–364.
Gastaldelli, A., Cusi, K., Pettiti, M., Hardies, J., Miyazaki, Y., Berria, R., Buzzigoli, E., Sironi, A. M., Cersosimo, E., & Ferrannini, E. (2007). Relationship between hepatic/visceral fat and hepatic insulin resistance in nondiabetic and type 2 diabetic subjects. Gastroenterology, 133, 496–506.
Gonciarz, Z., Besser, P., Lelek, E., Gundermann, K. J., & Johannes, K. J. (1988). Randomised placebo-controlled double blind trial on "essential" phospholipids in the treatment of fatty liver associated with diabetes. Medecine et Chirurgie Digestives, 17(1), 61–65.
Gundermann, K.-J., Gundermann, S., Drozdzik, M., & Mohan Prasad, V. G. (2016). Essential phospholipids in fatty liver: A scientific update. Clinical and Experimental Gastroenterology, 9, 105–117.
Hansen, H. H., Feigh, M., Veidal, S. S., Rigbolt, K. T., Vrang, N., & Fosgerau, K. (2017). Mouse models of nonalcoholic steatohepatitis in preclinical drug development. Drug Discovery Today, 22(11), 1707–1718.
Hazlehurst, J. M., Woods, C., Marjot, T., Cobbold, J. F., & Tomlinson, J. W. (2016). Non-alcoholic fatty liver disease and diabetes. Metabolism, 65(8), 1096–1108.
Kajikawa, S., Imada, K., Takeuchi, T., Shimizu, Y., Kawashima, A., & Harada, T. (2011). Eicosapentaenoic acid attenuates progression of hepatic fibrosis with inhibition of reactive oxygen species production in rats fed methionine- and choline-deficient diet. Digestive Diseases and Sciences, 56, 1065–1074.
Kim, W. (2017). [Treatment options in non-alcoholic fatty liver disease]. Korean Journal of Gastroenterology, 69(6), 353–358 (in Korean).
Lazo, M., Hernaez, R., Eberhardt, M. S., Bonekamp, S., Kamel, I., Guallar, E., Koteish, A., Brancati, F. L., & Clark, J. M. (2013). Prevalence of nonalcoholic fatty liver disease in the United States: The Third National Health and Nutrition Examination Survey, 1988–1994. American Journal of Epidemiology, 178, 38–45.
Lee, D. H. (2017). Imaging evaluation of non-alcoholic fatty liver disease: Focused on quantification. Clinical and Molecular Hepatology, 23, 290–301.
Lee, H. W., Kim, B. K., Kim, S. U., Park, J. Y., Kim, D. Y., Ahn, S. H., Kim, K. J., & Han, K. H. (2017). Prevalence and predictors of significant fibrosis among subjects with transient elastography-defined nonalcoholic fatty liver disease. Digestive Diseases and Sciences, 62(8), 2150–2158.
Li, J. H., Chen, X. Y., Zhong, C. F., & Min, J. (2000). A randomized controlled study of essential phospholipids (Essentiale capsules) in the treatment of fatty liver. Infectious Diseases Info, 13(4), 180–181.
Lombardi, R., Onali, S., Thorburn, D., Davidson, B. R., Gurusamy, K. S., & Tsochatzis, E. (2017). Pharmacological interventions for non-alcohol related fatty liver disease (NAFLD): An attempted network meta-analysis. Cochrane Database of Systematic Reviews, 3, CD011640pub2.
Loomba, R., & Sanyal, A. J. (2013). The global NAFLD epidemic. Nature Reviews Gastroenterology and Hepatology, 10, 686–690.
Lou, D. J., Zhu, Q. Q., Si, X. W., Guan, L. L., You, Q. Y., Yu, Z. M., & Zhang, A. Z. (2014). Serum phospholipid omega-3 polyunsaturated fatty acids and insulin resistance in type 2 diabetes mellitus and non-alcoholic fatty liver disease. Journal of Diabetes Complications, 28(5), 711–714.
Machado, M. V., & Cortez-Pinto, H. (2014). Non-alcoholic fatty liver disease: What the clinician needs to know. World Journal of Gastroenterology, 20(36), 12956–12980.
Magee, N., Zou, A., & Zhang, Y. (2016). Pathogenesis of nonalcoholic steatohepatitis: Interactions between liver parenchymal and nonparenchymal cells. BioMed Research International, 2016, 1–11.
Martínez-Rodríguez, L. A., Rojas, S. J., & Aldo, T. (2014). Siliphos selenium methionine alpha lipoic acid for non alcoholic fatty liver disease: Results of a pilot study. Journal of Clinical and Experimental Pharmacology, 4, 167.
Martin-Rodriguez, J. L., Gonzalez-Cantero, J., Gonzalez-Cantero, A., Arrebola, J. P., & Gonzalez-Calvin, J. L. (2017). Diagnostic accuracy of serum alanine aminotransferase as biomarker for nonalcoholic fatty liver disease and insulin resistance in healthy subjects, using 3T MR spectroscopy. Medicine (Baltimore), 96(17), e6770.
Maximos, M., Bril, F., Portillo Sanchez, P., Lomonaco, R., Orsak, B., Biernacki, D., Suman, A., Weber, M., & Cusi, K. (2015). The role of liver fat and insulin resistance as determinants of plasma aminotransferase elevation in nonalcoholic fatty liver disease. Hepatology, 61(1), 153–160.
Michelotti, G. A., Machado, M. V., & Diehl, A. M. (2013). NAFLD, NASH and liver cancer. Nature Reviews of Gastroenterology and Hepatology, 10(11), 656–665.
Musso, G., Gambino, R., Cassader, M., & Pagano, G. (2011). Meta-analysis: Natural history of non-alcoholic fatty liver disease (NAFLD) and diagnostic accuracy of non-invasive tests for liver disease severity. Annals of Medicine, 43, 617–649.
Newsome, P. N., Cramb, R., Davison, S. M., Dillon, J. F., Foulerton, M., Godfrey, E. M., Hall, R., Harrower, U., Hudson, M., Langford, A., Mackie, A., Mitchell-Thain, R., Sennett, K., Sheron, N. C., Verne, J., Walmsley, M., & Yeoman, A. (2018). Guidelines on the management of abnormal liver blood tests. Gut, 67, 6–19.
Nseir, W., & Mahamid, M. (2013). Statins in nonalcoholic fatty liver disease and steatohepatitis: Updated review. Current Atherosclerosis Reports, 15, 305.
Ohbayashi, H. (2004). Twelve-month chronic administration of polyenephosphatidylcholine (EPL®) for improving hepatic function of fatty liver patients. Progress of Medicine, 24(7), 1751–1756.
Padma, L., Mukaddam, Q., & Trailokya, A. (2013). An observational study of Essentiale-L in the treatment of patients with fatty liver disease. Indian Journal of Clinical Practice, 23, 735–739.
Patel, P. J., Hayward, K. L., Rudra, R., Horsfall, L. U., Hossain, F., Williams, S., Johnson, T., Brown, N. N., Saad, N., Clouston, A. D., Stuart, K. A., Valery, P. C., Irvine, K. M., Russell, A. W., & Powell, E. E. (2017). Multimorbidity and polypharmacy in diabetic patients with NAFLD: Implications for disease severity and management. Medicine (Baltimore), 96(26), e6761.
Perazzo, H., & Dufour, J. F. (2017). The therapeutic landscape of non-alcoholic steatohepatitis. Liver International, 37(5), 634–647.
Pivtorak, K. V. (2017). Features of nonalcoholic fatty liver disease pharmacotherapy in patients with overweight and obesity. Zaporozhye Medical Journal, 19(4), 520–524.
Poongothai, S., Karkuzhali, K., & Siva Prakash, G. (2005). Effect of essentiale in diabetic subjects with non-alcoholic fatty liver. International Journal of Diabetes in Developing Countries, 25(1), 12–19.
Riche, D. M., Fleming, J. W., Malinowski, S. S., Black, C. A., Miller, K. H., & Wofford, M. R. (2014). Resistant nonalcoholic fatty liver disease amelioration with rosuvastatin and pioglitazone combination therapy in a patient with metabolic syndrome. Annals of Pharmacotherapy, 48, 137–141.
Sanyal, A. J., Abdelmalek, M. F., Suzuki, A., Cummings, O. W., & Chojkier, M. (2014). EPE-A Study Group. No significant effects of ethyl-eicosapentanoic acid on histologic features of nonalcoholic steatohepatitis in a phase 2 trial. Gastroenterology, 147, 377–384.
Sas, E., Grinevich, V., Efimov, O., & Shcherbina, N. (2013). Beneficial influence of polyunsaturated phosphatidylcholine enhances functional liver condition and liver structure in patients with nonalcoholic steatohepatitis accompanied by diabetes type 2. Results of prolonged randomized blinded prospective clinical study [abstract]. Journal of Hepatology, 58, S549.
Schleicher, J., Guthke, R., Dahmen, U., Dirsch, O., Holzhuetter, H. G., Schuster, S. (2014). A theoretical study of lipid accumulation in the liver-implications for nonalcoholic fatty liver disease. Biochimica et Biophysica Acta, 1841(1), 62–69.
Sharma, M., Mitnala, S., Vishnubhotla, R. K., Mukherjee, R., Reddy, D. N., & Rao, P. N. (2015). The riddle of nonalcoholic fatty liver disease: Progression from nonalcoholic fatty liver to nonalcoholic steatohepatitis. Journal of Clinical and Experimental Hepatology, 5(2), 147–158.
Stankovic, M. N., Mladenovic, D., Ninkovic, M., Đuricic, I., Sobajic, S., Jorgacevic, B., de Luka, S., Vukicevic, R. J., & Radosavljevic, T. S. (2014). The effects of a-lipoic acid on liver oxidative stress and free fatty acid composition in methionine-choline deficient diet-induced NAFLD. Journal of Medicinal Food, 17(2), 254–261.
Stepanov, Y., Nedzvetskaya, N., Yagmur, V., & Kononenko, I. (2018). The significance of hepatic transaminases and ultrasound in the diagnosis of non-alcoholic fatty liver disease. Regulatory Mechanisms in Biosystems, 9(1), 105–111.
Stepanov, Y. M. (2016). The ese of essential phospholipids for the treatment of fatty liver disease. Gastroenterology, 62, 58–64.
Sumida, Y., Nakajima, A., & Itoh, Y. (2014). Limitations of liver biopsy and non-invasive diagnostic tests for the diagnosis of nonalcoholic fatty liver disease / nonalcoholic steatohepatitis. World Journal of Gastroenterology, 20(2), 475–485.
Takahashi, Y., & Fukusato, T. (2014). Histopathology of nonalcoholic fatty liver disease/nonalcoholic steatohepatitis. World Journal of Gastroenterology, 20(42), 15539–15548.
Verbeek, J., Cassiman, D., Lannoo, M., Laleman, W., van der Merwe, S., Verslype, C., Van Steenbergen, W., & Nevens, F. (2013). Treatment of non-alcoholic fatty liver disease: Can we already face the epidemic? Acta Gastro-Enterologica Belgica, 76(2), 200–209.
Williams, C. D., Stengel, J., Asike, M. I., Torres, D. M., Shaw, J., Contreras, M., Landt, C. L., & Harrison, S. A. (2011). Prevalence of nonalcoholic fatty liver disease and nonalcoholic steatohepatitis among a largely middle-aged population utilizing ultrasound and liver biopsy: a prospective study. Gastroenterology, 140, 124–131.
Wu, Y. (2009). Effective analysis of type 2 diabetic united adiposis hepatica with polyene phosphatidylcholine. Journal of Traditional Chinese Medicine, 29, 41–42.

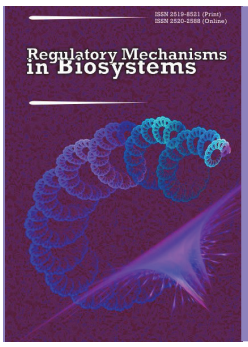

Regulatory Mechanisms in Biosystems

ISSN 2519-8521 (Print)
ISSN 2520-2588 (Online)
Regul. Mech. Biosyst., 9(3), 391–395
doi: 10.15421/021858

Change in magnesium concentration in erythrocytes in fish under stress

R. A. Zaprudnova

Papanin Institute for Biology of Inland Waters RAS, Borok, Russia

Article info

Received 12.07.2018
Received in revised form 18.08.2018
Accepted 20.08.2018

Papanin Institute for Biology of Inland Waters RAS, Borok, Yaroslavl oblast, 152742, Russia.
Tel.: +8-485-47-24-339.
E-mail: rimma@ibiw.yaroslavl.ru

Zaprudnova, R. A. (2018). Change in magnesium concentration in erythrocytes in fish under stress. Regulatory Mechanisms in Biosystems, 9(3), 391–395. doi:10.15421/021858

At present, the role of erythrocyte magnesium in the respiratory processes of fish (and other animals) under conditions of stress load is not known. This article presents the results of research on change in the concentration of magnesium in erythrocytes under the action of stressors of different quality and quantity for bream (*Abramis brama* L.), silver crucian carp (*Carassius auratus gabelio* Bloch) and tench, (*Tinca tinca* L.) in Rybinsk Reservoir. The concentration of magnesium ions was analyzed on an atomic absorption spectrometer AAS-1 manufactured by Carl Zeiss (Germany) in the absorption regime in an air-acetylene flame. For the first time, the dependence of the change in magnesium concentration in erythrocytes on the intensity of the stress load of different nature on the example of fishes was revealed. Weak and moderate strength effects (low doses of epinephrine, norepinephrine, small changes in water temperature, saline injection, injection into the abdominal cavity, short-term removal of fish from the water, short-term keeping of fish in a limited volume of water) increased the concentration of magnesium in erythrocytes up to 2.5 times. At the same time, an increase in the affinity of hemoglobin for oxygen and a decrease in oxygen consumption were observed. However, strong stressors such as catching, transporting fish to the laboratory (representing complex effects of hypoxia, limited water volume, mechanical effects, etc.), as well as a sharp and large change in water temperature, high doses of adrenaline reduced the concentration of magnesium in erythrocytes 3 times. At the same time, the hemoglobin affinity for oxygen decreased and oxygen absorption increased. However, before the death of fish (from exhaustion), with a low level of magnesium in erythrocytes the affinity of hemoglobin for oxygen increased and the intensity of gas exchange decreased. The research conducted allow us to consider the change in the concentration of magnesium ions in erythrocytes – which are positive modulators of the affinity of hemoglobin for oxygen – in fish exposed to stress as one of the mechanisms for reducing the gas exchange intensity for weak and medium short-term stress effects and increasing it for strong short-term ones. Especially important is the role of erythrocyte magnesium as a molecular mechanism for reducing oxygen uptake and, consequently, increasing anabolism and, thus, increasing the growth and development of animals under the action of mild, short-term stressors, i.e. with eustress. In addition, the concentration of magnesium in erythrocytes can serve as an indicator of the state of fish. A high level of this cation in erythrocytes (1.5–2.0 times higher and more than normal) is characteristic for strong, healthy animals in a state of eustress or physiological stress, and extremely low values of this indicator (1.5–2.0 and more times below the norm) are an indicator of reversible or permanent ill-being (distress or pathological stress). Weakened, exhausted animals are not capable of a response to eustress or physiological stress. The possible causes of low magnesium concentrations in human erythrocytes are discussed.

Keywords: bream; tench; crucian carp; affinity of hemoglobin to oxygen; gas exchange intensity; eustress; distress.

Introduction

An important property of erythrocytic magnesium is a positive modulating effect on affinity of hemoglobin for oxygen (Flatman, 2003; Wells, 2009), which manifests particularly in interspecies differences in concentrations of manganese in erythrocytes of fish, which differ by intensity of gas exchange and affinity of hemoglobin for oxygen, and also differences in seasonal dynamic of concentrations of manganese in red blood cells and affinity of hemoglobin for oxygen. Active swimmers which consume lots of oxygen have a lower level of erythrocytic magnesium and lower affinity of hemoglobin for oxygen compared to fish which are more resistant to oxygen deficiency (Soldatov, 1997; Zaprudnova & Kamshilov, 2008; Vornanenet al., 2009; Wells, 2009). During spawning (i.e. during activity), fish were recorded as having the highest level of manganese in erythrocytes during the year and the highest affinity of hemoglobin for oxygen. Minimum content of red blood cells and minimum affinity for hemoglobin and oxygen was recorded in summer, i.e. during maximum values of moving activity of fish and water temperature (Zaprudnova et al., 2016). Intensity of gas exchange and affinity of hemoglobin for oxygen changes also during stress (Wendelaar Bonga, 1997; Nikinmaa, 2003; Zaprudnova & Kamshilov 2010). Despite active study of physical-biochemical processes of fish during stress (Faught et al., 2016; Rodnick, & Planas, 2016; Takei & Hwang, 2016), at present there are no data on participation of erythrocytic magnesium related to breathing, in stress reaction of fish. There is no information on this issue for other (including Amniotes) vertebrates, despite intense study of the impact of magnesium on the organism of humans (see the special journal Magnesium Research published since 1988 and the international conferences described in it, and also numerous publications in other journals of physiological-biochemical and medical orientation). At the same time, most studies have concentrated on the positive effect of magnesium on the nervous and cardio-vascular systems of humans (Nechifor, 2008; Rosanoff & Wolf, 2016; Boyle et al., 2017). Often, the level of erythrocytic magnesium is used for determining deficiency of this ion in the organism, but the reason for change in concentration of magnesium in red cells is found usually to be related to some disease (Cox, et al., 1991; Widmer et al., 1995; Widmer et al., 1998; Kopitsyna et al., 2015).

The problem of stress is significantly related to such fundamental capacities of living organisms as ability to change the response reaction in relation to the extent (force and duration) of impact and initial conditi-

on of the organism. This dependency has been reflected in the theories of beneficial stress (eustress) and aversive (distress) stress (Dhabhar, 2008; Schreck, 2010; Schreck & Tort, 2016) or of physiological and pathological stress (Arshavskii, 1982). Pathological stress (or distress) occurs in response to activity of strong and/or long stressors and is followed by increase in catabolic processes, leading to decrease in resistance of an organism. Pathological stress is the stress as it is most commonly understood. Physiological stress occurs in response to short term stressors of low or average strength. During physiological stress, the intensity of anabolic processes and non-specific resistance of the organism increase. Earlier (Zaprudnova, 2017), it was demonstrated that under the impact of insignificant short term stressors (physiological stress), fish were observed to have changes in concentration of cations of sodium, calium, calcium and manganese in the internal environment towards increased ion concentration gradients on membranes of the cells and tissues, in particular hypernatremia in the environment on average equaled 10%. At impact of strong and/or long term stressors (pathological stress), changes in concentration of cations in the internal environment were orientated towards decrease of ion concentration gradients on membrane of the cells and tissues. During severe reversible and severe lethal stress, hyponatremia equaled up to 30% and 50% respectively, and during subsevere and chronic lethal stresses – up to 20% and 10% respectively. The objective of this study was the dynamic of the concentration of manganese in erythrocytes among some freshwater fish suffering stress of different intensity.

Materials and methods

We studied mainly mature or nearly mature individuals of bream (*Abramis brama* L.) in the Rybinsk Reservoir. Some of the tests were replicated on mature and nearly mature individuals of tench (*Tinca tinca* L.) and silver crucian carp (*Carassius auratus gabelio* Bloch). The body length of the studied bream, tench and silver crucian carp ranged from 350–386, 334–362 and 155–280 mm respectively. After caudectomy, blood was put in test tubes moistened with heparin and centrifuged at 1800 g 30 min. All plasma with the upper layer of leukocytes and erythrocytes was removed. Erythrocytes were dissolved in 500 times distilled water and held in refrigerator at 4 ºC no less than 2 days until full hemolysis. Concentration of magnesium ions was analyzed in absorptional regime on an atomic-absorptive spectrometer AAS-1 manufactured by Carl Zeiss (Jena, Germany) in air-acetylene flame.

The norm was considered to be the condition of fish adapted for no less than two weeks to the laboratory conditions in deep shaded basins (proportion of body weight and water was 1 : 200 and more). The control condition of fish was the level of natremia (Zaprudnova, 2017). As insignificant short term stressors (1–7), we used: intraperitoneal injection of 0.3–1.5 mg/kg of adrenalin (stressor 1), injection of normal saline (2), introduction of 0.2–1.3 mg/kg of noradrenalin (3), a prick with a needle in the abdominal cavity (4), extraction of fish from water for 1–2 min (5), gradual change in water temperature by 4–5 °C (6), putting fish for 20 min into a limited volume of water: the proportion of body weight and water equaled 1 : 15 (stressor 7, Table 1). As strong short term (2–20 min) stressors (8–11), we used a sharp increase in water temperature by 17–23 °C (stressor 8), introduction of high doses of adrenalin: 5–6 mg/kg (9), as short term strong complex stressor, we also used 15–20 min removal of fish from a natural water body in summer at the temperature of 18–23 °C (stressor 10a) and at water temperature of 2–9 °C in autumn-winter (10b). The work also analyzes literature data (Martemyanov, 1999) on roach (*Rutilus rutilus* L.), obtained in winter. The longer term strong complex stressors were removal of fish from their natural environment followed by transportation of fish to the laboratory during 1.0–1.5 h in a limited volume of water in summer (water temperature equaled 19–24 °C) in conditions of autogenic hypoxia (decrease in the content of oxygen in water to 3 mg/l) and increase in water temperature by 5–7 °C, when there was observed practically full exhaustion of hormones in chromaffin tissue (stressor 11a) and in autumn at lower temperatures (4–9–16 °C) − stressor 11b. Individuals which died in the conditions of stressor 11b were selected into a separate group 11c. Stressor 12 was 1.5 h imitation of transportation in summer of fish which were adapted to laboratory conditions (Table 2). Stressor 13 – severe stress: 9–15 days retention in laboratory conditions exposed to increased light and noise disturbance factors, with high placement density of (1 : 30), with periodic mechanical disturbance and elements of autogenic hypoxia. Stressor 14 – chronic stress: 1.0–1.5 months of retention in laboratory conditions with increased light and noise disturbance, with possible periodic low hypoxia. Also, fish in conditions of chronic stress were sometimes affected by low short term stressors: 1 (adrenalin in low doses), 2 (normal saline), 4 (prick), 7 (limited volume of water, Table 3). During the tests, fish were not fed.

The results of studying the concentration of manganese in erythrocytes of fish were compared with the intensity of gas exchange and the value of affinity of hemoglobin for oxygen, obtained earlier (Zaprudnova & Kamshilov, 2010) for the same species of fish and the same or similar stress conditions.

The work presents the average values of concentrations of manganese ions and mean error. The check of the norm of distribution in the selections was made using the Shapiro-Wilk criterion. The reliability of the differences were assessed using Student's criterion.

Results

Under the impact of insignificant short term stressors (in the research presented – stressors 1–7), i.e. under physiological stress, concentration of manganese in blood plasma increased by 9.2%, recovered after 1–2 days. The level of manganese in erythrocytes in the abovementioned conditions increased, reaching maximum values at the water temperature of 17–18 °C after 2 h after impact (Table 1). Subsequently, concentration of manganese in erythrocytes gradually reduced, returning to pre-stress values after 1–2 days. The amount and duration of deviation of erythrocytic cation increased from low to average stressors. Injection of hormones, introducing normal saline, injection and prick (stressors 1–4) should be probably classified as average stressors: recovery of the level of erythrocytic manganese occurred only after 2 days, and concentration of manganese in red blood cells increased by 2.33–2.56 times. Under the impact of the stressors 5–7 which were, obviously, weaker than the first four, concentration of manganese in erythrocytes increased by 1.83–2.20 times, and return to the normal values was observed after 24 hours. In summer, fish of the Rybinsk Reservoir, while rising from the bed to the surface heated by the sun, every day have the same load as at the impact of stressor 6. As the water temperature decreased, the reaction to the stressor slowed: in winter, at the temperature of acclimation of 0.2 °C, increase in the concentration of manganese of red blood cells by 1.82–2.11 times was observed a day after injection of adrenalin (stressor 1) and prick to the body (stressor 3). And, on the contrary, in summer, at the water temperature of 24 °C, maximum deviation of the level of manganese in erythrocytes occurred already an hour after injecting adrenalin (stressor 1) and normal saline (stressor 2): by 2.35 times on average.

Affinity of hemoglobin for oxygen of bream 1.5–2.0 h after the impact of short term insignificant stressors (low doses of adrenalin, injections, pricking, insignificant increase in water temperature, short term retention in small volume of water) increased by 1.34–1.71 times. In such conditionsб consumption of oxygen by bream, tench and and silver crucian carp decreased by 1.27–1.60 times (Zaprudnova & Kamshilov, 2010).

At severe reversible stress (stressors 8–12), i.e. at pathological stress, the concentration of sodium in blood plasma decreased by 28.3%. At the same time, the level of magnesium in erythrocytes decreased by 1.55–2.98 times. (Table 2). After 3–5 days (not studied before), we recorded normal level of this cation in erythrocytes: 9.6–11.1 mmol/l and recovery to pre-stress concentrations of sodium in blood plasma. During severe lethal stress (stressor 11c), the level of magnesium in erythrocytes was practically no different from that of fish which survived similar conditions.

Catching fish in the autumn-winter period caused a lower stress impact (stressor 10b) than in summer at higher temperatures (stressor 10a), and, therefore caused a smaller decrease in the level of magnesium in erythrocytes. Transportation of the fish was performed at a rather high temperature in autumn, therefore there are practically no differences between transportation of fish in summer. In the fish which adapted to

the laboratory conditions, and therefore were less sensitive to stressors, during the impact of stressors of an equal strength (stressor 12), deviation of concentration of manganese in red blood cells manifested less clearly, though the differences in relation to the norm were similarly significantly high ($P < 0.001$).

Table 1
Concentration of manganese in erythrocytes (mmol/l) of bream after the impact of insignificant short term stressors (total number of the studied fish – 115)

Stressors[x]	Time since end of exposure to stressors, hours					
	0.5	2.0	3.5	5.0	24	48
1 (adrenalin, 0.3–1.5 mg/kg)	14.5 ± 0.19***	26.1 ± 0.17***	22.3 ± 0.31***	18.1 ± 0.12***	16.1 ± 0.04***	10.1 ± 0.26***
2 (normal saline)	15.6 ± 0.20***	24.3 ± 0.15***	20.4 ± 0.19***	15.6 ± 0.26***	15.4 ± 0.08***	10.2 ± 0.15***
3 (noradrenalin, 0.2–1.3 mg/kg)	16.4 ± 0.18***	25.4 ± 0.22***	n.a.	14.7 ± 0.21***	n.a.	n.a.
4 (shoot)	14.2 ± 0.15***	23.8 ± 0.30***	n.a.	16.2 ± 0.12***	n.a.	n.a.
5 (extraction from water for 1–2 min)	n.a[xx].	22.5 ± 0.21***	n.a.	n.a.	9.9 ± 0.14***	n.a.
6 (gradual increase in temperature of water by 4–5 °C)	n.a.	18.7 ± 0.29***	n.a.	n.a.	10.3 ± 0.16***	n.a.
7(limited volume of water)	13.9 ± 0.16***	n.a.	n.a.	n.a.	n.a.	n.a.

Note: [x] – norm see in Table 2, *** – $P < 0.001$, compared to the norm; n.a. – not analyzed.

Table 2
Concentration of magnesium in erythrocytes (mmol/l) of some freshwater fish after exposure to significant stressors (the number of the studied bream – 54, tench – 32, crucian carp – 20)

Stressors	Bream	Tench	Crucian carp	Roach (Martemyanov, 1999)
Norm	10.2 ± 0.21	11.0 ± 0.30	12.4 ± 0.28	9.8–10.7
8 (sharp change in water temperature by17–23 °C)	4.1 ± 0.37*** 3.7 ± 0.51***	3.6 ± 0.42***	5.5 ± 0.40***	n.a.
9 (adrenalin 5–6 mg/kg)	3.8 ± 0.26***	3.9 ± 0.29***	n.a.	n.a.
10a (removal from the natural environment in summer)	4.4 ± 0.35*** 3.6 ± 0.40***	4.8 ± 0.41***	n.a.	n.a.
10b (removal from the natural environment in autumn and winter)	6.3 ± 0.38*** 4.9 ± 0.36***	6.2 ± 0.37***	6.3 ± 0.42***	6.6–7.0***
11a (catching and transportation to the laboratory in summer)	3.2 ± 0.45***	n.a.[x]	n.a.	n.a.
11b (catching and transportation to the laboratory in autumn)	4.1 ± 0.44***	4.3 ± 0.33***	4.6 ± 0.28***	n.a.
11c (lethal stress)	3.5 ± 0.46***	n.a.	n.a.	n.a.
12 (imitation of transportation in summer)	6.9 ± 0.39***	7.1 ± 0.36***	7.5 ± 0.41***	n.a.

Note: *** – $P < 0.001$ compared to the norm; [x] – n.a., not analyzed.

Table 3
Concentration of manganese in erythrocytes (mmol/l) of some fish exposed to subsevere and chronic stress and after impact of additional insignificant stressors (the number of the studied bream – 29, tench – 14, crucian carp – 20)

Stressors[x]	Bream	Tench	Crucian carp
13 (subsevere stress)	5.3 ± 0.40 ***	5.0 ± 0.38 ***	n.a.
14 (chronic stress)	7.2 ± 0.19 ***	7.4 ± 0.23 ***	7.6 ± 0.30 ***
14 (chronic stress) + 1 (adrenalin 0.3–1.5 mg/kg)	5.6 ± 0.32 *** - **	n.a.[xx]	n.a.
14 (chronic stress) + 2 (normal saline)	4.8 ± 0.37 *** ***	n.a.	n.a.
14 (chronic stress) + 4 (injection)	6.9 ± 0.35 ***	n.a.	5.6 ± 0.38 *** **
14 (chronic stress) + 7 (limited volume of water)	7.0 ± 0.36 ***	7.1 ± 0.33 ***	6.1 ± 0.43 *** * 6.9 ± 0.39 ***

Note: [x] – norm see in Table 2; *** – $P < 0.001$, ** – $P < 0.01$, * – $P < 0.05$ under dash – compared to the initial level at chronic stress, rest – compared to the norm, [xx] – n.a., not analyzed.

Affinity of hemoglobin for oxygen after exposure to strong short term stressors (catching, transporting, steep and high increases in water temperature) decreased by 1.23–1.35 times, and the consumption of oxygen increased on average by 1.50 times. However, the fish in a dying condition affinity of hemoglobin for oxygen increased compared the fish which were just caught: for example, bream – up to two times. Therefore, in these conditions, consumption of oxygen decreased: by 1.28–1.51 times (Zaprudnova & Kamshilov, 2010).

Subsevere and chronic stresses are also classified as pathological stress. Fish experiencing subsevere stress live 5 to 20 days, under chronic stress – 1–3 months. Having subsevere stress (stressor 13), hyponatremia equaled 19.5%, and concentration of magnesium in erythrocytes decreased by 2.06 times (Table 3). In fish with chronic stress (stressor 14), hyponatremia equaled 9.4%, and concentration of magnesium in erythrocytes was 1.51 times lower than the norm. However, affinity of hemoglobin for oxygen was close to the normal values: lower by 1.12–1.15 times. Also, reduced consumption of oxygen was recorded (Zaprudnova & Kamshilov, 2010).

In the conditions of chronic stress, 1.0–1.5 h after additional insignificant stress, the fish (when significant deviations in the concentration of erythrocytic magnesium should be observed) were in the half of the cases recorded as having a reliable decrease in the studied parameter, and in the rest – differences were not reliable for the initial level of manganese in red blood cells at chronic stress (Table 3). After additional insignificant stress, the level of natremia of fish decreased by 4.3–11.1%.

Discussion

The present research revealed the dependency of manganese concentration in red blood cells of fish on intensity of stressor loads of different types: level of erythrocytic manganese increased under the impact of insignificant and average stressors (at physiological stress) and decreased – under impact of significant loads (at pathological stress). The obtained data indicated also a broader range of fluctuations in magnesium concentrations in erythrocytes of stressed fish: a five-seven times change in the level of this cation. At the same time, similarly in both groups of significant and insignificant stressors, deviations became clearer after increasing load in duration and amount of magnesium concentration. Perhaps, there should be some load of intermediary value between average and significant stressors which does not cause deviations of magnesium concentrations in erythrocytes (condition of areactivity). It is possible that this phenomenon is related to absence of reaction of erythrocytic magnesium of people to intravenous injection of adrenalin (Ryzen et al., 1990). However, absence of reaction to the stressor in the abovementioned work could be also related to a particular latency in change of magnesium level in red blood cells during influence of an insignificant load. Practically instantly, during stress, change occurred only in concentration of erythrocytic sodium, along with the level of catecholamines which regulate it (Zaprudnova & Kamshilov, 2008).

The results of our work concur well with numerous studies by Konstantinov (1993) and his students on many species of fish, and also on amphibians in 1980–2000. The authors demonstrated that during insignificant fluctuations of practically all familiar abiotic factors (temperature, illuminance, oxygen, salinity, pH), i.e. at eustress or physiological stress, increase in growth and development of animals occurs, which is followed by decrease in consumption of oxygen and food. The present work states that at eustress or physiological stress, increase in concentration of magnesium of erythrocytes as a positive modulator occurs, contributing to increase in affinity of hemoglobin for oxygen and, therefore, reduction in gas exchange and, in consequence, increase in anabolism, growth and development of fish. And, by contrast, decrease in concentration of magnesium in erythrocytes during short term significant stress impacts (reaction of anxiety of general adaptation syndrome; distress or pathological stress) contributes to decrease in affinity of hemoglobin for oxygen and therefore increase in gas exchange, and, as a result, increase in catabolism. Under more prolonged impact of stressors (stage of exhaustion of general adaptation syndrome, subsevere and chronic stress), one should take into account the effect on the affinity of hemoglobin for oxygen and, therefore, intensity of gas exchange, decrease in the level of ATP in

erythrocytes (negative modulator of affinity of hemoglobin for oxygen) due to general exhaustion of the organism. Perhaps, this particular factor is related to relatively high affinity of hemoglobin for oxygen and decreased intensity of gas exchange, which were recorded before death among fish (at the end of pathological stress) with low concentration of magnesium in erythrocytes. It could be assumed that because of relatively high affinity of hemoglobin for oxygen and decrease in oxygen consumption during chronic stress, a condition of metabolic depression is maintained.

With deterioration of the condition (exhaustion, weakening, illness), and also against the background of the existing load, the fish reacted to insignificant short stressors in relation to type of physiological stress, i.e. increase in magnesium concentration in erythrocytes and change in the level of cations in the internal environment towards increase in ion concentration gradients on the membrane of cells and tissues (condition of areactivity). Moreover, in these conditions, changes by type of pathological stress can occur, i.e. decrease in concentration of magnesium in erythrocytes and change in the level of cations in the internal environment towards decrease in ion concentration gradients on the membrane of cells and tissues. Earlier (Zaprudnova, 2017), at impact of insignificant doses of noradrenaline and pricking, the fish suffering ichthyophthiriasis had hyponatremia. In other words, the pattern and extent of reaction to a stressor depended also on initial functional condition of the organism.

On the basis of the conducted studies, magnesium ions in erythrocytes as positive modulators of affinity of hemoglobin for oxygen are recommended to be considered as one of the molecular mechanisms which regulate processes of gas exchange, anabolism and catabolism of fish under stress. An especially significant role of erythrocytic magnesium is played by increase in anabolism and, therefore, growth and development of animals under impact of insignificant, short term stressors, i.e. under eustress or physiological stress.

Also, a significant role in mechanisms of excessive anabolism and increase in resistivity of an organism to the impact of unfavourable factors during eustress (or physiological stress) is played by energy of increased ion concentration gradients on the membrane of cells and tissues (Zaprudnova, 2017). Ion concentration gradients on the cellular membrane belong to the parameters of energetic condition of the organism. In particular, sodium potential belongs to the main "energetic currency" on the external membrane of animals` cells (Skulachev et al., 2010). Finally, ion concentration gradients can be considered an expression and mechanism of maintaining the stable metabolism of the organism. In natural conditions, insignificant short term stressors create the required condition of physiological stressors which cause a stimulating effect on all vital processes. Strong anabolic processes of fish during breeding also occur due to using energy of increased ion concentration gradients on the membrane of cells and tissues, and also minimization of energy discharge due to decrease in oxygen consumption. The latter is possible due to the high affinity of hemoglobin for oxygen because of increase of magnesium (the positive modulator) in erythrocytes (Zaprudnova & Kamshilov, 2016).

Energy released as result of decrease in ion concentration gradients at the impact of significant and/or long term stressors is used for maintaining life in extreme conditions.

Concentration of magnesium in erythrocytes of freshwater and marine fish is similar. For example, the fluctuation range of this parameter in marine fish equaled 9.8–12.8 mmol/l (Soldatov, 1997). However, it is interesting that the values of manganese in erythrocytes of humans are lower compared to fish: 1.4–2.3 mmol/l in the norm. This parameter is extremely low for many other mammals, for example, cattle < 1 mmol/l (Cox et al., 1991; Hinds et al., 1994; Flatman, 2003; Kopitsyna et al., 2015). It could be presumed that for humans, this reflects the condition of stress in regular life due to high psychological-emotional loads, intoxications, etc, which are typical for most of the population (Segerstrom & Miller, 2004). Moreover, people with psychologically borderline disorders have an erythrocytic magnesium level < 0.3 mmol/l (Kopitsyna et al., 2015). The conditions of laboratory animals before the study in vivaria are usually insufficiently favourable. Also, one should take into account the impact of stress procedures which are implemented prior to drawing blood from people and other mammals, which are more sensitive to stress than fish. With psychologically ill people, these procedures can have an especially frightening effect. It could be presumed that significantly different levels of erythrocytic magnesium (and even their oppositely orientated changes) among people with identical psychological illnesses mentioned in the works of a number of authors (Cox et al., 1991; Hinds et al., 1994; Widmer et al., 1995; Widmer et al., 1998; Kopitsyna et al., 2015) to a larger extent can be a manifestation of non-specific change of this cation in different stress conditions of patients rather than the specific impact of disease. From this perspective, six-fold differences (Flatman, 2003) in the concentrations of magnesium in red blood cells of swine and cattle could be explained. However, there is obviously a specific relationship between magnesium in red blood cells and some diseases, for example, sickle cell anemia (Flatman, 2003).

It should be recognized that until recently, the level of erythrocytic magnesium as a diagnostic parameter of animals (and humans) has remained underestimated. However, this question should be analyzed in more detail. In particular, the high variability of concentrations of erythrocytic magnesium of fish under stress (increases of up to 2.5 times and decreases of up to 3 times), to some extent limits the opportunity of its use as an accurate indicator of deficiency of this cation in the organism. An important recommendation for obtaining more reliable information on the condition of an organism is regular analysis of the level of manganese in red blood cells of animals (and humans) in different functional conditions. The results of our studies on fish demonstrated that high levels of this cation in erythrocytes (1.5–2.0 times higher and more than the norm) is distinctive for strong, healthy animals in a condition of eustress or physiological stress, and extremely low values of this parameter (1.5–2.0 times and more lower than the norm) are an indicator of both reversible and constant ill-being (distress or pathological stress). Absence of reaction of concentration of erythrocytic magnesium to insignificant short term stressors towards increase, and more important – change towards decrease in the level of this cation also indicates ill-being. Diagnosing the condition of animals in relation to the magnesium concentration in the internal environment of an organism is still complicated. First of all, this is related to the fact that during physiological stress, short term change in manganese concentration in blood plasma occurs towards increase in concentration gradients on the membrane of cells, i.e. hyponatremia, and during pathological stress, by contrast, more or less prolonged hypernatremia (Zaprudnova, 2017). Therefore, the observed hyponatremia of humans after internal injection of adrenalin is mistakenly determined by some authors (Ryzen et al., 1990) as a negative effect. A low level of erythrocytic magnesium is a more reliable characteristic of ill-being: temporarily or constant.

Conclusion

For the first time, the relationship of change in the concentration of magnesium in erythrocytes to the intensity of stress loads of different type was determined on the example of three species of fish: bream, tench, silver crucian carp. Insignificant and average loads (eustress or physiological stress) increased the concentration of magnesium in erythrocytes, while the same factors but in higher doses, and also complex effects of strong stressors (distress or pathological stress) decreased the content of magnesium in erythrocytes. During eustress, we observed increase in affinity of hemoglobin for oxygen and decrease of consumption of oxygen, and during distress – shift of dissociation curve to the right and intensification of gas exchange. On the basis of the conducted study, ions of magnesium in erythrocytes (as positive modulators of affinity of hemoglobin for oxygen) are recommended to be considered as one of the molecular mechanisms regulating the processes of gas exchange and catabolism of fish under stress. An especially significant role of these ions is intensifying anabolism and, therefore, growth and development of animals exposed to the influence of insignificant short stressors, i.e. to eustress or physiological stress. However, before death, the fish (at the end of pathological stress) at low concentration of magnesium in erythrocytes had increased affinity of hemoglobin for oxygen, and reduced intensity of gas exchange. Perhaps, in this situation, the essential role in the shift of dissociation curve to the left is played by decrease in the level of ATP – negative modulator of affinity

of hemoglobin for oxygen – due to the general exhaustion of organism. Concentration of magnesium in erythrocytes can be an indicator of the condition of fish, in particular, an extremely low level of magnesium in red blood cells always indicates temporary or constant ill-being. Weakened, exhausted, diseased animals are not able to react in response to type of eustress or physiological stress.

References

Arshavskii, I. A. (1982). Fiziologicheskie mekhanizmy i zakonomernosti individual'nogo razvitiya [Physiological mechanisms and patterns of individual development]. Nauka, Moscow (in Russian).

Boyle, N. B., Lawton, C., & Dye, L. (2017). The effects of magnesium supplementation on subjective anxiety and stress. A systematic review. Nutrients, 9(5), 429.

Cox, I. M., Cambell, M. J., & Dowson, D. (1991). Red blood cell magnesium and chronic fatigue syndrome. The Lancet, 337(8744), 757–760.

Dhabhar, F. S. (2008). Enhancing versus suppressive effects of stress on immune function: Implications for immunoprotection versus immunopathology. Allergy, Asthma and Clinical Immunology, 4, 2–11.

Faught, E., Aluru, N., & Vijayan, M. M. (2016). The molecular stress response. Biology of Stress in Fish. Fish Physiology, 35(4), 113–166.

Flatman, P. W. (2003). Magnesium transport. Red Cell Membrane Transport in Health and Disease, 16, 407–434.

Hinds, G., Bell, N. P., McMaster, D., & McCluskey, D. R. (1994). Normal red cell magnesium concentrations and magnesium loading tests in patients with chronic fatigue syndrome. Annals of Clinical Biochemistry, 31(5), 459–461.

Konstantinov, A. S. (1993). Vliyanie kolebaniy temperatury na rost, ehnergetiku i fiziologicheskoe sostoyanie molodi ryb [Influence of temperature fluctuations on the growth, energy and physiological state of juvenile fish]. Izvestiya AN RAN. Seriya Biologiya, 1, 55–63 (in Russian).

Kopitsyna, U. E., Grishina, T. R., Torshin, I. Y., Kalacheva, A. G., & Gromova, O. A. (2015). Sverkhnizkiy uroven' magniya v eritrotsitakh kak znachimyy faktor patogeneza pogranichnykh psikhicheskikh rasstroystv [Very low magnesium levels in red blood cells as a significant factor in the etiopathogenesis of borderline disorders]. Zhurnal Nevrologii i Psikhiatrii imeni S. S. Korsakova, 115(11), 85–96 (in Russian).

Martemyanov, V. I. (1999). Concentrations of cations in the plasma, erythrocytes, muscles, and gonads of *Rutilus rutilus* in nature and in those acclimated to laboratory conditions. Journal of Ichthyology, 39(2), 198–201.

Nechifor, M. (2008). Interactions between magnesium and psychotropic drugs. Magnesium Research, 21(2), 97–100.

Nikinmaa, M. (2003). Gas transport. Red Cell Membrane Transport in Health and Disease,16, 489–509.

Rodnick, K. J., & Planas, J. V. (2016). The stress and stress mitigation effects of exercise: Cardiovascular, metabolic, and skeletal muscle adjustments. Biology of Stress in Fish. Fish Physiology, 35(7), 251–294.

Rosanoff, A., & Wolf, F. I. (2016). A guided tour of presentations at the XIV International Magnesium Symposium "Magnesium in Health and Disease" Roma, Villa Malta, June 23–24, 2016. Magnesium Research, 29(3), 55–59.

Ryzen, E., Servis, K. L., & Rude, R. K. (1990). Effect of intravenous epinephrine on serum magnesium and free intracellular red blood cell magnesium concentrations measured by nuclear magnetic resonance. Journal of the American College of Nutrition, 9(2), 359.

Schreck, C. B. (2010). Stress and fish reproduction: The roles of allostasis and hormesis. General and Comparative Endocrinology, 165(3), 549–556.

Schreck, C. B., & Tort, L. (2016). The concept of stress in fish. Biology of Stress in Fish. Fish Physiology, 35(1), 1–34.

Segerstrom, S. C., & Miller, G. E. (2004). Psychological stress and the human immune system: A meta-analytic study of 30 years of inquiry. Psychological Bulletin, 130(4), 601–630.

Skulachev, V. P., Bogachev, A. V., & Kasparinskiy, F. O. (2010). Membrannaya bioenergetika [Membrane bioenergetics]. MGU, Moscow (in Russian).

Soldatov, A A. (1997). Kislorodno-dissotsionnye svoystva krovi i sostav vnutrieritrotsitarnoy sredy u morskikh ryb s razlichnoy dvigatel'noy aktivnost'yu. [Oxygen-dissociation properties of blood and composition of intra-erythrocytic medium in marine fishes with different motor activity] Zhurnal Evolyutsionnoy Biokhimii i Fiziologii, 33(6), 607–614 (in Russian).

Takei, Y., & Hwang, P.-P. (2016). Homeostatic responses to osmotic stress. Biology of Stress in Fish. Fish Physiology, 35(6), 207–249.

Vornanen, M., Stecyk, J. A.W., & Nilsson, G. E. (2009). The anoxia-tolerant crucian carp (*Carassius carassius* L.). Fish Physiology, 27(9), 397–441.

Wells, R. M. G. (2009). Blood-gas transport and hemoglobin function: Adaptation for functional and environmental hypoxia. Fish Physiology, 27(6), 255–299.

Wendelaar Bonga, S. E. (1997). The stress response in fish. Physiological Reviews, 77(3), 591–625.

Widmer, J., Féray, J.-C., Bovier, P., Hilleret, H., Raffin, Y., Chollet, D., Gaillard, J.-M., & Garay, R. (1995). Sodium-magnesium exchange in erythrocyte membranes from patients with affective disorders. Neuropsychobiology, 32, 3–18.

Widmer, J., Henrotte, J. G., Raffin, Y., Mouthon, D., Chollet, D., Stepanian, R., & Bovier, P. (1998). Relationship between blood magnesium and psychomotor retardation in drug-free patients with major depression. European Psychiatry, 13, 90–97.

Zaprudnova, R. A. (2017). Neprodolzhitel'noe deystvie nesil'nykh stressorov na kontsentratsiyu kationov v plazme krovi leshcha [Short-term effect of weak stressors on the concentration of cations in plasma of blood of the bream]. Trudy IBVV RAN, 78, 77–89 (in Russian).

Zaprudnova, R. A., & Kamshilov, I. M. (2008). Interspecific differences of respiratory functions of some freshwater fish species. Journal of Ichthyology, 48(6), 460–468.

Zaprudnova, R. A., & Kamshilov, I. M. (2010). Vliyanie stressovykh faktorov na dykhanie i dvigatel'nuyu aktivnost' ryb. Materialy Dokladov IV Vserossiyskoy Konferentsii [The influence of stress factors on the respiration and motor activity of fish]. Povedenie ryb. Akvaros, Moscow. Pp. 69–73 (in Russian).

Zaprudnova, R. A., & Kamshilov, I. M. (2016). Seasonal variations of functional properties of hemoglobin and ionic environment in the Freshwater fish: An example of bream, *Abramis brama* (Cyprinidae). Journal of Ichthyology, 56(2), 304–311.

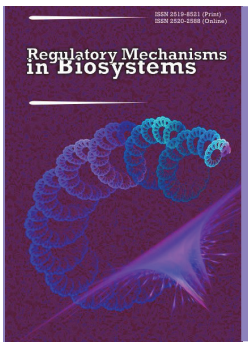

Regulatory Mechanisms in Biosystems

ISSN 2519-8521 (Print)
ISSN 2520-2588 (Online)
Regul. Mech. Biosyst., 9(3), 396–400
doi: 10.15421/021859

Bile acids from bile of rats of different sexes under testosterone

I. S. Chernuha, Y. M. Reshetnik, A. M. Liashevych, S. P. Veselsky, M. Y. Makarchuk

Taras Shevchenko National University of Kyiv, Kyiv, Ukraine

Article info

Received 19.06.2018
Received in revised form 15.07.2018
Accepted 17.07.2018

Taras Shevchenko National University of Kyiv, Glushkova st., 2, Kyiv, 03022, Ukraine. Tel.: +38-068-623-87-48. E-mail: chernuhairina17@gmail.com

Chernuha, I. S., Reshetnik, Y. M., Liashevych, A. M., Veselsky, S. P., & Makarchuk, M. Y. (2018). Bile acids from bile of rats of different sexes under testosterone. Regulatory Mechanisms in Biosystems, 9(3), 396–400. doi:10.15421/021859

Among the various functions of the liver, the formation of bile plays an important role. The optimal physiological ratio of bile components and the content of testosterone in the blood depend on various factors that can cause biliary system dysfunction and secretion. In experiments on different-sex rats, changes in bile acid contents of bile under the influence of testosterone propionate, which was injected intramuscularly 0.7 mg/kg, for 5 days were investigated. With the method of thin-layer chromatography, the basic fractions of bile acids conjugated in the bile were defined – taurocholic, taurochenodeoxycholic and taurodeoxycholic, glycocholic, glycochenodeoxycholic and glycodeoxycholic and free – cholic, chenodeoxycholic and deoxycholic acids. Conjugation rates were calculated (the ratio of the sum of conjugated cholates to the amount of free ones) and hydroxylation (ratio of the sum of trihydroxycholate bile acids to the sum of dihydroxycholanic) bile acids. In the bile of female rats almost all concentrations of cholates increased, except glycochenodeoxycholic and glycodeoxycholic acids. The calculated conjugation index on the whole did not undergo significant changes, but the hydroxylation factor increased, which may indicate an intensification of bile acid biosynthesis by neutral means, which is realized by 7α-hydroxylation of cholesterol. Under the influence of the hormone in male rats, the content of conjugated bile acids increased, and as for the free ones – a multidirectional effect of testosterone is observed, in particular, the concentration of cholic acid significantly decreased, indicating the activation of the poly-enzyme systems providing its conjugation with glycine and taurine. In connection with the wide use of the drug testosterone propionate and in view of its identified effects on the bile acid contents of the course of intramuscular administration, it is advisable to investigate the effect of this drug on the productive capacity of the liver.

Keywords: liver; cholates; conjugation index; hydroxylation index; testosterone propionate.

Introduction

In recent decades, there has been a tendency to increase in hepatobiliary pathology (Schirmer et al., 2005; Wang et al., 2008). Dysfunctional disorders of the biliary tract are found in most of the Ukrainian population, and the number of patients is steadily increasing (Gerbina et al., 2017). The liver is involved in metabolism of a number of hormones, therefore its disease may be accompanied by further hormonal disorders (Tomych, 2015). In particular, inflammatory processes in the liver affect metabolism of sex steroids, and may also suppress their binding with receptors throughout the whole body (Lee et al., 2017). Research has shown the complex relation of sex hormones with the liver, because it plays a role of mediator in a number of systemic effects on human and animal organisms (Klimyuk et al., 2010). Thus significant sex differences in liver functioning and metabolism discovered by many physiologists, suggest sex differentiation of liver functions (Rozen et al., 1991).

Recently, interest in the role of androgens in the development of obesity and obesity-related diseases such as diabetes, atherosclerosis and hypertension has increased. Testosterone regulates almost all intracellular transduction pathways directly involved in the metabolism of glucose and lipids, including key exchange enzymes (Bhandarkar et al., 2018; Yabiku et al., 2018; Yin et al., 2018; Palmisano et al., 2018). In particular, it has been shown that testosterone propionate changes lipid content of the bile of rats of different sex, that is, it affects the liver secretion function (Chernuha et al., 2017).

Medical studies indicate that cholelithiasis is more common in women than in men. It should be noted that Europeans are characterized by the formation of gallstones of a cholesterol nature. Women undergo the risk of their increase by physiologic rise in estrogen concentrations, which can be observed during pregnancy, the use of hormonal contraceptives and hormone substitution therapy in postmenopausal women (Novacek, 2006; Borovets et al., 2016). However, among men the number of hepatobiliary diseases is also increasing. The etiologies of their occurrence are nutrition and exogenous factors. Interestingly, the use of ethanol increases density of estrogen receptors in liver cells, which is believed to be a mechanism of feminization and the development of liver disease in alcoholism. There is also evidence that non-alcohol fatty liver disease is more common in men. Consequently, sex steroids are likely to play a role in its development. It is known that estrogens provide lipid homeostasis of the liver, and since androgens are predecessors of estrogen, then deviations in their ratio lead to pathological consequences (Boyer, 2013; Borovets et al., 2016; Mintziori et al., 2017).

The study of sex differences in the regulation of the bile-secretion function is considered as one of the most important trends in hepatology. And, since sex steroids are able to regulate the bile secretion function of the liver, their deficiency or excess can play a key role in the appearance of cholesterol gallstones (Ohshima et al., 1996). Therefore, nowadays considerable attention is paid to the study of the role of androgens in the development of pathologies of the hepatobiliary system. Intersexual differences in the formation of bile formation in liver tissue necessitate thorough experimental research on the effects of testosterone through various tests on the bile composition and the ratio of hepatitis secretion fractions in persons of different sex. And, because testosterone propionate is usually used intramuscularly for the treatment of a number of diseases, the purpose of our work is to detect the effect of the hormone on the bile acid composition of liver secretion of rats of both sexes.

Materials and methods

Experiments were carried out on 39 white non-breeding rats weighing 180–230 g. The study of the bile-secretion function of rats of both sexes was conducted in an acute experiment. The animals were kept in the accredited vivarium of the NSC "Institute of Biology and Medicine" of Kyiv Taras Shevchenko National University. All experiments were carried out in accordance with existing international and national requirements for the humane treatment of experimental animals.

The animals under investigation (males n = 9; females n = 9) were injected with a dose of 0.7 mg/kg body weight testosterone propionate for 5 days intramuscularly. The control group of male rats (n = 10) and females (n = 11) were daily injected intramuscularly with a solvent in the same volume as the amount of testosterone solution which each animal in the experimental group received daily for five days. For five days, the animals under study were kept in vivariums in four plastic specialized cells with a lattice iron lid in natural light, at a steady-state temperature regime and received a standard diet (feed for laboratory rats Vitamix, Ukraine) with free access to water.

Prior to surgical intervention, each animal was weighed and labeled. Sodium thiopental was used as an anesthetic in a dose of 60 mg/kg body weight of a rat. Injection of anesthesia was done intraperitoneally. After anesthetizing the animals, laparotomy with cannulation of the bile duct was carried out. Using this approach, we were able to record the volume of bile at 10, 30 minutes and 3 hours of the acute experiment. Subsequently, concentrations of bile acids in bile were determined by thin-layer chromatography, developed and improved in the Department of General Physiology of the Institute of Physiology named after Academician Petr Bogach of the National Institute of Biology and Medicine of Kyiv National Taras Shevchenko University (Veselsky et al., 1991). By the values of concentrations of conjugated and free choalates, the conjugation and hydroxylation factors of bile acids were calculated.

Statistical data processing was performed using the Statistica 7.0 (StatSoft Inc., USA). The reliability of the differences between the control and experimental groups was estimated by the ANOVA method. The results are also presented as median and upper and lower quartiles (Me [Q25; Q75]). Statistically significant differences were found for $P < 0.05$.

Results

In medical practice, in a number of diseases (hypogonadism, infertility, osteoporosis, etc.), testosterone is used intramuscularly in the course of treatment, an approach which we decided to reproduce under experimental conditions on the experimental animals. During intramuscular administration of testosterone (0.7 mg/kg) to female rats for 5 days, statistically significant changes in the studied characteristics of bile were observed during the whole acute experiment (Fig. 1). In the first half-hour interval, we observed an increase in the secretion of bile to 1.3 ± 0.3 µl/min·g of liver, i.e. by 128.2% ($P < 0.001$), in the second by 126.4% ($P < 0.001$) compared to the indicators of the control group of animals. The next half-hour intervals of the acute study were also characterized by a substantially statistically significant increase in the rate of choleresis, namely in the third by 137.1% ($P < 0.001$), the fourth by 164.4% ($P < 0.001$), fifth by 171.1% ($P < 0.001$) and the sixth by 173.2% ($P < 0.001$) in comparison with the control parameters (Fig. 1*a*). The experimental load of testosterone in female rats caused an increase in the level of bile produced by 147.1% ($P < 0.001$) compared with the control group (Fig. 1*b*).

In male rats, there were also statistically significant changes in the rate of choleresis, namely, after 0.5 hour of the acute experiment. In the second, the third, fourth, fifth and sixth intervals of the experiment, choleresis increased by 6.5% ($P < 0.05$), 11.1% ($P < 0.01$), 20.2% ($P < 0.001$), 21.3% ($P < 0.001$) and 20.1% ($P < 0.001$) compared to the control group of animals (Fig. 2*a*). The experimental load of exogenous testosterone on male rats caused an increase in the level of produced bile for all the time of the acute experiment by 12.4% ($P < 0.01$) compared with the control group (Fig. 2*b*).

Taking into account the fact that secretion of bile in rats is continuous and that, since they do not have a gall bladder, it immediately enters the duodenum, it can be assumed that the volume of allocated liver bile is the result of secretory activity of hepatocytes, and correspondingly, the participation of cholangiocytes in the synthesis of this secretion is less significant compared to other species. This specific feature of rats allows us, according to the dynamics of choleresis activity, to assess the regulatory effects of the hormone used on the external secretion activity of liver cells.

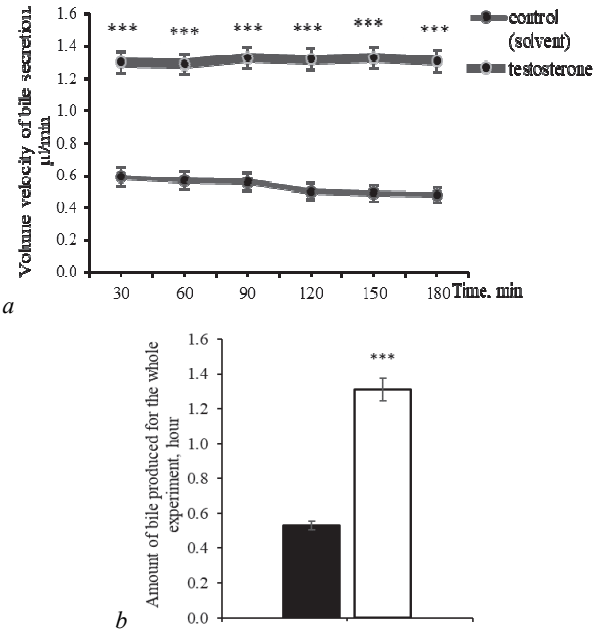

Fig. 1. Volume velocity of bile secretion in female rats in half hour intervals (*a*) and the amount of bile produced for the whole experiment (*b*) under control and after intramuscular administration of testosterone propionate (0.7 mg/kg) for 5 days (x ± SD): *** – $P < 0.001$; black – control (solvent, n = 11); white – testosterone (n = 9)

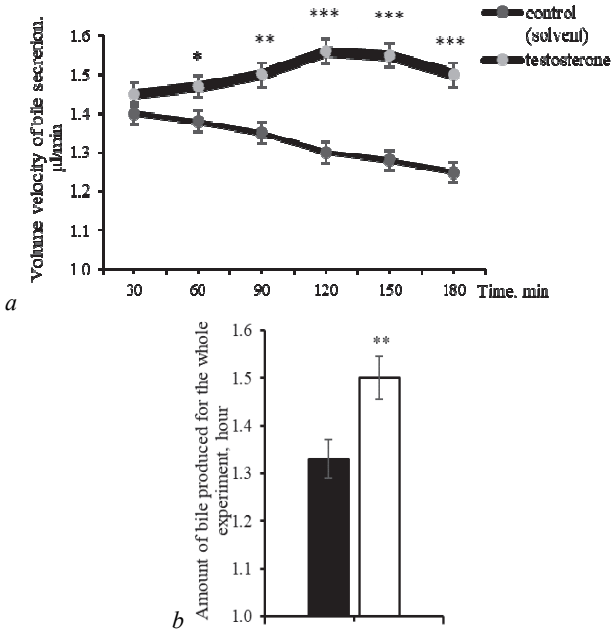

Fig. 2. Volume velocity of bile secretion in male rats at half hour intervals (*a*) and the amount of bile produced during the whole test (*b*) in the control and after intramuscular administration of testosterone propionate (0.7 mg/kg) for 5 days (x ± SD): * – $P < 0.05$, ** – $P < 0.01$, *** – $P < 0.001$; black – control (solvent, n = 10), white – testosterone (n = 9)

The main components of bile are bile acids, which are formed in the liver from cholesterol. In female rats, under influence of testosterone

propionate, the concentrations of the fractions of conjugated and free bile acids was statistically altered in comparison with the indicators of the control group of animals (Table 1). It turned out that in samples of bile in the studied group of animals, the content of taurocholic acid increased statistically significantly compared to the control after 1.5 h of acute experiment by 12.5% ($P < 0.05$) in the fourth sample of bile, in the fifth by 19.8% ($P < 0.01$), the sixth – 27.5% ($P < 0.001$). It is the increase in the concentration of taurocholic acid that must reduce the lithogenicity of the bile and the risk of the formation of gallstones (Levadianska et al., 2017; Pasternak et al., 2017). The content of taurochenodeoxycholic and taurodeoxycholic acids in the liver secretion increased only at the end of the experiment by 30.7% ($P < 0.01$) compared with the control indicators (Table 1). Concerning glycoconjugates of bile acids, the following is observed: concentration of glycocholic acid in the end of the acute experiment statistically significantly increased in the fifth sample of bile by 31.6% ($P < 0.01$), and in the sixth – by 53.9% ($P < 0.001$). The content of glycochenodeoxycholic and glycodeoxycholic acids decreased statistically significantly by 39.0% ($P < 0.001$) in the first sample of bile, the second by 43.5% ($P < 0.001$) in the third – 32.6% ($P < 0.01$) and in the fourth – 18.2% ($P < 0.05$) compared to the values of the control group of animals (Table 1).

After the course load on female rats with the studied hormone, significant fractions of free bile acids also occurred. Thus, the concentration of cholic acid statistically significantly increased in the second sample of the liver secretion by 48.2% ($P < 0.05$), on the third by 45.1% ($P < 0.05$) and the fourth by 37.5% ($P < 0.05$) compared to the control group. And the content of chenodeoxycholic and deoxycholic acids in the bile samples of female rats during the entire acute study statistically increased by 45.9% ($P < 0.05$) in the first bile test, in the second by 39.5% ($P < 0.05$), in the third by 23.3% ($P < 0.05$), the fourth by 45.4% ($P < 0.001$), in the fifth and sixth samples of the liver secretion by 66.7% ($P < 0.001$) and 69.2% ($P < 0.001$) compared to the control group of animals (Table 2).

Table 1

Concentration of conjugated bile acids in bile ducts (mg%) under testosterone (n = 9; 0.7 mg/kg; injected intramuscularly, over 5 days; x ± SD)

Samples of bile	Series of experiments	Fractions of conjugated bile acids			
		taurocholic acid	taurochenodeoxycholic + taurodeoxycholic acid	glycocholic acid	glycochenodeoxycholic + glycodeoxycholic acid
1	control	177.9 ± 18.7	98.7 ± 20.2	92.4 ± 21.4	36.5 ± 5.2
	testosterone	177.8 ± 8.6	94.5 ± 5.7	84.9 ± 6.7	22.2 ± 2.8***
2	control	177.6 ± 14.5	98.2 ± 17.4	91.5 ± 17.8	36.2 ± 5.2
	testosterone	179.1 ± 5.3	93.2 ± 7.5	81.4 ± 7.6	20.4 ± 2.1***
3	control	171.7 ± 14.0	95.9 ± 16.8	90.6 ± 16.1	34.2 ± 5.0
	testosterone	184.1 ± 4.8	99.4 ± 5.9	86.9 ± 7.2	23.0 ± 3.0**
4	control	167.3 ± 14.1	94.3 ± 14.2	85.3 ± 17.6	32.4 ± 4.1
	testosterone	189.3 ± 4.2*	106.4 ± 8.1	91.9 ± 6.0	26.5 ± 2.8*
5	control	163.1 ± 14.1	93.2 ± 16.5	81.1 ± 15.1	29.7 ± 4.1
	testosterone	195.3 ± 5.1**	113.6 ± 8.2	106.6 ± 6.4**	30.3 ± 2.8
6	control	159.7 ± 13.5	90.4 ± 14.1	77.8 ± 13.3	27.2 ± 4.1
	testosterone	203.6 ± 7.7***	118.1 ± 7.8**	119.8 ± 10.7***	33.0 ± 3.1

Notes: * – $P < 0.05$; ** – $P < 0.01$; *** – $P < 0.001$ statistically significant differences compared with the control group.

Table 2

Concentration of free bile acids in bile ducts (mg%) under influence of testosterone (n = 9; 0.7 mg/kg; injected intramuscularly, over 5 days; x ± SD)

Samples of bile	Series of experiments	Fractions of free bile acids	
		cholic acid	chenodeoxycholic + deoxycholic acid
1	control	16.8 ± 3.7	8.2 ± 1.9
	testosterone	23.8 ± 5.8	12.0 ± 2.2*
2	control	16.3 ± 3.1	7.7 ± 1.0
	testosterone	24.2 ± 5.0*	10.7 ± 1.7*
3	control	15.3 ± 3.1	7.9 ± 1.1
	testosterone	22.1 ± 4.5*	9.7 ± 0.8*
4	control	14.7 ± 2.6	7.6 ± 1.0
	testosterone	20.2 ± 3.9*	11.0 ± 1.1***
5	control	15.3 ± 2.8	7.5 ± 1.0
	testosterone	17.7 ± 3.5	12.6 ± 0.8***
6	control	15.7 ± 2.7	7.9 ± 1.4
	testosterone	15.8 ± 3.5	13.4 ± 2.0***

Notes: see Table 1.

In male rats which received testosterone propionate at the same dose as that of females, the concentration of bile acids statistically altered, namely: taurocholic, taurochenodeoxycholic and taurodeoxycholic, glycocholic, glycochenodeoxycholic and glycodeoxycholic (Table 3) and cholic (Table 4). The concentration of taurocholic acid increased throughout the acute experiment. In the first half-hour of the bile test, its content increased by 25.9% ($P < 0.001$) compared with control values. During the next 2.5 hours of the experiment, the concentration of taurocholic acid increased in a wavelike manner by 24.3% ($P < 0.001$), 23.1% ($P < 0.001$), 25.4% ($P < 0.001$), 24.6% ($P < 0.001$), 25.2% ($P < 0.001$) in comparison with the values of the control group of animals (Table 3). Statistically significant changes were observed in the concentration of taurochenodeoxycholic and taurodeoxycholic acids. Significant changes were noticeable in the beginning of the acute experiment and after 1.5 hours. In particular, their content under the action of the hormone increased by 17.4% ($P < 0.05$) in the first sample of the test sample, and in the second by 13.2% ($P < 0.05$) compared with the control parameters. After 1.5 hours of experiment, namely the fourth sample of liver secretion, the content of these acids increased by 31.5% ($P < 0.05$) compared with the control group of animals (Table 3).

Concerning concentration of glycocholic acid, statistically significant changes were observed only in the third and fourth samples of bile, that is, after 1 hour of acute experiment. The content of the investigated fraction in these samples increased by 10.2% ($P < 0.05$) compared with the control values. Statistically significant changes were observed throughout the experiment in concentrations of glycogenodeoxycholic and glycodeoxycholic acids. Their content in the studied samples of bile increased in a wavelike manner, namely 83.5% ($P < 0.001$) in the beginning of the experiments and 16.8% ($P < 0.001$) in the end of the acute experiment (Table 3). It should be noted that the course of testosterone in female rats resulted in a decrease in the concentration of glycogenodeoxycholic and glycodeoxycholic acids compared with control (Table 1). Only one fraction of free bile acids of the two studied underwent significant changes (Table 4).

Concentration of cholic acid changed statistically significantly throughout the experiment. In the beginning of the experiment, its content decreased by 38.6% ($P < 0.01$), and in the end of the acute experiment – 48.5% ($P < 0.001$) compared with the control indicators (Table 4). However, the concentration of cholic acid significantly increased in female rats under the influence of testosterone (Table 2).

The ratio of various components of bile, in particular, various bile acids are of great importance in the pathogenesis of many diseases of the hepatobiliary system. The conjugation indexes (the ratio of the sum of conjugated cholates to the amount of free ones) and hydroxylation (the ratio of the sum of trihydroxycholate bile acids to the sum of dihydroxycholate bile acids) are calculated by the concentrations of conjugated and free bile acids. In our experiment, testosterone in male rats did not cause statistically significant changes in the ratio of conjugated bile

acids to free ones. And, in the bile which was collected within an hour after the cannulation of the bile duct, the hydroxylation index increased statistically significantly by 13.9% ($P < 0.05$), indicating the stimulation of the biotransformation of dihydroxycholate acids to trihydroxycholate. In the following bile samples, no significant changes in the hydroxylation factor have been detected until the end of the experiment (Table 5).

Table 3
Concentration of conjugated bile acids in bile of male rats (mg%) under testosterone (n = 9, 0.7 mg/kg, injected intramuscularly, for 5 days, x ± SD)

Samples of bile	Series of experiments	Fractions of conjugated bile acids			
		taurocholic acid	taurochenodeoxycholic + taurodeoxycholic acid	glycocholic acid	glycogenodeoxycholic + glycodeoxycholic acid
1	control	180.8 ± 11.8	103.1 ± 8.2	141.8 ± 13.8	23.6 ± 6.2
	testosterone	227.7 ± 19.9***	120.7 ± 15.1*	153.0 ± 12.4	43.2 ± 5.9***
2	control	179.1 ± 10.1	104.5 ± 8.4	144.0 ± 8.4	21.9 ± 4.5
	testosterone	222.6 ± 14.7***	118.3 ± 13.3*	154.1 ± 10.2	44.6 ± 5.5***
3	control	175.7 ± 9.6	99.8 ± 8.5	137.2 ± 9.1	20.8 ± 5.0
	testosterone	216.1 ± 14.1***	127.1 ± 33.5	150.9 ± 10.0*	43.6 ± 6.0***
4	control	173.0 ± 9.9	95.9 ± 10.3	132.5 ± 11.6	19.1 ± 4.1
	testosterone	216.3 ± 15.6***	126.1 ± 33.3*	146.0 ± 10.5*	38.8 ± 5.5***
5	control	166.0 ± 1.0	92.7 ± 9.6	122.7 ± 16.1	20.4 ± 4.2
	testosterone	206.9 ± 12.5***	118.9 ± 31.0	136.5 ± 7.8	41.9 ± 6.2***
6	control	160.2 ± 10.5	89.6 ± 7.9	122.1 ± 16.0	17.4 ± 3.7
	testosterone	200.6 ± 12.6***	111.9 ± 32.3	136.1 ± 8.7	37.8 ± 5.1***

Notes: see Table 1.

Table 4
Concentration of free bile acids in bile of male rats (mg%) under testosterone (n = 9, 0.7 mg/kg, injected intramuscularly, for 5 days, x ± SD)

Samples of bile	Series of experiments	Fractions of free bile acids	
		cholic acid	chenodeoxycholic + deoxycholic acid
1	control	19.9 ± 4.8	8.3 ± 2.0
	testosterone	12.2 ± 1.8**	8.5 ± 0.8
2	control	19.8 ± 4.3	7.9 ± 1.3
	testosterone	11.6 ± 2.6***	8.6 ± 0.7
3	control	18.9 ± 4.5	7.5 ± 1.2
	testosterone	11.0 ± 2.3**	8.5 ± 1.2
4	control	18.5 ± 4.2	7.4 ± 1.1
	testosterone	10.6 ± 1.7***	7.9 ± 1.1
5	control	18.7 ± 3.8	7.4 ± 0.8
	testosterone	9.7 ± 1.2***	7.7 ± 0.8
6	control	18.3 ± 3.2	7.4 ± 0.8
	testosterone	9.4 ± 1.4***	7.8 ± 0.9

Notes: see Table 1.

Table 5
Bile acid conjugation factor and hydroxylation factor in bile of female rats under testosterone (0.7 mg/kg, injected intramuscularly; mg%; n = 9)

Samples of bile	Series of experiments	Conjugation factor	Hydroxylation factor
1	control	17.2 ± 5.9	2.0 ± 0.2
	testosterone	11.0 ± 2.8	2.2 ± 0.1
2	control	17.6 ± 5.1	2.0 ± 0.2
	testosterone	11.0 ± 2.4	2.3 ± 0.1*
3	control	16.8 ± 5.5	1.9 ± 0.3
	testosterone	12.6 ± 2.4	2.2 ± 0.1
4	control	17.7 ± 4.9	2.0 ± 0.1
	testosterone	13.5 ± 2.4	2.1 ± 0.1
5	control	16.7 ± 5.0	2.0 ± 0.2
	testosterone	14.9 ± 2.2	2.0 ± 0.1
6	control	16.0 ± 5.0	2.0 ± 0.1
	testosterone	16.0 ± 2.4	2.1± 0.1

Notes: see Table 1.

The conjugation factor under testosterone statistically significantly increased in male rats in the end of the acute test, i.e. in the fifth and sixth samples by 44.2% ($P < 0.05$) and 57.9% ($P < 0.05$) comparative with control. The increase in this factor indicates the activation of binding processes of free bile acids with taurine and glycine. The hydroxyllation coefficient also increased statistically significantly after 30-minutes of the acute test at 1.8–6.5% ($P < 0.05$) (Table 6).

Table 6
Bile acid conjugation factor and male bile hydroxylation in bile under testosterone (0.7 mg/kg, injected intramuscularly, mg%, Me [Q_{25}; Q_{75}], n = 9)

Samples of bile	Series of experiments	Conjugation factor	Hydroxylation factor
1	control	22.2 ± 7.1	2.4 [2.4; 2.4]
	testosterone	26.9 ± 5.9	2.3 [2.2; 2.4]*
2	control	22.7 ± 8.7	2.5 [2.4; 2.5]
	testosterone	27.4 ± 6.0	2.3 [2.2; 2.3]*
3	control	22.9 ± 8.0	2.5 [2.4; 2.6]
	testosterone	28.4 ± 6.1	2.3 [2.1; 2.4]*
4	control	22.5 ± 7.8	2.6 [2.5; 2.6]
	testosterone	29.4 ± 6.2	2.2 [2.1; 2.4]*
5	control	20.3 ± 7.0	2.5 [2.4; 2.7]
	testosterone	29.3 ± 4.8*	2.2 [2.2; 2.3]*
6	control	18.2 ± 5.6	2.6 [2.5; 2.7]
	testosterone	28.7 ± 4.9*	2.3 [2.2; 2.5]*

Notes: see Table 1.

Consequently, the course load of testosterone propionate in male and female rats resulted in a different effect of this hormone on the external secretion of the liver. This is primarily due to the different density of androgen receptors in the above-mentioned animals and, accordingly, the biotransformation of testosterone in the intramuscular administration, since it is known that the effects of steroid hormones are manifested not only for several hours but even days after their administration.

Discussion

Under the influence of exogenous testosterone, changes in the bile of male and female rats were observed, mainly increase in the concentrations of the main bile acid fractions, with the exception of glycochenodeoxycholic and glycodeoxycholic acid in females and cholic acid in males – their concentrations decreased compared to the control animals. Cholates regulate transport processes in liver cells at the transcription level of membrane transport proteins while interacting with nuclear hormonal receptors (Synelnyk et al., 2003). Regulatory substances that are capable of affecting the formation and secretion of bile acids can affect various levels of bile-acidic metabolism and transportation of organic constituents of bile. Taking into account that taurocholic acid reduces the risk of gallstone disease (Pasternak et al., 2017), the results may indicate the ability of the test hormone to reduce the lithogenicity of bile. And, the increase in the level of free cholic acid in bile, as observed in female rats, is primarily due to the lower efficiency of the work of the enzymes of this gender, which is responsible for its conjugation with taurine and glycine (Danchenko et al., 2014). One of the integrative indi-

cators of the coherent functioning of metabolic systems of transformations and transportation of bile acids, especially in hepatocytes, is the conjugation factor. It provides information on the solubilizing properties of bile, and the ratio of free and conjugated bile acid fractions is one of the criteria for assessing the lithogenicity of bile (Athamnah et al., 2015).

In our experiment, the conjugation rate in female rats did not undergo significant changes, whereas in males it significantly increased in the end of the acute experiment. Differences in the results may indicate that in males, the concentration of cholic acid during the acute experiment was statistically significantly reduced compared to the control group of animals. Stimulating the conjugation processes with high-polar compounds such as taurine and glycine also points to the enhancement of one of the methods of biological transformation of endo- and exogenous compounds. And, consequently, it may be an indication of improving the detoxification function of the liver (Reshetnik, 2012).

The bile acid hydroxylation coefficient of bile acids in male rats was significantly reduced, indicating that the test dose of testosterone promotes not only the activation of the poly-enzyme systems that provide conjugation of bile acids, but also increases their biosynthesis by "acidic" with the involvement of mitochondrial enzymes. The latter is associated with hormone activation of processes of tissue respiration in the liver (Borovets et al., 2016). An increase in the abovementioned ratio has been observed in female rats, in two bile samples, which may indicate the stimulatory effect of testosterone on the enzyme systems of liver cells, which provide hydroxylation of dioxocholanic bile acids in hepatocytes, as well as enhancement of the synthesis of trihydroxycholates. Thus, the study of the effect of testosterone on the content of cholates in bile provides the ability to establish the main links of bile formation, on which this hormone exhibits its regulatory effect. In addition, by changing the secretion of bile acids, the regulatory compound can be mediated through these same cholates, as through powerful endogenous cholic secretion regulators, and affect the bile-forming function of the liver of different sexes.

Conclusions

Testosterone propionate, when administered intramuscularly to male and female rats, significantly changed the concentration of bile acid in the bile, which may indicate its involvement in metabolic transformations and transport of cholates to the primary bile duct tubules.

In female rats, under the action of testosterone, there was an increase in biosynthesis processes of trihydroxycholate and certain dihydroxycholate bile acids in the liver. At the same time, the conjugation index did not undergo significant changes, and the hydroxylation factor increased, indicating a more pronounced synthesis of bile acids by the "classical" route, the key enzymatic reaction of which is the 7α-hydroxylation of cholesterol with the participation of CYP7A1.

The concentration of conjugated cholates in male rats, with the introduction of exogenous testosterone, increased significantly. The multidirectional effect of the hormone was on free bile acids, in particular the concentration of cholic acid dropped sharply, indicating the activation of the poly-enzyme systems that ensure its conjugation with glycine and taurine.

References

Atamnah, S., Reshetnik, J., Levadjans'ka, J., Baranovs'kyj, V., Vesel's'kyj, S., & Janchuk, P. (2015). Vplyv serotoninu na kon'jugaciju ta gidroksyljuvannja zhovchnyh kyslot u pechinci shhuriv [Serotonin effects on conjugation and hydroxylation of bile acid in the rats liver]. Naukovyj Visnyk Shidno-Jevropejs'kogo Universytetu Imeni Lesi Ukrai'nky, 2, 124–127 (in Ukranian).

Bhandarkar, N. S., Kumar, S. A., Martin, J., Brown, L., & Panchal, S. K. (2018). Attenuation of metabolic syndrome by EPA/DHA ethyl esters in testosterone-deficient obese rats. Marine Drugs, 16(6), e182.

Borovec', O., Bened', V., Reshetnik, J., Vesel's'kyj, S., & Makarchuk, M. (2016). Zhovchnosekretorna funkcija pechinky samok shhuriv v umovah blokady estrogenovyh receptoriv tamoksyfenom [Bile secretion liver function in the female rats at estrogen receptor tamoxifen blockade conditions]. Naukovyj Visnyk Shidno-Jevropejs'kogo Universytetu Imeni Lesi Ukrai'nky, 7, 194–199 (in Ukranian).

Boyer, J. L. (2013). Bile formation and secretion. Comprehensive Physiology, 3(3), 1035–1078.

Chernuha, I. S., Reshetnik, Y. M., & Vesel's'kyy, S. P. (2017). Doslidzhennja lipidnogo skladu zhovchi riznoi' stati pry dii' testosterone [Investigation of lipid composition of bile in different sexes rats under the testosterone influence]. ScienceRise: Biological Science, 4(7), 8–12 (in Ukranian).

Danchenko, N. M., Vesel's'kyj, S. P., & Cudzevych, B. O. (2014). Spivvidnoshennja zhovchnyh kyslot u zhovchi shhuriv za umov rozvytku aloksanindukovanogo cukrovogo diabetu [Correlations of bile acids in the bile of rats in conditions of alloxan induced diabetes melitus]. Ukrai'ns'kyj Biohimichnyj Zhurnal, 86(6), 147–153 (in Ukranian).

Gerbina, N. A., Ruban, O. A., Kutsenko, S. A., & Hontovaya, T. N. (2017). Perspektyvy zastosuvannja likars'koi' roslynnoi' syrovyny ta efirnyh olij pry patologijah biliarnogo traktu [Prospects of using medicinal herbs and essential oils for the treatment of the biliary tract]. Chasopys Fitoterapija, 1, 8–16 (in Ukranian).

Klymjuk, O., Bondzyk, O., Vesel's'kyj, S., & Makarchuk, M. (2010). Vplyv estronu na zovnishn'osekretornu funkciju pechinky shhuriv [Influence of estrone on the external secretion function of the liver of rats]. Visnyk Kyyivs'koho Natsional'noho Universytetu Imeni Tarasa Shevchenka, 56, 59–61 (in Ukranian).

Lee, S. R., Lee, S. Y., Kim, S. Y., Ryu, S. Y., Park, B. K., & Hong, E. J. (2017). Hydroxylation and sulfation of sex steroid hormones in inflammatory liver. Journal Biomedical Research, 31(5), 437–444.

Levadjans'ka, J., Reshetnik, J., Vesel's'kyj, S., & Janchuk, P. (2017). Zhovchnokyslotnyj spektr zhovchi samciv shhuriv pry dii' L-cystei'nu [Spectrum of bile acids in the bile of male rats after the administration of L-cysteine]. Naukovyj Visnyk Shidno-Jevropejs'kogo Universytetu Imeni Lesi Ukrai'nky, 7, 221–226 (in Ukranian).

Mintziori, G., Poulakos, P., Tsametis, C., & Goulis, D. G. (2017). Hypogonadism and non-alcoholic fatty liver disease. Minerva Endocrinologica, 42(2), 145–150.

Novacek, G. (2006). Gender and Gallstone disease. Wiener Medizinische Wochenschrift, 156(19–20), 527–533.

Ohshima, A., Cohen, B. I., Ayyad, N., & Mosbach, E. H. (1996). Effect of a synthetic androgen on biliary lipid secretion in the female hamster. Lipids, 31(8), 879–886.

Palmisano, B. T., Zhu, L., Eckel, R. H., & Stafford, J. M. (2018). Sex differences in lipid and lipoprotein metabolism. Molecular Metabolism, 45–55.

Pasternak, A., Bugajska, J., Szura, M., Walocha, J. A., Matyja, A., Gajda, M., Sztefko, K., & Gil, K. (2017). Biliary polyunsaturated fatty acids and telocytes in Gallstone disease. Cell Transplant, 26(1), 125–133.

Reshetnik, J. (2012). Vplyv blokady opioidnyh receptoriv na spivvidnoshennja holativ u zhovchi shhuriv iz eksperymentalnymalkogolnym gepatytom [Effect of opioid receptor blockade on the relation of cholates in bile of rats with experimental alcoholic hepatitis]. Tavrycheskyj Medyko-Byologycheskyj Vestnik, 15(3), 280–282 (in Ukranian).

Rozen, V. B., Mataradze, G. D., Smyrnova, O. B., & Smyrnov, A. N. (1991). Polovaja dyfferencyrovka funkcyj pecheny [Gender differentiation of liver function]. Medycyna, Moscow (in Russian).

Schirmer, B. D., Winters, K. L., & Edlich, R. F. (2005). Cholelithiasis and cholecystitis. Journal of Long-Term Effects of Medical Implants, 15(3), 329–338.

Synel'nyk, T. B., Synel'nyk, O. D., & Rybal'chenko, V. K. (2003). Zhovchni kysloty v procesah utvorennja kanal'cevoi' zhovchi [Bile acids the processes of canalicular bile formation]. Fiziologichnyj Zhurnal, 49(6), 80–93 (in Ukranian).

Tomych, M. I. (2015). Docil'nist' vykorystannja gepatoprotektoriv u kompleksnomu likuvanni dobrojakisnyh dysgormonal'nyh dysplazij molochnyh zaloz [Advisability of use of hepatoprotectors is in the treatment dishormonal dysplasia of breast]. Zdorov'e Zhenshhyny, 98, 101–103 (in Ukranian).

Vesel's'kyy, S. P., Lyashchenko, P. S., & Luk'janenko, Y. A. (1991). Sposob opredelenyja zhelchnyyh kyslot v byologycheskyh zhydkostjah [A method of determining bile acids in biological fluids]. Avtorskoe Svydetel'stvo 1624322 (in Ukranian).

Wang, H. H., Portincasa, P., & Wang, D. Q. (2008). Molecular pathophysiology and physical chemistry of cholesterol gallstones. Frontiers in Bioscience, 13(13), 401–423.

Yabiku, K., Nakamoto, K., & Tokushige, A. (2018). Reintroducing testosterone in the db/db mouse partially restores normal glucose metabolism and insulin resistance in a leptin-independent manner. BMC Endocrine Disorders, 18, 38.

Yin, L. J., & Wang, X. H. (2018). Research advance in the effects of androgen and its receptor on the development of obesity, obesity-related diseases and disorders of glucose and lipid metabolism. Sheng Li Xue Bao, 70(3), 319–328.

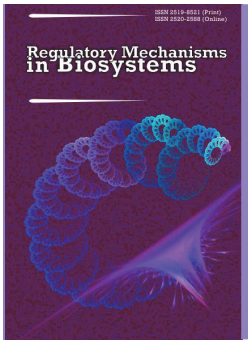

Regulatory Mechanisms in Biosystems

ISSN 2519-8521 (Print)
ISSN 2520-2588 (Online)
Regul. Mech. Biosyst., 9(3), 401–408
doi: 10.15421/021860

The characteristics, emergent properties and manner of spread in Ukraine of the Porcine Epidemic Diarrhea Virus

D. N. Masiuk*, V. S. Nedzvetsky*,**, A. I. Sosnitskiy*, A. V. Kokarev*, S. G. Koliada*

**Dnipro State Agrarian and Economic University, Dnipro, Ukraine*
***Bingol University, Bingol, Turkey*

Article info

Received 07.07.2018
Received in revised form 11.08.2018
Accepted 13.08.2018

Dnipro State Agrarian and Economic University, Sergei Efremov st., 25, Dnipro, 49600, Ukraine. Tel.+38-056-236-17-14. E-mail: plppm@ua.fm

Bingol University, Selahaddin-i Eyyubi Mah. Aydinlik Cad.,12000, Bingol, Turkey. E-mail: nedzvetskyvictor@gmail.com

Masiuk, D. N., Nedzvetsky, V. S., Sosnitskiy, A. I., Kokarev, A. V., & Koliada, S. G. (2018). The characteristics, emergent properties and manner of spread in Ukraine of the Porcine Epidemic Diarrhea Virus. Regulatory Mechanisms in Biosystems, 9(3), 401–408. doi:10.15421/021860

Study of the emergent properties and paths of spreading of PEDV was carried out in a model experiment on newborn non-immune piglets obtained from a PED virus-free pig-breeding enterprise. The piglets were kept in separate specialized containers, with a volume of 1.0 m^3, with access only through the opening at the top of the containers. The experimental group of the animals was infected with PEDV isolate extracted on one of the pig farms from the central region of Ukraine. Infection was carried out orally in a dose of 1–10 genome equivalents of virions. The control piglets, which were situated in the same room as the infected animals, were not deliberately infected. The study of biological material from piglets was carried out using the methods of bacteriology, histology and RT-PCR. To confirm the capability of PEDV to spread through house flies, specimens of *Musca domestica vicina* Mcq. were caught in the building where the experiment was carried out. The washings from the surface of their bodies were collected with sterile saline. Individually, 28 specimens of flies were selected. They were divided into two parts and the amount of virus in the homogenate of the fly bodies in these groups was determined with an interval between measurements of 72 hours. Study of PEDV in the washings and in flies body homogenates were carried out using RT-PCR. It is established that the field strain PEDV, belonging to the North American grouping II of the second group of the PED virus strains, is an emergent highly pathogenic agent for non-immune newborn piglets. In the model of piglets' infection it is established that the tested PEDV strain has a high virulence for newborn piglets, DCL is 1–10 virions and the incubation period is 18–26 hours. PED is acute with lethality to 100% within 68–72 hours after infection. According to the results of RT-PCR in washing from the surface of the bodies of flies, it is established that one of the ways piglets are infected and the environment contaminated with the PED virus is the spread of the pathogen by the flies *M. domestica vicina* Mcq. This leads to the induction of the emergent form of PED in piglets. The presence of PEDV in the homogenate from bodies of *M. domestica* caught in the focus of infection and the absence of virus reproduction in their body confirms the role of the house fly in the mechanical spread of PEDV in the external environment.

Keywords: PEDV; piglets; pathways; emergence; DCL; flies; *Musca domestica.*

Introduction

The virus of epidemic diarrhea of pigs (Porcine epidemic diarrhea virus – PEDV) was recently identified as a new infection and is considered as the causative agent of an emergent nosological unit in infectology. Epidemic diarrhea of pigs (PED) was first recorded in Europe at 1971, in South-East Asia 1995, in the Russian Federation 2005 and in Ukraine 2014 (Song et al., 2005; Martelli et al., 2008; Puranaveja et al., 2009; Strizhakova, 2013). In a relatively short time, the infection has assumed a global scope and tends to stagnate (Gerber et al., 2014; Vlasova et al., 2014; Wang et al., 2014; Dastjerdi et al., 2015).

Pigs of all age groups are affected by PED, though the most susceptible to PEDV are newborn piglets up to 10 days of age. In newborn piglets there is practically no immunity, and this is the main cause of their high susceptibility to infection with PEDV. In the early postnatal period, piglets develop debilitating watery diarrhea, dehydration, metabolic acidosis, intoxication and exhaustion during the course of the disease, which inevitably leads to death. From birth to 5 days, deaths reach 100%, from 6 to10 days – 60%, from 11 to 15 days – 30%, further 3% or less. When an infectious agent of PEDV reaches a farm, suckling piglets fall sick in the first days of life and die within 2–4 days. Such a progressive development of the infectious process determines the ineffectiveness and uselessness of vaccinating piglets. Under the circumstances of the infection propagation, the specific immune-biological protection with colostral immunoglobulins can form lactogenic immunity only (Annamalai et al., 2015).

Nowadays highly effective and biosafe methods of specific immune-prophylaxis and therapy are still not developed. Existing veterinary medications do not ensure eradication of the pathogen and are not effective against the expansion of PEDV on susceptible animals, therefore the development of epizootic PED is a difficult process to control (Choudhury et al., 2016). Both the practically total death of neonatal pigs and the absence of an etiopathogenetic correction of the infectious process are characteristic features of PEDV infection. The uncontrolled spread of the causative agent in swine herds can lead to enormous economic losses in industrial pig production. Together these facts give the grounds for considering PED as an emergent and especially dangerous infection in pig breeding (Gong et al., 2017).

The main path of infection of animals with the PED causative agent is oral-fecal with the subsequent replication of the virions in epithelial cells of the intestine, which leads to their prompt necrosis, tissue destruction and desquamation. After a short incubation period that varies in the range of 3–6 days, pathognomonic clinical signs of the disease appear in the form of diarrhea syndrome, which is accompanied by

watery diarrhea, vomiting, dehydration, increasing weakness, depression, exhaustion, intoxication and, as a rule, by death (Masiuk et al., 2017a). The excretion of PEDV with feces lasts 1–3 days, at the same time viral RNA is identified by molecular genetic methods within a month. After infection, a relatively short (up to 5 days) viremia period is usually detected. Viral antigens are detected in intestinal enterocytes as early as 12 hours after infection. Moreover, diagnosed concentration PEDV remains up to two weeks during the piglet infection (Lee, 2015).

The causative agent possesses unique biological properties that ensure the progressive growth of the infectious process (Boyko et al., 2009). The most important epizootic factors are high pathogenicity, extreme contagiousness, expressed enterotrophy and fatalities for newborn piglets, which together account for its emergent properties as a causative agent of a difficult to control infectious pathology (Kim & Chae, 2003; Martelli et al., 2008; Carvajal et al., 2015; Dastjerdi et al., 2015; Goede et al., 2015; Diel et al., 2016).

Given the fact that the virus causes non-curable diarrheal syndrome in newborn piglets, which leads to their total death, lactogenic immunity could prove to be the main method of their protection. It is impossible to form effective immunity without high immunogenic vaccines for sows. Modern anti-viral chemicals do not have sufficient protective activity for arresting the epizootic process of PED (Strizhakova, 2013; Langel et al., 2016; Tun et al., 2016; Srijangwad et al., 2017). Because of all of the above factors, the biological properties of PEDV field strains and epizootic patterns of PED, especially the emergent infectious pathology of piglets, this virus infection is recognized as one of the most urgent problems in animal infectious diseases. Quantitative characteristics of the pathogenicity of field strains of the PEDV, the paths of dissemination of this virus in the environment and the pathogenesis of PED have been insufficiently studied. The results of a detailed study of PEDV biology are extremely important as a methodological basis for developing strategies and tactics for combating and preventing its infectious pathology (Arriba et al., 2002; Stevenson et al., 2013; Goede & Morrison, 2016).

The aim of this study was to clarify the manner of the spread, the degree of pathogenicity and emergent properties of the PEDV field isolate in Ukraine in the model of native conditions of infection of non-colostrum, non-immune piglets.

Material and methods

The empirical component of the model experiment on the assessment of the emergent proprieties of PED infection was carried out in the vivarium of the Faculty of Veterinary Medicine of the Dnipro State Agrarian and Economic University (DSAEU). The laboratory research was carried out in the Scientific Research Center of Biosafety and Environmental Control in the Agro-Industrial Complex DSAEU.

Study of the biological properties of PEDV was performed using newborn non-immune piglets. Two groups of newborn piglets-analogues (6 experimental individuals and 3 control individuals) were randomly selected, before they started to consume colostrum. Piglets of cross-breeds ½ Pietren, ¼ Large White and ¼ Landras were obtained from a farm free from the PED virus, which was confirmed by preliminary screening studies on presence in the blood, colostrum and feces of both virus and antibodies to PED. Diagnostic analyses of sows' and piglets' samples were performed with RT-PCR and ELISA using commercial test kits "Bio-T kit®PEDV all – TGEV" ("Biosellal", France), "PED IgA ELISA" ("BioNote", Republic of Korea), and "Swinecheck® PED" ("Biovet", Canada).

The emergent characteristics of PEDV were determined in the samples collected in both the newborn non-colostrum piglets-analogous groups.

The piglets were kept in separate specialized insulated plastic containers, with a volume of 1.0 m^3. The access to both groups of piglets was operated only through the opening at the top of the containner. The distance from the upper plane of the container to the grill, on which the animals were kept, was not less than 70 cm. The maintenance of each container was carried out by personnel in individual overalls. Every staff person was subjected to additional sanitation just before any manipulation with the piglets. Containers were located about 2 m apart from each other in a separate vivarium room. In the room, the conditions were created to prevent active air movement, which was monitorred by the thermo-anemometer EA-2M (the range of measurement of the air speed within 0.1–5.0 m/s). The air temperature fluctuated in the range of 31–34 °C during the day and at night 17–23 °C. The conditions of the model experiment were as close as possible to industrial conditions. The experiment was carried out in August in the premises of the DSAEU vivarium without any measures to remove the house flies present – *Musca domestica vicina* Mcq. (Linnaeus, 1758).

The field strain of the PEDV which was isolated in one of the pig farms in the central region of Ukraine was used as a verified positive sample in the presented model of PED infection. The sequence-analysis showed the relation of this strain to the PED virus that was identified as a North American grouping II from the two group (Masiuk et al., 2017).

The piglets of the experimental group were exposed to the PEDV virus infection. The infection of animals was performed orally in a dose of virions of 1–10 genome equivalents. Control piglets were not infected, but they were kept in the same room as the infected animals. Every piglet before treatment with PEDV was tested for indices of health, especially locomotion and the body temperature. The locomotion of all animals was normal and temperature of the piglets of both the experimental and control groups was in the range 38.0–38.7 °C.

The piglets, that died by reason of diarrhea syndrome due to infection with PEDV, were dissected and the pathanoatomical changes were described. The infectious process was assessed with histological, bacteriological and PCR analyses in the tissue samples taken from the small intestine of the dead animals.

Fragments of the small intestine tissue from the dead piglets were fixed with 4% formalin solution in saline buffer. The tissue samples were paraffinized and 5 μm slices are prepared with a microtome. The slices were dried at room temperature and stained with both hematoxylin and eosin. The histological analysis of the objects was carried out with a microscope Leica DM 1000, digital camera Leica DFC 295, and the software Leica Qwin 3.0.

The samples for PCR analysis were prepared in a glass homogenizer with 100 mg tissue fragments of the small intestine. The extraction of nucleic acids (NA) from the biological material was carried out by the sorption method of these macromolecules on a silica-gel membrane with using columns BioExtract Column (Biosellal, France). The PED was diagnosed by polymerase chain reaction with real-time detection of the results (RT-PCR).

The reverse transcription of the RNA of the PED virus and the replication of the cDNA were performed using a kit Bio-T kit®PEDV all-TGEV (Biosellal, France) and CFX 96 Real-Time System (Bio Rad, USA) according to the temperature regime (Table 1).

Table 1
Temperature regime of amplification

Phase No.	Temperature, °C	Time, seconds	Number of cycles, pcs.
1	50	1200	1
2	95	300	1
3	95	10	45
4	60	45	

The fluorescence intensity in the samples was measured in real time at stage 4 of the temperature regime.

The analyses of the amplification results, as well as determination of the threshold cycle, C_t, were carried out using the Bio-Rad CFX Manager software.

Bacteriological study of the microorganism contents in the gastrointestinal tract of the animals was directed on both the indication and identification of microbionts of different taxonomic groups. To isolate aerobic bacteria, simple and enriched nutrient media were used, namely: meat-peptone broth and meat-peptone agar in a native form and with the addition of 10% blood serum, as well as on cardiac-brain broth, R. Hottinger's media, agar Endo, XLD agar. The anaerobic microorganisms were identified using both the Kit Tarozzi broth and the medium 5% agar with blood addition.

Morphology and biochemical data of field crops were studied by routine methods. The pathogenicity of the identified daily cultures of microorganisms was determined in a bioassay on white mice. The isola-

ted culture of microorganisms was administered subcutaneously in a volume 0.3 cm^3/animal to 5 white mice with a live weight of 18–20 g.

Fly individuals in the vivarium were selected to determine PEDV content in both the consumed matter and material absorbed from the body surface of the flies. The samples of PEDV content in the fly organism and absorbed on fly organism surface were studied separately. The flies caught in the vivarium were treated with sterile physiological saline solution to obtain the samples of absorbed PEDV. After individual washing of every fly the solutions were used for PEDV analyses with PCR-RT method. The second group of the flies selected in the vivarium was homogenized after the same washing. These samples were used to determine PEDV as fly consumption path. All samples of "fly consumption path" were randomly divided into two subgroups, which were studied with PCR-RT analysis twice with an interval of 72-hours.

Statistical analyses of the obtained results were carried out with using specialized software Statistica 6 (StatSoft Inc., USA). The reliability of the differences was evaluated after checking the obtained experimental data for the normal distribution using the Student test or its nonparametric analogue, the Wilcoxon test. The sample parameters indicated below in the text have the following notation: x is the selective mean, SE is the standard error of the mean.

Results

Non-immune newborn piglets which had not been fed colostrum were randomly selected in a pig enterprise immediately before the start of study. The screening studies of pigs for the presence of PED infection had been previously (2 weeks) carried out on the chosen pig farm (Table 2).

Table 2
The results of the PED infection screening in the donor farm of newborn piglets

The tested groups	ELISA				RT-PCR	
	serum		colostrum		feces	
	S/P, %	result	S/P, %	result	Ct	result
Sows 1–2 farrow	0.21 ± 0.04	–	0.47 ± 0.04	–	n.a.	–
Sows 3–4 farrows	0.21 ± 0.04	–	0.27 ± 0.07	–	n.a.	–
Sows 5 farrow and older	0.21 ± 0.05	–	0.43 ± 0.10	–	n.a.	–
Piglets of 35 days of age	0.28 ± 0.04	–	n.a.	n.a.	n.a.	–
Piglets of 75 days of age	0.17 ± 0.05	–	n.a.	n.a.	n.a.	–
Piglets 150 days old	0.18 ± 0.04	–	n.a.	n.a.	n.a.	–

Note: "–" – negative result; "n.a." – the absence of determined fluorescence.

The results of the screening study showed that the donor farm of the newborn piglets was free of PED infection. This conclusion is confirmed by the negative results of PCR analyses and determination of PEDV specific antibodies in the blood of both the sows and the piglets.

The results obtained in the model of experimental piglet's infection allowed us to assess the characteristics of distinctive temporal features of the growth and the length of the infectious PED process down to 100% mortality. The observed data showed the first typical features of this disease 18 hours after the induction of infection. One of the six piglets of the experimental group developed primary clinical signs of the disease – muscle weakness, lethargy, common inhibition of motor and reflex activity. In the following two hours, this individual had a manifestation of watery diarrhea, which is the main typical clinical sign of PED. Further clinical indicators of the severity of diarrhea syndrome progressively increased in every piglet of the infected group. The first lethal outcome was detected 60 hours after infection and 48 hours after visual manifestation of the clinical signs of PED.

The incubation period of the next 5 piglets infected with the PEDV developed continued for 6–8 hours longer than in the pig with the earliest symptoms, and was 24–26 hours. The infectious process developed typically in accord with clinical manifestations which fully correspond to the diarrhea syndrome of PED in newborn piglets. The deaths of animals of the experimental group were detected during the 68–72nd hours after infection. Analysis of clinical symptoms showed that every piglet infected with the pathogen had intensive diarrhea signs after an incubation period of the virion of about 22 ± 4 hours. The intensity of the pathological process progressively increased right up to the lethal outcome. The observed diarrhea symptoms were accompanied with continuous vomiting in every piglet, and some of them developed extremely painful symptoms. The observed feces immediately liquefied and turned into watery stools, colourless or greenish-yellow, without any admixture of blood. The main symptoms of diarrhea were identified in every infected animal. Moreover, diarrhea was prolonged, uninterrupted and quickly led to dehydration. The loss of animal weight was dramatic, which was visually noted, in particular, the piglets had clearly visible ribs and spine. The skin became wrinkled, inelastic, dry, and rough. General deterioration rapidly increased, the piglets noticeably weakened; toxic effects, metabolic acidosis and asthenia increased. During the 68–72nd hours of the development of diarrheal syndrome, on the background of hypothermia and progressive exhaustion, each of the infected pigs died. Thus, the lethality in the group of infected piglets was 100%.

Complex pathognomonic changes in the organism of the infected piglet group presented as the following abnormalities – severe general exhaustion, anemia and signs of severe intoxication combined with metabolic acidosis and alimentary asthenia. The signs of gastroenteritis and desquamation in the small intestine epithelium were meaningful and these features were pronounced in many areas of the gastrointestinal tract. Moreover, the pathogenetic signs of granular dystrophy were observed in the liver, kidneys and the heart muscle. Significant hyperplasia was discovered in the gastrointestinal lymph nodes. Every infected piglet had developed a number of anemic areas in the mucous membranes as well as an attenuation of the vessels, and depletion of the fat depot of the internal organs. In spite of all observed abnormalities, there was no indication of pathology of the spleen. The spleen tissue of the piglets infected with PEDV was not enlarged and the colour was bright-cherry, which reflects an absence of observed damage.

Histological analyses of fixed slices made from the samples of small intestine of both the control group piglets and the animals infected with PEDV indicated mucosal atrophy, swelling and infiltration of the intestinal wall with leukocytes (Fig. 1).

The results of histological analysis showed significant disorder in the structure of the small intestine, especially damage to the superficial and glandular epithelium. These changes are evidence of intestine dystrophy and predict local generation of necrotic areas. Moreover, strongly pronounced desquamation of the epithelial cells in the small intestine (a) accompanied with meaningful swelling (b) of the submucosa were detected in every sample of this piglet group.

Histology staining revealled the fragmentation, decay and vacuolation of muscle cells (Fig. 2a) as well as pyknosis and the translocation of nuclear matter also (Fig. 2b). The analysis of immune cells location showed intensive infiltration of lymphocytes and macrophages into the mucosa and submucosa of microvillies (Fig. 3).

Pathogens of both fungus and yeast microorganisms were not found in the intestinal contents of the orally infected group of piglets. The results of bacteriological analysis of fecal samples and intestinal contents of the experimental piglets infected with PEDV group showed the absence of pathogenic microorganisms (Table 3).

Neither fungus nor yeast microorganism pathogens were found in the intestinal contents of the orally infected group of piglets.

The kinds of elementary transient microflora that are usually are determined as being derived from the environment have been observed in the gullet. Particularly, the following bacteria families were dominant in this study – Enterobacteriaceae, Bacillaceae, Coccaceae. Prokaryotes species were identified according to their morphology and biochemical properties as typical fo newborn piglets. *Clostridium perfringens* showed an exceptionally high saccharolytic activity as well as anthracoid and coliform bacilli, while vulgar proteium developed extremely high proteolytic activity.

The test of pathogenic capability of isolated prokaryotic samples did not lead to the death of infected white mice for 5 days. Thus, all the identified prokaryotes were nonpathogenic.

Every small intestine sample from the piglets that had died as result of infection was analysed with RT-PCR to determine the PEDV content. The obtained results demonstrated meaningful C_t values in infected piglet samples, at average 21.33 ± 0.68. The data shown in Figure 4

indicate that the concentration of the content of the PED virus in piglets whose infection had a lethal outcome corresponds to the quantitative range of 10^5–10^6 genomic equivalents of the PEDV virions in 1 g extracted sample.

It should be noted that the piglets which were not infected with the field virus PEDV developed clinical manifestations of diarrhea syndrome as well as the infected piglet group. The clinical signs of PED detected in all piglets of the control group were similar to those in the experimental group. However, the manifestation of these symptoms was delayed for several days. The lethal outcome of all piglets of the control group occurred at a more distant period in comparison with the experimental group.

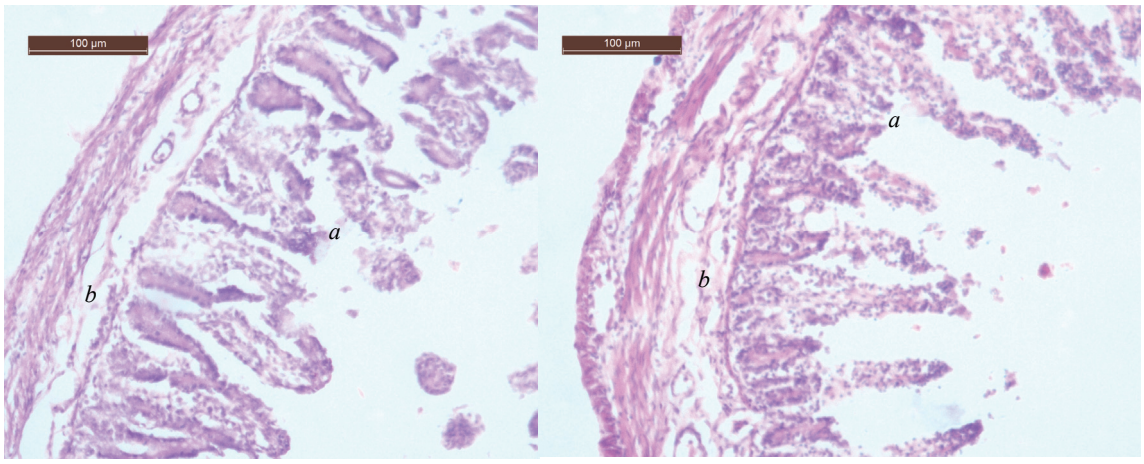

Fig. 1. Results of histology staining of the small intestine of piglet group infected with PEDV (hemotoxylin-eosin staining): *a* – desquamation of small intestinal epithelial cells; *b* – swelling of the submucosa

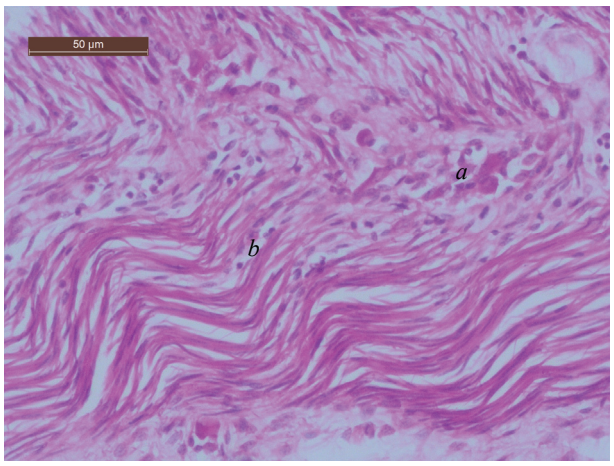

Fig. 2. The fragmentation of muscle in shell of small intestine (hemotoxylin-eosin staining): *a* – the destruction and vacuolization of myocytes; *b* –the pyknosis and rhexis of myocyte nucleis

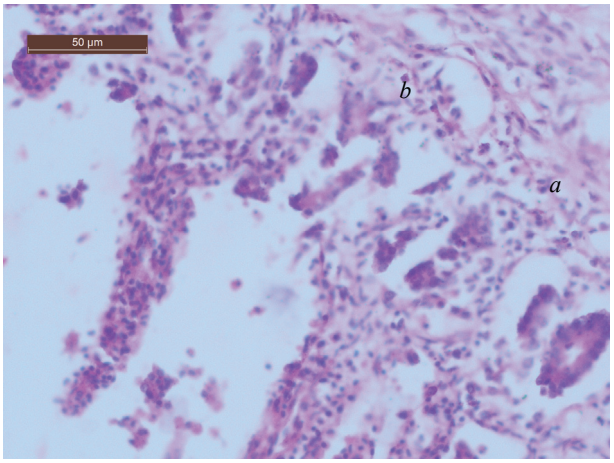

Fig. 3. The mucosa of the small intestine (hemotoxylin-eosin staining): *a* – lymphocytes infiltration; *b* – macrophage infiltration

Results of the RT-PCR analysis of the small intestine samples from the control group piglets showed a slightly lower PEDV content than the infected group. The C_t values for the samples obtained in the control group were 23.05 ± 1.31, which corresponds to 10^4–10^5 genome-equivalents of the virions of the PED exciter in 1 g of extract.

The first signs of the disease in the piglets of the control group appeared 36 hours after the start of the experiment. By contrast, for the infected group the time elapsing before appearance of the first symptoms did not exceed 18 hours. The result confirms the possibility of the virus spreading within the vivarium from the infected piglets to the piglets of the control group. The temporal differences in the lethal outcome between the groups correspond to the time difference in the manifestation of the first clinical signs.

Table 3

Species composition of the microbiocenosis of the intestines of piglets that died from PED (n = 9)

Name of microbiont	Number of biomaterial								
	test group						control group		
	1	2	3	4	5	6	1	2	3
Escherichia coli (Castellani and Chalmers, 1919)	+	+	+	+	+	+	+	+	+
Hemolysins *E. coli*	–	–	–	–	–	–	–	–	–
Proteus vulgaris (Hauser, 1885)	+	–	–	+	–	+	+	–	+
Pseudomonas aeruginosa (Migula, 1900)	+	–	+	+	–	–	+	+	–
Clostridium perfringens (Hauduroy et al., 1937)	–	+	–	+	+	+	–	+	–
Bacillus cereus (Frankland & Frankland, 1887)	+	–	+	–	+	–	+	+	–
Bacillus subtilis (Cohn, 1872)	–	–	–	+	–	+	+	–	+
Bacillus mycoides Flügge, 1886	+	+	–	+	+	–	–	+	+
Bacillus megaterium (de Bary, 1884)	–	–	+	–	–	+	+	–	+
Enterococcus spp. (Schleifer & Kilpper-Bälz, 1984)	+	+	–	+	–	+	–	+	–
Staphylococcus spp. (Rosenbach, 1884)	–	+	–	–	+	–	–	+	+
Streptococcus suis (Kilpper-Bälz & Schleifer, 1987)	–	+	–	–	–	+	+	–	–
Klebsiella spp. (Trevisan, 1885)	–	–	–	+	+	–	–	+	–

Note: "+" – presence of a microbiont; "–" – absence of microbiont determined content.

The time of the lethal outcome of the infected group was identified as within the 68–72nd hours. In the control group, the lethal outcome occurred 88–90 hours after the start of an experimental infection.

In all households, house flies are extremely common (*Musca domestica vicina* Mcq.), which in the conditions of the experiment (August, 2017) were also present in the vivarium in sufficient quantities. The flies could have been an effective PEDV carrier in these conditions. In favour

of this assumption is the correspondence between the time from infection till the appearance of clinical symptoms and the temporal difference in the lethal outcome of the infected and control groups. This assumption was confirmed by the results of PCR-RT analysis of the PED virus on the surface and in the body of houseflies. The samples of fly surface were tested on PEDV content. The results of studies of four group samples showed $C_t = 31.44 \pm 0.68$ (Fig. 5), which approximately corresponds to the quantitative range of 10^2–10^3 genome-equivalents of the virions of the PED exciter in 1 ml of flushing. The samples of flies were tested on PEDV content too. Two subgroups of individual fly samples were studied with PCR-RT analysis with a 72-hour postponement. The results of the analysis are shown in Figure 6.

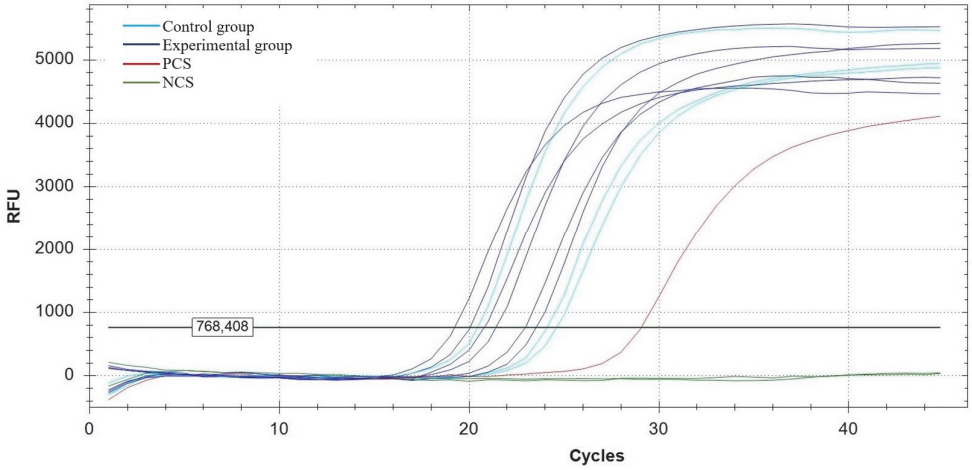

Fig. 4. The kinetics of cDNA amplification products of the PED virus extracted from the small intestine of piglets from the experimental and control groups: NCS – negative control samples RT-PCR, PCS – positive control sample RT-PCR

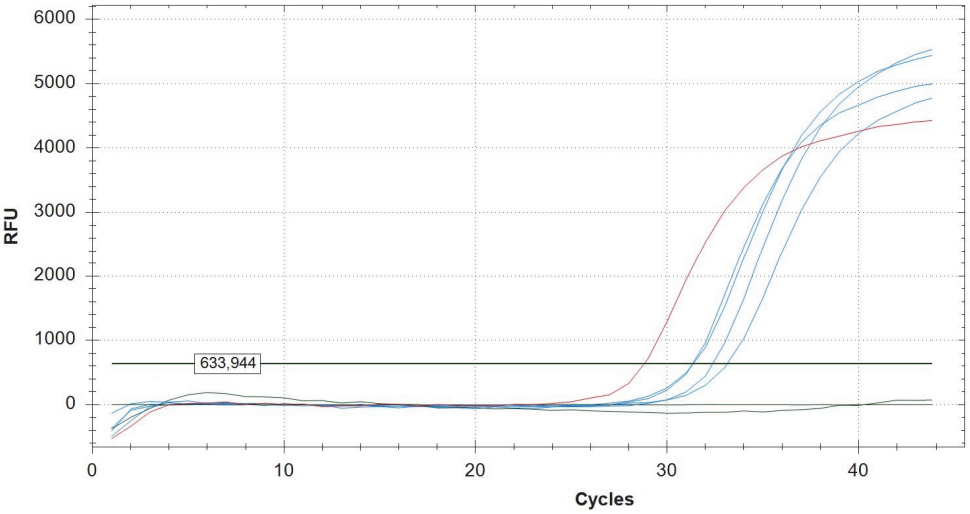

Fig. 5. The kinetics of cDNA amplification products of the PED virus extracted by washing of *Musca domestica vicina* Mcq.: NCS – negative PCR-RT control samples, PCS – PCR-RT positive control sample

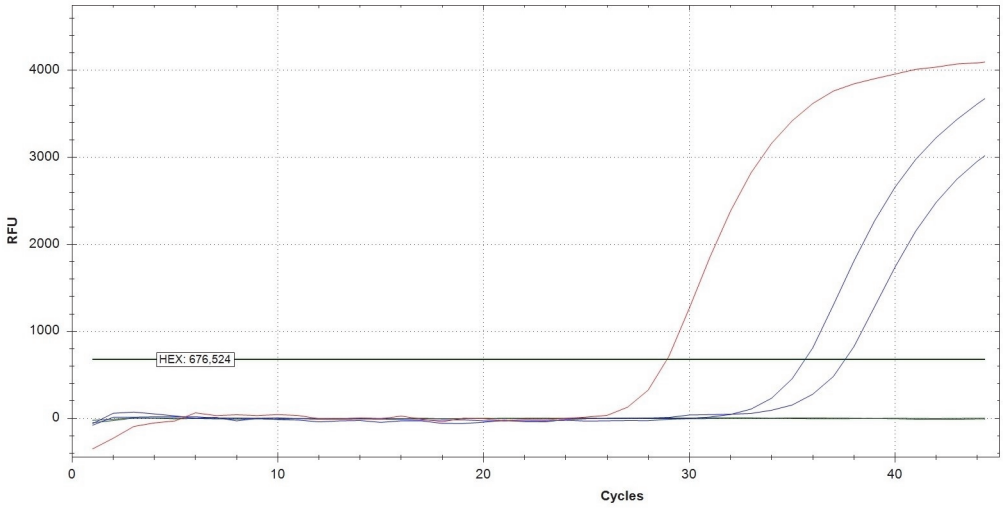

Fig. 6. The kinetics of cDNA amplification products of the PED virus extracted from the homogenate samples of *Musca domestica vicina* Mcq.: NCS – negative PCR-RT control samples, PCS – PCR-RT positive control sample

The content of virions revealed in both subgroups was almost identical and the statistical differences were not significant. The C_t value determined in the flies homogenate samples selected in the beginning of the experiment was 35.62. In the sample homogenized after 72 hours it was 37.57. The results obtained indicate that reproduction of the PED pathogen in the body of houseflies did not occur.

Discussion

Infection induced by PEDV was first identified only 5 years ago in Indiana (USA) in May 2013 (Snelson, 2014). Despite the short period since the discovery of PED disease this has become a separate nosological unit of infectious pathology. The risk of significant economic losses in pig farms caused by PED incidents is associated with high mortality of newborn piglets and a decrease in pig farming productivity of older age animal groups. Recently it has been shown that PEDV is an emergent highly pathogenic virus that induces a lethal diarrheal syndrome in newborn piglets (Stevenson et al., 2013). PED infection proceeds as a non-lethal enteral disorder in the cohort of adult animals (Wang et al., 2014; Alvarez et al., 2015; Choudhury et al., 2016).

PEDV differs from other representatives of the Coronaviridae family by its high contagiousness, which is due to the genetic features of this virus (Gong et al., 2017). In the course of one year after the discovery in North America a new variant of the PEDV strain with three deletions, one insertion and several mutations in the S (spike) 1 region was detected (Wang et al., 2014). Recent results obtained in the largest comparative analyses of 138 PEDV genomes have shown that this virus has a minimum of 6 subtypes (Jang et al., 2018). Groups 1 and 2 come from North America and groups 3–5 from Asia. According to Jang et al. (2018), the rate of the genome evolution is 3.38×10^{-4} site replacements per year, which is similar to other RNA-containing viruses.

In this way, the relatively high mutagenic ability of PEDV determines the difficulties of developing effective vaccines against PEDV. The lack of immunity in newborn piglets allows the virus to induce large-scale infection of piglets in a short period.

The spread of PEDV is also promoted by the fact that the virus can remain viable in the external environment for up to six months. At the same time, in the convalescent organism no viruses were revealed (Goede & Morrison, 2016). The high contagiousness and pathogenicity of PEDV along with significant economic losses caused by PEDV infection are the main causes of the special attention and intensive study of PED infection around the world. However, despite the progressive growth in the number of publications on the subject, the most important key biological characteristics of this pathogen remain too insufficiently studied to develop an effective strategy to cure PEDV infection.

The results of our study of the virulent activity characteristics of PEDV field isolated in Ukraine showed that the minimal infecting dose is 1–10 virions, which is equivalent to Dosis Certa Letalis (DCL). These data indicate that the PEDV strain isolated in Ukraine is an emergent highly virulent pathogen for newborn piglets. The results obtained in our work demonstrate that viral isolate induces infectious pathology in piglets according to the classic type of epizootic process, which is lethal for the newborns. Therefore, they act as a biological indicator of PEDV circulation in the focus of infection (Masiuk et al., 2017a).

High virulence of the PED pathogen has been shown in the realized experimental model, which contributes to the active spread of the virus to the nearest areas by mechanical transmission through transport, inventory, contaminated feed, insects, etc. (Yeruham et al., 1996; Sven et al., 2007; Förster et al., 2009).

Particular importance in the epidemiology of infectious diseases is given to flies as a separate biological carrier of microorganisms in animal populations, as well as translocation between animals and humans (Lecuona et al., 2005; Sven et al., 2007; Sukontason et al., 2007; Holt et al., 2007; Barin et al., 2010; Gestmann et al., 2012).

The biological features of *M. domestica* should be noted, which are important in providing an epizootic process of infectious diseases. The results presented by Dübendorfer et al. (2002) showed that the house fly *M. domestica vicina* Mcq. is a dipterous insect of the family of real flies, a common synanthropic organism, which almost does not occur in the wild environment. It is a diurnal insect. It feeds on organic waste of animals, but develops in their feces during the larval period, which contributes to their role as a mechanical carrier of infectious and parasitic pathogens. It has been proved that *M. domestica* is capable of transmitting several microorganisms, especially enterotoxic *E. coli*, *Klebsiella*, *Campylobacter*, *Providencia*, *Staphylococcus aureus*, *Streptococcus viridans*, etc. (Förster et al., 2012).

The epidemiological potential of *M. domestica* related to the mechanical propagation of the agents of pig infectious diseases is well known. The fly can spread various infectious agents, especially Aujeszky's disease (Medveczky et al., 1988), transmissible gastroenteritis (Saif & Wesley, 1999), mycobacteriosis (Fischer et al., 2001), reproductive-respiratory syndrome of pigs (Otake et al., 2004), as well as several parasitic diseases – *Ascaris suum*, *Strongyloides ransomi*, *Metastrongylus* sp., undetermined Strongylida is recorded (Förster et al., 2009).

Based on the results obtained in a study of the biological properties of *M. domestica*, Murvosh & Taggard (1966) identified two main propagation mechanisms of microorganisms which are mediated by this insect species. The first of them is the mechanical transfer of pathogens on the surface of insect bodies due to the adsorption of microorganisms and viruses on numbered setae and filaments. The second is carried out as a result of regurgitation of incompletely digested food which is contaminated with infectious agents.

In the world scientific literature there have been no reports that *M. domestica* may be a vector for the spread of PEDV. The results obtained in our study confirm the possibility of mechanical spreading of the PED virus transferred on the surface of the body of *M. domestica*. This is evidenced by the detection with the RT-PCR the genetic material of PEDV in the samples washed from the surface of the bodies of flies which had been in contact with the infected piglets.

Results of the study of homogenates from *M. domestica* bodies prepared at an interval of 72-hours with RT-PCR showed no PEDV replication in the flies. This is confirmed by the unchanged C_t value in the samples isolated from flies 3 days after the beginning of infection of the piglets. The results presented in our study indicate that flies can dominate only as a vector of mechanical transferring of PEDV.

The measurement of fly activity in the environment show that *M. domestica* has an average speed of 6.4 km/h and flight distance can be up to 40 km (Golding et al., 2001). The summer activity of flies could form one of the main factors of total environmental contamination with PEDV in a relatively short time period. Taking into account that newborn piglets have the lack of maternal immunity and that their own immune system is immature, they are extremely sensitive to PEDV infection propagated by flies. Generation of infection in piglets poses a serious threat to the spread of PEDV not only inside a farm, but it could be a source of infection in pigs in the farms located within a radius of several dozens of kilometers from the primary infected area.

According to data analysis of PubMed, ScienceDirect and Google Scholar publications, the positive results of infection of piglets by transmission of PEDV by house flies were obtained for the first time. The fact of mechanical spread of PEDV by house flies which contributes to the infection of piglets is experimentally established. The results of the study of the emergent properties of PEDV are fully consistent with the literature data on of the development of the PED disease. In the presented experimental model (summer, 2017) of acute intestinal disorder in the newborn piglets, typical features of PEDV infection developed within 36–48 hours after the injection of the strain of the virus isolated in Ukraine strain. The dosed infection of newborn piglets resulted in 100% lethal outcome. This fact is an important feature of the epizootic process of PED. The obtained results indicate that this manner of spreading of the virus could be one of the leading paths of infection on Ukrainian farms and a significant critical factor in the epidemiology of PED. These results have a great practical importance and can be used to develop a preventive strategy and to specify the therapy of PED infection in real pig farming conditions.

The presented results of the research on the emergent characters of PEDV infection point to the relevance of the problem of the viruses spreading on Ukrainian farms. The process of PEDV propagation on Ukrainian farms requires further detailed study, especially the pathoge-

nic proprieties of field isolated strains. The most significant issue is to determine the relation of the biological properties of PEDV field isolates with their genetic characteristics. First of all, biological properties of PEDV relate to the cause-effect relationship between the pathogenicity of the virus, the nucleotide sequence of its genome and the epizootic features of the infectious pathology. The differences among all PEDV morbid events could be caused by various isolates of the pathogen which are circulating among the susceptible population. Thus PED infection in Ukraine requires urgent and widespread study.

The extremely limited data on the characteristics of the infectious process of PED in Ukraine compared with other countries indicates that further research should be conducted on the pathways and methods of PEDV spreading on farms. The features of the spread of PEDV in the environment, the duration of preservation of the viruses' virulent properties in the conditions of virions' adsorption on contaminated technological equipment and also in the organism of both susceptible and non-susceptible animals remain poorly studied.

Conclusions

In the model of PED piglets' infection it is established that the tested PEDV strain has a high virulence for newborn piglets, DCL is 1–10 virions and the incubation period is 18–26 hours. PED is acute with lethality to 100% within 68–72 hours after infection.

Based on the results of RT-PCR analyses in the samples washed from the surface of the bodies of flies, it is established that one of the ways piglets are infected and the environment contaminated with the PED virus is the spread of the pathogen by the flies *M. domestica vicina* Mcq. This leads to the induction of the emergent form of PED in piglets.

The presence of PEDV in the homogenate from *M. domestica vicina* Mcq. bodies caught in the focus of infection and the absence of virus reproduction in their body confirms the role of housefly in the mechanical spread of PEDV in the external environment.

References

Alvarez, J., Sarradell, J., Morrison, R., & Perez, A. (2015). Impact of porcine epidemic diarrhea on performance of growing pigs. PLoS One, 10(3), e0120532.

Annamalai, T., Saif, L. J., Lu, Z., & Jung, K. (2015). Age-dependent variation in innate immune responses to Porcine epidemic diarrhea virus infection in suckling versus weaned pigs. Veterinary Immunology and Immunopathology, 168, 193–202.

Arriba, M. L., Carvajal, A., Pozo, J., & Rubio, P. (2002). Isotype-specific antibody-secreting cells in systemic and mucosal associated lymphoid tissues and antibody responses in serum of conventional pigs inoculated with PEDV. Veterinary Immunology and Immunopathology, 84(1), 1–16.

Barin, A., Arabkhazaeli, F., Rahbari, S., & Madani, S. A. (2010). The housefly, *Musca domestica*, as a possible mechanical vector of Newcastle disease virusin the laboratory and field. Medical and Veterinary Entomology, 24, 88–90.

Boyko, A., Brygadyrenko, V., Shendryk, L., & Loza, I. (2009). Estimation of the role of antropo-zoonosis invasion agents in the counteraction to bioterrorism. Counteraction to Chemical and Biological Terrorism in East European Countries. NATO Science for Peace and Security Series A: Chemistry and Biology. Springer Nature, 309–315.

Carvajal, A., Argüello, H., Martínez-Lobo, F. J., Costillas, S., Miranda, R., de Nova, P. J. G., & Rubio, P. (2015). Porcine epidemic diarrhoea: New insights into an old disease. Porcine Health Management, 1(12), 1–8.

Choudhury, B., Dastjerdi, A., Doyle, N., Frossard, J. P., & Steinbach, F. (2016). From the field to the lab – An European view on the global spread of PEDV. Virus Research, 226, 40–49.

Dastjerdi, A., Carr, J., Ellis, R. J., Steinbach, F., & Williamson, S. (2015). Porcine epidemic diarrhea virus among farmed pigs, Ukraine. Emerging Infectious Diseases, 21(12), 2235–2237.

Diel, D. G., Lawson, S., Okda, F., Singrey, A., Clement, T., Fernandes, M. H. V., Christopher-Hennings, J., & Nelson, E. A. (2016). Porcine epidemic diarrhea virus: An overview of current virological and serological diagnostic methods. Virus Research, 226, 60–70.

Dübendorfer, A., Hediger, M., Burghardt, G., & Bopp, D. (2002). *Musca domestica*, a window on the evolution of sex-determining mechanisms in insects. International Journal of Developmental Biology, 46(1), 75–79.

Fischer, O., Mátlová, L., Dvorská, L., Švástová, P., Bartl, J., Melichárek, I., Weston, R. T., & Pavlík, I. (2001). Diptera as vectors of mycobacterial infections in cattle and pigs. Journal Medical and Veterinary Entomology, 15(2), 208–211.

Förster, M., Gestmann, F., Mehlhorn, H., Sievert, K., Messler, S., Neuhausen, N., Petersdorf, S., & Pfeffer, K. (2012). Flies as vectors of microorganisms potentially inducing severe diseases in humans and animals. Arthropods as Vectors of Emerging Diseases. Parasitology Research Monographs. Vol. 3. Springer, Berlin, Heidelberg.

Gerber, P. F., Gong, Q., Huang, Y. W., Wang, C., Holtkamp, D., & Opriessnig, T. (2014). Detection of antibodies against porcine epidemic diarrhea virus in serum and colostrum by indirect ELISA. The Veterinary Journal, 202(1), 3–36.

Goede, D., & Morrison, R. B. (2016). Production impact and time to stability in sow herds infected with Porcine epidemic diarrhea virus (PEDV). Preventive Veterinary Medicine, 123(1), 202–207.

Golding, Y. C., Roland Ennos, A., & Edmunds, M. (2001). Similarity in flight behaviour between the honeybee, *Apis mellifera* (Hymenoptera: Apidae) and its presumed mimic, the dronefly *Eristalis tenax* (Diptera: Syrphidae). Journal Experimental Biology, 204(1), 139–145.

Gong, L., J. Li, Q., Zhou, Z., Xu, L., Chen, Y., Zhang, C., Xue, Z., Wen, Y. C. (2017). A New Bat-HKU2-like coronavirus in swine, China, 2017. Emerging Infectious Diseases, 23(9), 1607–1609.

Holt, P. S., Geden, C. J., Moore, R. W., & Gast, R. K. (2007). Isolation of *Salmonella enterica* serovar *enteritidis* from houseflies (*Musca domestica*) found in rooms containing *Salmonella* serovar *enteritidis*-challenged hens. Applied and Environmental Microbiology, 73(19), 6030–6035.

Jang, J., Yoon, S. H., Lee, W., Yu, J., Yoon, J., Shim, S., & Kim, H. (2018). Time-calibrated phylogenomics of the Porcine epidemic diarrhea virus: Genome-wide insights into the spatio-temporal dynamics. Genes Genomics, 40(8), 825–834.

Kim, O., & Chae, C. (2003). Experimental infection of piglets with a Korean strain of Porcine epidemic diarrhoea virus. Journal of Comparative Pathology, 129(1), 55–60.

Langel, S. N., Paim, F. C., Lager, K. M., Vlasova, A. N., & Saif, L. J. (2016). Lactogenic immunity and vaccines for Porcine epidemic diarrhea virus (PEDV): Historical and current concepts. Virus Research, 226, 93–107.

Lecuona, R. E., Turica, M., Tarocco, F., & Crespo, D. C. (2005). Microbial control of *Musca domestica* (Diptera: Muscidae) with selected strains of *Beauveria bassiana*. Journal of Medical Entomology, 42(3), 332–336.

Lee, C. (2015). Porcine epidemic diarrhea virus: An emerging and re-emerging epizootic swine virus. Virology Journal, 12, 193.

Martelli, P., Lavazza, A., Nigrelli, A. D., Merialdi, G., Alborali, L. G., Pensaert, M. B. (2008). Epidemic of diarrhoea caused by Porcine epidemic diarrhoea virus in Italy. Veterinary Record, 162(10), 307.

Masiuk, D. M., Sosnitsky, O. I., Nedzvetsky, V. S., Kokarev, A. V., & Koliada, S. G. (2017a). Endemic course of epidemic diarrhea of pigs in the stabilized focus of infection. Regulatory Mechanisms in Biosystems, 8(3), 410–416.

Masiuk, D. M., Sosnitsky, O. I., Nedzvetsky, V. S., Kokarev, A. V., & Koliada, S. G. (2017b). Epidemiology, etiology and gene analysis of spike S protein of porcine epidemic diarrhea virus infection in Ukraine during 2016–2017. Regulatory Mechanisms in Biosystems, 8(4), 602–610.

Medveczky, I., Kovács, L., Kovács, F. Sz., & Papp, L. (1988). The role of the housefly, *Musca domestica*, in the spread of Aujeszky's disease (pseudorabies). Journal Medical and Veterinary Entomology, 2(1), 81–86.

Murvosh, C. M., & Taggard, C. W. (1966). Ecological studies of the housefly. Annals of the Entomological Society of America, 59, 534–547.

Otake, S., Dee, S. A., Moon, R. D., Rossow, K. D., Trincado, C., & Pijoan, C. (2004). Studies on the carriage and transmission of porcine reproductive and respiratory syndrome virus by individual houseflies (*Musca domestica*). Veterinary Record, 154(3), 80–85.

Puranaveja, S., Poolperm, P., Lertwatchharasarakul, P., Kesdaengsakonwut, S., Boonsoongnem, A., Urairong, K., Kitikoon, P., Choojai, P., Kedkovid, R., Teankum, K., & Thanawongnuwech, R. (2009.). Chinese-like strain of Porcine epidemic diarrhea virus, Thailand. Emerging Infectious Diseases, 15, 1112–1115.

Saif, L. J., & Wesley, R. D. (1999). Transmissible gastroenteritis and porcine respiratory coronavirus, in straw. Diseases of Swine. 8-th ed. Iowa State University Press, Ames. Pp. 295–326.

Song, D. S., Oh, J. S., Kang, B. K., Yang, J. S., Song, J. Y., Moon, H. J., Kim, T. Y., Yoo, H. S., Jang, Y. S., & Park, B. K. (2005). Fecal shedding of a highly cell-culture-adaptrd porcine epidemic diarrhea virus after oral inoculation in pigs. Journal of Swine Health and Production, 13(5), 269–272.

Srijangwad, A., Stott, C. J., Temeeyasen, G., Senasuthum, R., Chongcharoen, W., Tantituvanont, A., & Nilubol, D. (2017). Immune response of gilts to single and double infection with Porcine epidemic diarrhea virus. Archives of Virology, 162, 2029–2034.

Stevenson, G. W., Hoang, H., Schwartz, K. J., Burrough, E. R., Sun, D., Madson, D., Cooper, V. L., Pillatzki, A., Gauger, P., Schmitt, B. J., Koster, L. G., Killian, M. L., & Yoon, K. J. (2013). Emergence of Porcine epidemic diarrhea virus in the United States: Clinical signs, lesions and viral genomic sequences. Journal of Veterinary Diagnostic Investigation, 25, 649–654.

Strizhakova, O. M. (2013). Isolation and identification of epizootic diarrhea virus in pigs under outbreak at a large farm. Sel'skokhozyaistvennaya Biologiya, 4, 65–69.

Sukontason, K. L., Bunchoo, M., Khantawa, B., Piangjai, S., Rongsriyam, Y., & Sukontason, K. (2007). Comparison between *Musca domestica* and *Chrysomya megacephala* as carriers of bacteria in Northern Thailand. Journal of Tropical Medicine and Public Health, 38(1), 38–44.

Sven, F. M., Heinz, K. M., Kai, S. S., & Pfeffer, M. K. (2007). Pilot study on synanthropic flies (e.g. *Musca*, *Sarcophaga*, *Calliphora*, *Fannia*, *Lucilia*, *Stomoxys*) as vectors of pathogenic microorganisms. Parasitology Research, 101(1), 243–246.

Tun, H. M., Cai, Z., & Khafipour, E. (2016). Monitoring survivability and infectivity of Porcine epidemic diarrhea virus (PEDV) in the infected on-farm Earthen manure storages (EMS). Frontiers in Microbiology, 7, 265–276.

Vlasova, A. N., Marthaler, D., Wang, Q., Culhane, M. R., Rossow, K. D., Rovira, A., Collins, J., & Saif, L. J. (2014). Distinct characteristics and complex evolution of PEDV strains, North America, May 2013 – February 2014. Emerging Infectious Diseases, 20(10), 1620–1628.

Wang, L., Byrum, B., & Zhang, Y. (2014). New variant of Porcine epidemic diarrhea virus, United States. Emerging Infectious Diseases, 20(5), 917–919.

Yeruham, I., Braverman, Y., Shpigel, N. Y., Chizov-Ginzburg, A., Saran, A., & Winkler, M. (1996). Mastitis in dairy cattle caused by *Corynebacterium pseudotuberculosis* and the feasibility of transmission by houseflies. The Veterinary Quarterly, 18(3), 87–89.

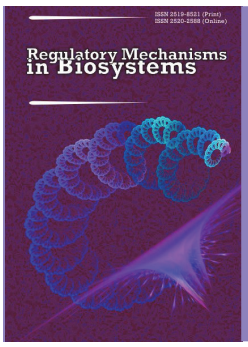

Regulatory Mechanisms in Biosystems

ISSN 2519-8521 (Print)
ISSN 2520-2588 (Online)
Regul. Mech. Biosyst., 9(3), 409–416
doi: 10.15421/021861

Comparative analysis of incidence of leptospirosis among farm animals and humans in Ukraine

V. V. Ukhovskyi*, N. B. Vydayko**, G. B. Aliekseieva***,
M. V. Bezymennyi*, I. M. Polupan***, I. P. Kolesnikova****

**Institute of Veterinary Medicine of National Academy of Agrarian Sciences of Ukraine, Kyiv, Ukraine*
***State Institution Ukrainian Center for Diseases Control and Monitoring of the Ministry of Health of Ukraine, Kyiv, Ukraine*
****State Scientific Research Institute of Laboratory Diagnostic and Veterinary Sanitary Expertise, Kyiv, Ukraine*
*****Bogomolets National Medical University, Kyiv, Ukraine*

Article info

Received 14.06.2018
Received in revised form 21.07.2018
Accepted 28.07.2018

Institute of Veterinary Medicine of National Academy of Agrarian Sciences of Ukraine, Donetska st., 30, Kyiv, 03151, Ukraine. Tel.:+38-067-981-52-26. E-mail: uhovskiy@ukr.net

State Institution Ukrainian Center for Diseases Control and Monitoring of the Ministry of Health of Ukraine, Yaroslavska st., 41, Kyiv, 04071, Ukraine.

State Scientific Research Institute of Laboratory Diagnostic and Veterinary Sanitary Expertise, Donetska st., 30, Kyiv, 03151, Ukraine.

Bogomolets National Medical University, T. Shevchenko blvd., 13, Kyiv, 01601, Ukraine.

Ukhovskyi, V. V., Vydayko, N. B., Aliekseieva, G. B., Bezymennyi, M. V., Polupan, I. M., & Kolesnikova, I. P. (2018). Comparative analysis of incidence of leptospirosis among farm animals and humans in Ukraine. Regulatory Mechanisms in Biosystems, 9(3), 409–416. doi:10.15421/021861

Leptospirosis remains one of the most widespread natural-focal, zoonotic infectious diseases in the world and in Ukraine. Leptospirosis is enzootic in the entire territory of Ukraine. Cases of diseases are registered in all regions of Ukraine. We initiated a study of comparative analysis of territorial distribution of leptospirosis outbreaks among animals and incidence in humans in Ukraine covering the years 2009–2016 inclusive. This study of the incidence of leptospirosis in Ukraine shows a significant circulation of leptospirosis both among humans and animals. Among cattle herds in Ukraine the percentage of positive animals was found to be 4.2% of the surveyed population. The dominant serovars of *Leptospira* were *kabura* (12.4%) and *polonica* (9.5%). Positive reactions with other serovars were observed less frequently: *tarassovi* – 5.1%, *bratislava* – 4.9%, *copenhageni* – 4.1%, *grippotyphosa* – 2.4%, *pomona* – 1.1%, *canicola* – 1.0%. In pigs, the percentage of positive animals amounted to 3.2%, the dominant serovars of *Leptospira* were *bratislava* (29.1%) and *copenhageni* (25.1%). Positive reactions with other serovars were observed less frequently: *tarassovi* – 4.3%, *canicola* – 3.0%, *pomona* – 2.7%, *grippotyphosa* – 1.3%, *polonica* – 1.2%, *kabura* – 0.6%. In horses, the percentage of positive animals amounted to 9.5% of the surveyed population. The serological range of *Leptospira* in horses was as follows: *copenhageni* – 14.2%, *bratislava* – 12.1%, *canicola* – 6.8%, *grippotyphosa* – 4.8%, *tarassovi* – 4.7%, *pomona* – 2.1%, *kabura* – 1.4%, *polonica* – 1.3%. Analysis of the results of research indicates extensive circulation of leptospirosis among humans in Ukraine as evidenced by the percentage of humans positively responding to MAT – 12.1% of the studied samples. The etiological structure of leptospirosis cases includes all the 14 serovars of the diagnostic set. The basis of the etiological spectrum was the serovar *copenhageni* – 37.3%. The share of other serovars as the etiological factor of leptospirosis in humans was different in different spans of the considered period. Most frequently, those were *kabura* – 12.3%, *grippotyphosa* – 11.7%, *canicola* – 9.5%, *pomona* – 9.1%. We mapped annual incidence of leptospirosis in animals and humans. Choropleth maps of annual leptospirosis incidence and cluster maps show opposite spatial patterns for animals and humans. The highest human rates were in the western and central parts of the country while the highest animal rates were mainly in the eastern part.

Keywords: *Leptospira*; etiological structure; microscopic agglutination test; mapping; GIS.

Introduction

Leptospirosis is an infectious disease that affects a large number of mammal species, as well as humans (Ko et al., 2009; Sykes et al., 2011). It has become widespread in many countries around the world (Levett, 2001; Lee et al., 2017; Daud et al., 2018). Leptospirosis is one of the most common and significant natural foci zoonoses and has been diagnosed on five continents (except Antarctica) in most countries of the world (Bharti et al., 2003). Leptospirosis causes huge economic losses in animal husbandry because of its significant incidence among animals, leading to mass abortions and a large number of still births, a decrease in animal productivity, and significant costs incurred in diagnostic research, treatment and prophylactic and quarantine measures (Hartskeerl et al., 2011; Pavlenko et al., 2011). Leptospirosis is a disease of great social significance because leptospirosis infected animals and host animals pose a direct threat to public health, characterized by high mortality of patients in recent years (Santos et al., 2018). Leptospirosis has been reported in over 150 mammalian species (Malalana et al., 2017; Brown et al., 2018; Miyama et al., 2018). In addition, antibodies against *Leptospira* strains can be identified in the blood sera of reptiles and amphibians (Levett, 2001; Adler & Moctezuma, 2010). Among farm animals, this zoonosis is often registered in cattle (Alonso-Andicoberry et al., 2001; Talpada et al., 2008), swine (Hartleben et al., 2013; Pyskun et al., 2016; Bertelloni et al., 2018) and horses (Brem et al., 1999; Arent & Kędzierska-Mieszkowska, 2013; Arent et al., 2016) throughout the world.

The majority of the leading specialists in the study of leptospirosis have studied the etiological structure of the disease, which of course, requires the constant monitoring both farm animals and dogs, synanthropic rodents and residents of natural foci (Stepna et al., 2016). At this stage, one of the main tasks of epidemiological and epizootic monitoring of natural focal infections is to determine enzootic areas of circulation of pathogens, including leptospirosis (Pavlenko et al., 2011).

Analyses of pathogenic *Leptospira* isolated in different countries shows that the etiological structure of leptospirosis in specific areas (dis-

tricts, regions, and countries) is heterogeneous in the number of various serotypes of *Leptospira*, and their ratios. The objective of our study was comparative analysis of the territorial confines of leptospirosis outbreaks among animals and its incidence in humans in Ukraine.

Materials and methods

Analysis of the etiological structure of leptospirosis based on data from animals. The spread and etiological structure of leptospirosis in animals was analyzed according to reports of the State Scientific Research Institute of Laboratory Diagnostics and Veterinary Sanitary Expertise during the years 2009–2016. Sero-prevalence for each region was calculated as the number of leptospirosis positive samples divided by the sample quantity in the region. Calculation of exact binomial 95% confidence intervals (BCI) was performed for sero-prevalence estimates using the R epitools package (https://cran.r-project.org).

Antigens. Cultures of reference strains of *Leptospira* consisting of 8 serovars: *canicola*, *grippotyphosa*, *kabura*, *copenhageni*, *pomona*, *polonica*, *tarassovi* and *bratislava*, were used to perform the microscopic agglutination test (MAT). These diagnostic strains of *Leptospira* used in serological studies on leptospirosis of animals were prepared by veterinary diagnostic laboratories in Ukraine. Leptospirae were cultivated in Korthof liquid medium at 28–30 ºC under aerobic conditions. The strains were subcultured every 7–10 days.

Microscopic agglutination test. The test was carried out according to OIE Manual of Standards for Diagnostic Tests and Vaccines and under the current Regulations (Nastanova z laboratornoi diahnostyky leptospirozu [Guidance on laboratory diagnosis of leptospirosis]. (1997). Zareiestrovana 11.01.1997, No 15–14/2. Ministerstvo Silskoho Hospodarstva i Prodovolstva Ukrainy, Kyiv). Briefly, the serum samples diluted 1 : 25 were mixed with an equal volume of each of the *Leptospira* culture. Serum dilution (including added antigen) used during preliminary examination was 1 : 50. For samples reacting in the preliminary examination with one or more serovars, series of twofold dilutions were prepared to reach the end point – 50% agglutination. The samples with titers equal or higher than 1 : 50 were recognized as positive.

Analysis of etiological structure of leptospirosis based on human data. Spreading and etiological structure of leptospirosis in humans and annual human incidence data per 100,000 population was analyzed according to reports of the State Institution Ukrainian Center for Diseases Control and Monitoring of the Ministry of Health of Ukraine during the years 2009–2016s.

Antigens. Cultures of reference strains of *Leptospira* consisted of 14 serovars: *canicola*, *grippotyphosa*, *kabura*, *copenhageni*, *pomona*, *polonica*, *tarassovi*, *bratislava*, *javanica*, *autumnalis*, *djatzi*, *ballum*, *pyrogenes* and *cynopteri*, were used to perform the MAT. These diagnostic strains of leptospires are used in serological studies on leptospirosis of animals that are conducted by the State Institution Regional Laboratory Center Ministry of Health of Ukraine.

Microscopic agglutination test. The test was carried out under the current Regulations (Protyepidemichni zakhody ta laboratorna diahnostyka leptospirozu. Metodychni vkazivky. MV 9.1.109–02 [Antiepidemic measures and laboratory diagnostics of leptospirosis. Methodological instructions. MI 9.1.109–02]. (2002). Zatverdzhena 11.12.2002, No 39, Kyiv). The serum samples diluted 1 : 50 were mixed with an equal volume of each of the *Leptospira* serovars. Final serum dilution (including added antigen) during preliminary examination was 1 : 100. For samples reacting in the preliminary examination with one or more serovars, a series of twofold dilutions were prepared to reach the end point – 50% of agglutination. The samples with titers equal or higher than 1 : 100 were recognized as positive.

Mapping and spatial analysis. Data on the incidence of leptospirosis in animals and humans in three regions for 2014–2016 were not available (AR Crimea, part of the Luhansk and Donetsk regions) and thus they were not mapped.

To calculate annual incidence per 100,000 animals, population data from the web site (www.ukrstat.gov.ua) of the State Statistics Service of Ukraine were used. The data on all three farm animal species (cattle, swine, horses) were summarized.

Annual incidence by region of both animals and humans was choropleth mapped in ESRI ArcGIS 10.3. Quantile classification with 5 classes of the data was chosen. With this classification, an equal number of regions fall into each class.

To find out and compare the patterns of incidence distribution among animals and humans at the regional level, we applied the local Moran I statistics at a statistical significance $P < 0.05$ using 999 permutations in the software GeoDa 1.10.0.8. In the analysis, we applied the first order rook contiguity matrix, where the regions adjoining their boundaries are considered neighbours. Local Moran I statistics reveals both clusters of similar values, and areas dissimilar to their neighbours – spatial outliers. On the maps B, areas with a high incidence rate, surrounded by high-value areas are designated High-High, areas with a low value surrounded by areas with a low values – Low-Low. Areas with a high incidence of disease surrounded by neighbours with low values are designated High-Low, areas with a low incidence rate surrounded by high values are Low-High.

Results

During the years 2009–2016, 1,238,876 samples of cattle sera were investigated by veterinary diagnostic laboratories of Ukraine and 52,310 reacted positive for leptospirosis. Analysis of the results indicates extensive circulation of leptospirosis among cattle herds in Ukraine as evidenced by the percentage of cattle positively responding to MAT, which is 4.2% (BCI, 4.2–4.3%) of the studied samples.

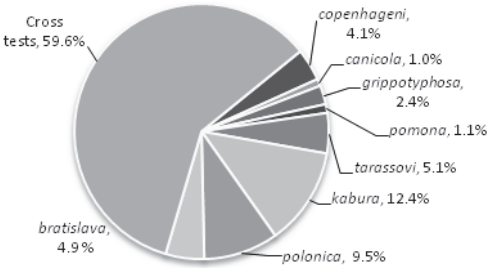

Fig. 1. Etiological structure of leptospirosis in cattle in Ukraine (2009–2016 years)

As shown in Figure 1 the dominant serovars of *Leptospira* were kabura (12.4%; BCI, 12.1–12.7%) and polonica (9.5%; BCI, 9.2–9.7%). Positive reactions with other serovars were observed less frequently: *tarassovi* – 5.1% (BCI, 4.9–5.3%), *bratislava* – 4.9% (BCI, 4.7–5.1%), *copenhageni* – 4.1% (BCI, 4.0–4.3%), *grippotyphosa* – 2.4% (BCI, 2.3–2.6%), *pomona* – 1.1% (BCI, 1.0–1.2%), *canicola* – 1.0% (BCI, 0.9–1.0%). The proportion of the cattle disease cases where antibodies to multiple serovars of *Leptospira* (cross tests) were detected was 59.6% (BCI, 58.9–60.2%).

During this period, 989,659 samples of pigs' sera were tested by veterinary laboratories in Ukraine and 31,181 samples were regarded as positive for leptospirosis, which amounted to 3.2% (BCI, 3.1–3.2%) of the surveyed population.

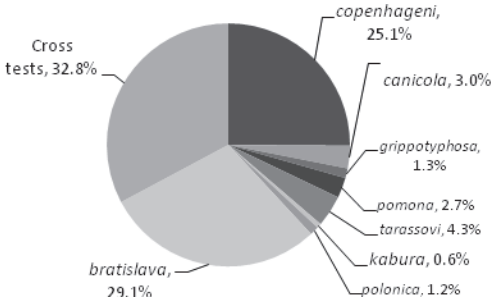

Fig. 2. Etiological structure of leptospirosis in pigs in Ukraine (2009–2016 years)

As shown in Figure 2, the dominant serovars of *Leptospira* were *bratislava* (29.1%; BCI, 28.5–29.7%) and *copenhageni* (25.1%; BCI,

24.6–25.7%). Positive reactions with other serovars were observed less frequently: *tarassovi* – 4.3% (BCI, 4.0–4.5%), *canicola* – 3.0% (BCI, 2.8–3.2%), *pomona* – 2.7% (BCI, 2.5–2.9%), *grippotyphosa* – 1.3% (BCI, 1.2–1.4%), *polonica* – 1.2% (BCI, 1.1–1.4%), *kabura* – 0.6% (BCI, 0.5–0.7%). The proportion of the pigs' disease cases where antibodies to multiple serovars of *Leptospira* a (cross tests) were detected was 32.8% (BCI, 32.1–33.4%).

During the years 2009–2016, 70,674 samples of sera from horses were examined in Ukraine and 6,734 samples were regarded as positive for leptospirosis. Analysis of the results of testing, indicates extensive circulation of leptospirosis among horses in Ukraine, which amounted to 9.5% (BCI, 9.3–9.8%) of the surveyed population.

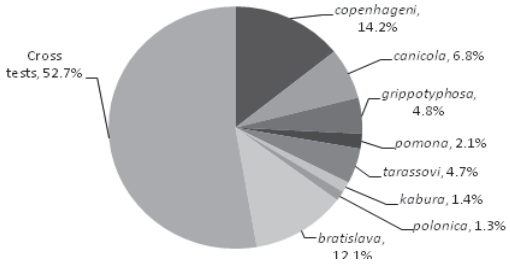

Fig. 3. Etiological structure of leptospirosis in horses in Ukraine (2009–2016 years)

The serological range of *Leptospira* in horses was as follows: *copenhageni* – 14.2% (BCI, 13.3–15.1%), *bratislava* – 12.1% (BCI, 11.3–13.0%), *canicola* – 6.8% (BCI, 6.2–7.4%), *grippotyphosa* – 4.8% (BCI, 4.3–5.3%), *tarassovi* – 4.7% (BCI, 4.2–5.2%), *pomona* – 2.1% (BCI, 1.7–2.4%), *kabura* – 1.4% (BCI, 1.1–1.7%), *polonica* – 1.3% (BCI, 1.1–1.6%). In 52.7% (BCI, 51.0–54.4%) of positively reacting sera, antibodies to *Leptospira* of multiple serovars were detected (Fig. 3).

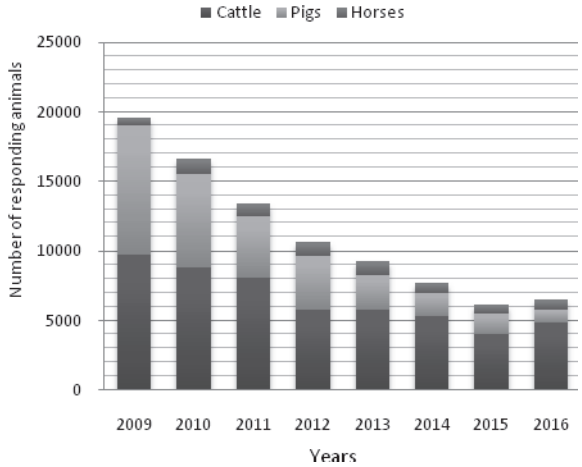

Fig. 4. Dynamics of leptospirosis infection in animals in Ukraine (2009–2016 years)

As shown in Figure 4, leptospirosis infection in animals for the analyzed period was the highest in 2009 – 19,611 positive samples of leptospirosis, the lowest in 2015 – 6,131 positive samples. During the period from 2009 to 2016, there has been a tendency towards reduction in cases of *Leptospira* infection in animals.

During the years 2009–2016, 24,990 samples of human sera were investigated by the State Institution Ukrainian Centre for Diseases Control and Monitoring of the Ministry of Health of Ukraine and 3,012 samples were regarded as positive for leptospirosis. Analysis of the results of research indicates extensive circulation of leptospirosis among humans in Ukraine as evidenced by the percentage humans of positively responding to MAT, which is 12.1% (BCI, 11.7–12.5%) of the studied samples. The etiological structure of leptospirosis cases included all the 14 serovars of the diagnostic set. As shown in Fig. 5, the basis of the etiological spectrum was the serovar *copenhageni* – 37.3% (BCI, 35.2–39.5%). The share of other serovars as the etiological factor of leptospirosis in humans was different in different spans of the considered period. Most frequently, those were *kabura* – 12.3% (BCI, 11.0–13.6%), *grippotyphosa* – 11.7% (BCI, 10.5–13.0%), *canicola* – 9.5% (BCI, 8.5–10.7%), *pomona* – 9.1% (BCI, 8.0–10.2%). Positive reactions with other serovars were observed less frequently: *bratislava* – 4.4% (BCI, 3.7–5.2%), *javanica* – 4.0% (BCI, 3.3–4.8%), *autumnalis* – 2.7% (BCI, 2.1–3.3%), *cynopteri* – 2.2% (BCI, 1.7–2.8%), *ballum* – 2.1% (BCI, 1.6–2.6%), *tarassovi* – 2.0% (BCI, 1.6–2.6%), *djatzi* – 1.4% (BCI, 1.0–1.9%), *pyrogenes* – 0.8% (BCI, 0.5–1.2%), *polonica* – 0.6% (BCI, 0.3–0.9%) (Fig. 5).

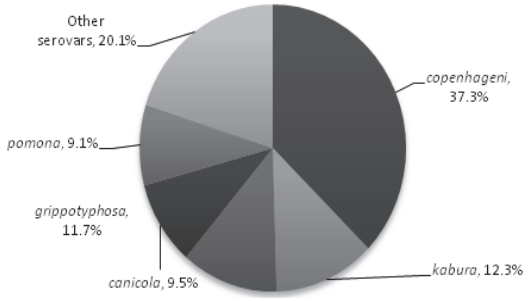

Fig. 5. Etiological structure of leptospirosis in humans in Ukraine (2009–2016 years)

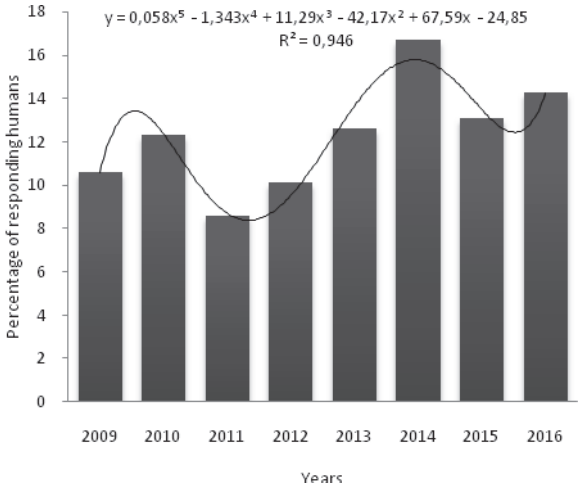

Fig. 6. Dynamics of leptospirosis infection in humans in Ukraine (2009–2016 years)

As shown in Figure 6, leptospirosis infection in humans for the analyzed period was the highest in 2014 – 16.7%, the lowest in 2011 – 8.6% positive samples. During the period from 2009 to 2016, there has been a tendency to increase in cases of leptospirosis infection in humans.

Choropleth maps of annual leptospirosis incidence and cluster maps show opposite spatial patterns for animals and humans (Fig. 7–14). The highest human rates are in western and central parts of the country while the highest animal rates are mainly in the eastern part.

The same opposite pattern was shown by cluster maps. Human High-High clusters are present for 2009–2010 and 2014 in the west. Human Low-Low clusters located in the east over all years but 2016. In 2016 no statistical significant human clusters were revealed.

Animal High-High clusters were found for all years in the east and Low-Low clusters located in western part of Ukraine.

Discussion

This study shows a significant circulation of leptospirosis both among humans and animals in Ukraine. Among cattle herds, the percentage of reacting positive animals is 4.2% (BCI, 4.2–4.3%), in pigs it amounted to 3.2% (BCI, 3.1–3.2%) and in horses it amounted to 9.5% (BCI, 9.3–9.8%) of the surveyed population. Analysis of the results of research indicates extensive circulation of leptospirosis among humans in Ukraine as evidenced by the percentage of positively responding to MAT humans – 12.1% (BCI, 11.7–12.5%) of the studied samples. It was established that the epizootic situation concerning animal leptospirosis and

incidence of leptospirosis in humans in different regions of Ukraine differ both in the etiological structure of agents, and the number of cases. During the analysis of the leptospirosis circulation, we examined for the period 2009–2016 a large number of specimens from animals and people from all over the country: cattle – 1,238,876 samples, pigs – 989,659, horses – 70,674 samples of sera and 24,990 samples of sera of humans.

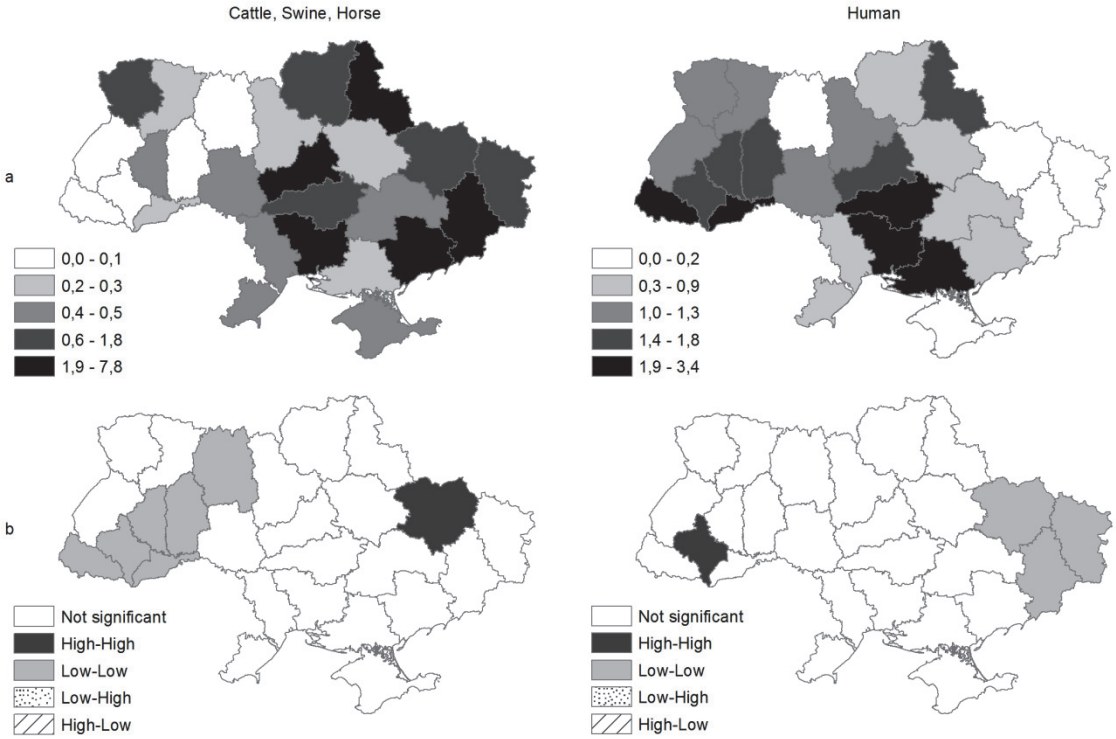

Fig. 7. Distribution of animal and human leptospirosis cases in Ukraine (2009 year): *a* – animal and human leptospirosis incidence per 100,000 at region level, *b* – cluster and outlier maps of animal and human leptospirosis incidence

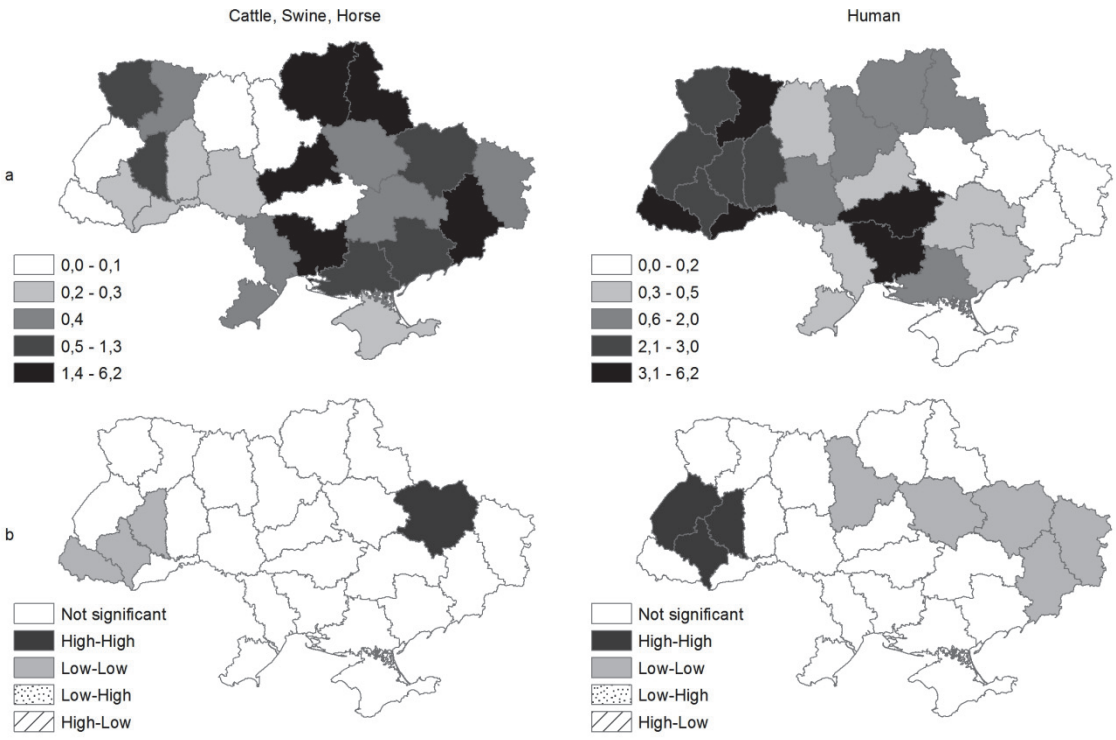

Fig. 8. Distribution of animal and human leptospirosis cases in Ukraine (2010 year): *a* – animal and human leptospirosis incidence per 100,000 at region level, *b* – cluster and outlier maps of animal and human leptospirosis incidence

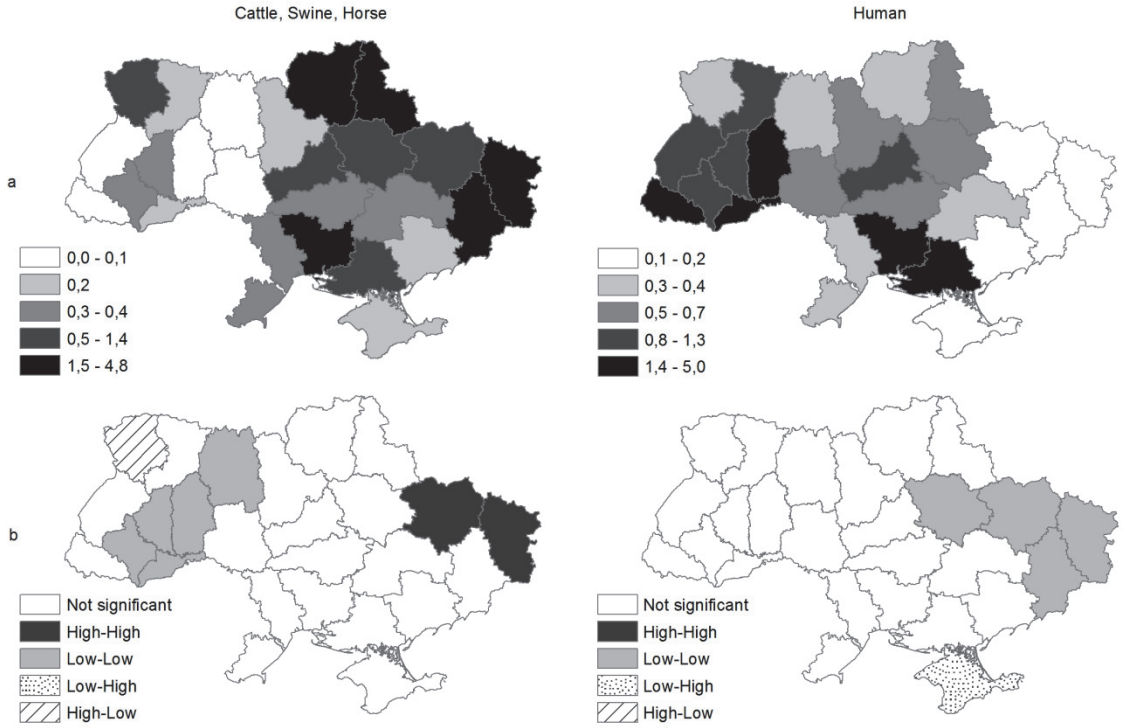

Fig. 9. Distribution of animal and human leptospirosis cases in Ukraine (2011 year): *a* – animal and human leptospirosis incidence per 100,000 at region level, *b* – cluster and outlier maps of animal and human leptospirosis incidence

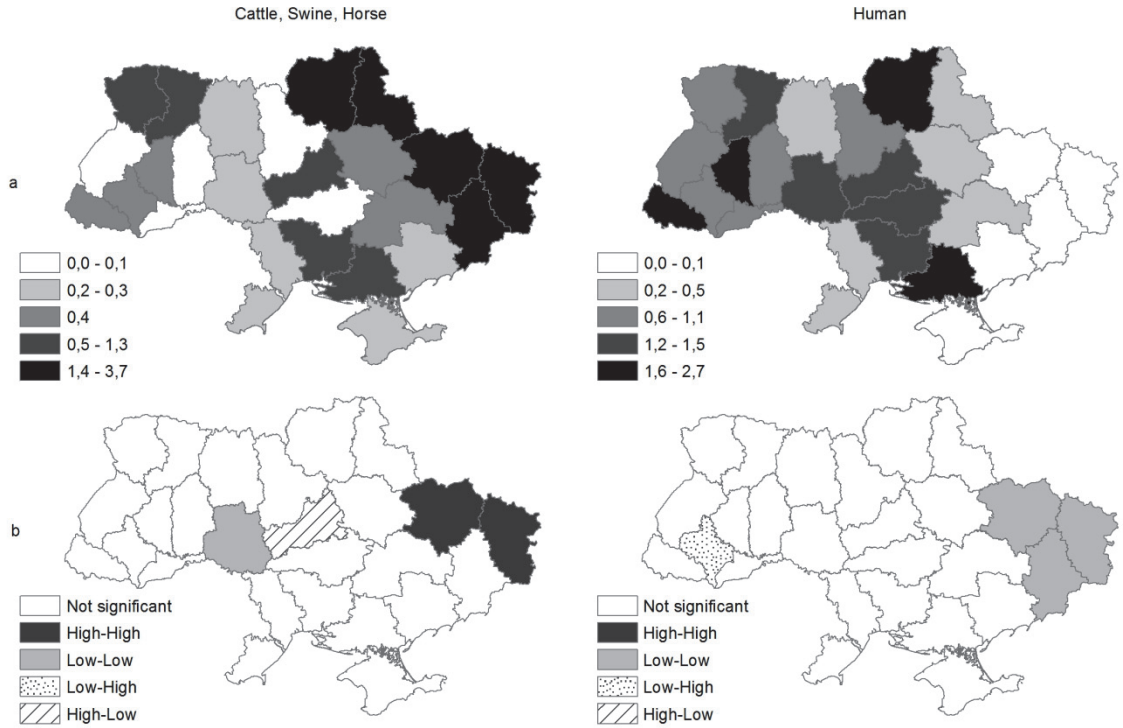

Fig. 10. Distribution of animal and human leptospirosis cases in Ukraine (2012 year): *a* – animal and human leptospirosis incidence per 100,000 at region level, *b* – cluster and outliers maps of animal and human leptospirosis incidence

Regarding the limitations of our research, it should be noted that we did not take into account the distribution and etiological structure of leptospirosis in dogs in Ukraine, since studies of leptospirosis in dogs are conducted mainly on the request of private veterinary clinics, and there is no official state programme for monitoring this disease in dogs. At the same time, leptospirosis in dogs constitutes a significant threat of transmission of leptospirosis to humans (Whitney et al., 2009; Sykes et al., 2011). Leptospirosis is a zoonosis, so cases of this disease in people are observed in areas where there are animals sick with leptospirosis or there are animal hosts (Witkowski et al., 2016; Guernier et al., 2017). Choropleth maps of annual leptospirosis incidence and cluster maps show opposite spatial patterns for animals and humans (Fig. 7–14). The highest human rates are in western and central parts of the country while the highest animal rates are mainly in the eastern part.

In our opinion, there are two main reasons for the opposite spatial patterns for animals and humans. The first reason is the difference in the causes of the spread of leptospirosis in humans and animals (Flores et al., 2017; Rajala et al., 2017). The most important reasons for the widespread distribution of leptospirosis in animals in Ukraine are inadequate animal welfare, and frequent and uncontrolled movement of them from farm to farm (Malakhov et al., 2000; Sykes et al., 2011). At the same time, natural conditions and rodent population have a secondary role in the occurrence of leptospirosis among animals. In contrast to animals, the main cause of infection in humans are rodents (rats and mice) (Stepna et al., 2016; Santos et al., 2018), insufficient rodent control and natural conditions. The main path of infection with *Leptospira* in Ukraine to humans, in contrast to leptospirosis of animals, is through water (swimming, fishing, working in wet areas, etc.) (Whitney et al., 2009; Barragan et al., 2016; Pinto et al., 2017). The proportion of people with leptospirosis associated with reservoirs and wet places is 50.7%; transmission through food related to the objects of epidemic – 2.2%; contact and household, connected with settlements – 31.9%; not established – 15.2% (Information report on the epidemic situation with leptospirosis in Ukraine in 2016).

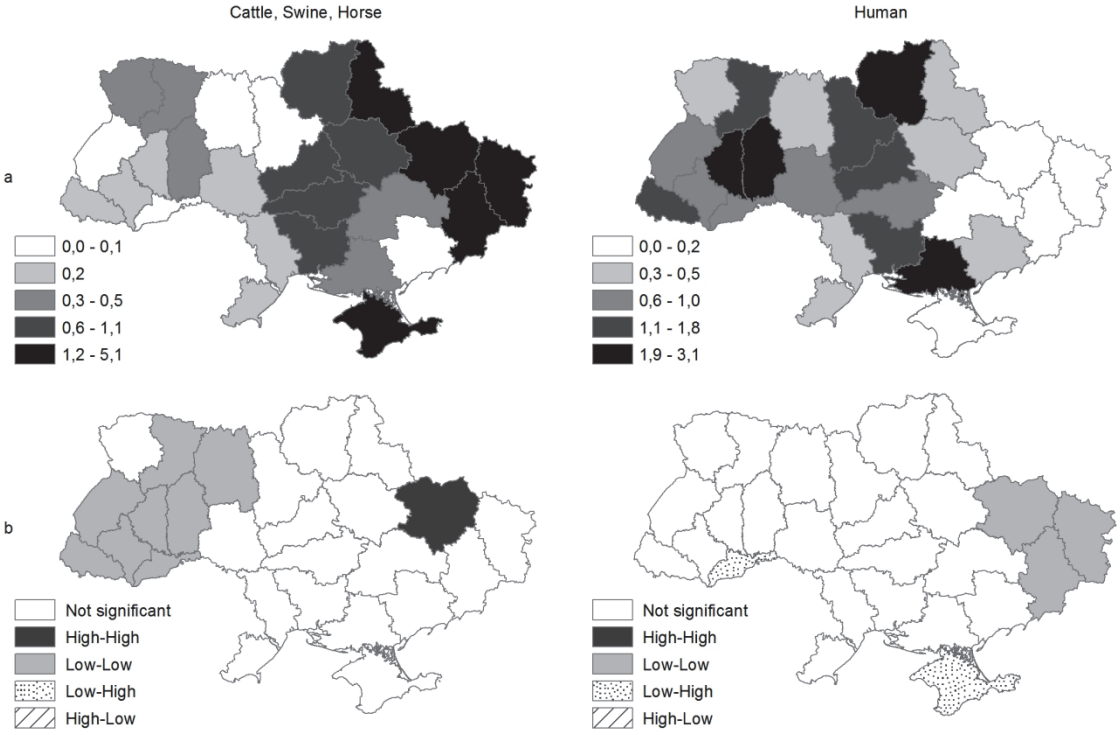

Fig. 11. Distribution of animal and human leptospirosis cases in Ukraine (2013 year): *a* – animal and human leptospirosis incidence per 100,000 at region level, *b* – cluster and outlier maps of animal and human leptospirosis incidence

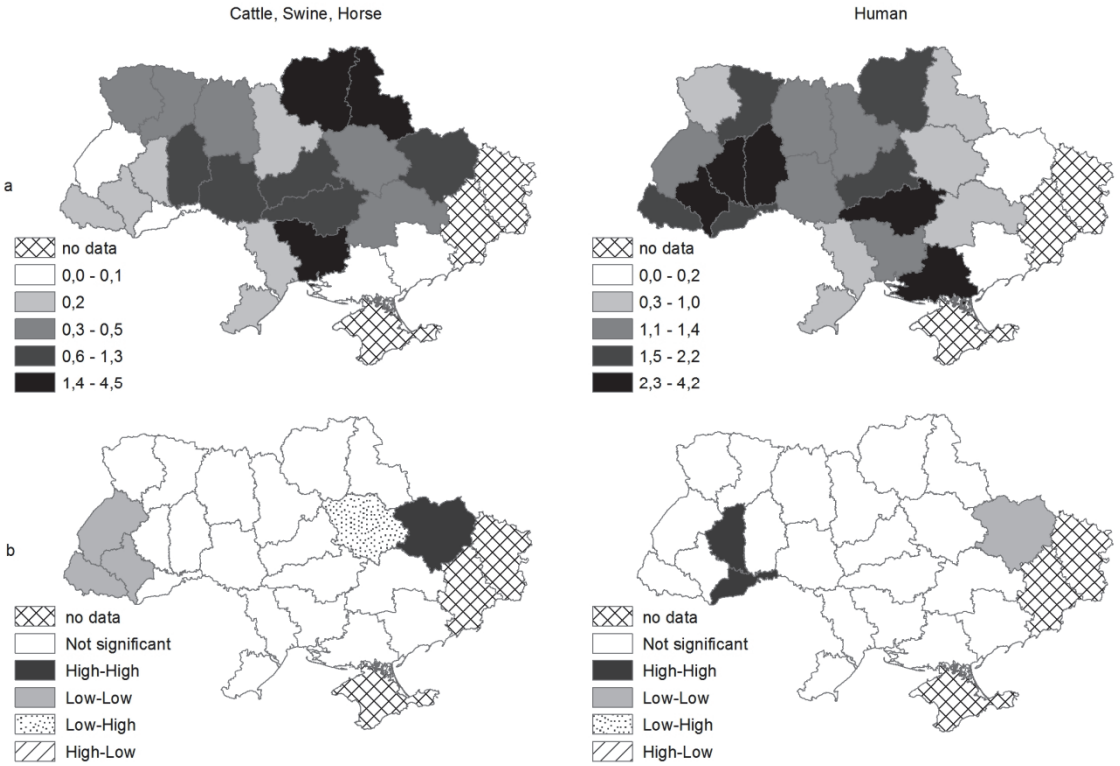

Fig. 12. Distribution of animal and human leptospirosis cases in Ukraine (2014 year): *a* – animal and human leptospirosis incidence per 100,000 at region level, *b* – cluster and outlier maps of animal and human leptospirosis incidence

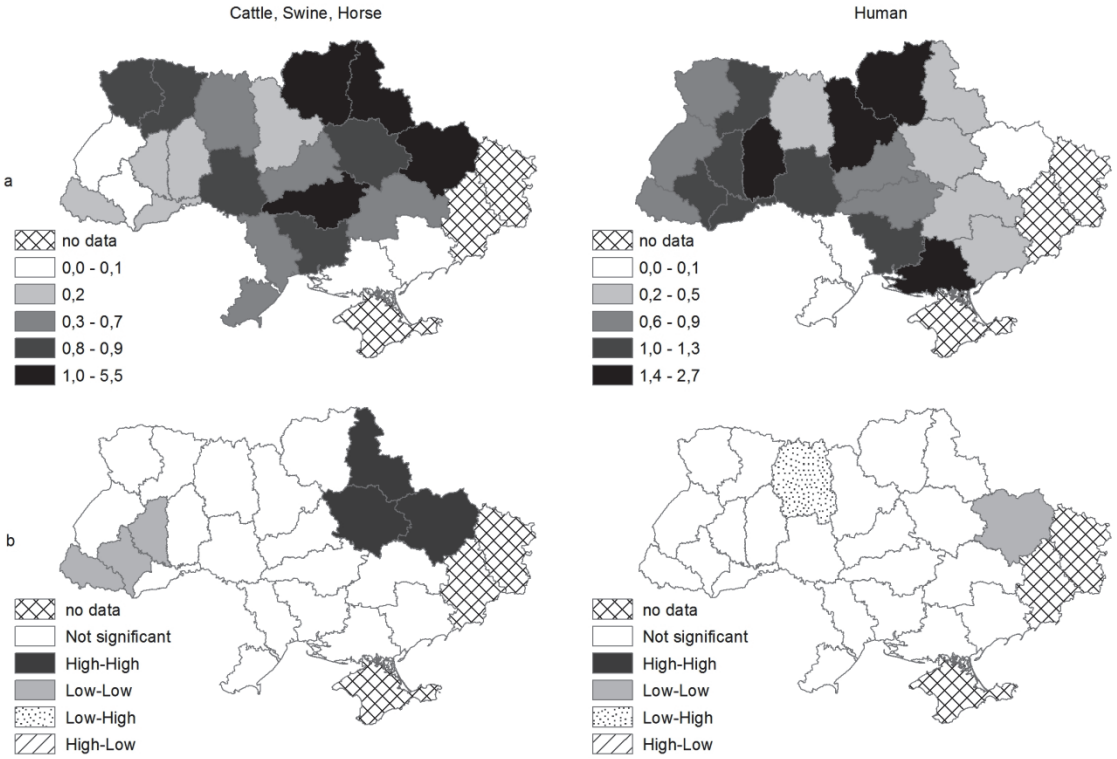

Fig. 13. Distribution of animal and human leptospirosis cases in Ukraine (2015 year): *a* – animal and human leptospirosis incidence per 100,000 at region level, *b* – cluster and outlier maps of animal and human leptospirosis incidence

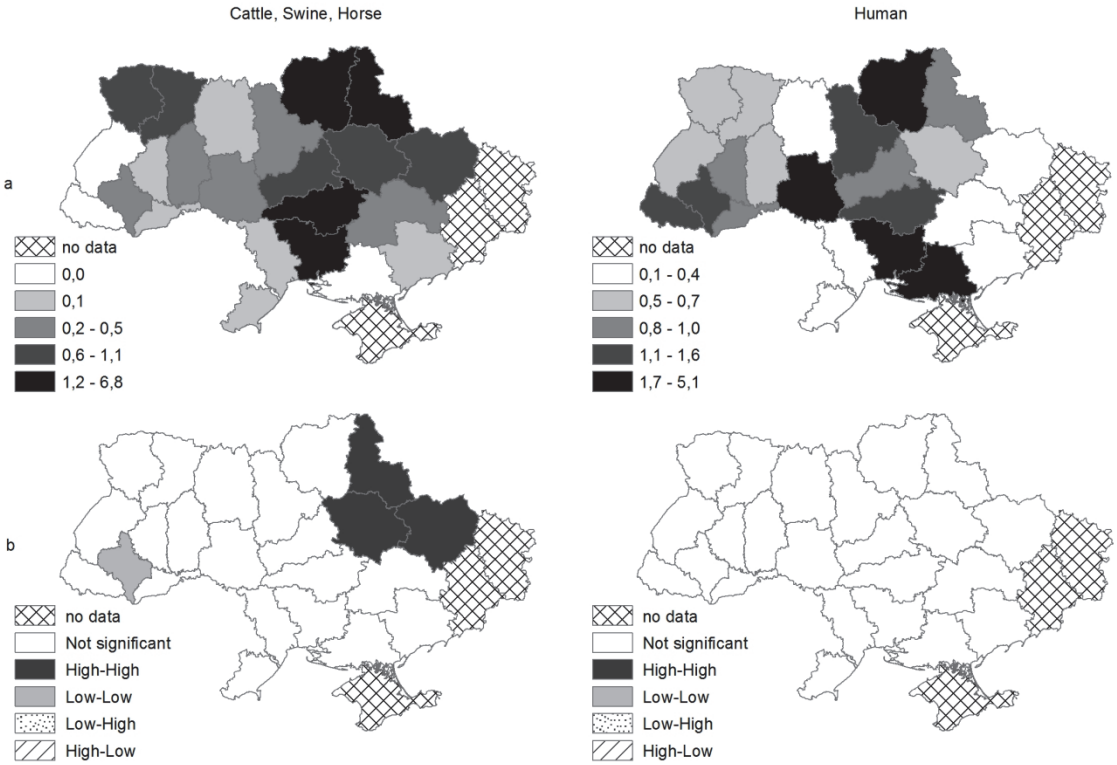

Fig. 14. Distribution of animal and human leptospirosis cases in Ukraine (2016 year): *a* – animal and human leptospirosis incidence per 100,000 at region level, *b* – cluster and outlier maps of animal and human leptospirosis incidence

The second reason, in our opinion, is underestimation and possible underreporting of cases in animals and insufficient monitoring of leptospirosis in animals. This applies particularly to the western regions of Ukraine (Ukhovskyi et al., 2015).

Conclusion

Based on the results of monitoring studies of the territory of Ukraine, we found that leptospirosis is widespread both among livestock and also among people. The average sero-prevalence for 8 years (2009–2016) was: among cattle herds – 4.2% of the surveyed population, in pigs up to 3.2%, in horses up to 9.5% and in humans – 12.1% of the studied samples. It was determined that the spectrum of leptospirosis of agricultural animals and humans in Ukraine had peculiarities both within the range of serovars and their significance for the total pathology of the disease. The dominant serovar *Leptospira* circulating within the territory of Ukraine were: in cattle – *kabura* and *polonica*, in pigs – *copenhageni* and *bratislava*, in horses – *copenhageni*, *bratislava* and *canicola*, in

humans – *copenhageni*. Based on the results of a comparative analysis of incidence of leptospirosis among farm animals and humans in the territory of Ukraine, it was established that animals and humans manifest opposite patterns. The highest animal leptospirosis rates were detected mainly in the eastern part while the highest human leptospirosis rates were in the western and central parts of the country. This information on the distribution of leptospirosis in animals and humans can help to improve and optimize the planning and development of specific preventive measures against leptospirosis in Ukraine.

References

Adler, B., & Moctezuma, A. (2010). *Leptospira* and leptospirosis. Veterinary Microbiology, 27, 287–296.

Alonso-Andicoberry, C., García-Peña, F. J., Pereira-Bueno, J., Costas, E., & Ortega-Mora, L. M. (2001). Herd-level risk factors associated with *Leptospira* spp. seroprevalence in dairy and beef cattle in Spain. Preventive Veterinary Medicine, 52(2), 109–117.

Anselin, L. (1995). Local indicators of spatial association – LISA. Geographical Analysis, 27, 93–115.

Arent, Z. J., & Kędzierska-Mieszkowska, S. (2013). Seroprevalence study of leptospirosis in horses in Northern Poland. Veterinary Record, 172(10), 269.

Arent, Z., Frizzell, C., Gilmore, C., Allen, A., & Ellis, W. A. (2016). *Leptospira interrogans* serovars *bratislava* and muenchen animal infections: Implications for epidemiology and control. Veterinary Microbiology, 190, 19–26.

Barragan, V., Chiriboga, J., Miller, E., Olivas, S., Birdsell, D., Hepp, C., Hornstra, H., Schupp, J. M., Morales, M., Gonzalez, M., Reyes, S., de la Cruz, C., Keim, P., Hartskeerl, R., Trueba, G., & Pearson, T. (2016). High *Leptospira* diversity in animals and humans complicates the search for common reservoirs of human disease in rural Ecuador. Neglected Tropical Diseases, 10(9), 49–59.

Bertelloni, F., Turchi, B., Vattiata, E., Viola, P., Pardini, S., Cerri, D., & Fratini, F. (2018). Serological survey on *Leptospira* infection in slaughtered swine in North-Central Italy. Epidemiology and Infection, 146(10), 1275–1280.

Bharti, A. R., Nally, J. E., Ricaldi, J. N., Matthias, M. A., Diaz, M. M., Lovett, M. A., Levett, P. N., Gilman, R. H., Willig, M. R., Gotuzzo, E., & Vinetz, J. M. (2003). Leptospirosis: A zoonotic disease of global importance. Lancet Infectious Diseases, 3, 757–771.

Brem, S., Gerhards, H., Wollanke, B., Meyer, P., & Kopp, H. (1999). 35 *Leptospira* isolated from the vitreous body of 32 horses with recurrent uveitis (ERU). Berliner und Münchener Tierärztliche Wochenschrift, 112(10–11), 390–393.

Brown, V. R., Bowen, R. A., & Bosco-Lauth, A. M. (2018). Zoonotic pathogens from feral swine that pose a significant threat to public health. Transboundary and Emerging Diseases, 65(3), 649–659.

Daud, A., Fuzi, N., Arshad, M., Kamarudin, S., Mohammad, W., Amran, F., & Ismail, N. (2018). Leptospirosis seropositivity and its serovars among cattle in Northeastern Malaysia. Veterinary World, 11(6), 840–844.

Flores, B. J., Pérez-Sánchez, T., Fuertes, H., Sheleby-Elías, J., Múzquiz, J. L., Jirón, W., Duttmann, C., & Halaihel, N. (2017). A cross-sectional epidemiological study of domestic animals related to human leptospirosis cases in Nicaragua. Acta Tropica, 170, 79–84.

Guernier, V., Richard, V., Nhan, T., Rouault, E., Tessier, A., & Musso, D. (2017). *Leptospira* diversity in animals and humans in Tahiti, French Polynesia. Neglected Tropical Diseases, 11(6), 56–76.

Hartleben, C. P., Leal, F. M., Monte, L. G., Hartwig, D. D., Seixas, F. K., Vasconcellos, S. A., Brihuega, B., & Dellagostin, O. A. (2013). Serological analysis by enzyme-linked immunosorbent assay using recombinant antigen LipL32 for the diagnosis of swine leptospirosis. Current Microbiology, 66(2), 106–109.

Hartskeerl, R. A., Collares-Pereira, M., & Ellis, W. A. (2011). Emergence, control and re-emerging leptospirosis: Dynamics of infection in the changing world. Clinical Microbiology and Infection, 17, 494–501.

Ko, A. L., Goarant, C., & Picardeau, M. (2009). Leptospira: The dawn of the molecular genetics era for an emerging zoonotic pathogen. Nature Reviews Microbiology, 7, 737–747.

Lee, H. S., Khong, N. V., Xuan, H. N., Nghia, V. B., Nguyen-Viet, H., & Grace, D. (2017). Sero-prevalence of specific *Leptospira* serovars in fattening pigs from 5 provinces in Vietnam. BMC Veterinary Research, 13(1), 125.

Levett, P. (2001). Leptospirosis. Clinical Microbiology Reviews, 14(2), 296–326.

Malakhov, Y., Panin, A., & Soboleva, G. (2000). Leptospiroz zhivotnyh [Leptospirosis of animals]. DIA-press, Yaroslavl (in Russian).

Malalana, F., Blundell, R. J., Pinchbeck, G. L., & Mcgowan, C. M. (2017). The role of *Leptospira* spp. in horses affected with recurrent uveitis in the UK. Equine Veterinary Journal, 49(6), 706–709.

Miyama, T., Watanabe, E., Ogata, Y., Urushiyama, Y., Kawahara, N., & Makita, K. (2018). Herd-level risk factors associated with *Leptospira* Hardjo infection in dairy herds in the Southern Tohoku, Japan. Preventive Veterinary Medicine, 149, 15–20.

Pavlenko, A. L., Hajtovich, A. B., Kovalenko, I. S., & Shvarsalon, N. K. (2011). Ekoregionalnye osobennosti ehnzootichnyh territorij leptospiroza v Ukraine [Ecological end regional features of enzootic areas of leptospirosis in Ukraine]. Profilaktychna Medycyna, 14, 63–69 (in Russian).

Pinto, P. S., Libonati, H., & Lilenbaum, W. (2017). A systematic review of leptospirosis on dogs, pigs, and horses in Latin America. Tropical Animal Health and Production, 49(2), 231–238.

Pinto, P. S., Pestana, C., Medeiros, M. A., & Lilenbaum, W. (2017). Plurality of *Leptospira* strains on slaughtered animals suggest a broader concept of adaptability of leptospires to cattle. Acta Tropica, 172, 156–159.

Pyskun, A. V., Spiridonov, V. G., Ukhovskyi, V. V., Rybalchenko, D. Y., & Homenko, Y. V. (2016). The validation of enzyme-linked immunosorbent assay for diagnosis leptospirosis among dogs, pigs and cattle. Veterinary Medicine, Biotechnology and Biosafety, 2(1), 11–15.

Rajala, E. L., Sattorov, N., Boqvist, S., & Magnusson, U. (2017). Bovine leptospirosis in urban and peri-urban dairy farming in low-income countries: A "one health" issue? Acta Veterinaria Scandinavica, 59(1), 83.

Santos, I. O., Landi, M. F., Lima, E. M., Cruz, L. M., Bofill, M. I., Santos, D. E., & Castro, M. B. (2018). Socio-epidemiological characterization of human leptospirosis in the Federal District, Brazil, 2011–2015. Revista da Sociedade Brasileira de Medicina Tropical, 51(3), 372–375.

Stepna, O., Rodyna, N., Ukhovskyi, V., & Kulikova, V. (2016). The research of circulation of pathogenic *Leptospira* among populations urban brown rats in Kyiv, Ukraine. Veterinary Medicine, Biotechnology and Biosafety, 2(1), 5–10.

Sykes, J. E., Hartmann, K., Lunn, K. F., Moore, G. E., Stoddard, R. A., & Goldstein, R. E. (2011). 2010 ACVIM small animal consensus statement on leptospirosis: Diagnosis, epidemiology, treatment and prevention. Journal of Veterinary Internal Medicine, 25(1), 1–13.

Talpada, M. D., Garvey, N., Sprowls, R., Eugster, A. K., & Vinetz, J. M. (2003). Prevalence of leptospiral infection in Texas cattle: Implications for transmission to humans. Vector Borne and Zoonotic Diseases, 3(3), 141–147.

Ukhovskyi, V. V., Alekseeva, G. B., Bezymennyy, M. V., & Kulykova, V. V. (2015). Analysis of the circulation of pathogens on leptospirosis in catle in Ukraine using GIS-technology. Veterinary Biotechnology, 26, 250–262.

Whitney, E. A., Ailes, E., Myers, L. M., Saliki, J. T., & Berkelman, R. L. (2009). Prevalence of and risk factors for serum antibodies against *Leptospira* serovars in US veterinarians. Journal of the American Veterinary Medical Association, 234(7), 938–944.

Witkowski, L., Cywinska, A., Paschalis-Trela, K., Crisman, M., & Kita, J. (2016). Multiple etiologies of equine recurrent uveitis – A natural model for human autoimmune uveitis: A brief review. Comparative Immunology, Microbiology and Infectious Diseases, 44, 14–20.

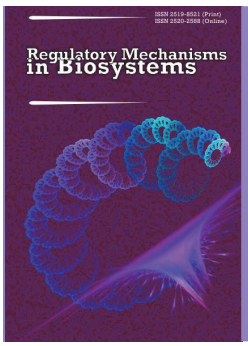

Regulatory Mechanisms in Biosystems

ISSN 2519-8521 (Print)
ISSN 2520-2588 (Online)
Regul. Mech. Biosyst., 9(3), 417–425
doi: 10.15421/021862

The features of summary background electric activity of the hypothalamus of rats under conditions of chronic caffeine alimentation

T. G. Turitskaya*, S. N. Lukashev**, V. P. Lyashenko*, G. G. Sidorenko***

**Oles Honchar Dnipro National University, Dnipro, Ukraine*
***Regional Clinical Hospital n.a. Mechnikov, Dnipro, Ukraine*
****Dnipro National University of Railway Ttransport n.a. Academician V. Lazaryan, Dnipro, Ukraine*

Article info

Received 09.07.2018
Received in revised form 14.08.2018
Accepted 17.08.2018

Oles Honchar Dnipro National University, Gagarin ave., 72, Dnipro, 49010, Ukraine. Tel.: +38-056-372-58-76. E-mail: tatyana.turickaya@gmail.com

Regional Clinical Hospital n.a. Mechnikov, Soborny District, 14, Dnipro, 49005, Ukraine. Tel.: +38-056-246-65-55. E-mail: dr.lukashev@gmail.com

Dnipro National University of Railway Transport n.a. Academician V. Lazaryan, Lazaryana st., 2, Dnipro, 49010, Ukraine. Tel.: +38-056-776-59-47. E-mail: morepisem83@gmail.com

Turitskaya, T. G., Lukashev, S. N., Lyashenko, V. P., & Sidorenko, G. G. (2018). The features of summary background electric activity of the hypothalamus of rats under conditions of chronic caffeine alimentation. Regulatory Mechanisms in Biosystems, 9(3), 417–425. doi:10.15421/021862

One of the factors of the environment which essentially shifts homeostasis is diets which contain caffeine. The aim of the study was to find out the basic characteristics of background electrical activity of trophotrophic and ergotrophic zones of the hypothalamus in conditions of chronic caffeine alimentation. Experiments were carried out on non-linear white male rats. The first group consisted of control animals (n = 22). The second group (n = 24) was represented by the animals that were given pure caffeine in an amount of 150 mg/kg/day with their meal. The registration on a electrohypothalamogram was carried out in conditions of acute experiment, every 2 weeks for 12 weeks. The spectral (mkV^2) and the normalized power (%) of electrohypothalamogram waves were analyzed within the common frequency band. The analysis of the results allowed us to establish a certain specificity of the reaction of the neuronal system of the trophotropic and ergotropic zones of the rat hypothalamus to the effect of chronic caffeine alimentation. The main difference in the reactive state of electrophysiological indices in the trophotrophic zone of rats is the lack of a typical desynchronization from the 4th to the 8th week of the study and the hypersynchronization after 12 weeks of the experiment. The most probable mechanism that explains the results obtained is the ultra-powerful GABA-ergic modulation of this zone, the main energy-accumulating center. Perhaps, this powerful inhibitory resource in this cerebral locus is the main stress-limiting factor that makes this zone of the central nervous system of rats less sensitive to caffeine exposure. Instead, under the influence of chronic caffeine load in the ergotropic zone of the hypothalamus, after 6 weeks of the experiment desynchronous high-frequency rhythms dominated. During the subsequent time of the experiment, we observed a decrease in both low-frequency and high-frequency components of the electrohypothalamogram of this zone. This gives reason to assume that the key component of the neurophysiological response of the posterior hypothalamus of rats to the caffeine ration is the powerful glutamatergic effects on the pre-synaptic and post-synaptic neurons under conditions of reactive exhaustion of local neurosynthetics. Caffeine depletion of the hypothalamic neurotransmission at the end of the experiment is replaced by an effective adaptive ergotropic restoration of neurosynthetic activity in this locus of the central nervous system of rats. Thus, caffeine has a powerful activating effect on the ergotropic function of the posterior hypothalamus of rats. Such a difference in the chronic effect of caffeine on the trophotropic and ergotropic zone of the rat hypothalamus is primarily due to the different mediator support of these zones underlying their physiological purpose. GABA is the main mediator of the trophotropic zone and the main neurotransmitter of its synchronous activity. At the same time, neurotransmitter support of the ergotropic zone is represented by glutamate, which, along with other agents, implements its desynchronous activity. Since caffeine stimulates excitation, activating the pathways traditionally associated with motivational and motor reactions in the brain, it can be assumed that this explains the fact of a more powerful influence of caffeine precisely on the ergotrophic zone of the hypothalamus.

Keywords: brain activity; trophotropic and ergotropic zone of the hypothalamus; sodium caffeine benzoate; rat; chronic caffeine alimentation.

Introduction

The hypothalamus plays a key role in controlling a wide range of vegetative, humoral and behavioral responses. From this point of view, the complex of such reactions has rather prolonged and ambiguous homeostatic consequences (Yoo & Blackshaw, 2018). At the same time, the hypothalamus is quite sensitive to the metabolic status of the organism. Using the principle of negative feedback, this structure still prenatally controls the hormonal axis of the sexual, adrenal steroid hormones and thyroid hormones (Sominsky et al., 2018). The hypothalamus is the central chain of maintenance of a certain vegetative tone and the provision of any activity. Functional classification of the hypothalamus identifies the areol nuclei of the ergo- and trophotropic zones that control the autonomic balance and have different neurotransmitter assistances. The gamma of neuro-endorrhizal reactions of the hypothalamus is also manifested in a certain emotional state and in the direction of complex behavioral reactions (Kalsbeek et al., 2014). It is known that the launch and regulation of stress reactions are carried out by the structures of the reticulum-limbic-neo-cortical system of the brain, the leading role in which belongs to the hypothalamus. There are many scientific papers that highlight the role of these nervous structures in providing adaptive-compensatory responses in organ systems and adaptive behavior formation (Meerson, 1993; Pshennikova, 2000; Vejn, 2003; Baldwin, 2006; Kazakov & Natrus, 2005). With the help of biochemical, mor-

phological, genetic and to a lesser extent, neurophysiological methods, it has been shown that these reactions are primarily carried out directly in the human brain and animals that are characterized by a large variety in the chronic effects of arbitrary factors (Lucassen et al., 2006; McEwen, 2008; Gunnar et al., 2009). That is why the hypothalamus has long been recognized as fundamental in the control and coordination of homeostatic activity. Historically, this was seen from the point of view of the large neuroendocrine control system, resulting from the processing of signals by the hypothalamus and the transfer of their results to the pituitary gland. Through these actions, the endocrine signals are integrated throughout the body, modulating a wide range of physiological processes. More recently, control of the hypothalamus over the autonomic nervous system was increasingly recognized as a powerful additional modulator of peripheral tissues. Nevertheless, the neuroendocrine and autonomic control pathways emerging from the hypothalamus are not separate processes. They act as the only integrated regulatory system, much more subtle and complex, than when every process is considered in isolation. Consequently, hypothalamic regulation should be considered as a summation of neuroendocrine and vegetative effects. It is believed that neural regulation is targeted and rapid, while hormonal regulation is more stable and widespread.

The direct recording of the electrical activity of neuronal populations is an extremely important diagnostic tool in the study of the functional activity of a certain central nervous system structure that is widely used throughout the world. The standard procedures for recording and analyzing brain electrical activity are widely recognized, but there is still a question about the interpretation of the results, especially of deep brain structures, such as the hypothalamus, which are involved in a large number of physiological reactions. That is why it is quite difficult to systematize and compare the findings of various researchers and scientific laboratories. We decided to solve this issue partially by means of chronic animal studies.

One of the factors of the environment, which essentially shifts homeostasis, is diets that include caffeine. Over the last decade, the use of such products has become massive, especially for coffee and tea. Today, coffee is one of the most popular beverages in the world, whose consumption has doubled over the past thirty five years (9.5 billion kg per year) (Ploshchyk, 2013; Kryvokulskyy & Kondras, 2014; Bunn et al., 2015). It is well known that coffee is one of the few beverages of natural origin, consisting of substances of both organic and inorganic origin, which substantially affect almost all structures and systems of the human body (Fernstrom, 2000; Geel et al., 2005; Grosso et al., 2017; Poole et al., 2017). Establishing links between coffee consumption and different states and diseases has become widely studied (Grosso et al., 2017), but often with contrasting outcomes. The main safety problems arise in the ratio of caffeine (trimethylxanthine) as the main constituent of coffee. A toxic dose is 10 g of caffeine per day for adults (one cup of coffee contains 80–175 mg of caffeine, depending on the preparation and type of grains). *Coffea arabica* contains twice as much caffeine as *Coffea robusta*. The highest content of caffeine is in Espresso coffee (100 mg 50 ml).

Caffeine is the most studied component, since it acts in a cell through several mechanisms and has several application points. It is an adenosine receptor antagonist (Ralevic & Burnstock, 1998), an inhibitor of phosphodiesterase, a calcium channel synthesizer, an antagonist of GABA-ergic receptors (Daly, 2007). Physiological features of the action of caffeine on the central nervous system have been investigated by I. P. Pavlov and his collaborators. It has been shown that caffeine has a directed effect on the processes of inhibition and excitation of the cerebral cortex and may be an indicator of the strength of the nervous processes. In addition, optimal doses of caffeine normalize the processes of nervous activity with their violations. It has been shown that at a concentration of 3.3 mg/kg it improves mental activity (Battig & Welzl, 1993). Paraxanthin, a major product of caffeine metabolism, is an even more active blocker of adenosine receptors (Viani, 1993). The action of adenosine on its own receptors depends on the type of receptor and the tissue or cell where the receptor is located. When blocking the adenosine receptors with caffeine, the concentration of adenosine in the plasma increases, due to which its systemic effects become more active. At the systemic level, adenosine enhances sympathetic tone, increases the concentration of catecholamines, the overall peripheral vascular resistance and production of renin. There is evidence (Scher et al., 2004) that during migraine attacks, the concentration of adenosine in the head and neck vessels increases by 68%. Since caffeine is a blocker of several types of adenosine receptors, the effects of adenosine after taking caffeine should be less pronounced, which is likely to weaken the attack. But one should not forget that in some cases, the use of a large amount of caffeine may be the opposite of a trigger headache. This is due to increased cerebral blood flow and stimulation of the sympathetic nervous system (Echeverri et al., 2010). That is, coffee and caffeine can have both a positive and a negative effect on the system and the body as a whole, due to the content of other biologically active substances. On the one hand, there is strong evidence of positive effects of coffee/caffeine consumption for a number of chronic diseases, including some types of cancer (endometrium, prostate, colorectal and hepatic), cardiovascular diseases, and metabolic-related conditions (type 2 diabetes, metabolic syndrome), neurological conditions (Parkinson's disease, Alzheimer's disease, depression) (Grosso et al., 2017). On the other hand, caffeine is the most compromised physiological stimulant, which has side effects (Zulli et al., 2016), which can affect the state of the cardiovascular system. In addition, there is an increased risk of stroke and heart attacks without significant atherosclerotic damage to cerebral arteries. More importantly, prolonged traditional use of caffeine-based products and drinks can lead to apoptotic neurodegeneration, which will primarily be reflected in electrophysiological characteristics of the brain.

To date, there is no complete picture of the mechanisms of adapting the functional activity of the central structures to the long-term effects of environmental factors. In turn, the study of this issue can have significance as an essential aspect of the theory of adaptation processes and its practical application. Therefore, the purpose of the study was to elucidate the basic characteristics of the background electrical activity of the hypothalamus in conditions of chronic caffeine alimentation.

Materials and methods

The research has been carried out in accordance with the existing international requirements and norms of humane attitude towards animals. Experiments were performed on non-linear white male rats. At the beginning of the study their body mass was 125–140 g. The animals lived in common sanitary conditions with a standard diet (Zapadnjuk et al., 1983). To obtain heterogeneity of emotional-stress reactions and their comparison in animals of the studied groups, preliminary testing was conducted to identify individual patterns of their behaviour (Gray, 1974). In addition, we tried to use rats with a more or less homogeneous genotype (from some parents). The first group consisted of control animals (n = 22), which during the whole experiment lived under standard conditions. The second group (n = 24) was represented by animals that received food "Caffeine sodium benzoate" (Darnitsa) in the amount of 150 mg/kg·day (Govindwar et al., 1984; Georgiev et al., 1993; Yadegari et al., 1995; Antonelli-Ushirobira et al., 2010; Yadegari et al., 2016).

The registration of the background electrical activity of the hypothalamus was carried out using the stereotactic biopotential withdrawal method (Buresh et al., 1962) in an acute experiment in a subgroup of 3–4 animals, every two weeks during the entire 12-week study. In addition, from the investigated areas of the rat's hypothalamus, 10–12 recordings of background electrical activity were made. As is known (Trahtenberg, 2001), for the majority of biological indicators used in studies, the minimum number of observations is 25. Also, this approach is convenient for clinical practice (Metodycheskye rekomendacyy, 1999). After each experiment, the localization of the electrode tip at the frontal sections of the brain was verified (Buresh et al., 1962). The cuts into the brain (Fig. 1) of the rats were made using a freezing microtome. This procedure allowed reduction in the number of "extra" records in the subsequent statistical processing of data, thereby ensuring the reliability of the results. Surgical preparation for withdrawal of the electrohypothalamogram was performed after intra-abdominal administration of 20 mg/kg of ketamine and 50 mg/kg of sodium thiopental (Abramov, 1986; Derymedved' et al., 2001). The anesthetised animal was fixed in a stereotactic SEZ-2 device

(on the design of Y. M. Belenov), which was located in a shielded room. The trepanation of the skull was carried out over the posterodial subzone of the cortical region at coordinates: 2–3 mm ulterior to the bregma and 5–6 mm lateral to the sagittal suture in the region of the intersection of the Bregma point with the horizontal and interraural axis. A prerequisite for a clear separation of the electrical activity of the hypothalamus was the fairly rigid mounting of the rat's head at three points (jaw and two auditory holes). After trepanation of the skull, a unipolar electrode (platinum, diameter 100 μm) was inserted into the ergotrophic and trophotropic zones of the hypothalamus in accordance with the stereotactic coordinates of the rat atlas (Paxinos and Watson, 1986). The reference electrode was placed on the anus of the animal, and grounding – in the region of the tail.

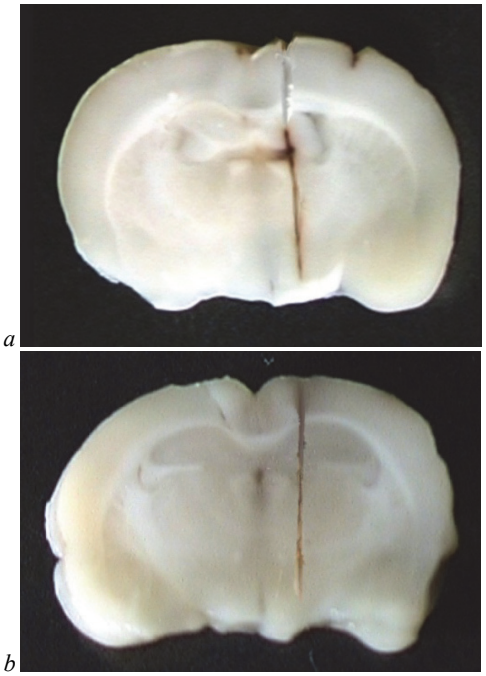

Fig. 1. Verification of localization of electrodes (frontal cuts of the brain of the rat): *a* – anterior hypothalamic area, *b* – dorsal hypothalamic area

The coordinates of the structures were determined by the stereotactic atlas (Paxinos & Watson, 2013). Coordinates of the anterior hypothalamic area: bregma = –1.4 cm, lateral axis = 0.8 cm, interraural axis = 9.0 cm, the coordinates of the drooping hypothalamic area: bregma = –2.3 cm, lateral axis = 0.3 cm, interraural axis = 8.0 cm. After the restoration of the motor activity of the rat, which was determined by the disappearrance of the background electrical activity of narcotic spindles, the recording of the electrohypothalamogram began. In order to exclude short-term effects of caffeine on the ergotrophic and trophotropic zone of the hypothalamus, the registration of electrical activity was carried out 24–26 hours after the last administration of the substance.

The background electric activity of the hypothalamus was recorded using a standard complex electrophysiological equipment with a 16-bit ADC with a sampling frequency of 512 Hz (OO Bohomolets Institute of Physiology, Kyiv). The frequency characteristics of the amplifiers were chosen to ensure adequate recording of low-frequency oscillations (delta-range). The epoch of registration at removal of background electrical activity from each zone was 1–2 minutes. Before digitizing, the signals received were amplified with the help of an amplifier (O. Bohomolets Institute of Physiology, Kyiv). The results were processed using the Math CAD 2014 application package. Through the software, in all records of the main rhythms of the FEA, the duration of the analysis period was 10 s with sampling frequency of df, which was 0.1 Hz. Rhythms and their power were obtained by the Fourier digital conversion method. To remove edge effects, a Hamming window was used. The spectral (absolute) power (mV^2) and the normalized (relative) power (%) of electropyographic wave volumes within the generally accepted frequency ranges were analyzed (Vorob'eva & Koljadko, 2007). The statistical processing of the results of the study was conducted using the Origin 6.0 Professional program using the method of pair comparisons and correlation analysis; the methods of variation statistics using the computer program Statistica 5.0 (StatSoft Inc., USA). The reliability of the differences between control and experimental data was determined using the non-parametric Mann-Whitney criterion for $P < 0.05$.

Results

The first stage of this work was registration with a further analysis of the native records of background electrical activity of the trophotropic zone of the rat hypothalamus in the studied groups (Fig. 2). Already at this stage of the work it was possible to visually note the difference in time between the experimental parameters of experimental rats. As we can see from Figure 2*d*, there was an increase in wavelengths both in the low-frequency range (0.3–7.0 Hz) and in the high-frequency range (8–30 Hz) compared with the data obtained in this group of animals in two weeks. The increase in the power of low-frequency waves may indicate, in our opinion, the species-specific features of the neurotransmitter in this species, which was reflected in the modulation of the background electrical activity of the trophotropic zone of the hypothalamus.

Analysis of the obtained data should be further elaborated on the dynamics of the basic rhythms of background electrical activity, which was recorded in the trophotropic zone of the hypothalamus. The statistical processing of all bioelectric signals of the anterior zone of the hypothalamus of the rat experimental group allowed us to reveal the following.

The rhythm with a frequency of oscillations of 0.5–4.0 Hz remained the dominant in the total electrohypothalamogram (trophotropic zone) of the animals of the experimental group during the whole time of the study. The analysis of spectral power in this frequency range showed the following. In the characteristic of the general dynamics of absolute power parameters of the delta-like activity of the caffeine group rats, it was possible to identify three phases with periods of 2–4, 6–8 and 10–12 weeks from the beginning of the experiment. The maximum values were recorded, respectively, in 2 (23.9 ± 3.2 mV^2), 6 (30.2 ± 2.2 mV^2) and 12 (36.9 ± 4.1 mV^2) weeks of the experiment. Comparing the result with control data (Fig. 3), the following should be highlighted. Only in the beginning (after 2 weeks) and at the end (after 12 weeks) of observation, were absolute power indices of delta-like activity in the total electrohypothalamogram of rats in the experimental group significantly higher ($P < 0.05$) for the corresponding control values. And from 4 to 10 weeks of the experiment, on the contrary – the value of the control group reliably ($P < 0.05$) exceeded the data of the experimental group.

In contrast to the spectral power, the dynamics of relative power indices in the frequency range of 0.5–4.0 Hz in the total electrohypothalamogram of rats in the experimental group was biphasic with periods of 2–6 and 8–12 weeks from the beginning of the experiment. For each phase, a gradual increase in the percentage of the delta-like activity from the minimum to the maximum values was characteristic. In general, the percentage of delta-rhythm in the total background electrical activity of the trophotrophic zone of the hypothalamus of the caffeine group rats varied between 62–78% during the experiment. Comparing the obtained result of the experimental group of rats with similar control data (Fig. 4), one can distinguish the following. In the first phase of the experiment (2–6 weeks), there was a tendency to increase the relative performance of the delta-like activity in the total electrohypothalamogram of the caffeine group rats in relation to control. For the second phase, after 8–10 weeks of the experiment, there was a characteristic tendency to reduction in these data relative to the control values, which only at the end of the observation (after 12 weeks) were significantly ($P < 0.05$) higher than the control data.

In contrast to the dynamics of spectral power in the frequency range of 0.5–4.0 Hz, changes in the spectral power parameters of experimental rats for the range of 4–8 Hz were biphasic. The first phase lasted from 2 to 8 weeks of the study, which was characterized by a gradual decrease in absolute power index of theta-like activity in the total electrohypothalamogram from 9.3 to 3.7 mV^2. The second phase lasted from 10 to 12 weeks of observation, during which these values decreased from 6.4 to 5.9 mV^2. Comparing the result of the experimental group's

rats to the control data (Fig. 3), the following should be noted. Only in the beginning (after 2 weeks) and at the end (after 12 weeks) was the absolute power performance of the theta-like activity of the caffeine group rats significantly ($P < 0.05$) higher than similar control data. In the period from 4 to 10 weeks from the beginning of the experiment on the contrary – it was significantly ($P < 0.05$) lower.

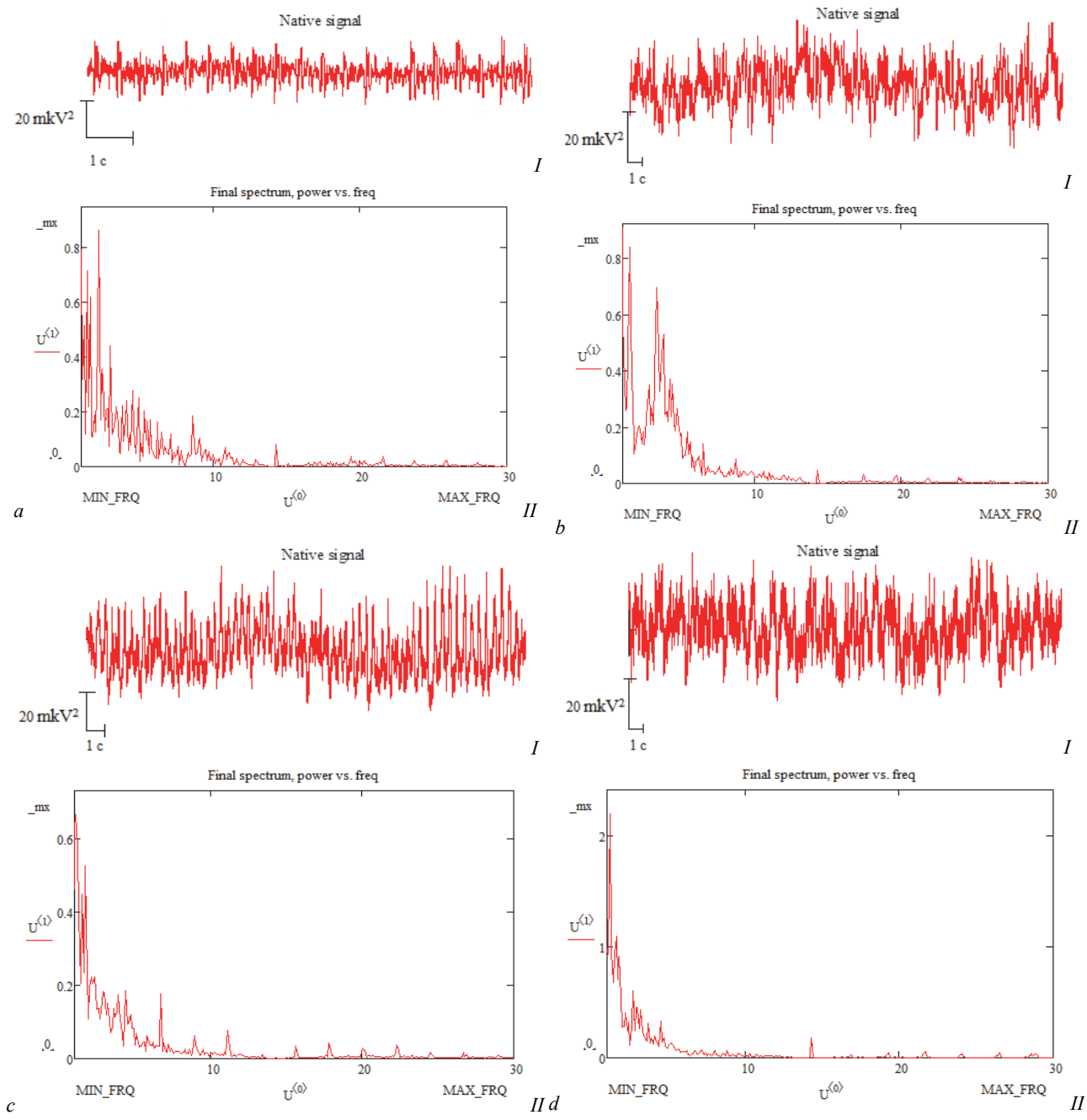

Fig. 2. The native recording (*I*) and the spectral graph (*II*) of the total background electrical activity of the trophotropic zone of the hypothalamus in animals of control (*a*, *b*) and experimental (*c*, *d*) groups: *a*, *b* – after 2 weeks of study, *c*, *d* – after 10 weeks of study

The dynamics of percentage power indices in the frequency spectrum of 4–8 Hz in the total electrohypothalamogram of the caffeine group rats was also biphasic with periods of 2–6 and 8–12 weeks from the beginning of the experiment. For each phase, a gradual decrease in the percentage of the theta-rhythm in the total background electrical activity of the trophotropic zone of the hypothalamus from the maximum to the minimum values was characteristic. In general, this indicator fluctuated within 10-24%. Attention is drawn to the fact that only after 2 and 10 weeks of the experiment, was the percentage of theta-like activity in the electrohypothalamogram of rats in the experimental group significantly ($P < 0.05$) higher than the similar control parameters (Fig. 4).

Similar to the dynamics of theta-like activity, there were changes in both spectral and normalized power parameters in the total electrohypothalamogram of the caffeine group rats in the frequency range of 8–13 Hz. These changes were biphasic, with time periods of 2–6 and 8–12 weeks from the start of the experiment. In addition, both absolute and relative values varied from maximum to minimum. At the same time, the spectral indices of the power of alpha-like activity in the total electrohypothalamogram of rats in the experimental group fluctuated within 1.00–2.86 mV^2, and normalized – within 2.6–8.7%. In addition, in most cases, the observed result in caffeine group rats was significantly ($P < 0.05$) lower than similar control data (Fig. 3, 4).

The rhythm with a frequency of 13–35 Hz was the least expressed in the total background electrical activity of the ergotrophic zone of the hypothalamus of experimental rats. The overall dynamics of both spectral and normalized power parameters of beta-like activity was three-phase. For absolute power indicators, the time periods of each phase changed after 2–6, 8–10 and 12 weeks from the beginning of the observation. At the same time, they underwent a gradual increase from the minimum to the maximum values. In general, this indicator varied within

the range of 1.6–2.5 mV^2. Comparing the results of the caffeine group rats with the control data, it should be noted that only at the end of the experiment were these values significantly ($P < 0.05$) greater than the result of control (Fig. 3). And in the period from 2 to 8 weeks – it was significantly lower ($P < 0.05$). For the relative power indices, the time periods of each phase changed after 2–4, 6–8 and 10–12 weeks from the beginning of the experiment. If the first two phases were characterized by a gradual increase in the percentage of beta-like activity in the total electrohypothalamogram of caffeine group rats from the minimum to maximum values, then at the end of the observation (the third phase), on the contrary, their decrease. In general, the percentage of beta-rhythm in the total electrohypothalamogram varied within 4–7%. Comparing the result with control data (Fig. 4), it should be noted that only 8–10 weeks from the beginning of the experiment, these values were significantly greater than control.

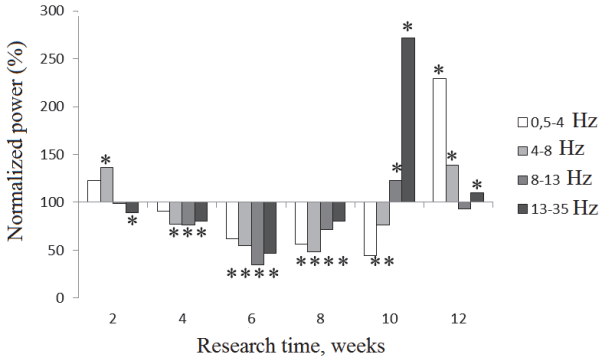

Fig. 3. Changes in normalized power indexes of the waves of the total background electrical activity of the trophotropic zone of the hypothalamus of animals of the experimental group relative to the values of this indicator in the control group rats in the correspondding weeks of the experiment (%): the stars above the columns represent a significant change in the background electrical activity of the trophotrophic zone of the hypothalamus in the experimental group animals relative to the control of the Mann-Whitney criterion ($P < 0.05$)

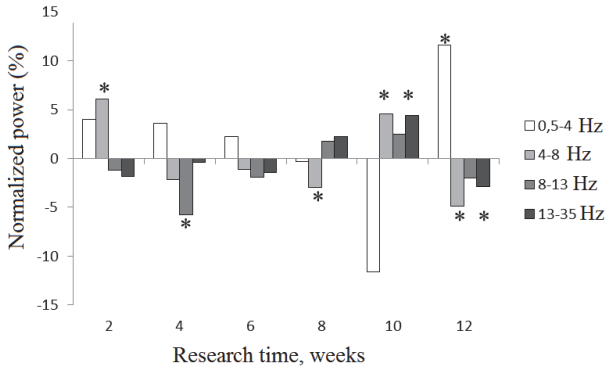

Fig. 4. Changes in normalized power indexes of the waves of the total background electrical activity of the trophotropic zone of the hypothalamus of animals of the experimental group relative to the values of this indicator in the control group rats in the corresponding weeks of the experiment (%): the designations are the same as in Fig. 3

The second stage of this work was registration with further analysis of the native records of the background electrical activity of the ergotrophic zone of the hypothalamus of the rats of the studied groups (Fig. 5), where certain differences were also noted. Over time, the study showed an increase in the power spectrum by 1.5 times, which was reflected in the frequency distribution of power (Fig. 5*g*). But it should be noted that in the beginning and at the end of the study, the dominant power values were recorded in low frequency bands (0.3–3.0 Hz), and the lowest values were recorded in the range of 14–30 Hz. Further mathematical analysis allowed us to reveal the following.

Delta-like activity remained the dominant over the entire time of the study in both the spectral and the normalized ratio in the total electrohypothalamogram (ergotropic zone). In the dynamics of spectral power indexes in the frequency range of 0.5–4.0 Hz, three phases with maxima were identified at 2, 6 and 12 weeks from the beginning of the observation. The power values in these time periods were 26.2 ± 1.4, 31.9 ± 2.3 and 40.0 ± 3.2 mV^2, respectively. Comparing the result with similar control indicators, the following should be noted (Fig. 6). Only in the beginning (after 2 weeks) and at the end of the experiment (after 12 weeks) were the absolute values of delta-rhythm power in the total electrohypothagramogram significantly ($P < 0.05$) greater than the corresponding control values. In another time period (after 6–10 weeks), the data of the animals of the caffeine group were significantly ($P < 0.05$) lower than the data of control.

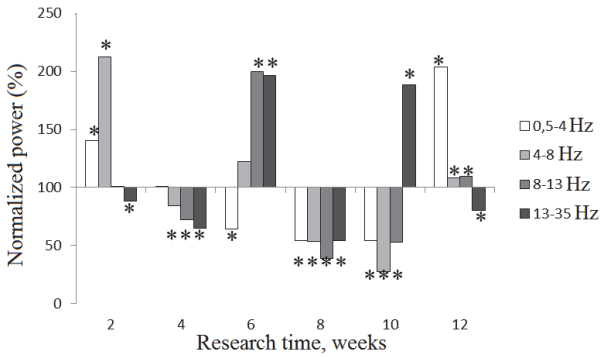

Fig. 6. Changes in normalized power indexes of the waves of the total background electrical activity of the ergotropic zone of the hypothalamus of animals of the experimental group relative to the values of this indicator in the control group rats in the corresponding weeks of the experiment (%): the stars above the columns represent a significant change in the background electrical activity of the ergotrophic zone of the hypothalamus in the experimental group animals relative to the control of the Mann-Whitney criterion ($P < 0.05$)

In contrast to the dynamics of spectral power parameters in the frequency range of 0.5–4.0 Hz, the changes in normalized power performance were biphasic: the first phase lasted from 2 to 6 weeks of experiment, the second – from 8 to 12 weeks from the beginning of the study. In addition, in these time periods, a gradual increase in the percentage of delta-like activity in the total electrohypothalamogram was noted, with the registration of maximum values for each phase through 6 (65.7 ± 3.8%) and 12 (77.3 ± 6.1%) weeks of experiment. The minimum values for this frequency range were recorded 8 weeks after the start of observation, when the percentage of delta rhythm in the total electrohypothalamogram of the erythropoies of the hypothalamus did not exceed 43.8 ± 2.1%. When comparing the result of the rats to which caffeine was administered with similar control data, the following should be highlighted (Fig. 7). In general, the importance of the percentage of delta-rhythm in the total electrohypothalamogram of animals in the experimental group was close to the control. Only 6, 8 and 12 weeks from the beginning of the experiment, were they significantly ($P < 0.05$) different.

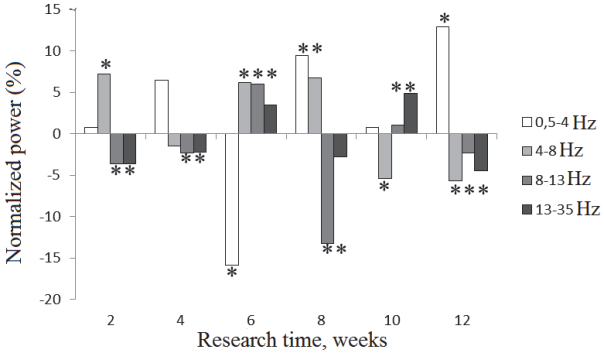

Fig. 7. Changes in normalized power indexes of the waves of the total background electrical activity of the ergotropic zone of the hypothalamus of animals of the experimental group relative to the values of this indicator in the control group rats in the corresponding weeks of the experiment (%): the designations are the same as in Fig. 6

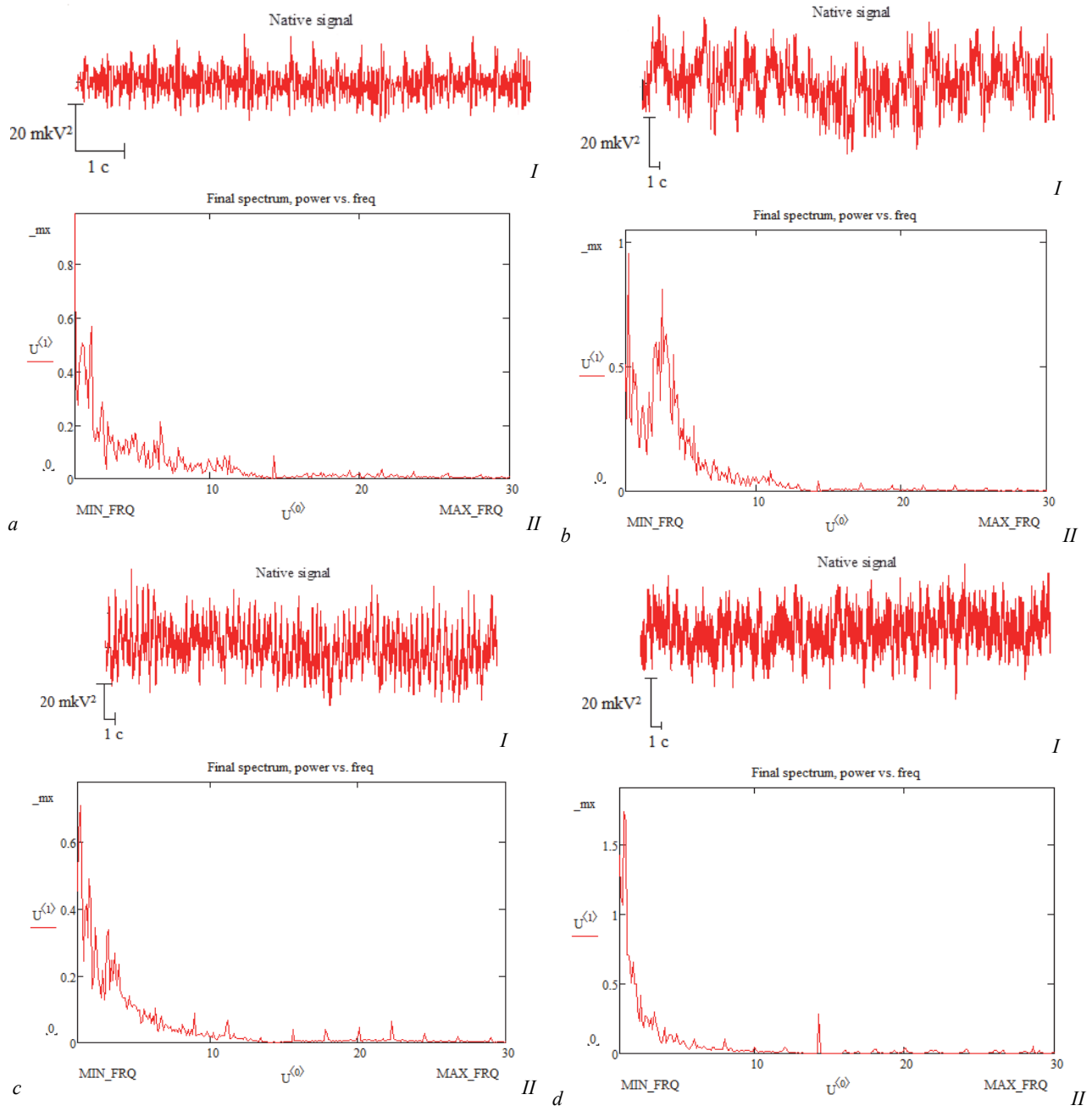

Fig. 5. The native recording (*I*) and the spectral graph (*II*) of the total background electrical activity of the ergotropic zone of the hypothalamus in animals of control (*a*, *b*) and experimental (*c*, *d*) groups: the designations are the same as in Fig. 2

Almost twice as much theta-like activity was expressed in the total electrohipothalamogram of rats in the experimental group. The dynamics of absolute power indices in the frequency range of 4–8 Hz was three-phase with periods of 2–4, 6–10 and 12 weeks from the beginning of the study. The maximum power indexes were recorded at the beginning of the experiment (after 2 weeks) and amounted to 13.6 ± 0.8 mV^2, and the minimum – after 4 and 10 weeks, where they did not exceed 5–6 mV^2. Comparing the obtained result of experimental rats with similar control indices, it should be noted that only in the beginning (after 2 weeks) and at the end (12 weeks) from the beginning of the experiment, was the spectral power of the theatrical rhythm in the total electrohypotalamogram significantly higher ($P < 0.05$) for control values (Fig. 1). In the middle of the study (after 4–10 weeks), on the contrary, there was a significant ($P < 0.05$) decrease in the investigated indicator in relation to control.

The dynamics of normalized power parameters in the frequency range of 4–8 Hz was almost the same as the spectral power in the total electrohypothalamogram of the caffeine group rats. In general, three phases could also be distinguished in changes in the percentage of theta-rhythm in the total electrohypothalamogram. The first phase lasted from 2 to 6 weeks of the experiment and was characterized by a gradual decrease of these parameters from 29.0% to 17.7%. The second phase (8–10 weeks) was characterized by a sharp increase in the percentage of theta-like activity up to 33.2% (which was the maximum for this frequency band), which further decreased threefold and did not exceed 11% (10 weeks of experiment). At the end of the observation (12 weeks) there was a slight restoration of the percentage of theta-rhythm in the total electrohypothagramogram to 14.0%. Comparing the results for the experimental group of animals to similar control data, one can distinguish the following (Fig. 7). For the time period from 2 to 8 weeks the study was characterized by a significant ($P < 0.05$) increase in the percentage of theta rhythm in the total electrohypothalamogram of the ergotrophic zone of the hypothalamus of the caffeine group rats in relation to control. Only at the end of the observation (after 10–12 weeks) was this indicator significantly ($P < 0.05$) lower than the similar values of control.

The least high-frequency rhythm was expressed in the total electrohypothalamogram of rats in the experimental group. Thus, for the frequency range of 8–13 Hz in the dynamics of absolute power parameters, three phases of the data changes, which lasted from 2 to 4, from 6 to 10

and 12 weeks of experiment, were characteristic. The maximum absolute values of the power of alpha-like activity in each of the time periods were recorded, respectively, in 2 (4.0 ± 0.2 mV^2), 6 (4.8 ± 0.7 mV^2) and 12 (2.7 ± 0.2 mV^2) weeks from the beginning of the study. And the smallest result for the frequency range of 8–13 Hz in the total electrohypothalamogram of the caffeine group rats was recorded after 10 weeks, where it was 2.0 ± 0.9 mV^2. In relation to control (Fig. 6), the values mentioned above, characteristic for the experimental group, almost always significantly differed ($P < 0.05$) among themselves.

In the dynamics of the percentage of alpha-like activity in the total electrohypothalamogram of the caffeine group rats from 2 to 8 weeks of experiment, a gradual increase in the data from 8 to 13% was observed. After 10 weeks of the experiment, a sharp decrease in the percentage of alpha rhythm to 4.5 ± 0.5% was observed, which at the end of the observation (after 12 weeks) although recovered to 5.6 ± 0.3%, did not exceed the initial values. Comparing the obtained result with similar control values (Fig. 7), it should be noted that almost always (except for 6 and 10 weeks) normalized power parameters in the frequency range of 8–13 Hz of experimental rats were significantly lower ($P < 0.05$).

The most stable and similar in dynamics both of absolute and relative power indices in the total electrohypothalamogram of the caffeine group rats were changes in the frequency range of 13–35 Hz. It was characterized by a gradual increase in both the spectrum and the percentage of beta-like rhythm from 2 to 8 weeks from the beginning of the experiment. Moreover, at the beginning of the observation (after 2 weeks), these data were minimal, and after 8 weeks - the maximum. At the end of the experiment (after 10–12 weeks) there was a gradual decrease in both absolute and relative power indices of beta-like activity in the total electrohypothalamogram. Comparing the result obtained in experimental rats with similar control data, it should be noted that these differences were always valid (Fig. 6, 7).

Discussion

The role of the hypothalamus in providing vital functions and maintaining homeostasis is beyond doubt. The fact that it is an important center for integrating the physiological functions of the body has been confirmed by many authors (Agadzhanjan, 1983; Malyshev & Manuhina, 1998; Morita et al., 2005). In addition, the hypothalamus acts as the central link, which first reacts to the action of arbitrary stress factors and provides adaptation of the organism to new conditions (Meerson, 1993; Pshennikova, 2000).

On the basis of numerous studies in the hypothalamus, the zones with mostly sympathetic (ergotropic hypothalamic region) and parasympathetic (trophotropic) effects were identified, and the hypothalamus itself was considered as the center of integration of the vegetative system (Talalaenko et al., 2002; Vejn, 2003; Gasser et al., 2006). Such a distribution on the ergotropic and trophotropic zone is functional and biological in character, indicating participation in the provision of functional activity. Thus, in the anterior zone of the hypothalamus, a cholinergic synaptic transmission predominates, and in the posterior region there is a catecholateral synaptic transmission. Changing the prevalence under certain conditions of neurotransmitters in the brain may serve as a strong modulator of background electrical activity (Majkova et al., 2004). It is likely that under the conditions of various stressors, the resistance of a living organism will be determined by the features of the central neurochemical organization in the ergotropic and trophotropic zones of the hypothalamus. Investigation of neurochemical mechanisms of stress state showed the participation of adrenergic systems in their neurotransmitter maintenance and the participation of cholinergic systems in their inhibition. In turn, under conditions of stressors, activation of the catecholateral neurotransmitter in the brain is observed. This is accompanied by an increase in mediation of norepinephrine in the paraventricular nucleus of the hypothalamus and mediated norepinephrine activation of the hypothalamic-pituitary-adrenal axis (Darlington et al., 1992; Bartamesz et al., 1994; Pacak et al., 1995). However, a continued mismatch between these neurotransmitter systems can lead to the development of negative stress states, which is accompanied by a change in vegetative functions and paroxysmal activity of background electrical activity, which originnally occurs on the hypothalamus. The electrical activity of the hypothalamus, in turn, is one of the indicators of the functional state, which plays an important role in the adaptive-compensatory reactions of the organism. In addition, incredibly complex functional bonds exist not only between different zones of the hypothalamus, but also between its nerve and endocrine elements. All this allows the body to adapt in the optimal and most energy-saving way. Caffeine is one of the most important stimulant drugs (Dimpfel, 2013). The use of caffeine in our studies allowed us to assess the state of the trophic and ergotropic zones of the hypothalamus and the possible mechanisms for their participation in adaptation processes.

An analysis of electrohypothalamograms showed that in the trophotropic zone of the hypothalamus, after two weeks of caffeine alimentation, an increase in the absolute and normalized power of the main delta-rhythm was observed. Our previous studies (Turic'ka et al., 2015, 2016) showed that this growth is much smaller than in the neocortex and hippocampus under similar conditions, but is clearly indicative of the activation of mediator synthetic systems. The most specific for this focus of the rat brain is the significant inhibition of both the power and the representation of high-frequency rhythms of the electrohypothalamogram after 4–8 weeks of the experiment. This is probably due to an increase in the reactivity of GABA-ergic modulation in hypermedia neurotransmitters. After 8–10 weeks of the experiment, there is a tendency to increase desynchronizing effects due to the probable exhaustion of the GABA resource, which is again sharply restored after 12 weeks – in the period of a significant increase in absolute and normalized theta-rhythm power in contrast to the high-frequency rhythms. It can be assumed that this mechanism is unique to the trophotropic zone of the rat hypothalamus in connection with its functional purpose of the energy storage center, which is dominated by the synergistic effects of GABA. Perhaps such a powerful inhibitory resource in this cerebral locus is the main stress-limiting factor that makes this zone of the central nervous system of rats less sensitive to caffeine exposure.

In the ergotropic zone of the hypothalamus, after a week of caffeine loading, a significant increase in the absolute and normalized power of the dominant synchronous rhythms was observed. This may be due to hypermediative neurosynthetic activity of presynaptic neurons due to activation of intracellular rianoindin receptors by caffeine. After 2–4 weeks of the experiment in the ergotropic zone, there was a decrease in the absolute and normalized power of both synchronous and desynchronous rhythms, indicating the onset of primary exhaustion of neurotransmission. But after 6 weeks, the power and the presence of high-frequency rhythms are likely to increase, which is most likely due to the modulating effect of glutamate on post-synaptic responses as a result of the activation of cambial postsynaptic receptors. In the continuation of 8 10 weeks, this effect disappears and the hypodemic neurotransmitter is restored. This is confirmed by the relative decrease in power of both the dominant low-frequency and high-frequency rhythms. The last two weeks of the experiment clearly demonstrate the initial adaptive-adaptive reversion of presynaptic neurosynthetic, thus providing an ergotropic ultra low-frequency sympathetic resource of the posterior hypothalamus. This is evidenced by the restoration of the initial physiological domination of low-frequency rhythms, both in absolute and in normalized power.

Such a difference in the chronic effect of caffeine on the trophic and ergotropic zone of the rat hypothalamus is primarily due to the different mediator support of these zones, which underlies their physiological purpose. GABA is the main mediator of the trophotropic zone and the main neurotransmitter of its synchronous activity. At the same time, neurotransmitter support of the ergotropic zone is represented by glutamate, which, along with other agents, implements its desynchronous activity. Studies in rats have shown (Lazarus et al., 2011) that caffeine stimulates excitation by activating pathways traditionally associated with motivational and motor reactions in the brain. To such paths, in a certain way, belongs also the ergotropic zone of the hypothalamus, which regulates the vegetative provision of the indicated processes. Perhaps this explains the fact of the more powerful influence of caffeine precisely on the ergotropic zone of the hypothalamus.

It is also impossible to ignore the different part of the investigated structures in the hypothalamic-pituitary-adrenocortical axis. Since caf-

feine is a nonselective adenosine antagonist, it can modulate the metabolic pathways in this axis (Nabbi-Schroeter et al., 2018; Karaismailoglu et al., 2017; Xu et al., 2012), which will somehow affect the adaptive responses. First of all, it concerns adrenal glands that react sensitively to the formation and implementation of adaptive-compensatory reactions.

Conclusions

The results of the experiment prove some specificity of the reaction of the neuronal system of the tropho- and ergotropic zones of the rat hypothalamus to the effect of chronic caffeine alimentation.

The main difference in the reactive state of electrophysiological indices in the trophotropic zone of rats is the absence of a typical desynchronization from the 4th to the 8th week of the study and the hypersynchronization after 12 weeks of the experiment. The most likely mechanism that explains the results obtained is the ultra-powerful GABA-ergic modulation of this zone, the main energy-accumulating center. Stress-limiting GABA-ergic resource of the indicated zone significantly reduces its sensitivity to caffeine exposure in rats.

Under the influence of chronic caffeine load in the ergotropic zone of the hypothalamus, after 6 weeks of study desynchronous high-frequency rhythms dominated. During the rest of the study, we observed a decrease in both the low-frequency and high-frequency components of the electrohypothalamogram of this zone. This forms the view that the key component of the neurophysiological response of the posterior rat hypothalamus to the caffeine diet is the powerful glutamatergic effects on the pre- and post-synaptic neurons under conditions of reactive exhaustion of local neurosynthetic. Caffeine depletion of the hypothalamic neurotransmission at the end of the experiment is replaced by an effective adaptive-adaptive ergotropic restoration of neurosynthetic activity in this locus of the central nervous system of rats. Thus, caffeine has a powerful activating effect on the ergotropic function of the posterior rat hypothalamus.

References

Agadzhanjan, N. A. (1983). Adaptacija i rezervy organizma [Adaptation and body reserves]. Fizkul'tura i Sport, Moscow (in Russian).

Antonelli-Ushirobira, T. M., Kaneshima, E. N., Gabriel, M., Audi, E. A., Marques, L. C., & Mello, J. C. (2010). Acute and subchronic toxicological evaluation of the semipurified extract of seeds of guaraná (*Paullinia cupana*) in rodents. Food and Chemical Toxicology, 48(7), 1817–1820.

Baldwin, A. L. (2006). Mast cell activation by stress. Methods in Molecular Biology, 315, 349–360.

Bartamesz, V., Aubry, J. M., & Steimer, T. (1994). Stressor-specific increase of vasopressin mRNA in paraventricular hypophysiothrophic neurons. Neuroscience Letters, 170, 35–38.

Battig, K., & Welzl, H. (1993). Psychopharmacological profile of caffeine. In: Garatini, S. (Ed.). Caffeine, coffee and health. Raven Press, New York. Pp. 213–253.

Berthou, F., Goasduff, T., Dréano, Y., & Ménez, J. F. (1995). Caffeine increases its own metabolism through cytochrome P4501A induction in rats. Life Sciences, 57(6), 541–549.

Bunn, C., Läderach, P., Rivera, O. O., & Kirschke, D. (2015). A bitter cup: Climate change profile of global production of Arabica and Robusta coffee. Climatic Change, 129(1–2), 89–101.

Buresh, J., Petran', M., & Zahar, I. (1962). Jelektrofiziologicheskie metody isledovanija [Electrophysiological methods of investigation]. Izdatel'stvo Inostrannoj Literatury, Moscow (in Russian).

Daly, J. W. (2007). Caffeine analogs: Biomedical impact. Cellular and Molecular Life Sciences, 64(16), 2153–2169.

Darlington, D. N., Barraclough, C. A., & Gann, D. S. (1992). Hypotensive hemorrhage elevates corticotrophin-releasing hormone messenger ribonucleic acid (mRNA) but not vasopressin mRNA in the rat hypothalamus. Endocrinology, 130, 1281–1288.

Derimedved', L. V., Percev, I. M., & Shuvalova, E. V. (2001). Vzaimodejstvie lekarstv i jeffektivnost' farmakoterapii [Interaction of drugs and the effectiveness of pharmacotherapy]. Megapolis, Kharkov (in Russian).

Dimpfel, W. (2013). Pharmacological classification of herbal extracts by means of comparison to spectral EEG signatures induced by synthetic drugs in the freely moving rat. The Journal of Ethnopharmacology, 149(2), 583–589.

Echeverri, D., Montes, F. R., Cabrera, M., Galán, A., & Prieto, A. (2010). Caffeine's vascular mechanisms of action. International Journal of Vascular Medicine, 2010, article ID 834060.

Fernstrom, J. D. (2000). Can nutrient supplements modify brain function? American Journal of Clinical Nutrition, 71(6), 1669S–1675S.

Gasser, P. J., Lowry, C. A., & Orchinik, M. (2006). Corticosterone-sensitive monoamine transport in the rat dorsomedial hypothalamus: Potential role for organic cation transporter 3 in stress-induced modulation of monoaminergic neurotransmission. Journal of Neuroscience, 26(34), 8758–8766.

Geel, L., Kinnear, M., & de Kock, H. L. (2005). Relating consumer preferences to sensory attributes of instant coffee. Food Quality and Preference, 16, 237–244.

Georgiev, V., Johansson, B., & Fredholm, B. B. (1993). Long-term caffeine treatment leads to a decreased susceptibility to NMDA-induced clonic seizures in mice without changes in adenosine A1 receptor number. Brain Research, 612(1–2), 271–277.

Govindwar, S. P., Kachole, M. S., & Pawar, S. S. (1984). *In vivo* and *in vitro* effects of caffeine on hepatic mixed-function oxidases in rodents and chicks. Food and Chemical Toxicology, 22(5), 371–375.

Gray, J. (1972). Tne psychology of fear and stress. Academic Press, New York.

Grosso, G., Godos, J., Galvano, F., & Giovannucci, E. L. (2017). Coffee, caffeine, and health outcomes: An umbrella review. The Annual Review of Nutrition, 37, 131–156.

Gunnar, M. R., Herrera, A., & Hostinar, C. E. (2009). Stress and early brain development. Encyclopedia on Early Childhood Development. Centre of Excellence for Early Childhood Development, Montreal, Quebec. Pp. 1–8.

Kalsbeek, A., Bruinstroop, E., Yi, C. X., Klieverik, L., Liu, J., & Fliers, E. (2014). Hormonal control of metabolism by the hypothalamus-autonomic nervous system-liver axis. Frontiers of Hormone Research, 42, 1–28.

Karaismailoglu, S., Tuncer, M., Bayrak, S., Erdogan, G., Ergun, E. L., & Erdem, A. (2017). The perinatal effects of maternal caffeine intake on fetal and neonatal brain levels of testosterone, estradiol, and dihydrotestosterone in rats. Naunyn-Schmiedeberg's Archives of Pharmacology, 390(8), 827–838.

Kazakov, V. N., & Natrus, L. V. (2005). Modulation of neuronal impulse activity of the anterior hypothalamus as a functional basis of the mechanisms underlying hypothalamic control. Neurophysiology, 37, 463–474.

Krivokul's'kij, O. B., & Kondras', N. M. (2014). Osnovni tendenciji spozhivannja kavi v sviti ta Ukraini: Suspilno-geografichnij aspect [Major trends of coffee consumption in the world and Ukraine: Human-geographical aspect]. Ekonomichna ta Social'na Geografija, 69, 299–307 (in Ukrainian).

Lazarus, M., Shen, H. Y., Cherasse, Y., Qu, W. M., Huang, Z. L., Bass, C. E., Winsky-Sommerer, R., Semba, K., Fredholm, B. B., Boison, D., Hayaishi, O., Urade, Y., & Chen, J. F. (2011). Arousal effect of caffeine depends on adenosine A2A receptors in the shell of the nucleus accumbens. The Journal of Neuroscience, 31(27), 10067–10075.

Lucassen, P. J., Heine, V. M., Muller, M. B., van der Beek, E. M., Wiegant, V. M., De Kloet, E. R., Joels, M., Fuchs, E., Swaab, D. F., & Czeh, B. (2006). Stress, depression and hippocampal apoptosis. CNS and Neurological Disorders Drug Targets, 5(5), 531–546.

Majkova, T. N., Lukashjov, S. N., & Piramidov, M. A. (2004). Javlenie samoreguljacii elektrogeneza central'noj nejronal'noj predachi mozga cheloveka [The phenomenon of self-electrogenesis central neuronal predachi human brain]. Vestnik Rossijskoj Akademii Estestvenih Nauk, 4(1), 64 (in Russian).

Malyshev, J. I., & Manuhina, E. B. (1998). Stress, adaptacija i oksid azota [Stress, adaptation and nitric oxide]. Biohimija, 63(7), 992–1006 (in Russian).

McEwen, B. S. (2008). Understanding the potency of stressful early life experiences on brain and body function. Metabolism, 57(2), 11–15.

Meerson, F. Z. (1993). Adaptacionnaja medicina: Mehanizmy i zashhitnye effekty adaptacii [Adaptation medicine: Mechanisms and protective effects of adaptation]. Hypoxia Medical LTD, Moscow (in Russian).

Metodicheskie rekomendacii po klinicheskomu ispytaniju lekarstvennyh sredstv v Ukraine (1999) [Methodical recommendations for the clinical trial of medicinal products in Ukraine]. Kyiv (in Russian).

Morita, K., Sekiyama, A., & Rokutan, K. (2005). Stress and central neuroendocrine networks. No To Shinkei, 57(5), 397–406.

Nabbi-Schroeter, D., Elmenhorst, D., Oskamp, A., Laskowski, S., Bauer, A., & Kroll, T. (2018). Effects of long-term caffeine consumption on the adenosine A1 receptor in the rat brain: An *in vivo* pet study with [^{18}F]CPFPX. Molecular Imaging and Biology, 20(2), 284–291.

Pacak, K., Palkovits, M., & Kvetnasky, R. (1995). Effects of various stressors on *in vivo* notepinephrine release in the hypothalamic paraventricular nucleus and on the pituitary-adrenocortical axis. Annals of the New York Academy of Sciences, 771, 115–130.

Paxinos, G., & Watson, C. (2013). The rat brain in stereotaxic coordinates. 7th ed. Academic Press, Imprint.

Ploshchyk, N. (2013). The world coffee sector under conditions of the second wave of the economic recession. Journal of Intercultural Management, 3(5), 91–101.

Poole, R., Kennedy, O. J., Roderick, P., Fallowfield, J. A., Hayes, P. C., & Parkes, J. (2017). Coffee consumption and health: Umbrella review of meta-analyses of multiple health outcomes. British Medical Journal, 359, j5024.

Pshennikova, M. G. (2000). Fenomen stressa [The phenomenon of stress]. Patologicheskaja Fiziologija i Eksperimental'naja Terapija, 2, 24–31 (in Russian).
Ralevic, V., & Burnstock, G. (1998). Receptors for purines and pyrimidines. Pharmacological Reviews, 50(3), 413–492.
Scher, I., Stewart, W. F., & Lipton, R. B. (2004). Caffeine as a risk factor for chronic daily headache: A population-based study. Neurology, 63(11), 2022–2027.
Sominsky, L., Jasoni, C. L., Twigg, H. R., & Spencer, S. J. (2018). Hormonal and nutritional regulation of postnatal hypothalamic development. The Journal of Endocrinology, 237(2), 47–64.
Talalaenko, A. N., Pankrat'ev, D. V., & Goncharenko, N. V. (2002). O mono-aminergicheskih i aminokislotergicheskih mehanizmah zadnego gipotalamusa v realizacii antiaversivnyh effektov anksiossedativnyh i anksioselektivnyh sredstv na razlichnyh modeljah trevogi [About monoaminergic and amino-acidic mechanisms of the posterior hypothalamus in the realization of anti-inversion effects of anksiosedative and anxioselective agents in various anxiety models]. Jeksperimental'naja i Klinicheskaja Farmakologija, 65(5), 22–26 (in Russian).
Trahtenberg, I. M. (Ed.). (2001). Osnovnye pokazateli fiziologicheskoj normy u cheloveka [The main indicators of physiological norm in humans]. Avicena, Kyiv (in Russian).
Turic'ka, T. G., Lukashov, S. M., & Ljashenko, V. P. (2016). Efekty vplyvu hronichnoji kofejinovoji alimentaciji na pokazniky fonovoji elektrychnoji aktivnosti neokorteksu shhuriv [Effects of chronic caffeine alimentation on the performance indicators of rat neocortex background electrical activity]. Experimental Physiology and Biochemistry, 75(3), 11–16.
Vejn, A. M. (2003). Vegetativnye rasstrojstva [Autonomic dysfunction]. MIA, Moscow (in Russian).
Viani, R. (1993). The composition of coffee. In: Garatini, S. (Ed). Caffeine, coffee and health. Raven Press, New York. Pp. 17–41.
Vorob'eva, T. M., & Koljadko, S. P. (2007). Jelektricheskaja aktivnost' mozga (priroda, mehanizmy, funkcional'noe znachenie) [The electrical activity of the brain (the nature, mechanisms, functional significance)]. Eksperimental'-naja i Klinicheskaja Medicina, 2, 4–11 (in Ukrainian).
Xu, D., Zhang, B., Liang, G., Ping, J., Kou, H., Li, X., Xiong, J., Hu, D., Chen, L., Magdalou, J., & Wang, H. (2012). Caffeine-induced activated glucocorticoid metabolism in the hippocampus causes hypothalamic-pituitary-adrenal axis inhibition in fetal rats. PLoS One, 7(9), e44497.
Yadegari, M., Khazaei, M., Anvari, M., & Eskandari, M. (2016). Prenatal caffeine exposure impairs pregnancy in rats. International Journal of Fertility and Sterility, 9(4), 558–562.
Yoo, S., & Blackshaw, S. (2018). Regulation and function of neurogenesis in the adult mammalian hypothalamus. Progress in Neurobiology, in press.
Zapadnjuk, I. P., Zapadnjuk, E. A., Zaharija, E. A., & Zapadnjuk, B. V. (1983). Laboratornye zhivotnye: Razvedenie, soderzhanie, ispol'zovanie v eksperi-mente [Laboratory animals: Breeding, content, use in experiment]. Vishha Shkola, Kyiv (in Russian).
Zulli, A., Smith, R. M., Kubatka, P., Novak, J., Uehara, Y., Loftus, H., Qaradakhi, T., Pohanka, M., Kobyliak, N., Zagatina, A., Klimas, J., Hayes, A., La Rocca, G., Soucek, M., & Kruzliak, P. (2016). Caffeine and cardiovascular diseases: Critical review of current research. European Journal of Nutrition, 55(4), 1331–1343.

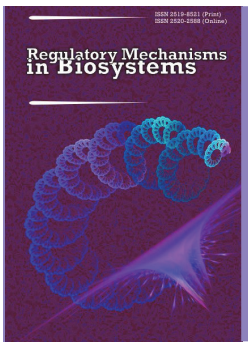

Regulatory Mechanisms in Biosystems

ISSN 2519-8521 (Print)
ISSN 2520-2588 (Online)
Regul. Mech. Biosyst., 9(3), 426–429
doi: 10.15421/021863

Choosing selective factors for the cultivation of *Aerococcus viridans* symbiont strains

D. O. Stepanskyi, I. P. Koshova, G. M. Kremenchutskyi, O. V. Khomiak

SE "Dnepropetrovsk Medical Academy of Ministry of Health of Ukraine", Dnipro, Ukraine

Article info

Received 15.06.2018
Received in revised form 23.07.2018
Accepted 28.07.2018

SE "Dnepropetrovsk Medical Academy of Ministry of Health of Ukraine", Vernadsky st., 9, Dnipro, 49000, Ukraine.
Tel.: +38-067-797-84-97.
E-mail: dstepanskiy@gmail.com

Stepanskyi, D. O., Koshova, I. P., Kremenchutskyi, G. M., & Khomiak, O. V. (2018). Choosing selective factors for the cultivation of Aerococcus viridans symbiont strains. Regulatory Mechanisms in Biosystems, 9(3), 426–429. doi:10.15421/021863

Aerococci have certain cultivation characteristics. A well-known method of aerococcal cultivation uses indicator media which included the complex "oxolinic acid – etonium", but data indicating cases of conditionally pathogenic flora contamination due to the accumulation of microorganisms that are resistant to this complex have been obtained. Therefore, there was a need to search for new substances that would have a wide range of antagonistic activity in relation to the conditionally pathogenic flora and at the same time would not inhibit the growth of aerococci, and which would also be available and safe. The sensitivity of the *A. viridans* symbionts and conditionally pathogenic flora to the substances with antimicrobial activity of different groups was determined by the method of "wells". For research, *A. viridans* symbionts isolated from different microbiocenoses have been used. *P. aeruginosa*, *S. aureus*, *K. pneumoniae*, *E. coli* and *C. albicans* were used as conditionally pathogenic flora. Norfloxacin, pefloxacin, ofloxacin, gatifloxacin, levofloxacin, miramistin, decamethoxine, chlorhexidine, octenidine and boric acid were used as investigational drugs. Also, the optimal concentration of drugs which would suppress the growth of conditionally pathogenic flora, and would not show a negative effect on *A. viridans* was determined by serial dilutions. It was found that miramistin, norfloxacin and boric acid meet the necessary criteria. The serum dilutions method was used to determine the minimum inhibitory concentration (MIC) of these drugs in the experiment. Norfloxacin in a dosage of 12.5–50.0 μg/ml effectively inhibited the growth of the conditionally pathogenic flora, but also reduced the number of aerococci. The dose of 8.3 μg/ml met the criteria we needed, namely suppressing the growth of the conditionally pathogenic flora and not affecting aerococci. The concentration of miramistin and boric acid in a culture medium that showed a stong depressant effect on conditionally pathogenic flora and practically did not affect *A. viridans* was 50 μg/ml. In addition, miramistin and boric acid exhibited fungicidal action against *C. albicans*. Antimicrobial effects of the investigated drugs on the conditionally pathogenic flora was not complete in some cases, or inhibited the growth of aerococci at higher doses, so the effect of their rational combination on the conditionally pathogenic flora was investigated. As a result, an antimicrobial complex with optimal concentrations of substances (norfloxacin 8.3 μg/ml, myramistin 50 μg/ml, boric acid 50 μg/ml), which effectively suppresses UPMF and does not affect the growth of symbionic *A. viridans*, was determined. The specified antimicrobial complex can be used for the production of modified media for isolation, cultivation and study of biochemical activity of *A. viridans* microorganisms. Properties of aerococci, grown on the nutrient medium with the studied drugs did not differ from aerococci, grown on nutrient media without additives.

Keywords: aerococci; autosymbionts; cultivation of aerococci; indicator media; modified media.

Introduction

Aerococcus viridans is a bacterium that is present in the environment and was initially isolated from the air. Other types of *Aerococcus* have been obtained from different parts of the human body and animals (Collins et al., 1999; Nobukazu Saishu et al., 2009). Aerococci are components of normal gut microbiota of animals (Wise & Siragusa, 2007; Senneby et al., 2016) and human intestinal flora. Along with this, there are cases of allocation of aerosols in humans and animals in various pathologies and these are associated, as a rule, with immuno-deficiency states. Initially, the *Aerococcus* genus, which included a single species – *Aerococcus viridans* was described. Subsequently, five new *Aerococcus* species: *Aerococcus urinae*, *A. sanguinicola*, *A. christensenii*, *A. urinaeequi* and *A. urinaehominis* (Facklam&Elliot, 1995) have been identified. The clinical significance of these species was clearly established for *A. urinae* and *A. viridans* (Shelton-Dodge et al., 2011; Rasmussen et al., 2013; Humphries et al., 2014; Senneby et al., 2015).

A. viridans are ubiquitous microorganisms, and have certain peculiarities of cultivation (Williams & Hirch, 1953; Rizhenko et al., 2002; Facklam et al., 2003). Research carried out used displaying medias through which the allocation, identification and differentiation of aerococci were conducted (Good et al., 1966; Devrise et al., 1999; Kremenchuckij et al., 2003, 2009). The composition of the aforementioned media for the selective allocation of various types of aerococci included the complex "oxolinic acid – etonium", which gave a selective effect of predominant aercocci growth in concentrations: oxalic acid – 50 μg/ml, etonium – 5 μg/ml. In the process of use of these media, data indicating cases of conditionally pathogenic flora (CPF) contamination due to the accumulation of microorganisms that are resistant to the "oxolinic acid – etonium complex" were obtained. The above-mentioned facts and increased incidence of infections caused by hospital strains with multi-resistance to chemotherapy (Uh et al., 2002; Yasukawa et al., 2014; Gonzalez et al., 2017), especially methicillin-resistant *Staphylococcus aureus* (MRSA) (Cho & Chung, 2017), have also created a need to search for new substances that would have a wide range of antagonistic activity in turn on the CPF and inhibit the growth of aerococci at the same time and which should also be accessible and safe.

The experimental method (Stepanskyi & Kremenchutskyi, 2014) made it possible to discover the sensitivity of the *A. viridans* symbionts to fluoroquinolones and determined that norfloxacin at a dosage of 8.3 μg/ml practically did not affect the growth of aerococci and effectively suppresses the CPF. However, it was important to enhance the

selective effect of norfloxacin with other antimicrobial agents in order to receive stronger suppression of CPF. Therefore, the purpose of the study was to select a selective antibacterial complex that would suppress the growth of UPMF and would not affect the growth of *A. viridans*, with the possibility of using it for the production of modified media for isolation, cultivation and study of the biochemical activity of *A. viridans* microorganisms.

Materials and methods

The determination of the *A. viridans* symbionts and CPF sensitivity to the substances of different groups with antimicrobial activity was carried out by the method of "wells" (Habriev, 2005; CLSI, 2010). As a dense nutrient medium, the Mühler-Hinton agar was used, in which the wells with a diameter of 8 mm were used, the "lawn" was sown with test strips and the test specimens (0.01 ml) were placed. The inoculation was incubated at 37 °C for 24 hours. The results of the experiment were recorded by measuring the diameter of the growth inhibition zone in mm.

A. viridans symbionts isolated from different human and animal microbiocenoses were used for the study: *A. viridans* E34 (human intestine), *A. viridans* O36 (human oral cavity), *A. viridans* 5m2015 (mouse feces), *A. viridans* 3k2015 (rat feces), *A. viridans* 23 (human tonsils). As CPF, *Pseudomonas aeruginosa* ATCC 27853, *Staphylococcus aureus* 209-p, *Klebsiella pneumoniae* ATCC 700603, *Escherichia coli* ATCC 8739 and *Candida albicans* ATCC 885-653 were taken. Norfloxacin, pefloxacin, ofloxacin, gatifloxacin, levofloxacin, miramistin, decamethoxine, chlorhexidine, octenidine, boric acid were used as investigational drugs. The number of studies was 5 for each microorganism.

After determining the optimal, in terms of the purpose of the study, drugs, in order to minimize selective factors in nutrient media for growing aerococci, the optimal concentration of drugs was determined by the method of serial dilutions, which would suppress the growth of CPF, and would not show a negative effect on *A. viridans*. For inoculation, a standard microbial suspension equivalent to 0.5 on the Mc Farland standard diluted 100 times on a nutrient broth was used, after which the concentration of the microorganism in it was approximately 10^6 CFU/ml. 0.5 ml of inoculum was injected into each test tube containing 0.5 ml of the appropriate dilution of the test substance and into one test tube containing 0.5 ml of the nutrient broth without the test drug ("negative" control). The final concentration of the microorganism in each test tube reached the requirements – approximately $5 \cdot 10^5$ CFU/ml. The test tubes were sealed with sterile cotton gauze plugs, test tube test tubes, except "negative" control for the test tube, incubated in a normal atmosphere at 37 °C for 24 hours. The "negative" control tube was placed in a refrigerator at +4 °C, where the results were stored.

To determine the presence of microorganism growth, tubes with inoculate were reviewed in transmitted light. In addition, further research on aerococci properties grown on media with the addition of study drugs and without them was conducted.

Under the normal distribution law, the indicators are represented as an arithmetic average (M), a standard error of the average (m). Comparison of statistical characteristics of different groups and dynamics observation was conducted using parametric and nonparametric criteria: assessment of the likelihood difference means for unrelated samples by Mann-Whitney (U), connected to multiple comparison – ANOVA with post-hoc analysis based on the Scheffe test and Dunnett test. The probability of differences in relative quantities is according to Fisher's exact two-tailed criterion (Fisher exact P, two-tailed). Statistically significant differences were considered when $P< 0.05$.

Results

Miramistin and boric acid were found to meet the necessary criteria in addition to norfloxacin in previous experiments. In the further experiment, the minimum inhibitory concentrations (MICs) of drugs that suppressed the CPF growth and did not show a negative effect on *A. viridans* were determined by serial dilutions. Results of the norfloxacin study are presented in Table 1. Norfloxacin in a dosage of 12.5–50.0 μg/ml effectively inhibited the growth of the CPF, but also decreased the number of aerococci. The dose of 8.3 μg/ml met the criteria we needed, namely suppressing the growth of the CPF and not affecting aerococci. However, it was alarming that the dose of norfloxacin 6 μg/ml left a viable UPPF of 10^3–10^4 CFU/ml. To prevent the emergence of resistant to norfloxacin CPF strains when cultivating aerococci, as well as to enhance the action of the latter, attention was drawn to preparations of surface-active substances with bactericidal and fungicidal properties, safe and widely used in medical practice (miramistin and boric acid). In addition, no data were found on the resistance of microorganisms to these substances. It turned out that the sensitivity of the CPF to the aforementioned substances is different in the strength and spectrum of bactericidal action. The optimal concentrations of these substances that suppressed the growth of the CPF and did not affect the growth of aerococci were determined (Table 2, 3).

Table 1
Influence of norfloxacin on the opportunistic microflora and multibiotopic *A. viridans* co-cultivation (n = 5; number of microorganisms after 24 hours of cultivation, M ± m)

Microorganisms (7 lg CFU/ml)	Dosage of the preparation, μg/ml				
	6.0	8.3	12.5	25.0	50.0
Aerococcus viridans E34 (human intestine)	6.60 ± 0.16	6.36 ± 0.11	6.18 ± 0.12	5.18 ± 0.12**	3.32 ± 0.15**
Aerococcus viridans O36 (human oral cavity)	6.56 ± 0.16	6.48 ± 0.07	5.37 ± 0.10**	3.10 ± 0.10**	2.96 ± 0.13
Aerococcus viridans 5м2015 (mouse feces)	6.30 ± 0.09	6.46 ± 0.07	5.31 ± 0.09**	5.16 ± 0.10*	3.40 ± 0.11**
Aerococcus viridans 3к2015 (rat feces)	6.62 ± 0.04	6.46 ± 0.06	5.04 ± 0.13**	3.45 ± 0.12**	3.20 ± 0.14
Aerococcus viridans 23 (human tonsils)	6.53 ± 0.08	6.42 ± 0.12	5.34 ± 0.10**	3.37 ± 0.10**	3.05 ± 0.17
Staphylococcus aureus	3.31 ± 0.09	--**	--	--	--
Klebsiella pneumoniae	4.62 ± 0.11	--**	--	--	--
Escherichia coli	3.57 ± 0.04	--**	--	--	--
Pseudomonas aeruginosa	4.71 ± 0.11	--**	--	--	--

Note: * – $P < 0.05$; ** – $P < 0.001$ compared to the previous dosage of the drug (Scheffe's criterion).

As shown by the analysis of the data obtained (Table 2), the concentration of myramistin in the culture medium, which showed a strong depressant effect in relation to the conditionally pathogenic microflora and practically did not affect *A. viridans*, was 50 μg/ml. *P. aeruginosa* and *K. pneumoniae* were the most resistant to the investigated drug microorganisms in this concentration. Myramistin at concentration of 75 mg/ml effectively inhibited all pathogenic microflora, but at the same time reduced the aerococci concentration (10^3–10^4 CFU/ml). In addition, myramistin exhibited a fungicidal effect in relation to *C. albicans*.

Similar results were obtained in the study of the effects of boric acid (Table 3). Boric acid concentration in the culture medium, which had a strong depressant effect on CPF and practically did not affect *A. viridans* was 50 μg/ml. *P. aeruginosa* and *E. coli* were the most resistant to the studied drug in this concentration microorganisms. Boric acid at a concentration of 75 μg/ml effectively suppressed all of the CPF, but at the same time lowered the concentration of aerococci (10^5 CFU/ml). In addition, miramistin and boric acid exhibited fungicidal action against *C. albicans*. All studied aerococcus autosymbionts tolerated even the highest investigated concentrations of myramistin well without losing their properties (morphological, physiological, tinctorial, etc.).

Despite the active antimicrobial effects of the investigated drugs on the CPF, this was not complete in some cases, or inhibited the growth of aerococci at higher doses, so the effect of their rational combination on the CPF was investigated. The results are presented in Table 4. The complex of all three drugs completely suppressed the CPF, which may be due to the summation of antimicrobial effects, with virtually no effect on the aerococci growth. Properties of aerococci grown on the nutrient medium with the studied drugs did not differ from aerococci grown on nutrient media without additives. That is why all these drugs were

combined into a single antimicrobial complex for the production of modified media for the isolation, cultivation and study of biochemical activity of *A. viridans* microorganisms.

Table 2
Effect of miramistin on the opportunistic microflora and multibiotopic *A. viridans* co-cultivation (n = 5; number of microorganisms after 24 hours of cultivation (Ig CFU/ml, M ± m)

Microorganisms, 7 lg CFU/ml	Dosage of the preparation, μg/ml				
	10	25	50	75	100
Aerococcus viridans E34 (human intestine)	6.61 ± 0.09	6.54 ± 0.07	6.22 ± 0.09	4.40 ± 0.13**	3.42 ± 0.19**
Aerococcus viridans O36 (human oral cavity)	6.48 ± 0.14	6.37 ± 0.10	5.31 ± 0.15**	3.17 ± 0.12**	2.77 ± 0.10
Aerococcus viridans 5m2015 (mouse feces)	6.57 ± 0.08	6.53 ± 0.11	5.31 ± 0.13**	3.43 ± 0.06**	3.08 ± 0.15
Aerococcus viridans 3k2015 (rat feces)	6.63 ± 0.09	6.61 ± 0.12	6.64 ± 0.11	4.57 ± 0.08**	3.40 ± 0.06**
Aerococcus viridans 23 (human tonsils)	6.80 ± 0.09	6.63 ± 0.05	5.48 ± 0.08**	3.30 ± 0.14**	3.47 ± 0.13
Staphylococcus aureus	3.31 ± 0.09	0.86 ± 0.13**	--**	--	–
Klebsiella pneumoniae	4.52 ± 0.09	2.37 ± 0.10**	1.17 ± 0.12**	–**	–
Escherichia coli	3.53 ± 0.11	--**	--	--	–
Pseudomonas aeruginosa	4.71 ± 0.18	2.31 ± 0.15**	1.02 ± 0.08**	–**	–
Aerococcus viridans E34 (human intestine)	4.48 ± 0.08	2.16 ± 0.10**	--**	--	–

Note: see Table 1.

Table 3
Effect of boric acid on the opportunistic microflora and multibiotopic *A. viridans* (n = 5; number of microorganisms after 24 hours of cultivation (Ig CFU/ml, M ± m)

Microorganisms (7 lg CFU/ml)	Dosage of the drug, μg/ml				
	10	25	50	75	150
Aerococcus viridans E34 (human intestine)	6.49 ± 0.09	6.38 ± 0.12	6.22 ± 0.09	5.08 ± 0.10*	3.32 ± 0.15*
Aerococcus viridans O36 (human oral cavity)	6.61 ± 0.06	6.54 ± 0.07	6.38 ± 0.12	5.16 ± 0.10*	3.52 ± 0.09*
Aerococcus viridans 5m2015 (mouse feces)	6.59 ± 0.15	6.48 ± 0.12	6.40 ± 0.13	5.32 ± 0.11*	3.50 ± 0.08*
Aerococcus viridans 3k2015 (rat feces)	6.48 ± 0.08	6.46 ± 0.07	6.31 ± 0.15	5.19 ± 0.12*	3.43 ± 0.13*
Aerococcus viridans 23 (human tonsils)	6.61 ± 0.06	6.52 ± 0.13	6.42 ± 0.12	5.30 ± 0.13*	3.36 ± 0.11*
Staphylococcus aureus	3.31 ± 0.15	--*	--	--	–
Klebsiella pneumoniae	4.43 ± 0.09	2.49 ± 0.05*	–*	--	–
Escherichia coli	4.48 ± 0.08	2.47 ± 0.15*	1.08 ± 0.10*	–*	–
Pseudomonas aeruginosa	4.60 ± 0.08	2.40 ± 0.11*	1.12 ± 0.07*	–*	–
Aerococcus viridans E34 (human intestine)	2.48 ± 0.08	–*	--	--	–

Note: see Table 1.

Discussion

Selective antimicrobial additives are widely used to prepare nutrient media in microbiology for the cultivation of various microorganisms. Korean researchers Chon et al. (2014) have been successfully used polymyxin as a selective additive for the cultivation of *Bacillus cereus*. British scientists Hill et al. (2013) achieved good results in isolating *C. difficile* from environmental objects using cefoxitin-cycloserin-egg yolk agar with lysozyme.

In the absence of commercially available selective agents designed to isolate certain microorganisms, it is possible to use media with selective factors, including antibiotics. One study (Glass et al., 2009) evaluated the sensitivity and selectivity of four media for the isolation of *Burkholderia mallei* and *B. pseudomallei* (Ashdown agar – a special selective medium for isolation of *B. pseudomallei*, well described in the literature but not commercially available; three commercially available media: *Burkholderia cepacia* selective agar (BCSA), oxidation-fermentative-polymyxin B-bacitracin-lactose (OFPBL) agar and *Pseudomonas cepacia* (PC) agar for isolation of *B. cepacia*). The authors came to the conclusion that Ashdown agar was the most sensitive medium for the isolation of *B. pseudomallei*, but it was unable to support the growth of *B. mallei*. The Czech authors Bunesova at al. (2015) successfully used environments supplemented by mupirocin to isolate and identify Bifidobacterium.

Table 4
Influence of norfloxacin, myramystine and boric acid on opportunistic microflora and *A. viridans* (n = 5, M ± m)

Drug	*Aerococcus viridans*symbionts (7 lgCFU/ml)	*Staphylococcus aureus* (7 lgCFU/ml)	*Klebsiella pneumoniae* (7 lgCFU/ml)	*Escherichia coli* (7 lgCFU/ml)	*Pseudomonas aeruginosa* (7 lgCFU/ml)	*Candida albicans* (7 lgCFU/ml)
Norfloxacin, 8.3 μg/ml	6.43 ± 0.06	–	–*	–#	–*#	–
Miramistin, 50 μg/ml	6.46 ± 0.07	–	1.17 ± 0.12	–#	1.02 ± 0.08	–
Boric acid, 50 μg/ml	6.40 ± 0.06	–	–*	1.08 ± 0.10	1.12 ± 0.07	–
Norfloxacin + Miramistin + boric acid	6.41 ± 0.11	–	–*	–#	–*#	–

Notes: * – P < 0.001 relative to the corresponding indicator when using miramistin at a dose of 50 μg/ml; # – P < 0.001 relative to the corresponding indicator for using boric acid at a dose of 50 μg/ml (Scheffer criterion).

In another study (Vlková et al., 2015) a new selective medium with mupirocin, acetic acid and norfloxacin was proposed and evaluated. Among other things, the authors sought to identify an antibiotic that would suppress the growth of clostridia and allow the growth of bifidobacteria, as well as use of the identified substance to develop a selective culture for the cultivation of bifidobacteria. The susceptibility of bifidobacteria and clostridia to 12 antibiotics was tested on an agar by disk diffusion method. Only norfloxacin inhibited the growth of clostridia and did not affect the growth of bifidobacteria. Using both pure cultures and fecal specimens from infants, adults, calves, lambs and piglets, the optimal concentration of norfloxacin in hard growth media was determined as 0.2 mg/ml. The results showed that a hard medium containing norfloxacin (0.2 mg/ml) in combination with mupirocin (0.1 mg/ml) and acetic acid (0.001 ml/ml), is suitable for the isolation of bifidobacteria from fecal specimens of various origins. The authors recommend norfloxacin as a selective factor that inhibits the growth of fecal clostridia. Well-known selective media for the isolation of *Fusobacterium* spp. from clinical material include josamycin, vancomycin and norfloxacin (JVN) (3, 4, and 1 microgram per ml, respectively) as selective agents, plus 5% defibrinated horse blood. British researchers (Brazier et al., 1991) have successfully isolated the strains of *F. naviforme*, *F. nucleatum* and *F. necrophorum* from the respiratory membrane of healthy volunteers and *F. varium* and *F. mortiferum* strains from fecal suspensions contaminated by these organisms using JVN medium.

The experimental method (Stepanskyi & Kremenchutskyi, 2014) made it possible to discover the sensitivity of the *A. viridans* symbionts to fluoroquinolones and determined that norfloxacin at a dosage of 8.3 μg/ml practically did not affect the growth of aerococci and effectively suppresses the CPF. However, it was important to enhance the selective effect of norfloxacin with other antimicrobial agents in order to receive stronger suppression of CPF. Therefore, the purpose of the study was to select a selective antibacterial complex that would suppress the growth of UPMF and would not affect the growth of *A. viridans*, with the possibility to use it for the production of modified media for isolation, cultivation and study of the biochemical activity of *A. viridans* microorganisms.

The complex of all three drugs completely suppressed the CPF, which may be due to the summation of antimicrobial effects, with virtually no effect on the aerococci growth. Properties of aerococci grown on the nutrient medium with the studied drugs did not differ from aerococci grown on nutrient media without additives. That is why all these drugs were combined into a single antimicrobial complex for the production of modified media for the isolation, cultivation and study of biochemical activity of *A. viridans* microorganisms.

Due to the growing resistance to antibiotics, constant monitoring of the effectiveness of antimicrobial additives, especially antibiotics is clearly needed. The use of these additives as substances to which there are no cases of resistance has obvious advantages. Prior to the creation of an antimicrobial complex for the cultivation of *A. viridans* (norfloxacin 8.3 μg/ml, miramistin 50 μg/ml, boric acid 50 μg/ml), we did not find cases of resistance to miramystin or boric acid, which is an unconditional advantage in combination with minimal resistance to norfloxacin and a positive experience with the use of this antibiotic as a selective supplement.

Conclusions

A complex of all three drugs (norfloxacin, miramistin, boric acid) completely suppresses the conditionally pathogenic microflora, which may be due to the summation of antimicrobial effects, with virtually no effect on the growth of aerococci. An antimicrobial complex with optimal concentrations of substances (norfloxacin 8.3 μg/ml, miramistin 50 μg/ml, boric acid 50 μg/ml) which effectively suppresses CPF and does not affect the symbiontic *A. viridans* growth was determined.

References

Brazier, J. S., Citron, D. M., & Goldstein, E. J. (1991). Aselective medium for *Fusobacterium* spp. Journal of Applied Bacteriology, 71(4), 343–346.

Bunesova, V., Musilova, S., Geigerova, M., Pechar, R., & Rada, V. (2015). Comparison of mupirocin-based media for selective enumeration of Bifidobacteria in probiotic supplements. Journal of Microbiological Methods, 109, 106–109.

Cho, S. Y., & Chung, D. R. (2017). Infection prevention strategy in hospitals in the era of community-associated methicillin-resistant *Staphylococcus aureus* in the Asia-Pacific region: A review. Clinical Infectious Diseases, 64(2), S82–S90.

Chon, J. W., Song, K. Y., Kim, H., & Seo, K. H. (2014). Comparison of 3 selective media for enumeration of *Bacillus cereus* in several food matrixes. Journal of Food Science, 79(12), 2480–2484.

CLSI (2010). Performance standards for antimicrobial susceptibility testing: 20th informational supplement. CLSI document M100-S20. Clinical and Laboratory Standards Institute, Wayne, PA.

Collins, M. D., Jovita, M. R., Hutson, R. A., & Ohlén, M. (1999). *Aerococcus christensenii* sp. nov., from the human vagina. International Journal of Systematic Bacteriology, 49, 1125–1128.

Devriese, L. A., Hommez, J., Laevens, H., Pot, B., Vandamme, P., & Haesebrouck, F. (1999). Identification of aesculin-hydrolyzing streptococci, lactococci, aerococci, and enterococci from subclinical intramammary infections in dairy cows. Veterinary Microbiology. (70), 87–94.

Facklam, R., & Elliott, J. A. (1995). Identification, classification, and clinical relevance of catalase-negative, gram-positive cocci, excluding the streptococci and enterococci. Clinical Microbiology, 8, 479–495.

Facklam, R., Lovgren, M., Shewmaker, P. L., & Tyrrell, G. (2003). Phenotypic description and antimicrobial susceptibilities of *Aerococcus sanguinicola* isolates from human clinical samples. Journal of Clinical Microbiology, 41(6), 2587–2592.

Glass, M. B., Beesley, C. A., Wilkins, P. P., & Hoffmaster, A. R. (2009). Comparison of four selective media for the isolation of *Burkholderia mallei* and *Burkholderia pseudomallei*. The American Journal of Tropical Medicine and Hygiene, 80(6), 1023–1028.

González Ramallo, V. J., Mirón Rubio, M., Estrada Cuxart, O., & García Leoni, M. E. (2017). Usefulness of hospital at home in nosocomial infections: Advantages and limitations. Revista Española de Quimioterapia, 30(1), 61–65.

Good, N. E., Winget, G. D., Winter, W., Connolly, T. N., Izawa, S., & Singh, R. M. (1966). Hydrogen ion buffers for biological research. Biochemistry, 5, 467–477.

Habriev, R. U. (2005). Rukovodstvo po jeksperimental'nomu (doklinicheskomu) izucheniju novyh farmakologicheskih veshhestv [Manual on experimental (preclinical) study of new pharmacological substances]. Medicina, Moscow (in Russian).

Hill, K. A., Collins, J., Wilson, L., Perry, J. D., & Gould, F. K. (2013). Comparison of two selective media for the recovery of *Clostridium difficile* from environmental surfaces. Journal of Hospital Infection, 83(2), 164–166.

Humphries, R. M, & Hindler, J. A. (2014). *In vitro* antimicrobial susceptibility of *Aerococcus urinae*. Journal of Clinical Microbiology, (52), 2177–2180.

Kremenchuckij, G. N., Ryzhenko, S. A., Val'chuk, S. I. (2003). Rol' mikrojekologii organizma cheloveka i principy ejo korrekcii [The role of microecology of the human body and the principles of its correction]. Porogi, Dnepropetrovsk (in Russian).

Kremenchuckyj, G. N., Jurgel', L. G., Sharun, O. V., & Stepans'kyj, D. O. (2009). Metody vydilennja ta identyfikacii' grampozytyvnyh katalazonegatyvnyh kokiv [Methods of selection and identification of gram-positive catalase-negative cocci]. Kyiv (in Ukrainian).

Rasmussen, M. (2013). Aerococci and aerococcal infections. Journal of Infection, 66(6), 467–474.

Rizhenko, S. A., Chernjaev, S. A., & Kremenchuc'kij, S. G. (2002). Zmina biologichnyh vlastyvostej useredini populjaciji *Aerococcus viridans* [Changing biological properties within the population Aerococcus viridans]. Medychni Perspektyvy, 7(2), 18–21 (in Ukrainian).

Saishu, N., Morimoto, K., Yamasato, H., Ozaki, H., & Murase, T. (2015). Characterization of *Aerococcus viridans* isolated from milk samples from cows with mastitis and manure samples. Journal of Veterinary Medical, 77(9), 1037–1042.

Senneby, E., Göransson, L., Weiber, S., & Rasmussen, M. (2016). A population-based study of aerococcal bacteraemia in the MALDI-TOF MS-era. European Journal of Clinical Microbiology and Infectious Diseases, 35(5), 755–762.

Senneby, E., Petersson, A. C., & Rasmussen, M. (2015). Epidemiology and antibiotic susceptibility of aerococci in urinary cultures. Diagnostic Microbiology and Infectious Disease, 81(2), 149–151.

Shelton-Dodge, K., Vetter, E. A., Kohner, P. C., Nyre, L. M., &Patel, R. (2011). Clinical significance and antimicrobial susceptibilities of *Aerococcus sanguinocola* and *Aerococcus urinae*. Diagnostic Microbiology and Infectious Disease, 70, 448–451.

Uh, Y., Son, J. S., Jang, I. H., Yoon, K. J., & Hong, S. K. (2002). Penicillin-resistant *Aerococcus viridans* bacteremia associated with granulocytopenia. Journal of Korean Medical Science, 17, 113–115.

Vlkova, E., Salmonova, H., Bunešova, V., Geigerova, M., Rada, V., & Musilova, Š. (2015). A new medium containing mupirocin, acetic acid, and norfloxacin for the selective cultivation of bifidobacteria. Anaerobe, 34, 27–33.

Williams, R. E., & Hirch, S. T. (1953). Cowan *Aerococcus* – a new bacterial genus. Journal of General Microbiology, 8, 475–480.

Wise, M. G., & Siragusa, G. R. (2007). Quantitative analysis of the intestinal bacterial community in one- to three-week-old commercially reared broiler chickens fed conventional or antibiotic-free vegetable-based diets. Journal of Applied Microbiology, 102, 1138–1149.

Yasukawa, K., Afzal, Z., Mbang, P., Stager, C. E., & Musher, D. M. (2014). Aerococcal infection at three US Tertiary Care Hospitals. Southern Medical Journal, 107(10), 642–647.

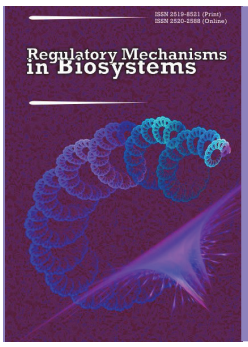

Regulatory Mechanisms in Biosystems

ISSN 2519-8521 (Print)
ISSN 2520-2588 (Online)
Regul. Mech. Biosyst., 9(3), 430–434
doi: 10.15421/021864

Optimization of the 9α-hydroxylation of steroid substrates using an original culture of *Rhodococcus erythropolis*

V. A. Andryushina, N. V. Karpova, T. S. Stytsenko, V. V. Yaderets, E. D. Voskresenskaya, V. V. Dzhavakhia

Federal Research Center "Fundamentals of Biotechnology", Russian Academy of Sciences, Moscow, Russian Federation

Article info

Received 07.06.2018
Received in revised form 12.07.2018
Accepted 16.07.2018

Federal Research Center "Fundamentals of Biotechnology", Russian Academy of Sciences, Leninsky prospect, 33/2, Moscow, 119071, Russian Federation.
Tel.: +7-499-135-30-49.
E-mail: andryushina@rambler.ru

Andryushina, V. A., Karpova, N. V., Stytsenko, T. S., Yaderets, V. V., Voskresenskaya, E. D., & Dzhavakhia, V. V. (2018). Optimization of the 9α-hydroxylation of steroid substrates using an original culture of Rhodococcus erythropolis. Regulatory Mechanisms in Biosystems, 9(3), 430–434. doi:10.15421/021864

To obtain inoculation material (cultivation stage 1), the biomass of *Rhodococcus erythropolis* VKPM AC-1740 was transferred from agar slants into 750 ml conic flasks containing 100 ml of vegetation media of the following composition (g/l): medium 1 – yeast extract, 10.0; glucose, 10.0; soybean flour, 10.0; KH_2PO_4, 2.0; Na_2HPO_4, 4.0 (pH 6.8–7.4); medium 2 – corn extract, 15.0; glucose, 10.0; KH_2PO_4, 2.0; Na_2HPO_4, 4.0 (pH 6.8–7.4). The culture was grown on a rotary shaker (220 rpm) for 68–72 h at 28–29 °C. To obtain a working biomass (cultivation stage 2), the inoculum obtained at the stage 1 was transferred into flasks containing the same media (the volume of seed material was 20% of the medium volume) and grown under the same conditions for 23–25 h. During a study of the effect of the inducer concentration on the rate of 9α-OH-AD formation, different concentrations (0.25, 0.50, and 1 g/l) of the AD solution in dimethylformamide (DMF) were added to the vegetation medium after 6 h of incubation. To perform AD transformation at a load of 5 g/l, 10 ml of *Rh. erythropolis* cells at the age of 23–25 h were transferred into 750 mL flasks with baffles containing 40 mL of vegetation medium supplemented with the steroid. AD was added in the form of microcrystals or suspension with a surfactant or DMF. The process was carried out at 28–29 ºC and with constant mixing (220 rpm). During AD transformation at a load of 10–30 g/l, the steroid was preliminarily precipitated from DMF solution. The resulting paste was mixed with a surfactant and transformation medium. The obtained homogeneous suspension was poured in equal amounts into the flasks with baffles, and then a concentrated cell mass was added (25 vol.%). To obtain a cell concentrate, cells were centrifuged for 1 h at 1500 rpm at the age of 23–25 h. The resulting biomass was homogenized, supplemented with a fresh medium to the required volume, and added into transformation flasks. The amount of a biomass required for AD transformation at a load of 10 g/l was 3.13 g/l (dry weight); in the case of a 30 g/l load, the biomass was added by two equal portions, and its total amount was 6.2 g/l (dry weight). The amount of 9α-OH-AD in a culture broth was evaluated by a thin-layer chromatography (TLC) and high-performance liquid chromatography (HPLC). Steroids were extracted by ethylacetate. To perform TLC, Sorbifil plates (Russia) and benzol: acetone mix (3 : 1) were used. HPLC was performed on a Gilson chromatographer (United States) equipped with a Silasorb C-18 column (10 μm, 4.0 × 250 mm); the flow rate was 0.8 ml/min. The mobile phase was MeOH : H_2O mix (70 : 30). The absorbance was measured at 260 nm. Replacement of corn extract, which has an unstable composition, by yeast extract and soybean flour and the use of glucose as an optimal carbon source for a *Rh. erythropolis* culture have provided a high-yield production of 9α-hydroxy-4-ene-3,17-dione with increased AD loads. Use of such techniques as the inoculum induction and application of surfactants have provided a positive effect on the AD transformation with a load exceeding 10 g/l. During 9α-hydroxylation of AD with a load of 30 g/l, a target product with the yield of 83% has been obtained.

Keywords: fluorinated corticoids; AD; 9α-OH-AD; *Rhodococcus erythropolis* VKPM AC-1740; surfactants; inducer.

Introduction

Deterioration of environmental conditions and the corresponding increase in the number of allergic and inflammatory diseases on the global scale gives rise to a growing need for steroid preparations of different therapeutic action. According to analytic forecasts, the volume of the steroid market in 2021 will reach 4.480 million US dollars (Fernandez-Cabezon et al., 2018; Barredo & Herráiz, 2017, Fernandes et al., 2003). Thus, despite the existing achievements in the biotechnology of steroid production, the development of effective methods of synthesis of androgenic, gestagenic, mineral, and glucocorticoid steroid preparations from natural plant products still remains relevant (Brzezinska et al., 2013; Guevara et al., 2017a; Fernandez-Cabezon et al., 2018).

The main indications for glucocorticosteroid therapy of humans include rheumatoid arthritis, bronchial asthma, neurodermatitis and other skin and allergic diseases, acute adrenal insufficiency, and also various shock states (post-rheumatic, operational, toxic, burn, etc.). Today the most common anti-inflammatory steroids represent structural modifications of natural compounds and are characterized by improved therapeutic properties and weaker side effects. Among such preparations, fluorinated corticosteroids (dexamethasone, sinaflan, triamcinolone, fluticasone, etc.) are in the greatest demand (Mashkovskiy, 2012).

9α-hydroxy-4-ene-3,17-dione (9α-OH-AD) is the basic intermediate in the synthesis of the aforementioned drug preparations from sterols (Fernández de las Heras et al., 2012; Mohn et al., 2012; Jakočiunas et al., 2016; Mondaca et al., 2017). According to the existing data, 9α-hydroxylation, which represents a key reaction in the synthesis of fluorinated corticoids, cannot be realized via chemical synthesis (Guevara et al., 2017). Therefore, a cost-efficient large-scale production of this class of drugs is possible only with the use of microorganisms able to perform a highly selective targeted transformation of steroid molecules of a given structure under ecologically safe conditions and without any need for preliminary protection of the functional groups of the initial molecule (Mutafova et al., 2016; Smitha et al., 2017).

It is known that some lower fungi (*Ascochyta*, *Helicostilum*, *Circinella*) and many bacteria, especially actinobacteria (*Arthrobacter*, *Corynebacterium*, *Mycobacterium*, *Nocardia*, *Rhodococcus*) are able to introduce 9α-hydroxygroups into a steroid molecule. However, steroid hydroxylation with fungi does not provide a sufficient selectivity of the process. Along with the formation of a target hydroxysteroid, fungi also produce a number of side mono- and dihydroxy-products, which complicates the further isolation of the target product and significantly reduces its yield. In addition, both position and orientation of an introduced hydroxyl group strongly depends on the structure of the steroid molecule (Donova & Egorova, 2012; Andryushina et al., 2013; Barredo & Herráiz, 2017).

Unlike fungi, bacteria perform 9α-hydroxylation reaction regardless of the steroid structure and presence of additional bonds and substituents. Therefore, actinobacteria capable of providing a high-selective introduction of a hydroxy group at the 9α-position of a steroid molecule may be considered as the most promising bioreagents, since the corresponding bacterial enzyme shows the lower substrate specificity than steroid 9α-monooxygenase of a fungal origin (Petrusma et al., 2009, 2011; Lee et al., 2016; Nielsen & Keasling, 2016). However, 9α-hydroxylation activity was detected only in bacteria which were able to use steroids as a carbon source since this reaction represents an intermediate stage of a complete cleavage of steroid molecules to CO_2 and H_2O, at which the simultaneous action of 3-ketosteroid-1,2-dehydrogenase and 9α-hydroxylase is observed (Petrusma et al., 2014; Donova & Egorova, 2012; Rodina et al., 2009). The analysis of published data showed that the selective 9α-hydroxylation without any destruction of a steroid nucleus can be performed using bacterial strains carrying mutations, which block the biosynthesis of 1,2-dehydrogenase or prevent the functioning of this enzyme. In our previous study, we obtained a highly-selective *Rhodococcus erythropolis* strain VKPM AC-1740 with improved 9α-hydroxylating activity (Rodina et al., 2009; Carpova-Rodina et al., 2011). Using this strain, we developed efficient technologies for the production of 9α-hydroxy-steroid derivatives (Vojshvillo et al., 2007) and developed several efficient methods for 9α-OH-AD production from sterols including the mixed culture method (Andryushina et al., 2011) or the use of original biocatalyst representing *R. erythropolis* VKPM AC-1740 cells immobilized in a PVA cryogel (Carpova-Rodina et al., 2011).

A common disadvantage of all methods for 9α-hydroxylation of steroids, which were previously developed by our team, was the dependence of the hydroxylating activity of *R. erythropolis* VKPM AC-1740 on a nutrient medium composition, namely, the quality of the corn extract used as the main nitrogen source (Ribeiro et al., 2017; van der Geize et al., 2001, 2001, 2008). The composition of a corn extract is determined by several factors, such as the grain quality, scheme and mode of its soaking, and the extract thickening procedure. Corn extract may contain some impurities, which provide a negative effect on microorganisms and reduce their enzymatic activity. Because of fluctuations in the activity of a culture grown on such medium, there is a need to select an alternative nitrogen source with the further optimization of the hydroxylation process under new fermentation conditions. At this stage of our work, yeast extract was chosen as a stable and available source of organic nitrogen.

Thus, the aim of this study was to evaluate the 9α-hydroxylating activity of *R. erythropolis* VKPM AC-1740, grown on media containning yeast extract and soybean flour as the main nitrogen sources, in relation to the production of 9α-OH-AD from AD at the initial AD concentration equal to 10–30 g/l.

Materials and Methods

Strain, nutrient media and cultivation conditions. The earlier developed *R. erythropolis* VKPM AC-1740 strain characterized by a high 9α-hydroxylating activity in relation to Δ4-3-ketosteroids, was used in the study. The culture was stored on solid agar medium of the following composition (g/l): yeast extract, 10.0; glucose, 10.0; KH_2PO_4, 1.0 (pH 6.8–7.2). To obtain inoculation material (cultivation stage 1), the biomass of *R. erythropolis* was transferred from agar slants into 750 ml conic flasks containing 100 ml of vegetation media of the following composition (g/l): medium 1 – yeast extract, 10.0; glucose, 10.0; soybean flour, 10.0; KH_2PO_4, 2.0; Na_2HPO_4, 4.0 (pH 6.8–7.4); medium 2 – corn extract, 15.0; glucose, 10.0; KH_2PO_4, 2.0; Na_2HPO_4, 4.0 (pH 6.8–7.4). The culture was grown on a rotary shaker (220 rpm) for 68–72 h at 28–29 °C.

To obtain a working biomass (cultivation stage 2), the inoculum obtained at the stage 1 was transferred into flasks containing the same media (the volume of seed material was 20% of the medium volume) and grown under the same conditions for 23–25 h. During the study of the effect of the inducer concentration on the rate of 9α-OH-AD formation, different concentrations (0.25, 0.50, and 1 g/l) of the AD solution in dimethylformamide (DMF) were added to the vegetation medium after 6 h of incubation.

Biotransformation conditions. To perform AD transformation at a load of 5 g/l, 10 ml of *R. erythropolis* cells at the age of 23–25 h were transferred into 750 ml flasks with baffles containing 40 ml of vegetation medium supplemented with the steroid. AD was added in the form of microcrystals or suspension with a surfactant or DMF. The process was carried out at 28–29 ºC and a constant mixing (220 rpm).

During AD transformation at a load of 10–30 g/l, the steroid was preliminarily precipitated from the DMF solution. The resulting paste was mixed with a surfactant and transformation medium. The obtained homogeneous suspension was poured in equal amounts into the flasks with baffles, and then a concentrated cell mass was added (25 vol.%).

To obtain a cell concentrate, cells were centrifuged for 1 h at 1500 rpm at the age of 23–25 h. The resulting biomass was homogenized, supplemented with a fresh medium to the required volume, and added into transformation flasks. The amount of a biomass required for AD transformation at a load of 10 g/l was 3.13 g/l (dry weight); in the case of a 30 g/l load, the biomass was added by two equal portions, and its total amount was 6.2 g/l (dry weight).

Transformation efficiency assessment. The amount of 9α-OH-AD in a culture broth was evaluated by a thin-layer chromatography (TLC) and high-performance liquid chromatography (HPLC). Steroids were extracted by ethylacetate. To perform TLC, Sorbifil plates (Russia) and benzol: acetone mix (3 : 1) were used. HPLC was performed on a Gilson chromatographer (United States) equipped with a Silasorb C-18 column (10 μm, 4.0 × 250 mm); the flow rate was 0.8 ml/min. The mobile phase was MeOH : H_2O mix (70 : 30). The absorbance was measured at 260 nm.

Results

Selection of Nitrogen and Carbon Sources. At the first stage of a nutrient medium optimization, a comparative 9α-hydroxylation of AD with a 5 g/l load was carried out using media 1 and 2. The obtained results were identical for both media: a complete conversion of the initial compound with the formation of 4.7–4.8 g/l of 9α-OH-AD occurred within 20–22 h. Replacement of a carbon source in the medium 1 provided a more significant impact on the AD biotransformation process (Table 1). According to the obtained data, the best result was obtained using a modified medium containing soybean flour, yeast extract, and glucose. After 21 h of the AD transformation (5 g/l load) in a modified medium, almost complete substrate conversion was observed with the formation of 9α-OH-AD as an individual compound. Therefore, this medium was chosen as the basic one for the further optimization of the conversion process.

Table 1
Effect of various carbon sources on the production of 9α-OH-AD by *Rhodococcus erythropolis* VKPM AC-1740

Carbon source (5 g/L)	Average steroid content in a culture broth, %	
	9α-OH-AD	AD
Control (no carbon source)	68 ± 1.5	30 ± 1.5
Glucose	98 ± 1.0	2 ± 1.0
Fructose	15 ± 1.3	84 ± 1.3
Sucrose	40 ± 0.8	60 ± 0.8
Lactose	12 ± 1.5	85 ± 1.5

Note: hereinafter, the experimental error (±) was determined as a random error of direct measurements using the following formula: $\Delta x = (x_{max} - x_{min})/2$, where x_{max} и x_{min} are the maximum and minimum values obtained by the series of repeated measurements.

Effect of the AD introduction method on the 9α-OH-AD output. As we have mentioned earlier, one of the main problems of microbiological transformations of steroid substrates is the high hydrophobic property of steroid molecules; the solubility of steroids belonging to the androstane group does not exceed 20 mg/l (Goetschel & Bar, 1992). To solve this problem, we added AD into a medium either in the form of a fine-dispersed suspension with various surfactants, or dissolved in DMF (Table 2).

Table 2
Effect of various surfactants on the production of 9α-OH-AD by *Rhodococcus erythropolis* VKPM AC-1740

Surfactant used for introduction of ground AD into fermentation medium	Average steroid content in a culture broth (TLC), %	
	9α-OH-AD	AD
Tween 21*	97 ± 1.5	3 ± 1.5
Tween 40	96 ± 1.3	4 ± 1.3
Tween 61	96 ± 1.4	4 ± 1.4
Tween 80	99 ± 0.3	1 ± 0.3
Triton 100	95 ± 1.6	5 ± 1.6
Span 20	98 ± 1.3	2 ± 1.3
Span 80	97 ± 1.5	3 ± 1.5
Emulan EL	90 ± 1.3	10 ± 1.3
DMF**	95 ± 1.3	5 ± 1.3
Control	98 ± 0.5	2 ± 0.5

Note: * – surfactant : AD ratio is 1 : 4; ** – DMF 4 vol.%.

According to the obtained results, the most efficient AD transformation at a 5 g/l load was observed in the variant with Tween 80. However, the control variant (i.e., without addition of any surfactant or solvent) demonstrated a quite comparable result.

Effect of the Inducer on a Microbiological 9α-Hydroxylation by R. erythropolis VKPM AC-1740. 3-Ketosteroid-9α-hydroxylase (9-KSH) is a two-component non-heme iron-dependent Rieske monooxygenase consisting of a KshA oxygenase and a KshB reductase. 9-KSH is one of the key enzymes involved into a microbiological degradation of steroids and is of a great physiological importance for a wide range of steroid-transforming bacteria (Petrusma et al., 2014). The presence of a 3-keto group and also Δ1 and / or Δ4-double bonds in the A ring of the steroid nucleus is a necessary condition for a 9α-hydroxylase activity (Akhrem & Titov, 1970).

To study the stimulation of a 9-KSH biosynthesis, the inoculum of *R. erythropolis* VKPM AC-1740 was grown on a medium supplemented with AD as an inducer (0.25, 0.50, and 1.0 g/l). The AD solution was added 6–7 h after inoculation by a second-generation culture. The total time of incubation was 23–25 h. The amount of the inoculum used for transformation of AD (5 g/l) was 20% of the medium volume. The result of the experiment is shown in Table 3.

Table 3
Consumption of AD (5 g/l) and accumulation of 9α-OH-AD by *R. erythropolis* VKPM AC-1740 grown in the presence of various concentrations of the inducer

Time, h	Average steroid content in a culture broth, %							
	control		inducer concentration, g/L					
			0.25		0.50		1.00	
	AD	9α-OH-AD	AD	9α-OH-AD	AD	9α-OH-AD	AД	9α-OH-AD
0	5.0	–	5.0	–	5.0	–	5.0	–
2	5.0	–	4.9	0.1	4.8	0.1	4.7	0.2
4	5.0	–	4.7	0.2	4.6	0.2	4.5	0.3
6	4.8	0.1	4.4	0.3	4.4	0.3	4.3	0.4
12	1.9	2.9	1.5	3.2	1.3	3.4	1.2	3.3
14	1.4	3.5	0.9	3.1	0.9	3.3	0.8	3.0
16	1.0	3.9	0.4	3.0	0.3	3.1	0.2	2.9
18	0.6	4.3	–	2.5	–	2.6	–	2.5
20	0.1	4.7	–	2.1	–	2.4	–	2.0

The 9α-hydroxylating activity of *R. erythropolis* VKPM AC-1740 in the presence of the inducer was observed already after 2 h of transformation, whereas in the control variant it was registered only after 6 hours of transformation. For all variants with induced seed material, we observed an active destruction of the target product during transformation. A probable explanation is that the induction of a 9-KSH biosynthesis may result in the induction of 1,2-dehydrogenase, responsible for the next reaction in the steroid nucleus degradation pathway.

Results obtained in this experiment were used for the study of the AD transformation at a load of 10–30 g/l. AD transformation into 9α-OH-AD at a substrate load of 10 g/l. The effect of induction on the AD transformation at a load of 10 g/l was examined using a concentrated *R. erythropolis* VKPM AC-1740 biomass (3.13 g/l of dry weight). The transformation time was 19–20 h. The yield of 9α-OH-AD equal to 94.3% and 94.0% (as determined by HPLC) was obtained in the case of the inducer concentration equal to 0.5 g/l; this yield exceeded that of the control by 10% (Fig. 1). A slight destruction of the target product was observed at the inducer concentration equal to 1.0 g/l (Figs. 1, 2).

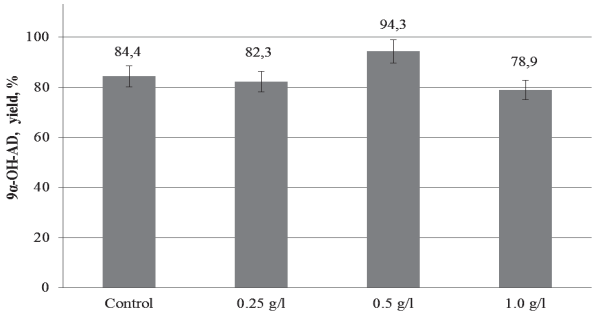

Fig. 1. Effect of various inducer concentrations on the yield of 9α-OH-AD at the end of the AD transformation by *Rhodococcus erythropolis* VKPM AC-1740: for all variants, the AD concentration was 10 g/l

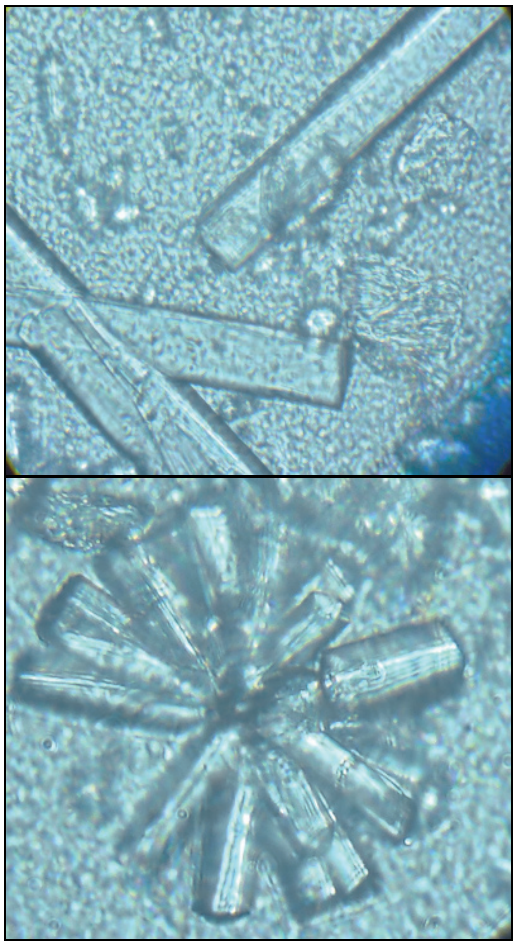

Fig. 2. 9α-OH-AD crystals in a culture broth AD transformation into 9α-OH-AD at a substrate load of 30 g/l

The AD transformation at a load of 30 g/L was carried out under conditions selected in the previous experiments. To improve the biotrans-

formation process, an additional portion of a concentrated inoculum and a glucose solution (5 g/l) were added during the process (Fig. 3).

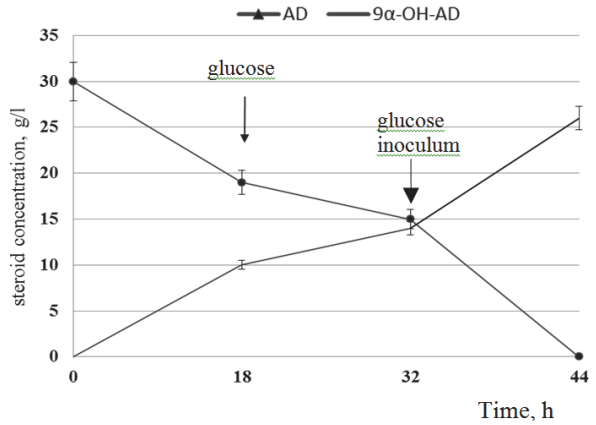

Fig. 3. Dynamics of 9α-OH-AD accumulation at the AD load of 30 g/l

According to this experiment, the substrate was completely transformed into 9α-hydroxyproduct within 44 h of incubation. The yield of a technical 9α-OH-AD substance reached 83%, while its content determined by HPLC was 93.6%.

Discussion

According to many authors, nutrient medium composition influences the direction of the steroid reaction and on the rates of consumption of the initial substrate and accumulation of the target product. For example, changes in the concentration or the origin of organic nitrogen in a nutrient medium directly affect the biomass accumulation rate and can change the hydroxylating activity of cells. It was shown that the use of non-dehydrated nitrogen sources, such as casein, gelatin, and meat extract, provided a biomass possessing the higher transformational activity (Angelova et al., 1995). Soybean flour contains fatty acids, which positively influence the permeability of a bacterial cell wall and improve the availability of lipophilic substrates, such as steroid compounds, for enzymes of steroid-transforming microorganisms. Soybean flour also contains lecithin, a natural emulsifier preventing aggregation of steroid particles.

The results obtained in our study revealed no correlation between the biotransformation ability of *Rh. erythropolis* VKPM AC-1740 and the nitrogen source. The effect of a carbon source on the yield of a target 9α-OH-AD was more significant. We showed that the absence of glucose (preferred carbon source) in the medium resulted in a decreased 9α-hydroxylation rate as compared with the glucose-containing medium (Table 1). We also observed the inhibition of a 9α-hydroxylase activity in the media containing lactose or fructose as a carbon source. Our results agree with the data obtained by Angelova et al. (1995), who also showed the maximum biomass accumulation and a high substrate conversion rate in a glucose-containing medium.

A high hydrophobic property of steroid substrates in aqueous media results in a low degree of conversion of the initial substrate and a low yield of the target reaction product. Traditional approaches to reducing mass transfer limitations include the use of a fine-grain substrate and various surfactants or solvents able to mix with water, such as dimethyl sulfoxide, DMF, methanol, acetone, and 1,2-propanediol. To prevent deactivation of the biocatalyst, the amount of the added solvent usually does not exceed 1.5–5.0% (v/v) (Fernandes et al., 2003). In addition, it is known that solvents may provide different effects, such as changes in the rate and direction of hydroxylation, as well as the stimulation or suppression of the by-product formation. According to some authors, microorganisms can include some solvents into their metabolic pathways to regenerate reduced cofactors (Angelova et al., 1995). Avramova et al. (2010) showed that the presence of Tween 80 in a glucose-containing medium accelerated the process of the 9α-hydroxylation of AD.

In this study we showed that the surfactant presence in the nutrient medium during the AD transformation at a load within 5 g/l did not result in an expected increase in the 9α-OH-AD generation rate as compared to the control (Table 2). A probable reason is that the strain itself may be able to emulsify and degrade hydrophobic substrates. According to the existing publications, such ability is determined mainly by specific structural features of the cell membrane of this microorganism, which is lipophilic, i.e., has a high affinity to hydrophobic substrates (Tsitko et al., 1999). The surface activity and hydrophobic character of the cell membrane promote interaction between the cells and insoluble substrate, which makes it possible to overcome a limited diffusion during the substrate uptake into a cell (Kostina, 2008). In addition, the composition of soybean flour includes lecithin, a natural emulsifier preventing aggregation of steroid particles (Petrusma et al., 2009; 2011; Jakočiunas et al., 2016; Liu et al., 2016). It is known that Δ1-2-dehydrogenation and 9α-hydroxylation reactions resulting in the opening of the B ring of the steroid structure are the key reactions in the process of steroid utilization as carbon sources (Marques et al., 2010; Wilbrink et al., 2011; Brzezinska et al., 2013; Yeh et al., 2014). Data shown in Table 3 allow us to assume that the induction of the 9α-KSH synthesis resulted in the induction of 1,2-dehydrogenase, responsible for the next reaction in steroid nucleus degradation pathway. This hypothesis may provide an explanation of the observed active 9α-OH-AD destruction. A possible reason for the lack of any undesirable 9α-OH-AD degradation (which was observed at the AD load of 5 g/l) during the AD transformation at a load of 10 g/l is that the increased AD load resulted in the accumulation of 9α-OH-AD in the culture broth in the form of crystal-like structures (Fig. 3) unavailable for the further microbial destruction (Rodina et al., 2009). During this study we selected optimal conditions providing AD transformation at a load of 30 g/L and obtaining a high output of a technical product. Our results suggest that further work is needed on the nutrient medium optimization and study of the effect of optimized media on the 9α-KSH activity of *R. erythropolis* VKPM AC-1740 to provide the further increase of the AD load and to obtain a high yield of 9α-OH-AD.

An obvious advantage of the proposed technology is acceleration of the transformation process due to a high substrate availability and use of a concentrated biomass that makes it possible to transform AD under high loads and under non-sterile conditions.

Conclusion

Replacement of corn extract with yeast extract and soybean flour, as well as the choice of glucose as a carbon source provided reduction of the duration of transformation while still maintaining a high 9α-OH-AD yield. At the same time, the effect of surfactants and the effect of 9-KSH-mediated induction of *R. erythropolis* VKPM AC-1740 were positive only if they were applied for transformation with an increased substrate load. A 44-h AD transformation at a load of 30 g/l by *R. erythropolis* VKPM AC-1740 resulted in the production of 9α-OH-AD with the yield of 83.0%; the content of the target compound determined by HPLC was 93.6%.

This study was supported by the programme of the Presidium of the Russian Academy of Sciences "Development of new biotechnological methods for obtaining highly active fluorinated corticosteroids of anti-inflammatory and antiallergic action from phytosterols via 9α-hydroxy-AD using biologically modified immobilized biocatalysts" (project 1201371077).

References

Akhrem, A. A., & Titov, Y. A. (1970). Steroids and microorganisms. Nauka, Moscow (in Russian).

Andryushina, V. V, Stytsenko, T. S., Voishvillo, N. E., Iaderetz, V. V., & Druzhinina, A. V. (2013). Effect of the steroid molecule structure on the direction of its hydroxylation by the fungus *Curvularia lunata*. Applied Biochemistry and Microbiology, 49(4), 382–390.

Angelova, B., Mutafov, S., Avramova, T., Dimova, I., & Boyadjie, L. (1996). 9α-Hydroxylation of 4-androstene-3,17-dione by resting *Rhodococcus* sp. cells. Process Biochemistry, 31(2), 179–184.

Arnell, R., Johannisson, R., Lindholm, J., Fornstedt, T., Ersson, B., Ballagi, A., & Caldwell, K. (2007). Biotechnological approach to the synthesis of 9alpha-hydroxylated steroids. Preparative Biochemistry and Biotechnology, 3, 309–321.

Avramova, T., Spassova, D., Mutafov S., Momchilova S., Boyadjieva, L., Damyanova, B., & Angelova, B. (2010). Effect of Tween 80 on 9a-steroid

hydroxylating activity and ultrastructural characteristics of *Rhodococcus* sp. cells. World Journal of Microbiology and Biotechnology, 26, 1009–1014.
Barredo, J.-L., & Herráiz, I. (Eds.). (2017). Microbial steroids: Methods and protocols. Methods in Molecular Biology. Springer Science + Business Media LLC, 1645, 373.
Bhatti, H. N., & Khera, R. A. (2012). Biological transformations of steroidal compounds: A review. Steroids, 77, 1267–1290.
Brzezinska, M., Szulc, I., Brzostek, A., Klink, M., Kielbik, M., Sulowska, Z., Pawelczyk, J., & Dziadek, J. (2013). The role of 3-ketosteroid 1(2)-dehydrogenase in the pathogenicity of *Mycobacterium tuberculosis*. BMC Microbiology, 13, 43.
Carpova-Rodina, N. V., Andryushina, V. A., Yaderetz, V. V., Druzhinina, A. V., Stytsenko, T. S., Shaskol'skiy, B. L., Lozinsky, V. I., Huy Luu, D., & Voishvillo, N. E. (2011). Transformation of Δ4-3-ketosteroids by free and immobilized cells of *Rhodococcus erythropolis* actinobacterium. Applied Biochemistry and Microbiology, 47(4), 386–392.
Donova, M. V. (2017). Steroid bioconversions. Methods in Molecular Biology, 1645, 1–13.
Egorova, O. V., Nikolayeva, V. M., Sukhodolskaya, G. V., & Donova, M. V. (2009). Transformation of C_{19}-steroids and testosterone production by sterol-transforming strains of *Mycobacterium* sp. Journal of Molecular Catalazysis B: Enzymatic, 57, 198–203.
Fernández de las Heras, L., van der Geize, R., Drzyzga, O., Perera, J., & Navarro-Llorens, M. J. (2012). Molecular characterization of three 3-ketosteroid-Δ(1)-dehydrogenase isoenzymes of *Rhodococcus ruber* strain Chol-4. Journal of Steroid Biochemistry and Molecular Biology, 132, 271–281.
Fernandez-Cabezon, L., Galán, B., & García, J. L. (2018). New insights on steroid biotechnology. Frontiers in Microbiology, 9, 958.
Guevara, G., Fernández de las Heras, L., Perera, J., Navarro, M., & Llorens, J. (2017b). Functional differentiation of 3-ketosteroid Δ1-dehydrogenase isozymes in *Rhodococcus ruber* strain Chol-4. Microbial Cell Factories, 16(1), 42.
Guevara, G., Heras, L. F. L., Perera, J., & Llorens, J. M. N. (2017a). Functional differentiation of 3-ketosteroid 9α-hydroxylases in *Rhodococcus ruber* strain Chol-4. Journal of Steroid Biochemistry and Molecular Biology, 7, 176–187.
Haußmann, U., Wolters, D. A., Fränzel, B., Eltis, L. D., & Poetsch, A. (2013). Physiological adaptation of the *Rhodococcus jostii* RHA1 membrane proteome to steroids as growth substrates. Journal of Proteome Research, 12, 1188–1198.
Jakočiunas, T., Jensen, M. K., & Keasling, J. D. (2016). CRISPR/Cas9 advances engineering of microbial cell factories. Metabolic Engineering, 34, 44–59.
Knol, J., Bodewits, K., Hessels, G. I., Dijkhuizen, L., & van der Geize, R. (2008). 3-Keto-5alpha-steroid delta(1)-dehydrogenase from *Rhodococcus erythropolis* SQ1 and its orthologue in *Mycobacterium tuberculosis* H37Rv are highly specific enzymes that function in cholesterol catabolism. Biochemistry Journal, 410, 339–346.
Lee, J. Y., Na, Y. A., Kim, E., Lee, H. S., & Kim, P. (2016). The actinobacterium *Corynebacterium glutamicum*, an industrial workhorse. Journal of Microbiology and Biotechnology, 26, 807–822.
Li, H., Sun, J., & Xu, Z. (2017). Biotransformation of DHEA into 7α,15α-diOH-DHEA. Methods in Molecular Biology, 1645, 289–295.
Liu, Y., Shen, Y., Qiao, Y., Su, L., Li, C., & Wang, M. (2016). The effect of 3-ketosteroid-Δ(1)-dehydrogenase isoenzymes on the transformation of AD to 9α-OH-AD by *Rhodococcus rhodochrous* DSM 43269. Journal of Industrial Microbiology and Biotechnology, 43, 1303–1311.
Marques, M. P. C., Carvalho, F., de Carvalho, C. C. C. R., Cabral, J. M. S., & Fernandes, P. (2010). Steroid bioconversion: Toward green processes. Food and Bioproduct Processing, 88, 12–20.
Mashkovskiy, M. D. (2012). Medicinal products. New Wave, Moscow (in Russian).
Mohn, W. W., Wilbrink, M. H., Casabon, I., Stewart, G. R., Liu, J., van der Geize, R., & Eltis, L. D. (2012). Gene cluster encoding cholate catabolism in *Rhodococcus* spp. Journal of Bacteriology, 194, 6712–6719.
Mondaca, M. A., Vidal, M., Chamorro, S., & Vidal, G. (2017). Selection of biodegrading phytosterol strains. Methods in Molecular Biology, 1645, 143–150.
Murphy, K. C., Papavinasasundaram, K., & Sassetti, C. M. (2015). Mycobacterial recombineering. Methods in Molecular Biology, 1285, 177–199.
Mutafova, B., Mutafov, S., Fernandes, P., & Berkov, S. (2016). Microbial transformations of plant origin compounds as a step in preparation of highly valuable pharmaceuticals. Journal of Drug Metabolism and Toxicology, 7(2), 1–11.
Nielsen, J., & Keasling, J. D. (2016). Engineering cellular metabolism. Cell, 164, 1185–1197.
Petrusma, M., Dijkhuizen, L., & van der Geize, R. (2009). *Rhodococcus rhodochrous* DSM 43269 3-ketosteroid 9alpha-hydroxylase, a two-component iron-sulfur-containing monooxygenase with subtle steroid substrate specificity. Applied and Environmental Microbiology, 75, 5300–5307.
Petrusma, M., Hessels, G., Dijkhuizen, L., & van der Geize, R. (2011). Multiplicity of 3-ketosteroid-9α-hydroxylase enzymes in *Rhodococcus rhodochrous* DSM 43269 for specific degradation of different classes of steroids. Journal of Bacteriology, 193, 3931–3940.
Petrusma, M., van der Geize, R., & Dijkhuizen, L. (2014). 3-Ketosteroid 9a-hydroxylase enzymes: Rieske non-heme monooxygenases essential for bacterial steroid degradation. Antonie van Leeuwenhoek, 106, 157–172.
Ribeiro, A. L., Sánchez, M., Hidalgo, A., & Berenguer, J. (2017). Stabilization of enzymes by using thermophiles. Methods in Molecular Biology, 1645, 297–312.
Rodina, N. V., Andryushina, V. V, Stytsenko, T. S., Turova, T. P., Baslerov, R. V., Panteleeva, A. N., & Voishvillo, N. E. (2009). The introduction of the 9α-hydroxy group into androst-4-en-3,17-dione using a new actinobacterium strain. Applied Biochemistry and Microbiology, 45(4), 395–400.
Smitha, M. S., Singh, S., & Singh, R. (2017). Microbial biotransformation: A process for chemical alterations. Journal of Bacteriology and Mycology, 4(2), 85.
Tsitko, I. V., Zaitsev, G. M., & Lobanok, A. G. (1999). Effect of aromatic compounds on cellular fatty acid composition of *Rhodococcus opacus*. Applied and Environmental Microbiology, 65(2), 853–855.
van der Geize, R., Hessels, G. I., Nienhuis-Kuiper, M., & Dijkhuizen, L. (2008). Characterization of a second *Rhodococcus erythropolis* SQ1 3-ketosteroid 9alpha-hydroxylase activity comprising a terminal oxygenase homologue, KshA2, active with oxygenase-reductase component KshB. Applied and Environmental Microbiology, 74, 7197–7203.
van der Geize, R., Hessels, G. I., van Gerwen, R., van der Meijden, P., & Dijkhuizen, L. (2001). Unmarked gene deletion mutagenesis of kstD, encoding 3-ketosteroid delta1-dehydrogenase, in *Rhodococcus erythropolis* SQ1 using sacB as counter-selectable marker. FEMS Microbiological Letters, 205, 197–202.
van der Geize, R., Hessels, G. I., van Gerwen, R., Vrijbloed, J. W., van Der Meijden, P., & Dijkhuizen, L. (2000). Targeted disruption of the kstD gene encoding a 3-kestosteroid Δ(1)-dehydrogenase isoenzyme of *Rhodococcus erythropolis* strain SQ1. Applied and Environmental Microbiology, 66, 2029–2036.
Voishvillo, N. E., Rodina, N. V., Andrjushina, V. A., Stytsenko, T. S., & Skryabin, K. G. (2007). Strain *Rhodococcus erythropolis* VKPM Ac-1740 for 9alpha-hydroxysteroids. Patent RU 2351645 (in Russian).
Wei, J. H., Yin, X., & Welander, P. V. (2016). Sterol synthesis in diverse bacteria. Frontiers in Microbiology, 7, 990.
Wilbrink, M. H., Petrusma, M., Dijkhuizen, L., & van der Geize, R. (2011). FadD19 of *Rhodococcus rhodochrous* DSM 43269, a steroid-coenzyme. A ligase essential for degradation of C-24 branched sterol side chains. Applied and Environmental Microbiology, 77, 4455–4464.
Yeh, C. H., Kuo, Y. S., Chang, C. M., Liu, W. H., Sheu, M. L., & Meng, M. (2014). Deletion of the gene encoding the reductase component of 3-ketosteroid 9α-hydroxylase in *Rhodococcus equi* USA-18 disrupts sterol catabolism, leading to the accumulation of 3-oxo-23,24-bisnorchola-1,4-dien-22-oic acid and 1,4-androstadiene-3,17-dione. Microbial Cell Factories, 13, 130.

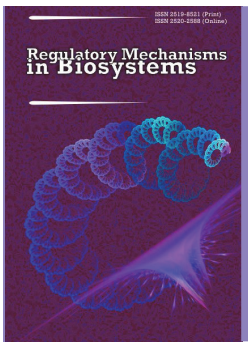

Regulatory Mechanisms in Biosystems

ISSN 2519-8521 (Print)
ISSN 2520-2588 (Online)
Regul. Mech. Biosyst., 9(3), 435–439
doi: 10.15421/021865

Influence of formic acid on the vitality of *Strongyloides papillosus*

O. O. Boyko*, O. G. Gavrilina*, P. N. Gavrilin*, Y. A. Gugosyan*, V. V. Brygadyrenko*, **

**Dnipro State Agrarian and Economic University, Dnipro, Ukraine*
***Oles Honchar Dnipro National University, Dnipro, Ukraine*

Article info

Received 14.06.2018
Received in revised form 27.07.2018
Accepted 29.07.2018

Dnipro State Agrarian and Economic University, Sergey Yefremov st., 25, Dnipro, 49600, Ukraine. Tel.: +38-099-405-51-98. E-mail: boikoalexandra1982@gmail.com

Oles Honchar Dnipro National University, Gagarin ave., 72, Dnipro, 49010, Ukraine. Tel.: +38-050-93-90-788. E-mail: brigad@ua.fm

Boyko, O. O., Gavrilina, O. G., Gavrilin, P. N., Gugosyan, Y. A., Brygadyrenko, V. V. (2018). Influence of formic acid on the vitality of Strongyloides papillosus. Regulatory Mechanisms in Biosystems, 9(3), 435–439. doi:10.15421/021865

Formic acid (methanoic acid, HCOOH) is an organic compound which belongs to saturated monobasic acids. In natural conditions, it is secreted from the glands of ants, and also extracted from the leaves of stinging nettles. It is soluble in water in any proportions, which makes it practical to use for making aquatic solutions. It is broadly used as a preservative in the food industry – E_{236} food additive (Codex Alimentarius), as a bactericide in medicine and veterinary medicine, and is also used against agricultural pest species of insects and mites. The *in vitro* and *in vivo* experiments revealed the anthelmintic properties of the acid against *Strongyloides papillosus* nematodes, parasites of the gastrointestinal tract of Ruminantia and rabbits. In the conditions of *in vitro*, 100% of (L_1, L_2, L_3) nematode larvae died from a 1% solution of formic acid (10 g/l) after 24 hours exposure. When exposed to less strong concentrations of the acid (1, 0.1, 0.01, 0.001 g/l), vital forms of L_3 *S. papillosus* were found. Non-invasive stages (L_1, L_2) are less resistant to the impact of the acid – death of 100% of the larvae was observed under the impact of 0.1% solution and up to 60% of larvae died at 0.01% solution of formic acid in the same conditions. LD_{50} for L_3 invasive larvae of *S. papillosus* equaled 0.47%, and 0.0076% for L_1, L_2 non-invasive larvae of *S. papillosus*. In the conditions of *in vivo* experiment (with guinea pigs), the effective dose of formic acid was 0.4% ml/kg of the animal`s body weight. The results of the coproscopy after the treatment demonstrated absence of the helminth larvae in the feces of the laboratory animals during 10 days and their occurrence only on days 15–20 with a low intensity (90 larvae/g of feces on average). During an external examination of the corpses of the animals of the experimental group, no pathological changes were found. The intestine, the heart, the lungs and the liver of the animals from this group had no macroscopic changes – they were of natural colour and size. The hepatocytes looked normal and the structure of the liver lobes was maintained. In the tissues of the liver of the animals from the experimental and control groups, we found processes of passive congestion, and an insignificant degree of signs of hepatic steatosis.

Keywords: nematodes; *Strongyloides*; antiparasitic activity; flavouring agents; formic acid.

Introduction

Currently, the requirements of society for quality products of animal origin is growing. Due to the popularizing of the data on the negative impact of the synthetic substances, most people more and more often demand ecologically pure products. During the production of these products, no substances of artificial origin are used. Due to the fact that the helminthiases regularly cause economic losses to livestock enterprises, manufacturers have begun searching for new methods against agricultural pests and parasites of animals, such as using agents of natural origin. The main property of such substances would be safety. They should not affect the quality of the production, therefore they should be safe for the consumer (Safiullin, 1997; Cabaret et al., 2002; Rahmann & Seip, 2006; Rinaldi et al., 2007; Burke et al., 2009; Charlier et al., 2009; Lu et al., 2010).

One of the preparations used currently as an anthelminthic agent is gentian violet. This substance has antimicrobial and anthelmintic properties. By toxicity, gentian violet belongs to the group of substances which are insignificantly toxic for animals. During its usage, there is no need to expect removal of the preparation from the organism of animals. The products of such animals can be used without any limitations. However, during its usage, one can face its main disadvantage – the substance significantly colours the mucous membranes and tissues pink. This property is the main reason why this substance cannot be used for animals intended for slaughter (Mashkovskij, 2000). Currently, many studies are oriented towards the search of substances of natural origin, plants, different food additives, which could be used against pests. Also, phytopreparations are becoming used more and more often. This is related to the fact that they have the least negative effect on the organisms of animals in general, therefore on the products obtained from the animals (Burke et al., 2009; Belletti et al., 2010; Boyko & Brygadyrenko, 2016, 2018).

The results of the studies by Faye et al. (2003), which were performed on goats by adding food additives to their food demonstrated not only significant effect on weight gain during the goats' pregnancy and during lactation. The goats that received the additives were observed to have increased milk production. The animals which were fed using the additives demonstrated a decrease in the number of eggs of helminths in their feces. It is well known that formic acid is also used against insects in insecticide compositions. The organic acids cause no harm to the environment due to the fact that they are pure substances of natural origin (Okhanov, 2000).

The studies on the impact of flavourings on pathogenic microorganisms have already been conducted. These studies revealed that apigenin, linalool and ursolic acid is extracted from *Ocimum sanctum*, and have a broad range of antiviral properties. Also, a mixture of these substances was found to have the ability to inhibit the growth of pathogenic microflora (Chiang et al., 2005). Apart from the impact on microorga-

nisms, scientists have proved the lethal effect of some of these substances on the larval forms of pathogens of nematode infections (Boyko & Brygadyrenko, 2016). Boyko & Brygadyrenko (2016) performed experiments on the comparative helminthocidal effect of the following flavourings: benzaldehyde, natural citral, D-limonene and B-iodine. Research on the larvae of *Strongyloides ransomi*, parasitic nematodes of swine, revealed that after a 24 hour exposure, these substances have an anthelmintic effect. Especially good results were obtained from experiments with benzaldehyde, which at 0.01–1% concentrations caused death of over 90% of the larvae. Currently, formic acid is becoming broadly used against parasitic organisms. Formic acid is a colourless substance with a distinctive odour. In natural conditions, it is secreted from the glands of ants, and it also can be extracted from some plants, for example leaves of stinging nettles. It can be dissolved in water in any proportions. This makes it good for preparing aquatic solutions. However, in concentrated form, this acid can leave burns on the skin. There are no data on using formic acid as an anthelmintic preparation. Therefore, it is important to study the impact of formic acid on helminths and analyze the possibility of including it in fodders as a food additive with anthelmintic properties.

Materials and methods

The study was performed in two stages during 2017–2018: determining a lethal dose of formic acid for *S. papillosus* larvae *in vitro*, determining the possibility of using this substance as a food additive with anthelmintic properties for laboratory animals (guinea pigs).

For the first stage of the experiment (*in vitro*), we used *S. papillosus* of small cattle and rabbits. Feces of these animals were examined for the eggs of strongyloidiasis pathogens using the McMaster method for further cultivation of the larvae (Zajac & Conboy, 2011). The cultivated material was centrifuged (by 4 ml in test tubes for 4 minutes, 1500 rotations/minute), the sediment with the larvae was uniformly mixed and put in 1.5 ml plastic test tubes by 0.1 ml. Then, 1 ml of the formic acid solution was added to each of the tubes. Five concentrations of aquatic solution of the substance were used in the experiment: 10, 1, 0.1, 0.01 and 0.001 g/l, and also the control (distilled water) in eight replications. The exposure time during the experiment was 24 hours at the temperature of 22–24 °C.

During the second stage of the experiment, 6 guinea pigs were used. The animals were kept in separate cages. The animals were fed regularly and fully. The diet consisted of fresh vegetables, fruits, greens, and also meadow hay. The animals had free access to water in individual water bowls. As litter, sawdust was used and changed daily. Normal saline solution with *S. papillosus* larvae (by 0.5 ml) of rabbits was introduced to the guinea pigs subcutaneously and orally. Then, monitoring of the infestation of the laboratory animals was performed by periodic selection of the feces and coprological study of it once every 10 days.

After the infestation, the guinea pigs were divided into two groups: experimental and control. The solution of formic acid was introduced to the guinea pigs orally using a laboratory pipette. To prepare the solution, a concentrated formic acid and distilled water was used. The first group of animals received 1% solution of formic acid in 15 ml dose twice in 10 and 5 ml doses at 2 hours interval. The control group of animals did not receive the substance. The litter was changed every 24 hours. Initially, examination of the feces for nematode larvae was made every three days until the pathogen was found, and then once in 10 days . 80 days after the beginning of the second stage of the experiment, a pathoanatomical autopsy was performed on the laboratory animals, which had been euthanized using ether. An external examination of the corpses was performed. During the pathoanatomical autopsy, the condition of the liver, the intestine, and the heart was determined.

To study the liver, we used the classical method of preparing paraffin sections using a rotary microscope and staining the sections with hematoxylin and eosin. The histological study consisted of the following stages: selecting the samples, fixating the material in 10% solution of neutral buffered formalin, dehydration of the samples, incorporation of paraffin over the samples, preparing histological sections of 3–5 μm thickness, with subsequent staining of them with hematoxylin and eosin, incorporating the sections in balsam, and microscopic examination of the preparations (Bancroft & Stevensens, 1990).

Results

All (100%) of the larvae of *S. papillosus* nematodes died during exposure to 1% solution of the acid. First and second stage larvae of the studied nematode species were exposed to the acidic solution of 0.1% concentration. After 24 hours in the formic acid solution, about 10% of the nematode larvae remained viable. Almost 100% of the invasive larvae survived in 0.1% concentration of formic acid. The next level of decrease in the concentration of the studied substance also had no positive result against the invasive larvae of the studied species of helminth. In 0.01% concentration, 100% of the invasive larvae remained vital. Up to 60% of the L_1 and L_2 died in 0.01% concentration. Only up to 30% of these larvae died in 0.001% acidic solution (Fig. 1).

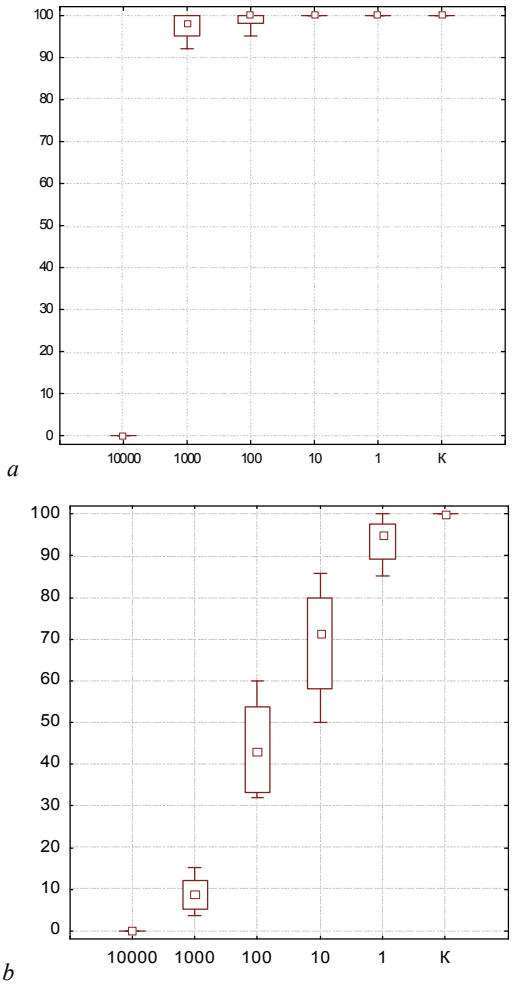

Fig. 1. The effect of formic acid on the viability of larvae of nematodes of Ruminantia: *a* – L_3 invasive larvae of *S. papillosus*; *b* – L_1, L_2 non-invasive larvae of *S. papillosus*; the ordinate axis indicates the percentage of living nematode larvae in the course of the 24-hour experiment; the abscissa axis indicates the concentration of the solution's active substance (%); *K* – control, where the concentration of the active substance is 0%; small square in the centre corresponds to the median, lower and upper edge of the large rectangle correspond to first and third quartiles, respectively, the vertical segments, directed upward and downward from the rectangles, correspond to minimum and maximum values (n = 8)

LD_{50} L_3 invasive larvae of *S. papillosus* on average does not exceed 0.47%, for L_1, L_2 non-invasive larvae of *S. papillosus* – 0.0076% (Table 1).

Table 1
LD_{50} (%, x ± SD) for the experiment on determining the impact of the chemical substance on the viability of nematode larvae in the laboratory experiment after one day

Substance	L_3 invasive larvae of *S. papillosus*	L_1, L_2 non-invasive larvae of *S. papillosus*
Formic acid	0.47 ± 0.29	0.0076 ± 0.0065

Thus, minimal concentration of the formic acid solution, in which 100% of invasive nematode larvae of *S. papillosus* died *in vitro* – 10 g/l.

Pathogens of strongyloidiasis among the guinea pigs were found in the coprological examination on days 25–50. We observed fluctuations of the infestation intensity from 283 to 1244 larvae/g of feces. On the 35th day of the experiment, the number of larvae increased on average by 592 per 1 g of excrement compared to the 25th day. On the 45th day, the infestation was reduced on average by 398 larvae/g of feces compared to the 35th day. However, these indicators were higher compared to the 25th day on average by 195 larvae/g of feces. The next examination was performed after 5 days. It revealed a significant increase in the invasion. On the 45th day, the infestation increased on average by 767 larvae/g of feces. Therefore, on the 50th day, the highest level of infestation of the guinea pigs was recorded – 1244 larvae/g of feces.

On the 56th day, the animals received treatment. The experimental group received 1% solution of formic acid in the dose of 0.40 ml/kg of body weight. The results of coprological examinations after the treatment indicated absence of the helminths in the animals over 10 days. On the 15th day after the treatment, the helminths were found in the guinea pigs' feces again in the amount of 13 larvae/g of feces. However, throughout the monitoring, their intensity was no higher than 90 larvae/g of feces on average.

External examination of the corpses of the experimental group animals revealled no pathological changes . The coat was dense, fur was glossy and fixed well in the skin, and no alopecia was observed. During the autopsy, no pathomorphological changes were found in the internal organs of the guinea pigs. The lungs were of regular form, pink colour, elastic consistency, moderately filled with blood. The pleura were smooth, moist, glossy. The small and large intestine of the animals were in the correct positions in the abdominal cavity. The mucous membrane of the intestine was pale-pink, moist, with no hyperemia (Fig. 2). The liver of all of the animals in the experimental group was of normal dark-brown colour, not enlarged, had a smooth and glossy surface, elastic consistency and was moderately filled with blood.

Fig. 2. The organs of the abdominal cavity of the experimental group animals (after peroral introduction of 1% solution of formic acid)

According to the results of the histological analysis of the liver of the experimental group animals , the organ had a typical lobed structure with insignificantly developed interlobular connective tissue. The hepactic tubules were clearly seen in the form of radial bands, sinusoid capillaries contained insignificant amount of erythrocytes. The hepatocytes had a many-sided form, with no clearly manifested signs of grainy texture and no fat droplets in the hepatocytes' cytoplasma. There were singular perivascular lymph nodes on the periphery of the lobes and no polymerphocellular accumulations (Fig. 3).

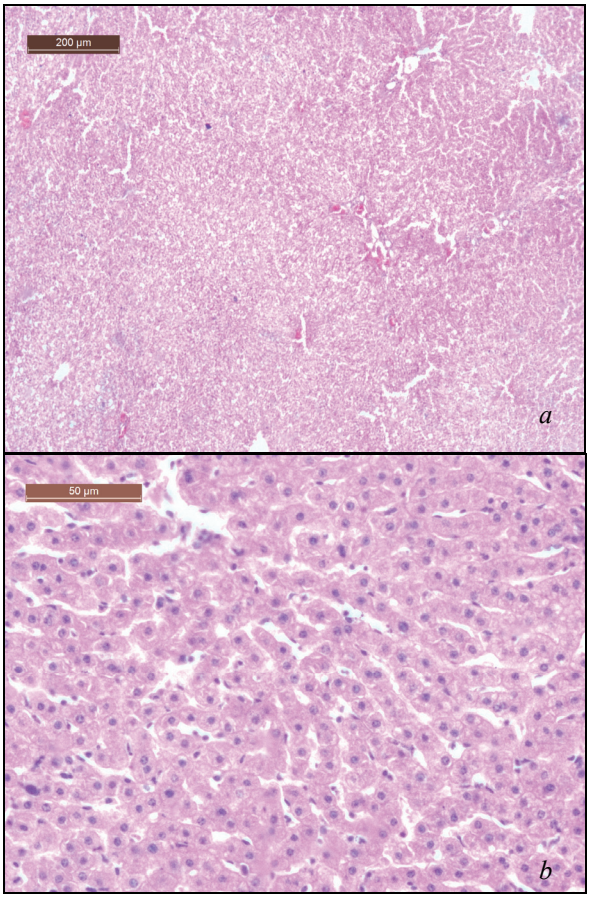

Fig. 3. Microscopic image of the liver of the animals from the experimental group: *a* – clear lobular structure of the liver parenchyma, *b* – hepactic tubules in the form of radial bands; hematoxylin and eosin

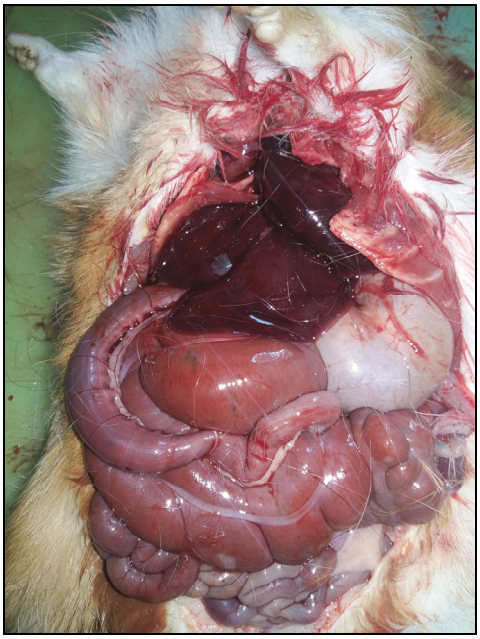

Fig. 4. The organs of the abdominal cavity of the animals from the control group

During an external examination of the corpses of the animals from the control group, we observed moderately manifested pathological changes in the coat. The hair was observed to be tarnished, mussed, not closely attached to the skin, thinned-out in the upper and lower spine. During the autopsy, we determined that the organs and serous membranes were not changed. In the small and large intestine, we observed signs of severe catarrhal inflammation (catarrh). The mucous membrane of the intestine was swollen, had areas with hyperemia of spotted or striped forms, which was especially clearly seen on the tops of its folds. In the mucous membrane of the small intestine, we found petechial hemorrhaging. The surface of the mucous membrane was covered with viscous, half-liquid slime. The aggregates of the lymph nodes of the mucous membrane were swollen and appear in lumen of intestine. The liver was insignificantly increased in size, pale-yellow flabby areas of different size were observed under the organ's capsula and on the section (Fig. 4).

During the histological examination of the liver of the animals of the control group, we determined that in the changed pale yellow areas of parenchyma of the organ, the tubular structure of the liver lobes was disrupted, hepatocytes were increased in size, and were mostly of rounded shape. The cytoplasm of the hepatocytes was alveolar. The alveoles were different in size. The hepatocytes' nuclei were positioned in the centers of the cells, had clear signs of karyopyknosis, some nuclei had become lysed. As a result of lysis, fat necrosis areas were formed. We observed perivascular proliferates of macrophages, fibroblasts and lymphocytes. In general, the pathomorphological condition of the liver in the animals of the control corresponds to the focal form of degenerative obesity (focal fat deposition) (Fig. 5).

Thus, at the macrolevel, formic acid in the tested concentrations had no negative effect on the internal organs of the studied animals. During the histological examination, the parameters of the liver of animals from the experimental group were better compared to the parameters of the control. The processes of fatty degeneration were possibly caused by helminths. Passive hyperemia which was found in all samples of the experimental group, was, probably, a consequence of using ether for euthanizing the animals.

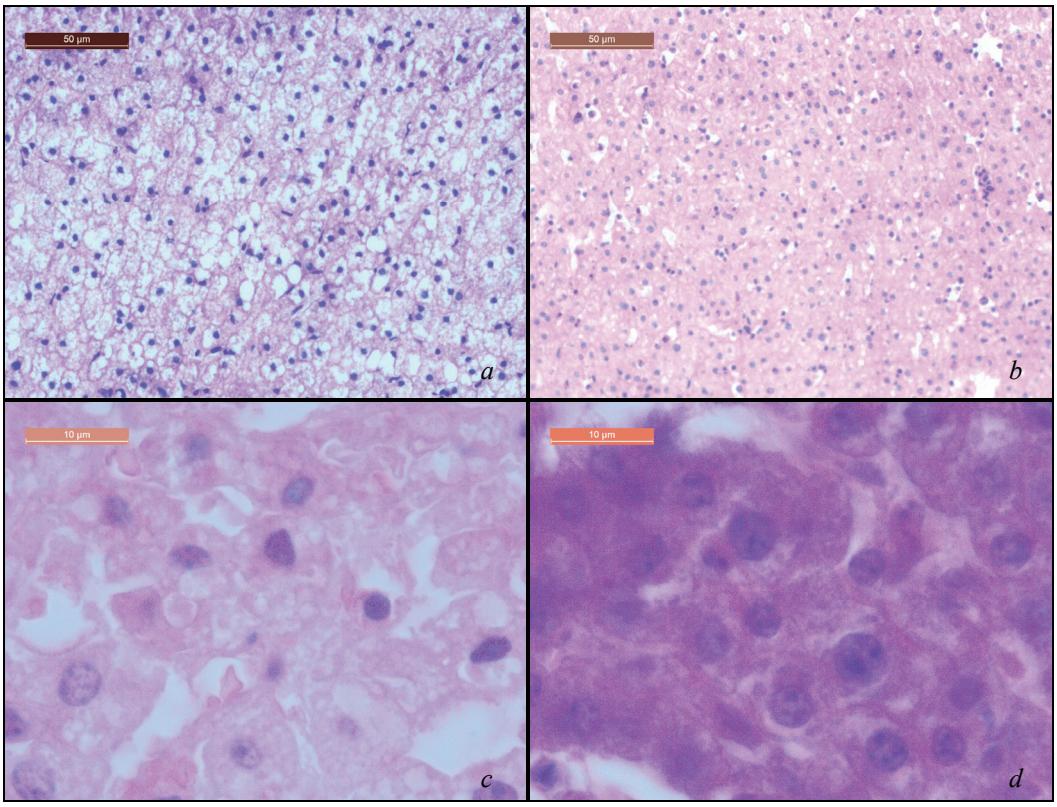

Fig. 5. Microscopic image of the liver of the animals in the control group: *a* – degenerative obesity of the hepatocytes, *b* – disorders in the tubular structure of liver lobes, *c* – the nuclei of the hepatocytes with signs of karyopyknosis and karyolysis, *d* – non-uniform structure of the cytoplasm of the hepatocytes; hematoxylin and eosin

Discussion

Mature *S. papillosus* helminths parasitise the small intestine, their larvae migrate through the body of animals. They cause mechanical, allergic and inoculative effects (Thamsborg et al., 2016). The results of experimental infestation of rabbits with *S. papillosus* larvae caused disorders in the gastrointestinal tract and led to development of anorexia, loss of weight and ultimately the death of the animals. Decrease in the body weight and daily food consumption were observed in a combination with heightened EPG in the infested animals (Kobayashi & Horii, 2008). The researchers have determined that infestation of non-typical hosts – Mongolian gerbils (*Meriones unguiculatus*) with mature individuals of *S. papillosus* led to increase in mortality in the experimental group and decrease in their life expectancy. At the same time, the main cause of death was disorders in the peristalsis – paralytic disruption of the normal propulsive ability of the gastrointestinal tract (Paralytic ileus) (Kobayashi et al., 2009). Apart from the infestation of the intestine with mature individuals, larvae of *S. papillosus* migrate in the organs and tissues, causing allergic processes with release of biologically active substances and development of eosinophilia of the infested animals (Nakanishi et al., 1993). Kváč & Vítovec (2007) determined that the main cause of death of calves infested with *S. papillosus* was pathological changes in the lungs, caused by the migration of larvae. They histologically determined the development of purulent granulomatous inflammation with the new connective tissue and predominance of eosinophils in the inflammatory infiltrates (Kváč & Vítovec, 2007). Therefore, parasitism of *S. papillosus* worsens the quality of life of animals and even causes their death. Therefore the development of effective methods against them is relevant.

Formic acid is widely used in the food industry as a preservative. This substance affects the taste and the aroma of food products and is used for making semi-finished fruit products, and also for preservation of vegetables and fruits. Currently, formic acid (E_{236}, Codex Alimentarius) and its salts (E_{237} sodium formate and E_{238} calcium formate) are used as a salt substitute (food additives). Formic acid is quickly metabo-

lized and removed from the organism. Therefore, in the solutions with low concentration, E_{236} additive has local irritant, anesthetic and anti-inflammatory effects. Currently, formic acid is used for disinfection. Its impact mostly targets yeasts and some bacteria. Mold and lactic bacteria are resistant to it. In Europe, formic acid is used mostly as a preservative of cattle fodder due to its strong bactericidal property. It is used as a spray for hay, therefore inhibiting the decomposition processes. Fodder maintains its nutrient qualities (Waldo et al., 1969; Castle & Watson, 1970). Also, there are data on using this substance in the compounds used against coccidiosis (Muzi & Rahman, 2005). One way of using formic acid is using it against *Varroa destructor* parasitic mites of bees. According to the researchers, effective destruction of these parasites was reached after treating the infested bees with formic acid in 0.08 and 0.16 mg/l concentrations as a fumigate (Underwood & Currie, 2003). Larvae L_3 *S. papillosus* and *H. contortus* were more resistant to the impact of formic acid. Our studies revealed the effectiveness of this substance in vitro only at 10 g/l concentration.

Conclusions

At the current stage, one can presume that systematic treatment of animals with formic acid (once in 10 days) in a dose of 0.40 ml/kg of body weight can achieve anthelmintic effect against the strongyloidiasis pathogen without any damage to the health of animals. This property of the studied substance is especially relevant in organic animal husbandry. Therefore, the anthelmintic properties of formic acid as a food additive need to be studied further.

References

Bancroft, J. D., & Stevensens, A. (1990). Theory and practice of histological technigues. Livingstone, London.

Belletti, N., Kamdem, S. S., Tabanelli, G., Lanciotti, R., & Gardini, F. (2010). Modeling of combined effects of citral, linalool and β-pinene used against *Saccharomyces cerevisiae* in citrus-based beverages subjected to a mild heat treatment. International Journal of Food Microbiology, 136(3), 283–289.

Boyko, O. O., & Brygadyrenko, V. V. (2016). Influence of water infusion of medicinal plants on larvae of *Strongyloides papillosus* (Nematoda, Strongyloididae). Visnyk of Dnipropetrovsk University. Biology, Ecology, 24(2), 519–525.

Boyko, O. O., & Brygadyrenko, V. V. (2018). The impact of certain flavourings and preservatives on the survivability of larvae of nematodes of Ruminantia. Regulatory Mechanisms in Biosystems, 9(1), 118–123.

Burke, J. M., Wells, A., Casey, P., & Kaplan, R. M. (2009). Herbal dewormer fails to control gastrointestinal nematodes in goats. Veterinary Parasitology, 160, 168–170.

Cabaret, J., Bouilhol, M., & Mage, C. (2002). Managing helminths of ruminants in organic farming. Veterinary Research, 33(5), 625–640.

Castle, M. E., & Watson, J. N. (1970). Silage and milk production, a comparison between wilted and unwilted grass silages made with and without formic acid. Grass and Forage Science, 25(4), 278–284.

Charlier, J., Höglund, J., Samson-Himmelstjerna, G., Dorny, P., & Vercruysse, J. (2009). Gastrointestinal nematode infections in adult dairy cattle: Impact on production, diagnosis and control. Veterinary Parasitology, 164, 70–79.

Chiang, L.-C., Ng, L.-T., Cheng, P.-W., Chiang, W., & Lin, C.-C. (2005). Antiviral activities of extracts and selected pure constituents of *Ocimum basilicum*. Clinical and Experimental Pharmacology and Physiology, 32(10), 811–816.

Cringoli, G., Veneziano, V., Jackson Vercruysse, J., Claerebout, E., Schnieder, T., Strube, C., Ducheyne, E., Hendrickx, G., & Charlier, J. (2009). The use of bulk-tank milk ELISAs to assess the spatial distribution of *Fasciola hepatica*, *Ostertagia ostertagi* and *Dictyocaulus viviparous* in dairy cattle in Flanders (Belgium). Veterinary Parasitology, 165, 51–57.

Faye, D., Leak, S., Nouala, S., Fall, A., Losson, B., & Geerts, S. (2003). Effects of gastrointestinal helminth infections and plane of nutrition on the health and productivity of F1. Small Ruminant Research, 50, 153–161.

Kobayashi, I., & Horii, Y. (2008). Gastrointestinal motor disturbance in rabbits experimentally infected with *Strongyloides papillosus*. Veterinary Parasitology, 158(1–2), 67–72.

Kobayashi, I., Kajisa, M., Farid, A. S., Yamanaka, A., & Horii, Y. (2009). Paralytic ileus and subsequent death caused by enteric parasite, *Strongyloides papillosus*, in Mongolian gerbils. Veterinary Parasitology, 162(1–2), 100–105.

Kváč, M., & Vítovec, J. (2007). Occurrence of *Strongyloides papillosus* associated with extensive pulmonary lesions and sudden deaths in calves on a beef farm in a highland area of South Bohemia (Czech Republic). Helminthologia, 44(1), 10–13.

Lu, C. D., Gangyi, X., & Kawasc, J. R. (2010). Organic goat production, processing and marketing: Opportunities, challenges and outlook. Small Ruminant Research, 89, 102–109.

Mashkovskij, M. D. (2000). Lekarstvennye sredstva [Medicinal products]. New Wave, Moscow.

Muzi, S., & Rahman, S. A. (2005). Urea and thiourea compounds useful for treatment of coccidiosis. US Patent No. 6875764B1. New Pharma Research Sweden AB.

Nakanishi, N., Nakamura, Y., Ura, S., Tsuji, N., Taira, N., Tanimura, N., & Kubo, M. (1993). Sudden death of calves by experimental infection with *Strongyloides papillosus*. III. Hematological, biochemical and histological examinations. Veterinary Parasitology, 47(1–2), 67–76.

Okhanov, V. V. (2000). Insektoakaritsidnoe sredstvo [Insectoacaricide]. U.S. Patent No. 2157182 RF.

Rahmann, G., & Seip, H. (2006). Alternative strategies to prevent and control endoparasite diseases in organic sheep and goat farming systems: A review of current scientific knowledge. In: Rahmann, G. (Ed.). Ressortforschung für den Ökologischen Landbau, 298. Pp. 49–90.

Rinaldi, L., Veneziano, V., & Cringoli, G. (2007). Dairy goat production and the importance of gastrointestinal strongyle parasitism. Transactions of the Royal Society of Tropical Medicine and Hygiene, 101, 103–105.

Safiullin, R. T. (1997). Rasprostranenie i ehkonomicheskij ushherb ot osnovnykh gel'mintozov zhvachnykh zhivotnykh [Distribution and economic damage from the basic helminthiases of ruminant animals]. Veterinary Medicine, 6, 28–32.

Sato, K., Krist, S., & Buchbauer, G. (2006). Antimicrobial effect of trans-Cinnamaldehyde, (–)-Perillaldehyde, (–)-Citronellal, Citral, Eugenol and Carvacrol on airborne microbes using an airwasher. Biological and Pharmaceutical Bulletin, 29(11), 2292–2294.

Somolinos, M., Garcia, D., Pagan, R., & Mackey, B. (2008). Relationship between sublethal injury and microbial inactivation by the combination of high hydrostatic pressure and citral or tert-butyl hydroquinone. Applied and Environmental Microbiology, 74(24), 7570–7577.

Thamsborg, S. M., Ketzis, J., Horii, Y., & Matthews, J. B. (2016). *Strongyloides* spp. infections of veterinary importance. Parasitology, 144(3), 274–284.

Underwood, R. M., & Currie, R. W. (2003). The effects of temperature and dose of formic acid on treatment efficacy against *Varroa destructor* (Acari: Varroidae), a parasite of *Apis mellifera* (Hymenoptera: Apidae). Experimental and Applied Acarology, 29, 303–313.

Veneziano, V., Rubino, R., Fedele, V., Rinaldi, L., Santaniello, M., Schioppi, M., Cascone, C., Pizzillo, M., & Cringoli, G. (2004). The effects of five anthelmintic treatment regimes on milk production in goats naturally infected by gastrointestinal nematodes. South African Journal of Animal Science, 34, 238–240.

Waldo, D. R., Smith, L. W., Miller, R. W., & Moore, L. A. (1969). Growth, intake, and digestibility from formic acid silage versus hay. Animal Husbandry Research Division, 52(10), 1609–1616.

Waller, P. J., & Thamsborg, S. M. (2004). Nematode control in 'green' ruminant production systems. Trends in Parasitology, 20(10), 493–497.

Zajac, A. M., & Conboy, G. A. (Eds.). (2011). Veterinary clinical parasitology, 8th ed. John Wiley and Sons, UK.

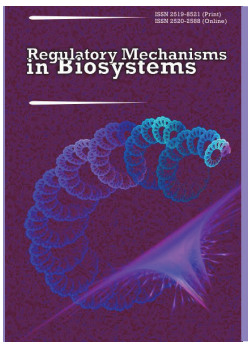

Regulatory Mechanisms in Biosystems

ISSN 2519-8521 (Print)
ISSN 2520-2588 (Online)
Regul. Mech. Biosyst., 9(3), 440–445
doi: 10.15421/021866

Influence of solution of lactoprotein with sorbitol on ultrastructural changes in lungs of rats in the condition of burn shock

A. O. Ocheretnyuk, O. V. Palamarchuk, D. A. Lysenko, G. I. Vashchuk, G. I. Stepanyuk

National Pirogov Memorial Medical University, Vinnytsya, Ukraine

Article info

Received 24.07.2018
Received in revised form 21.08.2018
Accepted 23.08.2018

National Pirogov Memorial Medical University, Pirogov st., 56, Vinnytsya, 21000, Ukraine.
Tel.: +38-067-90-90-930.
E-mail: anna.ocheretniuk@gmail.com

Ocheretnyuk, A. O., Palamarchuk, O. V., Lysenko, D. A., Vashchuk, G. I., & Stepanyuk, G. I. (2018). Influence of solution of lactoprotein with sorbitol on ultrastructural changes in lungs of rats in the condition of burn shock. Regulatory Mechanisms in Biosystems, 9(3), 440–445. doi:10.15421/021866

This article gives a theoretical substantiation and a new experimental solution of a scientific problem aimed at increasing the effectiveness of pharmacotherapy on the morphofunctional state of the lungs of rats under conditions of burn shock by using a combined colloid-hyperosmolar infusion solution – lacto-protein with sorbitol. The administration of the test solution at a dose of 10 ml/kg for 7 days in rats with modelled burn shock reduced ultrastructural changes in the lungs triggered by burn shock. It has been proved that in the conditions of shock, colloid-hyperosmolar infusion lacto-protein with sorbitol solution facilitates the restoration of vascular endothelium and fluid retention in the microcirculatory channel and improves the morphofunctional state of the aerohematic barrier of the lungs, stimulates the activity of the alveolar macrophages and the secretory function of the type II alveolocytes producing surfactant. At day 7 of burn shock, when 0.9% of NaCl was injected, significant changes were observed in the respiratory unit: part of the alveoli had considerably enhanced clearance of blood capillaries, which had platelets, neutrophils and altered forms of erythrocytes. At day 7 of burn shock in the lungs of the rats given an infusion of colloid-hyperosmolar solution – lactoprotein with sorbitol, the ultrastructure of the components of the lung cells had improved in comparison with 3 days. Luminosity of the hemocapillary parts was moderate, mainly with erythrocytes. The walls of endothelial cells had elongated nuclei with invaginations of nuclear membranes and clear contours. Their cytoplasmic regions were not widespread, with moderate electron densities. In type II alveolocytes, during this experiment, a lower degree of damage to the nucleus and organelles in the cytoplasm was established, and there were signs of a renewal of the secretory function of these cells. In the cytoplasm, hypertrophied mitochondria with clear crystals, different sizes of secretory granules, which had a different density, indicating their formation, were observed. According to the magnitude of the cytoprotective effect on lung cells under conditions of burn shock, the lactoprotein with sorbitol solution was shown to be superior in comparison with the physical solution (0.9% NaCl). The study of functional, biochemical and molecular genetic parameters that characterize the state of the aerohematic barrier under the conditions of using lactoprotein with sorbitol solution in the case of burn injuries of the skin will allow researchers to comprehensively evaluate the mechanisms of the pulmonary protective effect of this preparation and to experimentally substantiate the expediency of its use in clinical practice for pharmaco-correction of burn shock.

Keywords: thermal damage; skin; infusion therapy; pulmonary injuries.

Introduction

Burn injuries and the various types of damage to the organs and systems of the body to which it leads is one of the pressing problems of modern medicine throughout the world and in Ukraine, in particular (Fuzaylov et al., 2015; Gamelli et al., 2015). Burn illness is a symptom complex when there are functional and morphological changes in vital organs and systems, violation of metabolic and neurohumoral processses, burn shock (BS) (Snell et al., 2013; Nielson et al., 2017). The development of pulmonary complications contributes to an increase in mortality of up to 50%, which raises the issue of early diagnosis and prevention of lung injuries in burn shock as an important problem of combustiology (Cox et al., 2015).

The lungs are a target organ in burn chock, damage to lungs occurs as a result of the development of several pathogenesis units, which constitute a mosaic picture of severe damage and violation of the whole homeostasis of the body and require effective pharmacotherapy, in the first place, adequate correction of disorders in the early stages of burn injury (Porter et al., 2016). Pathogenesis of development and cellular mechanisms of lung damage is the least studied aspect of this problem, which, in turn, hinders the development of adequate and sufficiently effective methods of treatment of this pathology (Kaddoura et al., 2017). In the literature, morphofunctional changes in the structure of the lungs are not sufficiently studied, attention is not paid to the dynamics of these disorders, depending on the period of burn disease, and their relationship, which requires further research (Jacob et al., 2015; Sousse et al., 2015).

An analysis of the clinical picture of lung injury on the background of burns indicates the diversity of its forms, but more often two of its main varieties are distinguished (Cox et al., 2015). The first of these is associated with the effect of high temperatures on the mucous membrane of the respiratory tract. This form of lung inflammation according to some authors stands out as "primary burn pneumonia" (Shaver & Bastarache, 2014). One of the targets of these factors is the lung cells in which there is a decrease in the activity of synthetic processes, a more active response to apoptotic stimuli, their functioning is disturbed, which creates the preconditions for the development of clinical manifestations of lung injury on the background of thermal damage (Herold et al., 2015).

The development of lung injury is also associated with the polyfactor effect of thermal damage and has the character of a chain reaction. Burn shock causes the destruction of the phospholipid layer of mem-

branes under the action of histamine and kinins and violations of tissue respiration, permeability of the alveolar-capillary membranes, edema and fluid exudation from the vascular bed to the interstitial space and lumen of the alveoli, lung tissues, vascular spasm, small thrombi and plasmatic percolation, neutrophil infiltration, diffuse damage to the walls of the alveoli, hyaline dystrophy (Jacob et al., 2015). Oxygen-metabolic explosion of leukocytes becomes pathological, damaging cells and macromolecular compounds. In the pathogenesis of burn shock, the impairment of the hemodynamics of the small circle of blood circulation and the gas transportation function of the lungs is important. The pronounced disturbances of peripheral blood flow in certain areas of the lungs contribute to the formation of infiltrates, and later bronchopneumonia. In a morphological study of lungs (Sousse et al., 2015), it is possible to observe in the alveolus a protein-rich fluid with acuminate alveolocytes, macrophages, red blood cells, and fibrin cones. In cases of burn shock, functional activity decreases and the alveolar macrophage ultrastructure changes (Zhang et al., 2018). On the basis of violations of hemodynamics and rheological properties of blood, as well as hypoxia, action of biogenic amines and bacterial toxins in the lungs, dystrophic changes take place in the level of necrosis (Shaver & Bastarache, 2014).

The above changes have a certain sequence and at a certain stage of burn shock develop an irreversible nature, which requires timely correction or preventive intervention. It is important to use means that reduce the toxic effects of burn injury, or completely alleviate the negative factors, this being the goal of modern pathogenetic therapy in burn injury (Abdullahi & Jeschke, 2014; Snell et al., 2013; Kaddoura et al., 2017). The pathogenesis of development and cellular mechanisms of damage are the least studied, especially in the period after the day of injury, which, in turn, hinders the development of adequate and sufficiently effective methods of treatment of this pathology.

The high incidence of lung injury as a result of burn injury, the severity of this pathology, the high percentage of lung injury in this case, in particular the development of acute respiratory distress syndrome, and the known property of infusion solutions based on hyperosmolytic colloidal solutions, along with the correction of hypovolemic shock and septicemia, to suppress the increase in the amount of fluid in the lungs, without disturbing the gas exchange in them, gives relevance to the research and study of new combined colloid-hyperosmolytic infuseon solutions (Abdullahi & Jeschke, 2014).

One such drug is a solution of lactoprotein with sorbitol (LPS), which was created at the Lviv Institute of Blood Pathology and Transfusion Medicine (Covalchuk & Cherkasov, 2014). The results of preclinical study of the drug established its ability to support the vital functions of the body of rats and provide organoprotective effects in the conditions of experimental burn injuries of the skin (Cherkasov et al., 2015). The effect of the drug on ultrastructural changes in the lungs in the period of burn shock is unknown, which necessitates research in this direction.

The goal of our research was to find out the effect of the solution of lactoprotein with sorbitol on the ultrastructural organization of pulmonary tissues in rats with burn shock (BS).

Materials and methods

Experimental studies were performed on 256 white male rats weighing 160–180 g in accordance with the requirements of modern standards, as reflected in the international rules of the "European Convention for the Protection of Vertebrate Animals", the methodological recommendations of the Ministry of Health of Ukraine on "Preclinical Research of Medicinal Products" (Directive 2010/63/EC of the European Parliament and of the Council of 22 September 2010 on the Protection of Animals used for Scientific Purposes, 2010).

The animals were catheterized and divided into three groups: I group – intact animals, II, III groups – rats with BS, which were infused respectively: 0.9% NaCl solution, lactoprotein with sorbitol. Burn shock of moderate severity in animals caused thermal burns of the second degree (21–23%) by method (Regas & Ehrlich, 1992).

Infusion of the investigated solutions in a dose of 10 ml/kg was carried out in aseptic conditions in the femoral vein for 5 minutes. One hour after the infliction of burn shock; the following infusions – once a day for 7 days. A catheter with a diameter of 1–2 mm, mounted in the femoral vein, was placed under the skin, and its lumen was filled with titrated heparin solution (0.1 ml of heparin per 10 ml of 0.9% NaCl solution) throughout the length after each injection of the solutions studied. Shaving of the animals, catheterization of major vessels, infliction of burns and decapitation of the animals were carried out under conditions of propofol anesthesia at a dose of 60 mg/kg intraperitoneally (Abdullahi et al., 2014).

Two schemes of pharmacological correction of opioid shock were investigated in this work: 1) 0.9% solution of NaCl (produced by the Kyiv JSC Biofarma) – control pathology; 2) the investigated drug lactoprotein with sorbitol – protein and salt complex containing as a colloidal basis donor albumin – 5.0%, as well as polyatomic sorbitol – 6.0%, sodium lactate – 2.1%, sodium chloride – 0.8%, calcium chloride – 0.01%, potassium chloride – 0.0075%, sodium bicarbonate – 0.01%. Osmolarity of the drug – 1020 mOsmol/l (Registration certificate No 464/09-300200000 JSC Biofarma). Lactoprotein with sorbitol belongs to the group colloidal hyperosmolar solutions and is the closest in composition, transfusion potential and pharmacodynamic properties to blood plasma.

For electron microscopy, tracheotomy was performed in the rats under propofol anesthesia. After two-sided incisions along the intercostal spaces, the lungs collapsed, and then in the trachea about 1.5 ml of 2.5% glutaraldehyde solution on the phosphate buffer was immediately administered. After opening of the chest in situ, the right lung was irrigated with a 2.5% glutaraldehyde solution for 15–20 minutes. Sections from the lower lobe of the right lung were cut into small blocks and continued to be fixed in the same solution for an hour. After standard wiring, the material was poured into an epoch. Ultra-thin sections of the lung tissue produced on ultramicrotome LKB-3 were prepared with uranyl acetate and lead citrate by the Reynolds method and the lung structure studied under the electron microscope PEM-125K (Regas & Ehrlich, 1992).

Results

The longitudinal nuclei of endothelial cells and respiratory alveolocytes had invaginations, which are formed by the nuclear membranes. The wall of the aerogematous barrier was uneven due to edema and illumination of the cytoplasmic part of the respiratory epitheliocytes, their plasmolemma were wavy. Cell cytoplasm had a small number of pynocystic bubbles, there were separate vacuoles, and organelles were numb and destructively altered.

The thickness of the basement membrane was uneven, there were locally thickened areas. The cytoplasmic part of the endothelial cells had a different thickness, formed a leak in the lumen of the blood capillary. In the cytoplasm of the endothelial cells there were destructively altered organelles – hypertrophied mitochondria had places that were luminous matrix, damaged crystals, granular endoplasmic mesh channels were fragmented, thickened, on the surface of their membranes, there were few ribosomes.

Ultrastructure of type II alveolots was noticeably changed – there were small nuclei with uneven contours of the nuclear membrane. In the karyoplasm, there were many heterochromatin, they form a cluster and are located more along the nuclear membrane. In the cytoplasm, small numbers of mitochondria were hypertrophied, had a homogeneous matrix, in which the crystals were poorly visible, the channels of the granular endoplasmic mesh were deformed, uneven, on the surface of their membranes there were few ribosomes, and the cisternae in the dictyosomes of the Golgi complex were single. On the apical part of the plasmalema there were small microvilli, most of which is exposed. Such a state of secretory alveolocytes indicates their low functional activity (Fig. 1*b*). In the cytoplasm of the alveolar macrophages, many primary, small lysosomes and large secondary phagosomes were noted. The nucleus appeared diminished, the nuclear membranes formed invaginations, areas of heterochromatin were present in the karyoplasm. Cytoplasmic germs were present on separate areas of the surface, plasmolemma in them fuzzy, rippled, indicating a violation of the functional activity of alveolar macrophages (Fig. 1*c*).

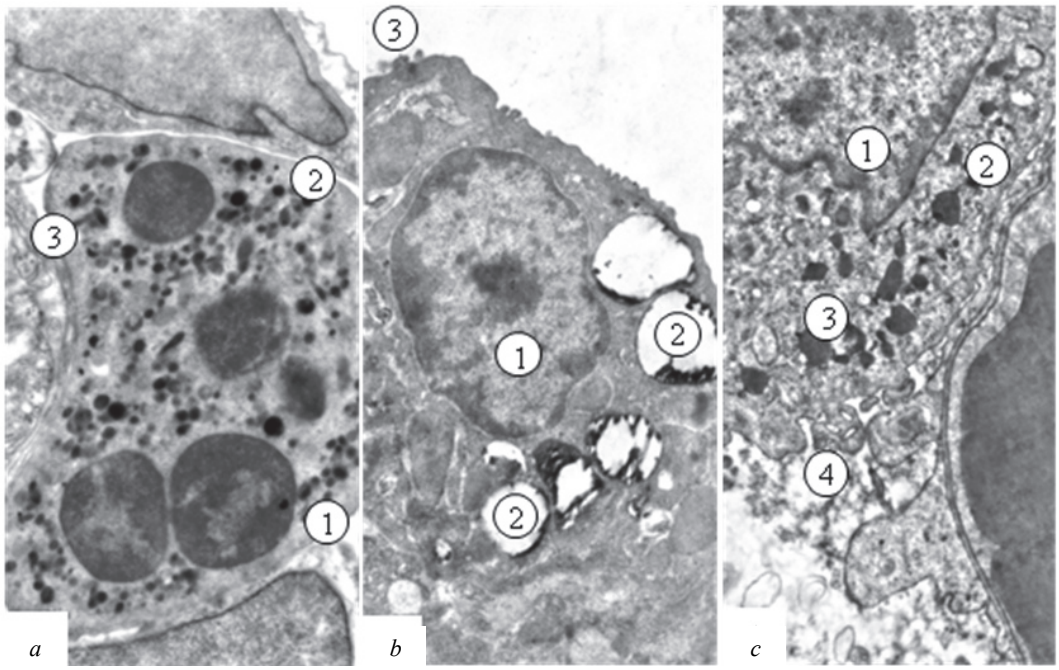

Fig. 1. Sub-microscopic changes in the respiratory lung unit for day 3 of burn shock when 0.9% NaCl solution was administered (the scale bar was 100 μm): *a* – alveol: 1 – lumen of hemocapillary with blood cells, *2* – endothelial cell, *3* – aerogemic barrier; *b* – alveolocytes: *1* – nucleus, *2* – vacuole-shaped lamellar bodies, *3* – single microvilli on the surface of the cell; *c* – alveolar macrophage: *1* – kernel with invaginations of the cariolomas, *2* – primary lysosomes, *3* – secondary lysosomes, *4* – cytoplasmic growths

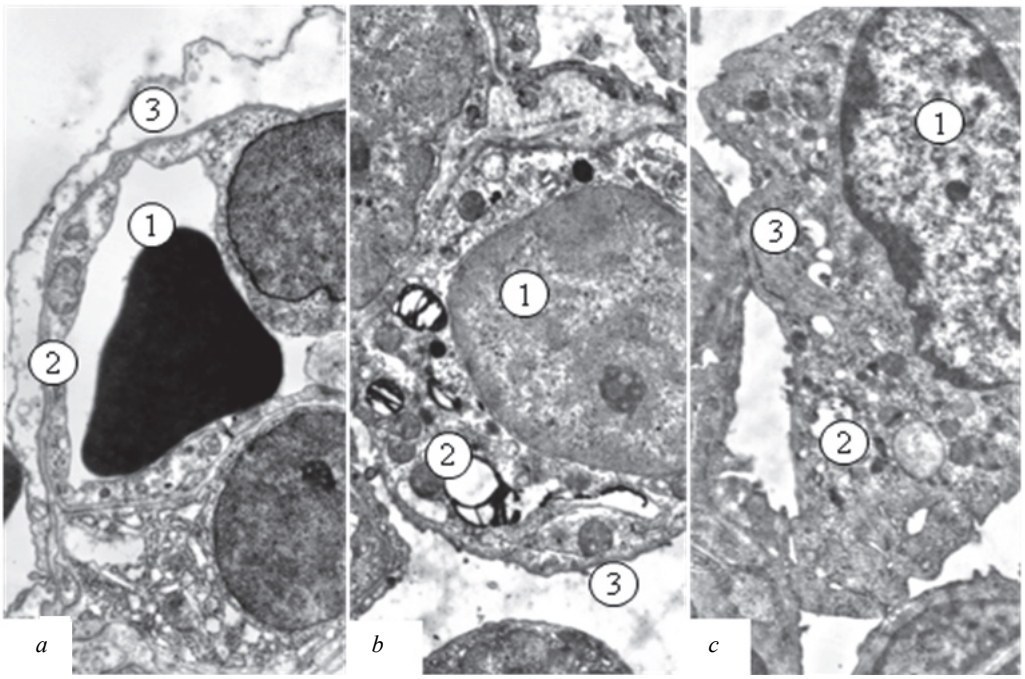

Fig. 2. Sub-microscopic changes in the respiratory lung unit on day 3 of burn shock when 0.9% NaCl solution was injected (the scale bar was 100 μm): *a* – alveoli: *1* – lumen of haemocapillary with blood cells, *2* – endothelial cell, *3* – aerogemic barrier; *b* – alveolocytes: *1* – nucleus, *2* – vacuole-shaped lamellar bodies, *3* – single microvilli on the surface of the cell; *c* – alveolar macrophage: *1* – kernel with invaginations of the karyolemmas, *2* – primary lysosomes, *3* – secondary lysosomes, *4* – cytoplasmic growths

At day 7 of burn shock, with 0.9% NaCl solution, significant changes were observed in the respiratory unit: part of the alveoli had considerably expanded blood flow of capillaries, which had platelets, neutrophils and altered erythrocytes. The wall of these alveoli had substantially thickened areas due to the of the edema cytoplasm of respiratory alveols and endothelial cells. In the aerohematic barrier there was a narrow basement membrane. The cytoplasmic parts of the endothelial cells were of different thicknesses. The nuclei of the endothelial cells were small, moderately osmeophilic. Organelles were single and damaged and occupied a small area. Respiratory epithelial cells had unevenly thickened, electron-transmitted cytoplasmic areas. Their outer membrane formed protuberance and invagination, pynocystic bubbles and caveolae were insufficient. Such a state of the aerohematic barrier, destructive changes in the structure's components indicates a significant deterioration of gas exchange in the respiratory lung (Fig. 2*a*). The ultrastructure of type II alveolocytes was significantly altered – there were violations of the karyolemmas, perinuclear space was expanding due to the detachment of the outer nuclear membrane, and a few nuclear pores in the cariolum. In the cytoplasm, the destruction of organelles was found: platelets were few, some of them were large with electron-translucent portions, contained little osmiumophi-

lic material; in the mitochondria there was an osmiophilic homogenized matrix in which the crystals were not detected; unevenly expanded and partially fragmented tubules of a granular endoplasmic net and Golgi complexes resembling vacuoles; at the apical portion of plasmolem, single microvilli (Fig. 2*b*). In the cytoplasm of alveolar macrophages, there were many different electronic densities of phagos, primary lysosomes were small, they were small, rounded, osmotic, their plasmolem is uneven, but cytoplasmic germs were small (Fig. 2*c*), which indicates the accumulation of phagocyte material in them.

At day 3 of burn shock in the background of administration of a solution of lactobacilli with sorbitol, less damage was done to the structures of the respiratory lung than in the group of rats which was fed a 0.9% solution of NaCl. The basement membrane looked like a light, moderate thickness of the tape, but in some areas it was not clearly contoured (Fig. 3*a*).

In uneven cytoplasmic areas of respiratory epitheliocytes, there were more pynocystic bubbles and caveoles, plasmolem formed bubbling and microvilli. Cytoplasmic areas of endothelial cells were of uneven thickness, they had few organelles (Fig. 3*b*).

During this period, the ultrastructure of type II alveolocytes and alveolar macrophages was similar to that of a group of animals that was fed a 0.9% solution of NaCl after infliction of the burn. Thus, in the cytoplasm of the secretory epithelial cells there were few platelets, they were large, electron-transparent, osmiophilic layered material was rarely observed. Mitochondria were small, osmiophilic, had a homogeneous matrix, crystals were poorly contoured.

On the apical part of the cells in plasmolomy there were microvilli, most of it was exposed. Such a state of secretory alveolocytes reflects their low functional activity. However, the nuclei of the secretory epitheliocytes had a rounded form, euchromatin predominated in their karyoplasm, and the kariolemmas were clearly contoured (Fig. 3*b*). This is a sign of the onset of intracellular regenerative processes. The cytoplasm of the alveolar macrophages had many primary small lysosomes and secondary phagos. Plasma cell cultures in selected areas were lacerated, fuzzy, cytoplasmic germs were present.

At day 7of burn shock in the lungs of rats which were injected with lactoprotein solution with sorbitol, the ultrastructure of the components of the aerohematic barrier had improved in comparison with 3 days. Luminosity of the hemocapillary parts was moderate, mainly with erythrocytes. Endothelial cells in their walls had elongated nuclei with invaginations of the nuclear membranes and clear contours. Their cytoplasmic regions were not wide-ranging, with moderate electron density.

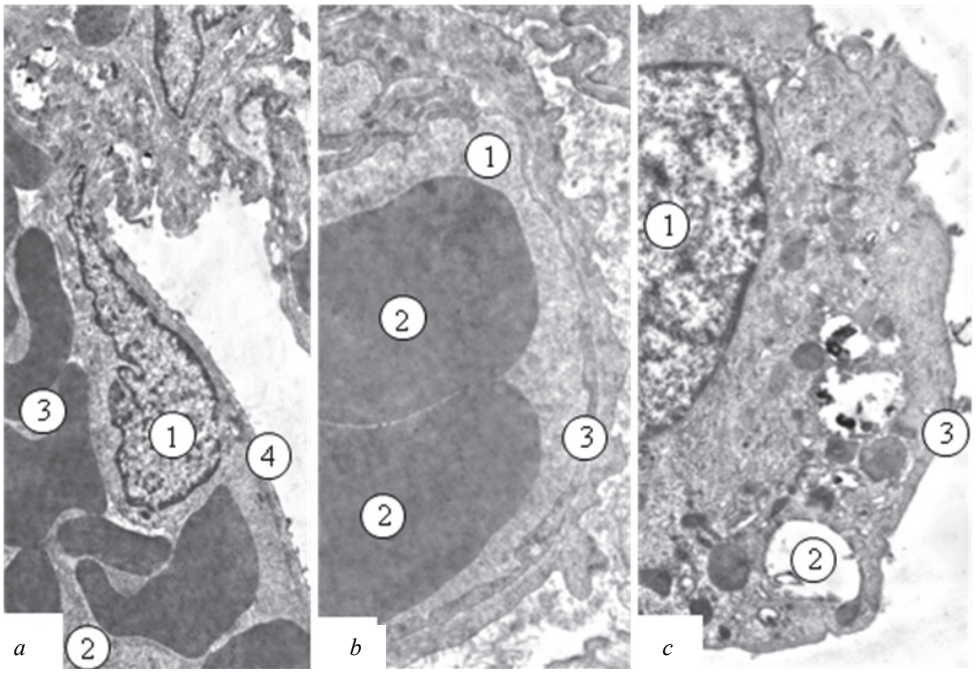

Fig. 3. Submicroscopic changes in the respiratory lung unit after 3 days of burn shock when lactoprotein and sorbitol were administered (the scale bar was 100 μm): *a* – alveoli: *1* – nucleus, *2* – lumen of hemocapillary, *3* – form elements of blood, *4* – aerohematic barrier; *b* – the walls of the alveoli: *1* – the lumen of the hemocapillary, *2* – red blood cells, *3* – aerohematic barrier; *c* – type II alveolocyte: *1* – nucleus, *2* – light secretory bodies, *3* – apical section of plasmolomy with microvilli

The basement membrane in the aerohematic barrier was relatively uniform, not wide, light, and from the side of the stroma was thickened and uneven. In the respiratory alveolocytes, cytoplasmic areas were of uneven thickness, plasmolemma, which limits wavelengths (Fig. 4*a*). However, the swelling of the cytoplasm and its illumination were not as significant as in this period when 0.9% solution of NaCl was introduced. In the part of cytoplasm segments of type I alveolocytes, many bubbles and caveolae were observed. Part of the blood capillaries remainned with enlarged, blood-filled lumens.

In type II alveolocytes, during this trial, a lower degree of damage to the nucleus and organelles in the cytoplasm was established and there were signs of a renewal of the secretory function of these cells. In the cytoplasm, we observed hypertrophied mitochondria with clear crystals, components of the Golgi complex, different size of secretory granules, which showed different densities, indicating their formation (Fig. 4*b*).

Near the wall of the alveoli, alveolar macrophages with many cytoplasmic germs were observed, some of them were branched. In the cytoplasm of the alveolar macrophages, there were many mitochondria, lysosomes present in small primary and larger secondary form. Such an ultrastructural organization of alveolar macrophages testifies to their functional activity and participation in protective reactions (Fig. 4*c*).

Discussion

Lungs play an important role in causing systemic homeostasis disorders against a background of burn shock (Shaver & Bastarache, 2014; Nielson et al., 2017); increased permeability of the capillaries, their dilatation, a decrease in the volume of circulating blood, deterioration of rheological properties and the development of microthrombosis, decreased intrapulmonary blood flow as a result of hypoxic lung injury. However, further elucidation of the ultrastructural mechanism of homeostasis in the lungs will allow us to assess both early changes in the body and the effectiveness of the applied therapy. In general, the ultrastructural changes detected in the application of the physiological solution on days 3 and 7 indicate an inadequate effect of this type of infusion therapy in preventing cellular damage in the lungs, this is compared

with the data regarding the development of pulmonary complications in the application of 0.9% NaCl solution to burn patients and in experimental studies (Jacob et al., 2015; Sousse et al., 2015). The obtained data correspond to ultrastructural changes recorded in other experimental studies regarding cellular lung injury on the background of thermal burns (Zhang et al., 2018).

During electron microscopic examination of the respiratory part of the lungs on day 3 of burn shock against the background of the use of 0.9% NaCl solution, reactive changes in the alveoli were determined, mainly destructive – necrotic, indicating a significant defeat of the organ in this period of thermal burn of the skin. We also revealed ultrastructural changes in alveolocytes which indicate their low functional activity. The changes observed correspond to the data obtained in other studies in the period of burn shock (Sousse et al., 2015; Zhang et al., 2018). At day 7 of burn shock, using 0.9% of NaCl solution, signs of progression of destructive changes in the components of the aerohematic barrier were observed, indicating the weak protective effect of 0.9% NaCl solution.

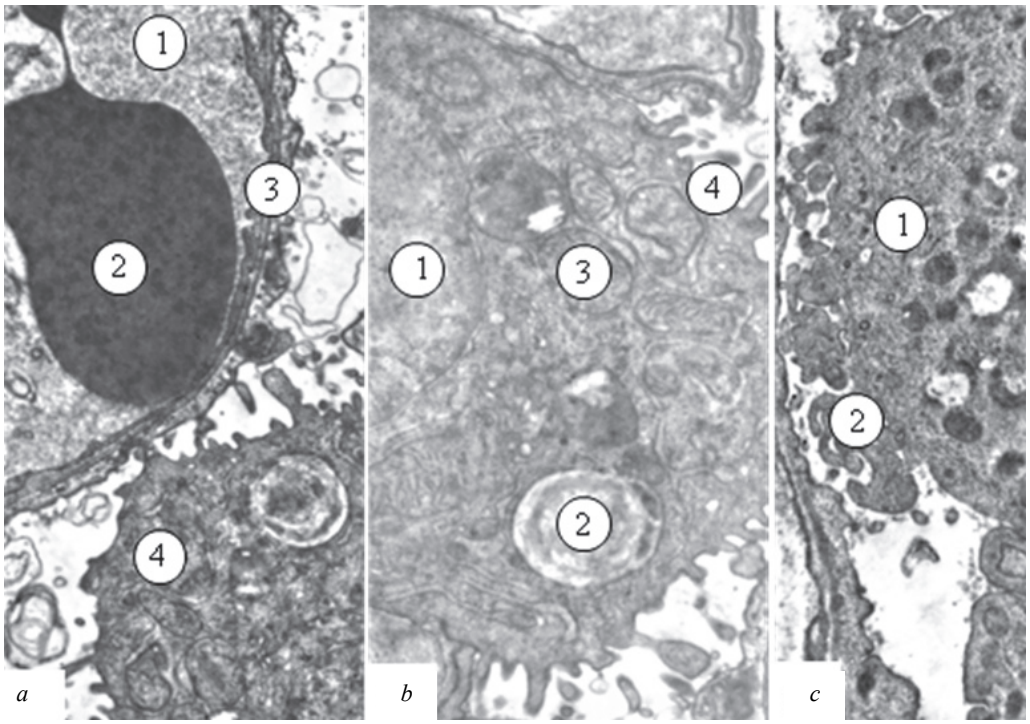

Fig. 4. Submicroscopic changes in respiratory lung part after 7 days of burn shock upon administration of lactobacilli with sorbitol: *a* – walls of the alveoli: *1* – lumen of the hemocapillary, *2* – erythrocyte, *3* – the wall of the alveoli, *4* – macrophage (×9,000); *b* – type II alveolocyte: *1* – rounded nucleus, *2* – secretory granules, *3* – hypertrophied mitochondria, *4* – apical section of plasmolymy with microvilli (×15,000); *c* – alveolar macrophage: *1* – fragment of the cytoplasm, *2* – cytoplasmic germs (×9,000)

When studying the corrective effect of lactoprotein with sorbitol solution after 3 days of burn shock in rats, ultrastructural data did not differ from the group of rats when 0.9% solution of NaCl was introduced. However, the nuclei of the secretory epitheliocytes had a rounded form, euchromatin predominated in their karyoplasma, clearly defined nuclear membranes, well-expressed nucleoli are signs of the onset of intracellular regenerative processes. At day 7 under the action of the solution of lactoprotein with sorbitol, changes in the aerohematic barrier were less pronounced than against the background of 0.9% NaCl solution. In type II alveolocytes there were signs of a renewal of the secretory function, the ultrastructural organization of alveolar macrophages testifyed to their functional activity and participation in protective reactions.

Thus, it was found at the subcellular level that the colloidal hyperosmolar solution of lactoproteins with sorbitol in the magnitude of the cytoprotective effect on lung cells with modelled burn shock prevails over the action of 0.9% NaCl solution, which is consistent with the literature on the effect of this drug on other organs (Cherkasov et al., 2015). However, it should be noted that in contrast to other organs, where changes in organs are recorded from practically the first day of burn shock (Guminskiy et al., 2017). In our study, the greatest positive effect on the cellular structures of lungs of lactoprotein solution with sorbitol was established 7 days after skin burn. We can explain this by the fact that the lungs against the background of burn shock are an effector organ in which an inflammatory reaction with marked cellular damage develops (Chong et al., 2014), against which apoptosis is activated in damaged lung cells (Dong et al., 2015; Rose & Chan, 2016). Therefore, the use of infusion solutions on lung cells is likely to exert its influence by activating synthetic processes that upgrade the cell population by replacing apoptotic cells as is established in other organs (Guo et al., 2015). It should also be noted that ultrastructural changes in the lungs with burn shock are noticed before the manifestation of clinical symptoms (Shaver & Bastarache, 2014), which suggests it is precisely the effect of lactoprotein solution with sorbitol on lung cells, which in the long run may improve the results of the therapy of this pathological condition.

Such results of an experimental study allow us to differentiate the changes caused by burn shock from changes caused by the drug itself, proving the safety of the drug and the possibility of its use in this pathology. It is known (Perel et al., 2013) that prolonged use of only one crystalloid solution has a number of undesirable reactions: the need to increase the volume of infusion, insignificant duration of circulatory effect, cell dehydration, significant overload of the body with sodium ions, increased edema in the burn area, deepening systemic acidosis, decreased blood lactate levels, a sharp drop in potassium ions, and a negative inotropic effect on the myocardium. Therefore, the feasibility of their use is questioned because they are not able to align the hemodynamic status.

Unlike hypertonic solutions of sodium chloride, combined hyperosmolar solutions have a number of benefits that provide a comprehensive pharmacological action: detoxification, intestinal, energy, moderate dehydration, and are characterized by a lower risk of side effects: pulmonary edema, hypocoagulation, impaired filtration ability of the kidneys (Abdullahi & Jeschke, 2014). Their effect is sufficiently studied (Perel et al., 2013), it is found that these solutions, which simultaneously affect the various parts of the burn shock, have a number of advantages over monotherapy: they can be used from the first hours of burn shock,

minimizing the negative effects inherent in the early application of colloids, they include solutions for the correction of metabolic acidosis, which is an important factor in the overall damage to thermal skin burns (Shaver & Bastarache, 2014; Nielson et al., 2017).

According to the results of an ultrastructural study, it was found in rats without burns which were injected a 0.9% solution of NaCl for 7 days and a lacto-protein with sorbitol that the structure of the aerohematic barrier remained unchanged: most of the lung cuts occupy the alveoli that formed alveolar strokes and alveolar sacs. In the cytoplasm of type II alveolocytes, a well-developed Golgi complex, elements of a granular endoplasmic net, numerous mitochondria, free ribosomes and polysomes, as well as lamellar bodies with surfactant, alveolar macrophages were introduced in the intervertebral septa, in their cytoplasm developed cisterns and electron-transparent vesicles of the Golgi complex, numerous mitochondria, primary and secondary lysosomes and vacuoles.

In contrast, the use of lactoprotein with sorbitol positively influenced the processes of renewal of cells in the lungs against the background of burn shock and intracellular structures more clearly from 7 days, which proves the advantage of this type of solution in the treatment of burn injury for tread effect on the lungs, which can and should be recommended for use according to modern guidelines (Snell et al., 2013; Abdullahi & Jeschke, 2014; Kaddoura et al., 2017) requiring the use of solutions with rapid recovery of circulating blood volume and positive effect on microcirculation and tissue oxygenation. The use of such solutions optimizes the functioning of organs. The data we obtainned allow us to confirm the positive effect of the solution of lactobacillus with sorbitol on the ultrastructure of the lungs with thermal damage to the skin and the development of burn shock.

Conclusions

As a result of the study of the influence of the solution of lactoprotein with sorbitol on the ultrastructure of the tissues of the lungs in rats with burn shock, we can state the advantage of this preparation over the use of physiological (0.9% NaCl) solution. In conditions of burn shock, the use of a solution of lactoprotein with sorbitol for 7 days is accompanied by a maximum pulmonoprotective action (as evidenced by ultrastructural changes in the lungs) in comparison with the control group using 0.9% NaCl solution.

The positive effect of the solution of lactoprotein with sorbitol on the ultrastructure of the lungs in the event of burn injuries of the skin is realized through the restoration of the endothelium of blood vessels, hemocapillaries, basement membrane, fluid retention in the microcirculatory channel, improvement of the aerohematic barrier, stimulation of the activity of alveolar macrophages and the secretory function of type II alveolocytes. The most distinct changes were observed at 7 days after induction of burn shock in the lungs of the rats which were injected with a solution of lactoprotein with sorbitol, the ultrastructure of the components of the aerohematic barrier improved compared with the first 3 days of the experiment using a similar solution.

The study of functional, biochemical and molecular genetic parameters that characterize the state of the aerohematic barrier following the use of a solution of lactoprotein with sorbitol in patients with a burn injury to the skin will allow a comprehensive assessment of the mechanisms of the pulmonary protective effect of this drug and experimenttally substantiate the feasibility of its use in clinical practice for pharmacocorrection of burn shock.

References

Abdullahi, A., & Jeschke, M. G. (2014). Nutrition and anabolic pharmacotherapies in the care of burn patients. Nutrition in Clinical Practice, 29(5), 621–630.

Abdullahi, A., Amini-Nik, S., & Jeschke, M. (2014). Animal models in burn research. Cellular and Molecular Life Sciences, 71(17), 3241–3255.

Cherkasov, V. G., Kovalchuk, A. I., Dzevulskaya, I. V., & Cherkasov, E. V. (2015). Evaluation of the effect of infusion of composite hyperosmolar solutions on the structure of the neuroimmunoendocrine system organs in burn disease. European International Journal of Science and Technology, 4(9), 51–61.

Chong, S. J., Wong, Y. C., Wu, J., Tan, M. H., Lu, J., & Moochhala, S. M. (2014). Parecoxib reduces systemic inflammation and acute lung injury in burned animals with delayed fluid resuscitation. International Journal of Inflammation, 2014, 972645.

Cox, R. A., Jacob, S., Andersen, C. R., Mlcak, R., Sousse, L., Zhu, Y., & Hawkins, H. K. (2015). Integrity of airway epithelium in pediatric burn autopsies: Association with age and extent of burn injury. Burns, 41(7), 1435–1441.

Directive 2010/63/EC of the European Parliament and of the Council of 22 September 2010 on the protection of animals used for scientific purposes (2010). Official Journal of the European Union, 276, 33–79.

Dong, Z. W., Chen, J., Ruan, Y. C., Zhou, T., Chen, Y., Chen, Y., & Peng, Y. Z. (2015). CFTR-regulated MAPK/NF-κB signaling in pulmonary inflammation in thermal inhalation injury. Scientific Reports, 5, 15946.

Fuzaylov, G., Anderson, R., Knittel, J., & Driscoll, D. N. (2015) Global health: Burn outreach program. Journal of Burn Care and Research, 36(2), 306–309.

Gamelli, L., Mykychack, I., Kushnir, A., Driscoll, D. N., & Fuzaylov, G. (2015) Targeting burn prevention in Ukraine: Evaluation of base knowledge in burn prevention and first aid treatment. Journal of Burn Care and Research, 36(1), 225–231.

Glik, J., Kawecki, M., Kitala, D., Klama-Baryła, A., Łabuś, W., Grabowski, M., & Kasperczyk, A. (2017). A new option for definitive burn wound closure-pair matching type of retrospective case-control study of hand burns in the hospitalised patients group in the Dr Stanislaw Sakiel Centre for Burn Treatment between 2009 and 2015. International Wound Journal, 14(5), 849–855.

Guminskiy, Y. I., Gunas, I. V., Ocheretna, N. P., & Bashinska, O. I. (2017). Micromorphometric changes in rats' spleen in the first 7 days after skin burns and under application of infusion solutions. Reports of Morphology, 23(2), 240–244.

Guo, S.-X., Fang, Q., You, C.-G., Jin, Y.-Y., Wang, X.-G., Hu, X.-L., & Han, C.-M. (2015). Effects of hydrogen-rich saline on early acute kidney injury in severely burned rats by suppressing oxidative stress induced apoptosis and inflammation. Journal of Translational Medicine, 13, 183.

Herold, S., Gabrielli, N. M., & Vadász, I. (2013). Novel concepts of acute lung injury and alveolar-capillary barrier dysfunction. American Journal of Physiology – Lung Cellular and Molecular Physiology, 305(10), L665–L681.

Jacob, S., Zhu, Y., Kraft, R., Cotto, C., Carmical, J. R., Wood, T. G., & Cox, R. A. (2015). Physiologic and molecular changes in the tracheal epithelium of rats following burn injury. International Journal of Burns and Trauma, 5(1), 36–45.

Kaddoura, I., Abu-Sittah, G., Ibrahim, A., Karamanoukian, R., & Papazian, N. (2017). Burn injury: Review of pathophysiology and therapeutic modalities in major burns. Annals of Burns and Fire Disasters, 30(2), 95–102.

Nielson, C. B., Duethman, N. C., Howard, J. M., Moncure, M., & Wood, J. G. (2017). Burns: Pathophysiology of systemic complications and current management. Journal of Burn Care and Research, 38(1), e469–e481.

Perel, P., Roberts, I., & Ker, K. (2013). Colloids versus crystalloids for fluid resuscitation in critically ill patients. Cochrane Database of Systematic Reviews, 2(2), CD000567.

Porter, C., Tompkins, R. G., Finnerty, C. C., Sidossis, L. S., Suman, O. E., & Herndon, D. N. (2016). The metabolic stress response to burn trauma: Current understanding and therapies. Lancet, 388(10052), 1417–1426.

Regas, F. C., & Ehrlich, H. P. (1992). Elucidating the vascular response to burns with a new rat model. The Journal of Trauma, 32(5), 557–563.

Rose, L. F., & Chan, R. K. (2016). The burn wound microenvironment. Advances in Wound Care, 5(3), 106–118.

Rowan, M. P., Cancio, L. C., Elster, E. A., Burmeister, D. M., Rose, L. F., Natesan, S., & Chung, K. K. (2015). Burn wound healing and treatment: Review and advancements. Critical Care, 19, 243.

Shaver, C. M., & Bastarache, J. A. (2014). Clinical and biological heterogeneity in acute respiratory distress syndrome: Direct versus indirect lung injury. Clinics in Chest Medicine, 35(4), 639–653.

Snell, J. A., Loh, N.-H. W., Mahambrey, T., & Shokrollahi, K. (2013). Clinical review: The critical care management of the burn patient. Critical Care, 17(5), 241.

Sousse, L. E., Herndon, D. N., Andersen, C. R., Zovath, A., Finnerty, C. C., Mlcak, R. P., Cox, R. A., Traber, D. L., & Hawkins, H. K. (2015). Pulmonary histopathologic abnormalities and predictor variables in autopsies of burned pediatric patients. Burns, 41(3), 519–527.

Zhang, D., Chang, Y., Han, S., Yang, L., Hu, Q., Yu, Y., & Chai, J. (2018). The microRNA expression profile in rat lung tissue early after burn injury. Turkish Journal of Trauma and Emergency Surgery, 24(3), 191–198.

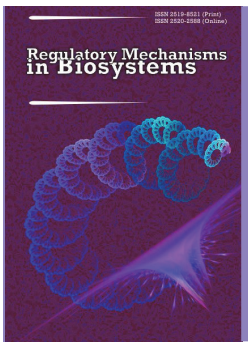

Regulatory Mechanisms in Biosystems

ISSN 2519-8521 (Print)
ISSN 2520-2588 (Online)
Regul. Mech. Biosyst., 9(3), 446–452
doi: 10.15421/021867

Cytogenetic anomalies of winter wheat cells, induced by chemical contamination of the territory of Kalush industrial district

V. V. Morgun, R. A. Yakymchuk

Institute of Plant Physiology and Genetics, NAS of Ukraine, Kyiv, Ukraine

Article info

Received 29.06.2018
Received in revised form 07.08.2018
Accepted 13.08.2018

Institute of Plant Physiology and Genetics, NAS of Ukraine, Vasylkivska st., 31/17, Kyiv, 03022, Ukraine.
Tel.: +38-097-341-89-12.
E-mail: peoplenature16@gmail.com

Morgun, V. V., & Yakymchuk, R. A. (2018). Cytogenetic anomalies of winter wheat cells, induced by chemical contamination of the territory of Kalush industrial district. Regulatory Mechanisms in Biosystems, 9(3), 446–452. doi:10.15421/021867

Mass accumulation of toxic waste near inhabited localities has changed some regions of Ukraine, in particular Kalush industrial area (Ivano-Frankivsk region), into zones of ecological disaster. Research on cytogenetic anomalies caused by chemical soil contamination of the territories of toxic chemical warehouses will be useful in determining the level of mutagenic activity of xenobiotics when they enter the environment and potential mechanisms of the induction of chromosome reconstructions by them and mitosis disorders. The aim of the research is to study frequency and spectrum of the types of cytogenetic disorders in *T. aestivum* L. under the prolonged effect on the seeds of soil contaminated with hexachlorinebenzene from territories of toxic waste warehousing and to determine the level of their mutagenic activity as compared with the effect of moderate and high concentrations of N-nitrozo-N-methylurea (NMU). Seeds of winter wheat cultivars Al'batros odes'kyi and Zymoiarka were sprouted in the soil samples taken from the toxic waste ground of LLC "Oriana Halev", its recultivated area and the dump area of Dombrovskyi potash ore mine, situated near Kalush city. Hexachlorobenzene concentrations in the soil of the studied areas exceeded CPC by 1233–18350 times. Soil samples from a tentatively clean area of Svatky village, Hadiach district, Poltava region were taken as the control. To study cytogenetic consequences of the effect of moderate and high concentrations of NMU, wheat seeds were kept in a mutagen water solution at concentrations 0.005%, 0.010%, 0.025%. Frequency and spectrum of cytogenetic anomalies were determined in the cells of sprout root meristem using the anatelophase technique. Chemical contamination of the soil exhibited high mutagenic activity which, by induction frequency of cytogenetic anomalies, exceeded the control level by 1.8–3.8 times and equalled mutagenic activity of NMU in moderate concentrations. The highest level of cytogenetic disorders, which exceeded spontaneous indicators by 3.4–3.8 times, was found when the soil contamination of the territory of the toxic waste ground with hexachlorobenzene was the most intensive. Traces of hexachlorobenzene in the soil of the recultivated plot of the ground continue to manifest high cytogenetic activity and pose a threat for the genomes of living organisms. Frequency of chromosome aberrations at a low hexachlorobenzene concentration in the soil of the disposal area of Dombrovskyi mine exceeded spontaneous indicators by 1.8–2.4 times, which is the result of its complex effect with natural-mineral compounds of mining-chemical raw materials. The increase of some bridges and acentric chromosome rings – markers of a radiation effect – among the types of cytogenetic disorders, induced by the soil contamination with hexachlorobenzene, confirms the radiometric properties of the xenobiotic, which were identified at high concentrations of NMU. The increase in the number of the cells with multiple aberrations, induced by the hexachlorobenzene contamination of the soil holding the studied objects proves the high genotoxicity of the chemical compound and the threat of serious genetic consequences if it enters the environment.

Keywords: *Triticum aestivum* L.; toxic waste; mitosis disorders; chromosome aberrations; mutagenic activity.

Introduction

Mutative changes of organisms are a required factor of evolution, they make the genome dynamic and flexible, help active response to environmental changes and are an adaptive feature of species (Lynch, 2016; Gervais & Roze, 2017; La Croixetal., 2017). In the conditions of increasing techno-genic load in the form of physical and chemical mutagens, controlling systems of genomic reconstructions fail to ensure their stable spontaneous level. Induced genetic disorders are revealed by genome destabilization (Chan et al., 2014; Kumar & Pandey, 2015), kinds of development (Aoki, 2017; Yahaya et al., 2017), the increase of genetic load in the populations, changes in the trends of natural selection (Sirohi et al., 2014; Henn et al., 2015), the decrease of lifespan (Chen et al., 2013; Correia et al., 2013), disorder of sexual dimorphism, individual death (Doorn, 2014; Kumar & Pandey, 2015).

Based on the generalization of the research results concerning the factors of chemical pollution of the environment, it has been established that wastes of danger category, 1–3, 8 mln t of which are annually formed in Ukraine, show the highest genotoxicity. Their mass accumulation in the ground near inhabited localities have changed some regions of Ukraine, in particular Kalush city and adjacent villages Kropyvnyk and Sivka-Kaluska in Ivano-Frankivsk region, into zones of ecological disaster (Al-Naber et al., 2016). Intensive soil, water and air contamination of Kalush industrial district with highly toxic substances from the largest deposit of toxic waste in Europe – LLC "Oriana Halev" and Dombrovskyi potash ore mine, where 11,087.6 t of hexachlorobenzene are stored according to official data (about 50% of all the available waste of danger category I in the territory of Ukraine) (Lysychenko et al., 2015), have caused an increase in the level of genetic pathology, inborn anomalies, new formations, and somatic diseases of the main organ systems among local residents (Rozhko et al., 2014). Based on the estimation of the UN international experts, recultivation of the ground of the territory and removal of toxic waste for further utilization outside the country caused additional contamination of the region with highly toxic chemi-

cal compounds and some concern of the world community as to a potential risk of trans-border ecological-technological disasters (Yakymchuk & Valyuk, 2018).

Most research has focussed on monitoring and identifying the amount of xenobiotic concentration in the soil, water and foodstuffs (Parpan et al., 2016; Febbraio, 2017; Dent & Dmytruk, 2017). The determination of the level of mutagenic danger to organisms of chemical soil contamination within areas of toxic waste warehousing is among the unsolved problems. To study their mutagenic activity and to define the mechanisms of occurrence of genetic disorder, it is important to research the effect of gene-toxicants on the functioning of a nucleus cell apparatus and frequency of cytogenetic disorders (Altwaty et al., 2016). The study of frequency and spectrum of cytogenetic anomalies, induced by chemical soil contaminants of the natural environment in comparison with the effect of different concentrations of the comprehensively-studied super-mutagens, among which are N-nitrozo-N-methylurea (NMU), is of great practical significance, and will make it possible to identify the level of mutagenic activity of the discovered xenobiotics and possible mechanisms of their induction of chromosome reconstructions and mitosis disorders.

When the effect of environmental harmful factors on the genetic apparatus of living organisms, including man, is studied, in most cases plant test-objects are used, as they facilitate the identification of various mutation types, they do not require serious financial expenses, and the experiments using them can be conducted in a shorter time (Firbas & Amon, 2014; Babatunde & Anabuike, 2015; Kumar & Srivastava, 2015). The aim of the research is to study frequency and spectrum of the types of cytogenetic disorders in *Triticum aestivum* L. under the prolonged effect on the seeds of the soil contaminated with hexachlorobenzene in the territories of toxic waste warehousing and to determine the level of their mutagenic activity as compared with the effect of moderate and high concentrations of N-nitrozo-N-methylurea.

Materials and methods

Cytogenetic activity of soil chemical contamination in the territory of the toxic waste ground of LLC "Oriana Halev" and Dombrovskyi potash ore mine (Kalush city, Ivano-Frankivsk rgn.) was studied on winter wheat sprouts of cv. Al'batros odes'kyi and Zymoiarka with help of anatelophase method. Seeds were sprouted at 25 ºC in soil samples moistened with distilled water and taken by standard technique (Bekker & Agaev, 1989) from the area within the toxic waste ground (49°04' N, 24°19' E), its recultivated area (49°05' N, 24°19' E) and dump of Dombrovskyi mine (49°01' N, 24°20' E) (Fig. 1). Hexachlorobenzene concentrations in the soil were 550.5, 292.0 and 37.0 mg/kg, respectively, and exceeded CPC by 1233–18350 times (0.03 mg/kg). Soil samples from a provisionally clean area of Svatky village, Hadiach district, Poltava region were taken as the control.

To study cytogenetic consequences of the effect of moderate and high concentrations of N-nitrozo-N-methylurea (NMU), wheat seeds were kept for 18 hours in water solution at concentrations 0.005%, 0.010%, 0.025%, after which they were placed in Petri dishes on filtered paper, moistened with distilled water. Seeds moistened in distilled water were taken as the control.

Primary rootlets, 0.8–1.0 cm long, were fixed during 4 hours in Clark holder. Their chemical maceration was done during 1 minute in 1 n solution of hydrochloric acid. When maceration was over, the rootlets were exposed to 23–25 ºC for 24 hours in aceto-orcein solution. Temporary crushed cytological preparations were used for microscopic analysis according to standard technique (Pausheva, 1988). Microscopic study of root meristem cells was carried out using the microscope Jenaval (Carl Zeiss Jena) at magnification 600^x. When identifying frequency of chromosome aberrations and mitosis disorders, cells which were in anaphase and early telophase were examined. Microphotography was done with help of Olympus SP–500 UZ integrated into a microscope at microscope magnification 900^x and software Quick Photo Micro 2.3 for Windows (Olympus). Sampling for each variant used at least 1000 cells, which were analyzed in 20 and more primary rootlets. Frequency of aberrant cells was considered as a percentage of cells in anaphase and early telophase which had chromosome disorders. When average number of aberrations per aberrant cell was calculated, cells with 0, 1, 2 and multiple chromosome aberrations (>2 aberrations) were taken into account. Statistical processing of experimental data was done by standard technique. Percentage shares of chromosome aberrations and average errors of sampled arithmetic averages are given in the tables.

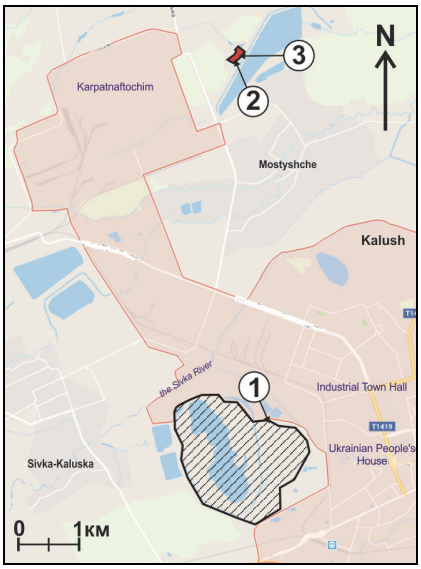

Fig. 1. Soil sampling areas near Kalush city, Ivano-Frankivsk rgn.: *1* – dumps of Dombrovskyi mine, *2* – toxic waste ground of LLC "Oriana Halev", *3* – recultivated area of the toxic waste ground of LLC "Oriana Halev"

Results

The prolonged effect of chemical factors of soil contamination from the territory of the toxic waste ground of LLC "Oriana Halev" and Dombrovskyi potash ore mine in Kalush city on wheat seeds caused the frequency increase of chromosome aberrations in primary rootlets of winter wheat, which was 1.51–2.35% for cultivar Al'batros odes'kyi and 1.37–2.51% for cultivar Zymoiarka, and it exceeded the control level by 1.8–3.8 times (Table 1). Its highest indicators – 2.35% for Al'batros odes'kyi and 2.51% for Zymoiarka – were recorded on the most intensively hexachlorobenzene contaminated soil area of the toxic waste ground. Frequency of cytogenetic disorders exceeded the control level by 3.4–3.8 times. The concentration of residual amount of hexachlorobenzene in the soil of a recultivated plot of the ground decreased twice, as compared with a previous variant. However, chemical contamination continued to maintain high mutagenic activity, which was confirmed by a statistically reliable induced increase in the number of aberrant cells of root meristem by 2.6–3.0 times. The frequency decrease of cytogenetic disorders regardless of the genotype of a winter wheat cultivar only by 1.3 times in the conditions of a doubled decrease of mutagen concentration proves that there is no direct correlation between the intensity of hexachlorobenzene soil contamination and the level of cytogenetic anomalies.

The level of cytogenetic disorders, induced by soil contamination near the dump of Dombrovskyi potash ore mine, exceeded control indicators by 1.8–2.4 times. The soils of Dombrovskyi mine dump contain bare-lying rocks, which include halite, kainite, langbanite, sylvite, kieserite, polyhalite, anhydrite, shungite, leonite and compounds Ni, Fe, Mn, Pb, Cr, Me, the concentrations of which exceed standard admissible rates considerably (Haidin et al., 2014). Besides, within the dump area of the mine, unsanctioned storage of thousands of tons of especially dangerous chemical substances – hexachlorobenzene and amines – took place, and they, being improperly isolated, enter the superficial soil layers. Hence, the preservation of high frequency of chromosome aberrations with further intensity decrease of soil hexachlorobenzene contamination by 8 times is classified as the result of the cumulative and synergetic effect of a complex impact of low concentrations of xenobiotics with natural mineral compounds of mining-chemical raw materials.

When the water solution of NMU was at the lowest concentration – 0.005%, the level of induced cytogenetic disorders in the cells of root meristem increased by 3.5–10 times: it was 2.74% for cultivar Al'batros odes'kyi and 5.82% for cultivar Zymoiarka, control indicators were 0.78% and 0.58%, respectively (Table 2). Further doubling of NMU concentration (0.01%) caused the increase of chromosome reconstruction level in sprout cells of cultivars Al'batros odes'kyi and Zymoiarka of up to 3.92% and 7.13%, respectively, which exceeded the control level by 5.0–12.3 times. However, no statistically reliable difference between the indicators of aberrant cell frequency, induced by NMU in concentrations 0.005% and 0.010%, was recorded. Further increase of NMU concentration by 2.5 times (0.025%) was followed by the induction of the highest level of cytogenetic disorders in meristem cells of primary rootlets – 19.0% for cultivar Al'batros odes'kyi and 23.1% for cultivar Zymoiarka, which exceeded the control level by 24.4–39.7 times. A considerable increase of the number of cells with chromosome reconstructions shows a radiomimetic effect of the chemical mutagen impact in a high concentration.

The spectrum of the types of cytogenetic anomalies in winter wheat cells under the effect of contamination of the soil and NMU water solutions from the studied areas with hexachlorobenzene, except for acentric fragments and bridges, which were typical for the control variant, contained micronuclei, ring and lagging chromosomes (Fig. 2*a*, *b*). The correlation between frequency of induction of several types of chromosome aberrations and the genotype of the plants and the concentration of the active substance was recorded. The increase in frequency of chromosome aberrations in the cells of sprout root meristem under the effect of contamination of soil with hexachlorobenzene in the highest concentration (the territory of the toxic waste ground) is due to the induction of single acentric fragments (1.18%) in cultivar Al'batros odes'kyi and that of chromatide and chromosome bridges (1.07%) in cultivar Zymoiarka (Table 3). As a result of the effect of contamination of soil with hexachlorobenzene in lower concentrations on wheat root meristem, which is typical for a recultivated plot of the toxic waste ground, frequency of the cells with acentric fragments remained at the level of a previous variant and was 0.88% for Al'batros odes'kyi and 0.90% for Zymoiarka (Fig. 3). But the share of bridges in total frequency of cytogenetic disorders decreased to the indicators of the control level. The increase of the number of clastogenic disorders in meristem cells of primary rootlets of wheat sprouts under soil chemical contamination near Dombrovskyi mine resulted from the formation of mainly acentric fragments in Al'batros odes'kyi and dicentric chromosomes in Zymoiarka.

Table 1

Frequency of anatelophase aberrations in winter wheat, induced by toxic waste contamination of soil (x ± SE)

Soil sampling area	Studied anatelophase mitoses, pcs	Mitoses with cytogenetic disorders		Studied anatelophase mitoses, pcs	Mitoses with cytogenetic disorders	
		pcs	%		pcs	%
	Al'batros odes'kyi			Zymoiarka		
Svatky village, Poltava rgn. (control)	1291	8	0.62 ± 0.22	1200	9	0.75 ± 0.25
Toxic waste ground of LLC "Oriana Halev"	1107	26	2.35 ± 0.46**	1592	40	2.51 ± 0.39**
Recultivated area of the toxic waste ground of LLC "Oriana Halev"	1133	21	1.85 ± 0.40*	1219	24	1.97 ± 0.40*
Dombrovskyi potash ore mine	1126	17	1.51 ± 0.36*	1166	16	1.37 ± 0.34

Notes: * – difference as to the control is statistically reliable at $P < 0.05$, ** – at $P < 0.01$.

Table 2

Frequency of anatelophase aberrations in winter wheat, induced by NMU

Mutagen concentration	Studied anatelophase mitoses, pcs	Mitoses with cytogenetic disorders		Studied anatelophase mitoses, pcs	Mitoses with cytogenetic disorders	
		pcs	%		pcs	%
	Al'batros odes'kyi			Zymoiarka		
Water (control)	1409	11	0.78 ± 0.23	1210	7	0.58 ± 0.22
NMU, 0.005%	1239	34	2.74 ± 0.46*	1117	65	5.82 ± 0.70*
NMU, 0.010%	1122	44	3.92 ± 0.60*	1319	94	7.13 ± 0.71*
NMU, 0.025%	1067	203	19.03 ± 1.20*#	976	225	23.05 ± 1.35*#

Notes: * – difference as to the control is statistically reliable at $P < 0.01$; # – difference as to variant NMU 0.005% and NMU 0.010% is statistically reliable at $P < 0.01$.

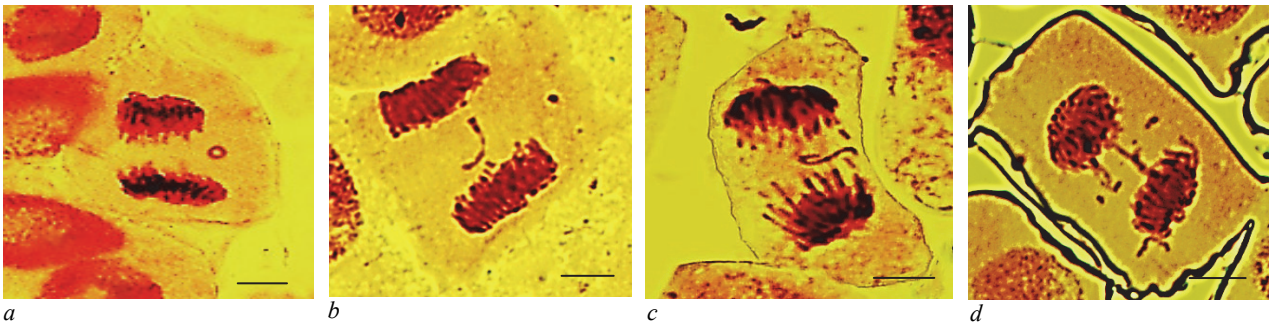

a *b* *c* *d*

Fig. 2. Chromosome aberrations and mitosis disorders in root meristem of winter wheat, induced by toxic waste contamination of soil: *a* – ring chromosome, *b* – lagging chromosome, *c* – pair acentric fragments and lagging chromosome, *d* – multiaberrations; bar – 5 μm

The frequency variation of fragments and bridges depending on the genotype of the plants and the concentration of mutagen was also recorded under the effect of NMU on winter wheat (Table 4). The effect of the supermutagen in concentration 0.005% caused a serious increase of both acentric fragments and chromatide bridges in mitotic cells of root meristem of wheat sprouts of cultivar Zymoiarka (2.78% and 0.89%, respectively, the control level was 0.33% and 0.25%), whereas in the cells of root meristem of cultivar Al'batros odes'kyi only frequency of acentric fragments increased (1.69%, the control level was 0.43%) (Fig. 4). The increase of NMU concentration to 0.01% was followed by a considerable increase of fragment and bridge frequency in the cells of root meristem of cultivar Zymoiarka, but a decrease of the number of cells with acentric fragments (0.89%) and increase in cells with dicentrics (1.25%) was seen in cultivar Al'batros odes'kyi. A serious increase in acentric fragments (8.34–9.02%) was recorded under the effect of NMU in high concentrations (0.025%) for both cultivars; most of them were pair ones. The frequency indicator of anatelophase cells with chromatide bridges, as compared with the previous variant of mutagen effect, did not change significantly.

Thus, the appearance of a great number of cells with dicentrics in wheat root meristem, induced by hexachlorobenzene contamination of the soil near the toxic waste ground, confirms the radiomimetic properties of the chemical compound. According to the results of studying cytogenetic consequences of NMU impact, the abovementioned type of chromosome aberrations with high frequency may occur under moderate and high concentrations of mutagen.

Contamination of the soil of the studied territories with hexachlorobenzene caused the appearance of the cells with ring chromosomes, which may point to the lack of affinity of chemical mutagens with genetic cell structures and the mechanism of their effect by a principle of a

target – accidentally. The spectrum of the types of cytogenetic disorders, as NMU concentration increased, extended with the appearance of ring chromosomes. They are markers of radiation effect (Ryu et al., 2016; Marković et al., 2017), which is why the appearance of such chromosome aberrations, affected by NMU in concentration 0.025% and hexachlorobenzene contamination of the soil in the areas of its storage with frequency 0.19–0.51% and 0.06–0.19% respectively, confirm radiomimetic properties of the studied xenobiotics.

Table 3

Spectrum of types of anatelophase chromosome aberrations in winter wheat, induced by toxic waste contamination of soil (x ± SE)

Soil sampling area	Frequency of types of mitosis disorders and chromosome aberrations, %						Number of aberrations per aberrant cell
	fragments	bridges	fragments and bridges	micronuclei	lagging chromosomes	chromosome rings	
Al'batros odes'kyi							
Svatky village, Poltava rgn. (control)	0.08 ± 0.08	0.54 ± 0.20	0	0	0	0	1.00
Toxic waste ground of LLC "Oriana Halev"	1.18 ± 0.32*	0.99 ± 0.30	0	0.09 ± 0.09	0	0.09 ± 0.09	1.19*
Recultivated area of the toxic waste ground of LLC "Oriana Halev"	0.88 ± 0.28*	0.53 ± 0.21	0	0	0.26 ± 0.15	0.18 ± 0.12	1.05
Dombrovskyi potash ore mine	0.53 ± 0.21	0.62 ± 0.23	0	0	0.36 ± 0.18*	0	1.18*
Zymoiarka							
Svatky village, Poltava rgn. (control)	0.42 ± 0.18	0.33 ± 0.16	0	0	0	0	1.00
Toxic waste ground of LLC "Oriana Halev"	0.88 ± 0.23	1.07 ± 0.26*	0.12 ± 0.08	0	0.38 ± 0.15*	0.06 ± 0.06	1.45**
Recultivated area of the toxic waste ground of LLC "Oriana Halev"	0.90 ± 0.27	0.66 ± 0.23	0.08 ± 0.08	0	0.25 ± 0.14	0.08 ± 0.08	1.38**
Dombrovskyi potash ore mine	0.43 ± 0.19	0.69 ± 0.24	0	0.09 ± 0.09	0.09 ± 0.09	0.09 ± 0.09	1.19

Notes: *– difference as to the control is statistically reliable at $P < 0.05$, ** – at $P < 0.01$.

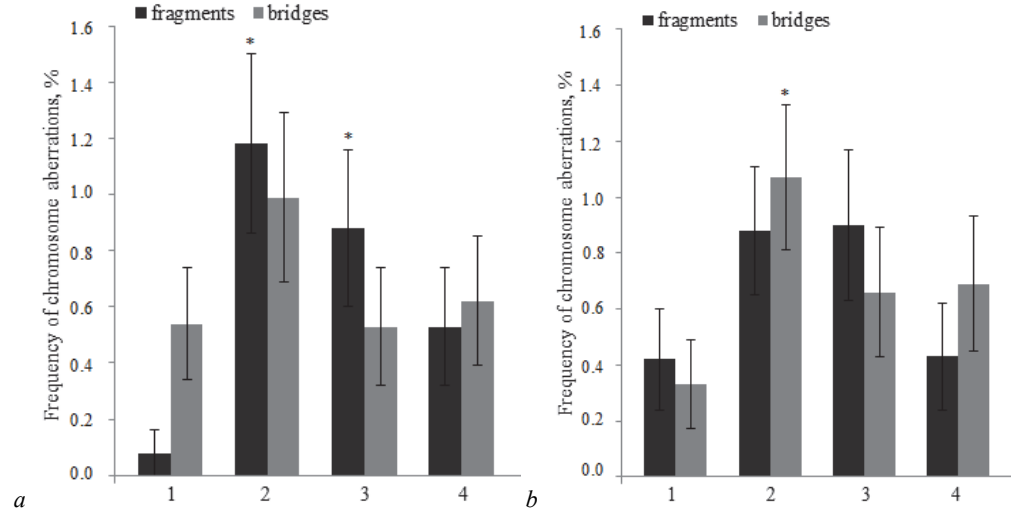

Fig. 3. Induction of acentric fragments and bridges by toxic waste contamination of soil in the cells of root meristem of winter wheat, cultivars Al'batros odes'kyi (*a*) and Zymoiarka (*b*): *1* – Svatky village, Poltava rgn. (control), *2* – toxic waste ground of LLC "Oriana Halev", *3* – recultivated area of the toxic waste ground of LLC "Oriana Halev", *4* – Dombrovskyi potash ore mine; * – $P < 0.05$ compared to the control; n = 1000, x ± SE

Chemical soil contaminants in the territory of the toxic waste ground and Dombrovskyi mine show the ability to cause aneuploid cells at frequency 0.09–0.38%. A statistically reliable increase of the level of lagging chromosomes caused by chemical contamination of the soil of the toxic waste ground and the dump of Dombrovskyi mine was 0.38% for cultivar Zymoiarka and 0.36% for cultivar Al'batros odes'kyi, respectively. Analysis of frequency of aneugenic effects under the impact of NMU in concentration 0.005% and 0.010% established that the level of the cells with lagging chromosomes is in direct correlation with the concentration of supermutagen. Frequency of the formation of the cells with lagging chromosomes in sprout root meristem of cultivars Al'batros odes'kyi and Zymoiarka was 0.65–1.33% and 1.70–2.12%, respecttively. A considerable increase in cytogenetic disorder frequency due to the induction of the cells with lagging chromosomes was observed at high concentration of chemical mutagen (0.025%), which was 8.34% for cultivar Al'batros odes'kyi and 11.47% for cultivar Zymoiarka.

Cells with more than two chromosome reconstructions were found among the aberrant cells, induced by soil contamination with chemical mutagens. The highest number of indicators of aberrations per aberrant cell, which were equal to the indicators, found at moderate and high concentrations of NMU, was characteristic of the cells of primary rootlet meristem of winter wheat sprouts of cultivar Zymoiarka, which were affected by contamination of the soil of the toxic waste ground (1.45) and its recultivated area (1.38) with hexachlorobenzene. Complex cytogenetic disorders in meristem cells of cultivar Al'batros odes'kyi were formed with lower frequency, however, under the effect of hexachlorobenzene in the highest and lowest concentrations, which is typical for soil contamination near the toxic waste ground and dumps of Dombrovskyi potash ore mine, the indicator of aberration number per aberrant cell reliably exceeded the control level. The majority of cytogenetic anomalies in the cells with multiple aberrations were presented with acentric fragments and lagging chromosomes. Also cells were found which included three acentric fragments at the same time, two lagging chromosomes, a single acentric fragment and a bridge, pair acentric fragments and a bridge, pair acentric fragments and a lagging chromosome (Fig. 2*c*, *d*). Heavy cytogenetic disorders, induced by low hexachlorobenzene concentrations in the soil, can be associated with a cumulative or synergetic effect of their combined impact with chemical factors of natural origin.

Discussion

Based on the results of numerous trials it has been established that chemical mutagens increase natural plant variability by tens of thousands times, cause a great variation of inherited changed forms. The advantage of chemical compounds in low and moderate concentrations, as compared with radiation, is high induction frequency of point mutations

and a low level of chromosome reconstructions (Venken & Bellen, 2014; Oladosu et al., 2016). But chemical mutagens in high concentrations produce an opposite effect, mostly inducing damage of the nuclear cell apparatus in the form of chromosome and aneuploid reconstructions, which corresponds to a severe effect of ionizing radiation. Although some believe that frequency of gene mutations increases along with the increase of the concentration of chemical mutagen factors, their identification in a phenotype is hindered by chromosome aberrations, mitosis anomalies, abiosis (Jejges, 2013). Taking into account the specificity of effect of mechanisms of chemical mutagens, connected with the correspondence of dipole moments of their molecules with dipole moments of certain molecular cell structures – preceding ones of DNA and protein synthesis, a predominant type of genetic material disorders is mutations of some chromosome loci (Bulathsinghala & Shaw, 2014).

Table 4

Spectrum of types of anatelophase chromosome aberrations in winter wheat, induced by NMU (x ± SE)

Mutagen concentration	Frequency of types of mitosis disorders and chromosome aberrations, %						Number of aberrations per aberrant cell
	fragments	bridges	fragments and bridges	micronuclei	lagging chromosomes	chromosome rings	
Al'batros odes'kyi							
Water (control)	0.43 ± 0.17	0.57 ± 0.20	0	0	0.07 ± 0.07	0	1.09
NMU, 0.005%	1.69 ± 0.36**	0.40 ± 0.18	0	0	0.65 ± 0.23*	0	1.21
NMU, 0.010%	0.89 ± 0.28	1.25 ± 0.33	0.18 ± 0.12	0.09 ± 0.09	1.33 ± 0.34**	0.18 ± 0.12	1.14
NMU, 0.025%	8.34 ± 0.84**	1.31 ± 0.35	0.66 ± 0.25*	0.19 ± 0.13	8.34 ± 0.84**	0.19 ± 0.13	1.52**
Zymoiarka							
Water (control)	0.33 ± 0.16	0.25 ± 0.14	0	0	0	0	1.14
NMU, 0.005%	2.78 ± 0.49**	0.89 ± 0.28*	0.09 ± 0.09	0.36 ± 0.18	1.70 ± 0.39**	0	1.47
NMU, 0.010%	3.18 ± 0.48**	1.37 ± 0.32**	0.15 ± 0.11	0.23 ± 0.13	2.12 ± 0.40**	0.08 ± 0.08	1.40
NMU, 0.025%	9.02 ± 0.92**	1.33 ± 0.36**	0	0.72 ± 0.27**	11.47 ± 1.02**	0.51 ± 0.23*	1.48*

Notes: * – difference as to the control is statistically reliable at P < 0.05, ** – at P < 0.01.

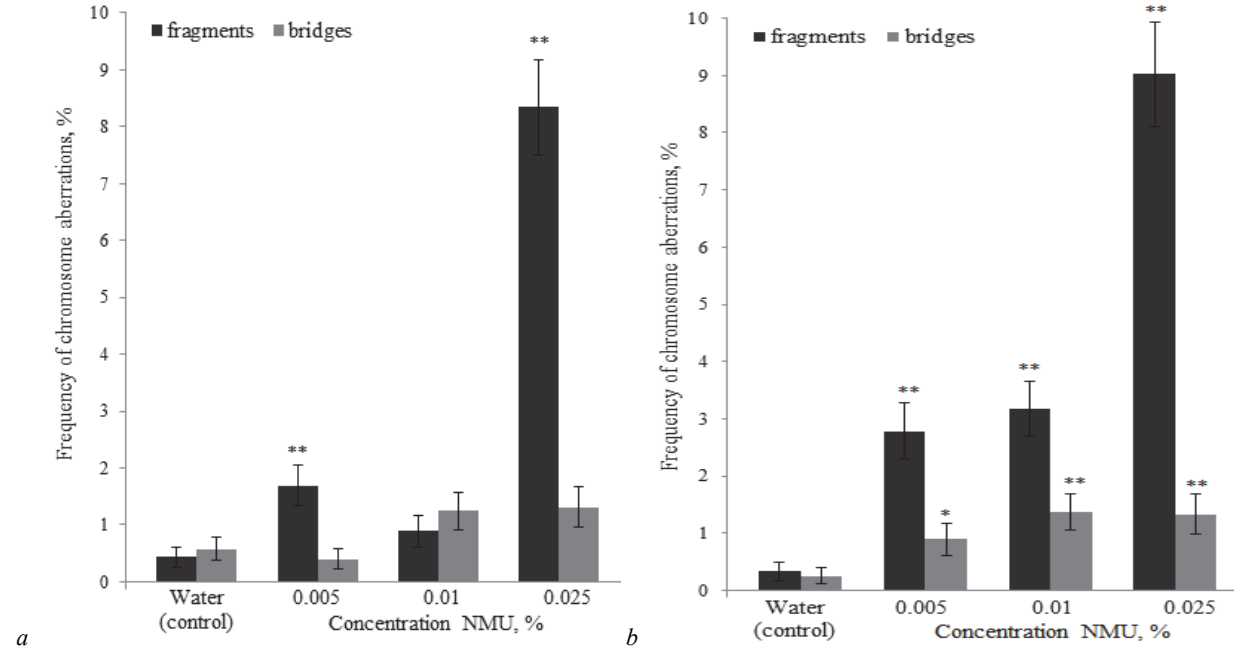

Fig. 4. Induction of acentric fragments and bridges under the effect of N-nitrozo-N-methylurea in the cells of root meristem of winter wheat, cultivars Al'batros odes'kyi (*a*) and Zymoiarka (*b*): * – P < 0.05 compared to the control, ** – P < 0.01; n = 1000, x ± SE

This point of view was grounded on the results of study of mutagenic activity of alkylating compounds in low and moderate concentrations. It is under these conditions that one can expect the induction of high frequency of point mutations and a low level of chromosome aberrations, which gives preferences to extended and efficient usage of chemical mutagens in breeding practice. Chemical mutagens in high concentrations produce a more occasional effect; they induce serious damage to genetic cell apparatus and the appearance of numerous cytogenetic disorders. Which is why one can assume that the lack of a serious difference between frequency of cells with chromosome aberrations under the effect of NMU in concentrations 0.005% and 0.010% and the effect of hexachlorobenzene contamination of soil near the toxic waste ground and its recultivated area is connected with the increase of specific genetic disorders at higher mutagen concentrations of point mutations, which are not identified with help of cytogenetic analysis and require research on mutative plant variability at the level of phenotype and molecular-genetic inherited changes. A non-linear dependence of genetic disorders on the concentration of chemical mutagens is also associated with the varied efficiency of reparation processes and different ways of their biotransformation (Budinsky et al., 2013). NMU is considered to make its main contribution to mutagenic effect as a result of the response of the interaction of decay products with biopolymers and, as one of the consequences, blocking the threads of spindle separation rather than through a direct mutagen attack of DNA molecules (Usatov et al., 2005). Chemical mutagen in high concentrations directly affects chromosome heterochromatin in the area of the centromere which causes chromosome lagging in a mitosis anatelophase (Jejges, 2013). Considering the insufficient study of the mechanisms of chemical interaction of hexachlorobenzene with inherited cell structures, one can assume that its high mutagenic activity is explained by the formation of a set of highly toxic compounds resulting from mutagen metabolism in a plant cell.

The high frequency of cytogenetic anomalies which was recorded when wheat seeds were sprouted in the dump soil of Dombrovskyi potash ore mine can be explained by the effect of synergetic interaction between low concentrations of hexachlorobenzene residues and a complex of heavy metals and natural mineral compounds of mining-chemical

raw materials. Synergetic responses of biological systems are observed when factors different in their nature act together: gamma-rays and chemical mutagens, heavy metals and radio nuclides, heavy metals and hypothermia, chemical mutagens and ultra-violet rays, laser radiation and magnetic field, etc. (Ang et al., 2016; Song et al., 2016; Kayalvizhi et al., 2017). The existence of a synergetic effect, under the impact of chemical environmental factors, which are particularly seen in small concentrations, was proved on lentils (*Lens culinaris* Medik.) (Laskar & Khan, 2017), winter cherry (*Physalis peruviana* L.) (Gupta et al., 2018), nematodes (*Caenorhabditis elegans*) (Guo et al., 2014), human cells (Devid et al., 2016). It has been established that synergetic effects are seen more often in a range of low dose loads than in the case of strong impacts. The processes of a direct mutagenic effect become of great importance when concentrations are high.

As a rule, the induction with high frequency of bridges, in particular chromosome ones, is a typical cytogenetic consequence of the effect of ionizing radiations (M'kacher et al., 2015; Syaifudin et al., 2017). The formation of a great number of cells with dicentrics in wheat root meristem, induced by the effect of hexachlorobenzene contamination of soil in the area of the toxic waste ground near Kalush city, confirms the radiomimetic properties of the chemical compound, which, based on the results of the research aimed at studying mutagenic NMU activity, can be seen under the impact of high mutagen concentrations. When seeds were sprouted in the samples of the studied soil objects, contaminated with chemical factors, single cases of ring chromosomes were observed – indicators of radiation impact, which prove the lack of the relationship of chemical mutagens with genetic cell structures and the mechanism of their effect by a principle of a target – accidentally (Oladosua et al., 2016). Their formation can be explained by the loss of telomere fragments, which leads to the loss of the connection of chromosomes with the nucleus wall and destruction of the architectonics of the nucleus (Zuccarello et al., 2010; Guilherme et al., 2011).

The effect of chemical mutagens is considered to lead to gene mutations or damages of mitotic spindle (Mohapatra et al., 2014). A serious increase in frequency of chromosome segregation disorders, which is found under the effect of hexachlorobenzene contamination of the soil of the toxic waste ground and Dombrovskyi mine, can be a consequence of the interaction of mutagen not only with microtube protein of spindle separation, but also with heterochromatin of nearby-centromere areas of chromosomes. A chemical mutagen in high concentrations directly affects chromosome heterochromatin in the area of the centromere which causes chromosome lagging into a mitosis or meiosis anatelophase (Jejges, 2013). It is with this mechanism of the appearance of cytogenetic disorders that a considerable increase in the number of aneuploid cells, under the effect of NMU in a high concentration, is connected.

Some authors connect the induction of multiple aberrations in the cells of wheat root meristem with chemical factors, which include a complex of chromosome reconstructions or chromosome reconstructions and mitosis anomaly, with many-sided chemical interaction of mutagens and biopolymeric nucleus structures. In particular, it has been shown for plant objects that the wide spectrum of NMU effect is caused not only by alkylating, but also by nitrating and carbonating, i.e., the compound has a complex impact on macromolecules (Usatov et al., 2005). Thus, further research aimed at studying mechanisms of the chemical effect of hexachlorobenzene on DNA molecule and enzymes of the repair system will help identify the potential level of xenobiotic mutagenic activity on the level of point mutations and predict distant genetic consequences of its impact in the series of organisms of the generations-to-come.

Conclusions

Chemical soil contamination of the toxic waste ground and dumps of Dombrovskyi potash ore mine near Kalush city leads to high mutagenic activity, which, by the induction level of cytogenetic anomalies in winter wheat root meristem, exceeds the control indicators by 1.8–3.8 times and is equal to mutagenic activity of N-nitrozo-N-methylurea in moderate concentrations. Hexachlorobenzene contamination of the soil of a recultivated area of the toxic waste ground results in the increase of aberrant cell frequency by 2.6–3 times, and it continues to be a threat to the genome of living organisms. Hexachlorobenzene contamination of the soil together with natural mineral compounds of mining-chemical raw materials, even in low concentrations, ensures high mutagenic activity. The spectrum of chromosome aberrations which contained acentric fragments that are typical for chemical mutagenesis expanded in the form of bridge induction, ring chromosomes and micronuclei. A considerable increase of the share of the cells with dicentric chromosomes in the spectrum of the types of chromosome disorders caused by the effect of hexachlorobenzene contamination of the soil of the toxic waste ground can confirm the radiomimetic properties of the chemical genotoxicant. The increase in the number of cells with multiple aberrations, induced by the effect of hexachlorobenzene contamination of the soil within the area of the studied objects, points to the high genotoxicity of the chemical compound and the threat it poses of serious genetic consequences if it penetrates into the environment.

References

Al-Naber, H. M. F., Slenzak, A., Stranadko, N., Tykhyy, V., Sulukhia, T., Lvovsky, K., Fan, Q., & Ahmed, K. (2016). Ukraine country environmental analysis. The World Bank, Washington.

Altwaty, N. H., El-Sayed, O. E., Aly, N. A. H., Baeshen, M. N., & Baeshen, N. A. (2016). Molecular and cytogenetic assessment of *Dipterygium glaucum* genotoxicity. Anais da Academia Brasileira de Ciências, 88(1), 623–634.

Ang, J., Song, L. Yu., D'Souza, S., Hong, I. L., Luhar, R., Yung, M., & Miller, J. H. (2016). Mutagen synergy: Hypermutability generated by specific pairs of base analogs. Journal of Bacteriology, 198(20), 2776–2783.

Aoki, Y. (2017). Evaluation of *in vivo* mutagenesis for assessing the health risk of air pollutants. Genes and Environment, 39, 1–12.

Babatunde, B., & Anabuike, F. (2015). *In vivo* cytogenotoxicity of electronic waste leachate from Iloabuchi electronic market, Diobu, Rivers state, Nigeria on *Allium cepa*. Challenges, 6, 173–187.

Bekker, A. A., & Agaev, T. B. (1989). Ohrana i control' zagrjaznenija prirodnoj sredy [Protection and control of environmental pollution]. Gidrometeoizdat, Leningrad (in Russian).

Budinsky, R., Gollapudi, B., Albertini, R. J., Valentine, R., Stavanja, M., Teeguarden, J., Fensterheim, R., Rick, D., Lardie, T., McFadden, L., Green, A., & Recio, L. (2013). Nonlinear responses for chromosome and gene level effects induced by vinyl acetate monomer and its metabolite, acetaldehyde in TK6 cells. Environmental and Molecular Mutagenesis, 54(9), 691–768.

Bulathsinghala, A. T., & Shaw, I. C. (2013). The toxic chemistry of methyl bromide. Human and Experimental Toxicology, 33(1), 81–91.

Chan, Y. A., Hieter, P., & Stirling, P. C. (2014). Mechanisms of genome instability induced by RNA-processing defects. Trends in Genetics, 30(6), 245–253.

Chen, Y., Ebenstein, A., Greenstone, M., & Li, H. (2013). Evidence on the impact of sustained exposure to air pollution on life expectancy from China's Huai River policy. Proceedings of the National Academy of Sciences of the United States of America, 110(32), 12936–12941.

Correia, A. W., Pope, C. A., Dockery, D. W., Wang, Y., Ezzati, M., & Dominici, F. (2013). The effect of air pollution control on life expectancy in the United States: An analysis of 545 US counties for the period 2000 to 2007. Epidemiology, 24(1), 23–31.

David, R., Ebbels, T., & Gooderham, N. (2016). Synergistic and antagonistic mutation responses of human MCL-5 cells to mixtures of benzo[a]pyrene and 2-amino-1-methyl-6-phenylimidazo[4,5-b]pyridine: Dose-related variation in the joint effects of common dietary carcinogens. Environmental Health Perspectives, 124(1), 88–96.

Dent, D., & Dmytruk, Y. (Eds.). (2017). Soil science working for a living. Springer Nature.

Doorn, G. S. (2014). Patterns and mechanisms of evolutionary transitions between genetic sex-determining systems. Cold Spring Harbor Perspectives in Biology, 6(8), 1–17.

Febbraio, F. (2017). Biochemical strategies for the detection and detoxification of toxic chemicals in the environment. World Journal of Biolgical Chemistry, 8(1), 13–20.

Firbas, P., & Amon, T. (2014). Chromosome damage studies in the onion plant *Allium cepa* L. Caryologia, 67(1), 25–35.

Gervais, C., & Roze, D. (2017). Mutation rate evolution in partially selfing and partially asexual organisms. Genetics, 207(4), 1561–1575.

Guilherme, R. S., Meloni, V. F. A., Kim, C. A., Pellegrino, R., Takeno, S. S., Spinner, N. B., Conlin, L. K., Christofolini, D. M., Kulikowski, L. D., & Melaragno, M. I. (2011). Mechanisms of ring chromosome formation, ring instability and clinical consequences. BMC Medical Genetics, 12(1), 1–7.

Guo, X., Bian, P., Liang, J., Wang, Y., Li, L., Wang, J., Yuan, H., Chen, S., Xu, A., & Wu, L. (2014). Synergistic effects induced by a low dose of diesel particulate

extract and ultraviolet-A in *Caenorhabditis elegans*: DNA damage-triggered germ cell apoptosis. Chemical Research in Toxicology, 27(6), 990–1001.

Gupta, A. K., Singh, S. P., Singh, M., & Marboh, E. S. (2018). Mutagenic effectiveness and efficiency of gamma rays and EMS on cape gooseberry (*Physalis peruviana* L.). International Journal of Current Microbiology and Applied Sciences, 7(2), 3254–3260.

Haidin, A. M., Diakiv, V. O., & Chikova, I. V. (2014). Kalush – programa revitalizacii' [Kalush – revitalization program]. Technogenic and Ecological Safety, 10(2), 102–107 (in Ukrainian).

Henn, B. M., Botigue, L. R., Bustamante, C. D., Clark, A. G., & Gravel, S. (2015). Estimating the mutation load in human genomes. Nature Reviews Genetics, 16, 333–343.

Jejges, N. S. (2013). Istoricheskaja rol' Iosifa Abramovicha Rapoporta v genetike. Prodolzhenie issledovanij s ispol'zovaniem metoda himicheskogo mutageneza [The historical role of Joseph Abramovich Rapoport in genetics. Continuation of studies using the method of chemical mutagenesis]. Vavilov Journal of Genetics and Selection, 17(1), 162–172 (in Russian).

Kayalvizhi, K., Kannan, M., & Ganga, M. (2017). Effect of physical and chemical mutagens on morphological characters in M1V2 generation of tuberose (*Polianthes tuberosa* L.). International Journal of Current Microbiology and Applied Sciences, 6(4), 2492–2499.

Kumar, G., & Pandey, A. (2015). Heavy metal induced genomic distortion in root meristems of coriander (*Coriandrum sativum* L.). International Journal of Research Plant Sciences, 4(5), 47–53.

Kumar, G., & Srivastava, A. (2015). Clastogenic and mito-inhibitory effect of heavy metals in root meristems of *Vicia faba*. Chromosome Botany, 10(1), 23–29.

La Croix, R. A., Palsson, B. O., & Feist, A. M. (2017). A model for designing adaptive laboratory evolution experiments. Applied and Environmental Microbiology, 83(8), 1–14.

Laskar, R. A., & Khan, S. (2017). Mutagenic effectiveness and efficiency of gamma rays and HZ with phenotyping of induced mutations in lentil cultivars. International Letters of Natural Sciences, 64, 17–31.

Lysychenko, G., Weber, R., Kovach, V., Gertsiuk, M., Watson, A., & Krasnova, I. (2015). Threats to water resources from hexachlorobenzene waste at Kalush City (Ukraine) – a review of the risks and the remediation options. Environmental Science and Pollution Research, 22(19), 14391–14404.

M'kacher, R., Maalouf, E. E., Terzoudi, G., Ricoul, M., Heidingsfelder, L., Karachristou, I., Laplagne, E., Hempel, W. M., Colicchio, B., Dieterlen, A., Pantelias, G., & Sabatier, L. (2015). Detection and automated scoring of dicentric chromosomes in nonstimulated lymphocyte prematurely condensed chromosomes after telomere and centromere staining. International Journal of Radiation Oncology, Biology, Physics, 91(3), 640–649.

Marković, S. Z., Nikolić, L. I., Hamidović, J. L., Grubor, M. G., Grubor, M. M., & Kastratović, D. A. (2017). Chromosomes aberations and enviromental factors. Hospital Pharmacology, 4(1), 486–490.

Mohapatra, T., Robin, S., Sarla, N., Sheshashayee, M., Singh, A. K., Singh, K., Singh, N. K., Mithra, S. V. A., & Sharma, R. P. (2014). EMS induced mutants of upland rice variety Nagina22: Generation and characterization. Proceedings of the Indian National Science Academy, 80(1), 163–172.

Oladosua, Y., Rafii, M. Y., Abdullaha, N., Hussind, G., Ramlie, A., Rahimf, H. A., Miaha, G., & Usmana, M. (2016). Principle and application of plant mutagenesis in crop improvement: A review. Biotechnology and Biotechnological Equipment, 30(1), 1–16.

Parpan, V. I., Shumska, N. V., Rudeichuk-Kobzeva, M. J., & Mylenka, M. M. (2016). Syntaxonomy of vegetation of Kalush hexachlorobenzene toxic waste landfill (Ivano-Frankivsk region). Biosystems Diversity, 24(2), 364–370.

Pausheva, Z. P. (1988). Praktikum po citologii rastenij [Workshop on plant cytology]. Agropromizdat, Moscow (in Russian).

Rozhko, M. M., Bilec'ka, E. M., Shmatkov, G. G., Erstenjuk, G. M., Kryzhanivs'ka, A. I., Onyshchenko, S. V., Rud'ko, G. I., Samojlik, M. S., Semchuk, J. M., & Solovjov, V. V. (2014). Rozrobka ta vprovadzhennja systemy zmenshennja tehnogennogo navantazhennja na terytorii' i naselennja ekologichno kryzovyh terytorij [Development and implementation of a system for reducing the man-caused load on the territory and population of ecologically crisis areas]. Ecology and Nature Management, 18, 97–110 (in Ukrainian).

Ryu, T. H., Kim, J.-H., & Kim, J. K. (2016). Chromosomal aberrations in human peripheral blood lymphocytes after exposure to ionizing radiation. Genome Integrity, 7(1), 1–5.

Sirohi, S., Mago, P., Gunwal, I., & Singh, L. (2014). Genetic pollution and biodiversity. International Journal of Recent Scientific Research, 5(6), 1152–1155.

Song, L. Y., D'Souza, S., Lam, K., Kang, T. M., Yeh, P., & Miller, J. H. (2016). Exploring synergy between classic mutagens and antibiotics to examine mechanisms of synergy and antibiotic action. Antimicrobial Agents and Chemotherapy, 60(3), 1515–1520.

Syaifudin, M., Lusiyanti, Y., Purnami, S., Lee, Y. S., & Kang, C. M. (2017). Assessment of ionizing radiation induced dicentric chromosome and micronuclei in human peripheral blood lymphocytes for preliminary reconstruction of cytogenetic biodosimetry. Atom Indonesia, 43(1), 47–54.

Usatov, A. V., Mashkina, E. V., & Gus'kov, E. P. (2005). Vlijanie okislitel'nogo stressa na mutagenez u podsolnechnika *Helianthus annuus* L., inducirovannyj nitrozometilmochevinoj [Influence of oxidative stress on sunflower *Helianthus annuus* L. mutagenesis induced by nitrosomethylurea]. Genetics, 42(1), 63–70 (in Russian).

Venken, K. J. T., & Bellen, H. J. (2014). Chemical mutagens, transposons, and transgenes to interrogate gene function in *Drosophila melanogaster*. Methods, 68(1), 15–28.

Yahaya, T., Obaroh, I., & Oladele, E. O. (2017). The roles of environmental pollutants in the pathogenesis and prevalence of diabetes: A review. Journal of Applied Science and Environmental Management, 21(1), 5–8.

Yakymchuk, R. A., & Valyuk, V. F. (2018). Soil mutagenic activity in hazardous waste site of Kalush City (Western Ukraine). Ukrainian Journal of Ecology, 8(1), 880–886.

Zuccarello, D., Dallapiccola, B., Novelli, A., & Foresta, C. (2010). Azoospermia in a man with a constitutional ring 22 chromosome. European Journal of Medical Genetics, 53(6), 389–391.

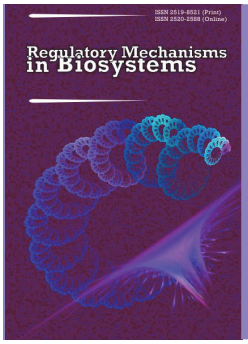

Regulatory Mechanisms in Biosystems

ISSN 2519-8521 (Print)
ISSN 2520-2588 (Online)
Regul. Mech. Biosyst., 9(3), 453–459
doi: 10.15421/021868

Influence of the type of autonomic tone on the volume of the mucous membrane of the small intestine of laying hens

A. Tybinka, H. Blishch, O. Shchebentovska

Stepan Gzhytskyi National University of Veterinary Medicine and Biotechnologies, Lviv, Ukraine

Article info

Received 03.06.2018
Received in revised form 14.07.2018
Accepted 19.07.2018

Stepan Gzhytskyi National University of Veterinary Medicine and Biotechnologies, Pekarska st., 50, Lviv, 79010, Ukraine.
Tel.: +38-067-353-03-20.
E-mail: a.m.tybinka@gmail.com

Tybinka, A., Blishch, H., & Shchebentovska, O. (2018). Influence of the type of autonomic tone on the volume of the mucous membrane of the small intestine of laying hens. Regulatory Mechanisms in Biosystems, 9(3), 453–459. doi:10.15421/021868

The connection between the separate structural parts of the mucous membrane of the small intestine of laying hens and the typological features of the autonomic tone were investigated. The studies were conducted on adult chickens of the cross-breed "Isa-Brown", which were divided into two groups: sympathicotonic chickens and sympathico-normotonic chickens, by the methods of electrocardiography and variation-pulsometry research. In the small intestine of the poultry of each group, the linear dimensions were determined first, and then the volume of the entire mucous membrane and its separate parts (villi, crypt, muscular plate), as well as the volume of connective tissue fibers in the crypt region. Research has shown that the villi account for ¾ of the volume of the entire mucous membrane. The volume of villi in the entire small intestine is more important in sympathico-normotonic chickens. This same poultry group has an advantage in the indicators of the volume of the muscular plate, but only in the duodenum and jejunum. In indicators of crypt volume, it turned out to be quite the opposite of the relationship with the typology of autonomous influences. In all studied intestines, the higher values of this indicator belong to the sympathotonic chickens. However, in terms of the volume of the entire mucous membrane, larger values still correspond to sympathico-normotonic chickens. Sympathicotonic chickens are inferior to them in the duodenum – at 1,005 mm^3, in the jejunum – at 2,699 mm^3 and in the ileum – only 78 mm^3. Investigating the structure of the villi, we established that the volume of their epithelium in all three sections of the small intestine has higher values in the sympathico-normotonic chickens, and the larger volume of the lamina propria of the villi in the sympathicotonic chickens. At the same time, the connection with the type of autonomic tone is reflected in the ratio between the two layers of villi. In all three sections of the small intestine of sympathicotonic chickens, the ratio between the epithelium and the lamina propria was, on average, 65%/35%, or 2/1. In sympathico-normotonic chickens, this ratio varied and, on average, equalled 75%/25%, or 3/1. The increase in the tone of sympathetic centers contributes to the growth of volume both as the total amount of fibers of connective tissue, and also as separate elastic fibers in the area of crypt. According to the data,indicators of the sympathico-normotonic chickens are inferior to those of sympathicotonic chickens in all of the small intestine. It was also found that in both groups of poultry the volume of elastic fibers was approximately half the volume of all fibers of the connective tissue of the duodenum. In other sections of the small intestine, this figure was reduced to about ⅓. Consequently, the typological features of the autonomic tone, providing various trophic-regulatory effects on the mucous membrane of the small intestine, cause the formation of differences in its volume.

Keywords: small intestine of chickens; sympathicotonic chickens; sympathico-normotonic chickens; volume of villi; volume of connective tissue fibers.

Introduction

The mucous membrane of the intestine of birds, similarly to other types of animals, is an active structure which is closely connected to other membranes and in the condition of dynamic balance. It constantly adapts to variable conditions of internal and especially external media. The most intensive changes in the structure of the intestine certainly take place during the embryonic period, when at the beginning, cellular-tissue components form, which unite into a morphological-functional composition (Shyer et al., 2013; Wali & Kadhim, 2014; Lilburn & Loeffler, 2015). Therefore, by the time a bird hatches, the intestine as well as most of the digestive organs is sufficiently formed according to the main indicators of structure and chemical composition, so chickens can consume food on their own (Sklan, 2001; Uni et al., 2003; China et al., 2017). Morphological changes in the structure of the mucous membrane in the postnatal period of ontogenesis are significantly related to genetic factors (Forder et al., 2012; Khalid et al., 2014; Mabelebele et al., 2014; Okpe et al., 2016), and characteristics of diet consumed by poultry in different periods of their life. This especially manifests in commercial poultry whose diet as they grow to a certain age is changed in accordance with technology of their rearing (Laudadio et al., 2012; Nasrin et al., 2012; Sittiya & Yamauchi, 2014). Changes in the structure of the mucous membrane also take place when birds feed during intensely or experience hunger (Incharoen et al., 2010), are subject to manipulations (Yamauchi et al., 2010) involving addition of medical preparations of feed additives to their diet (Wijtten et al., 2012; Tsirtsikos et al., 2012; Incharoen, 2013; Cheled-Shoval et al., 2014) and stress situations (Varasteh et al., 2015; Marchini et al., 2016). At the same time, excessive impacts on the intestinal wall can cause pathological processes instead of adaptive reactions (Heak et al., 2017; Wang et al., 2018). A significant parameter for determining the efficiency of the digestive organs is the age formation of the nervous system (Goldstein & Nagy, 2008; Heanue et al., 2016; Chevalier et al., 2017). Without the regulatory action of the autonomic nervous system, the activity of the intestinal wall is observed to have a certain chaotic character. Therefore, the functioning of the intestinal epithelium of chickens before the formation of submucous plexus is characterized by an undetermined polyphase pattern. After the plexus is activated, the

functioning of the epithelium of 17–18 day old fetuses obtains rhythmicity in the form of two-phase daily rhythms (maximum – night, minimum – day) (Sokolov & Chukalovskaja, 1980; Aubert et al., 2004). The submucous plexus of the intestine is structurally and functionally related to other plexuses of the intestinal wall (intramuscular, mucous and subserous) and all of them together form the complex nervous system of the intestine (Hao et al., 2016; Uesaka et al., 2016). The basis of the submucous plexus is composed mostly of bunches of unmyelinated nerve fibers which form large loops and contain small clusters with a small amount of nerve cells (up to ten neurons). Also, one can find average-sized single clusters of nerve fibers with a few dozen cells. Also, the mucous plexus contains thinner bunches of nerve fibers, which form smaller loops. In general, the mucous plexus can be conditionally divided into two parts: nervous plexus of villi and nervous plexus of crypts (Ali & McLelland, 1978; Fekete & Csoknya, 1987; Doyle et al., 2004). However, in general, all neurons of the intestine can be united into two groups: mobile and sensitive, though according to ultrastructural, hystochemical, biochemical and pharmaceutical properties of these neurons, ten or even more different types are distinguished (Furness & Costa, 1980; Furness, 2000; Yang et al., 2013). During ontogenesis, all nerve cells of the intestinal wall derive from the cells of neural crests (Sasselli et al., 2012). Therefore, in the process of age formation of the autonomic nervous system and establishment of its functional properties, the regulatory impacts on all organs modify, leading to their structural adaptation. Total tone of sympathetic and parasympathetic centers has an important role in this process. We have found very few studies in the scientific literature which examine the influence of this tone on the morphology of particular organs of animals (Kononenko & Zaitsev, 2009), including the intestine of chickens (Tybinka et al., 2016). At the same time, we found no literature data on the relationship between the typological peculiarities of the tone of autonomic nervous system and the parameters of volume of separate layers and the entire mucous membrane of chickens. Thus, we focused our study on these parameters.

Materials and methods

For the study, we selected a group of clinically healthy 1 year old ISA Brown cross chickens, which were reared in a poultry farm. Using electrocardiographic and variation-pulsometric examination (Baevskij et al., 1984), we determined the peculiarities of the muscular tone of the autonomic nervous system for each of the birds. Using the results of this examination, the poultry were divided into two groups. The first group consisted of 16 chickens with high clearly manifested sympathetic tone – sympathicotonic chickens (ST). The second group was formed of 17 chickens, the autonomous tone of which was characterized by deviation from the manifested sympathicotonia towards normotonia – sympathico-normotonic chickens (ST-NT). After euthanasing the birds, the small intestine was extracted and divided into its separate sections (duodenum, jejunum and ileum). For each of them, we determined length and perimeter (circular length), and also selected samples of the intestinal wall, which were fixated in Bouin's solution and then processed into paraffinised sections. For total detection of connective tissue fibers, histosections were stained using the methods of Van Gieson and Pacini (Mulisch & Welsch, 2010), and also for separate detection of elastic fibers only, we performed staining according to Weigert (Mulisch & Welsch, 2010). Using the prepared histopreparations and the method of computer morphometry, we analyzed the thickness of both the entire mucous membrane and its separate layers (muscular panel, crypt and villi). Taking into account the obtained parameters, we calculated the volume of the entire mucous membrane and its particular layers. In the villi, using the ratio of epithelium and lamina propria, we determined the volumes of these structures. Also, in the area of crypts, first we determined the percentage content, and then, on its basis, we calculated the volume of the fibers of the connective tissue. For statistical analysis of the study results, we used StatPlus 2008 program. Comparison of mean values of these groups was made on the basis of Student's t-criterion. Digital material in the tables and text is presented in the following form: $x \pm SE$, where x – sample mean, SE – standard error of average value.

Results

Having conducted a complex of planned morphometric research, we found that the results are characterized by a certain dependence on the type of the total tone of the autonomous centers. High sympathetic tone of ST-chickens caused higher values of the perimeter of the jejunum and ileum and the length of duodenum. Increase in parasympathetic tone of ST-NT chickens led to formation of higher parameters of perimeter of the duodenum and length of the jejunum and ileum. The presented patterns indicate compensatory relationships between these two parameters, when greater length of intestine corresponds to its lower perimeter. This indicates the peculiarities of formations of sizes of the intestine in relation to tone-trophic influence caused by the autonomic nervous system. Similar patterns are also typical for separate membranes of the intestinal wall (mucous and muscular), and also other particular layers of these membranes. At the same time, in all studied intestinal sections, the height of the villi and thickness of the lamina propriae were higher among the sympathico-normotonic chickens. At the same time, sympathicotonic chickens showed higher parameters of crypt depth and thickness of the epithelium of the villi. Chickens of this group were characterized by higher percentage content of the total number of connective tissue fibers, and also of elastic fibers separately. This again indicates formation of certain compensatory-adaptive relationships between certain parameters, but at the level of the mucous membrane. At the same time, all examined parameters, on the one hand, supplement one another and allow detailed analysis of particular aspects of the regulatory mechanisms of the autonomic nervous system. However, on the other hand, higher values of these parameters among different groups of chickens complicates the formation of the general characteristic of the impact of different tone of the autonomous centers on the intestinal wall on the whole and the mucous membrane in particular. Nevertheless, in general, all mentioned peculiarities are orientated towards provision of optimum parameters of digestion during corresponding type of the autonomic tone.

Therefore, we calculated more complex parameters based on the previous data and characterized the volume of the entire mucous membrane and its layers in particular sections and in the entire small intestine (Table 1). Along with the absolute volume of certain layers, which was expressed in mm^3, we also determined their percentage in the structure of mucous membrane, the volume of which was accepted as 100%. Certainly, the determining impact on the parameters of volume in different sections depends on the length of these sections. Therefore, the largest volumes of different layers of the mucous membrane were in the jejunum, these parameters were 3–4 times lower in the duodenum and 1.5–2.0 times lower in the ileum. However, thickness of these layers also makes adjustments to the parameters of volume.

The smallest part of mucous membrane is its lamina propriae. Along the small intestine, the dependence of its volume on the typology of autonomic tone is not of the same type. Over most of the area of the small intestine, the volume of the lamina propriae was higher among ST-NT chickens (Table 1). In the duodenum, their prevalence over the other poultry group was 10.1 mm^3, and 65.6 mm^3 in the jejunum. Only in the ileum were the parameters of both groups almost equalized and minimum domination (3.3 mm^3) of sympaticotonic chickens was observed. However, the mean parameter of the three sections was higher by 24.2 mm^3 among sympatico-normotonic chickens. A similar situation was also observed with total volume of lamina propriae of the entire small intestine. There, the prevalence of the second group of birds over the first one increased to 72.4 mm^3.

As for the percentage of the studied parameter within the entire mucous membrane, it was approximately the same in both groups of birds. However, in all sections of the small intestine, the ST-chickens had the minimum prevalence. This indicates higher dependence of the lamina propriae in the process of digestion during heightened tone of the sympathetic centers. Another interesting fact is the gradual two-fold increase in the share of lamina propriae in the volume of mucous membrane along the intestine. This process does not manifest a relationship with the typology of autonomous impacts and was observed in both groups.

Table 1
Absolute and relative parameters of volume of particular layers of mucous membrane of chickens' intestine (x ± SD)

Part of intestine	Type of ANS	Volume of lamina propriae in mm^3 (% of volume of entire mucous membrane)	Volume of crypts, mm^3 (% of volume of entire mucous membrane)	Volume of villi, mm^3 (% of volume of entire mucous membrane)
Duodenum	ST	246 ± 21 (2.8%)	1,919 ± 128 (21.9%)	6,598 ± 244 (75.3%)
	ST–NT	257 ± 28 (2.6%)	1,765 ± 115 (18.1%)	7,748 ± 269** (79.3%)
Jejunum	ST	1,066 ± 92 (4.2%)	5,428 ± 249 (21.4%)	18,923 ± 305 (74.4%)
	ST–NT	1,131 ± 116 (4.0%)	4,392 ± 221*** (15.6%)	22,593 ± 297***(80.4%)
Ileum	ST	218 ± 19 (5.7%)	914 ± 65 (23.9%)	2,688 ± 128 (70.4%)
	ST–NT	215 ± 19 (5.5%)	690 ± 55* (17.7%)	2,994 ± 149* (76.8%)
Mean parameter of three sections	ST	510 ± 42 (4.0%)	2,754 ± 128 (21.7%)	9,403 ± 294 (74.3%)
	ST–NT	534 ± 38 (3.8%)	2,282 ± 112** (16.4%)	11,112 ± 329* (79.8%)
Total parameter for small intestine	ST	1,530 ± 123 (4.0%)	8,262 ± 313 (21.7%)	28,208 ± 374 (74.3%)
	ST–NT	1,603 ± 115 (3.8%)	6,847 ± 276*** (16.4%)	33,335 ± 407* (79.8%)

Notes: * – P < 0.05, ** – P < 0.01, *** – P < 0.001.

A similar relationship with the type of autonomic muscular tone is also a characteristic of the volume of villi of the mucous membrane. However, unlike the volume of the lamina propriae, greater values of this parameter among sympatico-normotonics were found not only in the duodenum and jejunum, but over the entire small intestine. At the same time, their domination over sympathicotonic chickens was proportional to the length of the intestine, i.e. it was highest in the jejunum – 3,670 mm^3 (P < 0.001), intermediate in the duodenum (1,150 mm^3, P < 0.01) and the lowest in the ileum (306 mm^3, P < 0.05). The mean value of villi volume in these three small intestine sections of sympathicotonic chickens was lower compared to sympathico-normotonic chickens by 1,709 mm^3 (P < 0.05). Also, the total volume of villi of the mucous membrane of the entire small intestine of ST chickens and ST-NT chickens differed far more significantly and equaled 5,126 mm^3 (P < 0.05).

Characterising the percentage content of the villi in the volume of mucous membrane of the small intestine revealed that the villi account for ¾ of the total volume. The minimum share of villi was found in the ileum of ST chickens (70.4%), and the maximum in the jejunum of ST-NT chickens (80.4%). The dependence of this parameter on the type of autonomic tone is close to the absolute parameters expressed in mm^3. Therefore, along the entire intestine, its higher values corresponded to the sympathico-normotonic chickens.

Fig. 1. Fragment of mucous membrane of the jejunum of a ST-NT chicken: lamina propriae of mucous membrane (*1*), crypts of mucous membrane (*2*), villi of mucous membrane (*3*); Van Gieson staining

A totally contrasting dependence on the typological peculiarities of autonomic impacts was seen in the volume of the crypts. Higher values of this parameter in all studied sections of the small intestine were observed among sympathicotonic chickens, they prevailed over sympathico-normotonic chickens by 155 mm^3 – in the duodenum, and by 1,036 mm^3 (P < 0.001) – in the jejunum and by 224 mm^3 (P < 0.05) in the ileum. Therefore, the mean value of this parameter in the studied intestines of chickens of both groups differed by 472 mm^3 (P < 0.01). However, the clearest dominance of the chickens of the first group over the birds of the second group was manifested in total parameters of volume of the crypts of the entire small intestine. At the same time, the difference between the ST and ST-NT chickens equaled 1,416 mm^3 (P < 0.001).

The percentage of crypts in the structure of the mucous membrane had no clear pattern in the studied groups of birds. Therefore, the ST chickens had intermediate values of the share of crypts in the duodenum, minimum in the jejunum, and maximum in the ileum. Also, sympathico-normotonic chickens were characterized by the highest share of crypts in the duodenum, the lowest in the jejunum and intermediate in the ileum.

The previously described parameters of volumes of the lamina propriae, crypts and villi together form the volume of the entire mucous membrane. Therefore, on the basis of these parameters alone, even without a morphometric examination of the entire mucous membrane, we can see that in the entire small intestine, the highest parameters of its volume correspond to sympathico-normotonic chickens. Further study fully proved this presumption. In the duodenum and jejunum, the dominance of the second group of chickens (9,769 ± 313 and 28,116 ± 462 mm^3 respectively) over the first group (8,764 ± 292 and 25,417 ± 448 mm^3 respectively) was quite significant and equaled 1,006 (P < 0.05) and 2,699 mm^3 (P < 0.01) respectively. This was conditioned by the larger sizes of these sections (especially the jejunum) and also the fact that ST-NT chickens had higher values of both volume of villi and lamina propriae. Also, by contrast, in small ileums higher values of volumes of lamina propriae and crypts were observed among ST chickens. For this reason, by the volume of mucous membrane of this section, the domination of chickens of the second group (3,899 ± 158 mm^3) over the chickens of the first group (3,821 ± 197 mm^3) manifested insignificantly and equaled only 78.4 mm^3. However, by mean values of the volume of mucous membrane of the studied intestines, the domination of ST-NT chickens (13,928 ± 352 mm^3) over ST chickens (12,667 ± 316 mm^3), remained quite significant – 1,261 mm^3 (P < 0.05). Therefore, the largest difference between the groups of birds was observed in total values of the volume of the mucous membrane of the entire small intestine. By this parameter, ST chickens (38,001 ± 405 mm^3) were behind the ST-NT chickens (41,784 ± 437 mm^3) by 3,783 mm^3 (P < 0.001).

Because the dominant part of the mucous membrane of the intestine is the villi, along with determination of their total volume, we also analyzed the volumes of particular layers of these villi – epithelium cover and the lamina propria. Similarly to previous parameters, along with absolute sizes expressed in mm^3, we determined the percentage of each layer in the volume of villi (Table 2).

Morphometric examinations determined that in all three sections of the small intestine, the volume of epithelium of the villi had higher values among sympathico-normotonic chickens (Fig. 2). This group of birds dominated over the other group by 1,322 mm^3 (P < 0.01) in the duodenum, by 3,997 mm^3 (P < 0.05) in the jejunum and by 473 mm^3 (P < 0.05) in the ileum. At the same time, the mean parameter of differences between the groups of birds equaled 1,931 mm^3 (P < 0.05). And usually, the largest difference between the parameters of ST and ST-NT chickens is formed by the parameter of total volume of epithelium of the entire small intestine – 5,793 mm^3 (P < 0.01).

Unlike the previous parameter, higher values of the volume of the lamina propria of the villi, by contrast, correspond to sympathicotonic

chickens. In the duodenum, the parameter of sympathico-normotonic chickens was lower by 172 mm^3, by 327 mm^3 in the jejunum, and by 167 mm^3 in the ileum. Average volume of lamina propria of all three sections of the small intestine of chickens of the first and the second group differed by 222 mm^3. The total volume of lamina propria in the entire intestine of ST and ST-NT chickens differed by 666 mm^3.

The distinctive effect of typological peculiarities of the autonomic tone was observed in the percentage content of certain layers of villi. In all three small intestine sections of sympathicotonic chickens, the ratio of epithelium and lamina propria on average equaled 65% / 35%, or 2/1. In sympathico-normotonic chickens, this ratio on average equaled 75% / 25%, or 3/1. These proportions indicate the peculiarities of functional characteristics of villi of the small intestine in relation to the typology of effects of the autonomic nervous system. Also, the demonstrated results prove the higher activity of the epithelium layer compared to the lamina propria.

Table 2

Absolute and relative parameters of volume of structural parts of villi of mucous membrane of the intestine of chickens (x ± SE)

Part of intestine	Type of ANS	Volume of epithelium of villi, mm^3 (% of the total volume of villi)	Volume of lamina propria of villi, mm^3 (% of the total volume of villi)
Duodenum	ST	4,341 ± 122 (65.8%)	2,256 ± 71 (34.2%)
	ST–NT	5,663 ± 165** (73.1%)	2,084 ± 66 (26.9%)
Jejunum	ST	13,037 ± 409 (68.9%)	5,884 ± 198 (31.1%)
	ST–NT	17,035 ± 395* (75.4%)	5,558 ± 155 (24.6%)
Ileum	ST	1,763 ± 95 (65.6%)	924 ± 57 (34.4%)
	ST–NT	2,236 ± 119* (74.7%)	757 ± 44 (25.3%)
Mean values for three sections	ST	6,381 ± 227 (66.8%)	3,022 ± 187 (33.2%)
	ST–NT	8,312 ± 301* (74.4%)	2,799 ± 152 (25.6%)
Total value for small intestine	ST	19,142 ± 309 (67.9%)	9,065 ± 339 (32.1%)
	ST–NT	24,935 ± 347** (74.8%)	8,399 ± 295 (25.2%)

Notes: * – P < 0.05, ** – P < 0.01, *** – P < 0.001.

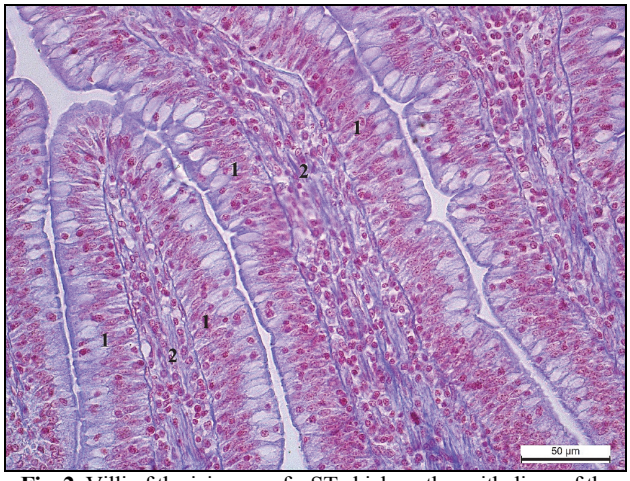

Fig. 2. Villi of the jejunum of a ST chicken: the epithelium of the villi (*1*), lamina propria of mucous membrane (*2*); Pacini staining

An important and integral part of the mucous membrane is its fiber connective tissue component. The examinations conducted prove that these fibers most densely localize in the area of crypts and their number is reliably affected by the type of autonomous tone (Table 3).

Analysis of the volume of total number of connective tissue fibers reveals that in all studied sections of the small intestine, sympathicotonic chickens showed higher values of this parameter (Fig. 3). In the duodenum, they prevailed over sympathico-normotonic chickens by 13 mm^3, by 238 mm^3 (P < 0.01) in the jejunum and by 42 mm^3 (P < 0.001) in the ileum. It should be mentioned that in the latter section, the difference between the groups was the clearest in the percentage expression and equaled 39%. The mean value of the three sections in ST and ST-NT chickens differed by 98 mm^3 (P < 0.01), and the total volume of connective tissue fibers in the entire small intestine of chickens of the second group was 293 mm^3 (P < 0.01) lower than in the first group. Along with the volume of the total number of connective tissue fibers in the crypt area, we performed a separate study of the volume of elastic fibers (Fig. 4). The data in Table 3 demonstrates that in both groups of birds, the volume of elastic fibers equals approximately half of the volume of all fibers of the duodenum connective tissue. In other sections, this parameter decreases approximately to ⅓.

Table 3

Volume of connective tissue fibers in the area of crypts of mucous membrane of the intestine of chickens (x ± SE)

Section of intestine	Type of ANS	Volume of all connective tissue fibers, mm^3	Volume of elastic fibers, mm^3
Duodenum	ST	111.3 ± 8.3	56.6 ± 3.4
	ST–NT	98.6 ± 7.6	50.3 ± 4.9
Jejunum	ST	665.0 ± 32.4	224.7 ± 17.7
	ST–NT	426.9 ± 28.7**	167.8 ± 12.2*
Ileum	ST	108.5 ± 7.1	30.5 ± 1.9
	ST–NT	66.5 ± 4.8***	21.4 ± 1.4*
Mean indicator of three sections	ST	295.0 ± 20.7	104.0 ± 8.5
	ST–NT	197.3 ± 15.9**	79.8 ± 4.8*
Total parameter of small intestine	ST	884.8 ± 51.5	311.9 ± 23.6
	ST–NT	592.0 ± 37.7**	239.5 ± 19.1**

Notes: * – P < 0.05, ** – P < 0.01, *** – P < 0.001.

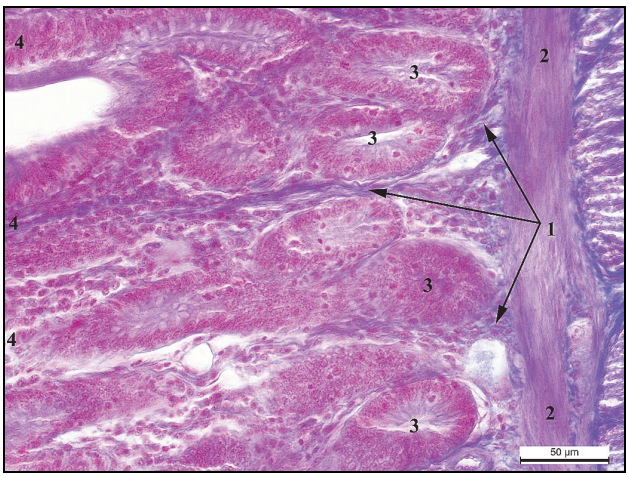

Fig. 3. The area of the crypts of ileum of a ST chicken: connective tissue fibers (*1*), lamina propria of mucous membrane (*2*), crypts (*3*), villi (*4*); Pacini staining

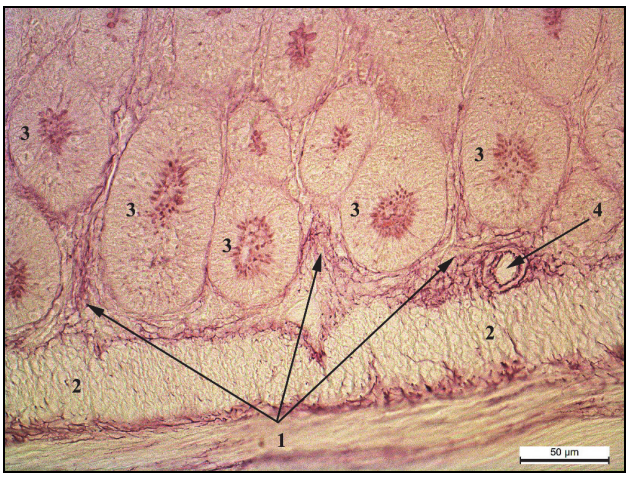

Fig. 4. The area of crypts of duodenum of a ST-NT chicken: elastic fibers (*1*), lamina propria of mucous membrane (*2*), crypts (*3*), blood vessel (*4*); Weigert staining

As for the relationship with the typology of autonomic tone, we observed full similarity with the previous parameter. I.e. along the entire small intestine, the sympathicotonic chickens were characterized by higher values of elastic fibers' volume. Therefore, these values were lower for sympathico-normotonic chickens by 6.3 mm^3 – in the duodenum, by

56.9 mm^3 ($P < 0.05$) – in the jejunum and by 9.1 mm^3 ($P < 0.05$) – in the ileum. Mean values of this parameter in the studied intestines of both groups of chickens differed by 24.2 mm^3 ($P < 0.05$). By total volume of elastic fibers in the entire small intestine, sympathicotonic chickens prevailed over sympathico-normotonic chickens by 72.4 mm^3 ($P < 0.01$).

Discussion

Combination of structural components and functional peculiarities of each system of an organism occurs in such way that it provides the optimum conditions for the metabolic processes in it, achievement of maximum efficiency in performing its tasks and quick adaptation to varying conditions of internal and external media (Bahr, 2008; Taylor et al., 2014; Palmquist-Gomes et al., 2016). To achieve all goals at the same time, each morpho-functional system should be in a certain way flexible and adaptive to opportunities. This is possible through regulatory impacts of the endocrine system and the autonomic nervous system. At the same time, each of the systems is observed to have a clearly manifested specialization in regulating only a certain area of an organism's activity (Crossley & Altimiras, 2000; Scanesa & Pierzchala-Koziec, 2014; Bedecarrats et al., 2016; Dennis, 2016).

One of the main distinctive features of the nervous system is its sensitivity, which manifests in the constant tone of the nerve centers. As we know, the sympathetic and parasympathetic sections of the autonomic nervous system are often characterized by antagonistic impacts on particular organs and systems of the organism. Decrease or increase of the tone in one of the sections causes an opposite effect in the same organ. Obviously, such fluctuations in tone are possible in both sections at the same time, therefore the final regulatory impact caused by the autonomic nervous system is determined by total tone of both sections. This leads to formation of a certain type of autonomic tone in animals' organisms, which is determined in the process of ontogenesis and conditions a complex of structural adaptations in all its systems (Shah et al., 2010; Kjaer & Jorgensen, 2011; Tybinka et al., 2016; Sheng & Zhu, 2018). Such adaptation reactions at different levels of structural organisation of an organism condition the formation of homeostasis both at these levels and in the entire organism. The studies of this state and determination of its quantitative equivalents result in formation of a parameter such as "norm". The total of such particular parameters form the general condition of an organism, which is called "health" (Jeurissen et al., 2002; Borell et al., 2007; Yegani & Korver, 2008; Scanes, 2017).

The results of our studies indicate that in the intestinal wall of the small intestine of chickens, as in any typical morpho-functional system, self-regulating processes and adaptation to regulatory impacts take place. This is related to a certain type of autonomic tone. Depending on the functional tasks of each intestine in the digestion, the sizes of its structural units change, with the general structure of the intestinal wall remaining the same. Therefore, providing digestive process during different typology of autonomous impacts is characterized by different morphological orientation. At the same time, there are often seen compensatory phenomena in sizes of particular layers of the intestinal wall, when one group of birds has higher values of one parameter combined with lower values of another in all intestines. However, compensation is not full because each parameter is determined by a certain range of values. Greater depth and volume of crypts in sympathicotonic chickens cannot compensate for greater height and volume of villi in sympathico-normotonic chickens. This, finally, manifests in larger values of volume of mucous membrane of the entire intestine in sympathico-normotonic chickens. The morphometric analysis we conducted helps us understand the ways of formation of this advantage.

Also, it should be mentioned that dependence of particular structural elements of the intestinal wall on autonomous impacts is not uniform in its extent. This can be seen in the level of reliability between the values of particular parameters of chickens of the studied groups. For example, the impact of the type of autonomic tone on the parameters of epithelium volume is much more significant than on the volume of lamina propria. This is indicated by significant and reliable differences between the groups of birds in the first parameter, and relatively insignificant and not reliable differences in the second parameter. The pattern we found proves the significant role of the epithelium layer in the processes of adaptation of the intestinal wall to certain typology of autonomous impacts. Therefore, the values of lamina propriae in this process are much lower. Considering the determining role of epithelium in the processes of near wall digestion (Geyra et al., 2001; Esmail, 1988; Theerawatanasirikul et al., 2017), it is clear that change in sizes of epithelium layer will affect this process. According to the same principle, we can also see that the lamina propriae of the mucous membrane, compared to crypts and villi is less significant in the process of adaptation of the mucous membrane to the corresponding type of autonomic tone.

The described pattern and other results of studies demonstrate that efficient assessment of different morphological structures can be made only by taking into account their functional characteristics because even slight changes in the structure cause a certain change of function (Yamauchi, 2002; Lavin et al., 2008; Verdal et al., 2010).

An integrated part of the intestinal wall is connective tissue which, by forming interlayers between certain groups of cells or layers of other tissues, unites all these structures in an integrated morpho-functional composition. It also accumulates biologically active substances, immune cells (Casteleyn et al., 2010; Revajova et al., 2013), and blood vessels and nerves lie across it. Connective tissue in general and its fiber component in particular is a part of the trophic complex of a certain area (Zeng et al., 2003; Pandit et al., 2018). For this reason, connective tissue is considered to play an important role in formation of homeostasis (Borda-Molina et al., 2018; Kogut et al., 2018). The presence of reliable differences in the parameters of volume of connective tissue fibers in the studied groups of poultry, proves the important role of connective tissue in the processes of adaptation of the structure of the intestinal wall to peculiarities of regulatory impacts caused by the autonomic nervous system. At the same time, the stimulatory effect of sympathetic tone is clearly manifested on the volumes of both total number of connective tissue fibers and elastic fibers in particular.

A certain influence on the studied processes is caused by the area of the intestinal wall due to significant length of intestine, and also peculiarities of digestive processes in its particular parts (Uni et al., 1998; Yamauchi, 2007; Svihus, 2014). However, according to our results, the general tendency of the impact of the typology of autonomic tone on most parameters is similar over the entire length of the small intestine.

Conclusions

Formation of a particular type of autonomic tone in the organism of chickens conditions the corresponding pattern of tone-trophic influence on their intestine. This, finally, is reflected both in the linear parameters of the intestine and parameters of volume of its mucous membrane. The intensity of the relationship with the typology of autonomic tone is not the same for all layers of the mucous membrane, which indicates their different role in the processes of adaptation of the intestinal wall in general and the mucous membrane in particular to regulatory impacts caused by the autonomic nervous system. A certain increase in parasympathetic tone among sympathico-normotonic chickens provides higher values of villi volume, therefore of the entire mucous membrane, because villi are ¾ of its volume. High sympathetic tone in ST chickens conditions higher values of volume of all connective tissue fibers, and elastic fibers particularly. On the whole, all determined morphological peculiarities of the mucous membrane indicate its significant and differently orientated properties in the process of adaptation to the pattern of regulatory impacts caused by the autonomic nervous system.

References

Ali, H. A., & McLelland, J. (1978). Avian enteric nerve plexuses. A histochemical study. Cell and Tissue Research, 189, 537–548.

Aubert, A. E., Beckers, F., Ramaekers, D., Verheyden, B., Leribaux, C., Aerts, J.-M., & Berckmans, D. (2004). Heart rate and heart rate variability in chicken embryos at the end of incubation. Experimental Physiology, 89(2), 199–208.

Baevskij, R. M., Kirilov, O. I., & Kleckin, S. Z. (1984). Matematicheskij analiz serdechnogo ritma pri stresse [Mathematical analysis of cardiac rhythm in stress]. Nauka, Moscow (in Russian).

Bahr, J. M. (2008). The chicken as a model organism. Sourcebook of Models for Biomedical Research, 161–167.
Bedecarrats, G. Y., Baxter, M., & Sparling, B. (2016). An updated model to describe the neuroendocrine control of reproduction in chickens. General and Comparative Endocrinology, 227, 58–63.
Borda-Molina, D., Seifert, J., & Camarinha-Silva, A. (2018). Current perspectives of the chicken gastrointestinal tract and its microbiome. Computational and Structural Biotechnology Journal, 16, 131–139.
Borell, E., Langbein, J., Despres, G., Hansen, S., Leterrier, C., Marchant-Forde, J., Marchant-Forde, R., Minero, M., Mohr, E., Prunier, A., Valance, D., & Veissier, I. (2007). Heart rate variability as a measure of autonomic regulation of cardiac activity for assessing stress and welfare in farm animals – A review. Physiology and Behavior, 92, 293–316.
Casteleyn, C., Doom, M., Lambrechts, E., Van den Broeck, W., Simoens, P., & Cornillie, P. (2010). Locations of gut-associated lymphoid tissue in the 3-month-old chicken: A review. Avian Pathology, 39(3), 143–150.
Cheled-Shoval, S. L., Withana Gamage, N. S., Amit-Romach, E., Forder, R., Marshal, J., Van Kessel, A., & Uni, Z. (2014). Differences in intestinal mucin dynamics between germ-free and conventionally reared chickens after mannan-oligosaccharide supplementation. Poultry Science, 93, 636–644.
Chevalier, N. R., Fleury, V., Dufour, S., Proux-Gillardeaux, V., & Asnacios, A. (2017). Emergence and development of gut motility in the chicken embryo. PLoS One, 12(2), e0172511.
China, A. M., Hill, D. R., Aurorac, M., & Spencea, J. R. (2017). Morphogenesis and maturation of the embryonic and postnatal intestine. Seminars in Cell and Developmental Biology, 66, 81–93.
Crossley, D., & Altimiras, J. (2000). Ontogeny of cholinergic and adrenergic cardiovascular regulation in the domestic chicken (*Gallus gallus*). American Journal of Physiology. Regulatory, Integrative and Comparative Physiology, 279, 1091–1098.
Dennis, R. L. (2016). Adrenergic and noradrenergic regulation of poultry behavior and production. Domestic Animal Endocrinology, 56, 94–100.
Doyle, A. M., Roberts, D. J., & Goldstein, A. M. (2004). Enteric nervous system patterning in the avian hindgut. Developmental Dynamics, 229, 708–712.
Esmail, S. H. M. (1988). Scanning electron microscopy of intestinal villous structures and their putative relation to digestion and absorption in chickens. Reproduction Nutrition Development, 28(6A), 1479–1487.
Fekete, E., & Csoknya, M. (1987). Fluorescence characterization of the nerve plexuses in the small intestine of the chicken. Acta Biologica Szegediensis, 33, 97–104.
Forder, R. E., Nattrass, G. S., Geier, M. S., Hughes, R. J., & Hynd, P. I. (2012). Quantitative analyses of genes associated with mucin synthesis of broiler chickens with induced necrotic enteritis. Poultry Science, 91, 1335–1341.
Furness, J. B. (2000). Types of neurons in the enteric nervous system. Journal of the Autonomic Nervous System, 81(1–3), 87–96.
Furness, J. B., & Costa, M. (1980). Types of nerves in the enteric nervous system. Commentaries in the Neurosciences, 235–252.
Geyra, A., Uni, Z., & Sklan, D. (2001). Enterocyte dynamics and mucosal development in the posthatch chick. Poultry Science, 80(6), 776–782.
Goldstein, A. M., & Nagy, N. (2008). A bird's eye view of enteric nervous system development: Lessons from the avian embryo. Pediatric Research, 64(4), 326–333.
Hao, M. M., Foong, J. P. P., Bornstein, J. C., Li, Z. L., Vanden Berghe, P., & Boesmans, W. (2016). Enteric nervous system assembly. Functional integration within the developing gut. Developmental Biology, 417, 168–181.
Heak, C., Sukon, P., Kongpechr, S., Tengjaroenkul, B., & Chuachan, K. (2017). Effect of direct-fed microbials on intestinal villus height in broiler chickens: A systematic review and meta-analysis of controlled trials. International Journal of Poultry Science, 16, 403–414.
Heanue, T. A., Shepherd, I. T., & Burns, A. J. (2016). Enteric nervous system development in avian and zebrafish models. Developmental Biology, 417(2), 129–138.
Incharoen, T. (2013). Histological adaptations of the gastrointestinal tract of broilers fed diets containing insoluble fiber from rice hull meal. American Journal of Animal and Veterinary Sciences, 8(2), 79–88.
Incharoen, T., Yamauchi, K., Erikawa, T., & Gotoh, H. (2010). Histology of intestinal villi and epithelial cells in chickens fed low-crude protein or low-crude fat diets. Italian Journal of Animal Science, 9(4), 429–434.
Jeurissen, S. H. M., Lewis, F., Klis, J. D., Mroz, Z., Rebel, J. M. J., & Huurne, A. A. H. M. (2002). Parameters and techniques to determine intestinal health of poultry as constituted by immunity, integrity, and functionality. Current Issues in Intestinal Microbiology, 3, 1–14.
Khalid, K. K., Zuki, A. B., Noordin, M. M., Mohd, A. B., & Mohd, Z. S. (2014). Light and scanning electron microscopy of the small intestine of young Malaysian village chicken and commercial broiler. Pertanika Journal of Tropical Agricultural Science, 37(1), 51–64.
Kjaer, J. B., & Jorgensen, H. (2011). Heart rate variability in domestic chicken lines genetically selected on feather pecking behavior. Genes, Brain and Behavior, 10, 747–755.
Kogut, M. H., Genovese, K. J., Swaggerty, C. L., He, H., & Broom, L. (2018). Inflammatory phenotypes in the intestine of poultry: Not all inflammation is created equal. Poultry Science, 97(7), 2339–2346.
Kononenko, V. S., & Zaitsev, A. A. (2009). Analiz makromorfometrichnih parametriv sercja ovec' z riznim tonusom avtonomnih centriv [An analysis of macromorphometric parameters of heart of sheep with different tone of autonomous centers]. Naukovij Visnik L'vivs'kogo Nacional'nogo Universitetu Veterinarnoji medicini ta biotehnologij imeni S. Z. Gzhic'kogo, 11(2), 165–169 (in Ukrainian).
Laudadio, V., Passantino, L., Perillo, A., Lopresti, G., Passantino, A., Khan, R. U., & Tufarelli, V. (2012). Productive performance and histological features of intestinal mucosa of broiler chickens fed different dietary protein levels. Poultry Science, 91, 265–270.
Lavin, S. R., Karasov, W. H., Ives, A. R., Middleton, K. M., & Garland, T. Jr. (2008). Morphometrics of the avian small intestine compared with that of nonflying mammals: A phylogenetic approach. Physiological and Biochemical Zoology, 81(5), 526–550.
Lilburn, M. S., & Loeffler, S. (2015). Early intestinal growth and development in poultry. Poultry Science, 94, 1569–1576.
Mabelebele, M., Alabi, O. J., Ng'ambi, J. W., Norris, D., & Ginindza, M. M. (2014). Comparison of gastrointestinal tracts and pH values of digestive organs of Ross 308 broiler and indigenous venda chickens fed the same diet. Asian Journal of Animal and Veterinary Advances, 9(1), 71–76.
Marchini, C. F. P., Cafe, M. B, Araujo, E. G., & Nascimento, M. R. B. M. (2016). Physiology, cell dynamics of small intestinal mucosa, and performance of broiler chickens under heat stress: A review. Revista Colombiana de Ciencias Pecuarias, 29, 159–168.
Mulisch, M., & Welsch, U. (2010). Mikroskopische technik. Spektrum Akademischer Verlag.
Nasrin, M., Siddiqi, M. N. H., Masum, M. A., & Wares, M. A. (2012). Gross and histological studies of digestive tract of broilers during postnatal growth and development. Journal of the Bangladesh Agricultural University, 10(1), 69–77.
Okpe, C. G., Abiaezute, N. C., & Adigwe, A. (2016). Evaluation of the morphological adaptations of the small intestine of the African pied crow (*Corvus albus*). The Journal of Basic and Applied Zoology, 75, 54–60.
Palmquist-Gomes, P., Guadix, J. A., & Perez-Pomares, J. M. (2016). A chick embryo cryoinjury model for the study of embryonic organ development and repair. Differentiation, 91(4–5), 72–77.
Pandit, K., Dhote, B. S., Mahanta, D., Sathapathy, S., Tamilselvan, S., Mrigesh, M., & Mishra, S. (2018). Histological, histomorphometrical and histochemical studies on the large intestine of Uttara Fowl. International Journal of Current Microbiology and Applied Sciences, 7(3), 1477–1491.
Revajova, V., Slaminkova, Z., Gresakova, L., & Levkut, M. (2013). Duodenal morphology and immune responses of broiler chickens fed low doses of deoxynivalenol. Acta Veterinaria Brno, 82, 337–342.
Sasselli, V., Pachnis, V., & Burns, A. J. (2012). The enteric nervous system. Developmental Biology, 366, 64–73.
Scanes, C. G. (2017). Grand and less grand challenges in avian physiology. Frontiers in Physiology, 222, 1–5.
Scanesa, C. G., & Pierzchala-Koziec, K. (2014). Biology of the gastro-intestinal tract in poultry. Avian Biology Research, 7(4), 193–222.
Shah, R., Greyner, H., & Dzialowski, E. M. (2010). Autonomic control of heart rate and its variability during normoxia and hypoxia in emu (*Dromaius novaehollandiae*) hatchlings. Poultry Science, 89(1), 135–144.
Sheng, Y., & Zhu, L. (2018). The crosstalk between autonomic nervous system and blood vessels. International Journal of Physiology, Pathophysiology and Pharmacology, 10(1), 17–28.
Shyer, A. E., Tallinen, T., Nerurkar, N. L., Wei, Z., Gil, E. S., Kaplan, D. L., Tabin, C. J., & Mahadevan, L. (2013). Villification: How the gut gets its villi. Science, 342, 212–218.
Sittiya, J., & Yamauchi, K. (2014). Growth performance and histological intestinal alterations of sanuki cochin chickens fed diets diluted with untreated whole-grain paddy rice. The Journal of Poultry Science, 51(1), 52–57.
Sklan, D. (2001). Development of the digestive tract of poultry. World's Poultry Science Journal, 57, 415–428.
Sokolov, V. I., & Chukalovskaja, R. N. (1980). Proliferativnye processy i citohimicheskie osobennosti kishechnogo jepitelija cypljat [Proliferative processes and cytochemical features of the intestinal epithelium of chickens]. Morphology of farm animals. Collection of Scientific Papers, 60, 74–78 (in Russian).
Svihus, B. (2014). Function of the digestive system. The Journal of Applied Poultry Research, 23(2), 306–314.
Taylor, E. W., Leite, C. A. C., Sartori, M. R., Wang, T., Abe, A. S., & Crossley, D. A. (2014). The phylogeny and ontogeny of autonomic control of the heart and cardiorespiratory interactions in vertebrates. The Journal of Experimental Biology, 217, 690–703.
Theerawatanasirikul, S., Koomkrong, N., Kayan, A., & Boonkaewwan, C. (2017). Intestinal barrier and mucosal immunity in broilers, Thai Betong, and native

Thai Praduhangdum chickens. Turkish Journal of Veterinary and Animal Sciences, 41, 357–364.
Tsirtsikos, P., Fegeros, K., Balaskas, C., Kominakis, A., & Mountzouris, K. C. (2012). Dietary probiotic inclusion level modulates intestinal mucin composition and mucosal morphology in broilers. Poultry Science, 91, 1860–1868.
Tybinka, A., Zaitsev, O., & Blishch, G. (2016). Impact of autonomic tonus typological features on the duodenum structure of chickens. Veterinary Medicine – Open Journal, 1(1), 12–17.
Uesaka, T., Young, H. M., Pachnis, V., & Enomoto, H. (2016). Development of the intrinsic and extrinsic innervation of the gut. Developmental Biology, 417, 158–167.
Uni, Z., Ganot, S., & Sklan, D. (1998). Posthatch development of mucosal function in the broiler small intestine. Poultry Science, 77(1), 75–82.
Uni, Z., Tako, E., Gal-Garber, O., & Sklan, D. (2003). Morphological, molecular, and functional changes in the chicken small intestine of the late-term embryo. Poultry Science, 82, 1747–1754.
Varasteh, S., Braber, S., Akbari, P., Garssen, J., & Fink-Gremmels, J. (2015). Differences in susceptibility to heat stress along the chicken intestine and the protective effects of galacto-oligosaccharides. PLoS One, 10(9), e0172511.
Verdal, H., Mignon-Grasteau, S., Jeulin, C., Le Bihan-Duval, E., Leconte, M., Mallet, S., Martin, C., & Narcy, A. (2010). Digestive tract measurements and histological adaptation in broiler lines divergently selected for digestive efficiency. Poulty Science, 89, 1955–1961.
Wali, O. N., & Kadhim, K. K. (2014). Histomorphological comparison of proventriculus and small intestine of heavy and light line pre- and at hatching. International Journal of Animal and Veterinary Advances, 6(1), 40–47.
Wang, F., Zuo, Z., Chen, K., Gao, C., Yang, Z., Zhao, S., Li, J., Song, H., Peng, X., Fang, J., Cui, H., Ouyang, P., Zhou, Y., Shu, G., & Jing, B. (2018). Histopathological injuries, ultrastructural changes, and depressed TLR expression in the small intestine of broiler chickens with aflatoxin B1. Toxins, 10(4), 131–147.
Wijtten, P. J. A., Langhout, D. J., & Verstegen, M. W. A. (2012). Small intestine development in chicks after hatch and in pigs around the time of weaning and its relation with nutrition: A review. Acta agriculturae Scandinavica, A 62, 1–12.
Yamauchi, K. (2002). Review on chicken intestinal villus histological alterations related with intestinal function. The Journal of Poultry Science, 39(4), 229–242.
Yamauchi, K. (2007). Review of a histological intestinal approach to assessing the intestinal function in chickens and pigs. Animal Science Journal, 78, 356–370.
Yamauchi, K. E., Incharoen, T., & Yamauchi, K. (2010). The relationship between intestinal histology and function as shown by compensatory enlargement of remnant villi after midgut resection in chickens. The anatomical record, 293(12), 2071–2079.
Yang, P., Gandahi, J. A., Zhang, Q., Zhang, L. L., Bian, X. G., Wu, L., Liu, Y., & Chen, Q. S. (2013). Quantitative changes of nitrergic neurons during postnatal development of chicken myenteric plexus. Journal of Zhejiang University-Science B (Biomedicine and Biotechnology), 14(10), 886–895.
Yegani, M., & Korver, D. R. (2008). Factors affecting intestinal health in poultry. Poultry Science, 87(10), 2052–2063.
Zeng, Y.-J., Qiao, A.-K., Yu, J.-D., Zhao, J.-B., Liao, D.-H., Xu, X.-H., & Gregersen, H. (2003). Collagen fiber angle in the submucosa of small intestine and its application in gastroenterology. World Journal of Gastroenterology, 9(4), 804–807.

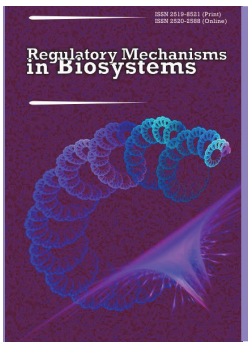

Regulatory Mechanisms in Biosystems

ISSN 2519-8521 (Print)
ISSN 2520-2588 (Online)
Regul. Mech. Biosyst., 9(3), 460–468
doi: 10.15421/021869

Pathomorphology of peripheral organs of immunogenesis in cats with spontaneous feline infectious peritonitis

M. R. Khalaniia, G. I. Kotsyumbas, V. V. Pritsak

Stepan Gzhytskyi National University of Veterinary Medicine and Biotechnologies, Lviv, Ukraine

Article info

Received 29.06.2018
Received in revised form 07.08.2018
Accepted 09.08.2018

Lviv National University of Veterinary Medicine and Biotechnologies named after S. Z. Gzhytskyj, Pekarska st., 50, Lviv, 79010, Ukraine. Tel.:+ 38-032-260-28-89. E-mail: martadocvet@gmail.com

Khalaniia, M. R., Kotsyumbas, G. I., & Pritsak, V. V. (2018). Pathomorphology of peripheral organs of immunogenesis in cats with spontaneous feline infectious peritonitis. Regulatory Mechanisms in Biosystems, 9(3), 460–468. doi:10.15421/021869

This article presents the results of pathomorphological research on the spleen and mesenteric lymph nodes of 23 dead cats aged from 3 months to 7 years, which in their lifetimes (according to anamnesis, clinical signs, laboratory-instrumental methods of examination and VetExpert FCoV Ab express test) had been diagnosed with infectious peritonitis. All the animals were domestic. Blood was drawn from the subcutaneous vein of the forelimb of the diseased cats. We determined ESR, morphological parameters of blood and content of hemoglobin. For histological and histochemical examinations, we selected samples of spleen and mesenteric lymph nodes, which were fixated in 10% aqueous solution of neutral formalin, Carnoy's and Bouin's solutions. The prepared histological sections were stained using haematoxylin and eosin, Van Gieson's stain, methyl green-pironin stain (Brashe), PAS-reaction (McManus), alcian blue and Congo red. Hematological parameters during 3 weeks of clinical progression of the disease among the cats demonstrated a decrease in the hemoglobin content and in the number of erythrocytes and leukocytes. Possible decrease in the number of lymphocytes indicated the development of an immune-deficiency state. Also, during the development of disease, the animals had possible increase in ESR, which indicated the development of an inflammatory process in the organism and decrease in the number of thrombocytes, which conditioned development of disseminated intravascular coagulation. The anatomical pathology autopsy showed that in most animals the spleen was diminished in size, the surface of the organ was tuberous, the capsule was wrinkled and mat, the edges were sharpened. The histostructural change was accompanied by a sharp depletion of the lymph nodes and reduction in the number of micro- and macrophages, which indicated the reduction of white pulp, rapid inhibition of the activity of T- and B-lymphocytes, plasmacytic and macrophage reaction and manifested in development of immune-deficient condition of the organism. In this process, the reticular carcass of the lymph nodes saturated with PAS-positive and eosinophilic masses was clearly manifested, which indicated formation of fibrinoid. In the spleen of 5 individuals, during staining using Congo red, we found deposition of amyloid masses both in the intima of the blood vessels and along the reticulary fibers of the lymph nodes. In the cytoplasm of macrophages, we found pyroninophilic formations. In two cases, we observed blood accumulation of red pulp and bleeding following the reduction of white pulp, and in one case fibrinogenous perisplenitis. In the mesenteric lymph nodes of most of the cats which had suffered from infectious peritonitis, we determined that edema, exposure of the reticular soft skeleton (stroma) of adrenal and paracortical zones, dilation of the border and central sinuses and thrombosis of vessels were followed by steep decrease in the number of T- and B-lymphocytes, plasma cells, micro- and macrophages, which indicated the development of atrophic processes of lympoid tissue and immune-suppression. In three cases, in mesenteric lymph nodes of cats, we determined development of sinus histiocytosis. The changes determined in the spleen and lymph nodes of the cats which had suffered from FIP indicate immune-suppressed condition and steep decrease in the functional ability of the organs and organism in general.

Keywords: spleen; lymph nodes; lymphocytes; macrophages; reticular carcass.

Introduction

Feline infectious peritonitis (FIP) is an immune-conditioned disease of domestic and wild cats, which is caused by the virulent cat coronavirus, which is one of the main infectious causes of death of young cats, and which threatens the survival of wild cats (Baydar et al., 2014; Kim et al., 2016; Ziółkowska et al., 2017). Occurrence of cases of cats suffering FIP is several times higher among the adult and young cats, which are kept in research centers or animal shelters. 80% of FIP cases are observed among young cats up to two years old, and 50% among kittens up to 7 months. Outbreaks of FIP can also occur in places where cats concentrate, where previously not a single case had been recorded (Knotek et al., 2000; Pedersen et al., 2009, 2014, 2016).

Despite the fact that pathogenesis is complicated and not fully clear, the pathogen is FIP (FIPV) virus, monocytic / macrophago-tropic mutated feline enteric coronavirus (FECV), which is widely distributed among cats all over the world (Crawford et al., 2017, Pedersen, 2014a, b). Macrophages with the virus cause a significant inflammatory reaction, leading to multisystemic pyogranulomatous vasculitis. Over time, the histiocytic population is replaced by a lymphoplasmatic population (Crawford et al., 2017).

Feline coronovirus (FCoV) belong to the genus *Alphacoronavirus* and usually causes mild symptoms of disorders of the gastrointestinal tract in cats. A low percentage of seropositive animals (5% to 12%) can develop feline infectious peritonitis (FIP). There are two known serotypes, among which type I is the commonest (80–95%), whereas the less common type II of FCoV may have formed due to a double process of recombination between type I of FCoV and type II of canine coronavirus (CCoV) (Le Poder et al., 2013; Bálint et al., 2014).

The critical factor in FIP pathogenesis is the function of cell-conditioned immunity, which can either prevent or allow full development of clinical disease among the infected animals. In the first case, the patient

can develop a latent infection, making him a carrier of a virus (Knotek et al., 2000). Cats with high humoral immunity and low or absent cellular-conditioned immune response against FIPV, obtain stable viremia and exudative form of FIP. The exudative form of the disease occurs as a result of broad sedimentation of immune complexes in the walls of blood vessels and activation of the complement which causes damage to the vessels, development of vasculitis and secretion of serum and protein in the body cavities. Cats with partial cellular-conditioned immune responses combined with humoral immune reactions develop a more chronic non-exudative form of FIP, which is characterized by immune-conditioned (hypersensitivity of delayed type) granulomatosis, often with perivascular damage to organs of the abdominal cavity, lungs, brain and eyes (Baydar et al., 2014).

FIPV can infect monocytes and macrophages, causing systemic infections and fatal diseases, whereas FECV only replicates in mature intestinal epithelium, which mainly causes non-symptomatic infection (Hora et al., 2016). Currently, it is known that the main links of the FIP pathogenesis are a systemic infection with FIPV, effective and stable replication of the virus in monocytes and activation of infected monocytes. This activation of monocytes and macrophages leads directly to pathological peculiarities of FIP, including vasculitis, secretions into the body cavities, with development of fibrinogenous and granulomatous inflammatory damage (Kipar et al., 2014). It is considered that the overwhelming of the immunity is conditioned by disorders in the co-working of T-lymphocytes and macrophages infected with FIP. Certainly, stress or immune suppression play an important part in manifestation of FIPV (Knotek et al., 2000).

The level of organism protection depends on the efficiency of the immune system which is the most important component of animal health, therefore the study of the defects of organs of immune system, which occur in the case of infectious diseases is one of the main orienttations in researching the development of pathological state of animals. Due to the important role of the immune system in development of FIP, the objective of our study was to determine the pathomorphological changes in the peripheral organs of the immune system of cats suffering from infectious peritonitis. Spleen and lymph nodes constantly interact with antigens in the blood of animals, therefore structural changes which follow the development of FIP can help in determining some aspects of the mechanism of development of immune-pathological processes in cats.

Materials and methods

For determination of hematological parameters, blood was drawn twice out of the subcutaneous vein of the forelimb of 5 diseased animals. Prior to this, the fur was cut and the skin was disinfected. As an anticoagulant, we used EDTA K2. The number of erythrocytes and leukocytes in the blood was determined using the standard method with a hemocytometer. Content of hemoglobin was determined colormetrically using the hemoglobin-cyanide unified method, ESR – using Panchenkov's method (Kondrahin, 2014; Uillard et al., 2014). The data was statistically analyzed using the StatPlus program, reliability of the obtained data was determined using ANOVA.

The pathomorphological studies were conducted at the Department of Normal and Pathological Morphology and Veterinary Forensics of Lviv Stepan Gzhytskyi National University of Veterinary Medicine and Biotechnologies and the Deartment of Pathologies of the University of Wrocław (Republic of Poland) during 2016–2018. We conducted a pathoanatomical study of the bodies of 23 cats aged from 3 months to 7 years, who while still alive had been diagnosed with FIP (based on anamnesis, clinical signs, laboratory-instrumental methods of study and express-diagnostics (VetExpert FCoV Ab express test).

For histological study, we cut fragments of the spleen and mesenteric lymph nodes of 1 x 1 cm size, then put them in 10% aqueous solution of neutral formalin for fixation, with a layer of cheesecloth for full submergence. The fixated patho-material was washed in tap water during 24 h, and using a sharp blade, thin 2 mm thick panels were accurately cut. Further, the cut fragments of the selected tissues were dehydrated in spirits in the order of increasing content of alcohol (70^o, 80^o, 90^o, 96^o – I and 96^o – II) for 24 hours in each spirit. After dehydrating the samples, they were put for an hour into a mixture of 96^o spirit and chloroform in 1 : 1 proportion, and then into pure chloroform-I for an hour and chloroform-II for an hour. Then, the patho-material was put into a melted mixture of chloroform and paraffin in 1 : 1 proportion for an hour in a thermostat at +37 ^{o}C. Next , the tissue fragments were put in two portions of melted paraffin for 2 hours in each, in a thermostat at +56 ^{o}C. The patho-material fragments from the paraffin-II were transferred into forms, which were further filled with melted paraffin and cooled in cold water. The obtained paraffin blocks were glued to wooden blocks. For histological study, the samples of the studied tissues were fixated in Carnoy's and Bouin's solutions. Out of paraffin blocks, 7 μm thick histological sections were made on MS-2 sliding microtome. The obtained histological sections were removed from the knife with a soft brush and transferred into warm distilled water (40 degrees C), submerging it starting from the surface which contacted the knife. After becoming spread in the warm water, the histological sections were taken out with a microscope slides. The microscope glasses with histological sections were put into thermostat for 24 h at a temperature of +37 ^{o}C. The histological sections stained with haematoxylin and eosin were deparaffinated in two portions of xylene for 2 min in each portion, transferred to spirits at decreasing concentration for 2 min in each concentration (96°, 80°, 70°) and put into distilled water for 3 min, and then transferred to Ehrlich's hematoxylin for 5 min, rinsed in distilled water over 3 s. Then the sections were transferred to tap water for 5 min. The differentiation was made in 1% solution of hydrochloric acid (3 s), rinsed in tap (5 min) and distilled (3 s) water. The histological sections were put in 0.1% aqueous solution of eosin for 0.5 min and washed with distilled water. The histological sections were dehydrated in spirits in order of increasing concentration (70°, 80°, 96°) – by 2 min, cleared in two portions of xylene for 2 min and put into Canada balsam. Also, the histological sections were stained with Van Gieson's solution, methyl green-pironin stain (Brashe), PAS-reaction (McManus method), alcian blue (Steedman's method) and Congo red for detection of amyloids (Pyrs, 1962; Merkulov, 1969; Goral's'kyj et al., 2005). The prepared histological preparations were analysed using a Leica DM-2500 (Switzerland) light microscope, photographed using a Leica DFC450C camera with Leica Application Suite Version 4.4 software.

Results

In veterinary clinics of Lviv, during the examination of diseased cats with signs of flaccidity, reduction of appetite, loss of weight and ascites, 5 animals were diagnosed with FIP. The palpatory mesenteric lymph nodes were enlarged, one cat was diagnosed with uveitis. The animals were monitored during a month. After the cats' owners had contacted the clinic for the first time, blood was drawn out of the subcutaneous vein of the cats' forelimbs. Over three weeks of clinical progression of the disease, the hematological parameters of the diseased cats significantly changed towards possible decrease in lymphocytes. During the first examination of the animals' blood parameters, we determined regenerative shift of neutrophils to the left and gradual increase in ESR. After a second examination 3 weeks later, we found nuclear shift of neutrophils to the right ($P < 0.01$) and possible decrease in the number of lymphocytes ($P < 0.01$) following a normal level of leukocytes. At the same time, the ESR increased by more than three times ($P < 0.01$), and the number of thrombocytes ($P < 0.05$) and the content of hemoglobin steeply decreased (Table 1).

The analysis of the obtained results allows us to state that over 3 week clinical progression of the disease, the monitored cats underwent a steep decrease in the hemoglobin concentration, number of erythrocytes and leukocytes. Possible decrease in the number of lymphocytes ($P < 0.01$) indicated the development of an immune-deficiency condition. Also, in the process of the disease's development, the animals possibly had an increase in ESR ($P < 0.01$), which indicates the development of inflammatory process in the organism, and decrease in the number of thrombocytes ($P < 0.05$) led to the development of disseminated intravascular blood coagulation (DIC syndrome). The general condition of the examined cats steeply declined Three of the cats were euthanized at the owners' request, the other two died.

Table 1
Hematological parameters of blood of cats during the clinical progression of FIP (n = 5; x ± SD)

Parameter	Norm	First examination	Replication after 3 weeks
Leukocytes, g/l	10.5–15.5	25.5 ± 1.9	5.9 ± 0.4***
Erythrocytes, corpuscles per liter	6.6–9.4	7.6 ± 0.4	5.6 ± 0.3***
Hemoglobin, g/l	90–155	114.6 ± 6.5	76.8 ± 5.3
Thrombocytes, g/l	200–600	465.0 ± 11.4	79.8 ± 2.8*
Leukogram			
Band neutrophils, %	3–9	14.4 ± 1.6	5.6 ± 1.2
Neutrophils with segmented nuclei, %	40–45	56.0 ± 2.4	84.4 ± 1.8**
Eosinophils, %	2–8	3.4 ± 2.7	0
Basophils, %	0–1	0	0
Monocytes, %	1–5	4.2 ± 1.2	5.4 ± 1.0
Lympocytes, %	36–51	22.0 ± 2.4	4.6 ± 0.9**
ESR, mm/h	2–6	22.6 ± 1.2	67.4 ± 3.4**

Note: * – P < 0.05, ** – P < 0.01,*** – P < 0.001 compared to the first study.

During the anatomical pathology autopsy of the bodies of 23 cats which died of infectious peritonitis over 2016–2018, the changes in spleen were not of the same type. In most cases, we observed a decrease in size of the spleen. The surface of the organ was tuberous, the capsule was wrinkled and mat, the edges were sharpened (Fig. 1).

During the histological examination of the histological preparations of such spleens, we determined disorganization of the connective-tissue stroma, atrophy of white pulp. The connective tissue capsule of the spleen was uneven, folded. Disruption of the fibers and edema of trabeculae and walls of vessels were followed by their saturation with PAS-positive protein masses. In this process, decreases in the volume of lymph nodes were clearest,which had no clearly distinguished zones and also were observed to have thinning or even reduction in lymph cords (Fig. 2).

Fig. 1. Shrunken spleen of a cat witht FIP: the surface is tuberous, the capsule was wrinkled, overlapped in some places

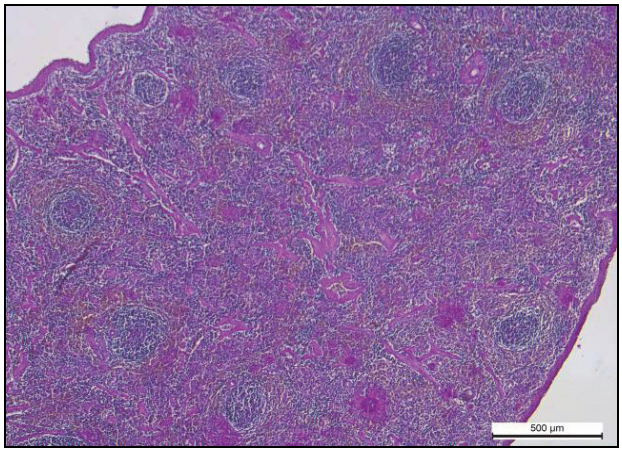

Fig. 2. Spleen of a cat with FIP: the capsule is folded; the saturation of trabeculae and walls of vessels with PAS-positive masses; PAS-reaction

It should be mentioned that the structure of the vessel walls of the organ was damaged. On the preparations stained with haematoxilin and eosin, the walls of central arteries of the lymph nodes either spread, the basal membrane was damaged, endothelial cells were turbid, the cytoplasm transilluminated, nuclei pyknotic or lysed, in some places desquamated. Damage to the endothelial cells led to increased penetrability and disorders in blood flow (Fig. 3). Alongside the changes in endothelial cells, plasmatic saturation of the walls and their fibrinoid swelling occurred. The enlarged vessel walls of the arterioles manifested clear alcianophilia and fuchsinophilia on the preparations stained using Steedman's and McMannus' methods. As they enlarged, their translumminance decreased, which reflected negatively in the rheological properties of the blood. Accumulations of glycosaminoglycans and glycoproteins indicated disorders of collagene and elastic fibers of the vessel walls and development of mesenchymal proteinosis. On the preparations stained with iodine acid-Schiff, the enlarged walls of arteries and arterioles demonstrated a bright PAS-positive reaction, which indicated the development of fibrinoid swelling of vessels (Fig. 4).

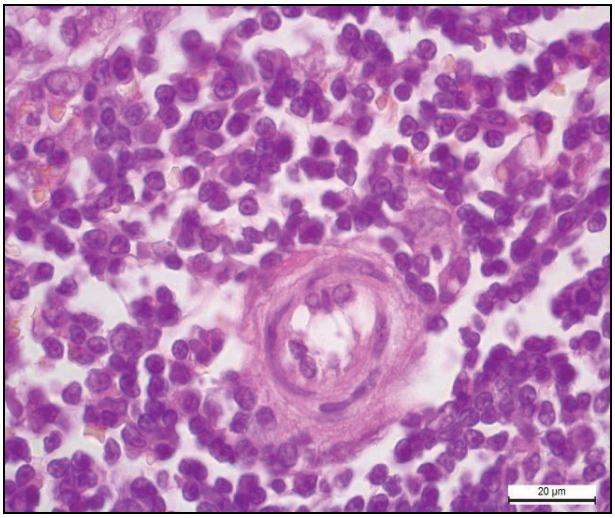

Fig. 3. Spleen of a cat with FIP: central artery of lymph node; endothelium cells of arterioles are turbid, desquamated at some places; hematoxilin and eosin

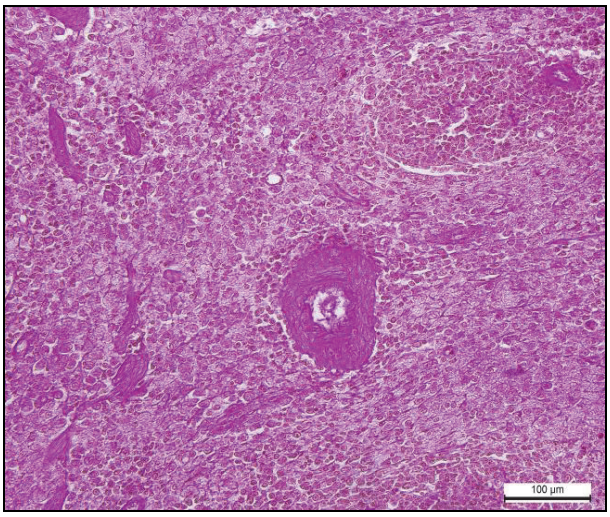

Fig. 4. Spleen of a cat with FIP: the depositions of PAS-positive protein mass in walls of arteries; PAS-reaction

Mostly small in volume, the lymph nodes were a sharply narrowed periarterial T-zone, where the cells were distributed. We observed disorders in the structure of white pulp and quantitative decrease of small, average lymphocytes and macrophages. A steep decrease in the lymphoid population of cells in the lymph nodes and decrease in the content of micro- and macrophages in red pulp was clearly observed in the preparations stained with methyl green-pyronin. A small accumulation of

T-lymphocytes stained in blue-green was freely positioned around the central artery of the lymph node. Lymphopoiesis and plasmacytic reactions were inhibited (Fig. 5). Often, turbid lymphocytes with decomposing nuclei were found among the cells of the periarterial zone. Along with decrease in the number of lymphocytes, we observed hyperplasia and hypertrophy of reticular cellular elements and their transformation into macrophages. Due to the fact that this zone is enriched with interdigitating cells – macrophages able to fixate complexes of antibodies and antigens on their surface, hypertrophied macrophages were found among the small population of spread lymphocytes. Cytoplasm of swollen, hypertrophied macrophages stably contained pirinophilic elements, and nuclei were in the state of pyknosis or lysis. Also, in the macrophages' cytoplasm, we found vacuoles of different size (Fig. 6). It is known that these particular macrophages are targeted cells, where the coronavirus replication takes place. During absence of adequate cellular immune reaction which occurs in FIP, and even with the presence of specific antibodies, the virus probably continues reproducing in the macrophages (Rjemsi & Tennant, 2005; Kudrjashov & Balabanova, 2011). We microscopically found pironinophilic elements in cytoplasm of macrophages of lymph nodes, which indicates that coronavirus replication takes place in macrophages.

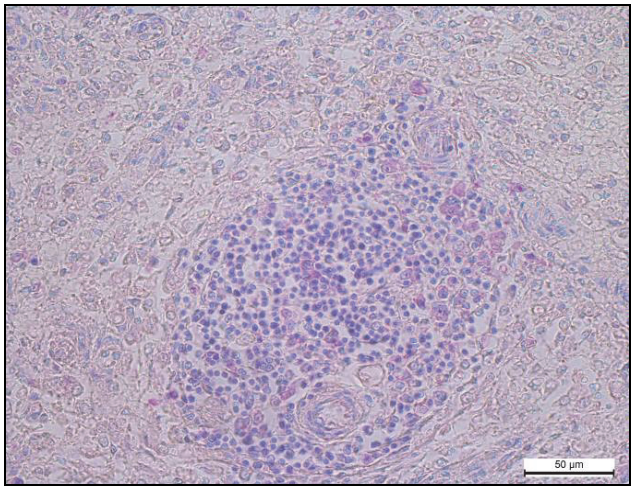

Fig. 5. Spleen of a cat with FIP: steep decrease in the number of lymphocytes in lymph nodes; methyl green pironin

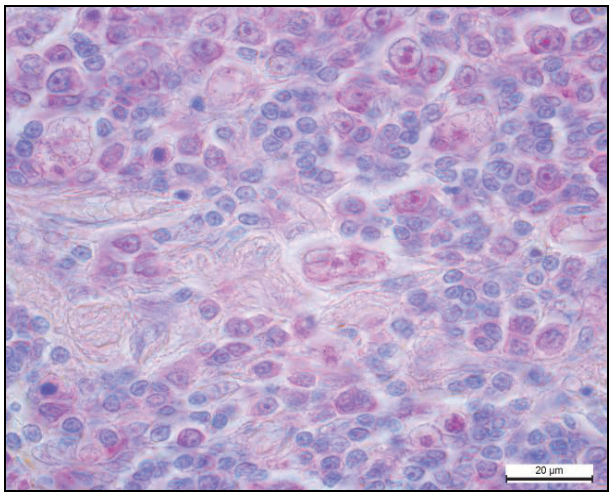

Fig. 6. Spleen of a cat with FIP: macrophages with pironin elements among lymphocytes in lymph node; methyl green-pironin

In the marginal (border) zone of a lymph node, which is the place where white pulp is replaced by red pulp, we found no subpopulations of lymphocytes, and the mantle zone contained single cellular elements. The reticular carcass of both marginal and mantle zone became exposed, and the number of micro- and macrophage cells in the red pulp sharply decreased.

During the monitoring of white pulp reduction, we determined that walls of sinusoids of small vessels in the border (marginal) zone and mantle zone demonstrated clear fuchsinophility on preparations stained with iodine acid-Schiff. The reticular carcass, walls of vessels and sinuses of lymph nodes of the spleen were saturated with PAS-positive protein masses, which in one case manifested highly intense fuchsinophility in the marginal and mantle zones, in other cases – in lymph nodes (Fig. 7). It is possible that damage in the structure of the walls of vessels of microcircular flow caused increase in penetrability in blood vessels, sinusoids, insudation of highly molecular proteins and glycoproteins of blood, leading to disorders in protein-carbohydrate composition of the main substance. At the same time, we observed partial decomposition of fiber structures of collagen fibers. In atrophied lymph nodes, we found accumulations of homogenous mass in the form of fuchsinophilic elements (Fig. 8).

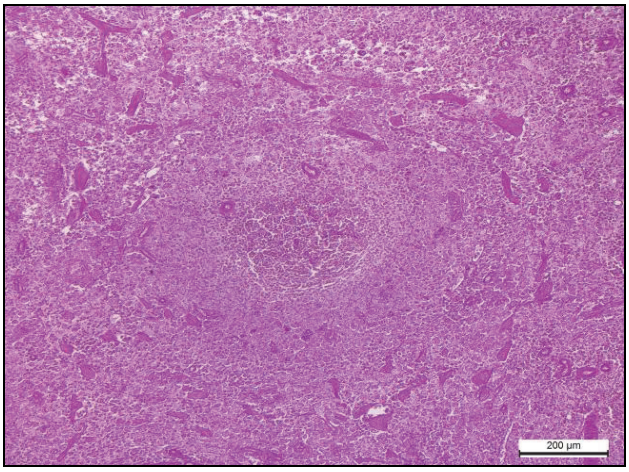

Fig. 7. Spleen of a cat with FIP: saturation of sinusoids and vessels of border zone of lymph node with PAS-positive protein mass; PAS-reaction

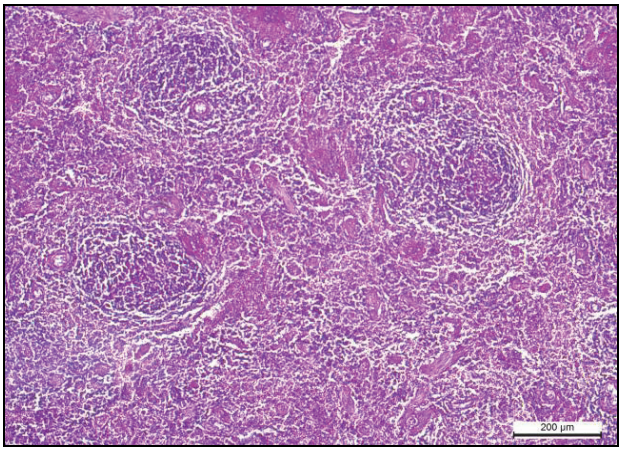

Fig. 8. Spleen of a cat with FIP: sedimentation of PAS-positive protein mass in the walls of arteries and reticular carcass of white pulp; PAS-reaction

On the preparations stained with haematoxylin and eosin, such elements in lymph nodes became of eosinphilic colour, which is caused by saturation of reticular structures and walls of vessels with proteins of blood plasma, including poorly dispersive protein – fibrinogen and leads to formation of untypical protein-polysugar complexes and was the basis for formation of fibrinoid (Fig. 9). During histochemical examination, this particular complex caused eosinphilic, PAS-positive reaction. Also, in five cases in reaction with Congo red, in the spleen of cats, we found accumulation of amyloid masses. Localization of amyloid masses was observed in the subendothelial layer of arterioles, along the reticular fibers of lymph nodes in the form of orange homogenous masses (Fig. 10). The spleens of two cats were enlarged, their edges became rounded, and

the capsule tensioned. Bleeding of different extent was observed under the capsule (Fig. 11). Histological examination of the spleen of the above-mentioned cats revealed a sharp decrease in hemodynamic, which was expressed in enlarging and oversaturation of the vessels with blood, stases and excessive saturation of red pulp with erythrocytes. Such marked plethora indicated increasing deposition of blood in the spleen (Fig. 12).

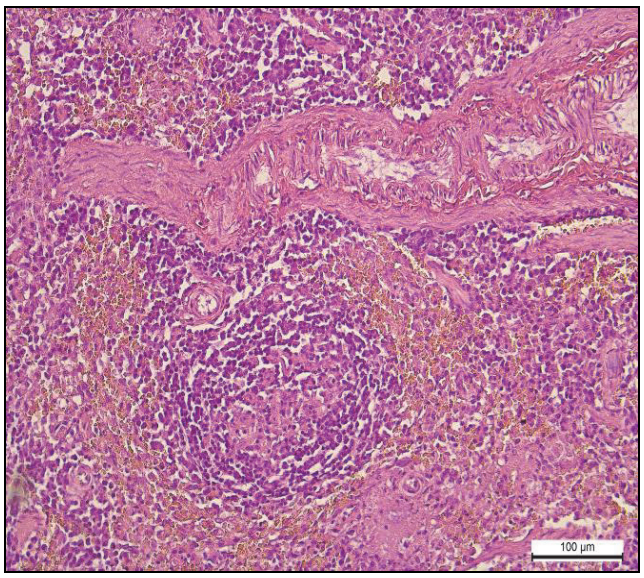

Fig. 9. Spleen of a cat with FIP: eosinophilic protein mass deposited along reticular fibers in the center of lymph node; haematoxilin and eosin

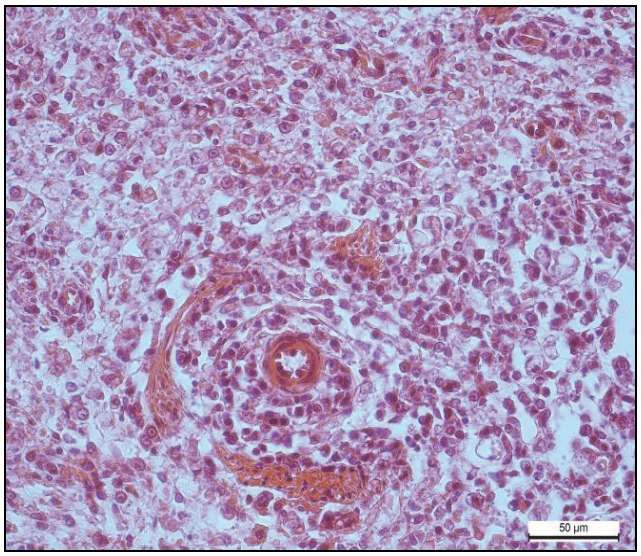

Fig. 10. Spleen of a cat with FIP: deposition of amyloid masses along the reticular fibers of lymph node and wall of blood vessel; Congo red

Disorders in capillary blood flow, increased transcapillary fluid exchange were caused by endotheliocytes. Destruction of endotheliocytes with disruption of the fibers in the wall of the vessels contributed to increase in their penetrability and was reflected in the phenomena of stromal, perivascular edemas of tissue and bleeding. Red pulp was filled with erythrocytes at different stages of decomposition. In the reticular structure of red pulp, we also observed thin cords formed by micro- and macrophages, but their number was much lower compared to the control animals. The number of megakaryocytes increased. Formation of megakaryocytes indicated increase in extramedullary haematopoiesis. As a result of plethora, the size of lymph nodes decreased. Perivascular edema and disruption of the fibers in the walls of vessels, steep accumulation of blood in red pulp contributed to increase in the organ's volume, which was observed during macroscopic examination. In one cat, the volume of the spleen increased, which was followed by fibrinous periplenitis. The surface was tuberous with layering, the capsule was wrinkled and covered with light-grey moderately fibrinous membranes, which at some places were hard to remove. Histological examination of the spleen revealed disruption of connective tissue fibers and saturation of capsules with fibrinous exudate. On the preparations stained using Van Gieson, among interlaced fibrin filaments, fiber structures of red colour were clearly distinguished, which indicated organisation of fibrin (Fig. 13).

Fig. 11. Spleen of cat with FIP: tubular surface with overlapping

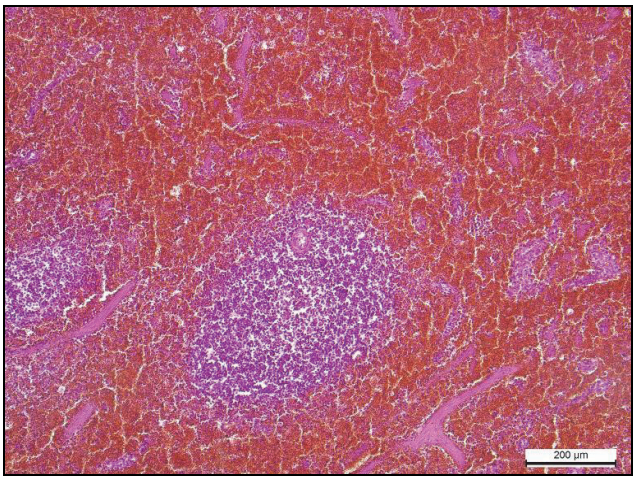

FIg. 12. Spleen of a cat with FIP: blood-filling of red pulp; depletion of lymph node; haematoxylin and eosin

In this organ, lymph nodes of white pulp were much larger compared to previous animals, but the mantle and marginal zones were unclear. In such lymph nodes, we clearly see the reticular carcass, where small groups of stretched lymphocytes were located in the periarterial zone (Fig. 14). The walls of the central arteries of lymph nodes were enlarged, the endothelium was at some places desquamated, which affected blood circulation. Centers of lymph nodes were stretched and deplated, observed to have karyorrhexis of cells of different intensity. The red pulp had moderate content of macrophages with grains of hemosiderin and cells of lysed nuclei.

Therefore, during the analysis of the results of pathomorphological examination of spleens of cats which suffered infectious peritonitis, we should mention that the structural changes were accompanied by steep depletion of lymph nodes by lymphocytes and decrease in the number of micro- and macrophages, which indicated reduction of white pulp, steep inhibition of activity of T- and B-lymphocytes, plasmacytic and macrophage reaction and manifested in development of immune-deficiency condition of the organism. Also, in the spleen, we observed mesenchymal disproteinosis, which was accompanied by fibrinoid

swelling and amyloidosis of walls of vessels and deposition of fibrinoid and amyloid along the reticular fibers of lymph nodes.

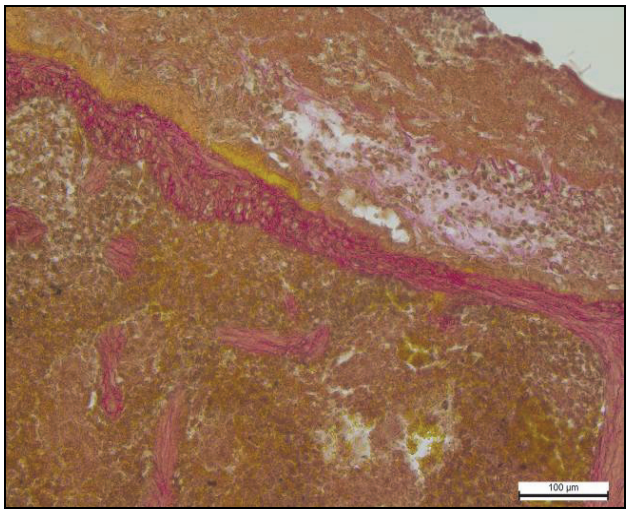

Fig. 13. Spleen of a cat with FIP: perisplenitis; organisation of fibrin; Van-Gieson

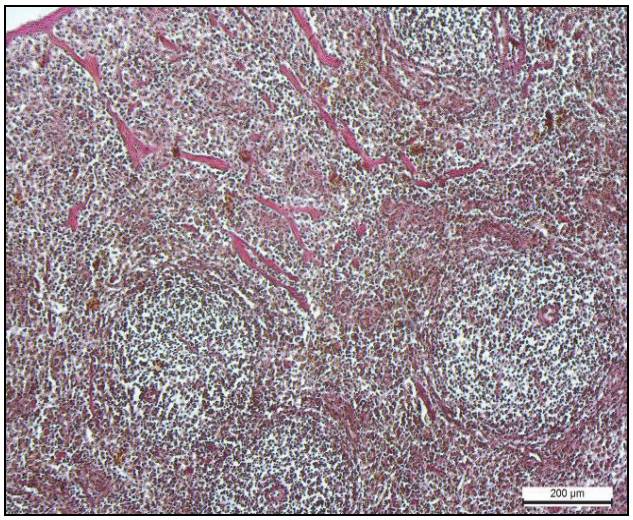

Fig. 14. Spleen of cat with FIP: periarterial zone of lymph nodes poorly filled with erythrocytes; Van-Gieson

Similar disorders in the system of T- and B-lymphocytes were observed also in mesenteric lymph nodes of cats suffering from FIP. During the histological examination, the capsula and stroma of lymph nodes were stretched, saturated with transudates rich in PAS-positive compounds (Fig. 15). Interstitial edema was followed by exposure of the reticular carcass of the adrenal and paracortical zone of lymph nodes and significant decrease in the subpopulation of blood elements in the organ. In the cortex, directly under the border sinuses, lymph nodes different in size but significantly decreased were clearly seen. At the same time, lymph nodes with reactive centers were not determined. At some places, between reticular fibers of paracortical zones, we could see single granulocytes, macrophages and small groups of apoptosis-changed lymphocytes. As we know, the paracortical zone is the T-dependant zone, through the postcapillary venules of which, migration of recirculating lymphocytes to parenchyma and lymph nodes occurs. We determined histostructural changes and severe inhibition of T-lymphocytes activity, and also weakening of cellular immunity (Fig. 15). On the preparations stained using iodine acid-Schiff, we determined significant fuchsinophility of not only the walls of vessels, sinusoids, reticular structures, and also detected PAS-positive filament structures in lumina of the vessels (Fig. 16).

Lower web-like alcianphilic structures were found in the vessels' lumina, sinuses, among aggregate erythrocytes on the preparations stained with alcian blue (Fig. 17). Presence of filament structures in lumina of the vessel system of lymph node indicates intravascular blood coagulation and blood circulation disorders during their life.

We observed dilatation of border and central sinuses and disorders in their structure. Walls of sinuses became exposed, at some places, there were seen singular endothelium cells. It seems that sinuses are formed by phagocytic cells, which are the first to contact the virus after the pathogens penetrate the organism, and then transform into macrophages. However, a small number of transformed cells became visible. Among turbid reticular cells, we found single macrophages. Quantitative composition of micro- and macrophages was sharply decreased. Lymph cords which branched from cortex and trabeculae were significantly narrowed and totally depleted, plasmatic cells were not found. Steep decrease in the number of T- and B-lymphocytes and plasma cells conditioned exposure of the reticular carcass of the paracortical and adrenal zones (Fig. 18). The determined changes in lymph nodes indicate development of clearly manifested atrophic processes of lymphoid tissue and immune-deficiency condition of the organism.

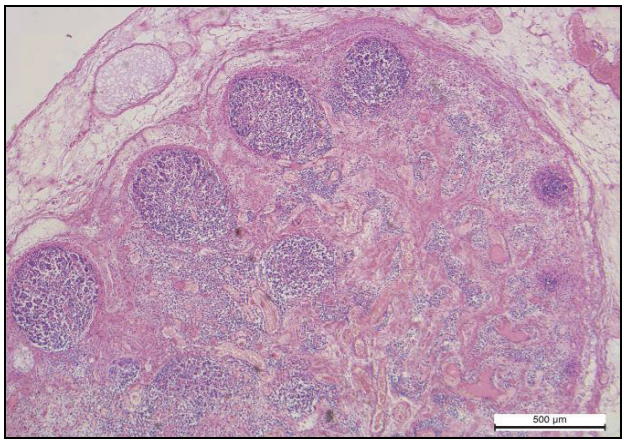

Fig. 15. Lymph node of a cat with FIP: different in size, but much smaller lymph nodes in the cortex zone

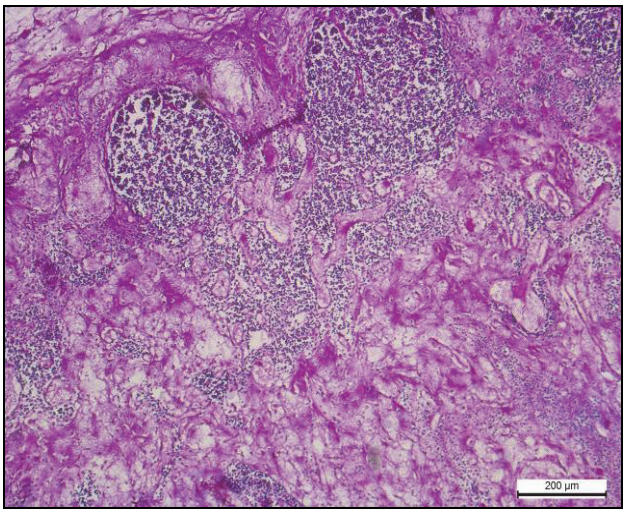

Fig. 16. Lymph node of a cat with FIP: the saturation of reticular carcass with PAS-positive masses; PAS-reaction

Analysis of the data obtained during histological examination of mesenteric lymph nodes of most of the cats which suffered feline infectious peritonitis demonstrated that edema and exposure of the reticular carcass of the adrenal and paracortical zones, dilatation of border and central sinuses were followed by a sharp decrease in the number of T- and B- lymphocytes, plasma cells, micro- and macrophages, which indicated development of atrophy processes of lymph tissue and immune-deficiency condition of the organism. Histostructural changes in lymphoid tissue were combined with thrombosis of the vessels. In the mesenteric lymph nodes of two cats that suffered from hemorrhagic hyperplasia of the spleen, atrophy of the lymph tissue was followed by

significant enlargement of the blood vessels, plethora of the blood vessels, central sinuses, stases and bleeding in the organ`s stroma (Fig. 19). The number of lymphocyte subpopulations both in the cortex, and in the adrenal zones steeply decreased. The lymph nodes were small and moderately filled with lymphocytes.

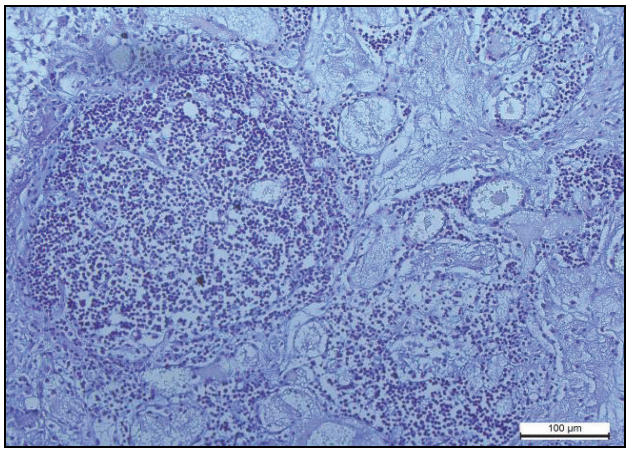

Fig. 17. Lymph node of a cat with FIP: exposure of reticular carcass of the paracortical zone; alcian blue

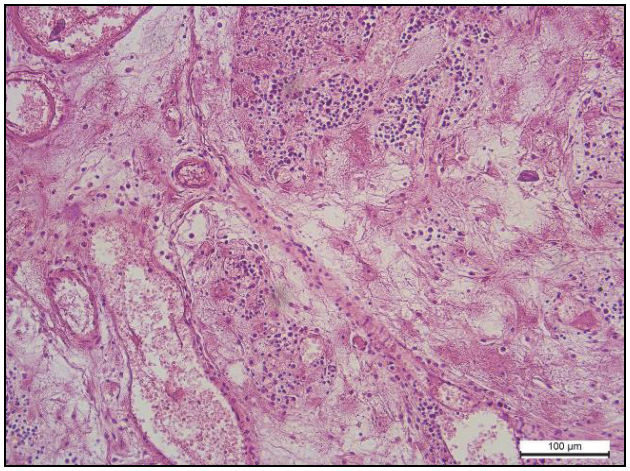

Fig. 18. Lymph node of a cat with FIP: depletion of lymph cords; haematoxilin and eosin

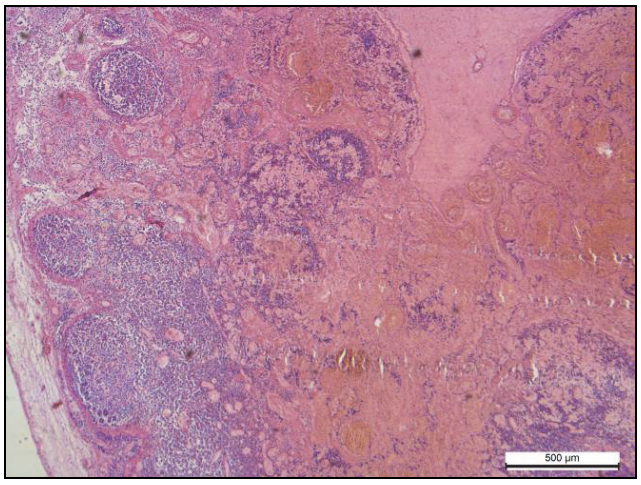

Fig. 19. Lymph node of a cat with FIP: enlargement and overfilling with blood of border and central sinuses, stasis and bleeding into stroma of the organ; haematoxilin and eosin

In three other cases, mesenteric lymph nodes of the cats were observed to show development of sinus histiocytosis. Cortex substance in lymph nodes was represented by poorly contoured, small lymph nodes. There were small lymphatic nodes with widely distributed lymphocytes. As a result of decrease in the number of cellular elements in the central part of the lymph nodes, some lymph nodes were found to have bright centers (in the form of "starry sky"), which is considered to be a clear resistance reaction to pathogens. Density of lymphocytes in the cortex and paracortical zones was low. The saturation of cellular elements of RNA was also sharply decreased. Reticular tissue of the adrenal zone was also luminant, with enlarged sinuses (Fig. 20).

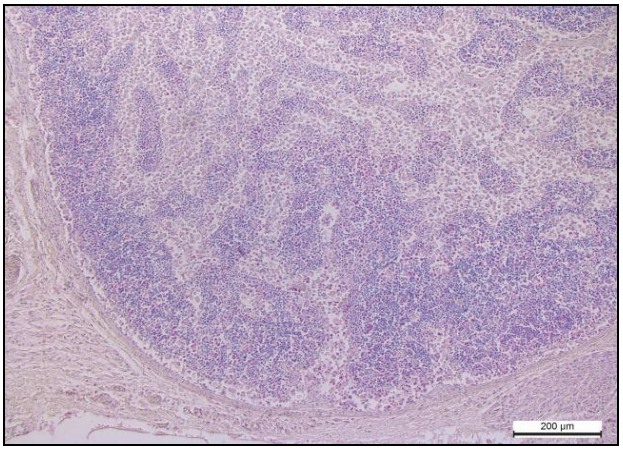

Fig. 20. Lymph node of a cat with FIP: narrowing of cortex; sharp decrease in lymph nodes; methyl green-pironin

Lymph cords were thinned, widely spread, and presented in the form of narrow tails filled with lymphoid elements. Compared to the previous animals, in the lymph cords, we found lymphocytes, lymphoblasts and a small number of plasmatic cells. The cytoplasm of the latter demonstrated moderate pirinophilic reaction during Brashe staining. There was a clear dilatation of the central sinuses, where the syncytial connection of endothelium cells was damaged. As we know, steep enlargement of sinuses is orientated towards strengthening of the processes of biological and mechanical filtration, phagocytosis and slowed flow of lymph through the enlarged sinuses. As a result of swelling and desquamation of sinusoidal endothelium cells, they were located in the lumina of sinuses in the form of rounded cells, among which single lymphocytes and macrophages were clearly distinguished. Many cells were in the state of necrobiosis (Fig. 21). Intense infiltration of sinuses by histiocytes at different stages of decomposition indicates development of sinusoidal histiocytosis.

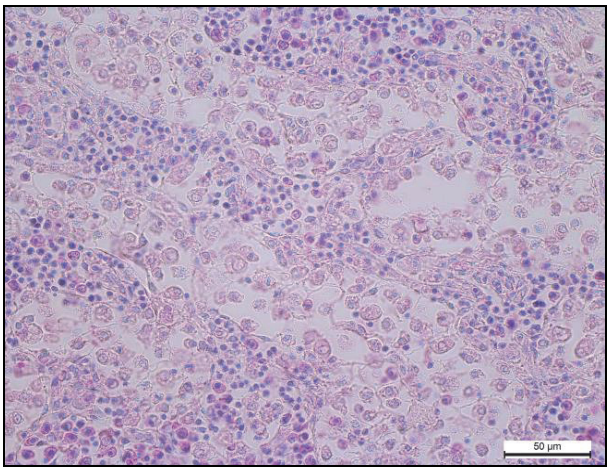

Fig. 21. Lymph node of a cat with FIP: lymph cords moderately filled with B-lymphocytes and single plasmatic cells; methyl green-pironin

During staining with iodine acid-Schiff, "shore" cells of the sinuses, which perform a filtration-phagocytic function, were seen on the preparations in the form of starry cells with mutually interlaced processes, often containing grainy fuchsinophilic elements. Clear fuchsinophilia was

determined also for walls of arterioles and damaged structures of reticular fibers (Fig. 22).

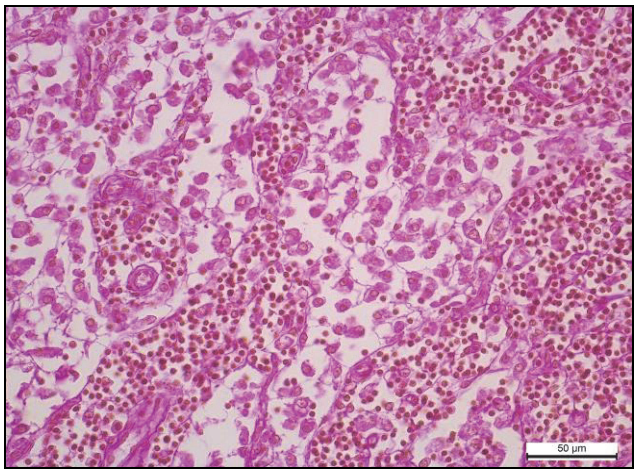

Fig. 22. Lymph node of a cat with FIP: lymph cords; fuchsinophilia of reticular fibers and walls of vessels; PAS-reaction

On the preparations stained with methyl green and pironin, we observed that sinus endothelial cells free of synthesis relations were present in the lumina of sinuses in the form of mostly rounded cells with poorly stained cytoplasm and nucleus, often with lysed nuclei. Small vacuoles were found in the cytoplasm and nuclei of most desquamated endothelial cells (Fig. 23). Also, we found cells with small pironinophilic elements in the cytoplasm (Fig. 24).

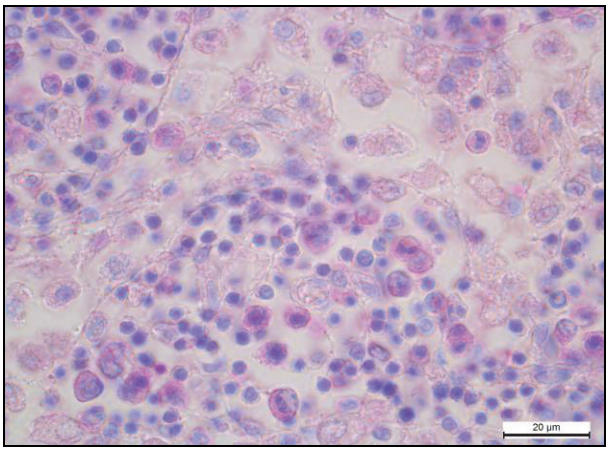

Fig. 23. Lymph node of a cat with FIP: lumen of sinuses of rounded cells, with poorly stained cytoplasm and nucleus; moderately filled with B-lymphocytes and single plasmatic cells; methyl green-pironin

Therefore, in the mesenteric lymph nodes of cats with FIP, edema and exposure of reticulary carcass and paracortical zone, dilatation of border and central sinuses were followed by steep decrease in the number of T- and B-lymphocytes, plasmatic cells, micro- and macrophages, which indicated development of atrophic processes in the lymphoid tissue and immune-suppressive condition of the organism. Histostructural changes in lymphoid tissue were combined with thrombosis of vessels. In two cases, the atrophy of lymphoid tissue was followed by dramatic enlargement and overfilling with blood of the blood vessels, central sinuses, stases and bleeding in the stroma of the organ, and three cats were recorded as having sinus histiocytosis.

Discussion

The peripheral organs of immunogenesis – spleen and lymph nodes are specific biological "filters" which disable antigens, and where antigen proliferation and differentiation of T- and B-lymphocytes takes place and where a particular immune response is formed. The main function of the spleen is its participation in many immunological processes, provision of development and activation of lymphocytes and their transformation into cells – primary producers of antibodies, or in cells which take part in the reaction of cellular immunity (Lucyk et al., 2003; Golovac'kyj et al., 2009; Kotsan et al., 2009; Vandevelde, 2015; Lucas, 2017; Golub et al., 2018).

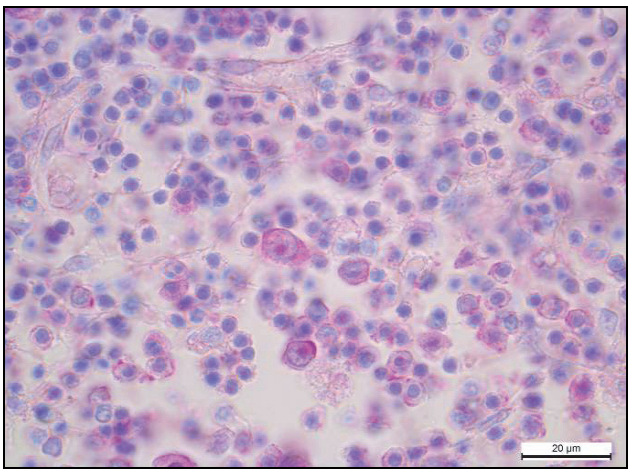

Fig. 24. Lymph node of a cat with FIP: cells with small pironinophilic elements in cytoplasm; methyl green-pironin

It has been determined that during infectious peritonitis, an excessive production of antibodies which are not controlled by suppressive lymphocytes occurs, leading to development of hypersensitivity of slowed type. Intensive production of defective neutralizing antibodies with formation of antigen-antibody complexes is distinctive for severe infectious peritonitis. Complexes in blood attach to macrophages and distribute them in the blood vessels. In the blood vessels, the antigen-antibody system is accompanied by the complement, and the complexes formed this way attach to the walls of vessels. These complexes are phagocytized by macrophages which stimulate accumulation of neutrophilic leukocytes through the factor of chemotaxis and lead to damage to endothelium and vessel wall, formation of thrombi (Hsieh et al., 2010; Brown, 2011; Kudrjashov & Balabanova, 2011; Han et al., 2014; Günther et al., 2018; Jaimes & Whittaker, 2018; Shirato et al., 2018).

In the case of structural changes in spleen, it should be mentioned that most of the studied animals were recorded having mesenchymal disproteinosis, which was followed by fibrinoid swelling, amyloidosis of walls of vessels and deposition of fibrinoid and amyloid along the reticular fibers of lymph nodes. I.e. in the spleen of the diseased cats, changes in the vessels of a non-inflammatory nature prevailed – angiopathy. One of the most important characteristics of development of pathological process in animals with infectious peritonitis is damage to the endothelium of vessels, which leads to heightened penetrability of the vessels, insudation of high molecular proteins and glycoproteins of blood, thus leading to disorders of protein-carbohydrate composition of the main substance (Rjemsi & Tennant, 2005; Kudrjashov & Balabanova, 2011). Formation of unusual protein-polysugar complexes became a basis for formation of fibrinoid which manifested significant eosinophilic PAS-positive reaction during histochemical examination. Also, during staining with Congo red, the spleens of the cats were observed to have deposition of amyloid masses in the intima of blood vessels and along the reticular fibers of lymph nodes.

Pathohistological changes in the spleen of the cats suffering from infectious peritonitis were characterized by steep depletion of lymph nodes by lymphocytes and decrease in the number of micro- and macrophages, which indicated reduction of white pulp, sharp inhibition of T- and B-lymphocytes' activity, which was possibly conditioned by long term persistence of the virus in the organism.

The morphological changes revealed in the mesenteric lymph nodes were mainly of one type, and slightly differed by extent of manifestation. We constantly found fuchsinophilic, alcianophilic filament structures in aggregated erythrocytes, which indicates the development

of disseminated thrombosis, a peculiarity of which is development of interstitial edema, which took place in the peripheral organs of immunogenesis. Edema and exposure of reticular carcass of the adrenal and paracortical zones, dilatation of border and central sinuses were followed by steep decrease in the number of T- and B-lymphocytes, plasmatic cells, micro- and macrophages, which indicated development of atrophic processes in the lymph tissue.

Therefore, in infectious feline peritonitis, the peripheral organs of immunogenesis manifested development of mesenchymal disproteinosis, disseminated thrombosis, depletion of lymph nodes by lymphocytes, steep inhibition of activity of T- and B-lymphocytes, plasmocytic and macrophage reaction, which indicated the development of an immune-deficient condition of the organism.

Conclusion

Hematological parameters during the three week clinical progression of the course of the disease in cats demonstrated reduction of the hemoglobin concentration, number of erythrocytes and leukocytes. A possible decrease in the number of lymphocytes indicated development of an immune-deficiency condition. Also, during development of the disease, the animals had a possible increase in ESR, which indicates the development of inflammatory process in the organism and reduction in the number of thrombocytes, which conditioned the development of disseminated intravascular coagulation (DIC).

The spleen of the cats which suffered from infectious peritonitis underwent histostructural changes were accompanied by steep depletion of lymph nodes by lymphocytes and decrease in the number of micro- and macrophages, which indicated reduction of white pulp, steep inhibition of activity of T- and B-lymphocytes, plasmocytic and macrophage reaction and manifested in development of immune-deficiency condition of the organism. Also, mesenchymal disproteinosis was observed in the spleen,which was asccompanied by fibrinoid swelling and amyloidosis of walls of vessels and deposition of fibrinoid and amyloid along the reticular fibers of the lymph nodes.

In the mesenteric lymph nodes of most of the cats which suffered infectious peritonitis, the following symptoms were observed; edema and exposure of reticular carcasses of the adrenal and paracortical zones, dilatation of border and central sinuses, thrombosis of vessels, followed by steep decrease in the number of T- and B-lymphocytes, plasmatic cells, micro- and macrophages, which indicated the development of atrophic processes in lymphoid tissue and immune-suppression. In three cases, we recorded sinus histiocytosis in the mesenteric lymph nodes of cats.

References

Bálint, Á., Farsang, A., Szeredi, L., Zádori, Z., & Belák, S. (2014). Recombinant feline coronaviruses as vaccine candidates confer protection in SPF but not in conventional cats. Veterinary Microbiology, 169(3–4), 154–162.

Baydar, E., Eröksüx, Y., & Timurkan, M. O. (2014). Feline infectious peritonitis with distinct ocular involvement in a cat in Turkey. Kafkas Universitesi Veteriner Fakultesi Dergisi, 20(6), 961–965.

Brown, M. A. (2011). Genetic determinants of pathogenesis by feline infectious peritonitis virus. Veterinary Immunology and Immunopathology, 143(3–4), 265–268.

Crawford, A. H., Stoll, A. L., Sanchez-Masian, D., Shea, A., Michaels, J., Fraser, A. R., & Beltran, E. (2017). Clinicopathologic features and magnetic resonance imaging findings in 24 cats with histopathologically confirmed neurologic feline infectious peritonitis. Journal of Veterinary Internal Medicine, 31(5), 1477–1486.

Gavrilin, P., Gavrilina, E., & Evert, V. (2017). Histoarchitectonics of the parenchyma of lymph nodes of mammals with different structure of intranodal lymphatic channel. Ukrainian Journal of Ecology, 7(3), 96–107.

Golovac'kyj, A. S., Cherkasov, A. S., Sapin, M. R., & Parahin, A. I. (2009). Anatomija ljudyny [Human anatomy]. Vol. 3. Nova Knyga, Vinnycja (in Ukrainian).

Golub, R., Tan, J., Watanabe, T., & Brendolan, A. (2018). Origin and immunological functions of spleen stromal cells. Trends in Immunology, 39(6), 503–514.

Goral's'kyj, L. P., Homych, V. T., & Konons'kyj, O. I. (2005). Osnovy gistologichnoi' tehniky i morfofunkcional'ni metody doslidzhen' u normi ta pry patologii' [Bases of histological technology and morphofunctional methods of research in norm and in pathology]. Polissja, Zhytomyr (in Ukrainian).

Günther, S., Felten, S., Wess, G., Hartmann, K., & Weber, K. (2018). Detection of feline *Coronavirus* in effusions of cats with and without feline infectious peritonitis using loop-mediated isothermal amplification. Journal of Virological Methods, 256, 32–36.

Han, J.-I., Kang, S.-Y., Yoon, K.-J., & Na, K.-J. (2014). Nucleic acid-based differential diagnostic assays for feline coronavirus. Journal of Virological Methods, 208, 21–25.

Hora, A. S., Tonietti, P. O., Taniwaki, S. A., Asano, K. M., Maiorka, P., Richtzenhain, L. J., & Brandao, P. E. (2016). Feline *Coronavirus* 3c protein: A candidate for a virulence marker. BioMed Research International, 2016, e8560691.

Hsieh, L.-E., Lin, C.-N., Su, B.-L., Jan, T.-R., Chen, C.-M., Wang, C.-H., Lin, D.-S., Lin, C.-T., & Chueh, L.-L. (2010). Synergistic antiviral effect of *Galanthus nivalis* agglutinin and nelfinavir against feline coronavirus. Antiviral Research, 88(1), 25–30.

Jaimes, J. A., & Whittaker, G. R. (2018). Feline coronavirus: Insights into viral pathogenesis based on the spike protein structure and function. Virology, 517, 108–121.

Kim, Y., Liu, H., Kankanamalage, A. C. G., Weerasekara, S., Hua, D. H., Groutas, W. C., Chang, K.-O., & Pedersen, N. C. (2016). Reversal of the Progression of fatal *Coronavirus* infection in cats by a broad-spectrum *Coronavirus* protease inhibitor. PLoS Pathogens, 12(3), e1005531.

Kipar, A., & Meli, M. L. (2014). Feline infectious peritonitis: Still an enigma? Veterinary Pathology, 51(2), 505–526.

Knotek, Z., Toman, M., & Faldyna, M. (2000). Clinical and immunological characteristics of cats affected by feline infectious peritonitis. Acta Veterinaria Brno, 69(1), 51–60.

Kondrahin, I. P. (2004). Metody veterinarnoj klinicheskoj laboratornoj diagnostiki [Methods of veterinary clinical laboratory diagnostics]. Kolos, Moscow (in Russian).

Kotsan, I. Y., Hrynchuk, V. O., Velemets, V. K., Shvarts, L. O., Pykaliuk, V. S. & Shevchuk, T. I. (2009). Anatomiia liudyny [Human anatomy]. Tsentr Uchbovoi Literatury, Kyiv (in Ukrainian).

Kudrjashov, A. A., & Balabanova, V. I. (2011). Patologoanatomicheskaja diagnostika boleznej sobak i koshek [Pathological diagnosis of diseases of dogs and cats]. Institut Veterinarnoj Biologii, Saint Petersburg (in Russian).

Le Poder, S., Pham-Hung d'Alexandry d'Orangiani, A.-L., Duarte, L., Fournier, A., Horhogea, C., Pinhas, C., Vabret, A., & Eloit, M. (2013). Infection of cats with atypical feline coronaviruses harbouring a truncated form of the canine type I non-structural ORF3 gene. Infection, Genetics and Evolution, 20, 488–494.

Lucas, S. B. (2017). Lymph node pathology in infectious diseases. Diagnostic Histopathology, 23(9), 420–430.

Lucyk, O. D., Ivanova, A. J., Kabak, K. S., & Chajkovs'kyj, J. B. (2003). Gistologija ljudyny [Human histology]. Knyga Pljus, Kyiv (in Ukrainian).

Merkulov, G. A. (1969). Kurs patologogystolohycheskoj tekhnyky [The course of pathohistological technique]. Medycyna, Leningrad (in Russian).

Pedersen, N. C. (2014a). An update on feline infectious peritonitis: Virology and immunopathogenesis. The Veterinary Journal, 201(2), 123–132.

Pedersen, N. C. (2014b). An update on feline infectious peritonitis: Diagnostics and therapeutics. The Veterinary Journal, 201(2), 133–141.

Pedersen, N. C., Liu, H., Dodd, K. A., & Pesavento, P. A. (2009). Significance of *Coronavirus* mutants in feces and diseased tissues of cats suffering from feline infectious peritonitis. Viruses, 1(2), 166–184.

Pedersen, N. C., Liu, H., Durden, M., & Lyons, L. A. (2016). Natural resistance to experimental feline infectious peritonitis virus infection is decreased rather than increased by positive genetic selection. Veterinary Immunology and Immunopathology, 171, 17–20.

Pedersen, N. C., Liu, H., Gandolfi, B., & Lyons, L. A. (2014). The influence of age and genetics on natural resistance to experimentally induced feline infectious peritonitis. Veterinary Immunology and Immunopathology, 162(1–2), 33–40.

Pyrs, J. (1962). Gistohimija [Histochemistry]. Izdatel'stvo Inostrannoj Literatury, Moscow (in Russian).

Rjemsi, J., & Tennant, B. (2005). Infekcionnye bolezni sobak i koshek [Infectious diseases of dogs and cats]. Akvarium, Moscow (in Russian).

Shirato, K., Chang, H.-W., & Rottier, P. J. M. (2018). Differential susceptibility of macrophages to serotype II feline coronaviruses correlates with differences in the viral spike protein. Virus Research, 255, 14–23.

Uillard, M., Tvedten, G., & Tornval'd, G. (2004). Laboratornaja diagnostika v klinike melkih domashnih zhivotnyh [Small animal clinical diagnosis by laboratory methods]. Akvarium, Moscow (in Russian).

Vandevelde, K. (2015). Immunological barriers: Functional histology of the spleen. The Veterinary Journal, 205(1), 3–4.

Ziółkowska, N., Paździor-Czapula, K., Lewczuk, B., Mikulska-Skupień, E., Przybylska-Gornowicz, B., Kwiecińska, K., & Ziółkowski, H. (2017). Feline infectious peritonitis: Immunohistochemical features of ocular inflammation and the distribution of viral antigens in structures of the eye. Veterinary Pathology, 54(6), 933–944.

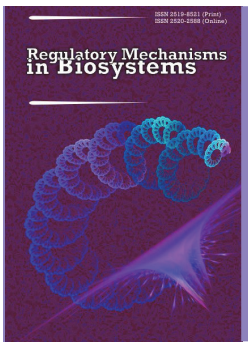

Regulatory Mechanisms in Biosystems

ISSN 2519-8521 (Print)
ISSN 2520-2588 (Online)
Regul. Mech. Biosyst., 9(3), 469–476
doi: 10.15421/021870

Enzyme-like activity of nanomaterials

S. I. Tsekhmistrenko*, V. S. Bityutskyy*, O. S. Tsekhmistrenko*, V. M. Polishchuk*, S. A. Polishchuk*, N. V. Ponomarenko*, Y. O. Melnychenko*, M. Y. Spivak**

**Bila Tserkva National Agrarian University, Bila Tserkva, Ukraine*
***Zabolotny Institute of Microbiology and Virology of NAS of Ukraine, Kyiv, Ukraine*

Article info

Received 11.06.2018
Received in revised form 07.07.2018
Accepted 08.07.2018

Bila Tserkva National Agrarian University, Soborna ploshcha, 8/1, Bila Tserkva, 09100, Ukraine. Tel.: +38-045-635-12-88.

Zabolotny Institute of Microbiology and Virology of NAS of Ukraine, Akad. Zabolotny st., 154, Kyiv, 03680, Ukraine. Tel.: +38-068-034-48-48. E-mail: svetlana.tsehmistrenko@gmail.com

Tsekhmistrenko, S. I., Bityutskyy, V. S., Tsekhmistrenko, O. S., Polishchuk, V. M., Polishchuk, S. A., Ponomarenko, N. V., Melnychenko, Y. O., & Spivak, M. Y. (2018). Enzyme-like activity of nanomaterials. Regulatory Mechanisms in Biosystems, 9(3), 469–476. doi:10.15421/021870

In modern conditions, nanomaterials, especially nanoparticles of metals and nonmetals, are increasingly used in various industries. Due to their unique properties, in particular, the ability of nanoparticles to exhibit an enzyme-like effect they are widely used in biology, medicine, biotechnology, the food industry and agriculture. Important advantages of nanoparticles are their size, which enables specific properties to be present: their large surface area, the ability to transfer molecules and the ability to protect them from degradation and release over a long time, the location of action and the specificity of interaction with biological structures. Nanoparticles play a special role in the processes of neutralizing the active forms of oxygen. It has been established that a number of nanoparticles, in particular, Fe, Mn, Zn, Ce, Si and Se oxides, have an enzyme-like activity mimicking that of some enzymes. By changing the degree of oxidation, these particles can regenerate and continuously catalyze the reaction of neutralizing superoxide anion radicals, thus fulfilling the function of SOD and being the first link in protecting tissues and cells from oxidative stress in physiological and pathological conditions. It is proved that nanoparticles Mn_3O_4, Fe_3O_4, Co_3O_4, CeO_2, $LaCoO_3$ and other elements can effectively dispose of hydrogen peroxide and other peroxides, showing catalase-like and peroxidase-like activity. Nanozymes are characterized that exhibit the activity of oxidases, peroxidases and phosphatase. The prospect of using mimetics for complex in vitro analyzes of high-sensitivity biomarker disease detection is shown. The possibility of effective multi-use of nanoparticles as antioxidants is indicated. There are good prospects for further research on properties and the use of polyfunctional particles that are easily synthesized, reliable and inexpensive. More work is needed to determine the interaction of enzymomimetics with biological molecules such as proteins, carbohydrates and lipids, and also to take into account the peculiarities of their metabolism, clearance, degradation, biocompatibility and side effects, since individual nanoparticles have the potential to be deposited in separate organs.

Keywords: mimetics; superoxide dismutase; catalase; oxidase; peroxidase; phosphatase.

Introduction

The 21st century is considered to be the period of global usage of nanotechnology, which deals with a set of theoretically sound and practical methods of research, analysis and synthesis, as well as the production and use of products with a predictable atomic structure through controlled manipulation of individual atoms and molecules (Gordon et al., 2007). Due to the extremely small dimensions (up to 100 nm) and the large surface area per unit volume, nanomaterials have specific chemical, physical and biological properties that are useful for many new applications. Many nanoparticles (NPs) have been found to exhibit enzymatic activity and are potentially capable of being used in various industries, particularly in the food industry, pharmacy, and biotechnology. The creation of artificial enzymes simulating the complexity and functioning of natural systems is one of the greatest achievements of the last two decades.

Use of nanoparticles

Rapid development of nanotechnology around the world has created numerous catalytically active nanomaterials (Cormode et al., 2018). Currently, nanomaterials of different origin are used in biology, medicine and biotechnology (Fig. 1). This category includes nanomaterials with enzyme-mimetic properties, such as nanoparticles of metals and nonmetals, their oxides, magnetic nanoparticles, liposomes, carbon and polymer nanomaterials. They are characterized as a potential alternative to natural enzymes and are widely used in many industries such as immunoassay, biosensorica, pharmaceutical processes, oncotherapy, the food industry, ecology, etc. (Chen et al., 2012, 2014; Fu, 2014; Lu et al., 2015; Li & Zhang, 2016). This demonstrates the great importance and commercial interest of using nanomaterials as enzyme mimetics. Compared to enzymes of natural origin, agonists or mimetics on the basis of nanomaterials can change catalytic activity, are stable in harsh conditions, their production is relatively easy and economically justified (Cheng et al., 2015). The cyclic action of nanoparticles and the possibility of recovery without significant loss in subsequent cycles of catalytic activity makes them unique compounds (Wei & Wang, 2013). In addition, the surface of nanomaterials, unlike natural enzymes which have only one active site in a molecule, may have more catalytic centers (Liu et al., 2015; Gao et al., 2017). These enzyme mimetics are of great importance in practice (Gordon et al., 2007; Wei & Wang, 2013; Lin et al., 2014; Xu et al., 2014).

The basic requirements for nanoparticles regarding their use in biology and medicine are low toxicity or absence of it, high biocompatibility, biodegradational property and the ability to be removed from the organism naturally (Fu, 2014; Kozik et al., 2016; Bityutskyy et al., 2017; Chekman et al., 2017).

The catalytic activity of nanoparticles and the ability to inactivate active forms of oxygen can be used to simulate the catalytic activity of natural enzymes. Different nanoparticles have been studied to date, and their enzymomimetic activity, in particular superoxide dismutase, oxidase-like, peroxidase-like, catalase- and phosphatase-like, have been determined (He et al., 2014; Cormode et al., 2018).

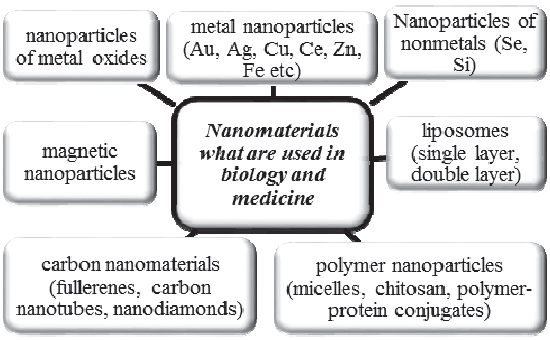

Fig. 1. Nanomaterials used in biology and medicine

General characteristics of mimetics

Agonists or mimetics are compounds that imitate the action of other substances, being similar to the ones formed in the organism (enzymes, hormones, mediators). Cell receptors react to mimetics as a substance which they interact with (Singh, 2016). According to physical and chemical properties, mimetics are similar to natural signaling molecules, but they have a number of important qualities (Fig. 2).

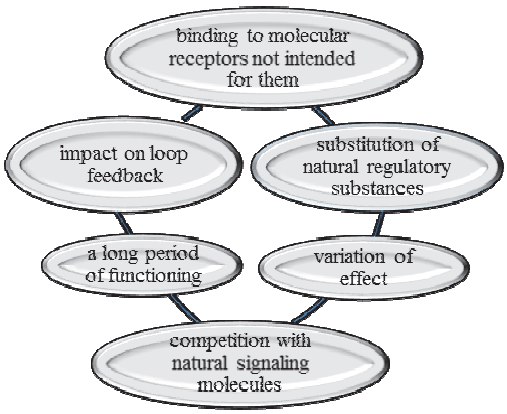

Fig. 2. Properties of mimetic enzymes

They bind to molecular receptors not intended for them, and substitute natural regulatory substances. Mimetics can act more strongly or weakly than the compounds that they replace, that is, their impact varies. They can compete with natural signaling molecules for binding to receptors (by concentration and affinity). The period of functioning of the mimetics in the unchanged state of the organism and the time of binding to the receptors are different from natural compounds. Formation in the body of its own regulatory substances due to the feedback between the concentration of regulators and their production is conditioned by the presence of mimetics (Chekman et al., 2017).

The term "nanozymes" was introduced for nanomaterials with their own enzyme-like activity to distinguish these nanocomplexes from immobilized enzymes (Wei & Wang, 2013). The development of highly effective non-protein analogues of enzymes is an relevant task for modern biology, biotechnology, medicine and agriculture (Dong et al., 2012; Bityutskyy et al., 2017). Currently, several types of artificial enzymes have been created to replace natural analogues (Kozik et al., 2016; Nelson et al., 2016; Wang et al., 2017).

Natural enzymes and mimetics have many properties in common: they accelerate the chemical reactions and can regenerate (Kozik et al., 2016; Chekman et al., 2017). Natural enzymes, unlike the artificial ones, require special environmental conditions, in particular a certain temperature and pH (Grulke et al., 2014). Such unique properties of nanomaterials can be used for the prevention, diagnosis and treatment of diseases. Many nanomaterials have powerful antioxidant properties that can potentially act as inhibitors of active forms of oxygen. However, it has also been proven that certain nanomaterials have prooxidant properties that contribute to the formation of active forms of oxygen, which can lead to the formation of oxidative stress, which is known to promote the development of various pathologies (Amani et al., 2017; Sims et al., 2017). One of the important features of nanoenzymes compared to the natural enzymes and other mimetics is that their activity can be regulated by altering the structure, size, surface modification, introduction of protective coverings, etc. (Liu et al., 2015; Kozik et al., 2016; Fa et al., 2018). A relationship between catalytic activity, therapeutic efficiency and biocompatibility of particular mimetics has been determined (Cormode et al., 2018). It was found that the smaller are the particles, the higher is their catalytic activity. This phenomenon is conditioned by the fact that smaller nanoparticles have a larger surface area for interaction with the substrate. This indicates the possibility of synthesizing nanoparticles with a particular activity and properties (Gao et al., 2017). The enzyme-mimetic activity of nanomaterials is influenced by several factors, in particular, their chemical composition, surface charge, particle size, and surface covering (Sharpe et al., 2011; Samuel et al., 2014; Verma, 2014; Sandhir et al., 2015; Cîrcu et al., 2016; Shah et al., 2017). However, both the positive and the toxic effects of NPs may be different, since the synthesis method, the choice of stabilizers which cover the particles, can lead to a different biological effect (Estevez et al., 2017). It is important to understand which physical-chemical properties correlate with biological activity, and are critical for determining the conditions that contribute to the positive effect and for determining the circumstances which lead to formation of toxic properties.

There is a prospect of using nanomaterials for medical and industrial purposes (Armstrong et al., 2013; Sandhir et al., 2015). It is believed that their significant activity provides more effective neutralization of various types of active forms of oxygen (Sandhir et al., 2015). Recently, antioxidant activity was determined for various metallic nanocomposites such as gold (Esumi et al., 2003; BarathManiKanth et al., 2010), platinum (Kajita et al., 2007; Kim et al., 2008; Moglianetti et al., 2016), iron (Paul et al., 2009; Szekeres et al., 2014; Toth et al., 2014; Shah et al., 2017), nickel (Saikia et al., 2010), cerium (Kim et al., 2012) and yttrium (Schubert et al., 2006). Nanoparticles (NPs) of metal oxides are intensively studied (Kozik et al., 2016; Tsekhmistrenko et al., 2018). They are successfully used in the treatment of a number of pathologies, have high colloidal resistance and biocompatibility (Grillone et al., 2017).

Nanoparticles with their antioxidant activity conditioned by the ability to exhibit enzyme-mimetic action, can be promising therapeutic agents that can be used for targeted drug delivery (Morry et al., 2017). However, with nanoparticles, one should take into account such issues as metabolism, clearance, degradation, biocompatibility and side effects, since individual nanoparticles have the potential for prolonged maintenance in the organs, in particular, the liver and spleen (Cormode et al., 2018). The interaction of nanoparticles with the local environment plays an important role in their distribution and long-term stability (Dhall et al., 2017).

Nanomaterials as SOD mimetics

Superoxide dismutase is an enzyme that functions for the catalytic conversion of a superoxide radical to oxygen and hydrogen peroxide. The catalytically active metal of this enzyme can be Cu, Fe, Mn.

A superoxide radical which is formed predominantly in mitochondria and, when protons are added is capable of being converted into hydroperoxide (Fig. 3), is one of the most destructive forms of oxygen (Lushchak, 2015; Wang et al., 2017). It is known that SOD inactivates superoxide anion in two stages with formation of hydrogen peroxide and oxygen (Shin et al., 2009). In this case, the general reaction of superoxide anion dismutation for nanoparticles also includes two stages (Korsvik et al., 2007).

SOD-like activity is typical for various metal oxide nanoparticles, in particular nano-TiO_2 (Zheng et al., 2017), ZnO (Li et al., 2018),

Fe_3O_4 (Khedri et al., 2018), NiO-NPs (Faisal et al., 2013), Mn_3O_4 (Yao et al., 2018), $LaCoO_3$ (Wang et al., 2017), CeNPs (Batinić-Haberle et al., 2010; Heckert et al., 2008), Pt (Wei & Wang, 2013), Au (Lin et al., 2014) and nonmetals: SiO_2 (Farhangi-Abriz et al., 2018; Soares et al., 2018) and Se (Guo et al. 2016). These mimetics provide considerable interest, as they are characterized by increased stability, multifunctionnality and regulated activity.

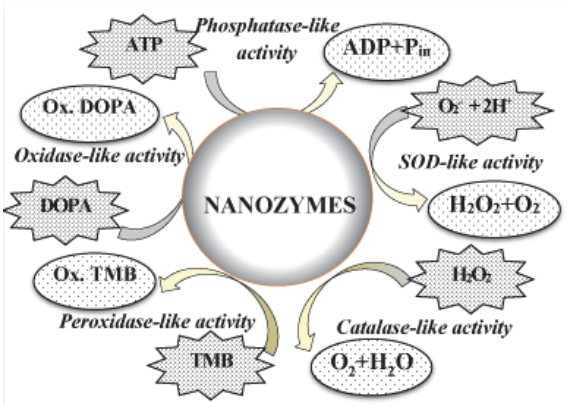

Fig. 3. Enzyme-like properties of nanomaterials: TMB (3,3,5,5-tetramethylbenzidine), DOPA (dihydroxyphenylalanine) (adopted from Singh, 2017)

One of the first superoxide dismutase activities determined was for cerium dioxide nanoparticles (Korsvik et al., 2007; Singh, 2016). In the case of superoxide anion dismutration, the formation of hydrogen peroxide and transitional compound – cerium hydroperoxide $Ce(OOH)(OH)_3$ on the surface of the nanodispersed cerium dioxide occurs, ie, three reactions actually occur (Batinić-Haberle et al., 2010):

Oxidation of $O_2^- - \bar{e} \rightarrow O_2$;

Restoration of $O^{2-} + \bar{e} + 2H^+ \rightarrow H_2O_2$;

Oxidation-reduction $Ce^{3+} + 4H_2O \leftrightarrow Ce(OH)_4 + 4H^+ + \bar{e}$.

The treatment of cerium nanoparticles with H_2O_2 causes a complete loss of SOD-like activity, but after a certain period of time, the activity is restored, which confirms the process of spontaneous regeneration of the nanoparticle surface (in relation to oxygen non-stoichiometry) and recovery to trivalent cerium (Gil et al., 2017; Baldim et al., 2018). The activity of nanoparticles depends on their size. NPs, the size of which is 3–5 nm, more intensively inactivate superoxide anion than larger nanoparticles (5–8 nm). The effectiveness of nanocerium to act as a SOD mimetic is proportional to the concentration of Ce^{3+} ions on the surface of particles (Nelson et al., 2016). The presence of other ions, in particular titanium ions, inhibits this activity (Zhu et al., 2012). SOD-like activity of nanoparticles depends on the ionic composition of the solution (McCormack et al., 2014). During the action of phosphate ions, phosphorylation of the surface of particles occurs, which reduces their ability to manifest the functions of SOD and catalase.

Nanomaterials as catalase mimetics

Along with superoxide radionuclide, hydrogen peroxide is also an active form of oxygen that is neutralized due to catalase. It was determined that a number of nanoparticles effectively protect the cells and tissues from the toxic effects of H_2O_2 (Grinko et al., 2015; Wang et al., 2017) and other peroxides (Sun et al., 2017).

Nanoparticles of Mn_3O_4 (Yao et al., 2018), Fe_3O_4, Co_3O_4 and CeO_2 (Wei & Wang, 2013), $LaCoO_3$ (Wang et al., 2017), NiO-NPs (Faisal et al., 2013), Au (Lin et al., 2014) simulate the activity of catalase. In conditions of physiological reactions, including the substrate, the optimal values of pH and temperature, some nanoparticles, particularly of ferrum oxide, demonstrate catalase- and peroxidase-like activity (Gao et al., 2017). The Fe_2O_3 and Fe_3O_4 nanoparticles decompose H_2O_2 in a neutral and alkaline medium, but it was found that Fe_3O_4 was characterized by higher catalase mimetic activity. Similarly to peroxidase-like activity, the pH range is essential in the effectiveness of this reaction (Chen et al., 2012; Gao et al., 2017). Singh et al. (2017) reported that the ability of graphenes to simulate the catalase function at pH > 7.2. The mechanism of mimetic action of nanoparticles is complex and remains incompletely studied. Grinko et al. (2015) mention that the process of decomposition of H_2O_2 by nanoparticles is similar to the mechanism of catalase activity. The intensity of the catalase-mimetic activity of nanoparticles of transition metals, in particular cerium, is conditioned by the number of ions of trivalent Ce on their surface (Das et al., 2013; Nelson et al., 2016; Yang et al., 2016). The reactivity of hydrogen peroxide is affected by the size of nanoparticles and surface ligands (Lee et al., 2013; Gil et al., 2017). Small CeO_2 nanoparticles, and those containing more oxide, exhibit increased reactivity to H_2O_2. Reaction of the decomposition is not hindered by the surface ligand. Concentrations of Ce^{3+} ions on the surface of CeO_2 nanoparticles have a proportional effect on their catalase-like activity (Nelson et al., 2016).

The possibility of effective use and reuse of CeO_2 nanoparticles as an antioxidant has been proved. Such effect occurs due to the fact that at first the Ce^{3+} ions located on the surface of nanoparticles, are oxidized with hydrogen peroxide, forming Ce^{4+}.

At the same time, H_2O_2 is irreversibly adsorbed on the surface of hydrated Ce^{4+} ions, forming cerium perhydroxide. Perhydroxide is decomposed with the formation of oxygen. After using all of the hydrogen peroxide in the system, part of the quaternary cerium ions due to the restoration (recovery) of the crystalline lattice of the nanoparticle returns to the initial Ce^{3+} state (Celardo et al., 2011; Grinko et al., 2015; Kozik et al., 2016). These processes are possible due to the occurrence of oxygen vacancies which contribute to the formation of oxygen non-stoichiometry and increase in the number of cerium atoms with the III degree of oxidation. The set of processes which occurs on the surface of cerium nanoparticles can be represented in the form of a scheme:

$$NP\text{-}Ce^{3+} + H_2O_2 \rightarrow NP\text{-}Ce^{4+}{=}O + H_2O,$$

$$NP\text{-}Ce^{4+}{=}O + H_2O_2 \rightarrow NP\text{-}Ce^{3+} + H_2O + O_2.$$

Ions of various metals can modify the catalase-like activity of nanoparticles (Tsai et al., 2007). Therefore, in the case of doping into a crystalline lattice of cerium dioxide of zirconium ions, there was observed the activation of the decomposition of hydrogen peroxide, which was directly proportional to the molar Zr/Ce ratio. Celardo et al. (2011) mentioned the opposite effect after introducing Samarium ions into the crystalline lattice of CeNPs. The authors observed a monotonic decrease in the speed of decomposition of hydrogen peroxide, which depended on the content of Samaria.

It was determined that nanopolyhedrons with a high concentration of Ce^{4+} ions contributed to the mimetic activity of catalase, while nanotubes and nanopowders with high concentration of Ce^{3+} ions increased the mimetic activity of SOD (Naganuma, 2017). These results should be used to construct nanoparticles aimed at enhancing enzyme mimetic activity for therapeutic purposes. It was determined that biomimetic artificial enzymes based on antioxidant CeO_2 nanoparticles become luminescent during their Eu^{3+} doping (Pratsinis et al., 2017).

Nanomaterials as oxidase mimetics

Over the recent decades, the enzyme-like properties of nanomaterials have been widely studied, but for the most part, attention has been paid to SOD-like, peroxidase- and catalase-like activity of these nanomaterials. Now, research is becoming focused on nanomaterials with oxidase-like properties.

Oxidases are enzymes from the oxidoreductase class, which catalyze the oxidation-recovery reaction, which includes molecular oxygen as an acceptor of electrons. In the course of reactions which are catalyzed by oxidase, the substrate oxidizes by molecular oxygen, forming water, hydrogen peroxide or free oxygen radicals (Singh, 2016). These enzymes catalyze a number of reactions:

$$Glucose + O_2 \rightarrow Gluconic\ acid + H_2O_2\ (Glucose\ oxidase)$$

$$Galactose + O_2 \rightarrow 1,6\text{-}Diadehyde + H_2O_2\ (Galactose\ oxidase)$$

$$Alcohol + O_2 \rightarrow Aldehyde + H_2O_2\ (Alcohol\ oxidase)$$

$$Cholesterol + O_2 \rightarrow Cholesteon + H_2O_2\ (Cholesterol\ oxidase)$$

$$Choline \rightarrow Betaine + H_2O_2\ (Choline\ oxidase)$$

Recently, research has increasingly focussed on the oxidase-mimetic activity of nanoparticles. The studies by Cao et al. (2017) revealed that

ruthenium nanoparticles (Ru) exhibit their own oxidase activity, catalyzing the oxidation of tetramethylbenzidine (TMB) and sodium L-ascorbate with dissolved oxygen. Similar activity was demonstrated by Pt nanoparticles (Deng et al., 2017), Au (He et al., 2011), Ir (Cui et al., 2017), $CoFe_2O_4$ (Zhang et al., 2013), $ZnFe_2O_4$ (Su et al., 2012), MnO_2 (Yan et al., 2017), CeO_2 (Dalapati, 2017; Estevez et al., 2017), $NiCo_2O_4$ (Song et al., 2018), Se (Guo et al., 2016) and other metals and composites. It was determined that the maximum mimetic activity depends on particular physical parameters. Thus, the nanoparticles of Se exhibited optimal catalytic activity at pH 4 and 30 °C, and the oxidase-like activity was higher as the concentrations increased and the size reduced (Guo et al., 2016). The maximum activity of iridium nanoparticles (IrNP) which were synthesized using sodium citrate and $NaBH_4$, occured at their average diameter of 2.5 nm (Cui et al., 2017). Chen et al. (2017) reported the first attempt of using graphene nanoparticles (GQD/AgNP hybrids). These NPs demonstrate high oxidase activity and remained stable in neutral media at temperature of up to 60 °C. The doping of CeO_2 nanoparticles by titanium caused no reduction in their oxidase mimetic activity, but was accompanied by a change in the shape of the spherical nanostructure (Zhu et al., 2012).

Nanomaterials as peroxidase mimetics

Peroxidase is an enzyme that catalyzes the oxidation of polyphenols and some aromatic amines with oxygen, hydrogen peroxide or organic peroxides. Peroxidase forms a complex compound with hydrogen peroxide, resulting in peroxide being activated and becoming able to act as an acceptor of hydrogen (Pandey et al., 2017).

$$2RH + H_2O_2 \rightarrow 2R + 2H_2O.$$

Peroxidases, as a cofactor in active centers, contain gem, or redox-active cysteine or selenium (van Bloois et al., 2010). There are several types of peroxidases, such as glutathione peroxidase, myeloperoxidase, haloperoxidase, lactoperoxidase, etc. (Pandey et al., 2017).

Since 2007, when the enzyme-like peroxidase activity of Fe_3O_4 nanoparticles was first recorded, over 40 nanomaterials have been identified (Jiang et al., 2018). It was determined that nanomaterials are characterized by peroxidase activity, including high stability and low cost of synthesis (He et al., 2014; Singh, 2016).

Peroxidation activity is characteristic for Co_3O_4 nanoparticles (Jia et al., 2016), Cu_2O (Chen et al., 2012; Guo et al., 2017), FeS (Dutta et al., 2012), CeO_2 (Sun et al., 2017), Au/CeO_2 (Bhagat et al., 2018), $CoFe_2O_4$ (Fan & Huang, 2012), $BiFeO_3$ (Luo et al., 2010), $MnFe_2O_4$ (Vernekar, et al., 2016), CdS (Garai-Ibabe et al., 2014), FeSe (Dutta et al., 2012), FeTe (Jiang et al., 2013), rhodium (Choleva et al., 2018), $ZnFe_2O_4$ (Zhao et al., 2013), graphene oxide (Vineh et al., 2017), fullerene (Voeikov & Yablonskaya, 2015) and carbon nanotubes (Wang et al., 2014). This allows them to be applied for immunoassay, glucose detection, protection against free radicals, etc. Significant enzymic activity of such nanoparticles (in the presence of the nucleus and the shell) is maintained at extreme values of pH (2–11) and high temperature (up to 90 °C), which indicates their superiority over natural enzymes.

Antioxidants based on selenium and tellurium can act as mimetics of glutathione peroxidase, can reduce oxidative stress during inflammatory processes and other pathological conditions (Huang et al., 2014; Lu et al., 2017; Hosnedlova et al., 2018). Nano-Se has a better antioxidant effect than other chemical forms of selenium, at the same time reducing the risk of its toxicity (Wang et al., 2007). The antioxidant properties of SeNPs nanoparticles are more effective compared to other selenium compounds and less toxic than selenomethionine (SeMet).

The internal triple enzyme-mimetic activity of nickel-palladium nanoparticles (NiPd HNPs) (Wang et al., 2016), $LaCoO_3$ was also studied (Wang et al., 2017) and V_6O_{13} (Li et al., 2018). The multimimetic particles of NiPd and V_6O_{13} exhibit oxidase-like, peroxidase-like and catalase-like activity, are reliable, inexpensive and easily synthesized. On the basis of oxidase-like and peroxidase-like activity, a colorimetric biosensor was developed to detect glutathione and a fluorescence system for the detection of H_2O_2 and glucose. Recently, there was discovered the "hidden talent" of gold to exhibit mimetic activity (Lin et al., 2014). Gold nanoparticles, similarly to the multimimetics, were observed simulating peroxidase, nucleases, esterases, glucose oxidases, catalase and superoxide dismutase. The authors mention that these enzyme-like characteristics are conditioned by nanogold itself or functional groups present in the surrounding monolayer.

Zhao et al. (2018) for the first time reported the construction of mesoporous nanostructures based on Co_3O_4 for the dispersion of catalytically active sites for the purpose of doping iron nanoparticles (FeNP). Composites (FeNP @ Co_3O_4 HNCs) have high peroxidase activity, which is significantly higher compared to iron nanoparticles (FeNP) and Co_3O_4. The high catalytic activity of FeNP @ Co_3O_4 nanoparticles occurs due to its porous-hollow structure, which is convenient for dispersion of formed nanoparticles and to reduction of agglomeration.

Nanoparticles Au, MnO_2, Fe_3O_4, CuO, Co_3O_4 NP and CeO_2 caused increased glutathione peroxidase activity (Wei & Wang, 2013). Liu et al. (2012) have shown that stabilized nanoparticles of MnO_2 imitate the activity of peroxidase, therefore they were started to be used in immunoassay for colorimetric measurements. New nanoparticles of Co_9S_8 type with effective intrinsic peroxidase activity can be used for colorimetric ionisation of copper ions (Mu et al., 2018).

Ions of transition metals, such as Fe, have peroxidase activity and can inactivate hydroxyl radicals using a general mechanism similar to Fenton's reaction (Singh, 2016; Gao et al., 2017). Khedri et al. (2018) mention that the peroxidase activity of chitosan coated Fe_3O_4NPs nanoparticles. Similarly to natural enzymes, the enzyme-mimetic activity of nanoparticles may be stimulated or inhibited by certain chemical compounds. Thus, nucleotides, in particular, AMP, can enhance the peroxidase activity of Fe_3O_4 nanoparticles at neutral pH by forming a complex (Yang et al., 2017). Inhibitors of this mimetic activity can be sodium azide, ascorbic acid and catecholamines (Liu et al., 2012). Liao et al. (2018) report that sulfide ions are capable of inhibiting peroxidase-like activity of copper nanoclusters (CuNCs).

It was determined that TiO_2 nanoparticles demonstrated mimetic activity, can be incorporated into a photosensitive biocatalytic cascade, activate alkaline phosphatase, and subsequently peroxidase (Li et al., 2018). Brominated graphene (GBR) containing about 3% bromine had a mimetic peroxidase activity in relation to 3,3', 5,5'-tetramethylbenzidine (TMB). The optimum activity was observed at pH 4.48 (Singh et al., 2016).

Nanomaterials as phosphate mimetics

Phosphatase catalyzes the hydrolysis of complex esters of phosphoric acid in living organisms. The function of phosphatase is maintaining the phosphate level required for various biochemical processes. Phosphatase is involved in biological processes such as cell proliferation, transduction of signals, metabolism, intercellular communication, etc. For the first time, phosphatase-like activity was studied in cerium nanoparticles (Kuchma et al., 2010). Nanoparticles of SeO_2 exhibit phosphatasomimetic activity in relation to the hydrolysis of organic phosphate esters, and the dependence between of the reaction speed on the pH of the medium was determined (Singh, 2016). It is assumed that in the case of this reaction, splitting of phosphate and its adsorption on the surface of nanoparticles occur. According to Kozik et al. (2016), cerium dioxide nanoparticles are not complete phosphatase analogues, since the phosphate group binds to the surface of the nanoparticle irreversibly. Subsequently, cerium phosphate is desorbed, and the surface of nanoparticles is able to be involved in catalytic reactions again. Nanodispersive cerium dioxide is used for concentration and quantitative dephosphorylation of phosphoproteins (Jia et al., 2012). It also can stimulate phosphorylation of mitogen-active protein kinase in human bronchial epithelial cells (Beas2B), manifesting pro-oxidant properties (Park et al., 2008).

The activation of the nuclear transcription factor NF-κB depends on phosphorylation of the protein-inhibitor of IκBα-kinases (IKK) (Popov et al., 2017). NF-κB functions as one of the most important intracellular messengers which combines a variety of environmental signals with the expression of numerous cellular genes. NF-κB regulates a variety of biological processes: cell growth, their survival, tissue development, immune response and inflammatory processes. Disorders in regulation of

signaling mechanisms which are based on NF-κB are associated with such severe human diseases as cancer, autoimmune diseases, chronic inflammation, metabolic disorders, diabetes and neurodegenerative diseases (Ghosh, 2007; Pushkarev et al., 2015).

The ability to purposefully regulate the activity of the factor NF-κB is promising for controlling and treating a large number of pathological processes in the cell. Research has shown that cerium dioxide nanoparticles inhibit phosphorylation of IκBα, thereby reducing the translocation of the p65 subunit, which occurs due to activation of NF-κB (Popov et al., 2017).

Nanoparticles with low ratios of the Ce^{3+}/Ce^{4+} oxidation state demonstrate both mimetic activity of catalase and phosphatase (Dhall et al., 2017). The ability to manifest the activity of acid phosphatase was observed for Pt nanoparticles (Deng et al., 2017), and the activity of alkaline phosphatase simulates fullerene nanoparticles (Voeikov & Yablonskaya, 2015). Reverse phosphorylation and dephosphorylation reactions are the basis of energy and signaling metabolism in the cells, and such molecular activity opens a new perspective in the evaluation and prediction of biological properties of nanoparticles (Celardo et al., 2011).

Conclusions

This paper demonstrates separate results on the study of the enzymatic activity of nanoparticles and their positive effects. However, there are a number of studies on the risks of their use (Bandas et al., 2015; Fu, 2014). As a result of the conducted analysis, we can state that nanoparticles have a large number of applications in various fields – biology, medicine, the food industry, etc. However, the development of new nanosystems raises a number of new questions. It has been found that nanoparticles are highly biologically active, which is determined by the polyfactor action, which needs to be determined. The interaction between nanoparticles and biological molecules, such as proteins, carbohydrates, and lipids, remain poorly studied. Practical application of nanoparticles in biology requires an integrated analysis of the duration of their stay in the organism and the need for targeted delivery to organs and tissues, which accelerates further spread (Grillone et al., 2017). Due to their mimetic properties, it is promising to use nanoparticles for the purpose of early diagnosis of dangerous diseases, development of fundamentally new methods and molecular instruments in therapy and surgery, as well as solving other biological and biotechnological problems. In future, research on this topic requires a safe, responsible and integrated approach with scientific research and assessments of possible medical-sanitary and environmental risks, which is the basis of the European Union policy in the field of nanotechnology (Regulation, 2012).

References

Amani, H., Habibey, R., Hajmiresmail, S. J., Latifi, S., Pazoki-Toroudi, H., & Akhavan, O. (2017). Antioxidant nanomaterials in advanced diagnoses and treatments of ischemia reperfusion injuries. Journal of Materials Chemistry B, 5(48), 9452–9476.

Armstrong, D., Bharali, D. J., Armstrong, D., & Bharali, D. (2013). Oxidative stress and nanotechnology. Methods and Protocols, 1028.

Baldim, V., Bedioui, F., Mignet, N., Margaill, I., & Berret, J. F. (2018). The enzyme-like catalytic activity of cerium oxide nanoparticles and its dependency on Ce^{3+} surface area concentration. Nanoscale, 10(15), 6971–6980.

Bandas, I. A., Krynytska, I. Y., Kulitska, M. I., & Korda, M. M. (2015). Nanoparticles: Importance today, classification, use in medicine, toxicity. Medychna ta Klinichna Khimiya, 17(3), 123–129 (in Ukrainian).

BarathManiKanth, S., Kalishwaralal, K., Sriram, M., Pandian, S. R. K., Youn, H. S., Eom, S., & Gurunathan, S. (2010). Anti-oxidant effect of gold nanoparticles restrains hyperglycemic conditions in diabetic mice. Journal of Nanobiotechnology, 8(1), 16.

Batinić-Haberle, I., Rebouças, J. S., & Spasojević, I. (2010). Superoxide dismutase mimics: Chemistry, pharmacology, and therapeutic potential. Antioxidants and Redox Signaling, 13(6), 877–918.

Bhagat, S., Vallabani, N. S., Shutthanandan, V., Bowden, M., Karakoti, A. S., & Singh, S. (2018). Gold core/Ceria shell-based redox active nanozyme mimicking the biological multienzyme complex phenomenon. Journal of Colloid and Interface Science, 513, 831–842.

Bityutskyy, V. S., Tsekhmistrenko, O. S., Tsekhmistrenko, S. I., Spyvack, M. Y., & Shadura, U. M. (2017). Perspectives of cerium nanoparticles use in agriculture. The Animal Biology, 19(3), 9–17.

Cao, G. J., Jiang, X., Zhang, H., Croley, T. R., & Yin, J. J. (2017). Mimicking horseradish peroxidase and oxidase using ruthenium nanomaterials. RSC Advances, 7(82), 52210–52217.

Celardo, I., Pedersen, J. Z., Traversa, E., & Ghibelli, L. (2011). Pharmacological potential of cerium oxide nanoparticles. Nanoscale, 3(4), 1411–1420.

Chaudhry, Q., & Castle, L. (2015). Safety assessment of nano- and microscale delivery vehicles for bioactive ingredients. Nanotechnology and Functional Foods: Effective Delivery of Bioactive Ingredients, 348–357.

Chekman, I. S., Horchakova, N. O. & Simonov, P. V. (2017). Biologically active substances as nanostructures: A biochemical aspect. Klinična Farmacìâ, 21(2), 15–22 (in Ukrainian).

Chen, H., Seiber, J. N., & Hotze, M. (2014). ACS select on nanotechnology in food and agriculture: A perspective on implications and applications. Journal Agricultural and Food Chemistry, 62(6), 1209–1212.

Chen, S., Quan, Y., Yu, Y. L., & Wang, J. H. (2017). Graphene quantum dot/silver nanoparticle hybrids with oxidase activities for antibacterial application. ACS Biomaterials Science and Engineering, 3(3), 313–321.

Chen, W., Chen, J., Feng, Y. B., Hong, L., Chen, Q. Y., Wu, L. F., Lin, X. H., & Xia, X. H. (2012). Peroxidase-like activity of water-soluble cupric oxide nanoparticles and its analytical application for detection of hydrogen peroxide and glucose. Analyst, 137(7), 1706–1712.

Chen, Z., Yin, J. J., Zhou, Y. T., Zhang, Y., Song, L., Song, M., Hu, S., & Gu, N. (2012). Dual enzyme-like activities of iron oxide nanoparticles and their implication for diminishing cytotoxicity. Acs Nano, 6(5), 4001–4012.

Cheng, H., Zhang, L., He, J., Guo, W., Zhou, Z., Zhang, X., Hie, S., & Wei, H. (2016). Integrated nanozymes with nanoscale proximity for *in vivo* neurochemical monitoring in living brains. Analytical Chemistry, 88(10), 5489–5497.

Choleva, T. G., Gatselou, V. A., Tsogas, G. Z., & Giokas, D. L. (2018). Intrinsic peroxidase-like activity of rhodium nanoparticles, and their application to the colorimetric determination of hydrogen peroxide and glucose. Microchimica Acta, 185(1), 22.

Cîrcu, M., Nan, A., Borodi, G., Liebscher, J., & Turcu, R. (2016). Refinement of magnetite nanoparticles by coating with organic stabilizers. Nanomaterials, 6, 228.

Cormode, D. P., Gao, L., & Koo, H. (2018). Emerging biomedical applications of enzyme-like catalytic nanomaterials. Trends in Biotechnology, 36(1), 15–29.

Cui, M., Zhao, Y., Wang, C., & Song, Q. (2017). The oxidase-like activity of iridium nanoparticles, and their application to colorimetric determination of dissolved oxygen. Microchimica Acta, 184(9), 3113–3119.

Dalapati, R., Sakthivel, B., Ghosalya, M. K., Dhakshinamoorthy, A., & Biswas, S. (2017). A cerium-based metal-organic framework having inherent oxidase-like activity applicable for colorimetric sensing of biothiols and aerobic oxidation of thiols. CrystEngComm, 19(39), 5915–5925.

Das, S., Dowding, J. M., Klump, K. E., McGinnis, J. F., Self, W., & Seal, S. (2013). Cerium oxide nanoparticles: Applications and prospects in nanomedicine. Nanomedicine, 8(9), 1483–1508.

Deng, H. H., Lin, X. L., Liu, Y. H., Li, K. L., Zhuang, Q. Q., Peng, H. P., Liu, A. L., Xia, X. H., & Chen, W. (2017). Chitosan-stabilized platinum nanoparticles as effective oxidase mimics for colorimetric detection of acid phosphatase. Nanoscale, 9(29), 10292–10300.

Dhall, A., Burns, A., Dowding, J., Das, S., Seal, S., & Self, W. (2017). Characterizing the phosphatase mimetic activity of cerium oxide nanoparticles and distinguishing its active site from that for catalase mimetic activity using anionic inhibitors. Environmental Science: Nano, 4(8), 1742–1749.

Dong, Z., Luo, Q., & Liu, J. (2012). Artificial enzymes based on supramolecular scaffolds. Chemical Society Reviews, 41(23), 7890–7908.

Dutta, A. K., Maji, S. K., Srivastava, D. N., Mondal, A., Biswas, P., Paul, P., & Adhikary, B. (2012). Synthesis of FeS and FeSe nanoparticles from a single source precursor: A study of their photocatalytic activity, peroxidase-like behavior, and electrochemical sensing of H_2O_2. ACS Applied Materials & Interfaces, 4(4), 1919–1927.

Estevez, A. Y., Stadler, B., & Erlichman, J. S. (2017). *In-vitro* analysis of catalase-, oxidase- and SOD-mimetic activity of commercially available and custom-synthesized cerium oxide nanoparticles and assessment of neuroprotective effects in a hippocampal brain slice model of ischemia. The FASEB Journal, 31(1 Supplement), 693–695.

Esumi, K., Takei, N., & Yoshimura, T. (2003). Antioxidant-potentiality of gold-chitosan nanocomposites. Colloids and Surfaces B: Biointerfaces, 32, 117–123.

Fa, M., Yang, D., Gao, L., Zhao, R., Luo, Y., & Yao, X. (2018). The effect of AuNP modification on the antioxidant activity of CeO_2 nanomaterials with different morphologies. Applied Surface Science, 2018, e277.

Faisal, M., Saquib, Q., Alatar, A. A., Al-Khedhairy, A. A., Hegazy, A. K., & Musarrat, J. (2013). Phytotoxic hazards of NiO-nanoparticles in tomato: A study on mechanism of cell death. Journal of Hazardous Materials, 250, 318–332.

Fan, Y., & Huang, Y. (2012). The effective peroxidase-like activity of chitosan-functionalized $CoFe_2O_4$ nanoparticles for chemiluminescence sensing of hydrogen peroxide and glucose. Analyst, 137(5), 1225–1231.
Farhangi-Abriz, S., & Torabian, S. (2018). Nano-silicon alters antioxidant activities of soybean seedlings under salt toxicity. Protoplasma, 2018, 1–10.
Fu, P. P. (2014). Introduction to the special issue: Nanomaterials-toxicology and medical applications. Journal of Food and Drug Analysis, 22(1), 1–2.
Gao, L., Fan, K., & Yan, X. (2017). Iron oxide nanozyme: A multifunctional enzyme mimetic for biomedical applications. Theranostics, 7(13), 3207–3227.
Garai-Ibabe, G., Möller, M., Saa, L., Grinyte, R., & Pavlov, V. (2014). Peroxidase-mimicking DNAzyme modulated growth of CdS nanocrystalline structures in situ through redox reaction: Application to development of genosensors and aptasensors. Analytical Chemistry, 86, 10059–10064.
Ghosh, S. (2006). Handbook of transcription factor NF-kappaB. CRC Press.
Gil, D., Rodriguez, J., Ward, B., Vertegel, A., Ivanov, V., & Reukov, V. (2017). Antioxidant activity of SOD and catalase conjugated with nanocrystalline ceria. Bioengineering, 4(1), 18.
Gordon, A. T., Lutz, G. E., Boninger, M. L., & Cooper, R. A. (2007). Introduction to nanotechnology: Potential applications in physical medicine and rehabilitation. American Journal of Physical Medicine and Rehabilitation, 86(3), 225–241.
Grillone, A., Li, T., Battaglini, M., Scarpellini, A., Prato, M., Takeoka, S., & Ciofani, G. (2017). Preparation, characterization, and preliminary in vitro testing of nanoceria-loaded liposomes. Nanomaterials, 7(9), 276.
Grinko, A. M., Brichka, A. V., Bakalinska, O. M., Brichka, S. Y., & Kartel, M. T. (2015). Hydrogen peroxide decomposition by nanocomposites kaolin clay – nanoceria. Poverkhnost', 7, 274–284 (in Ukrainian).
Grulke, E., Reed, K., Beck, M., Huang, X., Cormack, A., & Seal, S. (2014). Nanoceria: Factors affecting its pro- and antioxidant properties. Environmental Science: Nano, 1(5), 429–444.
Guo, L., Huang, K., & Liu, H. (2016). Biocompatibility selenium nanoparticles with an intrinsic oxidase-like activity. Journal of Nanoparticle Research, 18(3), 74.
Guo, Y., Wang, H., Ma, X., Jin, J., Ji, W., Wang, X., Song, W., Zhao, B., & He, C. (2017). Fabrication of Ag–Cu_2O/reduced graphene oxide nanocomposites as surface-enhanced raman scattering substrates for *in situ* monitoring of peroxidase-like catalytic reaction and biosensing. ACS Applied Materials and Interfaces, 9(22), 19074–19081.
He, W., Liu, Y., Yuan, J., Yin, J. J., Wu, X., Hu, X., Zhang, K., Liu, J., Chen, C., Ji, Y., & Guo, Y. (2011). Au@Pt nanostructures as oxidase and peroxidase mimetics for use in immunoassays. Biomaterials, 32(4), 1139–1147.
He, W., Wamer, W., Xia, Q., Yin, J. J., & Fu, P. P. (2014). Enzyme-like activity of nanomaterials. Journal of Environmental Science and Health, Part C, 32(2), 186–211.
Heckert, E. G., Seal, S., & Self, W. T. (2008). Fenton-like reaction catalyzed by the rare earth inner transition metal cerium. Environmental Science and Technology, 42(13), 5014–5019.
Hosnedlova, B., Kepinska, M., Skalickova, S., Fernandez, C., Ruttkay-Nedecky, B., Peng, Q., Baron, M., Melcova, M., Opatrilova, R., Zidkova, J., Bjørklund, G., Sochor, J., & Bjørklund, G. (2018). Nano-selenium and its nanomedicine applications: A critical review. International Journal of Nanomedicine, 13, 2107–2128.
Huang, B., Zhang, J., Hou, J., & Chen, C. (2003). Free radical scavenging efficiency of Nano-Se *in vitro*. Free Radical Biology and Medicine, 35(7), 805–813.
Jia, H., Yang, D., Han, X., Cai, J., Liu, H., & He, W. (2016). Peroxidase-like activity of the Co_3O_4 nanoparticles used for biodetection and evaluation of antioxidant behavior. Nanoscale, 8(11), 5938–5945.
Jia, W., Andaya, A., & Leary, J. A. (2012). Novel mass spectrometric method for phosphorylation quantification using cerium oxide nanoparticles and tandem mass tags. Analytical Chemistry, 84(5), 2466–2473.
Jiang, B., Duan, D., Gao, L., Zhou, M., Fan, K., Tang, Y., Xi, J., Bi, Y., Tong, Z., Gao, G. F., Xie, N., Tang, A., Nie, G., Liang M., & Xie, N. (2018). Standardized assays for determining the catalytic activity and kinetics of peroxidase-like nanozymes. Nature Protocols, 1.
Jiang, L., Yuan, R., Chai, Y., Yuan, Y., Bai, L., & Wang, Y. (2013). An ultrasensitive electrochemical aptasensor for thrombin based on the triplex-amplification of hemin/G-quadruplex horseradish peroxidase-mimicking DNAzyme and horseradish peroxidase decorated FeTe nanorods. Analyst, 138(5), 1497–1503.
Kajita, M., Hikosaka, K., Iitsuka, M., Kanayama, A., Toshima, N., & Miyamoto, Y. (2007). Platinum nanoparticle is a useful scavenger of superoxide anion and hydrogen peroxide. Free Radical Research, 41, 615–626.
Khedri, B., Shahanipour, K., Fatahian, S., & Jafary, F. (2018). Preparation of chitosan-coated Fe_3O_4 nanoparticles and assessment of their effects on enzymatic antioxidant system as well as high-density lipoprotein/low-density lipoprotein lipoproteins on wistar rat. Biomedical and Biotechnology Research Journal, 2(1), 68.
Kim, C. K., Kim, T., Choi. I.-Y., Soh, M., Kim, D., Kim, Y.-J., Jang, H., Yang, H.-S., Kim, J. Y., Park, H. K., Park, S. P., Park, S., Yu, T., Yoon, B.-W., Lee, S.-H., Hyeon, T. (2012). Ceria nanoparticles that can protect against ischemic stroke. Angewandte Chemie International Edition, 51, 11039–11043.
Kim, J., Takahashi, M., Shimizu, T., Shirasawa, T., Kajita, M., Kanayama, A., & Miyamoto, Y. (2008). Effects of a potent antioxidant, platinum nanoparticle, on the lifespan of *Caenorhabditis elegans*. Mechanisms of Ageing and Development, 129(6), 322–331.
Korsvik, C., Patil, S., Seal, S., & Self, W. T. (2007). Superoxide dismutase mimetic properties exhibited by vacancy engineered ceria nanoparticles. Chemical Communications, (10), 1056–1058.
Kozik, V. V., Shcherbakov, A. B., Ivanova, O. S., Spivak, N. Y., & Ivanov, V. K. (2016). Synthesis and biomedical applications of nanodispersed cerium dioxide. Izdatel'skiy Dom Tomskogo universiteta, Tomsk.
Kuchma, M. H., Komanski, C. B., Colon, J., Teblum, A., Masunov, A. E., Alvarado, B., Badu, S., Seal, S., Summy, J., & Baker, C. H. (2010). Phosphate ester hydrolysis of biologically relevant molecules by cerium oxide nanoparticles. Nanomedicine: Nanotechnology, Biology and Medicine, 6(6), 738–744.
Lee, S. S., Song, W., Cho, M., Puppala, H. L., Nguyen, P., Zhu, H., Segatori, L., & Colvin, V. L. (2013). Antioxidant properties of cerium oxide nanocrystals as a function of nanocrystal diameter and surface coating. ACS Nano, 7(11), 9693–9703.
Li, H., Wang, T., Wang, Y., Wang, S., Su, P., & Yang, Y. (2018). Intrinsic triple-enzyme mimetic activity of V_6O_{13} nanotextiles: Mechanism investigation and colorimetric and fluorescent detections. Industrial and Engineering Chemistry Research, 57(6), 2416–2425.
Li, J., Schiavo, S., Xiangli, D., Rametta, G., Miglietta, M. L., Oliviero, M., Changwen, W., & Manzo, S. (2018). Early ecotoxic effects of ZnO nanoparticle chronic exposure in *Mytilus galloprovincialis* revealed by transcription of apoptosis and antioxidant-related genes. Ecotoxicology, 2018, 1–16.
Li, M., & Zhang, C. (2016). γ-Fe_2O_3 nanoparticle-facilitated bisphenol A degradation by white rot fungus. Science Bulletin, 61(6), 468–472.
Li, P., Cao, G. X., Liu, Q., Guo, Y. Y., Dong, Y., Li, Z., & Wang, G. L. (2018). A novel strategy for amplified probing versatile biomolecules through a photoswitchable biocatalytic cascade. Sensors and Actuators B: Chemical, 262, 110–117.
Liao, H., Hu, L., Zhang, Y., Yu, X., Liu, Y., & Li, R. (2018). A highly selective colorimetric sulfide assay based on the inhibition of the peroxidase-like activity of copper nanoclusters. Microchimica Acta, 185(2), 143.
Lin, Y., Ren, J., & Qu, X. (2014). Nano-gold as artificial enzymes: Hidden talents. Advanced Materials, 26(25), 4200–4217.
Liu, B., Sun, Z., Huang, P. J. J., & Liu, J. (2015). Hydrogen peroxide displacing DNA from nanoceria: Mechanism and detection of glucose in serum. Journal of the American Chemical Society, 137(3), 1290–1295.
Liu, C. H., Yu, C. J., & Tseng, W. L. (2012). Fluorescence assay of catecholamines based on the inhibition of peroxidase-like activity of magnetite nanoparticles. Analytica Chimica Acta, 745, 143–148.
Liu, X., Wang, Q., Zhao, H., Zhang, L., Su, Y., & Lv, Y. (2012). BSA-templated MnO_2 nanoparticles as both peroxidase and oxidase mimics. Analyst, 137(19), 4552–4558.
Liu, Y., Wu, H., Chong, Y., Wamer, W. G., Xia, Q., Cai, L., Nie, Z., Fu, P. P., & Yin, J. J. (2015). Platinum nanoparticles: Efficient and stable catechol oxidase mimetics. ACS Applied Materials and Interfaces, 7(35), 19709–19717.
Lu, L., Wang, X., Xiong, C., & Yao, L. (2015). Recent advances in biological detection with magnetic nanoparticles as a useful tool. Science China Chemistry, 58(5), 793–809.
Lu, X., Mestres, G., Singh, V. P., Effati, P., Poon, J. F., Engman, L., & Ott, M. K. (2017). Selenium-and tellurium-based antioxidants for modulating inflamemation and effects on osteoblastic activity. Antioxidants, 6(1), 13.
Luo, W., Li, Y. S., Yuan, J., Zhu, L., Liu, Z., Tang, H., & Liu, S. (2010). Ultrasensitive fluorometric determination of hydrogen peroxide and glucose by using multiferroic $BiFeO_3$ nanoparticles as a catalyst. Talanta, 81(3), 901–907.
Lushchak, V. I. (2015). Free radicals, reactive oxygen species, oxidative stresses and their classifications. The Ukrainian Biochemical Journal, 87(6), 11–18.
McCormack, R. N., Mendez, P., Barkam, S., Neal, C. J., Das, S., & Seal, S. (2014). Inhibition of nanoceria's catalytic activity due to Ce^{3+} site-specific interaction with phosphate ions. The Journal of Physical Chemistry C, 118(33), 18992–19006.
Moglianetti, M., De Luca, E., Pedone, D., Marotta, R., Catelani, T., Sartori, B., Amenitsch, H., Retta, S. F., & Pompa, P. P. (2016). Platinum nanozymes recover cellular ROS homeostasis in an oxidative stress-mediated disease model. Nanoscale, 8(6), 3739–3752.
Morry, J., Ngamcherdtrakul, W., & Yantasee, W. (2017). Oxidative stress in cancer and fibrosis: Opportunity for therapeutic intervention with antioxidant compounds, enzymes, and nanoparticles. Redox Biology, 11, 240–253.
Mu, J., Li, J., Zhao, X., Yang, E. C., & Zhao, X. J. (2018). Novel urchin-like Co_9S_8 nanomaterials with efficient intrinsic peroxidase-like activity for colorimetric sensing of copper (II) ion. Sensors and Actuators B: Chemical, 258, 32–41.

Naganuma, T. (2017). Shape design of cerium oxide nanoparticles for enhancement of enzyme mimetic activity in therapeutic applications. Nano Research, 10(1), 199–217.

Nelson, B. C., Johnson, M. E., Walker, M. L., Riley, K. R., & Sims, C. M. (2016). Antioxidant cerium oxide nanoparticles in biology and medicine. Antioxidants, 5(2), 15.

Pandey, V. P., Awasthi, M., Singh, S., Tiwari, S., & Dwivedi, U. N. (2017). A comprehensive review on function and application of plant peroxidases. Biochemistry and Analytical Biochemistry, 6, 308.

Park, E. J., Choi, J., Park, Y. K., & Park, K. (2008). Oxidative stress induced by cerium oxide nanoparticles in cultured BEAS-2B cells. Toxicology, 245(1–2), 90–100.

Paul, S., Saikia, J., Samdarshi, S., & Konwar, B. (2009). Investigation of antioxidant property of iron oxide particlesby 1′-1′ diphenylpicryl-hydrazyle (dpph) method. Journal of Magnetism and Magnetic Materials, 321, 3621–3623.

Popov, A. L., Shcherbakov, A. B., Zholobak, N. M., Baranchikov, A. Y., & Ivanov, V. K. (2017). Cerium dioxide nanoparticles as third-generation enzymes (nanozymes). Nanosystems: Physics, Chemistry, Mathematics, 8(6), 760–784.

Pratsinis, A., Kelesidis, G. A., Zuercher, S., Krumeich, F., Bolisetty, S., Mezzenga, R., Leroux, J. C., & Sotiriou, G. A. (2017). Enzyme-mimetic antioxidant luminescent nanoparticles for highly sensitive hydrogen peroxide biosensing. ACS Nano, 11(12), 12210–12218.

Pushkarev, V. M., Kovzun, O. I., Pushkarev, V. V., Huda, B. B., & Tronko, N. D. (2015). Chronic inflammation and cancer. Role of nuclear factor NF-κB (review of literature and own data). Journal of the National Academy of Medical Sciences of Ukraine, 21(3–4), 287–298.

Regulation, E. U. (2012). No 528/2012 of the European Parliament and of the Council of 22 May 2012 concerning the making available on the market and use of biocidal products. Official Journal of the European Union L, 167.

Saikia, J. P., Paul, S., Konwar, B. K., & Samdarshi, S. K. (2010). Nickel oxide nanoparticles: A novel antioxidant. Colloids and Surfaces B: Biointerfaces, 78, 146–148.

Samuel, E. L. G., Duong, M. T., Bitner, B. R., Marcano, D. C., Tour, J. M., & Kent, T. A. (2014). Hydrophilic carbon clusters as therapeutic, high-capacity antioxidants. Trends in Biotechnology, 32, 501–505.

Sandhir, R., Yadav, A., Sunkaria, A., & Singhal, N. (2015). Nano-antioxidants: An emerging strategy for intervention against neurodegenerative conditions. Neurochemistry International, 89, 209–226.

Schubert, D., Dargusch, R., Raitano, J., & Chan, S.-W. (2006). Cerium and yttrium oxide nanoparticles are neuroprotective. Biochemical and Biophysical Research Communications, 342, 86–91.

Shah, S. T., A Yehya, W., Saad, O., Simarani, K., Chowdhury, Z., A Alhadi, A., & Al-Ani, L. A. (2017). Surface functionalization of iron oxide nanoparticles with gallic acid as potential antioxidant and antimicrobial agents. Nanomaterials, 7(10), 306.

Sharpe, E., Andreescu, D., & Andreescu, S. (2011). Artificial nanoparticle antioxidants. ACS Symposium Series, 1083, 235–253.

Shcherbakov, A. B., Zholobak, N. M., Ivanov, V. K., Tretyakov, Y. D., & Spivak, N. Y. (2011). Nanomaterials based on the nanocrystalline ceric dioxode: Properties and use perspectives in biology and medicine. Biotechnologia Acta, 4(1), 9–28 (in Russian).

Shin, D. S., Di Donato, M., Barondeau, D. P., Hura, G. L., Hitomi, C., Berglund, J. A., Getzoff, E. D., Cary, S. C., & Tainer, J. A. (2009). Superoxide dismutase from the eukaryotic thermophile *Alvinella pompejana*: Structures, stability, mechanism, and insights into amyotrophic lateral sclerosis. Journal of Molecular Biology, 385(5), 1534–1555.

Sims, C. M., Hanna, S. K., Heller, D. A., Horoszko, C. P., Johnson, M. E., Bustos, A. R. M., Reipa, V., Riley, K. R., & Nelson, B. C. (2017). Redox-active nanomaterials for nanomedicine applications. Nanoscale, 9(40), 15226–15251.

Singh, S. (2016). Cerium oxide based nanozymes: Redox phenomenon at biointerfaces. Biointerphases, 11(4), 04B202.

Singh, S. (2017). Catalytically active nanomaterials: Artificial enzymes of next generation. Nanoscience and Technology, 5(1), 1–6.

Singh, S., Mitra, K., Shukla, A., Singh, R., Gundampati, R. K., Misra, N., Maiti, P., & Ray, B. (2016). Brominated graphene as mimetic peroxidase for sulfide ion recognition. Analytical Chemistry, 89(1), 783–791.

Singh, S., Singh, M., Mitra, K., Singh, R., Gupta, S. K. S., Tiwari, I., & Ray, B. (2017). Electrochemical sensing of hydrogen peroxide using brominated graphene as mimetic catalase. Electrochimica Acta, 258, 1435–1444.

Soares, C., Branco-Neves, S., de Sousa, A., Azenha, M., Cunha, A., Pereira, R., & Fidalgo, F. (2018). SiO_2 nanomaterial as a tool to improve *Hordeum vulgare* L. tolerance to nano-NiO stress. Science of the Total Environment, 622, 517–525.

Song, Y., Zhao, M., Li, H., Wang, X., Cheng, Y., Ding, L., Fan, S., & Chen, S. (2018). Facile preparation of urchin-like $NiCo_2O_4$ microspheres as oxidase mimetic for colormetric assay of hydroquinone. Sensors and Actuators B: Chemical, 255, 1927–1936.

Su, L., Feng, J., Zhou, X., Ren, C., Li, H., & Chen, X. (2012). Colorimetric detection of urine glucose based $ZnFe_2O_4$ magnetic nanoparticles. Analytical Chemistry, 84(13), 5753–5758.

Sun, L., Ding, Y., Jiang, Y., & Liu, Q. (2017). Montmorillonite-loaded ceria nanocomposites with superior peroxidase-like activity for rapid colorimetric detection of H_2O_2. Sensors and Actuators B: Chemical, 239, 848–856.

Szekeres, M., Toth, I. Y., Illes, E., Hajdu, A., Zupko, I., Farkas, K., Oszlanczi, G., Tiszlavicz, L., & Tombacz, E. (2013). Chemical and colloidal stability of carboxylated core-shell magnetite nanoparticles designed for biomedical applications. International Journal of Molecular Sciences, 14, 14550–14574.

Toth, I. Y., Szekeres, M., Turcu, R., Saringer, S., Illes, E., Nesztor, D., & Tombacz, E. (2014). Mechanism of in situ surface polymerization of gallic acid in an environmental-inspired preparation of carboxylated core-shell magnetite nanoparticles. Langmuir, 30, 15451–15461.

Tsai, Y. Y., Oca-Cossio, J., Agering, K., Simpson, N. E., Atkinson, M. A., Wasserfall, C. H., Constantinidis, I., & Sigmund, W. (2007). Novel synthesis of cerium oxide nanoparticles for free radical scavenging. Nanomedicine, 2(3), 325–332.

Tsekhmistrenko, O. S., Tsekhmistrenko, S. I., Bityutskyy, V. S., Melnichenko, O. M., & Oleshko, O. A. (2018). Biomimetic and antioxidant activity of nanocrystalline cerium dioxide. Svit Medytsyny ta Biolohii, 63(1), 196–201.

van Bloois, E., Pazmiño, D. E. T., Winter, R. T., & Fraaije, M. W. (2010). A robust and extracellular heme-containing peroxidase from *Thermobifida fusca* as prototype of a bacterial peroxidase superfamily. Applied Microbiology and Biotechnology, 86(5), 1419–1430.

Verma, A. K. (2014). Anti-oxidant activities of biopolymeric nanoparticles: Boon or bane! Journal of Pharmacy Research, 8, 871–876.

Vernekar, A. A., Das, T., Ghosh, S., & Mugesh, G. (2016). A remarkably efficient $MnFe_2O_4$-based oxidase nanozyme. Chemistry – An Asian Journal, 11, 72–76.

Vineh, M. B., Saboury, A. A., Poostchi, A. A., Rashid, A. M. & Parivar, K. (2017). Stability and activity improvement of horseradish peroxidase by covalent immobilization on functionalized reduced graphene oxide and biodegradetion of high phenol concentration. International Journal of Biological Macromolecules, 17, 32776–32779.

Voeikov, V. L., & Yablonskaya, O. I. (2015). Stabilizing effects of hydrated fullerenes C_{60} in a wide range of concentrations on luciferase, alkaline phosphatese, and peroxidase *in vitro*. Electromagnetic Biology and Medicine, 34(2), 160–166.

Wang, G., Zhang, J., He, X., Zhang, Z., & Zhao, Y. (2017). Ceria nanoparticles as enzyme mimetics. Chinese Journal of Chemistry, 35(6), 791–800.

Wang, H., Li, S., Si, Y., Zhang, N., Sun, Z., Wu, H., & Lin, Y. (2014). Platinum nanocatalysts loaded on graphene oxide-dispersed carbon nanotubes with greatly enhanced peroxidase-like catalysis and electrocatalysis activities. Nanoscale, 6(14), 8107–8116.

Wang, H., Zhang, J., & Yu, H. (2007). Elemental selenium at nano size possesses lower toxicity without compromising the fundamental effect on selenoenzymes: Comparison with selenomethionine in mice. Free Radical Biology and Medicine, 42(10), 1524–1533.

Wang, K., Song, J., Duan, X., Mu, J., & Wang, Y. (2017). Perovskite $LaCoO_3$ nanoparticles as enzyme mimetics: Their catalytic properties, mechanism and application in dopamine biosensing. New Journal of Chemistry, 41(16), 8554–8560.

Wang, Q., Zhang, L., Shang, C., Zhang, Z., & Dong, S. (2016). Triple-enzyme mimetic activity of nickel-palladium hollow nanoparticles and their application in colorimetric biosensing of glucose. Chemical Communications, 52(31), 5410–5413.

Wei, H., & Wang, E. (2013). Nanomaterials with enzyme-like characteristics (nanozymes): Next-generation artificial enzymes. Chemical Society Reviews, 42(14), 6060–6093.

Xu, C., & Qu, X. (2014). Cerium oxide nanoparticle: A remarkably versatile rare earth nanomaterial for biological applications. NPG Asia Materials, 6(3), e90.

Yan, X., Song, Y., Wu, X., Zhu, C., Su, X., Du, D., & Lin, Y. (2017). Oxidase-mimicking activity of ultrathin MnO_2 nanosheets in colorimetric assay of acetylcholinesterase activity. Nanoscale, 9(6), 2317–2323.

Yang, Y. C., Wang, Y. T., & Tseng, W. L. (2017). Amplified peroxidase-like activity in iron oxide nanoparticles using adenosine monophosphate: Application to urinary protein sensing. ACS Applied Materials and Interfaces, 9(11), 10069–10077.

Yang, Y., Mao, Z., Huang, W., Liu, L., Li, J., Li, J., & Wu, Q. (2016). Redox enzyme-mimicking activities of CeO_2 nanostructures: Intrinsic influence of exposed facets. Scientific Reports, 6, 35344.

Yao, J., Cheng, Y., Zhou, M., Zhao, S., Lin, S., Wang, X., Wu, J., Li, S., & Wei, H. (2018). ROS scavenging Mn_3O_4 nanozymes for *in vivo* anti-inflammation. Chemical Science, 9(11), 2927–2933.

Zhang, X., He, S., Chen, Z., & Huang, Y. (2013). $CoFe_2O_4$ nanoparticles as oxidase mimic-mediated chemiluminescence of aqueous luminol for sulfite in white wines. Journal of Agricultural and Food Chemistry, 61(4), 840–847.

Zhao, J., Dong, W., Zhang, X., Chai, H., & Huang, Y. (2018). FeNPs@Co_3O_4 hollow nanocages hybrids as effective peroxidase mimics for glucose biosensing. Sensors and Actuators B: Chemical, 263, 575–584.

Zhao, M., Huang, J., Zhou, Y., Pan, X., He, H., Ye, Z., & Pan, X. (2013). Controlled synthesis of spinel $ZnFe_2O_4$ decorated ZnO heterostructures as peroxidase mimetics for enhanced colorimetric biosensing. Chemical Communications, 49(69), 7656–7658.

Zheng, W., Zou, H. F., Lv, S. W., Lin, Y. H., Wang, M., Yan, F., Sheng, Y., Song, Y. H., Chen, J., & Zheng, K. Y. (2017). The effect of nano-TiO_2 photocatalysis on the antioxidant activities of Cu, Zn-SOD at physiological pH. Journal of Photochemistry and Photobiology B: Biology, 174, 251–260.

Zhu, A., Sun, K., & Petty, H. (2012). Titanium doping reduces superoxide dismutase activity, but not oxidase activity, of catalytic CeO_2 nanoparticles. Inorganic Chemistry Communications, 15, 235–237.

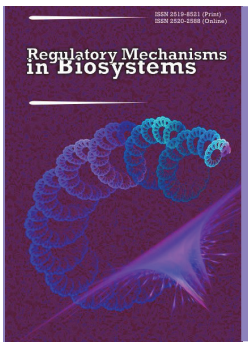

Regulatory Mechanisms in Biosystems

ISSN 2519-8521 (Print)
ISSN 2520-2588 (Online)
Regul. Mech. Biosyst., 9(3)

Table of Contents